



National Library
of Canada

Acquisitions and
Bibliographic Services Branch

395 Wellington Street
Ottawa, Ontario
K1A 0N4

Bibliothèque nationale
du Canada

Direction des acquisitions et
des services bibliographiques

395, rue Wellington
Ottawa (Ontario)
K1A 0N4

Your file Votre référence

Our file Notre référence

NOTICE

The quality of this microform is heavily dependent upon the quality of the original thesis submitted for microfilming. Every effort has been made to ensure the highest quality of reproduction possible.

If pages are missing, contact the university which granted the degree.

Some pages may have indistinct print especially if the original pages were typed with a poor typewriter ribbon or if the university sent us an inferior photocopy.

Reproduction in full or in part of this microform is governed by the Canadian Copyright Act, R.S.C. 1970, c. C-30, and subsequent amendments.

AVIS

La qualité de cette microforme dépend grandement de la qualité de la thèse soumise au microfilmage. Nous avons tout fait pour assurer une qualité supérieure de reproduction.

S'il manque des pages, veuillez communiquer avec l'université qui a conféré le grade.

La qualité d'impression de certaines pages peut laisser à désirer, surtout si les pages originales ont été dactylographiées à l'aide d'un ruban usé ou si l'université nous a fait parvenir une photocopie de qualité inférieure.

La reproduction, même partielle, de cette microforme est soumise à la Loi canadienne sur le droit d'auteur, SRC 1970, c. C-30, et ses amendements subséquents.

Canada

University of Alberta

DYNAMIC TWO-DIMENSIONAL RIVER WATER QUALITY MODELLING

by

Gordon James Putz



**A thesis submitted to the Faculty of Graduate Studies and Research in partial fulfillment of
the requirements for the degree of DOCTOR OF PHILOSOPHY**

in

Environmental Engineering

Department of Civil and Environmental Engineering

Edmonton, Alberta

Spring 1996



National Library
of Canada

Acquisitions and
Bibliographic Services Branch

395 Wellington Street
Ottawa, Ontario
K1A 0N4

Bibliothèque nationale
du Canada

Direction des acquisitions et
des services bibliographiques

395, rue Wellington
Ottawa (Ontario)
K1A 0N4

Your file Votre référence

Our file Notre référence

The author has granted an irrevocable non-exclusive licence allowing the National Library of Canada to reproduce, loan, distribute or sell copies of his/her thesis by any means and in any form or format, making this thesis available to interested persons.

L'auteur a accordé une licence irrévocable et non exclusive permettant à la Bibliothèque nationale du Canada de reproduire, prêter, distribuer ou vendre des copies de sa thèse de quelque manière et sous quelque forme que ce soit pour mettre des exemplaires de cette thèse à la disposition des personnes intéressées.

The author retains ownership of the copyright in his/her thesis. Neither the thesis nor substantial extracts from it may be printed or otherwise reproduced without his/her permission.

L'auteur conserve la propriété du droit d'auteur qui protège sa thèse. Ni la thèse ni des extraits substantiels de celle-ci ne doivent être imprimés ou autrement reproduits sans son autorisation.

ISBN 0-612-10627-6

Canada

University of Alberta

Library Release Form

Name of Author: Gordon James Putz

Title of Thesis: Dynamic Two-Dimensional River Water Quality Modelling

Degree: Doctor of Philosophy

Year this Degree Granted: 1996

Permission is hereby granted to the University of Alberta Library to reproduce single copies of this thesis and to lend or sell copies for private, scholarly, or scientific research purposes only.

The author reserves all other publication and other rights in association with the copyright in the thesis, and except as hereinbefore provided, neither the thesis nor any substantial portion thereof may be printed or otherwise reproduced in any material form whatever without the author's prior written permission.

A handwritten signature in dark ink, appearing to read "Gordon Putz", is written over a horizontal line.

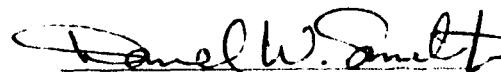
259 Sylvian Way
Saskatoon, Saskatchewan
S7H 5G1

Dated: 18 April, 1996

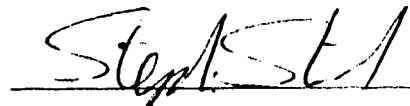
University of Alberta

Faculty of Graduate Studies and Research

The undersigned certify that they have read, and recommend to the Faculty of Graduate Studies and Research for acceptance, a thesis entitled **DYNAMIC TWO-DIMENSIONAL RIVER WATER QUALITY MODELLING** submitted by **GORDON JAMES PUTZ** in partial fulfillment of the requirements for the degree of **DOCTOR OF PHILOSOPHY** in **ENVIRONMENTAL ENGINEERING**.



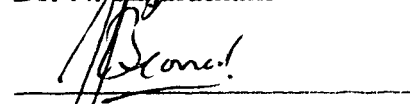
Dr. D.W. Smith



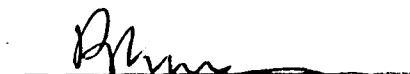
Dr. S.J. Stanley



Dr. N. Rajaratnam



Dr. J. Leonard



Dr. B.G. Krishnappan

Dated: 12 April 1996

Dedication

This thesis and the completion of my doctoral program is dedicated to my wife Susan. Her love, support and self sacrifice has allowed me to accomplish far more than I had ever imagined possible.

I also dedicate this work to the memory of my friend and mentor Dr. Larry Gerard. His commitment to academic and professional excellence continues to be a guiding example and the standard against which I measure my efforts.

Abstract

As background to the thesis work presented herein the following topics are initially reviewed:

- 1. The development of the governing mass balance equation describing the mixing and transport of dissolved, neutrally buoyant substances, discharged to a river system,**
- 2. Methods for determining and predicting transverse mixing coefficients,**
- 3. Solution methods for two-dimensional, steady state, river mixing problems, and**
- 4. Previous work on the development of modelling procedures for the simulation of two-dimensional river mixing with unsteady substance input.**

The development of a microcomputer-based, two-dimensional river mixing model capable of handling unsteady substance source input is described. The model is based upon the original work of Beltraos conducted in the late 1970's. The numerical method employed utilizes a calculation grid with optimized intervals to eliminate numerical dispersion and dissipation errors associated with the advective transport calculations.

The application of this modelling procedure to natural river systems is evaluated by comparing the model output to unsteady source conservative tracer studies conducted on three major rivers (North Saskatchewan, Peace and Slave Rivers). The verification studies conducted are the most extensive field verification of a two-dimensional unsteady input source model presented to date. On the basis of satisfactory results obtained in these three studies the modelling procedure is considered adequately verified for field conditions.

Modification of the modelling procedure to handle non-conservative (reactive) river water quality parameters is described. In particular modifications to simulate dissolved oxygen and biochemical oxygen demand in two-dimensions, downstream of an unsteady discharge are described in detail. Kinetic equations representing carbonaceous and nitrogenous biochemical oxygen demand, atmospheric reaeration, aquatic plant

photosynthetic oxygen production and respiration, and sediment oxygen demand are incorporated into the mixing model.

A verification study of the resulting dissolved oxygen model is presented. Model simulations of dissolved oxygen concentrations, downstream of a primary wastewater treatment plant discharging to the South Saskatchewan River, are compared to measured concentrations taken over a 48 hour period. Model performance was judged to be very good but additional field studies are warranted.

Finally, an adaptation of the mixing model to simulate the adsorption of an organic insecticide to suspended sediment and bed materials is presented. Comparison of the model output to field measurements, taken following a slug treatment of the Athabasca River, could not confirm a suspected loss of insecticide to the bed materials. However, the model study did illustrate the importance of a two-dimensional consideration of mixing and transport in comparison to a previous one-dimensional analysis.

Acknowledgments

I would like to express my sincere thanks to my supervisor, Dr. Daniel W. Smith, for his support and patience throughout my doctoral program. His guidance and encouragement were instrumental in the achievement of my goals.

I would also like to thank my examining committee members (Dr. N. Rajaratnam, Dr. S.J. Stanley, Dr. J. Leonard and Dr. B.G. Krishnappan) for their efforts and valuable suggestions. I am particularly pleased that Dr. B.G. Krishnappan was able to serve as my external examiner.

The following agencies and individuals kindly provided unpublished field data and information from their files:

Alberta Environmental Protection

Mr. G. Fennell

Mr. J. Charles

Trillium Engineering and Hydrographics Inc.

(formerly the Surface Water Engineering Section, Alberta Research Council)

Mr. D. Andres

Mr. J. Thompson

City of Saskatoon

Mr. C.P. Hwang

The efforts and assistance of these individuals is greatly appreciated. The information they provided was vital to the successful completion of my thesis.

Finally, I would like to thank the following organizations for financial support during my studies:

Natural Sciences and Engineering Research Council of Canada

Postgraduate Scholarship

Dr. D.W. Smith, Operating Grant

University of Alberta

Walter H. Johns Graduate Fellowship

University of Saskatchewan

Educational Leave Grants

TABLE OF CONTENTS

CHAPTER	PAGE
1. INTRODUCTION.....	1
1.1 PROBLEM OVERVIEW.....	1
1.2 RESEARCH OBJECTIVES.....	6
1.3 SCOPE OF THE INVESTIGATION.....	6
2. REVIEW OF TWO-DIMENSIONAL RIVER MIXING THEORY.....	7
2.1 GOVERNING EQUATIONS	7
2.1.1 Material Mass Balance Equation.....	7
2.1.2 Two Dimensional Mixing Equation for Prismatic Channels.....	12
2.1.2.1 Transverse mixing zone.....	16
2.1.2.2 Longitudinal mixing zone.....	15
2.2 TRANSVERSE MIXING COEFFICIENT	17
2.2.1 Determination from Tracer Tests.....	18
2.2.1.1 Method of moments analysis.....	18
2.2.1.2 Simulation methods.....	20
2.2.2 Prediction by Empirical Methods.....	20
2.2.2.1 Theoretical background.....	20
2.2.3 Transverse Mixing Coefficient Investigations.....	27
3. SOLUTION PROCEDURES FOR THE TWO-DIMENSIONAL MIXING EQUATION.....	34
3.1 TRANSVERSE COORDINATE TRANSFORMATION	35
3.2 ANALYTICAL SOLUTIONS	37
3.3 NUMERICAL SOLUTION CONSIDERATIONS.....	41
3.3.1 Truncation Error Analysis.....	43
3.3.2 Stability Analysis.....	44
3.3.3 Grid Resolution	46
3.3.4 Convergence.....	46

ION OPTIMIZED GRID METHOD.....	61
CTION.....	61
INVESTIGATIONS.....	62
DESCRIPTION.....	64
Streamtube Representation	65
Longitudinal Spacing of Streamtube Elements.....	66
Effective Flux.....	69
Dispersive Flux.....	69
AND STABILITY CONSIDERATIONS	72
Reaction Substep	72
Dispersion Substep.....	72
Boundary Error	73
Time Step and Transverse Grid Spacing Selection.....	74
IMPLEMENTATION	74
Processing Program STRMTUBE.....	75
Processing Program GRIDGEN.....	76
1 Program 2DMIX.....	78
Processing Program XSLICE.....	80
VERIFICATION STUDIES.....	82
CTION.....	82
VERIFICATION AGAINST ANALYTICAL METHODS	82
Effective Translation	82
Steady State Substance Source	85
VERIFICATION USING LABORATORY MEASUREMENTS.....	87
VERIFICATION USING FIELD TRACER STUDIES.....	92

5.4.1	Introduction.....	92
5.4.2	North Saskatchewan River downstream of Edmonton.....	95
5.4.2.1	Background	95
5.4.2.2	Hydrometric data	95
5.4.2.3	Model input and results.....	101
5.4.3	Peace River at Peace River.....	114
5.4.3.1	Background	114
5.4.3.2	Hydrometric data	114
5.4.3.3	Model input and results.....	115
5.4.4	Slave River downstream Fort Smith.....	126
5.4.4.1	Background	126
5.4.4.2	Hydrometric data	126
5.4.4.3	Model input and results.....	128
5.5	DISCUSSION OF FIELD VERIFICATION RESULTS	142
6.	MODELLING NON CONSERVATIVE SUBSTANCES.....	143
6.1	ADAPTATION OF THE AOG METHOD FOR NON-CONSERVATIVE SUBSTANCES.....	143
6.2	BOD AND DISSOLVED OXYGEN MODELLING	144
6.2.1	Background	144
6.2.2	Analytical verification	152
6.2.3	Field verification South Saskatchewan River downstream of Saskatoon.....	163
6.2.3.1	Background	163
6.2.3.2	Hydrometric data	163
6.2.3.3	Transverse mixing.....	165
6.2.3.4	Model input	169
	6.2.3.4.1 CBOD and NBOD	169
	6.2.3.4.2 Dissolved Oxygen	171
	6.2.3.4.3 Photosynthetic oxygen production and respiration rates	173
	6.2.3.4.4 Sediment Oxygen Demand	178
6.2.3.5	Model results for CBOD.....	179

6.2.3.6	Model results for NBOD.....	181
6.2.3.7	Model results for Dissolved Oxygen.....	184
6.2.3.8	Model results for Sediment Oxygen Demand.....	190
6.2.4	Discussion	191
6.3	MODELLING METHOXYCHLOR SEDIMENT INTERACTIONS.....	193
6.3.1	Methoxychlor.....	193
6.3.2	Field Verification Athabasca River downstream of Athabasca.....	193
6.3.2.1	Background	193
6.3.2.2	Hydrometric data	194
6.3.2.3	Mass conservative mixing simulation.....	197
6.3.2.4	Adsorption and mixing simulation	204
6.3.3	Discussion	206
7.	CONCLUSIONS AND RECOMMENDATIONS.....	208
8.	BIBLIOGRAPHY.....	210
APPENDIX A	Interpolation Procedure for Determining Element Lengths.....	218
APPENDIX B	AOG Method Error Analysis.....	220
APPENDIX C	Program Listings.....	225
	STRMTUBE.....	225
	GRIDGEN	228
	2DMIX.....	234
	XSLICE	242
APPENDIX D	Cross Sections	245
	North Saskatchewan River	246
	Peace River.....	296
	Slave River	312
	South Saskatchewan River.....	332
	Athabasca River.....	336
APPENDIX E	Concept of Dosage	354
APPENDIX F	Notes and Assumptions Regarding the Peace River Mixing Simulation	355

LIST OF FIGURES

	PAGE
Figure 1.1 Typical velocity gradients in a natural stream.....	2
Figure 1.2 Mixing due to differential advection.....	2
Figure 1.3 Typical spread of substance mass in the characteristic mixing regions.....	3
Figure 2.1 Control volume.	7
Figure 2.2 Coordinate system for spatial and velocity components.....	13
Figure 2.3 Velocity distribution in cartesian and transformed coordinates.	21
Figure 2.4 Typical secondary circulation and transverse velocity profile.....	28
Figure 2.5 Dimensionless mixing coefficient vs. aspect ratio.	29
Figure 2.6 Dimensionless mixing coefficient (W as length scale) vs. aspect ratio.....	30
Figure 3.1 Transverse coordinate transformation.	35
Figure 3.2 Image source method to simulate a no flux boundary.....	38
Figure 3.3 Dimensionless concentration vs. χ for a substance source at the left bank...	40
Figure 3.4 Numerical solution procedure.	41
Figure 3.5 Discretization grid.	42
Figure 3.6 Grid Resolution.	46
Figure 3.7 Numerical dispersion and dissipation analysis of a forward time, backward space explicit representation of the one-dimensional advection equation.....	52
Figure 3.8 Numerical dispersion.	53
Figure 4.1 Streamtube representation of cross sections.	65
Figure 4.2 Successive streamtube elements.....	66
Figure 4.3 Discretization grid optimized for advection.	68
Figure 4.4 Adjacent Streamtube Elements (Simple Case).....	70
Figure 4.5 Secondary advective flux.....	73
Figure 4.6 Schematic representation of the function of the GRIDGEN preprocessing program.	77
Figure 4.7 Organization of output from 2DMIX.....	79
Figure 4.8 Post processing of 2DMIX output data.....	81

Figure 5.1	Triangular section used for the advection test.	83
Figure 5.2	Advection test input waveforms.....	84
Figure 5.3	Comparison of concentrations predicted by analytical and numerical solutions for two dimensional steady state mixing.....	87
Figure 5.4	Fischer experiment channel characteristics and probe locations	88
Figure 5.5	Fischer Ser. 2800 Experiment, C-t curves at 16.07 m.....	90
Figure 5.6	Fischer Ser. 2800 Experiment, C-t curves at 26.11 m.....	91
Figure 5.7	Simulated vs. observed results, Athabasca River below Fort McMurray, ice covered, $x = 11.8$ km, - from Beltaos (1978).	94
Figure 5.8	Plan view of the North Saskatchewan study reach.....	97
Figure 5.9	North Saskatchewan River water surface profile.	99
Figure 5.10	Example cross section and flow distribution plot.....	100
Figure 5.11	North Saskatchewan River dosage distributions, slug input.	102
Figure 5.12	North Saskatchewan River, C-t curves at 8960 m, slug input.	104
Figure 5.13	North Saskatchewan River, C-t curves at 19550 m, slug input.	105
Figure 5.14	North Saskatchewan River, C-t curves at 48550 m, slug input.	106
Figure 5.15	North Saskatchewan River dosage distributions, time dependent source... ..	108
Figure 5.16	North Saskatchewan River, C-t curves at 8960 m, extended slug input. ...	109
Figure 5.17	North Saskatchewan River, C-t curves at 19550 m, extended slug input. .	110
Figure 5.18	North Saskatchewan River, C-t curves at 48550 m, extended slug input. .	111
Figure 5.19	Plan of the Peace River study reach.....	116
Figure 5.20	Peace River dosage distributions, extended slug input to the model.....	118
Figure 5.21	Peace River, C-t curves at 8300 m, extended slug input to the model.....	120
Figure 5.22	Peace River, C-t curves at 24800 m, extended slug input to the model....	121
Figure 5.23	Peace River, C-t curves at 42400 m, extended slug input to the model....	122
Figure 5.24	Plan of the Slave River study reach.....	127
Figure 5.25	Dead zone effect approximately 1800 m downstream of injection.....	130
Figure 5.26	Slave River dosage distributions, extended slug input to the model.	131
Figure 5.27	Slave River, C-t curves at 2000 m, extended slug input to the model.....	134
Figure 5.28	Slave River, C-t curves at 5500 m, extended slug input to the model.....	135

Figure 5.29	Slave River, C-t curves at 12000 m, extended slug input to the model.....	136
Figure 5.30	Slave River, C-t curves at 14200 m, extended slug input to the model.....	137
Figure 5.31	Slave River, C-t curves at 15800 m, extended slug input to the model.....	138
Figure 5.32	Slave River, C-t curves at 29100 m, extended slug input to the model.....	140
Figure 6.1	Comparison of model output and Streeter-Phelps analysis.....	154
Figure 6.2	Comparison of periodic BOD profiles computed using Li's solution and the Streeter-Phelps model.....	156
Figure 6.3	Trapezoidal channel sequence used for comparison to Li's solution.	158
Figure 6.4	Biochemical oxygen demand simulations vs. Li analytical solution, $b = 0.30$ for the numerical model, $E_x = 50 \text{ m}^2/\text{s}$ for the analytical model.....	160
Figure 6.5	Dissolved oxygen deficit simulations vs. Li analytical solution, $b = 0.30$ for the numerical model, $E_x = 50 \text{ m}^2/\text{s}$ for the analytical model.....	161
Figure 6.6	BOD and DO analytical solutions for $E_x = 10$ to $100 \text{ m}^2/\text{s}$ vs. numerical solution for $b = 0.3$.....	162
Figure 6.7	South Saskatchewan River downstream of Saskatoon.....	164
Figure 6.8	Diurnal variations in flow, Saskatoon Pollution Control Plant and South Saskatchewan River.....	166
Figure 6.9	Diurnal variations in chloride concentrations, Saskatoon Pollution Control Plant and South Saskatchewan River.	166
Figure 6.10	Effluent chloride mass flow, Saskatoon Pollution Control Plant.....	167
Figure 6.11	Chloride concentration measurements and simulations, South Saskatchewan River downstream of the Saskatoon Pollution Control Plant, input @ $q/Q = 0.36$ to 0.39	168
Figure 6.12	Diurnal variation in CBOD and TKN concentration, Saskatoon Pollution Control Plant and South Saskatchewan River.	170
Figure 6.13	Diurnal variation in CBOD and TKN mass flow, Saskatoon Pollution Control Plant.....	170
Figure 6.14	Diurnal variation in DO concentration, Saskatoon Pollution Control Plant and South Saskatchewan River.	172

Figure 6.15	Diurnal temperature cycle, South Saskatchewan River downstream of Saskatoon.....	172
Figure 6.16	Typical diurnal cycle of photosynthetic oxygen production.....	174
Figure 6.17	Average photosynthetic oxygen areal production rates, South Saskatchewan River downstream of Saskatoon.	176
Figure 6.18	Simulation of diurnal photosynthetic oxygen production.....	178
Figure 6.19	CBOD composite concentration measurements and simulations, South Saskatchewan River downstream of the Saskatoon Pollution Control Plant.....	180
Figure 6.20	TKN composite concentration measurements and simulations, South Saskatchewan River downstream of the Saskatoon Pollution Control Plant.....	182
Figure 6.21	Schematic representation of ammonia and methane generation in bottom sediments.	183
Figure 6.22	Dissolved oxygen measurements and simulations, South Saskatchewan River, Transect 5, 140 m downstream of the Saskatoon Pollution Control Plant.....	186
Figure 6.23	Dissolved oxygen measurements and simulations, South Saskatchewan River, Transect 6, 1130 m downstream of the Saskatoon Pollution Control Plant.....	187
Figure 6.24	Dissolved oxygen measurements and simulations, South Saskatchewan River, Transect 7, 4000 m downstream of the Saskatoon Pollution Control Plant.....	188
Figure 6.25	Dissolved oxygen measurements and simulations, South Saskatchewan River, Transect 8, 13000 m downstream of the Saskatoon Pollution Control Plant.....	189
Figure 6.26	Plan view of the Athabasca River study reach.....	195
Figure 6.27	Athabasca River, Methoxychlor C-t curves at 1760 m.....	199
Figure 6.28	Athabasca River, Methoxychlor C-t curves at 3740 m.....	200
Figure 6.29	Athabasca River, Methoxychlor C-t curves at 8770 m.....	201

Figure 6.30	Athabasca River, Methoxychlor C-t curves at 16670 m.....	202
Figure 6.31	Athabasca River, Methoxychlor C-t curves at 21470 m.....	203

LIST OF TABLES

	PAGE
Table 2.1	Dimensionless transverse mixing coefficients from several investigators..... 32
Table 4.1	STRMTUBE Input/output summary..... 76
Table 4.2	GRIDGEN Input/output summary..... 77
Table 4.3	2DMIX Input/output summary..... 80
Table 5.1	Half sine wave concentrations after the peak has moved 450 time steps. 84
Table 5.2	Rectangular waveform concentrations after 450 time steps. 84
Table 5.3	Half sine wave concentrations after the peak has moved 900 time steps. 85
Table 5.4	Rectangular waveform concentrations after 900 time steps. 85
Table 5.5	Rectangular channel characteristics for diffusion testing..... 86
Table 5.6	Comparison of concentrations predicted by analytical and numerical solutions for two dimensional steady state mixing..... 86
Table 5.7	Fischer experiment channel characteristics and probe locations. 88
Table 5.8	North Saskatchewan River tracer test estimated water surface elevations... 98
Table 5.9	North Saskatchewan River tracer mass recoveries..... 101
Table 5.10	North Saskatchewan River, dimensionless transverse mixing coefficients used in the model..... 112
Table 5.11	Peace River tracer mass recoveries. 117
Table 5.12	Peace River, dimensionless transverse mixing coefficients and shape factors..... 124
Table 5.13	Peace River , initial subreach diffusion factor calculations..... 125
Table 5.14	Peace River, dimensionless transverse mixing parameters..... 125
Table 5.15	Slave River tracer mass recoveries..... 133
Table 5.16	Slave River, dimensionless transverse mixing coefficients..... 141
Table 6.1	Parameters for model verification against Streeter Phelps solution. 154
Table 6.2	Parameters used for periodic BOD calculations..... 156
Table 6.3	Parameters used in the AOG model, Li's solution BOD DO deficit comparisons. 157

Table 6.4	South Saskatchewan River chloride mass recovery ratios.....	167
Table 6.5	South Saskatchewan River dimensionless mixing coefficients.....	169
Table 6.6	Average photosynthetic oxygen production rates, South Saskatchewan River downstream of Saskatoon.	175
Table 6.7	Sediment oxygen demand estimates.....	190
Table 6.8	Comparison of study reach characteristics.....	191
Table 6.9	Athabasca River cross sections.	197
Table 6.10	Summary of methoxychlor sorption and desorption rate coefficients.....	205

LIST OF SYMBOLS

$A_{i,m}$	is the side boundary area shared between element (i, j) and an adjacent element m
A^n	amplitude at time step n
A	amplitude ratio
A_s	source amplitude
c	concentration
\hat{c}	dimensionless concentration
\bar{c}	time-averaged concentration component
c'	time fluctuating concentration component
\tilde{c}	time and depth-averaged concentration component
c''	time-averaged depth fluctuating concentration component
c_∞	fully mixed concentration
C_r	Courant No.
C	dissolved oxygen concentration
C_t	total methoxychlor
C_w	dissolved washload concentrations
C_m	methoxychlor concentration adsorbed to suspended sediment
C_s	dissolved oxygen saturation concentration
CBOD	carbonaceous biochemical oxygen demand
d_z	local transverse diffusion factor
D	dissolved oxygen deficit
D_f	diffusion coefficient
D_z	transverse diffusion factor
E_x, E_z	mixing coefficients
f	fraction of the day between sunrise and sunset
g	gravitational constant
G	rate of flow energy dissipation
h	water depth
H	is the mean sectional depth
k	first order rate coefficient

K	proportionality constant
K_a	volumetric reaeration coefficient
K_b	first order adsorption rate coefficient between the water column and the bed
K_d	first order rate constant for CBOD exertion
K₁	first order rate constant for CBOD exertion in a standard bottle test
K_L	oxygen transfer coefficient,
K_n	first order rate constant for NBOD exertion
K_r	in-stream first order CBOD removal rate coefficient
K_w	first order adsorption rate coefficient to suspended sediment
K_{ws}	first order desorption rate coefficient from suspended sediment
L	CBOD concentration remaining
L₀	ultimate CBOD concentration
L_N	NBOD concentration remaining
M	mass
M_b	methoxychlor mass adsorbed to a bed surface area
M_{ws}	methoxychlor mass adsorbed to the suspended solids within a given water volume
M_A	mass of substance injected per unit area
\dot{M}	mass rate of transport
\bar{n}	normal unit vector
N	number of nodes per wavelength
NBOD	nitrogenous biochemical oxygen demand
P	photosynthetic oxygen production rate
q	cumulative flow
\vec{q}	flux density vector,
\vec{q}_a	advective mass flux vector
\vec{q}_d	diffusive mass flux vector
Q	total channel flow
r	local hydraulic radius
r_r	ratio = $E_z \Delta t / \Delta z^2$
\hat{R}	mass reaction rate per elemental volume

R_c	curve radius
R_h	channel hydraulic radius
Re	grid Reynold's number
R	rate of dissolved oxygen consumption by respiration
s	channel slope
S	rate of sediment oxygen demand
SOD	sediment oxygen demand
t	time
t_1	sunrise time
t_2	sunset time
T	time period
T_c	water temperature in °C
T_K	temperature in °K
TKN	total Kjeldahl nitrogen concentration
u, v, w	velocities in the x,y,z directions
$\bar{u}, \bar{v}, \bar{w}$	time-averaged velocity components in the x,y,z directions
u', v', w'	time fluctuating velocity components in the x,y,z directions
$\tilde{u}, \tilde{v}, \tilde{w}$	time and depth-averaged velocity components in the x,y,z directions
u'', v'', w''	time-averaged depth fluctuating velocity components in the x,y,z directions
u_*	local shear velocity
U	mean channel velocity
U_*	mean channel shear velocity
V	characteristic velocity scale
\forall	volume
\vec{V}	fluid velocity vector
W	section width
x	longitudinal distance
y	vertical distance
y_L	CBOD exerted
Y	height above sea level in metres
z	transverse distance

β	dimensionless mixing coefficient
γ	amplification factor
Γ	surface area
δ	$(4E_x)/(U^2T)$ in Li's solution
$\epsilon_x, \epsilon_y, \epsilon_z$	turbulent diffusion coefficients
η	dimensionless transverse cumulative flow
θ	phase angle error.
Θ	dosage
κ	von Karman's constant
λ	mixing length
Λ	characteristic length scale
v'	velocity fluctuation
ξ	transformed longitudinal coordinate
ρ	fluid density
σ^2	variance of a concentration distribution
σ_z^2	variance of a transverse concentration distribution
τ	shear stress
τ_o	boundary shear stress
ϕ	molecular diffusion coefficient
Φ	time in transformed system
χ	dimensionless longitudinal distance
ψ	shape factor
Ψ	dimensionless transverse distance
ω	waveform frequency, cycles per m
Ω	waveform frequency, radians per m

1. Introduction

1.1 Problem Overview

A critical component of modelling the environmental fate of a substance discharged to a river is to accurately predict its distribution in time and space in the absence of any environmental reactions acting upon it. Once this mass conservative distribution of the substance is defined, it can then be used as a benchmark against which the effects of environmental reactions can be judged. Without the benchmark information it is difficult to separate mixing and transport attenuation effects from the effects of environmental reactions.

A neutrally buoyant substance discharged into a stream will be mixed with the stream water by the processes of diffusion and mixing due to differential advection. At the same time the substance will be moved in the direction of flow by bulk movement (advection) of the fluid.

Diffusion is movement of the substance within the stream due to random motions in the presence of a substance mass concentration gradient. The substance mass moves from areas of high concentration to areas of lower concentration. The random motion may be molecular, a property of the fluid, or turbulent, a property of the fluid flow. In natural flow situations turbulent diffusion is the dominant diffusion mechanism.

Mixing due to differential advection is caused by velocity gradients in the bulk fluid flow. Most natural streams have significant vertical and transverse velocity gradients as shown in Figure 1.1. Mixing by differential advection occurs in conjunction with diffusion as shown in Figure 1.2. Diffusion creates a mass flux (mass flow) in the direction of the area of lower concentration. The velocity profile of the main fluid flow will cause substance mass moving upward due to random motion to increase in velocity, while substance mass moving downward will decrease in velocity. The end result is a spreading of the substance in the streamwise (longitudinal) direction. Similarly longitudinal spreading is also caused by the transverse velocity gradients. The differential advection process is often called 'longitudinal dispersion'.

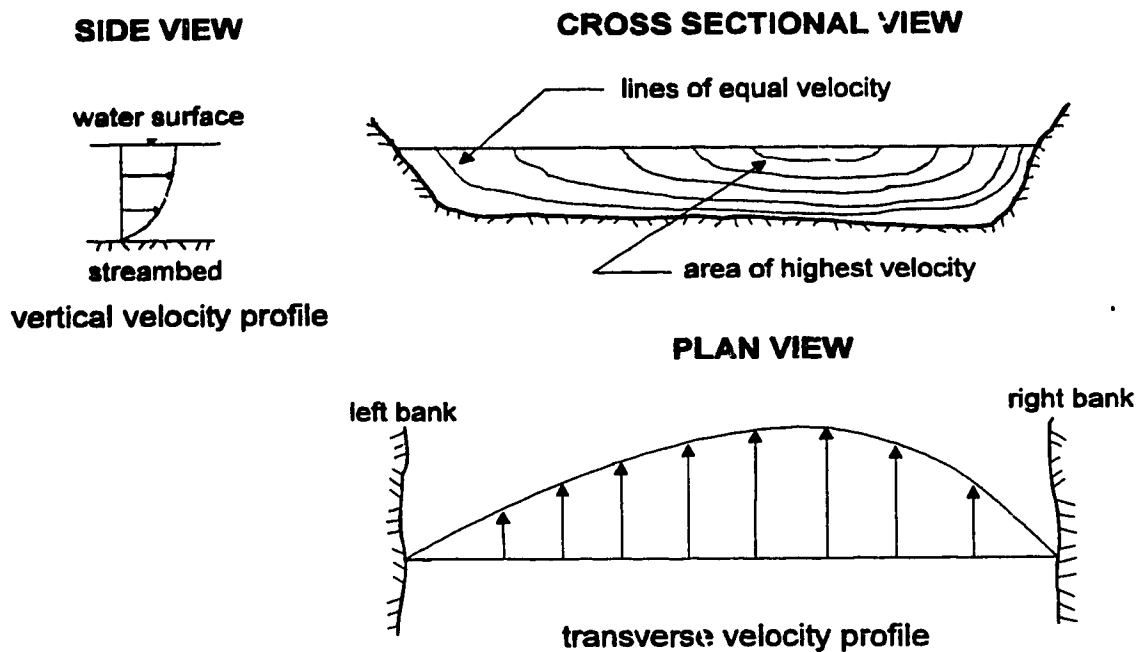


Figure 1.1 Typical velocity gradients in a natural stream.

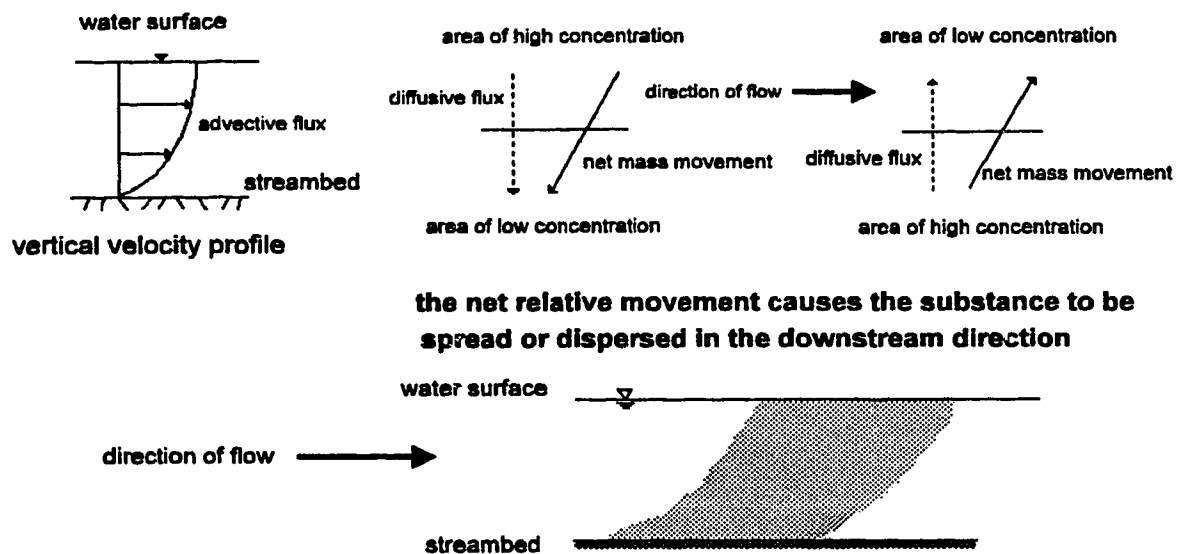


Figure 1.2 Mixing due to differential advection.

The interaction of diffusion, differential advection and channel geometry create several characteristic mixing regions in a river. Beltaos (1979) described these interactions with the aid of Figure 1.3. At time t_0 , a quantity of conservative substance is instantaneously released into the stream flow. The substance mass moves downstream at the local flow velocity, mixing in all directions, primarily by diffusion, and remaining a near uniform cloud until time t_1 corresponding to distance x_1 . Beyond x_1 the substance will encounter the streambed and velocities that are significantly different than the original local velocity at t_0 . The substance cloud then begins to distort due to differential advection.

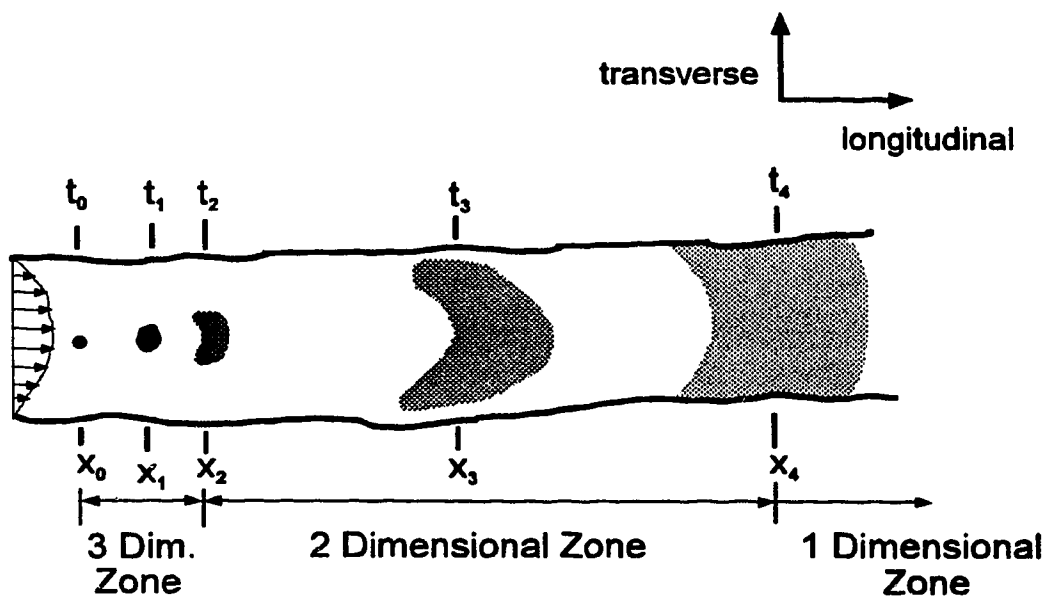


Figure 1.3 Typical spread of substance mass in each of the characteristic mixing regions - modified from Beltaos (1979).

At x_2 the main body of the substance cloud has become uniformly mixed in the vertical due to the 'no flux' boundary conditions of the streambed and the water surface. The cloud is stretched into a crescent shape under the influence of longitudinal dispersion and transverse diffusion. Transverse spreading of the substance mass continues until the edges of the cloud encounter the stream banks at x_3 , and eventually at x_4 near uniform concentrations are established across the stream. Beyond x_4 the cloud continues to stretch in the longitudinal direction.

The region x_0 to x_2 is called the three-dimensional mixing zone because concentration gradients exist in every direction. Between x_2 and x_4 significant concentration gradients only exist in the transverse and longitudinal directions. This region is called the two-dimensional or the transverse mixing zone because the transverse gradients are dominant. Beyond x_4 the dominant concentration gradients exist in the longitudinal direction and the region is called the one-dimensional or longitudinal mixing zone.

Many river mixing and transport models have been developed using the principles of fluid mechanics, mass transport and numerical methods. Most of the models reported in the literature have been verified with field studies. However, the majority of these models have been developed for the following specific situations:

1. one-dimensional, unsteady effluent source problems where the substance concentration changes in time and with distance in the downstream direction only (beyond x_4 in the discussion above), and
2. two-dimensional, steady-state effluent source problems where the substance concentration changes with distance in the downstream direction and with position across the stream in the transverse mixing zone (between x_2 and x_4 in the discussion above), but is invariant in time.

In other words, the models have been developed for simplified special cases of the overall problem in which the substance concentration changes in time, and in three dimensions.

Some simplifications are justified. Most rivers have a large width to depth ratio, and complete mixing in the vertical direction occurs rapidly in comparison to the across stream and downstream directions. As a result, most river mixing models are derived for a depth-averaged concentration, which reduces the overall problem to two spatial dimensions.

In addition, mixing models are generally derived for steady river flow. This is justified because critical situations, in terms of substance mixing, commonly occur under steady or quasi-steady state river flow conditions. Examples are low flow, open water

conditions, or ice-covered winter flow conditions. Although river flow is assumed steady, time dependency is introduced as a result of the characteristics of the waste discharge. Waste discharges may be instantaneous (i.e. a slug release), intermittent, or continuous. The latter two discharge situations commonly have a variable substance concentration in the effluent and/or variable effluent flow. Therefore the capability to handle time varying input conditions is an important feature of a river mixing model.

Two-dimensional capability is important because the transverse mixing zone in a river can extend for many kilometers downstream of the outfall location. A common rule of thumb is that the mixing zone will extend for approximately 100 to 300 river widths downstream of an outfall for a bank discharge. The substance distribution in a large river, resulting from an intermittent or continuously fluctuating discharge, can not be satisfactorily modelled within the two-dimensional zone using the existing special case models. In such cases, a more comprehensive two-dimensional unsteady effluent source model is required.

Two-dimensional, unsteady effluent source modelling techniques for mass conservative substances have been proposed by several authors. However, only limited data has been presented regarding the field verification of such models. One of the most promising techniques was first proposed by Fischer (1968) and later developed more extensively by Beltraos (1978). This method has been verified with several flume experiments, but with only one limited field test. Further, no work has been reported regarding the adaptation of a two-dimensional, unsteady effluent source mixing model for the prediction of common water quality parameters such as dissolved oxygen and biochemical oxygen demand within the transverse mixing zone.

1.2 Research Objectives

The work reported upon herein had the following objectives:

1. Develop a microcomputer-based set of computer programs for modelling two-dimensional, unsteady effluent source river mixing based upon the explicit method first proposed by Fischer (1968) and further developed by Beltraos (1978).
2. Verify this modelling approach using field data from three slug input tracer tests conducted on three major western Canadian rivers.
3. Demonstrate the ease of adaptability of this mixing model to the prediction of non-conservative parameters by the addition of subprograms to simulate typical environmental reactions.
4. Apply an adapted version of the model to the prediction of dissolved oxygen concentrations downstream of the outfall of a primary wastewater treatment plant.
5. Apply an adapted version of the model to the prediction of methoxychlor (an organic insecticide) concentrations downstream of a slug treatment discharge.

1.3 Scope of the Investigation

The scope of the investigation was limited to existing data which had previously been collected by federal, provincial and municipal government agencies and the University of Alberta. No new data was collected due to the prohibitive costs of conducting a comprehensive field program. Despite this restriction the quality of the data sets obtained is reasonable and encompasses five major studies conducted on five separate western Canadian rivers.

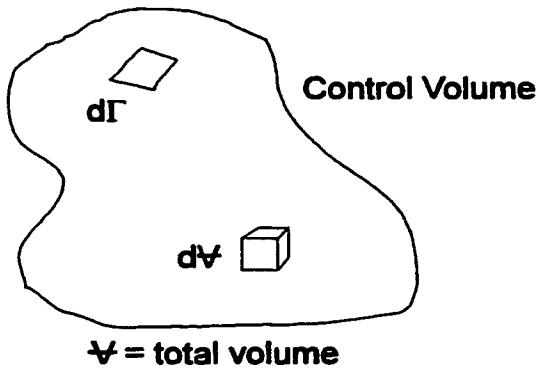
2. Review of Two-Dimensional River Mixing Theory

2.1 Governing Equations

2.1.1 Material Mass Balance Equation

The material mass balance equation is the basis of all mathematical descriptions of substance mixing within a fluid body. Considering a control volume within the fluid body (Csanady, 1973), mass conservation requires that:¹

Γ = total surface area



The time rate of change of total substance
mass in the control volume

=

The net influx of substance across the
surface area of the control volume

+

The time rate of 'creation' or 'decay' of
the substance within the control volume

Figure 2.1 Control volume.

The control volume is shown in Figure 2.1 where: V is the total volume, Γ is the total surface area, dV is an elemental volume and $d\Gamma$ is an elemental area on the surface of the control volume. The elemental volume dV is small enough that the substance concentration c , contained within dV , can be considered a constant throughout dV at any given time. The mass of substance within dV is the product cdV . The total mass of substance, M , within the control volume is given by the following volume integral:

$$M = \int_V c dV \quad [1]$$

¹ The equation development presented in this section is adapted from Steffler, 1991 and Rajaratnam, 1980.

The time rate of change of mass within the control volume is a derivative with respect to time:

$$\frac{dM}{dt} = \frac{d}{dt} \int_V c dV \quad [2]$$

Considering the control volume dimensions to be independent of time, and using the Leibnitz rule Equation [2] may be expressed as follows:

$$\frac{dM}{dt} = \int_V \frac{\partial c}{\partial t} dV \quad [3]$$

The net influx of substance mass through the surface area of the control volume is given by the expression:

$$\text{net influx} = \int_{\Gamma} (-\vec{q} \cdot \vec{n}) d\Gamma \quad [4]$$

where: \vec{q} is a flux density vector,
 \vec{n} is the normal unit vector to the control volume surface, which is positive outward, and
 $d\Gamma$ is an elemental surface area small enough such that \vec{q} is constant for the element at any given time

The net rate of mass reaction (creation or decay) within the control volume is given by the expression:

$$\text{net rate of reaction} = \int_V \hat{R} dV \quad [5]$$

where: \hat{R} is the mass reaction rate per elemental volume

Combining Equations [3], [4], and [5] gives a general integral expression for mass balance within the control volume:

$$\int_V \frac{\partial c}{\partial t} dV = \int_{\Gamma} (-\vec{q} \cdot \vec{n}) d\Gamma + \int_V \hat{R} dV \quad [6]$$

Analytical solution techniques for Equation [6] traditionally work with the differential rather than the integral form of the equation. Although it is possible to solve Equation [6] numerically, most numerical methods also work with the differential form. The divergence theorem can be used to combine all the terms of Equation [6] into the following volume integral equation:

$$\int_V \left(\frac{\partial c}{\partial t} + \nabla \cdot \bar{q} - \hat{R} \right) dV = 0 \quad [7]$$

where the divergence theorem has been used to convert the surface integral to a volume integral as follows:

$$\int_V \nabla \cdot \bar{q} dV = \int_\Gamma \bar{q} \cdot \bar{n} d\Gamma \quad [8]$$

Integrating Equation [7] gives a general differential expression for mass balance of the control volume.

$$\frac{\partial c}{\partial t} + \nabla \cdot \bar{q} - \hat{R} = 0 \quad [9]$$

In order to express Equation [9] in terms of concentration alone a 'constitutive relationship' is required for the flux and reaction variables. That is, an expression is required for the flux and reaction rate as a function of c . To illustrate the incorporation of the constitutive relationships consider a rectilinear control volume in cartesian coordinates. The flow is assumed to be steady and laminar. Turbulent flow will be considered later.

Mass may enter or leave the element as a result of advective or diffusive flux. Advective flux is mass transfer by bulk movement of the fluid and is given as the product of fluid velocity and concentration:

$$\bar{q}_a = \bar{V}c \quad [10]$$

where: \bar{V} is the fluid velocity vector

\bar{q}_a is the advective mass flux vector

Diffusive mass flux occurs as a result of random molecular motion in the fluid. It is analogous to heat flow in a substance and is described by Fick's Law. Diffusive flux

through an elemental area is equal to the product of the concentration gradient perpendicular to the area and a constant called the molecular diffusion coefficient. In vector notation Fick's gradient law can be expressed as follows:

$$\bar{q}_d = -\phi \nabla c \quad [11]$$

where: \bar{q}_d is the advective mass flux vector
 ∇ is the gradient vector
 ϕ is the molecular diffusion coefficient.

The reaction constitutive relationship will depend upon the characteristics of the substance and the fluid flow. For example, a first order decay reaction, which is often used to model the degradation of organic materials, is given as:

$$\hat{R} = -kc \quad [12]$$

where: k is a first order rate coefficient.

Substituting the expressions for mass flux into Equation [9], and switching from vector to scalar notation in cartesian coordinates, gives the following expression for substance mass balance:

$$\frac{\partial c}{\partial t} + \frac{\partial uc}{\partial x} + \frac{\partial vc}{\partial y} + \frac{\partial wc}{\partial z} = \frac{\partial}{\partial x} \left(\phi_x \frac{\partial c}{\partial x} \right) + \frac{\partial}{\partial y} \left(\phi_y \frac{\partial c}{\partial y} \right) + \frac{\partial}{\partial z} \left(\phi_z \frac{\partial c}{\partial z} \right) + \hat{R} \quad [13]$$

where: u, v, w are velocities in the x, y, z directions, and
 \hat{R} is the reaction term left as a general expression.

In the development of Equation [13] the velocity field is assumed to be known and steady. If the velocity field is unknown a relationship to predict its magnitude and direction is also required.

The selection of the constitutive laws, which describe the physical processes, is a critical part of the modelling process. If the constitutive laws poorly represent the phenomena the model will give poor results.

In natural streams the fluid flow is turbulent. In turbulent flow the velocities in the x, y , and z directions and the concentrations at a point are the sum of a time-averaged component and a randomly fluctuating component as shown below:

$$\begin{aligned}
u &= \bar{u} + u' \\
v &= \bar{v} + v' \\
w &= \bar{w} + w' \\
c &= \bar{c} + c'
\end{aligned}
\tag{14}$$

where the overbar indicates a time-averaged component and the prime indicates a fluctuating component.

If a turbulent variable in quasi-steady state flow is time-averaged at a point over a short interval, the average component is a constant and the resultant of the fluctuating component is zero. Substituting Equation [14] into Equation [13] and time averaging each of the terms gives:

$$\begin{aligned}
\frac{\partial \bar{c}}{\partial t} + \frac{\partial \bar{uc}}{\partial x} + \frac{\partial \bar{vc}}{\partial y} + \frac{\partial \bar{wc}}{\partial z} = \\
\frac{\partial}{\partial x} \left(\phi_x \frac{\partial \bar{c}}{\partial x} - \overline{u'c'} \right) + \frac{\partial}{\partial y} \left(\phi_y \frac{\partial \bar{c}}{\partial y} - \overline{v'c'} \right) + \frac{\partial}{\partial z} \left(\phi_z \frac{\partial \bar{c}}{\partial z} - \overline{w'c'} \right) + \hat{R}
\end{aligned}
\tag{15}$$

The time average terms $\overline{u'c'}$, $\overline{v'c'}$ and $\overline{w'c'}$ are the products of random fluctuations about the mean velocities and concentration. They represent substance mass transport via the random motion of discrete fluid packets or eddies (i.e. turbulent motion) superimposed on the mean advective transport. Experiments have shown that mass transport by turbulent motion produces Gaussian concentration distributions which are also a characteristic of the molecular diffusion process (Elder, 1959). Therefore the turbulent flux terms are generally expressed in the form of Fick's Law. For example the x direction component is:

$$\overline{u'c'} = -\epsilon_x \frac{\partial \bar{c}}{\partial x}
\tag{16}$$

where: ϵ_x is the turbulent diffusion coefficient in the x direction.

Further, the turbulent diffusive flux is much larger in magnitude than the molecular diffusive flux, i.e. $\epsilon_x \gg \phi_x$. Substitution of the gradient law expressions for the

turbulent flux terms in Equation [15] and dropping the molecular diffusion terms gives the material mass balance equation for turbulent flow:

$$\frac{\partial \bar{c}}{\partial t} + \frac{\partial \bar{uc}}{\partial x} + \frac{\partial \bar{vc}}{\partial y} + \frac{\partial \bar{wc}}{\partial z} = \frac{\partial}{\partial x} \epsilon_x \frac{\partial \bar{c}}{\partial x} + \frac{\partial}{\partial y} \epsilon_y \frac{\partial \bar{c}}{\partial y} + \frac{\partial}{\partial z} \epsilon_z \frac{\partial \bar{c}}{\partial z} + \hat{R} \quad [17]$$

The overbars in Equation [17] are frequently omitted on the understanding that all variables have been time-averaged.

2.1.2 Two-Dimensional Mixing Equation for Prismatic Channels

The three-dimensional material mass conservation equation was derived in the previous section. Equation [17] can be applied to any mixing problem provided the velocity field, diffusion coefficients, reaction term and boundary conditions are known. However, solutions in three-dimensions require complex algorithms and often require an enormous computing effort.

The initial problem definition can point to appropriate simplifications which can reduce the complexity and computing effort required without sacrificing accuracy. Appropriate simplifications depend upon the channel geometry, the velocity field characteristics and the distance downstream of the substance source.

Natural streams generally have a large aspect ratio (width to depth ratio). Substance mass released to the stream will initially mix in all directions but will rapidly encounter the stream bed and the water surface. The bed and the water surface are 'no flux' boundaries, therefore, the substance will quickly become uniformly mixed in the vertical in comparison to the longitudinal and transverse directions (see Figure 2.2 for the coordinate system definition). Generally the substance is well mixed in the vertical some 50 to 100 river depths downstream of the substance source.²

² Based upon analytical solutions to the three-dimensional pollutant mass balance equation. Experimental verification can be found in Nokes et al. (1984).

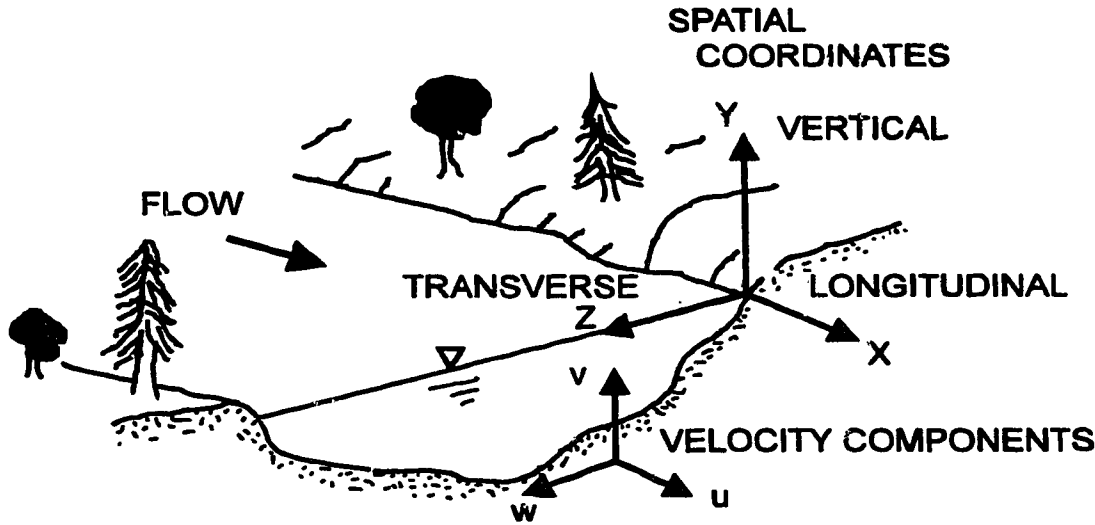


Figure 2.2 Coordinate system for spatial and velocity components.

For water quality modelling beyond the initial three-dimensional zone, it is advantageous to work with a depth-averaged equation. The depth averaging process reduces the problem to two dimensions.

The time-averaged velocities and concentration in Equation [17] can be expressed as the sum of two components, i.e.

$$\begin{aligned}
 \bar{u} &= \tilde{u} + u'' \\
 \bar{v} &= \tilde{v} + v'' \\
 \bar{w} &= \tilde{w} + w'' \\
 \bar{c} &= \tilde{c} + c''
 \end{aligned}
 \tag{18}$$

where the tilde indicates a depth-average component and the double prime indicates a spatially varying component whose depth-average is zero.

A number of terms may be eliminated from Equation [17] using the depth-averaging procedure and recognizing that the vertical advective and diffusive substance mass fluxes at the water surface and at the bed are zero. After substitution of Equation [18] into Equation [17] each term is integrated with respect to y and divided by the total depth h .

For example, depth averaging the second term on the right hand side of the equation gives:

$$\frac{1}{h} \int_0^h \frac{\partial}{\partial y} (\epsilon_y \frac{\partial \bar{c}}{\partial y}) dy = \frac{1}{h} \left[\epsilon_y \frac{\partial \bar{c}}{\partial y} \right]_0^h = 0 \quad [19]$$

The resulting equation after depth-averaging all the terms is:

$$\begin{aligned} \frac{\partial}{\partial t} (h\bar{c}) + \frac{\partial}{\partial x} (h\bar{u}\bar{c}) + \frac{\partial}{\partial z} (h\bar{w}\bar{c}) = \\ \frac{\partial}{\partial x} \left[h\epsilon_x \frac{\partial \bar{c}}{\partial x} + h(\overline{u''c''}) \right] + \frac{\partial}{\partial z} \left[h\epsilon_z \frac{\partial \bar{c}}{\partial z} + h(\overline{w''c''}) \right] + h\hat{R} \end{aligned} \quad [20]$$

where: $\overline{u''c''}$ and $\overline{w''c''}$ represent substance mass transport due to differential advection in the x and z directions respectively, $\overline{u''c''}$ resulting from vertical shear flow (i.e. the distribution of u in the vertical) and $\overline{w''c''}$ resulting from secondary circulation.

This method of analysis was originally developed by Taylor (1953, 1954) in radial coordinates for shear flow in pipes. Elder (1959) later adapted the method to idealized open channel flow in cartesian coordinates.

Generally the turbulent diffusive flux and the differential advective flux in the x and z directions are combined into single terms. This reduces Equation [20] to:

$$\begin{aligned} \frac{\partial}{\partial t} (h\bar{c}) + \frac{\partial}{\partial x} (h\bar{u}\bar{c}) + \frac{\partial}{\partial z} (h\bar{w}\bar{c}) = \\ \frac{\partial}{\partial x} \left(hE_x \frac{\partial \bar{c}}{\partial x} \right) + \frac{\partial}{\partial z} \left(hE_z \frac{\partial \bar{c}}{\partial z} \right) + h\hat{R} \end{aligned} \quad [21]$$

where: E_x and E_z are called mixing coefficients.

The mixing coefficients incorporate the dispersion effects of differential advection into Equation [21] assuming the process is also a direct function of concentration gradient.

The tildes are generally omitted with the understanding that all velocities and the concentration are time and depth-averaged.

Equation [21] is a general expression for two-dimensional mixing in a natural stream. For the case of a prismatic channel (i.e. h and u do not change in the x direction), Equation [21] may be modified to:

$$h \frac{\partial c}{\partial t} + hu \frac{\partial c}{\partial x} + \frac{\partial}{\partial z}(hwc) = h E_x \frac{\partial^2 c}{\partial x^2} + \frac{\partial}{\partial z}(h E_z \frac{\partial c}{\partial z}) + h \hat{R} \quad [22]$$

where: h and u have come outside the longitudinal (x direction) differentials.

Although natural streams can seldom be considered prismatic, they can be approximated by a series of subreaches or segments of constant geometry. The mixing in each subreach is then approximated by Equation [22]. A critical component of the modelling procedure is the acquisition and application of representative subreach geometry and velocity field information.

Additional simplifications to Equation [22] are discussed in the next section. These will further reduce the complexity and computational effort, however, the simplifications only apply to specific regions downstream of the substance source. The modeller must be careful to choose simplifications which are appropriate for the river reach of interest.

2.1.2.1 Transverse mixing zone

Observations of a slug release of substance in a Lagrangian reference frame (i.e. a reference frame moving at the mean advective velocity) within the region before the substance becomes uniformly mixed across the channel, indicate that the transverse spread of the plume is small in comparison to the longitudinal extent of the plume (Elder, 1959). Using order of magnitude analysis it can be shown that $\partial c / \partial z \gg \partial c / \partial x$ and therefore the diffusive flux in the z direction is much greater than in the x direction. For this reason the region is called the transverse mixing zone.

Applying this approximation to Equation [22] and assuming the mean advective transport in the z direction is negligible, i.e. $wc \approx 0$, gives:

$$h \frac{\partial c}{\partial t} + hu \frac{\partial c}{\partial x} = \frac{\partial}{\partial z} (h E_z \frac{\partial c}{\partial z}) + h \hat{R} \quad [23]$$

which describes two-dimensional time dependent mixing and reaction, of a neutrally buoyant substance in the transverse mixing zone for quasi-steady state stream flow.

If the substance mass flux of the source is steady state and the reaction is also steady, then a time independent concentration distribution will be established downstream of the source. In such a case Equation [23] may be further simplified by omitting the time differential giving:

$$hu \frac{\partial c}{\partial x} = \frac{\partial}{\partial z} (h E_z \frac{\partial c}{\partial z}) + h \hat{R} \quad [24]$$

2.1.2.2 Longitudinal mixing zone

Beyond the distance required to establish a near uniform concentration across the flow, the transverse concentration gradient is negligible compared to that in the longitudinal direction, i.e. $\partial c / \partial x \gg \partial c / \partial z$. Applying this approximation to Equation [22] and again assuming negligible transverse advective flux gives:

$$h \frac{\partial c}{\partial t} + hu \frac{\partial c}{\partial x} = h E_x \frac{\partial^2 c}{\partial x^2} + h \hat{R} \quad [25]$$

which describes one-dimensional transient mixing and reaction, of a neutrally buoyant substance in the longitudinal mixing zone for quasi-steady state stream flow.

The steady state expression for Equation [25] is the simplest example of transport and reaction of a neutrally buoyant substance. In this situation the longitudinal diffusive flux is negligible compared to the longitudinal advective flux, i.e. $E_x \partial c / \partial x \ll uc$. The concentration downstream of the source is then given by:

$$u \frac{\partial c}{\partial x} = \hat{R} \quad [26]$$

which is identical to the expression for a steady state plug flow reactor.

2.2 Transverse Mixing Coefficient

In order to use any of the equations presented in the previous section it is necessary to have a knowledge of the mixing coefficients. Several methods are available for the calculation or prediction of mixing coefficients. These include:

1. Change of moments analysis of measured concentration distributions.
2. Numerical or analytical solution of the governing differential equations, using trial and error values for the mixing coefficients, to obtain an optimum fit to measured concentration distributions.
3. Integration of the governing differential equations to solve for the mixing coefficients.
4. Empirical equations for the prediction of the mixing coefficients based upon turbulence theory, channel geometry and flow characteristics.

Methods 1 and 2 require measurements of the substance concentration, channel geometry and velocity distribution downstream of the source. The concentration distribution is often determined by means of a tracer test. Method 1 uses a relationship between substance or tracer plume spreading and diffusion theory to obtain a reach-averaged value of the mixing coefficient. The variance (second central moment) of the concentration distribution at each section is used as a measure of the plume spreading.

In method 2, the value of the mixing coefficients is deduced by trial and error fitting of an analytical or numerical solution of the governing mass balance equation, to measured concentration distributions downstream of the source. Optimum values of the mixing coefficient can be obtained for each subreach.

Method 3 is theoretically based and requires very accurate knowledge of the channel flow characteristics. Expressions or experimental data must be available which accurately define the velocity and shear stress distributions within the flow as well as the concentration distributions. As a result this type of analysis generally can only be applied to simple flow situations such as pipe flow or uniform flow in a infinitely wide channel.

Once the mixing coefficient has been determined, using methods 1,2 or 3 for a particular set of flow and channel characteristics, it may be used in the mass balance equation to predict concentration distributions for other substance discharge conditions. If the flow and channel conditions vary considerably a number of field tests will be required to define the mixing coefficient over the range of variation in flow conditions.

Method 4 uses turbulence theory and knowledge obtained in previous experimental studies to try to empirically relate the mixing coefficient to easily measured channel geometry and flow parameters. No prior knowledge of the concentration distributions is required.

Method 4 is the only truly predictive procedure. However, caution must be used in its application. At this point the empirical relationships are based upon a limited number of field measurements and actual values can vary widely. Method 4 is often satisfactory for first approximation mixing calculations, but coefficients derived from field tracer tests are generally required to confirm and/or improve model accuracy.

2.2.1 Determination from Tracer Tests

2.2.1.1 Method of moments analysis

The analytical solution to the one-dimensional diffusion equation, $\partial c / \partial t = D_f (\partial^2 c / \partial x^2)$, for an instantaneous point source injection of substance is the Gaussian distribution, i.e.

$$c(x,t) = \frac{M_A}{\sqrt{4\pi D_f t}} \exp\left[-\frac{x^2}{4 D_f t}\right] \quad [27]$$

where: x is the distance downstream of the injection point (m),
 t is the time after injection (s),
 D_f is the diffusion coefficient (m^2/s), and
 M_A is the total mass of substance injected per unit area (g/m^2).

For the Gaussian distribution or any other concentration distribution³ it can be shown that the change in variance of the distribution with time is a direct function of the diffusion coefficient, i.e.

$$\frac{d\sigma^2}{dt} = 2D_f \quad [28]$$

where: σ^2 is the variance of the concentration distribution at time t (m^2).

Using this principle, mixing coefficients can be determined from a series of measured concentration distributions by plotting σ^2 versus travel time or distance. For example Sayre and Chang (1968) determined the reach-averaged transverse mixing coefficient E_z for a number of continuous, point-source tracer experiments using the relationship:

$$E_z = \frac{U}{2} \frac{d\sigma_z^2}{dx} \quad [29]$$

where: E_z is the transverse mixing coefficient (m^2/s),
 σ_z^2 is the variance of the transverse concentration distribution (m^2),
 U is the mean channel velocity (m), and
 x is the distance from the tracer injection point (m).

Equation [29] applies to the region between the establishment of a uniform vertical concentration and the distance at which the edge of the tracer plume contacts the channel boundaries. This method of analysis and those similar to it are generally called the change of moments method. Examples of the application of the change in moments method to channels with a significant transverse advection component and to the region influenced by boundary reflections are given by Holley et al. (1972) and Beltraos (1980a).

³ Provided the mass diffusion conforms to Fick's Law and the concentration is zero at $x = \pm \infty$.

2.2.1.2 Simulation methods

As outlined earlier, mixing coefficients can also be determined by iterative solution of the governing mixing equation to give an optimized fit to measured concentration distributions. Specific analytical and numerical solutions will be discussed in the next chapter. Numerical simulations provide an opportunity to incorporate the influence of local variations in depth, velocity and the mixing coefficient into the solution. Examples of the determination of the transverse mixing coefficient using simulation methods are given by Yotsukura and Cobb (1972), Yotsukura and Sayre (1976), Lau and Krishnappan (1981) and Putz (1983).

2.2.2 Prediction by Empirical Methods

2.2.2.1 Theoretical background

Although method 3 is of limited value for predicting mixing coefficients in natural streams, a knowledge of the principles involved in the analysis greatly contributes to an understanding of the mixing process. A general introduction to method 3 for the longitudinal mixing coefficient is given by Fischer et al. (1979). A modified version of this analysis is presented here.

Consider uniform flow in an infinitely wide channel as shown in Figure 2.3. The flow is turbulent with velocity u in the x direction only. There are no changes in u or c in the z direction (into the plane of the paper). Also consider u and c to be time-averaged values. The time-averaged velocity and concentration vary in the vertical direction and can be expressed as the sum of a mean taken over the depth and a deviation from the mean as previously seen in [18]

The mass balance equation for this flow situation is:

$$\frac{\partial}{\partial t}(\bar{c} + c'') + (\bar{u} + u'')\frac{\partial}{\partial x}(\bar{c} + c'') = \epsilon_x \left[\frac{\partial^2}{\partial x^2}(\bar{c} + c'') \right] + \epsilon_y \frac{\partial^2 c''}{\partial y^2} \quad [30]$$

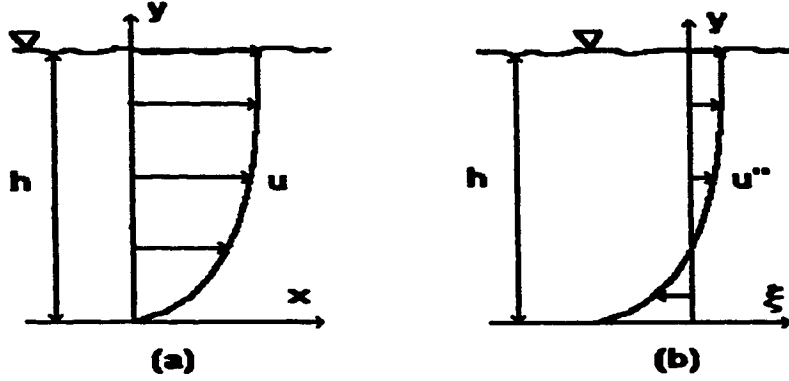


Figure 2.3 Velocity distribution in (a) cartesian coordinates and (b) transformed coordinates.

The analysis proceeds using a transformation of Equation [30] to a coordinate system whose origin moves at the mean velocity , where:

$$\xi = x - \bar{u}t, \quad \Phi = t \quad [31]$$

where ξ is the transformed longitudinal coordinate and Φ is the time in the transformed system.

The coordinate transformation (using the chain rule of calculus), and the assumption that the longitudinal differential advective flux is much larger in magnitude than the turbulent diffusive flux, reduces Equation [30] to:

$$\frac{\partial \tilde{c}}{\partial \Phi} + \frac{\partial c''}{\partial \Phi} + u'' \frac{\partial \tilde{c}}{\partial \xi} + u'' \frac{\partial c''}{\partial \xi} = \epsilon_y \frac{\partial^2 c''}{\partial y^2} \quad [32]$$

Note that in the moving coordinate system the only observable velocity is u'' .

Order of magnitude analysis is used to further simplify Equation [32] to:

$$u'' \frac{\partial \tilde{c}}{\partial \xi} = \epsilon_y \frac{\partial^2 c''}{\partial y^2} \quad \text{with} \quad \frac{\partial c''}{\partial y} = 0, \quad \text{at } y = 0, h \quad [33]$$

which implies a balance between longitudinal advective flux and vertical diffusive flux. However, this balance is only established after an initial elapsed time period due to the influence of the smaller magnitude terms dropped from the equation.

The solution to Equation [33] is:

$$c''(y) = \frac{\partial \bar{c}}{\partial x} \int_0^y \frac{1}{\epsilon_y} \int_0^y u'' dy dy + c''(0) \quad [34]$$

The rate of mass transport in the longitudinal direction, \dot{M} , (in the moving coordinate system) is the product of the velocity u'' and concentration c'' integrated over the depth of flow, i.e.:

$$\dot{M} = \int_0^h u'' c'' dy = \frac{\partial \bar{c}}{\partial x} \int_0^h u'' \int_0^y \frac{1}{\epsilon_y} \int_0^y u'' dy dy dy \quad [35]$$

Note that the second term of Equation [34] becomes zero when integrated over the depth of flow.

Equation [35] shows that the mass transport in the longitudinal direction, viewed in the moving coordinate system, is proportional to the concentration gradient in the longitudinal direction. A depth-averaged bulk transport equation can be written in the form of Fick's Law, analogous to molecular and turbulent diffusion, i.e.

$$\dot{M} = -h E_x \frac{\partial \bar{c}}{\partial x} \quad [36]$$

in which E_x is the longitudinal dispersion (mixing) coefficient. E_x plays the same role in expressions for depth-averaged mass transport as ϵ_x does in expressions describing diffusive flux at the elemental scale. The value of E_x can be calculated as follows:

$$E_x = -\frac{1}{h} \int_0^h \int_0^y \frac{1}{\epsilon_y} \int_0^y u'' dy dy dy \quad [37]$$

provided the velocity distribution and the distribution of the vertical turbulent diffusion coefficient are known.

Using E_x , a one-dimensional diffusion equation for the depth-averaged mass flux in the moving coordinate system is given as:

$$\frac{\partial \bar{c}}{\partial \Phi} = E_x \frac{\partial^2 \bar{c}}{\partial \xi^2} \quad [38]$$

Converting back to a cartesian coordinate system, the mean advective velocity is reintroduced and Equation [38] becomes:

$$\frac{\partial \bar{c}}{\partial t} + \bar{u} \frac{\partial \bar{c}}{\partial x} = E_x \frac{\partial^2 \bar{c}}{\partial x^2} \quad [39]$$

which is identical to Equation [25], the longitudinal dispersion equation discussed earlier, for a conservative substance (i.e. there is no reaction term).

This method of analysis to obtain an expression for the longitudinal dispersion (mixing) coefficient was developed by Taylor (1953,1954) for shear flow in a pipe.

Taylor's analysis uses the 'Reynold's analogy' which states that the diffusion coefficients for mass and momentum flux are equal in magnitude. The momentum diffusive flux through a unit surface area is equal to the shear stress τ at the surface divided by the fluid density ρ and is analogous to the mass diffusive flux q_d . Therefore, by the Reynold's analogy:

$$\varepsilon_y = \frac{\tau / \rho}{(\partial u / \partial y)} = \frac{q_d}{(\partial c / \partial y)} \quad [40]$$

Hence E_x can be calculated using Equation [37] provided the distribution of velocity and shear stress are known for the flow.

Taylor substituted experimentally-derived expressions for u'' and ε_y into an equation equivalent to Equation [37] derived for pipe flow and then numerically integrated the equation to obtain the following simple expression:

$$E_x = 10.1 r u_* \quad [41]$$

where: r is the hydraulic radius, for pipe flow $r = \text{pipe dia.}/4$ (m),
 u_* is the shear velocity given by $(\tau_o/\rho)^{1/2}$ (m/s) where,
 τ_o is the shear stress at the pipe wall (kg/m s^2 or N/m^2), and
 ρ is the fluid density (kg/m^3).

Elder (1959) applied Taylor's method of analysis to uniform flow in an infinitely wide channel and derived a simple expression for the longitudinal dispersion coefficient. Elder used the following logarithmic velocity profile for the calculations:

$$u = \bar{u} + u'' = \bar{u} + \frac{u_*}{\kappa} \left[1 + \ln \left(\frac{y}{h} \right) \right] \quad [42]$$

where: y is the distance from the bed, and
 κ is von Karman's constant, generally taken as ≈ 0.4 .

For open channel flow, the shear velocity is given by:

$$u_* = \sqrt{g R_h s} \quad [43]$$

where: g is the gravitational constant (m/s^2),
 R_h is the channel hydraulic radius (m), and
 s is the slope of the energy line (water surface slope for uniform flow).

The distribution of shear stress across the flow can be derived from a force balance and is given by:

$$\tau = \tau_0 \left[1 - \frac{y}{h} \right] \quad [44]$$

Substituting Equations [42] and [44] into Equation [40], and differentiating u with respect to y , gives the following expression for ε_y :

$$\varepsilon_y = \kappa \left[\frac{y}{h} \right] \left[1 - \frac{y}{h} \right] h u_* \quad [45]$$

Equation [45] and the expression for u'' from Equation [42] are then substituted into Equation [37] and the triple integral evaluated giving:

$$E_x = \left[\frac{0.404}{\kappa^3} \right] h u_* \quad [46]$$

Elder took κ to be 0.41 reducing the expression to:

$$E_x = 5.93 h u_* \quad [47]$$

Taylor's method of analysis could be applied to more complicated flow situations if the vertical and transverse variations in velocity and shear stress were described by mathematical expressions. If these expressions were available then the derived expression for E_x would have to be section-averaged rather than depth-averaged to account for variations in u'' in the transverse direction. A comparable expression could also be derived for E_z , the transverse mixing coefficient, if the distribution of w'' and the transverse shear stress distribution were known.

Unfortunately the complexity of natural stream flow and even flow within a flume is generally too great to handle using Taylor's method. As a result, empirical methods for predicting the magnitude of the mixing coefficients have been developed based upon turbulence theory and easily measurable flow parameters.

The general theory of turbulent diffusion (Taylor, 1921) states that turbulent diffusive flux is related to the random movement of fluid particles or packets called eddies. As shown above, the turbulent diffusion is analogous to molecular diffusion and can be quantified with a gradient expression in the same form as Fick's Law. Taylor's analysis shows the turbulent mixing coefficient is given as:

$$\epsilon_n = \lambda_n \left[(v')^2 \right]_n^{1/2} \quad [48]$$

where: ϵ_n is the turbulent diffusion coefficient in the n direction,
 λ_n is the effective eddy size in the n direction, often called the mixing length, and
 $[(v')^2]_n^{1/2}$ is the root mean square of the velocity fluctuations in the n direction, a measure of the intensity of the turbulence.

It is difficult to measure λ_n and v' . Therefore, more easily measured parameters are desirable to characterize the turbulence. Commonly selected parameters are generally a length scale, representative of the channel geometry and hopefully of the eddy size, and a velocity scale representative of the intensity of the turbulence of the flow in question. The turbulent diffusion coefficient is then given by:

$$\varepsilon = \beta \Lambda V \quad [49]$$

where: Λ is a characteristic length scale, (m)
 V is a characteristic velocity scale, and (m/s)
 β is a dimensionless coefficient.

The validity of this empirical approach for predicting the turbulent diffusion coefficient is evident in Elder's analysis of uniform flow in an infinitely wide channel. If Equation [45] is integrated over the flow depth with $\kappa = 0.41$, the depth-averaged vertical turbulent diffusion coefficient is given as:

$$\overline{\varepsilon_y} = 0.067 h u_* \quad [50]$$

where: h the flow depth, is the length scale, (m)
 u_* the shear velocity, is the velocity scale, and (m/s)
 β is the dimensionless diffusion coefficient = 0.067.

An empirical formulation is also representative of the mixing coefficients derived by Elder and Taylor as shown by Equations [41] and [47]. It must be remembered that Equation [47] was derived for idealized flow with no transverse velocity gradients. Natural streams always contain transverse velocity gradients due to the bank boundary shear. These gradients greatly contribute to the dispersion effect and as a result E_x is always much larger than predicted by Equation [47].

In order to predict E_x accounting for the transverse velocity gradients, expressions similar in format to Equation [47] are used with section-averaged, rather than depth-averaged parameters. An example proposed by Fischer (1975) is:

$$E_x = \frac{0.11 U^2 W^2}{H U_*} \quad [51]$$

where: U is the mean sectional velocity, (m/s)
 W is the section width, (m)
 H is the mean sectional depth, and (m)
 U_* is the mean sectional shear velocity. (m/s)

An alternative approach is to use the following relationship proposed by Kolomogoroff (1941) in which the intensity of the turbulence is characterized by energy dissipation rather than a velocity scale:

$$E_x = \beta G^{1/3} \lambda^{4/3} \quad [52]$$

where: G is the rate of flow energy dissipation per unit mass, and
 λ is the mixing length.

One-dimensional mixing and the longitudinal dispersion (mixing) coefficient have been extensively studied by many authors. Notable works are those by Fischer (1973) and Beltaos (1980b). The objective of the above discussions was to illustrate the determination of mixing coefficients by integration methods. An appreciation of these theoretic arguments are important because they form the basis for the structure of empirical formula's used for the prediction of transverse and longitudinal mixing coefficients.

As the major focus of this work is within the two-dimensional mixing zone no further discussion of one-dimensional longitudinal mixing will be presented. For further information on longitudinal mixing and the longitudinal mixing coefficient before and after the balance implied by Equation [33] the reader should consult the review paper by Elhadi et al. (1984) and the reference works by Fisher et al. (1979) and Rutherford (1994).

2.2.3 Transverse Mixing Coefficient Investigations

Within the two-dimensional mixing zone there are large concentration gradients in the transverse direction. Although the time and depth-averaged transverse velocity (i.e. \tilde{w}) is generally negligible, transverse mixing occurs due to turbulent diffusion and dispersion effects. The w' turbulent fluctuations create a diffusive flux while transverse velocity profiles of the type shown in Figure 2.4 cause a dispersion effect.

The transverse velocity profiles, often called 'secondary circulation', are induced by bank shear, especially where there are bends or large irregularities. It is very difficult to quantify or derive expressions for w' and w'' and therefore the transverse mixing coefficient is generally predicted using an empirical equation.

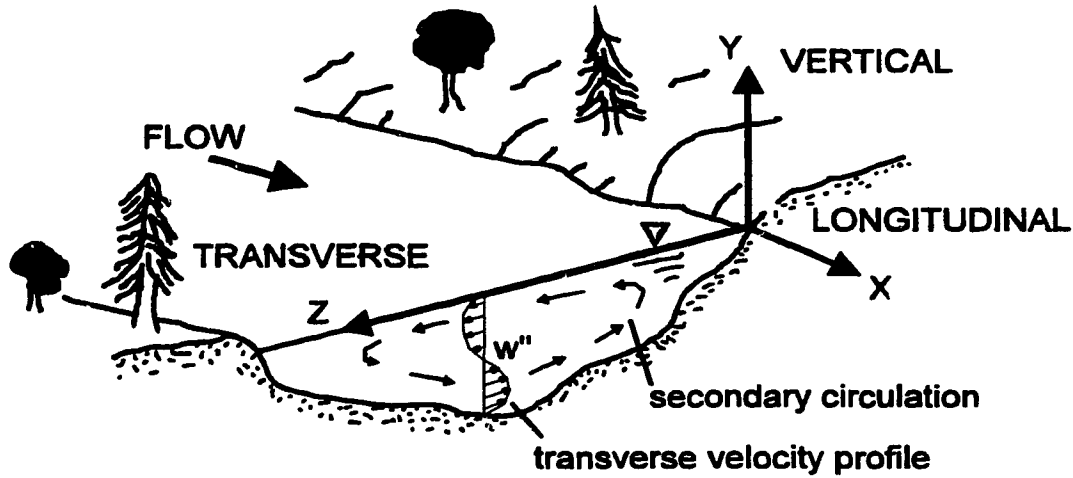


Figure 2.4 Typical secondary circulation and transverse velocity profile.

While investigating longitudinal dispersion in a wide rectangular channel Elder (1959) also observed the transverse concentration distributions resulting from a point source slug injection of tracer. He noted that the distributions were Gaussian in shape implying a Fickian diffusion type process and proposed an empirical expression similar to that for the vertical diffusion coefficient, i.e.

$$\varepsilon_z = \beta H U. \quad [53]$$

Elder estimated β to have a value of 0.23 on the basis of a best fit Gaussian curve to his experimental results.

Since Elder's original work the transverse mixing coefficient E_z (which includes turbulent diffusion and dispersion effects) has been extensively studied in straight rectangular channels (i.e. flumes) and in natural streams. Despite all the effort a great deal of uncertainty still exists regarding the factors which influence its magnitude.

Lau and Krishnappan (1977) presented a comprehensive summary of the results of approximately 50 transverse mixing experiments in straight rectangular channels. This data and the results of more recent experiments by Webel and Schatzmann (1984) and Nokes and Wood (1988) are shown in Figure 2.5. An approximate average for the experimental results using Elder's empirical formulation is $\beta = 0.14$.

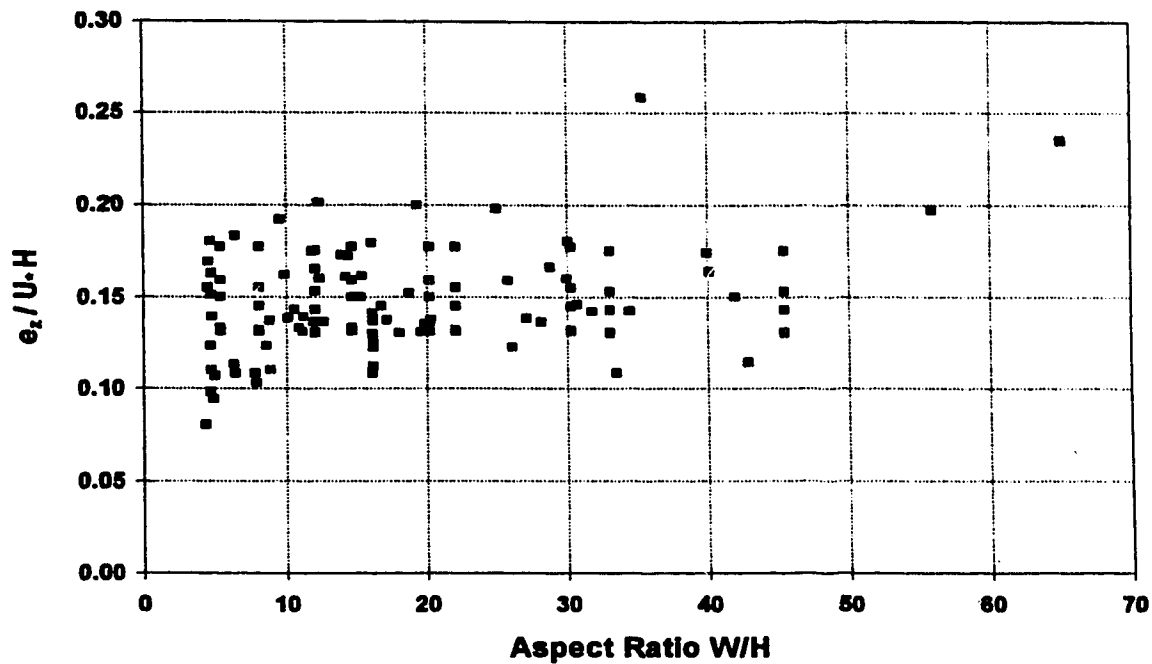


**Figure 2.5 Dimensionless Mixing Coefficient vs. Aspect Ratio
- modified from Lau and Krishnappan (1977).**

In an effort to explain some of the scatter in his experimental data Okoye (1970) suggested β may be a function of channel aspect ratio (i.e. W/H , the channel width to depth ratio). A dimensional analysis conducted by Lau and Krishnappan (1977) also suggested β may be a function of aspect ratio. The aspect ratio should be indicative of the possible magnitude of the secondary currents. If W/H is large the influence of side wall shear and thus secondary currents will be less significant than for small W/H .

Lau and Krishnappan (1977) could not confirm this relationship but proposed an alternative method to reduce the scatter in the data. They suggested using the channel width as the length scale in the empirical formula and plotted E_z/WU_* vs. channel aspect ratio. Using this approach all the data appears to collapse onto one consistent curve as shown in Figure 2.6.

There is some qualitative basis for suggesting a lateral length scale to characterize the transverse mixing. Fischer (1967), in commenting on the large magnitude of the transverse mixing in comparison to that in the vertical, had alluded to the fact that eddy

size is partially dependent upon the proximity of normal boundaries. Hence eddy size is less restricted in the transverse than in the vertical direction. Fischer (1967) suggested larger scale eddies in the transverse direction may provide more effective mixing explaining the larger coefficients measured in the transverse compared to the vertical.

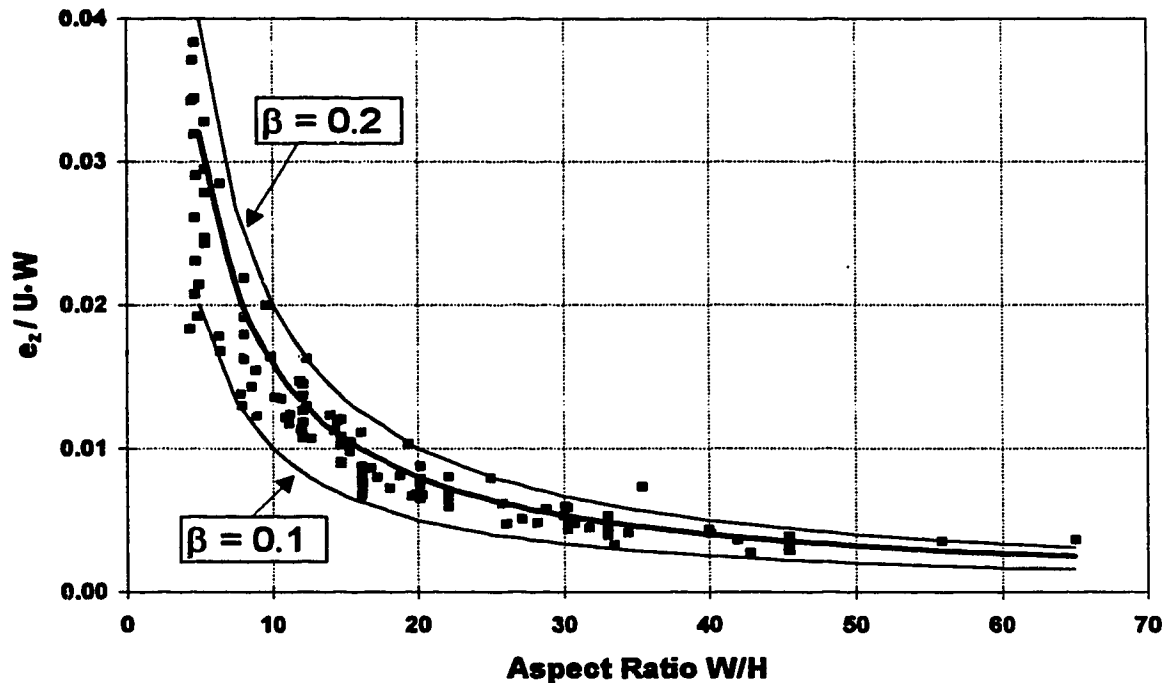


Figure 2.6 Dimensionless Mixing Coefficient (W as length scale) vs. Aspect Ratio - modified from Nokes and Wood (1988).

Webel and Schatzmann (1984) conducted a comprehensive laboratory study of the hydraulic and geometric parameters which dimensional analysis indicate could influence β . These included Froude No., Reynolds No., friction factor and aspect ratio. They concluded E_z/HU_* was independent of all parameters except friction factor. For smooth bed flow with friction factor < 0.08 , they observed an increase in E_z/HU_* .⁴ For friction factor > 0.08 , E_z/HU_* was constant with a value of about 0.13. Webel and Schatzmann

⁴ Values of friction factor < 0.08 are well below those found in natural streams.

concluded that the flow depth and not width was the most appropriate length scale for non-dimensionalizing E_z .

Nokes and Wood (1988) further studied the question of non-dimensionalizing E_z and also concluded that depth was the most appropriate length scale. They demonstrated that a plot of $E_z/WU_* = 0.16/(W/H)$ gives an excellent fit to the data presented by Lau and Krishnappan. In effect this curve is a plot of $E_z/HU_* = 0.16$ and therefore the curve of good fit is independent of aspect ratio and the channel width. The majority of the data shown in Figure 2.6 fall between the curves defined by $E_z/HU_* = 0.10$ and 0.20 .

Nokes and Wood (1988) qualified their finding by stating investigators must clearly define what processes E_z is intended to represent. If E_z is only intended to represent transverse turbulent diffusion, with negligible secondary circulation, then the depth is the correct parameter. They took great care in their experiments and in the selection of data from other investigators to eliminate secondary circulation from the analysis. Basically this meant they only used data with large aspect ratio (including Webel and Schatzmann's) which would minimize side wall induced secondary circulation. On this basis they concluded $\varepsilon_z = 0.134 HU_*$.⁵

While these results for rectangular channels are of academic interest they are not that useful for predicting the mixing in natural channels due to the ever present secondary circulations. This is confirmed by numerous field measurements where E_z/HU_* has been found to range from 2 to 40 times the value of 0.134. A summary of field results from a number of investigations is shown in Table 2.1.

In a field simulation, E_z attempts to account for diffusion by turbulent fluctuations, the dispersion effects of secondary circulation and possibly minor transverse advective effects which have been dropped from the mass balance equation. In these situations the secondary circulation is generally significant and highly variable and can induce transverse eddies on a scale much larger than the depth of flow.

⁵ Note ε_z has been used here rather E_z to denote a primarily turbulent diffusion process.

Table 2.1 Dimensionless transverse mixing coefficients from several investigators.

Stream Description	Investigators	W/H	E/HU.
Missouri River near Blair	Yotsukura and Cobb (1972)	66.7	0.50
South River	Yotsukura and Cobb (1972)	46.2	0.29
Ussel River	Holley and Abraham (1973)	17	0.51
Mackenzie River, Ft Simpson to Norman Wells	Mackay (1970)	185	0.66
Athabasca River below Ft. McMurray	Beltaos (1978)		
open water		170	0.75
ice-covered		131	0.58
Athabasca River below Athabasca	Beltaos (1978)		
open water		156	0.41
ice-covered		288	0.29
North Saskatchewan River below Edmonton	Beltaos (1978)	137	0.25
Bow River at Calgary	Beltaos (1978)	104	0.61
Beaver River near Cold Lake	Beltaos (1978)		
open water		45	1.03
ice-covered		64	1.27
Missouri River below Copper Generation Station	Sayre and Yeh (1975)	59	3.30
Grand River below Kitchener	Lau and Krishnappan (1981)	117	0.26
Slave River below Ft. Smith near bank region:	Putz(1983)		
open water		164	0.07
ice-covered		164	0.05
mid channel region:			
open water		161	0.88
ice-covered		163	0.47
Mississippi River below Monticello Generating Plant	Demetracopoulous and Stefan (1983)	171	0.24 to 4.65

Consequently for field studies there are still the following uncertainties regarding appropriate scales for non-dimensionalizing E_z :

1. Is a vertical or a horizontal length scale more representative of the eddies involved in the mixing process?
2. Are local values of the length and intensity scales more appropriate than section or reach averages?
3. Is the length scale a function of aspect ratio or proximity to shear boundaries?

At present most investigators using numerical models for mixing simulations use section-averaged or plume region values of flow depth and shear velocity to non-dimensionalize E_z within a sub-reach. Those using analytical models work with reach-averaged values. Aspect ratio or proximity to shear boundaries is generally not considered.

Some investigations on the influence of secondary circulation upon transverse mixing have been conducted. Fischer (1969) proposed the following relationship to quantify the enhanced transverse mixing resulting from bend-induced secondary circulation:

$$\frac{E_z}{HU_*} = K \left[\frac{U}{U_*} \right]^2 \left[\frac{H}{R_c} \right]^2 \quad [54]$$

where: U , H and U_* are section averages,
 R_c is the radius of the curve, and
 K is a proportionality constant.

Fischer found K to have a value of approximately 25 in a laboratory flume of constant curvature.

Yotsukura and Sayre (1976) recommended the right side of Equation [54] be multiplied by $(W/H)^2$. This modification of Equation [54] resulted in a better fit to tracer tests conducted on curved portions of the Missouri River.

Lau and Krishnappan (1981) proposed stream sinuosity as a possible parameter to characterize bend-induced transverse mixing. Their analysis of existing field data suggested that the non-dimensional mixing coefficient β may be proportional to sinuosity. However there is insufficient field data to formulate a quantitative relationship.

3. Solution Procedures for the Two-Dimensional Mixing Equation

The governing mass balance equation which describes two-dimensional mixing for a prismatic channel was derived in Section 2.1.2 (see Equation [22]). As indicated in Section 2.1.2.1 the transverse advection and the longitudinal diffusion terms are generally small and can be ignored as shown in Equation [23]. For steady state mixing and a steady reaction the time differential $\partial c/\partial t$ can be omitted from the equation as seen in Equation [24].

Several analytical solutions are available for simplified versions of Equation [23]. These assume the channel depth h , longitudinal velocity u , and transverse mixing coefficient E_z do not change with respect to z and therefore Equation [23] may be expressed as:

$$\frac{\partial c}{\partial t} + u \frac{\partial c}{\partial x} = E_z \frac{\partial^2 c}{\partial z^2} + \hat{R} \quad [55]$$

In natural channels h , u and E_z can change in the z direction, and as a result numerical solutions are required. Several numerical models have been developed for the general solution of Equation [22], and Equation [23] with steady and unsteady substance sources. Most of the models reported in the engineering literature use finite difference procedures. There are also a few examples of finite element models. The discussions presented here will focus on the finite difference method.

The primary advantage of the finite element method is its adaptability to irregular channel geometries in plan view. A transformation of the transverse spatial coordinate to a streamtube representation of the channel flow largely mitigates this problem for the finite difference method. However, the finite element method remains an excellent tool for estuary and lake models where the streamtube representation is not easily implemented. An example of the application of the finite element method is given by Lawrence et al. (1973).

3.1 Transverse Coordinate Transformation

The transverse changes in local stream depth and streamwise velocity (i.e. h and u change in the z direction) and the presence of transverse advective flux (i.e. $\partial(wc)/\partial z \neq 0$) can be accounted for by using a transverse coordinate transformation introduced by Yotsukura and Cobb (1972). A new transverse coordinate defined as cumulative flow, q (m^3/s), is given by:

$$q_{(z)} = \int_0^z uh \, dz \quad [56]$$

where: $z = 0$ represents the left bank as shown in Figure 3.1, and u is the depth-averaged velocity in the direction of flow.

At the right bank $z = W$, the total stream width, and $q = Q$, the total stream discharge. Equation [56] indicates a line of constant q represents a streamline and hence two adjacent lines of constant q define a streamtube.

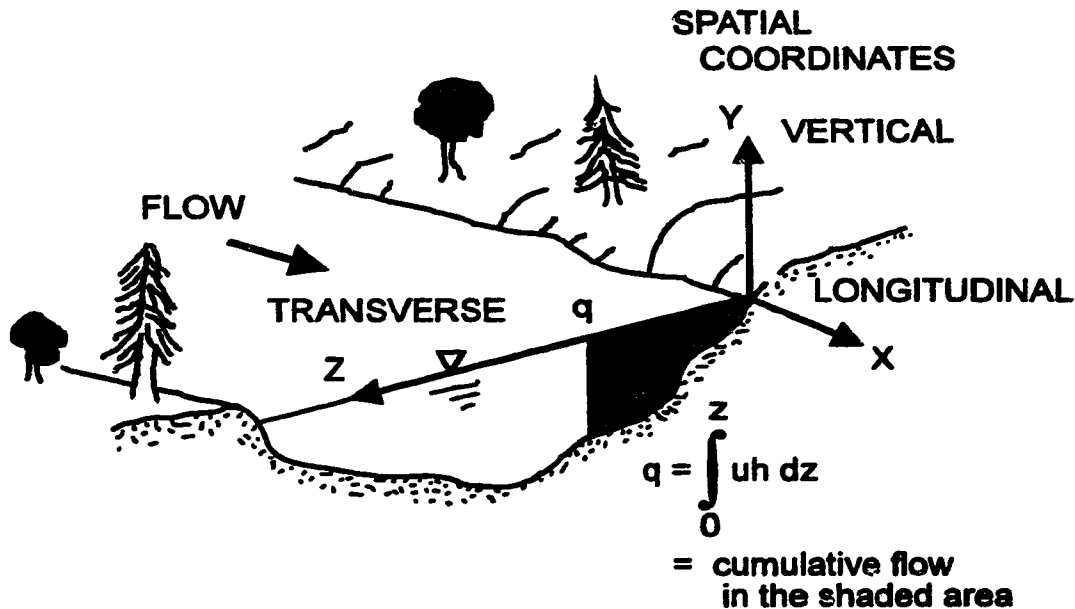


Figure 3.1 Transverse coordinate transformation.

Important features of the q transformation are:

- 1. there is no average flow across a line of constant q and therefore no depth-averaged transverse advection; and**
- 2. the plan view of a natural stream of variable width is transformed into a simple rectilinear form of constant width Q.**

Introduction of the q transformation into Equation [22] and neglecting the longitudinal diffusion and transverse advection terms gives:

$$\frac{1}{u} \frac{\partial c}{\partial t} + \frac{\partial c}{\partial x} = \frac{\partial}{\partial q} (uh^2 E_z \frac{\partial c}{\partial q}) + \frac{\hat{R}}{u} \quad [57]$$

Mixing equations are often expressed in a non-dimensional form. In this manner solutions to the equation may be applied to a number of substance input conditions.

Defining a dimensionless transverse coordinate η as:

$$\eta = q/Q \quad [58]$$

and, a dimensionless concentration \hat{c} as:

$$\hat{c} = c / c_{ref} \quad [59]$$

where: c_{ref} is a constant reference concentration.

The dimensionless form of Equation [57] is then given as:

$$\frac{1}{u} \frac{\partial \hat{c}}{\partial t} + \frac{\partial \hat{c}}{\partial x} = \frac{1}{Q^2} \frac{\partial}{\partial \eta} (uh^2 E_z \frac{\partial \hat{c}}{\partial \eta}) + \frac{\hat{R}}{u} \quad [60]$$

For steady state mixing of a conservative substance c_{ref} is generally defined as the fully mixed river concentration c_∞ of the substance which is given by:

$$c_\infty = c_o \frac{Q_o}{Q} \quad [61]$$

**where: Q_o is the effluent discharge to the river, and
 c_o is the substance concentration in the effluent**

3.2 Analytical Solutions

As noted above several analytical solutions are available for steady state versions of the two-dimensional mixing equation. These solutions have been derived for conservative substances, i.e. $\hat{R} = 0$. With these additional simplifications Equation [55] becomes:

$$u \frac{\partial c}{\partial x} = E_z \frac{\partial^2 c}{\partial z^2} \quad [62]$$

The solution for Equation [62], for an infinitely wide channel of constant depth and velocity and a point source input of substance is given by Fischer et al. (1979):

$$\frac{c(x,z)}{c_\infty} = \frac{1}{\sqrt{4\pi\chi}} \exp\left[-\frac{(z-z_0)^2}{4\chi}\right] \quad [63]$$

where: $c_\infty = c_0 Q_0 / (u h W)$,
 $\chi = x E_z / (u W^2)$, a dimensionless longitudinal distance,
 z_0 is the transverse coordinate of the source, and
 z is the transverse coordinate of the solution location.

Equation [63] can only be used as an approximate solution in the region before either edge of the effluent plume has come in contact with the bank. The banks are 'no flux' boundaries which must be accounted for in the solution beyond the point of contact. One method of accounting for the influence of the banks is to use superposition of image sources.

An image source is located beyond the bank, symmetric with respect to the real source (see Figure 3.2). The sum of the contributions from the real and image sources gives zero flux at the bank, i.e. the amount of substance flowing through the boundary is replaced by the substance from the image source. Multiple image sources are located at the left and right banks as required.

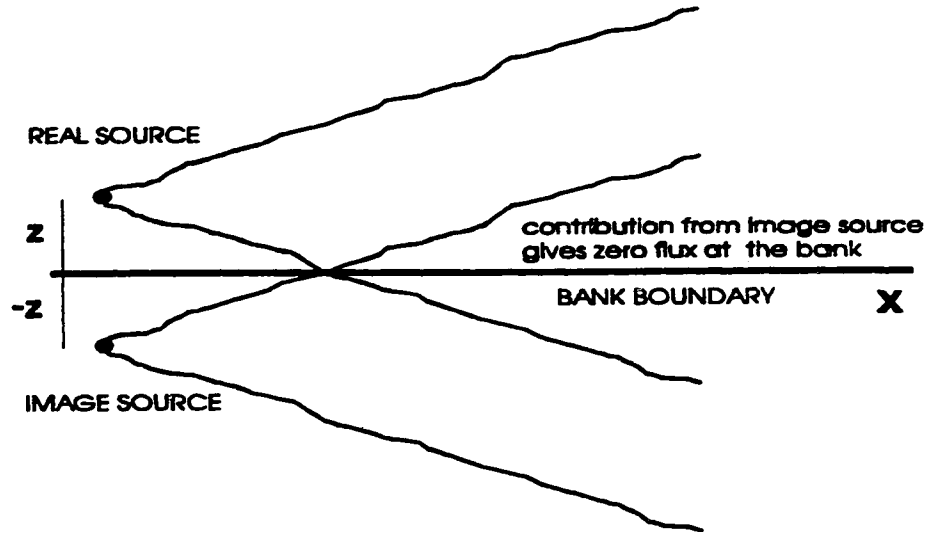


Figure 3.2 Image source method to simulate a no flux boundary.

Using the method of images a more complete representation of the mixing in the two-dimensional zone is given by:

$$\frac{c(x,z)}{c_{\infty}} = \frac{1}{\sqrt{4\pi\chi}} \sum_{m=-\infty}^{+\infty} \left\{ \exp\left[-\frac{(\Psi - 2m - \Psi_0)^2}{4\chi}\right] + \exp\left[-\frac{(\Psi - 2m + \Psi_0)^2}{4\chi}\right] \right\} \quad [64]$$

where: $\Psi = z/W$, a dimensionless transverse distance,
 Ψ_0 = the location of the source,
 $z = 0$ at the left bank, and
 m is an integer.

Each term in the infinite series represents a boundary reflection. In practise only one or two +ve and -ve terms are required for the solution to converge.

Yotsukura and Cobb (1972) demonstrated that numerical solutions to the steady state version of Equation [57] are relatively insensitive to transverse variations in the term uh^2E_z , especially for substance sources in the mid-stream region. They proposed replacing uh^2E_z with a constant section-averaged parameter called the diffusion factor D_z , given by:

$$D_z = \frac{1}{Q} \int_0^Q uh^2 E_z \, dq \quad [65]$$

The solution to Equation [57] for a steady state point source of conservative substance is given by Yotsukura and Cobb (1972) in dimensionless form as:

$$\frac{c(x,\eta)}{c_{\infty}} = \frac{1}{\sqrt{4\pi\chi}} \sum_{m=-\infty}^{+\infty} \left\{ \exp\left[-\frac{(\eta-2m-\eta_o)^2}{4\chi}\right] + \exp\left[-\frac{(\eta-2m+\eta_o)^2}{4\chi}\right] \right\} \quad [66]$$

where: $\chi = xD_z/Q^2 = xE_z/(uW^2)$ as in Equations [63] and [64],
 η_o is the transverse location of the source,
 η is the solution location, and
 m is an integer.

Yotsukura and Cobb (1972) also presented the following solution to Equation [57] for a steady state horizontal line source of substance:

$$\frac{c(x,\eta)}{c_{\infty}} = \frac{1}{2(\eta_2 - \eta_1)} \sum_{m=-\infty}^{+\infty} \left\{ \operatorname{erf}\left[\frac{(\eta_2 + 2m - \eta)}{2\sqrt{\chi}}\right] - \operatorname{erf}\left[\frac{(\eta_1 + 2m - \eta)}{2\sqrt{\chi}}\right] \right. \\ \left. + \operatorname{erf}\left[\frac{(\eta_2 + 2m + \eta)}{2\sqrt{\chi}}\right] - \operatorname{erf}\left[\frac{(\eta_1 + 2m + \eta)}{2\sqrt{\chi}}\right] \right\} \quad [67]$$

where: η_1 is the left side of the line source,
 η_2 is the right side of the line source, and
 erf designates the error function defined by:

$$\operatorname{erf}(x) = \frac{2}{\sqrt{\pi}} \int_0^x e^{-p^2} dp = \frac{2}{\sqrt{\pi}} \left[x - \frac{x^3}{3 \cdot 1!} + \frac{x^5}{5 \cdot 2!} - \frac{x^7}{7 \cdot 3!} + \dots \right] \quad [68]$$

The line source solution is particularly useful for approximating a multiple point source discharge to a stream as in a diffuser outlet structure.

It is interesting to note that the approximations for the crossing distance and the distance to establish a fully mixed condition can be derived from Equation [64]. A plot of c/c_{∞} vs. χ for a left bank injection of substance is shown in Figure 3.3. The crossing distance is the point at which the concentration at the right bank is approximately 0.1 times the concentration at the left bank. From Figure 3.3 this condition occurs at $\chi \approx 0.1$, therefore:

$$x = \frac{\chi u W^2}{E_z} = \frac{0.1 u}{\beta u \cdot h} W \approx 100W \quad [69]$$

where: u/u_∞ is in the order of 10,
 W/h is in the order of 50, and
 β is in the order of 0.5.

Similarly the distance to the fully mixed condition is the point at which the concentration at the right bank is approximately 0.9 times the concentration at the left bank. From Figure 3.3 this condition occurs at $\chi \approx 0.35$, therefore:

$$x = \frac{\chi u W^2}{E_z} = \frac{0.35 u}{\beta u \cdot h} W \approx 350W \quad [70]$$

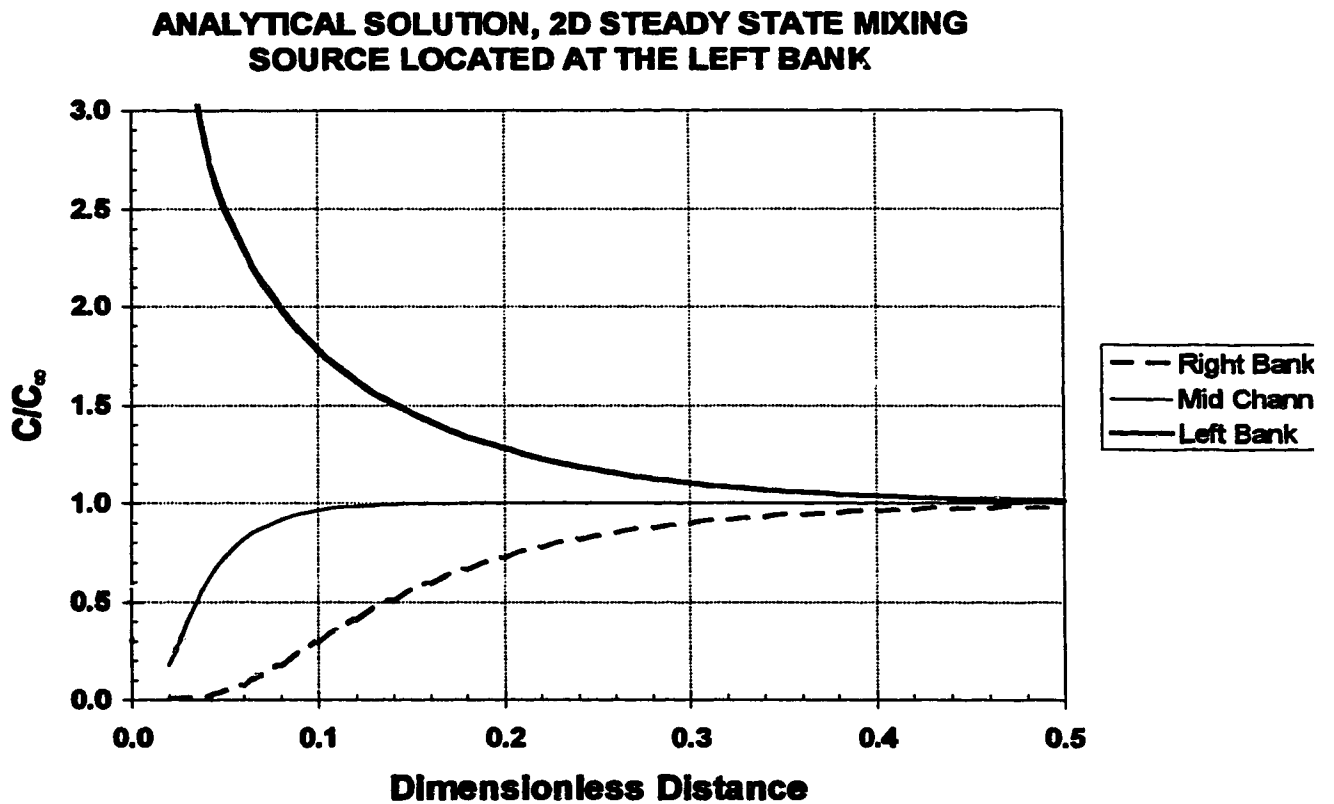


Figure 3.3 Dimensionless concentration vs. χ for a substance source at the left bank.

A search of the literature failed to identify any analytical solutions to the general two-dimensional mixing equation (i.e. Equation [22]) which can account for all three of the following:

1. an unsteady substance source
2. a reaction term, and
3. transverse variations in h , u , and E_z .

In order to accurately handle these situations a numerical solution procedure is required.

3.3 Numerical Solution Considerations

An overview of numerical solution procedures is shown in Figure 3.4.

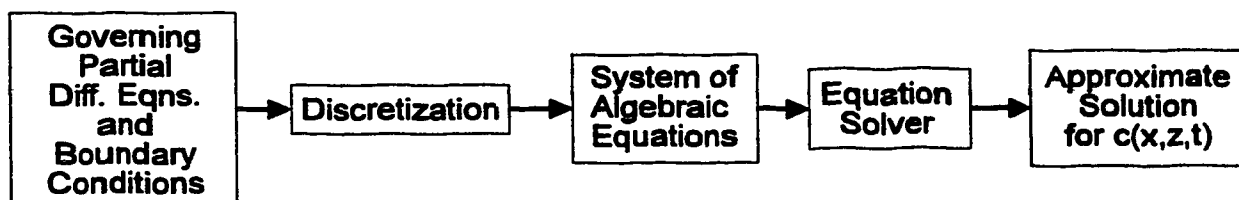


Figure 3.4 Numerical solution procedure.

The discretization stage consists of the following steps:

1. the establishment of a system of nodes called a grid which represents temporal and spatial increments,
2. approximation of the governing partial differential equation and any applicable boundary conditions at each node by replacement of the differentials with approximate algebraic expressions, and,
3. assembly of the complete system of algebraic equations representing each node in the grid system.

These steps are common to all discretization schemes whether they be finite difference, finite volume or finite element methods.

The second step in the numerical procedure is the solution of the system of algebraic equations. In general the system of equations must be solved simultaneously using matrix elimination or iterative techniques. Elementary matrix solution techniques can be found in introductory texts on numerical methods (for example see Gerald (1980)). The end result of the second step is an approximate solution to the governing mass balance equation at each grid node.

The simplest and the most direct means of discretization is to replace the governing equation differentials with finite difference expressions. For example, the one dimensional diffusion equation:

$$\frac{\partial c}{\partial t} = E_z \frac{\partial^2 c}{\partial z^2} \quad [71]$$

can be approximated as follows:

$$\frac{c_j^{n+1} - c_j^n}{\Delta t} = E_z \frac{(c_{j-1}^n - 2c_j^n + c_{j+1}^n)}{\Delta z^2} \quad [72]$$

The time and spatial steps Δt and Δz and the grid notation scheme for Equation [72] are shown in Figure 3.5.

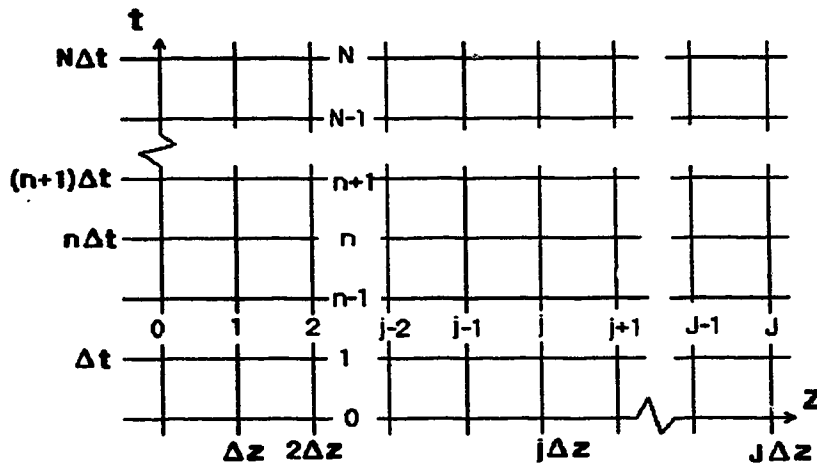


Figure 3.5 Discretization grid.

To solve Equation [72] the initial concentration distribution, i.e. $c_{(z,0)}$, and the boundary conditions at the edges of the grid system must be known. Given the initial concentration distribution and the boundary conditions c_j^{n+1} is the only unknown in Equation [72] and can be solved for directly. Discretization schemes of this type are called 'explicit'.

Equation [71] could also have been approximated as:

$$\frac{c_j^{n+1} - c_j^n}{\Delta t} = E_z \frac{(c_{j-1}^{n+1} - 2c_j^{n+1} + c_{j+1}^{n+1})}{\Delta z^2} \quad [73]$$

This discretization scheme results in three unknowns at the $n+1$ time level. The approximate governing equation at each node and the two boundary conditions at $j = 0$ and $j = J$ form a system of algebraic equations equal in number to the number of unknowns. The system must be solved simultaneously because the solution at each node is dependent upon the adjacent nodes. Discretization schemes of this type are called 'implicit'.

3.3.1 Truncation Error Analysis

It must be remembered that Equation [72] is only an approximation of Equation [71]. One method of assessing the error associated with the approximation is to use a Taylor series expansion about the $j\Delta x$, $n\Delta t$ node as follows:

$$\begin{aligned} c_j^n &= c \\ c_j^{n+1} &= c_j^n + \frac{\partial c}{\partial t} \Delta t + \frac{\partial^2 c}{\partial t^2} \frac{\Delta t^2}{2} + \frac{\partial^3 c}{\partial t^3} \frac{\Delta t^3}{6} + \dots \\ c_{j-1}^n &= c_j^n - \frac{\partial c}{\partial z} \Delta z + \frac{\partial^2 c}{\partial z^2} \frac{\Delta z^2}{2} - \frac{\partial^3 c}{\partial z^3} \frac{\Delta z^3}{6} + \frac{\partial^4 c}{\partial z^4} \frac{\Delta z^4}{24} - \dots \\ c_{j+1}^n &= c_j^n + \frac{\partial c}{\partial z} \Delta z + \frac{\partial^2 c}{\partial z^2} \frac{\Delta z^2}{2} + \frac{\partial^3 c}{\partial z^3} \frac{\Delta z^3}{6} + \frac{\partial^4 c}{\partial z^4} \frac{\Delta z^4}{24} + \dots \end{aligned} \quad [74]$$

If Equation [74] is substituted into Equation [72] it can be shown that the actual differential equation used to approximate Equation [71] is:

$$\frac{\partial c}{\partial t} = E_z \frac{\partial^2 c}{\partial z^2} - \left[\frac{\partial^2 c}{\partial t^2} \frac{\Delta t}{2} - E_z \frac{\partial^4 c}{\partial z^4} \frac{\Delta z^2}{6} + \dots \right] \quad [75]$$

Therefore the error associated with using Equation [72] to represent Equation [71] is 1st order in time and 2nd order in space. The approximation must also have the property of consistency, i.e. as Δt and $\Delta z \rightarrow 0$ the original equation must be recovered, in order to satisfactorily represent the original equation

The selection of Δt and Δz can play a role in the size of the truncation error. For example Δt and Δz can be chosen so the first set of error terms cancel each other. Using Equation [71] and changing the order of differentiation it can be shown that:

$$\frac{\partial^2 c}{\partial t^2} = E_z^2 \frac{\partial^4 c}{\partial z^4} \quad [76]$$

Then equating the leading error terms:

$$\frac{\partial^2 c}{\partial t^2} \frac{\Delta t}{2} = E_z^2 \frac{\partial^4 c}{\partial z^4} \frac{\Delta t}{2} = E_z \frac{\partial^4 c}{\partial z^4} \frac{\Delta z^2}{12} \quad [77]$$

gives:

$$\Delta t = \frac{\Delta z^2}{6 E_z}, \quad \text{i.e.} \quad E_z \frac{\Delta t}{\Delta z^2} = \frac{1}{6} \quad [78]$$

which will cancel the leading error terms and decrease the error to 2nd order in time and 4th order in space. Unfortunately this procedure is generally only possible for explicit discretization schemes. Grid size also plays a role in stability considerations as discussed below.

3.3.2 Stability Analysis

A discretization scheme must have stability. Stability means that small disturbances such as round off errors or spikes in the initial concentration distribution will not propagate and cause the solution to diverge. One method of stability analysis is the Fourier or von Neumann approach (see Fletcher, 1991).

Any concentration distribution can be represented by the summation of a number of simple waveforms. Each waveform can be expressed as a trigonometric function or as a product of the waveform amplitude and the base of the natural logarithms raised to an imaginary number. For example

$$C(z=j\Delta z, t=n\Delta t) = A^n e^{i2\pi\omega j\Delta z} \quad [79]$$

where: $2\pi\omega$ is the waveform frequency (radians/m),
 A^n is the amplitude at time step n , and,
 i is the imaginary unit $= \sqrt{-1}$.

To test a discretization scheme for stability it is only necessary to use a single waveform. The ratio of the amplitude of the selected waveform at successive time steps allows an assessment of stability. If expressions similar to Equation [79] are substituted into Equation [72] the following expression can be obtained:

$$\frac{A^{n+1}}{A^n} = \gamma_{num} = 1 + r_r(e^{-i2\pi\omega\Delta z} - 2 + e^{i2\pi\omega\Delta z}) \quad [80]$$

where: γ_{num} is the amplification factor, and
 $r_r = E_z \Delta t / \Delta z^2$

Converting to a trigonometric representation of the frequency gives:

$$\gamma_{num} = 1 + r_r(2 \cos(2\pi\omega\Delta z) - 2) \quad [81]$$

For stability $|\gamma_{num}| \leq 1$. Therefore, by varying the phase angle $2\pi\omega\Delta z$ and calculating r_r for $|\gamma_{num}| \leq 1$ bounds can be placed on the ratio of the time and space grid increments to ensure stability.

The shortest wavelength λ that can be resolved using a grid increment Δz corresponds to $\Delta z = \lambda/2$ (see Figure 3.6). Therefore to assess the stability of the smallest resolvable wavelength:

$$\text{phase angle} = 2\pi\omega\Delta z = (2\pi/\lambda)(\lambda/2) = \pi$$

Stability criteria for longer wavelengths can be assessed in the same manner. The minimum r value will be the governing stability criteria. For Equation [81], $r_r \leq 1/2$ governs.

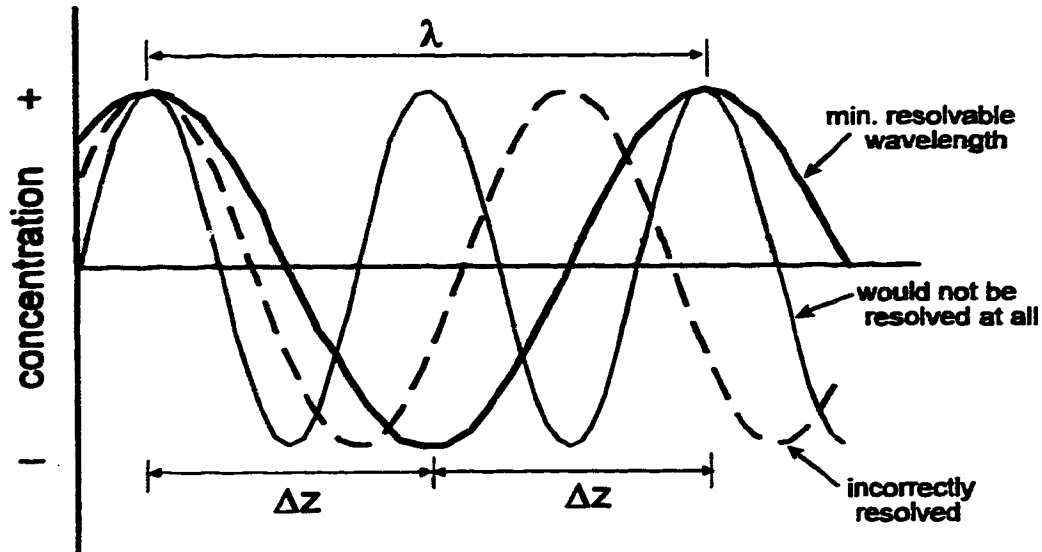


Figure 3.6 Grid Resolution.

3.3.3 Grid Resolution

The discussion of stability indicated there is a limit to the wavelength or scale of a waveform which can be resolved for a given grid increment. Therefore, in order to perform properly, a numerical solution must have sufficient grid resolution. The increment size must be small enough to adequately define steep concentration gradients with several nodal points. A general procedure for sizing the grid increments is to first select the spatial increment to provide sufficient resolution, then choose Δt to minimize the truncation error and finally check for stability.

3.3.4 Convergence

If the chosen discretization scheme and grid increment sizes have the properties of consistency and stability, then convergence of the numerical solution is implied.

In the discussions above the one-dimensional diffusion equation was used to introduce the concepts of discretization, truncation error, consistency, stability and grid resolution. These concepts are equally applicable to more general problems involving

advection and diffusion in several spatial dimensions. However, the error and stability analysis of more general problems becomes much more complex.

Two additional concepts must be introduced to complete this brief overview of numerical procedures. These are numerical diffusion and numerical dispersion.

3.3.5 Numerical Diffusion

The discretization of advection-diffusion problems can introduce an error term which behaves in similar fashion to the actual diffusion term in the original differential equation. Error of this type is called 'numerical' or 'artificial' diffusion. The error term is associated with forward difference approximations of the advective terms.⁶

For example, consider the one-dimensional steady state advection-diffusion equation:

$$U \frac{\partial c}{\partial x} = E_x \frac{\partial^2 c}{\partial x^2} \quad [82]$$

Which expressed in finite difference form using a forward difference for the advection term and a central difference for the diffusion term gives:

$$U \frac{(c_k - c_{k-1})}{\Delta x} = E_x \frac{(c_{k+1} - 2c_k + c_{k-1}))}{\Delta x^2} \quad [83]$$

Using a Taylor series expansion about node k gives:

$$U \frac{\partial c}{\partial x} - \left[U \frac{\partial^2 c}{\partial x^2} \frac{\Delta x}{2} + U \frac{\partial^3 c}{\partial x^3} \frac{\Delta x^2}{6} - \dots \right] = E_x \frac{\partial^2 c}{\partial x^2} + \left[E_x \frac{\partial^4 c}{\partial x^4} \frac{\Delta x^2}{12} + \dots \right] \quad [84]$$

Rearranging gives:

$$U \frac{\partial c}{\partial x} = U \frac{\Delta x}{2} \frac{\partial^2 c}{\partial x^2} + E_x \frac{\partial^2 c}{\partial x^2} + [\Delta x^2 \text{ error terms}] \quad [85]$$

⁶ Forward differences are generally preferred for approximating advective terms because central difference schemes can cause instability.

The error term $U(\Delta x/2)(\partial^2 c/\partial x^2)$ is called the numerical or artificial diffusion. The artificial diffusion term will cause the solution distributions to either spread more rapidly or less rapidly depending upon its sign.

The magnitude of the artificial diffusion can be assessed by introducing a parameter called the grid Reynold's number, $R_e = U\Delta x/E_x$,

$$\frac{U}{E_x} \frac{\partial c}{\partial x} = \left[\frac{R_e}{2} + 1 \right] \frac{\partial^2 c}{\partial x^2} \quad [86]$$

Therefore, if $R_e > 2$ then artificial diffusion at least as large as the real diffusion is introduced to the approximating equation.

The simplest method to reduce the artificial diffusion is to keep Δx small. However in practice this may substantially increase the computational effort required. As a result the modeller usually has to tolerate an acceptably small amount of artificial diffusion. An alternative is to use higher order discretization schemes (i.e. involving a greater number of nodal points to try to eliminate the artificial diffusion term. Unfortunately these schemes often have large truncation errors or have stability problems.

3.3.6 Numerical Dispersion and Dissipation

Consider the one-dimensional advection equation:

$$\frac{\partial c}{\partial t} + u \frac{\partial c}{\partial x} = 0 \quad [87]$$

which describes the simple translation of a waveform in the x direction. Using Fourier analysis it can be shown that one solution to Equation [87] is:

$$c(x,t) = B e^{-i\Omega\Delta t} e^{i\Omega\Delta x} = B e^{i\Omega(\Delta x - u\Delta t)} \quad [88]$$

where: $\Omega = 2\pi\omega = 2\pi/\lambda$, and
 B is a constant.

As shown in the discussion of stability, an amplification ratio may be defined as follows:

$$\gamma_m = \frac{c_k^{n+1}}{c_k^n} = \frac{B e^{i\Omega(k\Delta x - u(n+1)\Delta t)}}{B e^{i\Omega(k\Delta x - un\Delta t)}} = e^{-i \frac{2\pi u \Delta t}{\lambda}} \quad [89]$$

Further, defining N as the number of nodes per wavelength and Courant No., C_r , as the number of nodes per time step:

$$N = \frac{\lambda}{\Delta x} \quad [90]$$

$$C_r = u \frac{\Delta t}{\Delta x} \quad [91]$$

and substituting Equation [90] and Equation [91] into Equation [89] gives:

$$\gamma_m = e^{-i \frac{2\pi u \Delta t}{N \Delta x}} = e^{-i \frac{2\pi C_r}{N}} \quad [92]$$

Equation [92] shows that the amplification ratio is a function of N and C_r .

In general the amplification ratio for any solution to the governing mass balance equation can be given in either of the following formats:

$$\gamma = a + ib \quad [93]$$

where: a is an expression for the real portion of the amplification ratio
b is an expression for the imaginary portion of the amplification ratio

$$\gamma = A e^{i\theta} \quad [94]$$

where: A is the amplitude ratio $= (a^2 + b^2)^{1/2}$, and
 θ is the phase angle error $= \tan^{-1}(b/a)$.

The amplitude ratio is an indication of the growth or attenuation of the waveform amplitude at successive time steps. The phase angle error is an indication of the displacement of solutions in the x direction for successive time steps. Both are functions of N and C_r . For the analytical solution given above there is no growth or decay of amplitude, however solutions of different C_r and N may be out of phase.

Applying a forward time, backward space explicit discretization scheme, Equation [87] can be approximated as follows:

$$\frac{c_k^{n+1} - c_k^n}{\Delta t} = -u \frac{c_k^n - c_{k-1}^n}{\Delta x} \quad [95]$$

A stability analysis of Equation [95] gives the following expression for the numerical solution amplification ratio:

$$\gamma_{num} = 1 - C_r + C_r e^{i\frac{2\pi}{N}} = 1 - C_r + C_r \cos\left(\frac{2\pi}{N}\right) - i C_r \sin\left(\frac{2\pi}{N}\right) \quad [96]$$

From which the numerical solution phase angle error may be determined as:

$$\theta_{num} = \tan^{-1} \left[\frac{-C_r \sin\left(\frac{2\pi}{N}\right)}{1 - C_r + C_r \cos\left(\frac{2\pi}{N}\right)} \right] \quad [97]$$

The value of the phase angle error of the analytical (exact) solution is shown in Equation [92] as:

$$\theta_{an} = -\frac{2\pi C_r}{N} \quad [98]$$

Comparing Equation [97] and Equation [98] indicates that for $C_r = 1$ and any value of N (greater than the minimum grid resolution), $\theta_{num} = \theta_{an}$ and the numerical scheme produces an exact solution. Unfortunately, except for idealized channels it is not possible to set $C_r = 1$ everywhere in a symmetrical grid due to the variations in channel velocity. Therefore, it is important to check the stability of the numerical solution for the probable range of C_r and N .

The numerical solution amplitude ratio from [96] is:

$$\begin{aligned} A_{num} &= \sqrt{\left[1 - C_r + C_r \cos\left(\frac{2\pi}{N}\right)\right]^2 + \left[-C_r \sin\left(\frac{2\pi}{N}\right)\right]^2} \\ &= \sqrt{1 + 2C_r(1 - C_r)\left[\cos\left(\frac{2\pi}{N}\right) - 1\right]} \end{aligned} \quad [99]$$

The value of the amplitude ratio of the exact solution as shown in Equation [92] is 1, therefore A_{num}/A_{ex} is identical to the expression for A_{num} .

This type of analysis is common for assessing numerical schemes. The results are often shown as plots of A_{num}/A_{ex} and θ_{num}/θ_{ex} vs. N for various C_r . Examples for the analysis given above are shown in Figure 3.7.

The significance of θ_{num}/θ_{ex} is:

1. for $\theta_{num}/\theta_{ex} > 1$ the numerical solution for a particular N moves faster than the actual solution and errors will propagate in advance of the true waveform, and
2. for $\theta_{num}/\theta_{ex} < 1$ the numerical solution for a particular N moves slower than the actual solution and errors will lag behind the true waveform.

The effects of θ_{num}/θ_{ex} are shown in Figure 3.8.

Because all input waveforms are a composite of a number of wavelengths including small disturbances caused by errors, there is always the potential for separation to occur. This type of behaviour due to a phase error is called 'numerical dispersion'.

Similarly A_{num}/A_{ex} can cause the solution amplitude to grow or attenuate as a function of N . This process is called 'numerical dissipation' although it is often incorrectly referred to as numerical diffusion.

The discussion above introduced the concepts of numerical diffusion, dispersion and dissipation. The literature is ripe with proposed numerical procedures which attempt to minimize these types of errors. Often these procedures employ higher order discretization and more implicit schemes or play one type of error against another. A review and discussion of a number of these procedures is given by Fletcher (1991).

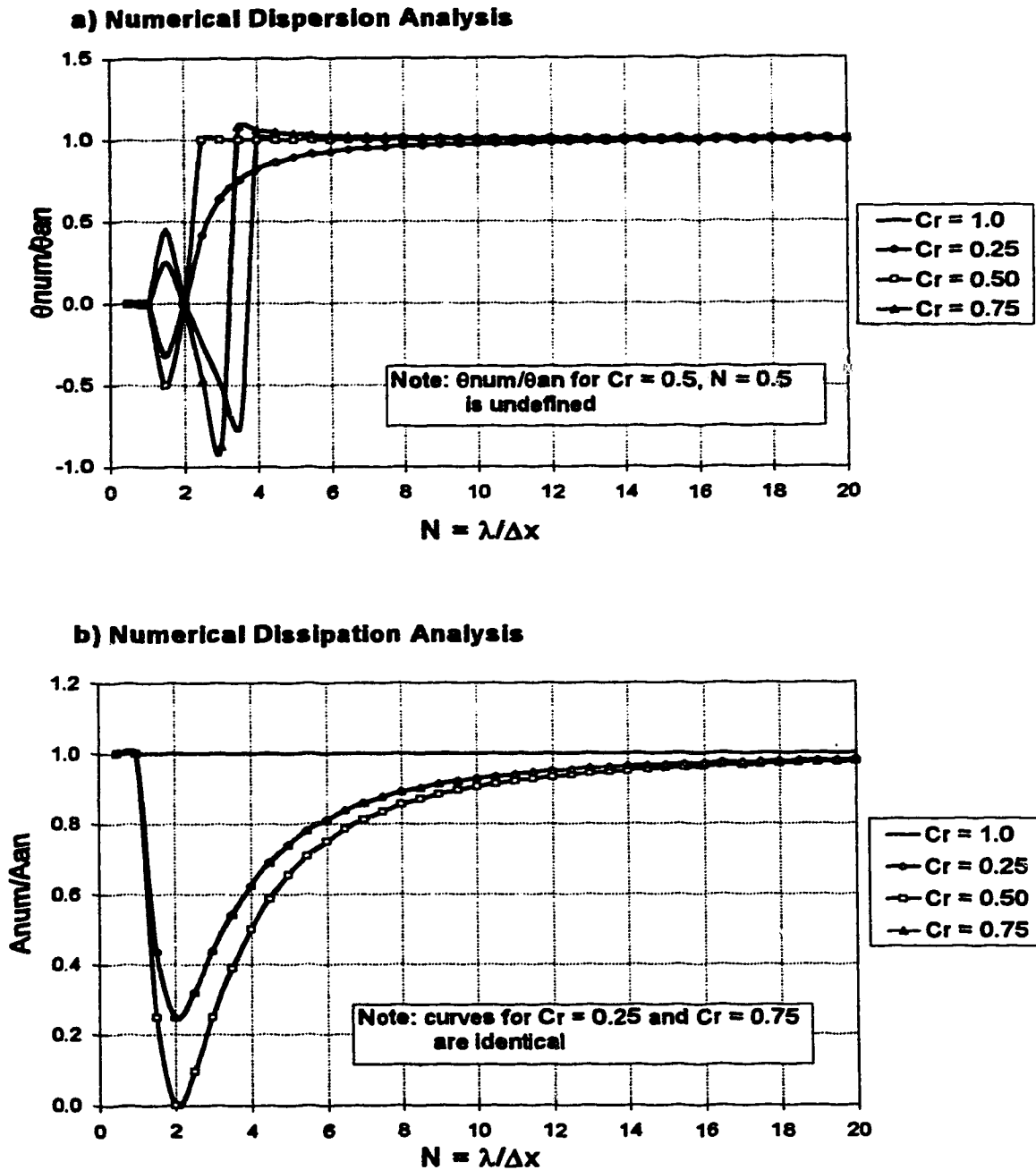


Figure 3.7 Numerical dispersion and dissipation analysis of a forward time, backward space explicit representation of the one-dimensional advection equation.

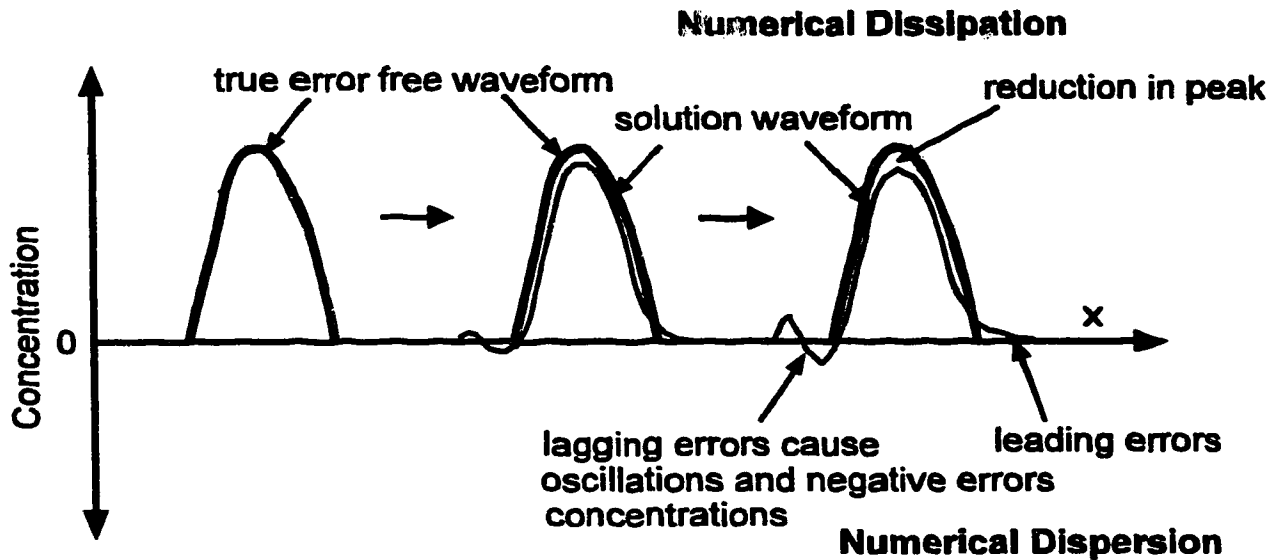


Figure 3.8 Numerical dispersion.

Further details of these concepts are beyond the scope of the present discussion. However, the reader should always keep in mind their significance. Model developers should thoroughly analyze their proposed procedures using these concepts and specify criteria for model use. Model users should be aware of the limitations imposed by these concepts and observe specified criteria in attempting to use a model.

3.4 Numerical Solution Methods for a Steady Substance Source

Wastewater outlets discharging to receiving streams are commonly located at or near one of the stream banks. For a steady-state, side discharge into a wide natural channel, the term uh^2E_z in Equations [57] and [60] cannot be replaced by a reach or section-averaged value of uh^2E_z as was the case for the analytical solutions. In the vicinity of the bank the local values of u , h , and E_z are generally small in comparison to the section averages for these parameters. As a result the mixing in this region is often much less efficient than that which occurs near mid channel. This phenomena has been observed by Lau and Krishnappan (1981) and Putz et al. (1982).

A numerical procedure is the only method of incorporating a consideration of local u , h , and E_z into solutions for Equations [57] and [60]. Numerical solution methods using explicit finite difference discretization schemes for Equation [24] with no reaction term were first introduced in the early 1970's (see for example Yotsukura et al. (1970)). Yotsukura and Sayre (1976) presented an explicit finite difference scheme adapted to the streamtube approach for the solution of Equation [57] with $\hat{R} = 0$.

The discretization scheme used by Yotsukura and Sayre (1976) used a forward difference expression for the $\partial c / \partial x$ term and a centred difference expression for the $\partial^2 c / \partial \eta^2$ term. An error analysis of the discretization scheme would reveal it is subject to a large truncation error and to numerical dispersion. No criteria were presented for the selection of Δx and $\Delta \eta$ to minimize these errors.

Yotsukura and Sayre (1976) also introduced a curvilinear orthogonal coordinate system which can more accurately approximate the flow distances along meandering rivers. The curvilinear coordinate system is implemented through the use of 'metric' coefficients. In cases where the channel to be modelled is relatively straight or only involves gentle curvature the use of the metric coefficients is not required.

An implicit finite difference scheme first proposed by Stone and Brian (1963) for the one-dimensional advective transport equation, was adapted to the solution of Equation [57] (with $\hat{R} = 0$) by Lau and Krishnappan (1981). The method was later extended to the solution of Equation [57] with a first order reaction term (Putz, 1983; Krishnappan and Lau, 1985).

The adaptation of the Stone and Brian method reduces much of the numerical error which was inherent in the explicit discretization. The Stone and Brian discretization procedure uses weighting coefficients and forward difference expressions evaluated over several grid points to approximate the $\partial c / \partial x$ and the $\partial c / \partial \eta$ derivatives. The second order derivative is approximated using a Crank-Nicolson expression. The Crank-Nicolson expression reduces the truncation error associated with the forward difference expression

for $\partial c/\partial x$. The values of the weighting coefficients were chosen by Stone and Brian in a comparison to analytical solutions to the one-dimensional advective transport equation.

Details of the discretization procedure for a conservative substance is given by Lau and Krishnappan (1981). The discretization procedure with a first order reaction term is presented by Putz (1983). The method is subject to solution oscillations and negative concentrations if coarse grid spacing is employed in areas with steep concentration gradients. Krishnappan and Lau (1982) suggest the longitudinal grid spacing be computed using the following in order to avoid solution oscillations:

$$\frac{(uh^2 E_z) \Delta x}{Q^2 \Delta \eta^2} \approx 1 \quad [100]$$

The boundary regions are the most instrumental in creating the oscillations and therefore $uh^2 E_z$ within this region should be used for selecting the grid increments.

Lau and Krishnappan (1981) used the Stone and Brian adaptation to investigate solution sensitivity to various formulations of the diffusion factor $uh^2 E_z$. Solution distributions from the model were compared to a steady state tracer test on the Grand River. They found the solutions were most sensitive to transverse variations in uh^2 . Formulations which allowed E_z to vary in the transverse direction did not significantly improve the solution and did not warrant the additional computational effort. Therefore E_z was set as a section average in each subreach, but was allowed to vary from subreach to subreach.

Putz et al. (1984) used the algorithm, including the reaction term, to investigate the die-off of indicator microorganisms in an ice-covered river.

3.5 Numerical Solution Methods for an Unsteady Substance Source

Relatively few numerical models have been presented in the literature for simulation of two-dimensional mixing of an unsteady substance source in a natural stream. Of those presented, most have only been verified with laboratory tests or with steady state field tests.

Yotsukura and Fiering (1964) presented an explicit finite difference algorithm to solve Equation [23] for a conservative tracer⁷. The algorithm utilized a forward difference expression for the time differential and central difference expressions for the advection and diffusion terms. As outlined in Section 3.3, simple explicit finite difference representations of the advection and diffusion terms of Equation [23] are subject to numerical errors. In order to minimize these errors, restrictions are required for the time increment and grid spacing. Yotsukura and Fiering (1964) specified that C_r must equal one to prevent numerical dispersion and dissipation associated with the approximation of the advective term. They also specified that $(E_x \Delta t)/(\Delta y)^2$ must be less than 0.5 to ensure stability for the approximation of the diffusive term.⁸

Yotsukura and Fiering (1964) noted that it was very difficult to select uniform grid intervals which would satisfy both criteria for all regions of the grid. After several trial combinations of time and spatial increments they concluded that the algorithm was highly subject to numerical dispersion errors and abandoned it for the development of an implicit method.

Fischer (1968) proposed a much simpler explicit procedure for solving Equation [22]. Fischer's approach used the streamtube concept and separated the mixing process into two substeps. First, the advective mass flux was simulated by simple

⁷ Yotsukura and Fiering (1964) were investigating the influence of velocity gradient in the vertical on longitudinal dispersion. Therefore Equation [23] was written for the x and y directions rather than x and z.

⁸ Note that the derivation of both these criteria were demonstrated in Section 3.3.

translation of the concentration by one longitudinal increment down each streamtube. Second, the transverse diffusion between adjacent stream tubes was simulated using a Fickian diffusion model. Fischer's method did not solve the governing differential equation directly and therefore may be criticized for a lack of mathematical rigour (Beltaos and Arora, 1988). However, the method is very appealing in that it seeks simplification through a physical understanding of the processes involved (Beltaos and Arora, 1988).

Fischer's method works, provided there is near complete mass exchange between successive streamtube elements for the advective substep (i.e. $C_r = u\Delta t/\Delta x \approx 1$). However, if Δx is consistent for each streamtube in a real channel, complete exchange is impossible to achieve overall. Fischer suggested selecting Δt on the basis of the stability requirement outlined above, then determining Δx using the maximum streamtube velocity across any given section. For streamtubes where there is incomplete advective exchange between successive elements (i.e. $C_r \neq 1$, $u < u_{\max}$), concentrations are assigned to the elements in inverse proportion to the distance traveled relative to Δx . Fischer successfully used this method to simulate the longitudinal dispersion of an instantaneous line source of tracer injected into the Green River.

Despite the successful application of the procedure outlined by Fischer (1968), Holly (1975) demonstrated that the proportioning scheme for the advective transfer between successive streamtube elements (where $C_r \neq 1$) is highly subject to numerical diffusion errors.⁹ This implies that for successful general application of Fischer's method to natural streams Δx must be varied for each streamtube in order to ensure $C_r = 1$ for each element.

Verboom (1973, 1975) presented a numerical approach for solving two-dimensional unsteady substance source mixing problems which utilized the 'fractional step method'. The fractional step method is essentially what Fischer (1968) had proposed

⁹ See Beltaos (1978) or Beltaos and Arora (1988) for a detailed demonstration of this effect.

by dividing each time step into an advective substep and a diffusive substep. Verboom worked in cartesian coordinates and included three substeps representing longitudinal advection, transverse advection and transverse diffusion. The advective steps were represented using a five point, fourth-order explicit finite difference scheme. The diffusive step was represented using a simple central difference explicit scheme.

Verboom (1975) presented a detailed 'acceptable' error analysis of his proposed scheme compared to a scheme using second order implicit representations of the advective and diffusive substeps. The result of the analysis was a graphical representation of feasible time and spatial grid increments. He concluded that the implicit representations were unnecessary as the explicit scheme was less susceptible to amplitude and phase errors, provided the stability criteria were observed ($C_r \geq 1$ and $(E_x \Delta t)/(\Delta y)^2 \leq 0.5$). Verboom (1975) also presented an 'acceptable' error analysis for selection of appropriate space and time increments for the simulation of two-dimensional unsteady mixing in a laboratory model of the Ijssel River. The model was used to simulate a steady state transverse mixing test in the laboratory channel with acceptable results.

A weakness in Verboom's 'acceptable' error analysis is the assumption that the input wavelength was spread over 10 nodes (i.e. $N = 10$). As shown in Figure 3.7 and Figure 3.8 for large N there is much less significant influence of C_r than for $N < 6$. Therefore, if the error analysis was repeated for a much shorter waveform while maintaining the same acceptable error criteria the feasible grid intervals would be much more restricted.

The alternative to wholly explicit algorithms is to utilize implicit, higher order (and thus more mathematically complex) discretization methods to attempt to minimize or eliminate the numerical errors caused by the uniformly spaced calculation grid. Models proposed by Holly (1975), Holly and Preissmann (1977) and Harden and Shen (1979) take this approach.¹⁰

¹⁰ These models retain the longitudinal diffusion term incorporating E_x in the governing mass balance equation.

Holly (1975) and Holly and Cunge (1975) used the streamtube concept and three substeps to solve the governing mass balance equation. The advective substep was represented by a half implicit, half explicit second order accurate method. Then the diffusive exchange in the longitudinal and transverse directions were simulated in separate substeps using an implicit finite difference algorithm. Although the method assured stability, the advective substep was subject to numerical dispersion, potentially causing phase errors, solution oscillations and negative concentrations similar to the behaviour shown in Figure 3.8 (Cunge et al., 1980).

Holly and Preissman (1977) developed a more accurate algorithm to solve the advective substep. Their algorithm uses the method of characteristics with non-linear interpolation to explicitly determine the advected concentration at the next longitudinal grid point. The algorithm was referred to as a 'two point, high order method'. The improved representation of the advective substep and the original implicit representations of the diffusive substeps were incorporated in to a two-dimensional unsteady substance source model called POLDER.

Holly and Nerat (1983) reported satisfactory results for a field calibration of the POLDER model against a steady state tracer test. No verification of the model using an unsteady substance source has been reported.

Harden and Shen (1979) used a nine-node, combined implicit/explicit finite difference scheme to solve the governing mass balance equation based upon the work of Stone and Brian (1963) and Peaceman and Rachford (1955). The solution proceeds in three substeps. First, an implicit algorithm is used to predict the longitudinal advection and diffusion. A second implicit algorithm is then used to predict the transverse diffusion. Finally the concentration at the time step $n+1$ is calculated using an explicit algorithm using the concentration values at time step n and the intermediate predictions from steps one and two.

The Harden and Shen model was tested with satisfactory results against data from a steady state tracer test on the Missouri River originally reported by Yotsukura et al. (1970). No verification of the model against an unsteady substance source tracer test or against an analytical solution to the one-dimensional advection equation was reported. In the absence of additional verification studies it is difficult to assess whether the method has any potential problems with numerical dispersion.

Harden and Shen (1979) also investigated the effects of omitting the longitudinal diffusion term from the governing mass balance equation (i.e. $E_x = 0$). They compared model results, with and without the longitudinal diffusion term, for the transient period during the development of the steady state concentration profile for the Missouri River data. Dropping the term had negligible effect on the solution profiles.

Sobey (1984) reviewed alternatives for numerically solving the advective transport equation. He concluded all numerical schemes based upon regular grid intervals are susceptible to numerical dispersion errors to some degree. Higher order methods can reduce the error but they are more complex and require a greater computational effort. Sobey (1984) further concluded that methods which utilize a moving coordinate system for the advective step effectively eliminate numerical dispersion problems without the need for higher order methods.

The optimized grid proposed by Fischer (1968), which ensures complete advective mass transport between successive longitudinal streamtube elements, is in effect a moving reference frame. Given the complexity and the lack of adequate verification of the higher order schemes discussed above, further investigation of Fischer's method is warranted. Further development of Fischer's method is discussed in detail in the next section.

4. Advection Optimized Grid Method

4.1 Introduction

The numerical procedure proposed by Fischer (1968) for solution of the two-dimensional unsteady substance source mass balance equation and its subsequent development by Beltaos (1978) and others will be termed the 'Advection Optimized Grid' or AOG method. As described previously, the major innovation of the AOG method is the selection of element lengths which ensure complete advective mass exchange from element to element down each streamtube, during each time step of the simulation. Using this approach, a simple explicit forward finite difference expression can be used to represent longitudinal advection and each calculation will have a Courant No. of one. In this manner the troublesome problems of numerical dispersion, dissipation and solution oscillations normally associated with numerical representations of the advective step can be avoided.

The work reported herein describes the development and verification of a microcomputer-based, two-dimensional unsteady mixing and reaction model. The mixing portion of the model utilizes the AOG method and is based upon the work of Beltaos (1978). Although the mixing portion of the model is based upon Beltaos's description of the AOG method, no portions of the original computer code were used or revised for use in the present model. Rather, all algorithms were completely written by the author to implement the method.

After development of a working model, the present study focuses on a much more extensive verification of the AOG method than has previously been reported. The verification studies utilize data from slug tracer tests conducted on three major western Canadian rivers. A more extensive field verification of the AOG algorithms is critically important to the overall project in order to be confident that the mixing and transport aspects of the model are accurate when applied in a practical engineering setting. Remarkably, there have been few attempts to verify two-dimensional unsteady substance source models with field, slug-injection tracer tests.

Once the AOG method was verified it was then coupled with reaction components and used for two-dimensional, unsteady, non-conservative modelling of water quality parameters. The verification studies for the AOG method are described in Chapter 5. The adaptation of the method for use with non-conservative parameters is described in Chapter 6. The remainder of this chapter describes previous investigations with the AOG method, presents a description of the basic algorithms used in the present model and describes the model implementation.

4.2 Previous Investigations

Beltaos (1978) and later Beltaos and Arora (1988) reported the development and verification of an explicit two-dimensional mixing model based upon the method originally devised by Fischer (1968). Following Fischer's method, the Beltaos model used the streamtube approach and separated each time step into two substeps for calculation of the advective and diffusive exchange between elements. However, rather than using the maximum of the streamtube velocities across a section for the selection of a common longitudinal grid spacing, a unique optimized longitudinal spacing was selected for each element. This further development of Fischer's original model ensured a Courant No. of one for each advective exchange calculation, for each element, for each time step in the simulation.

The transverse diffusive exchange was represented by the equivalent of an explicit central difference expression between adjacent streamtube elements. However, because of the optimized longitudinal grid, the diffusion calculations are more complex than for a consistent grid spacing, and potentially involve several streamtube elements depending upon their alignment in the grid. The calculation procedure for the advection and diffusion substeps of the AOG method will be discussed more fully in the next section.

Beltaos (1978) used two one-dimensional¹ and one two-dimensional² unsteady substance source laboratory experiments reported by other investigators and a field slug

¹ Test results reported by Fischer (1968)

injection test on the Athabasca River to verify the model. The model simulations of the laboratory tests produced good results. For the reported field test, concentration vs. time measurements were only obtained at a single transect across the river. The comparison of the model output to the field tracer measurements was satisfactory although there was some minor translation in the time scale of the measured and simulated concentration vs. time plots. Beltaos speculated that the discrepancy was due to inaccuracies in the estimated stream velocity distribution. These estimates were based upon gauging station records which routinely may involve 10 to 15% error.

Luk et al. (1990) describe the development and laboratory verification of an explicit two-dimensional unsteady substance source model very similar to that developed by Beltaos. The Luk model has the added features of metric coefficients to handle stream curvature, a first order reaction term and source-sink terms. The model was verified against analytical solutions of the one-dimensional advection equation and the two-dimensional advection-diffusion equation, and against two-dimensional unsteady tracer tests in a sinusoidally curved laboratory flume. The flume channel was 0.3 m wide and approximately 20 m long. The sine curves were 0.29 m in amplitude and 1.9 m in wavelength. The bed was composed of resin hardened sand which preserved the equilibrium scour pattern originally formed by the channel. Therefore the channel depth was variable and similar to a natural channel.

Luk et al. (1990) presented concentration vs. time plots at several transverse locations across the laboratory channel at distances of 4, 8 and 12m downstream of a central injection of tracer. A slug test and a variable rate injection test were conducted. Model simulations very closely matched the measured concentration vs. time plots for the two tests. Only minor translations in the time scales were evident and peak concentrations were very accurate.

² Test results reported by Sayre and Chang (1968). Two-dimensional in this experiment was in the vertical and longitudinal directions rather than the transverse and the longitudinal.

The laboratory study by Luk et al. (1990) is the most comprehensive test of the AOG method reported to date. However, two of the three channel transects measured in their study did not have very significant variations in peak concentration across the channel. This is an indication that the tracer was almost uniformly mixed across the channel and thus the measurements were taken within or very near the one-dimensional zone. It is unfortunate that measurements were not obtained at 2 m downstream which would have been well within the two-dimensional zone and thus would have represented a much more rigorous test of the model.

Despite the work of Beltaos and Luk et al., uncertainty remains regarding adequate verification of the AOG method for natural channels. It would be highly desirable to make comparisons of model simulations to tracer measurements taken from natural channels at several transects within the two-dimensional mixing zone, and for a time dependent tracer input. To date, Beltaos's single transect on the Athabasca River is the only comparison which meets this criteria.

4.3 Method Description

The governing mass balance equation (Equation [23]) is solved in fractional steps (Fischer, 1968; Verboom, 1975) therefore, the two-dimensional equation is separated into advection and diffusion substeps as follows:

$$\text{advective substep} \quad \frac{\partial c}{\partial t} = -u \frac{\partial c}{\partial x} \quad [101]$$

$$\text{diffusion substep} \quad \frac{\partial c}{\partial t} = \frac{\partial c}{\partial z} \left(E_z \frac{\partial c}{\partial z} \right) \quad [102]$$

The two substeps are solved in succession using explicit finite difference representations of Equations [101] and [102] at a series of points (nodes) within the channel.

In order to facilitate these calculations for the entire two dimensional extent of the channel a grid is established with nodes distributed in the transverse and longitudinal directions. The solution procedure utilizes a streamtube representation of the channel in

order to determine the transverse grid interval, however the calculations proceed using the cartesian z coordinate, rather than the transformed q coordinate.

4.3.1 Streamtube Representation

The hydraulic and geometric parameters of the river reach to be modelled must be represented by a series of surveyed or synthesized cross sections. At each cross section the channel geometry and velocity distribution must be known for the particular flow (i.e. Q) of interest as shown in Figure 4.1 a). Integration of the h and u curves according to Equation [56] and division by Q produces a dimensionless cumulative flow curve as shown in Figure 4.1 b). The channel is then divided into a series of adjacent streamtubes with boundaries at specified q/Q intervals. Sufficient streamtubes must be defined to obtain good definition of the channel within the expected plume region. At each cross section the width of the streamtubes is determined by subtraction of the z coordinate at the left and right q/Q boundaries of the tubes. The mean velocity and depth of each streamtube at the particular section is then determined by integration of the u vs. z and the h vs. z curve, between the streamtube z coordinate boundaries, and dividing by the streamtube width.

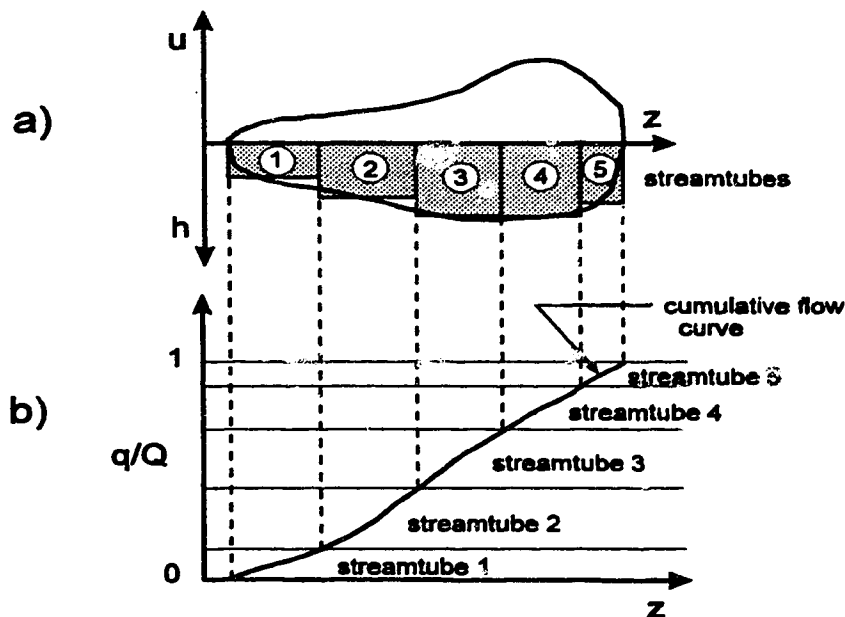


Figure 4.1 Streamtube representation of cross sections.

This process defines a series of nodes stretching in the transverse direction across each cross section. Each node represents the centroid of the streamtube with a set of associated mean parameters. Between defined cross sections the channel is divided into a series of streamtube segments or elements with a node representing the centroid of each element. The mean width, depth and velocity of each element is determined by linear interpolation between defined sections. However, the longitudinal position of the upstream and downstream element boundaries must be determined before this linear interpolation can proceed.

4.3.2 Longitudinal Spacing of Streamtube Elements

The longitudinal spacing of the streamtube element boundaries is variable, and is selected in order to optimize the advection calculations. To illustrate this procedure consider the streamtube elements shown in Figure 4.2 with centroids at position $(i-1, j)$ and (i, j) . The simple explicit forward time, backward space, finite difference expression for Equation [101] which represents advective exchange between the two elements is:

$$\frac{(c_{i,j,t+\Delta t} - c_{i,j,t})}{\Delta t} = -u \frac{(c_{i,j,t} - c_{i-1,j,t})}{\Delta x} \quad [103]$$

where Δx is the longitudinal distance between element centroids and u is the mean longitudinal velocity between the centroids.

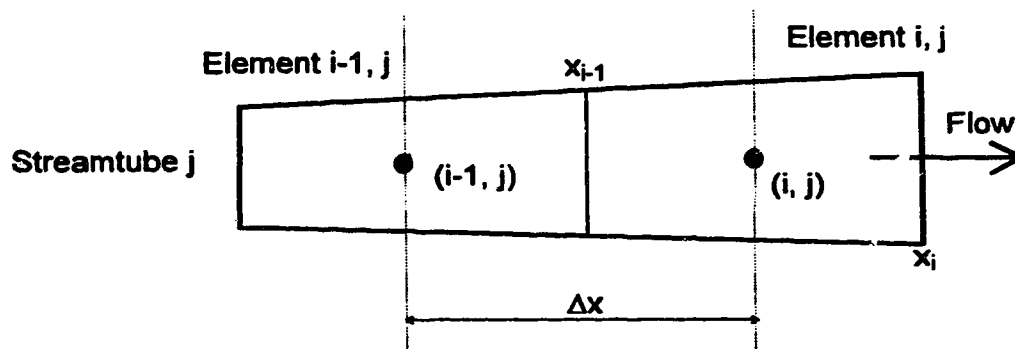


Figure 4.2 Successive streamtube elements.

Solving for the concentration at position (i, j) at time (t + Δt) gives:

$$c_{i,j,t+\Delta t} = c_{i,j,t} + \frac{(u\Delta t)}{\Delta x} (c_{i-1,j,t} - c_{i,j,t}) = c_{i,j,t} + C_r (c_{i-1,j,t} - c_{i,j,t}) \quad [104]$$

from which it can be seen that the extent of the mass exchange between elements element (i-1, j) and element (i, j) is a function of C_r . For $C_r \neq 1$ there is incomplete exchange of mass between element (i-1, j) and element (i, j) during the time step Δt. The incomplete exchange results in the numerical dispersion errors discussed previously. For $C_r = 1$ there is complete exchange and the numerical dispersion errors are eliminated. The basis of the AOG method is to select the upstream and downstream streamtube element boundaries to ensure $C_r = 1$ for each advective exchange between elements.

C_r can also be defined in terms of the volume of and the flow through each element as follows (Beltaos and Arora, 1988):

$$C_r = \frac{\Delta q_j \Delta t}{\Delta V_i} \quad [105]$$

where Δq_j is the flow within streamtube j and ΔV_i is the volume of element i. For complete advective exchange of mass between successive elements, during a time step, (i.e. $C_r = 1$) the volume of element (i-1, j) must equal the volume of element (i, j) because Δq_j and Δt are set values. The volume of each element is solely a function of the element length Δx because the element depth and width are linearly interpolated on the basis of longitudinal distance along the streamtube between defined sections. Therefore, the longitudinal length of each element must be carefully selected to ensure each element of a streamtube has the appropriate volume.

Details of the procedure for selection of the element lengths is given in Appendix A and follows the procedure outlined by Beltaos and Arora (1988). In brief, the cumulative volume to any point along a streamtube is a cubic function of longitudinal distance from the upstream boundary. For time step i the cumulative volume down a streamtube j from time zero would be $i\Delta q_j \Delta t$. In order to determine the downstream

boundary of the i th element the cubic function must be solved by successive substitutions to determine x_i . The element boundaries are then x_i and x_{i-1} (i.e. the boundary from the previous time step calculation).

Once x_i and x_{i-1} are known for the i th element, the mean value of h , h at the right boundary, Δz and E_z for the streamtube at these positions can be determined by linear interpolation between defined sections. The parameters values for the element centroid position are then determined by averaging the parameters values at x_i and x_{i-1} . The calculations proceed down the streamtube until the downstream boundary is reached. The procedure is then repeated for each streamtube. The result of these calculations is an asymmetrical grid pattern with non aligned elements in adjacent streamtubes. Each element has a volume which will ensure complete advective exchange with its upstream and downstream neighbours during a time step calculation. Each element also has an associated list of mean parameters for subsequent use in the mixing calculations. An example of the grid structure is shown in Figure 4.3.

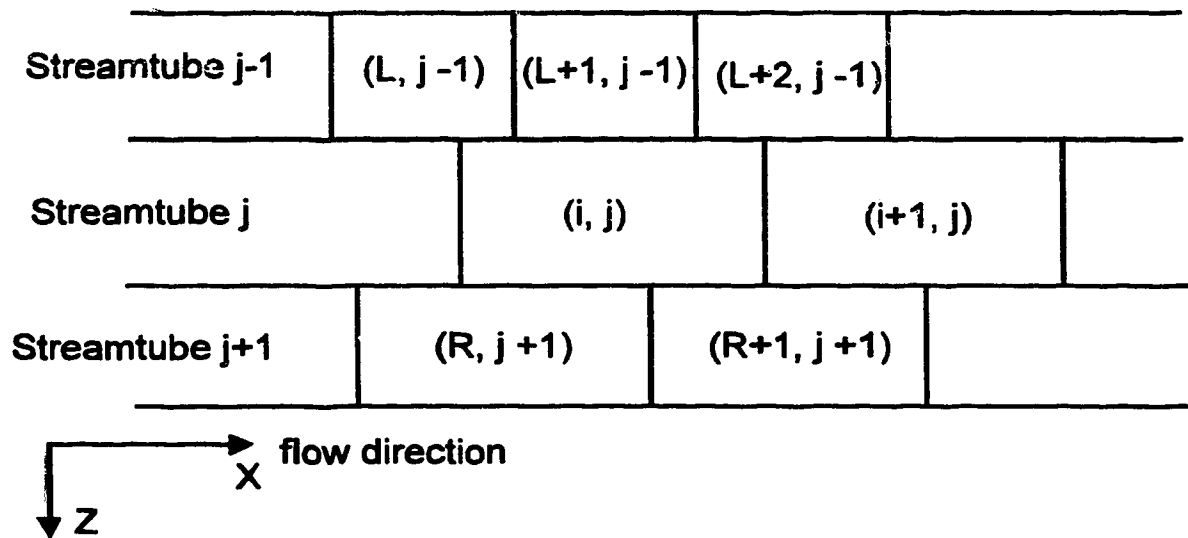


Figure 4.3 Discretization grid optimized for advection - modified from Beltaos and Arora (1988).

4.3.3 Advective Flux

Once the calculation grid is constructed as specified in the previous section the advective flux during each time step is simply a transfer of concentration from upstream elements to downstream elements, i.e.

$$c_{i,j,t+\Delta t} = c_{i-1,j,t} \quad [106]$$

where i varies from one, to the number of elements in tube j , and j varies from one, to the number of streamtubes. At the upstream boundary ($i=0$) the element concentrations are set to the desired input concentration at the beginning of each time step.

4.3.4 Diffusive Flux

The diffusion substep distributes mass laterally between streamtubes using an approximation of the governing differential equation. For the simple case where the elements of adjacent streamtubes are aligned, as shown in Figure 4.4, the approximation would be as follows:

$$\frac{(c_{i,t+\Delta t} - c_{i,t})}{\Delta t} = \frac{E_{z_{i,L}} \frac{(c_{L,t} - c_{i,t})}{\Delta z_{i,L}} - E_{z_{i,R}} \frac{(c_{i,t} - c_{R,t})}{\Delta z_{i,R}}}{\Delta z} \quad [107]$$

where $E_{z_{i,L}}$ and $E_{z_{i,R}}$ are mixing coefficients at the element sides determined as averages between the element centroids. Note that for $\Delta z_{i,L} = \Delta z_{i,R} = \Delta z$ and consistent E_x the approximation will reduce to a central difference expression for the differential $\partial^2 c / \partial z^2$.

The change in mass contained within the element during one time step is:

$$(c_{i,t+\Delta t} - c_{i,t})V_i = E_{z_{i,L}} \frac{(c_{L,t} - c_{i,t})}{\Delta z_{i,L}} A_{i,L} \Delta t - E_{z_{i,R}} \frac{(c_{i,t} - c_{R,t})}{\Delta z_{i,R}} A_{i,R} \Delta t \quad [108]$$

where V_i is the element volume and $A_{i,L}$ and $A_{i,R}$ are the average side areas through which the mass flux occurs.

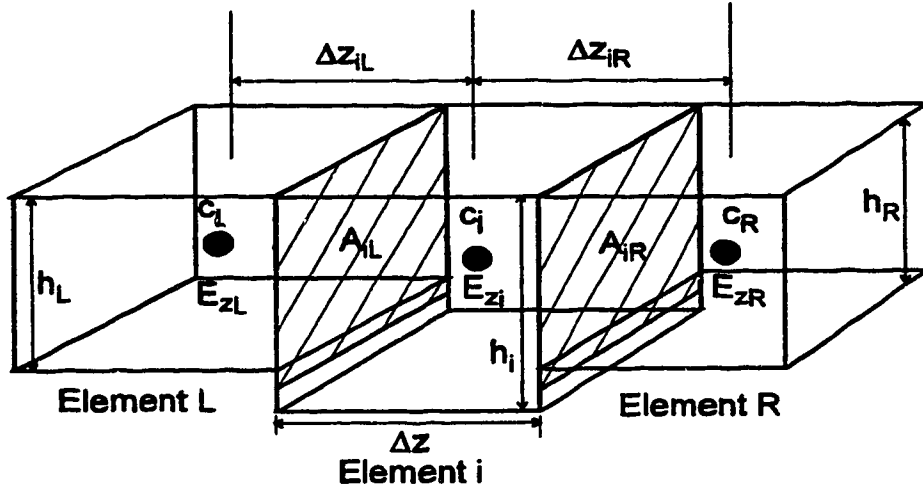


Figure 4.4 Adjacent Streamtube Elements (Simple Case).

In general the elements are not aligned due to the asymmetrical nature of the grid. For element (i, j) shown in Figure 4.3, the diffusive exchange with each neighbouring element sharing a portion of the side boundary is simulated as follows:

$$\begin{aligned}
 (c_{i,j}^* - c_{i,j}) V_{i,j} = & E_z^{i,L} \left[\frac{c_{L,j-1} - c_{i,j}}{\Delta z_{i,L}} \right] A_{i,L} \Delta t + E_z^{i,L+1} \left[\frac{c_{L+1,j-1} - c_{i,j}}{\Delta z_{L+1,i}} \right] A_{i,L+1} \Delta t \\
 & + E_z^{i,L+2} \left[\frac{c_{L+2,j-1} - c_{i,j}}{\Delta z_{i,L+2}} \right] A_{i,L+2} \Delta t + E_z^{i,R} \left[\frac{c_{R,j+1} - c_{i,j}}{\Delta z_{i,R}} \right] A_{i,R} \Delta t \\
 & + E_z^{i,R+1} \left[\frac{c_{R+1,j+1} - c_{i,j}}{\Delta z_{i,R}} \right] A_{i,R+1} \Delta t
 \end{aligned}
 \tag{109}$$

where: the asterisk represents concentration at time $t + \Delta t$, all other concentrations are for time t ,
 $V_{i,j}$ is the volume of element (i, j),
 $A_{i,m}$ is the side boundary area shared between element (i, j) and an adjacent element,
 $\Delta z_{i,m}$ is the average distance between centroids of adjacent elements,
 $E_z^{i,m}$ is the local transverse mixing coefficient between adjacent elements, and
 Δt is the size of the time step.

The concentration for element (i, j) at the next time step can be directly calculated using a rearranged version of Equation [109]. The values of $A_{i,m}$ and $\Delta z_{i,m}$ are calculated using the centroid parameters of each element which were determined during the grid generation process. The shared side area between adjacent elements is the product of the average depth and the shared length. $V_{i,j}$ is known for each element from the grid generation process. The local mixing coefficient is the average of the values at the centroid of the two adjacent elements.

The mixing coefficient at the centroid of each element is predicted using the empirical equation discussed earlier, i.e.

$$E_z = \beta h u_* \quad [110]$$

where: β is the dimensionless mixing coefficient,
 h is the average depth of the element,
 u_* is the local shear velocity or $\sqrt{g r s}$,
 r is the average hydraulic radius for the element, and
 s is the channel slope.

During the grid generation process values for β for each streamtube, and s the channel slope, are input at each defined section in a similar fashion as the streamtube depths, velocities and widths. The dimensional transverse mixing coefficient is then calculated for each streamtube at each section and is subsequently determined for the centroid of each streamtube element by interpolation between sections.

A calculation similar to that represented by Equation [109] is repeated for each element in the grid to complete the diffusion substep. Note that the only parameters that change with time in Equation [109] are the concentrations. Therefore, the position of adjacent elements, the overlapping areas, the Δz 's, and the mixing coefficients only have to be determined once at the beginning of a simulation. These parameters are then stored in a 'flux table' for each grid element and recalled as required in subsequent calculations.

4.4 Error and Stability Considerations

4.4.1 Advection Substep

Truncation error analysis and consistency checks for the forward time, backward space explicit representation of the one-dimensional advection equation are given in Appendix B. The error associated with the approximation is of the order of Δt and Δx used in the discretization.

The stability analysis for the forward time, backward space explicit representation of the one-dimensional advection equation was discussed in Chapter 3. The analysis is repeated for convenient reference in Appendix B. The stability analysis shows that for $C_r = 1$, for which the calculation grid is generated, the finite difference representation has no dissipation errors and no dispersion errors for $N > 4$. Because the model is started with a block input at the upstream boundary some minor dispersion may occur in the first couple of time steps until the waveform spreads.

4.4.2 Diffusion Substep

The truncation error analysis for the forward time, central difference explicit representation of the one-dimensional diffusion equation was discussed in Chapter 3. The analysis is repeated for convenient reference in Appendix B. The error associated with the approximation is of the order of Δt and Δz^2 used in the discretization.

The stability analysis for the forward time, central difference explicit representation of the one-dimensional diffusion equation is given in Appendix B. The results of the analysis indicate that for stability:

$$E_z \frac{\Delta t}{\Delta z^2} \leq \frac{1}{2} \quad [111]$$

otherwise negative concentrations can occur in the solution. This analysis confirms the recommendations of Yotsukura and Fiering (1964) discussed earlier. From the truncation error analysis discussed earlier it was determined that the error could be significantly reduced by cancellation of the leading error terms if:

$$E_z \frac{\Delta t}{\Delta z^2} = \frac{1}{6} \quad [112]$$

However, this state is impossible to achieve for all elements but indicates that values for the parameter of approximately 0.2 are preferable to those nearer 0.5.

4.4.3 Secondary Error

Beltaos and Arora (1988) note that the diffusion substep can cause a numerical diffusion error in the longitudinal direction if the $\Delta x/\Delta z$ ratio is too large (i.e. if the streamtube elements are too long and slender). When mass is exchanged between elements in the diffusion substep it is distributed uniformly over the element giving an average concentration. Depending upon the alignment of the elements the mass can be artificially advanced in the longitudinal direction. The effect is shown schematically in Figure 4.5.

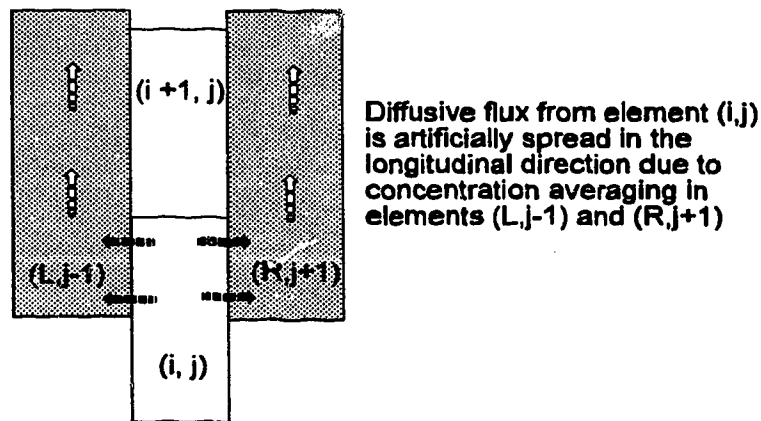


Figure 4.5 Secondary advective flux.

Beltaos and Arora (1988) report that this effect is minor in comparison to the longitudinal dispersion resulting from differential advection. However, in order to limit this effect, they recommend the element dimensions be limited to $\Delta x/\Delta z < 10$ for good results. Some artificial diffusion in the longitudinal direction may in fact be of benefit as it may compensate somewhat for neglecting the longitudinal dispersion term in the original mass balance equation.

4.4.4 Time Step and Transverse Grid Spacing Selection

A suggested strategy for selecting the appropriate time step and transverse grid spacing for the modelling procedure can be summarized as follows:

1. Select the streamtube spacing across the channel in terms of q/Q (and thus the Δz spacing) in order to obtain a reasonable number of points across the lateral extent of the effluent plume or slug release at the sections of interest. Remember the streamtube spacing in terms of q/Q must be consistent at each section. The streamtube spacing should also consider the location of midchannel bars and/or islands if they are to be considered in the simulation.
2. Select a proposed time step, then at each section using the mean velocity in each streamtube estimate Δx . Check that $\Delta x/\Delta z < 10$ for each streamtube at each section. If this condition is not met the time step must be shortened or the streamtube spacing revised.
3. Once the $\Delta x/\Delta z$ criteria is satisfied check the transverse diffusion stability criteria (i.e. $E_z \Delta t / \Delta z^2 < 0.5$) for each streamtube at each section. Again if this condition is not met the time step must be shortened or the streamtube spacing revised.

Beltaos and Arora (1988) demonstrated that the transverse diffusion stability requirement will generally be met automatically if the $\Delta x/\Delta z$ recommendation is observed. For this reason $\Delta x/\Delta z$ is checked first.

4.5 Method Implementation

The overall AOG method is implemented using a series of four programs. Two preprocessing programs are used to divide the channel into streamtubes and generate the optimized grid for the river reach of interest. A main program then conducts the mixing calculations using input of stored parameters from the preprocessing programs and input of upstream boundary concentrations. Finally, a post processing program is used to interpolate the output from the main program to obtain results at a specified distance

downstream of the input location. Each of these programs are briefly described in the following sections.

All the programs have been written in Microsoft Fortran for IBM compatible computing systems. The programs were compiled for use with Microsoft Windows. This offers two advantages:

1. The programs can address a significantly larger amount of memory than if they were compiled for use with MSDOS. This allows the use of very large array sizes with the only restriction being how they are organized within memory blocks.
2. The Windows environment allows easy manipulation of data files allowing cutting and pasting between files. In addition, screen output from any of the programs can be cut and pasted directly into a spreadsheet or word-processing program if desired.

4.5.1 Preprocessing Program STRMTUBE

The purpose of STRMTUBE is to take a series of cross sections with defined h , and q/Q vs. z curves and divide the channel into streamtubes with specified q/Q boundaries. The h and q/Q vs. z relationships are defined by a series of coordinates which are read into the program. The channel geometry and flow information must first be compiled from cross section surveys or synthesized using established river engineering principles. The majority of the compilations of this data are easily handled using a spreadsheet program from which the resulting data coordinates can be cut and pasted into the STRMTUBE input file.

The program takes the defined z , q/Q , h points at each section and interpolates between them at the requested q/Q boundaries in order to determine the streamtube z coordinates and depths. The program also assembles slope and dimensionless mixing coefficient data for each section. The output from STRMTUBE is in a format which is readily acceptable as input to the second preprocessing program.

The second important function of STRMTUBE is to check the combination of the proposed streamtube widths (i.e. the transverse grid spacing) and the time step against the

error criteria discussed above.³ A compilation of $(\Delta x/\Delta z)$ and $(E_x \Delta t/\Delta z^2)$ for each streamtube is output to a text file which can be reviewed by the user to ensure none of the error criteria have been exceeded.

The required input data for STRMTUBE and it's output are summarized in Table 4.1. A listing of the program is given in Appendix C.

Table 4.1 STRMTUBE Input/output summary.

Input	Output
for the reach:	for each section:
total flow, Q	streamtube avg. depths
time step, Δt	streamtube widths
q/Q streamtube boundaries	streamtube right boundary depth
for each section:	dimensionless mixing coefficient, β
downstream location, x	channel slope, s
series of h, z, q/Q coordinates	
dimensionless mixing coefficient, β	
channel slope, s	

4.5.2 Preprocessing Program GRIDGEN

The purpose of GRIDGEN is to take compiled streamtube information from the previous preprocessing program and generate the advection optimized grid for the river reach. The process is shown schematically in Figure 4.6.

The interpolation procedure discussed above, which uses element volumes to determine element longitudinal boundaries, is used in the grid generation process. The GRIDGEN program also determines a list of element parameters for use by the main mixing program. The output from GRIDGEN is stored in two data files. SIMDIMS.DAT contains the i,j designation of each element and a list of the element parameters. The information is organized so that there is one element per line beginning at position (1,1)

³ Once a section is divided into streamtubes the mean flow velocity u for each tube can be calculated from $u = \Delta x/\Delta t$.

and proceeding down each streamtube in succession. RCHCHAR.DAT contains reach information including the number of streamtubes, time step, number of elements in each tube, and the volume of the elements in each tube.

The required input data for GRIDGEN and its output are summarized in Table 4.2. A listing of the program is given in Appendix C.

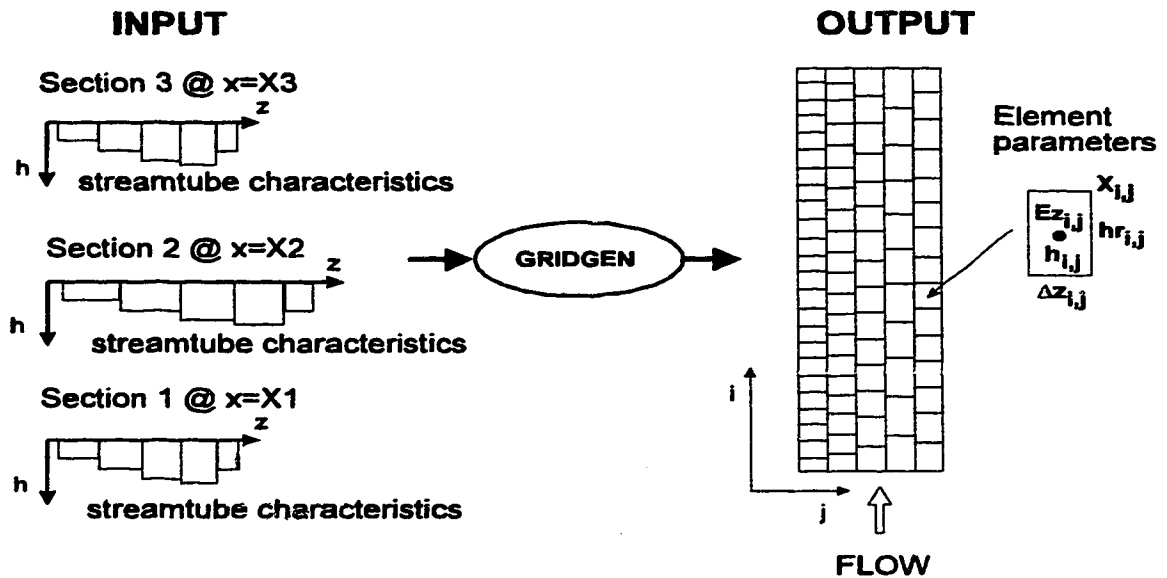


Figure 4.6 Schematic representation of the function of the GRIDGEN preprocessing program.

Table 4.2 GRIDGEN Input/output summary.

Input	Output
for the reach:	to SIMDIMS.DAT for each element:
no. of sections	avg. depth
no. of streamtubes	width
time step, Δt	right boundary depth
total flow, Q	dimensional mixing coefficient, E_z
q/Q streamtube boundaries	downstream boundary position x
for each section:	to RCHCHAR.DAT for the reach:
STRMTUBE output	no. of sections
	no. of streamtubes
	no. of elements in each streamtube
	vol. of elements in each streamtube

4.5.3 Main Program 2DMIX

The main program 2DMIX performs all the fractional time step mixing calculations on the grid established by the preprocessing programs. The tasks performed by 2DMIX may be summarized as follows:

1. Read the information from RCHCHAR.DAT and SIMDIMS.DAT into memory and establish an array containing an initial concentration for each element in the grid at time $t = 0$.
2. For each element in the grid, determine the shared area, mean E_z , and Δz between stream tube centrelines and the i, j coordinates of each transversely adjacent element. Store this information in an array in memory (a 'flux table') for subsequent recall during each time step.
3. Determine the longitudinal extent to which mass has been advected down the channel from time zero. Translate this longitudinal distance into limiting i coordinates for each streamtube in order to limit the mixing calculations to the region in which mass will be present. This procedure eliminates numerous redundant calculations in the early portion of the simulation.
4. Then for each time step perform the following substep operations:
 - a) Read the upstream boundary concentrations.
 - b) Perform the advective exchange operation for each element proceeding up each streamtube toward the upstream boundary concentration. An intermediate concentration is thus established for each element which replaces the original concentration at time t .
 - c) Perform the diffusion calculation for each element using the intermediate concentrations to determine the concentration gradient between adjacent elements. Note that the position of the adjacent elements and the required parameters for this calculation are recalled from an element's 'flux table'.

The resulting concentration for each element is stored in an array of concentrations for time $t+\Delta t$.

- d) The concentrations at $t+\Delta t$ are written to a data file called TIMECONC.DAT and then transferred in memory to the array holding the intermediate concentrations. This array then becomes the initial concentration for the next time step.

Repeat a) to d) until the requested number of time steps have been completed.

The output to TIMECONC.DAT is arranged as one long vector or series of records, one record for each element in each time step. Within a time step, the records progress from the first position in streamtube 1 (i.e. element(1, 1)), down the tube to the downstream boundary and then start over again at the next tube and continue until the last tube is traversed to the final i position (see Figure 4.7). The results from each new time step are stored in similar fashion and continue on in the file from the last record of the previous time step. The current version of the program has capacity for 2048 time steps and 20 streamtubes.

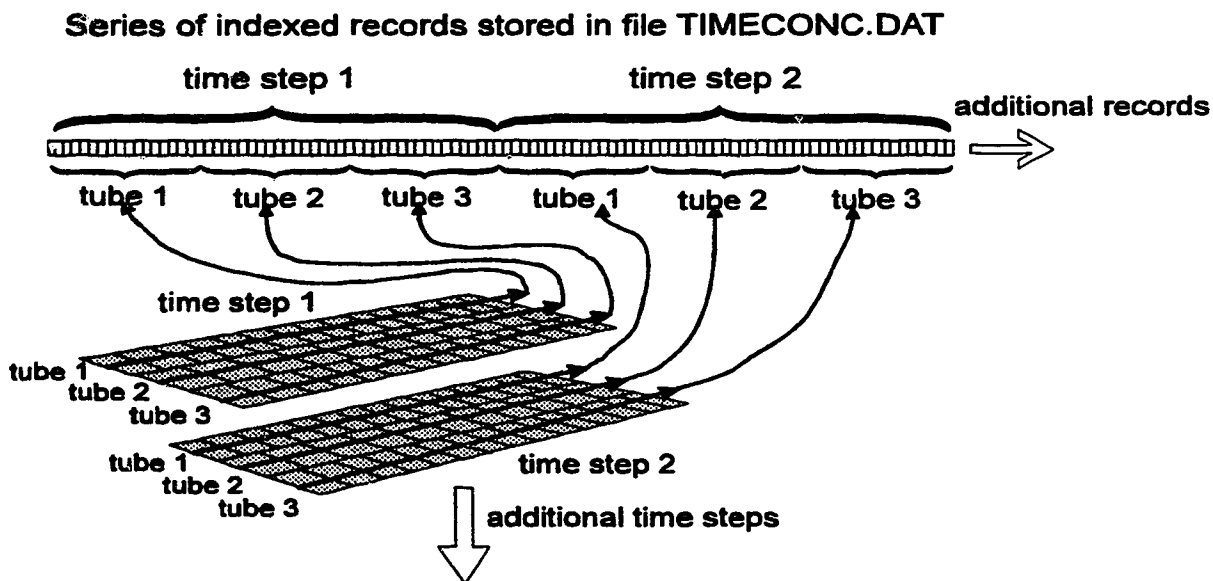


Figure 4.7 Organization of output from 2DMIX.

The left and right bank 'no flux' boundary conditions are easily handled in the program by only permitting exchange on one side of the elements which are adjacent to the left and right banks. No flux boundaries created by mid channel bars and islands can also be handled by locating sections at their upstream and downstream ends. The appropriate streamtube will then have a right boundary depth equal to zero which causes the calculations to result in zero diffusive flux.

The required input data for 2DMIX and it's output are summarized in Table 4.3. A listing of the program is given in Appendix C.

Table 4.3 2DMIX Input/output summary.

Input	Output
for the reach:	for each element and timestep:
total flow, Q	output concentrations, c
time step, Δt	elapsed time, t
q/Q streamtube boundaries	
input concentrations at each time step, c	
for each section:	
downstream location, x	
series of $h, z, q/Q$ coordinates	
dimensionless mixing coefficient, β	
channel slope, s	

4.5.4 Post Processing Program XSLICE

The purpose of the post processing program XSLICE is to retrieve records from TIMECONC.DAT to obtain concentration vs. time data for a specified longitudinal position in the river reach. XSLICE first determines the (i,j) position of the element in each streamtube which straddles the specified x location. The index numbers of the records in the first segment of TIMECONC.DAT which holds the concentrations of these elements are then determined. Next, the first time step concentrations in each streamtube are determined by linear interpolation between the appropriate upstream and downstream

centroid concentrations retrieved from the appropriate records. Finally, the interpolations are repeated for each time step. The appropriate record index numbers for successive time steps are easily determined as they are always offset by the total number of elements from the previous index number.

The post processing procedure is shown schematically in Figure 4.8. The interpolated results are output to a text file, one line per time step in the following format:

```
time 1, conc. in tube 1, conc. in tube 2, .....conc. in last tube.
time 2, conc. in tube 1, conc. in tube 2, .....conc. in last tube.
      :
      :
last time, conc. in tube 1, conc. in tube 2, .....conc. in last tube.
```

The text file is easily loaded into a spreadsheet program for plotting and/or further analysis.

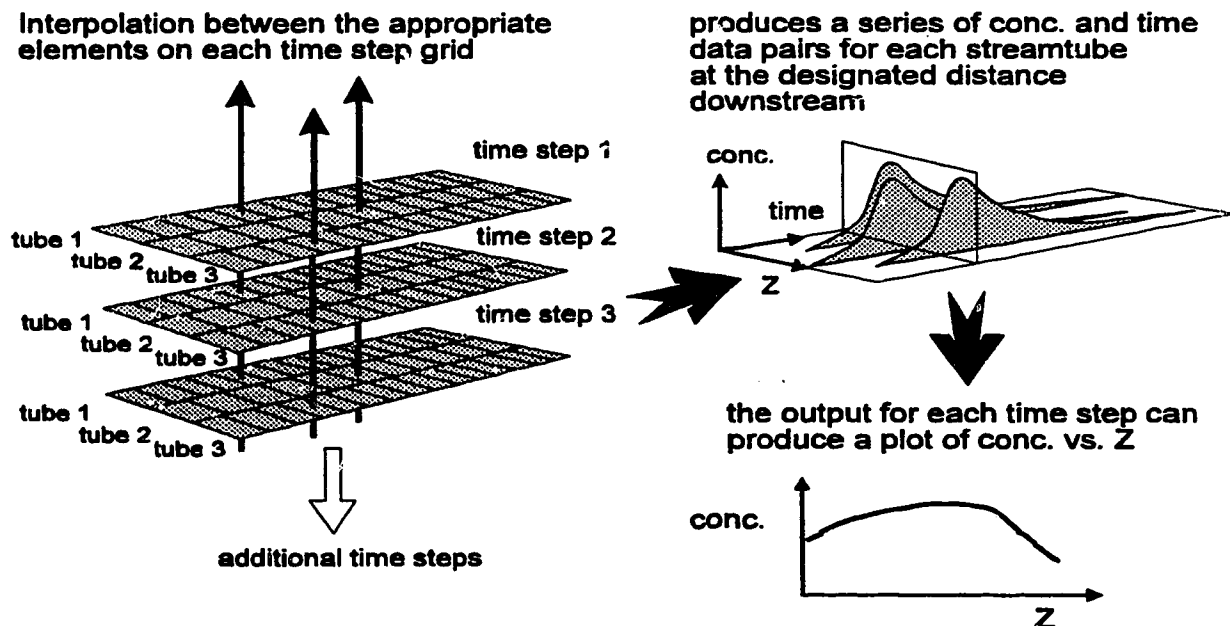


Figure 4.8 Post processing of 2DMIX output data.

5. Model Verification Studies

5.1 Introduction

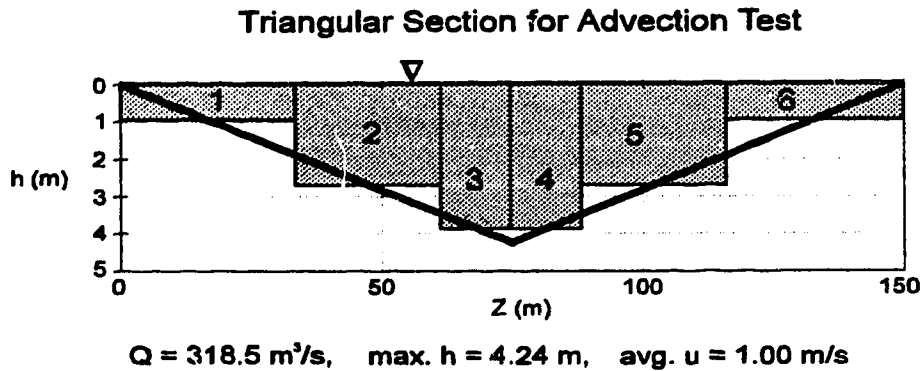
In order to confirm the accuracy of the present implementation of the AOG method, the algorithms were first tested against analytical solutions for simplified situations. These include: one-dimensional advective translation with no dispersion and steady state transverse mixing.

The algorithms were then tested against a laboratory study conducted by Fischer (1966) and reported by Beltraos (1978). Finally, and most significant, the present AOG model was tested against the results of three major slug tracer tests conducted on three large western Canadian rivers. The final stage of the verification is the most significant because only one field slug test has been reported in the literature to verify the AOG method. In the test which was reported by Beltraos and Arora (1988) tracer concentration data from only a single cross section are available. Clearly a more extensive verification of the AOG method in the field is desirable before it can be recommended for general use for conservative parameters. Once this verification is complete the method can be extended to non-conservative parameters.

5.2 Model Verification against Analytical Methods

5.2.1 Advective Translation

The advective substep of the model was tested using a slug input across a channel at its upstream boundary, and running the model for $\beta = 0$ (i.e. no transverse diffusion). The channel used for the test was triangular in cross section and divided into six stream tubes as shown in Figure 5.1. A triangular section was used to ensure the grid generated by the model had overlapping elements. This is a more stringent test than using a rectangular channel because transverse concentration gradients are produced due to the differential velocities between streamtubes. Any inaccuracies in the diffusion substep would distort the input waveform as a result of these gradients.



Streamtube Characteristics

Tube	h (m)	width (m)	q/Q	$\Delta q/Q$ (m³/s)	u (m/s)
1	0.98	34.1	0.0625	0.0625	0.5950
2	2.67	26.0	0.2800	0.2175	0.9968
3	3.78	14.9	0.5000	0.2200	1.2427
4	3.78	14.9	0.7200	0.2200	1.2427
5	2.67	26.0	0.9375	0.2175	0.9968
6	0.98	34.1	1.0000	0.0625	0.5950

Figure 5.1 Triangular section used for the advection test.

Two input waveforms were used for the test. A half sine wave and a rectangle as shown in Figure 5.2. The output waveforms were determined after 450 and 900 time steps. Because the output concentrations are interpolated between element centroids care must be taken to ensure the requested longitudinal distance aligns with the element centroid. The longitudinal distance corresponding to the desired number of time steps is:

$$((\text{no. time steps}) - 0.5) (\text{mean flow velocity of the streamtube})$$

The half time step back is required because the elements are initially aligned with their downstream boundaries at time zero.

The output waveform concentrations are listed in Table 5.1 to Table 5.4 compared to the input concentrations. The output is virtually identical to the input as would be expected if the algorithms are functioning correctly. Even the rectangular input which is defined by a single point is accurately transferred down the streamtubes.

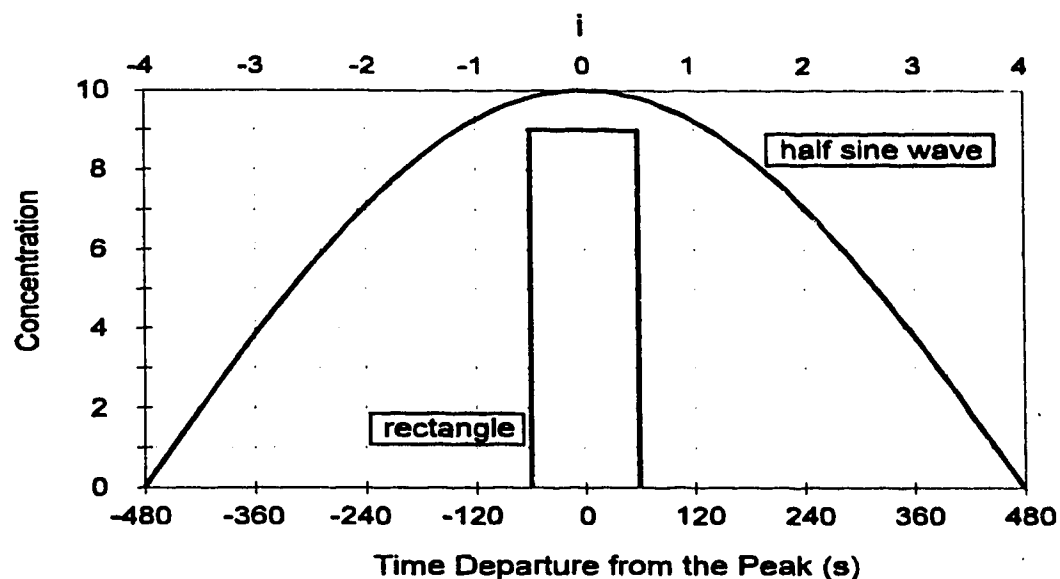


Figure 5.2 Advection test input waveforms.

Table 5.1 Half sine wave concentrations after the peak has moved 450 time steps.

Input	Position	Tube 1	Tube 2	Tube 3
0.0000	445.5uΔt	0.0000	0.0000	0.0000
3.8268	446.5uΔt	3.8267	3.8268	3.8268
7.0711	447.5uΔt	7.0710	7.0711	7.0711
9.2388	448.5uΔt	9.2387	9.2388	9.2388
10.0000	449.5uΔt	10.0000	10.0000	10.0000
9.2388	450.5uΔt	9.2388	9.2388	9.2388
7.0711	451.5uΔt	7.0712	7.0711	7.0711
3.8268	452.5uΔt	3.8269	3.8269	3.8268
0.0000	453.5uΔt	0.0000	0.0000	0.0000

note: $\Delta t = 120$ sec

Table 5.2 Rectangular waveform concentrations after 450 time steps.

Input	Position	Tube 1	Tube 2	Tube 3
0.0000	448.5uΔt	0.0000	0.0000	0.0000
9.0000	449.5uΔt	8.9998	8.9997	9.0000
0.0000	450.5uΔt	0.0002	0.0003	0.0000

note: $\Delta t = 120$ sec

Table 5.3 Half sine wave concentrations after the peak has moved 900 time steps.

Input	Position	Tube 1	Tube 2	Tube 3
0.0000	895.5uΔt	0.0000	0.0000	0.0000
3.8268	896.5uΔt	3.8268	3.8268	3.8271
7.0711	897.5uΔt	7.0711	7.0711	7.0713
9.2388	898.5uΔt	9.2388	9.2388	9.2389
10.0000	899.5uΔt	10.0000	10.0000	9.9999
9.2388	900.5uΔt	9.2388	9.2388	9.2386
7.0711	901.5uΔt	7.0711	7.0711	7.0708
3.8268	902.5uΔt	3.8268	3.8268	3.8264
0.0000	903.5uΔt	0.0000	0.0000	0.0000

note: $\Delta t = 120$ sec

Table 5.4 Rectangular waveform concentrations after 900 time steps.

Input	Position	Tube 1	Tube 2	Tube 3
0.0000	898.5uΔt	0.0000	0.0000	0.0000
9.0000	899.5uΔt	9.0000	8.9976	8.9991
0.0000	900.5uΔt	0.0000	0.0024	0.0009

note: $\Delta t = 120$ sec

5.2.2 Steady State Substance Source

The diffusion substep of the model was tested using a steady state line source across a portion of the channel. The output from the model is compared to the analytical solution for continuous line sources developed by Yotsukura and Cobb (1972) (see Equation [67]). The channel used for the numerical simulation was rectangular in shape and divided into 20 streamtubes. The channel and streamtube characteristics are listed in Table 5.5. A rectangular section was used because the analytical solution was developed for an idealized channel with constant depth and velocity.

The output from the analytical and numerical simulations are shown in Table 5.6 and plotted in Figure 5.3. Note the numerical solution concentrations are means for the streamtubes and are plotted at the streamtube centrelines. Therefore, the boundary concentrations cannot be predicted by the numerical method. The numerical and analytical solutions are in very close agreement.

Table 5.5 Rectangular channel characteristics for diffusion testing.

 Rectangular channel divided into 20 equal streamtubes, $\Delta q/Q = 0.05$

 Continuous line source between 0 and 0.1 q/Q , $c=10.0$
 $\Delta t = 10 \text{ sec}$
 $\beta = 0.35, s = 0.0001$

Channel characteristics	Streamtube characteristics
$W = 20 \text{ m}$	$\Delta z = 1 \text{ m}$
$H = 1 \text{ m}$	$h = 1 \text{ m}$
$U = 0.4 \text{ m/s}$	$u = 0.4 \text{ m/s}$
$U_* = \sqrt{gHs}$	$u_* = \sqrt{ghs}$
$E_z = \beta H U_* = 0.0110 \text{ m}^2/\text{s}$	$E_z = \beta h u_* = 0.0110 \text{ m}^2/\text{s}$

Table 5.6 Comparison of concentrations predicted by analytical and numerical solutions for two-dimensional steady state mixing.

$x =$ q/Q	50m		100m		200m		400m	
	Model	Anal.	Model	Anal.	Model	Anal.	Model	Anal.
0.000	-	7.72	-	6.06	-	4.54	-	3.30
0.025	7.54	7.51	5.98	5.96	4.51	4.49	3.29	3.28
0.075	6.02	6.01	5.18	5.17	4.15	4.14	3.15	3.15
0.125	3.75	3.78	3.87	3.88	3.53	3.53	2.89	2.89
0.175	1.80	1.82	2.50	2.52	2.76	2.77	2.54	2.54
0.225	0.66	0.66	1.39	1.40	2.00	2.00	2.14	2.14
0.275	0.19	0.17	0.67	0.67	1.33	1.34	1.72	1.73
0.325	0.04	0.03	0.28	0.27	0.82	0.82	1.33	1.34
0.375	0.01	0.00	0.10	0.10	0.46	0.47	0.99	0.99
0.425			0.03	0.03	0.24	0.24	0.70	0.70
0.475			0.01	0.01	0.12	0.12	0.48	0.48
0.525					0.05	0.05	0.31	0.31
0.575					0.02	0.02	0.19	0.19
0.625					0.01	0.01	0.12	0.12
0.675							0.07	0.07
0.725							0.04	0.04
0.775							0.02	0.02

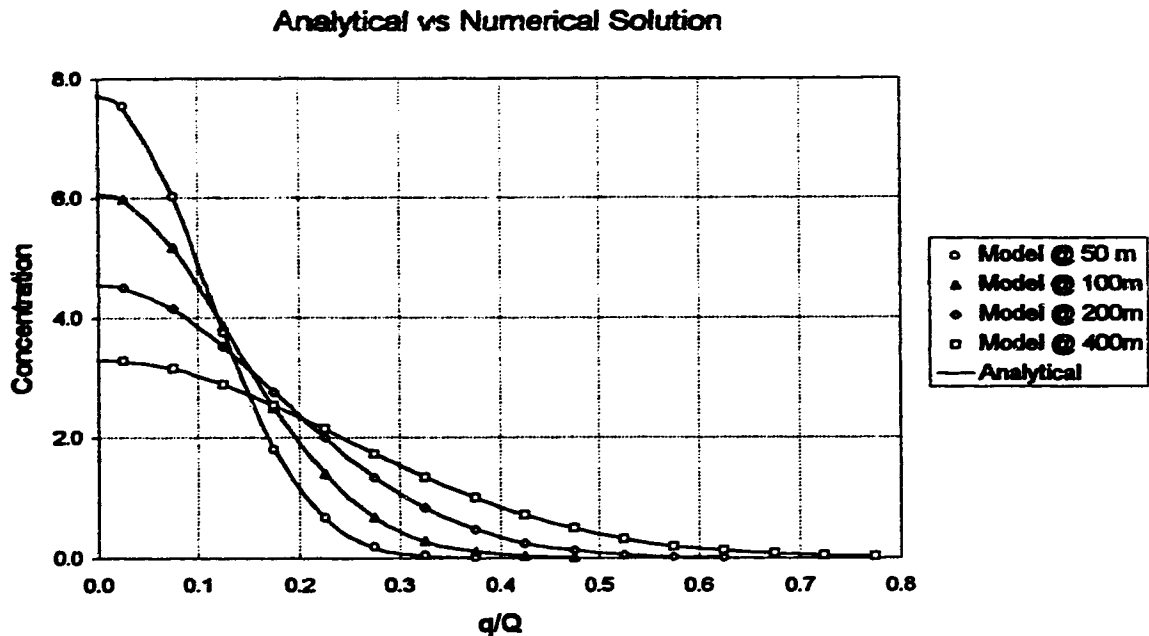


Figure 5.3 Comparison of concentrations predicted by analytical and numerical solutions for two-dimensional steady state mixing.

5.3 Model Verification using Laboratory Measurements

Fischer (1966) reported the results of longitudinal dispersion studies in a trapezoidal flume. In one experiment granular fill was placed on the side slopes of the flume in order to create more significant transverse velocity gradients. The fill in effect created a rectangular channel with roughened sides. Tracer was input in a line across the channel, as a slug, and was monitored at two downstream sections at several transverse locations. Beltaos (1978) used Fisher's experiment as one of the laboratory verifications of the AOG method. The exercise was repeated for the current implementation of the AOG method using Fischer's data taken from Beltaos's report.

The monitoring (probe) locations and the characteristics of the flume channel are shown in Figure 5.4 and listed in Table 5.7. This section was used to characterize the full length of the flume. The total flow was determined using the channel dimensions and the velocity distribution reported by Fischer and is estimated to $0.00329 \text{ m}^3/\text{s}$.

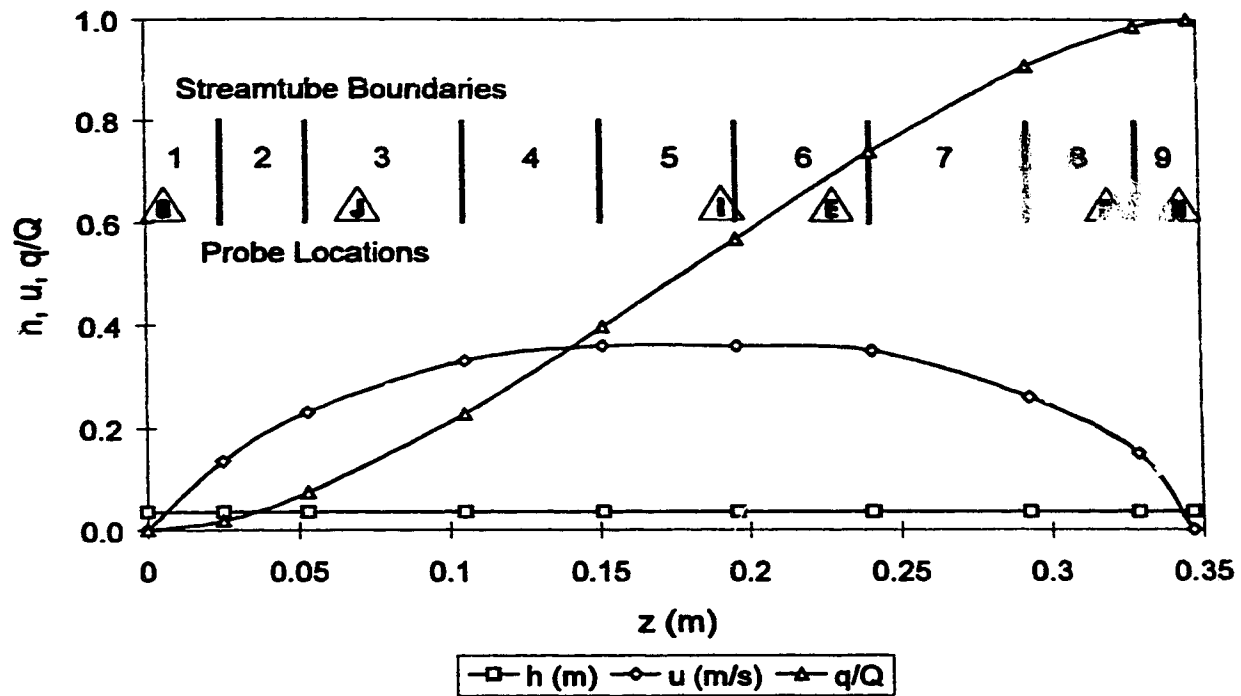


Figure 5.4 Fischer experiment channel characteristics and probe locations - modified from Beltaos (1978).

Table 5.7 Fischer experiment channel characteristics and probe locations.

Streamtube Boundary Locations and Characteristics					Probe Locations	
Tube	z (m)	q/Q	h (m)	u (m/s)	Probe	q/Q
	0.000	0.000	0.035	0.000	G	0.005
1	0.025	0.018	0.035	0.135	J	0.120
2	0.053	0.072	0.035	0.230	I	0.555
3	0.105	0.227	0.035	0.330	E	0.690
4	0.151	0.396	0.035	0.360	F	0.960
5	0.196	0.568	0.035	0.360	H	0.995
6	0.241	0.738	0.035	0.350		
7	0.293	0.907	0.035	0.260		
8	0.329	0.986	0.035	0.150		
9	0.347	1.000	0.035	0.000		

Tracer measurements were taken by Fischer at 16.11 and 26.07 m downstream and were reported in relative concentrations. In order to determine the total mass input in relative concentrations, the measured concentration vs. time plots (the C-t plots) were integrated with respect to time and the z direction. The results of these integrations showed there was some discrepancy between the total mass recovery at the two monitored sections. This indicates that the measurements may have been taken for two separate injections and hence the need to report the results in relative concentrations.

In order to overcome these difficulties the model was run twice, once for the relative mass recovery obtained at 16.11 m (6.04 units), and once for the relative mass recovery obtained at section 26.07 m (9.99 units)). A uniform concentration (1837 and 3036 units/m³ respectively) was placed in the first element of each streamtube to begin each simulation. The input concentration was equal to the product of the total mass input, the total flow rate and the time step. The model was initially run using $E_z = 1.63 \text{ cm}^2/\text{s}$ as reported by Beltaos (1978), however a revised value of $E_z = 1.79 \text{ cm}^2/\text{s}$ produced a better fit to the measured data. The model results and the measured concentrations are shown in Figure 5.5 and Figure 5.6.

The model accurately predicts the measured concentrations with only minor discrepancies near the banks. Beltaos (1978) obtained similar results and speculated that the poorer match near the banks may be due to the presence of dead zones. Tracer trapped in the dead zones is slowly released over time hence the attenuation in the peak concentration and the elongated time base of the measured waveform in comparison to that predicted by the model.

As noted in Chapter 4, Luk et al. (1990) completed an extensive laboratory verification study of the AOG method in a sinusoidally meandering flume channel with variable cross section geometry. Under these conditions the model also performed very well. A minor weakness of this study was that the channel reach in which tracer had not yet approached the side boundaries was not sampled. Hence the model was not rigorously tested in the two-dimensional mixing zone. The same is true for the Fischer experiment since the mass was input as a line source across the channel. Despite this the model can be considered adequately and independently verified for laboratory conditions.

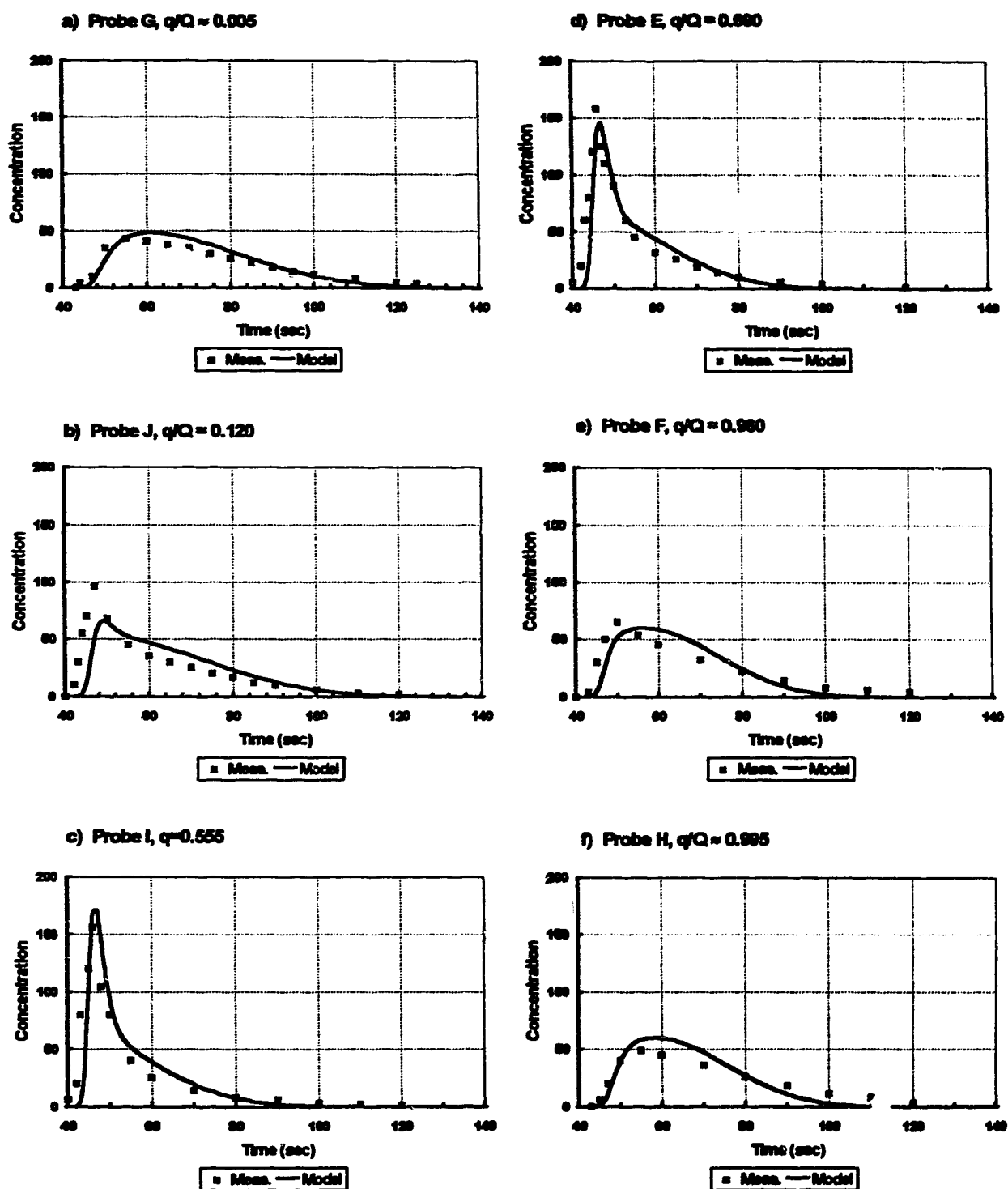


Figure 5.5 Fischer Ser. 2800 Experiment, C-t curves at 16.07 m.

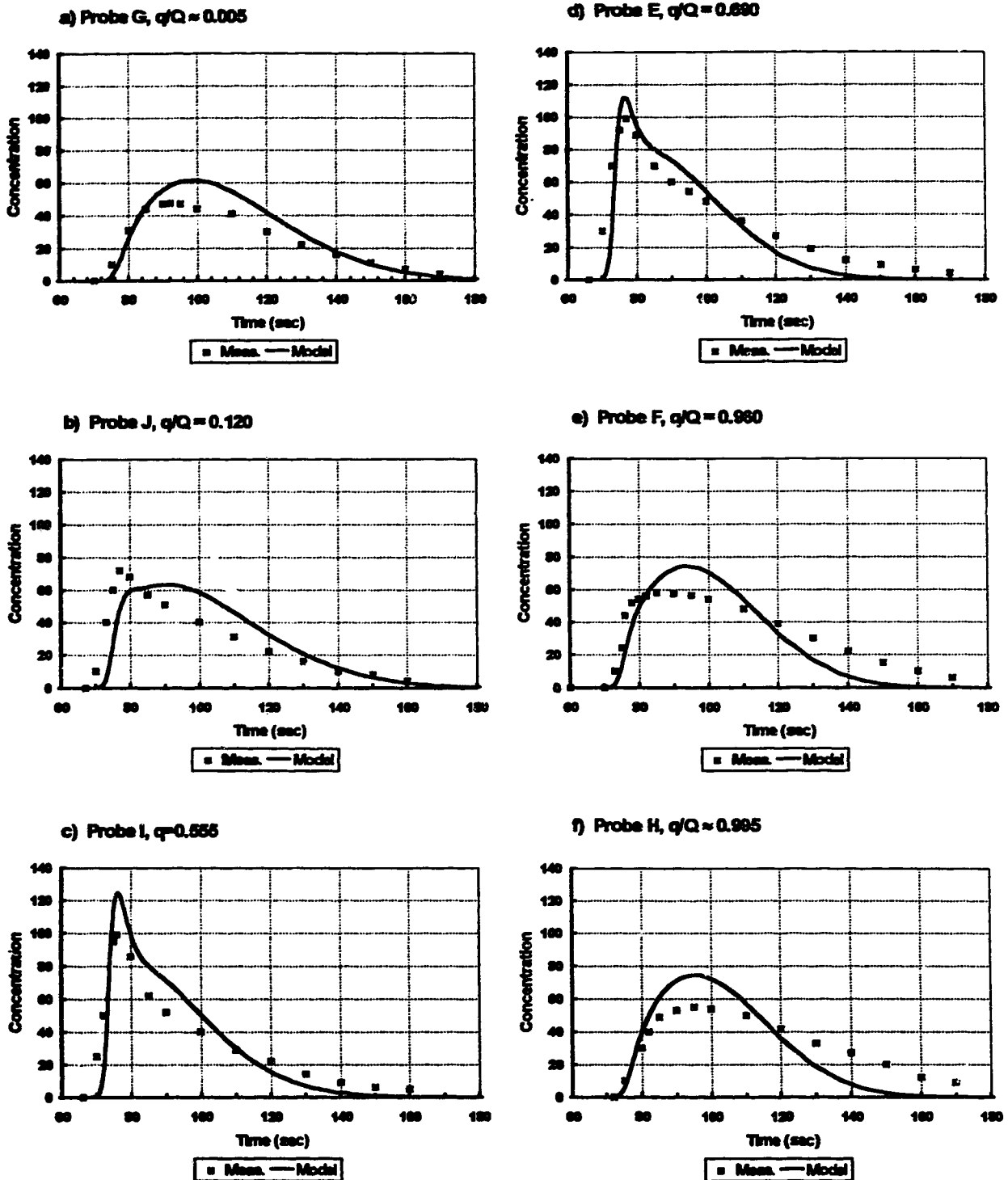


Figure 5.6 Fischer Ser. 2800 Experiment, C-t curves at 26.11 m.

5.4 Model Verification using Field Tracer Studies

5.4.1 Introduction

The next step in the verification process was to test the AOG method against several tracer tests conducted in the field. Field verification is vital in order to have confidence that the model can be applied to practical effluent disposal problems.

The comparison of the model output to the laboratory investigations described in the previous section indicates the AOG method is satisfactory for modelling the mixing conditions which occur in channels with limited secondary currents. Secondary currents are always present in natural channels due to the variable cross section geometry created by bends, bars, outcrops etc. The result is enhanced transverse mixing conditions. The AOG method must be able to directly handle the variations in cross section geometry (i.e. the u and h variations both transversely and longitudinally) and to indirectly handle the enhanced transverse mixing by means of the dimensionless transverse mixing coefficient (i.e. the β coefficient).

An additional phenomenon which commonly occurs in natural streams is the presence of dead zones (backwater) near the banks of the stream. This effect was evident in the Fischer laboratory experiment discussed above. Mass entering the dead zone becomes temporarily trapped and is slowly released over time. Thus a C-t waveform entering the backwater tends to have its peak attenuated and its time base stretched. The presence of this effect can hamper the model accuracy within the near-shore region. The seriousness of these inaccuracies must be considered in the assessment of model performance.

Beltaos and Arora (1988) reported the results of a verification test of the AOG method using data collected on the Athabasca River downstream of Fort McMurray under ice-covered conditions (see Beltaos (1978) for details of the field test). The study reach was 11.8 km long and characterized by cross sections located at 1.9, 3.1, 4.3, 6.3, 7.8, 9.7 and 11.8 km downstream of the injection point. Tracer was injected as a slug near the left bank of the river. Tracer concentrations were measured across the channel at 6.3 and

11.8 km. Unfortunately, the slug passed by 6.3 km too quickly to obtain accurate C-t plots. The AOG method was used to simulate the tracer concentrations measured at 11.8 km using the appropriate channel parameters taken from the cross section surveys. A reach-averaged value of $E_z = 0.04 \text{ m}^2/\text{s}$ was used in the simulation.

The results of the simulation are shown in Figure 5.7. As noted by Beltaos and Arora (1988) there were some minor discrepancies in the time of travel predicted by the model and that observed in the field. These discrepancies could easily be the result of gauging station error in reporting total flow (as proposed by Beltaos) or due to reduced cross sectional area due to accumulation of frazil ice¹ and or cut off of shallower sections of the river by ice cover. In addition, the shapes of the C-t curves near the left bank are significantly different. Beltaos speculated that this difference was due to the presence of dead zones near the left bank. This would be consistent with the attenuated peak and elongated time scale of the observed C-t plot.

This single slug test on the Athabasca River appears to be the only time-dependent field verification of a two-dimensional unsteady substance source model documented in the literature. All other investigators have used either laboratory studies or steady state tracer tests for verification. Verification of the current AOG model against three major field tracer studies are presented in the following sections. The completion of these verification studies represents a major step toward general acceptance of the AOG method for the simulation of plumes resulting from unsteady effluent discharges to natural rivers.

¹ Ice pellets which form in open water during freeze-up conditions and attach to the underside of ice floes. Once the river freezes over the frazil ice is redistributed under the ice cover.

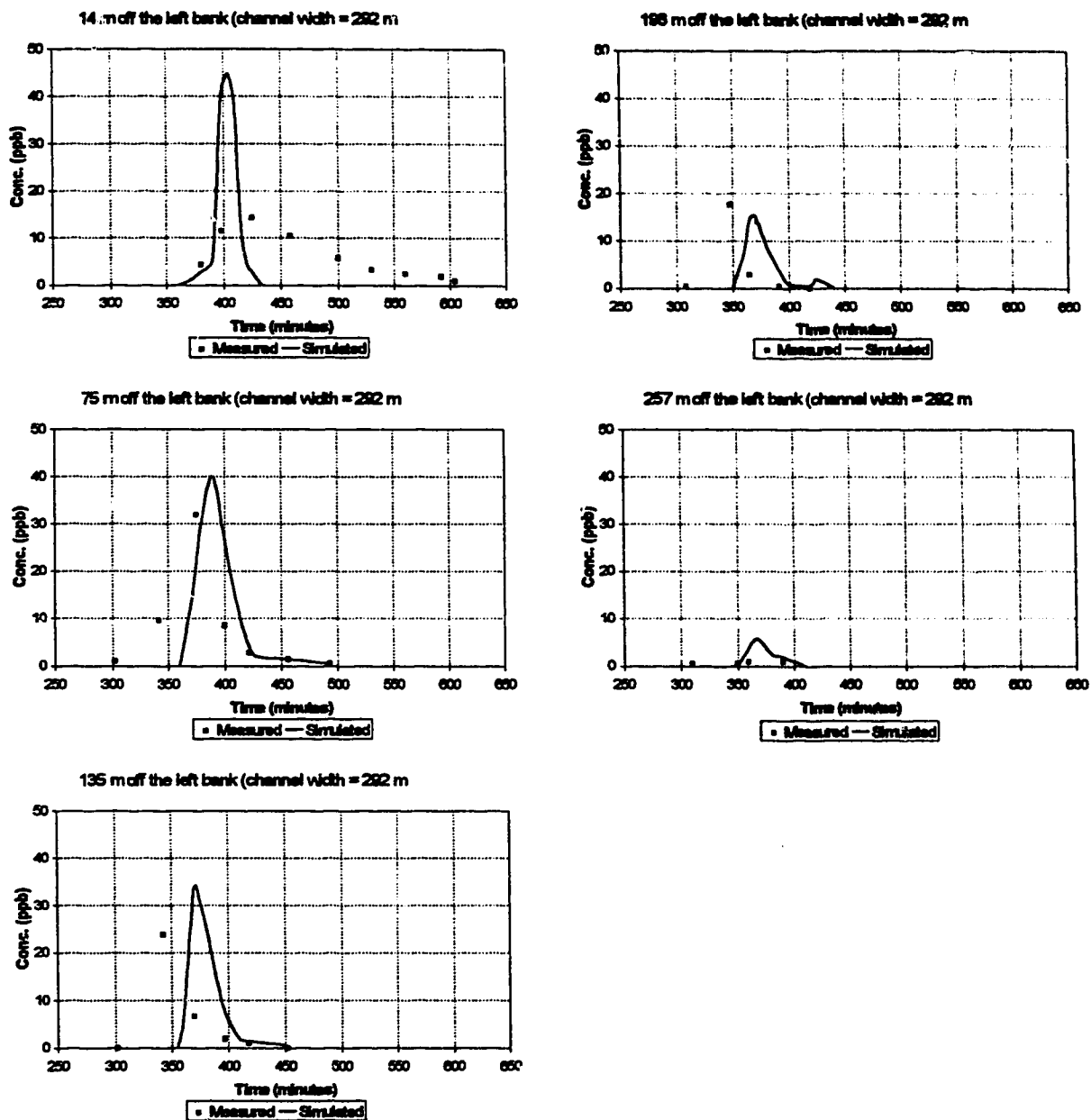


Figure 5.7 Simulated vs. observed results, Athabasca River below Fort McMurray, ice-covered, $x = 11.8$ km - modified from Beltaos (1978).

5.4.2 North Saskatchewan River downstream of Edmonton

5.4.2.1 Background

In October 1977 the Alberta Research Council (ARC) conducted a slug injection tracer test on the North Saskatchewan River downstream of Edmonton. The results of this tracer study, and an analytical analysis of the transverse mixing characteristics of this reach of the North Saskatchewan River, were reported by Beltaos and Anderson (1979). The study reach was approximately 75 km long and was characterized by eight cross-section surveyed at the time of the test. Tracer concentrations vs. time were measured at several transverse locations across four of the cross sections and presented in the report.

The ARC analysis of the concentration vs. time data used the dosage² concept and the method of moments to determine the transverse mixing coefficient. This approach is equivalent to the analysis procedure that would be used for a steady state tracer test. The authors noted that a true one-dimensional state of transient mixing had not been established within the study reach. However, they reported a one-dimensional approach could be used to predict concentrations in the lower portion of the reach to within a factor of two. No attempt was made to model the two-dimensional transient mixing in the upper portion of the reach. The work presented here will deal with the upper 50 km of the reach in the two-dimensional mixing zone.

5.4.2.2 Hydrometric data

An initial attempt to model the mixing in the upper portion of the reach using only the hydrometric data presented in the ARC report achieved limited success. The poor results can largely be attributed to a lack of sufficient cross section information required to adequately define the transverse and longitudinal variations in local depth and velocity.

Additional cross-section information for the upper portion of the study reach was obtained from the River Engineering Branch of Alberta Environmental Protection (AEP).

² The dosage concept is explained in Appendix E.

Approximately forty additional cross sections were available from flood plain and river ice studies conducted since the ARC tracer test. The AEP cross sections were all tied to geodetic elevations and their longitudinal position was specified in distance along the river from the Alberta Saskatchewan border. Prominent locations such as bridges and major tributaries aided the process of longitudinal alignment of the AEP and ARC sections. A plan view of the study reach and a number of the cross-section locations are shown in Figure 5.8.

A much larger effort was required to align the sections in regard to elevation. Unfortunately, the original ARC sections had not been tied to geodetic elevation. In order to use the additional AEP cross sections the geodetic water surface elevation had to be estimated at each section for the date of the tracer test (October 17, 1977). The first step was to attempt to match the transverse bed profiles at several locations common to the ARC and AEP surveys. The water surface at other AEP locations could then be estimated using the slope of the water surface through the reach.

A survey of the water surface slope through the reach was not conducted during the ARC study. The ARC analysis relied upon average slope information presented by Kellerhals et al. (1972). Attempts to project this average slope information through the AEP cross sections yielded unreasonable depths at many locations. Fortunately AEP had conducted a slope survey through the reach in 1990 at a flow close to that which was measured during the tracer test ($242 \text{ m}^3/\text{s}$ compared to $142 \text{ m}^3/\text{s}$)³. This slope information and the transverse bed profile matching procedure at the common sections was used to estimate the water surface elevation at each section. This method is not precise and several adjustments were necessary to obtain reasonable agreement between tracer time of travel and mean cross section velocities. The estimated water surface elevation and the longitudinal location of each cross section is presented in Table 5.8. A plot of the estimated water surface elevations and a portion of the AEP slope survey is shown in Figure 5.9.

³ Kellerhals et al. (1972) list the 2 year flood discharge as $1190 \text{ m}^3/\text{s}$.

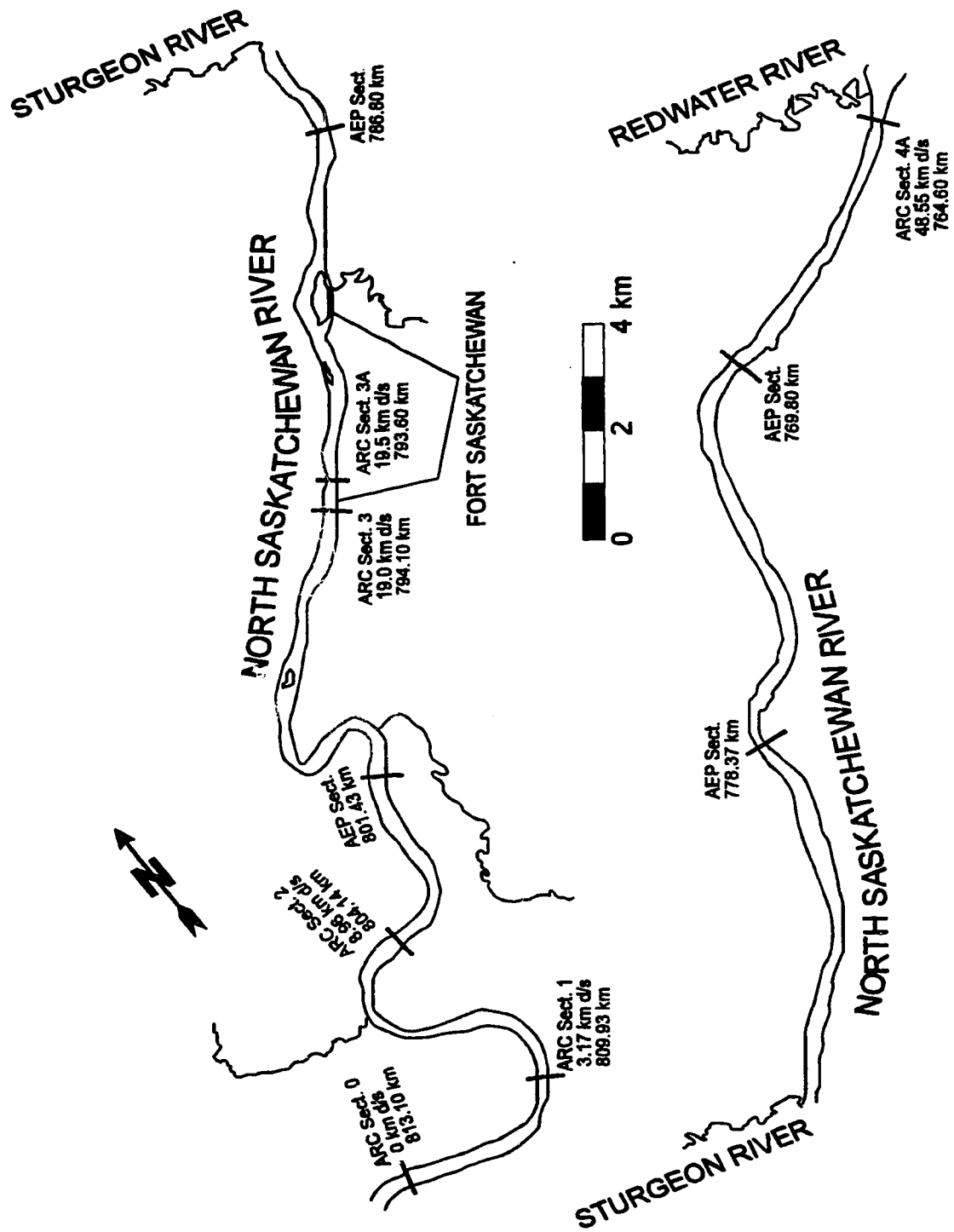


Figure 5.8 Plan view of the North Saskatchewan study reach.

Table 5.8 North Saskatchewan River tracer test estimated water surface elevations.

Location (km)	Dist. from Injection (m)	Geodetic Water Level (m)	Description and Comments
815.80	-2700	-	AE Aug 14,1990 slope survey point
813.24	-140	607.58	AE Hec 2 Section
813.10	0	607.53	ARC Section 0, Injection Site
812.89	210	607.45	AE Hec 2 Section
812.54	560	607.32	AE Hec 2 Section
812.14	960	607.17	AE Hec 2 Section
811.81	1290	607.04	AE Hec 2 Section
811.40	1700	606.89	AE Hec 2 Section
811.08	2020	606.76	AE Hec 2 Section
810.69	2410	606.62	AE Hec 2 Section
810.37	2730	606.50	AE Hec 2 Section
809.93	3170	606.33	ARC Section 1, Sampling Site, AE Hec 2 Section, geodetic elevation selected by comparing sections
809.64	3460	606.22	AE Hec 2 Section
809.29	3810	606.08	AE Hec 2 Section
809.04	4060	605.98	AE Hec 2 Section
808.70	4400	605.85	AE Hec 2 Section
808.36	4740	605.71	AE Hec 2 Section
808.05	5050	605.59	AE Hec 2 Section
807.76	5340	605.48	AE Hec 2 Section
807.31	5790	605.30	AE Hec 2 Section
807.08	6020	-	AE Aug 14,1990 slope survey point
806.90	6200	605.14	AE Hec 2 Section
806.57	6530	605.01	AE Hec 2 Section
806.22	6880	604.87	AE Hec 2 Section
805.89	7210	604.74	AE Hec 2 Section
805.53	7570	604.60	AE Hec 2 Section
805.12	7980	604.44	AE Hec 2 Section
804.66	8440	604.25	AE Hec 2 Section
804.21	8890	604.08	AE Hec 2 Section
804.14	8960	604.05	ARC Section 2 geodetic elevation selected by comparing sections
803.90	9200	603.94	AE Hec 2 Section
803.56	9540	603.79	AE Hec 2 Section
803.20	9900	603.63	AE Hec 2 Section
802.10	11000	603.14	AE Hec 2 Section
801.82	11280	603.02	AE Hec 2 Section
801.43	11670	602.84	AE Hec 2 Section
798.15	14950	601.39	AE Hec 2 Section
795.55	17550	600.23	AE Hec 2 Section, AE Aug 14,1990 slope survey point
794.10	19000	599.68	ARC Section 3
793.60	19500	599.49	ARC Section 3A, Sampling Site
791.95	21150	598.87	AE Hec 2 Section, AE Aug 14,1990 slope survey point
789.45	23650	597.75	AE Hec 2 Section
786.80	26300	596.56	AE Hec 2 Section, AE Aug 14,1990 slope survey point
783.25	29850	595.10	AE Hec 2 Section
781.47	31630	594.37	AE Hec 2 Section
778.37	34730	593.09	AE Hec 2 Section, AE Aug 14,1990 slope survey point
769.80	43300	589.41	AE Hec 2 Section, AE Aug 14,1990 slope survey point
764.60	48500	588.39	ARC Section 4, AE Hec 2 Section, geodetic elevation selected by comparing sections
764.55	48550	588.35	ARC Section 4A, Sampling Site
761.40	51700	585.51	AE Hec 2 Section, AE Aug 14,1990 slope survey point

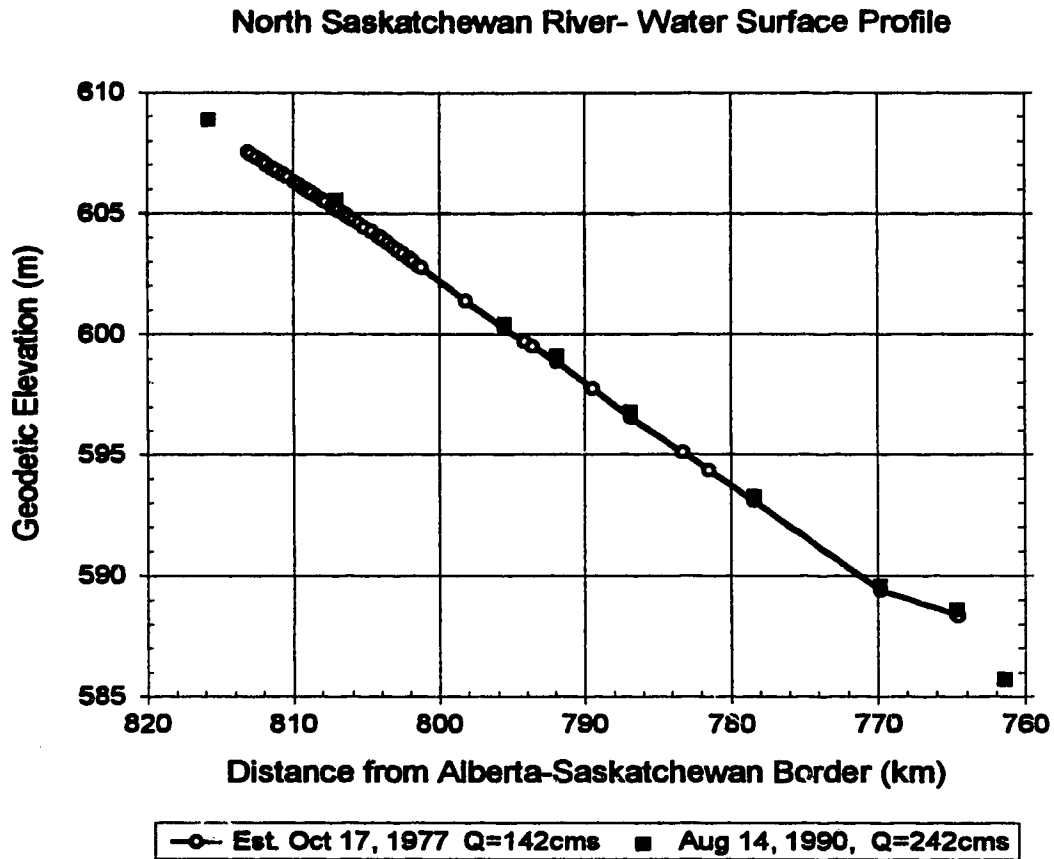


Figure 5.9 North Saskatchewan River water surface profile.

Once the water surface elevation at each section was set the mean depth and velocity could be determined. The local velocities and flow distribution were then estimated using a resistance equation relationship. A tabulation of these calculations, a cross section plot, and the estimated flow distribution for each section are presented in Appendix D. An example tabulation and cross section plot is shown in Figure 5.10.

X-SECTION N. Sask. River, 812.14 km

DATE October 18, 1977

DISCHARGE m^3/s 142.00

WIDTH m 234.93

MEAN DEPTH m 0.89

AREA m^2 209.84

MEAN VELOCITY m/s 0.677

HEC2 Section from Alberta Env.

Est. Water Surface Elev. 607.17

LB 607.81 607.17

RB 842.74 607.17

Sta. m	Elev. m		h m	w/W	u m/s	dq est. m^3	norm. q/Q	Area adjusted u m^2	
607.81	607.17	607.81	0.00	0.000	0.000	0.00	0.00000	0.0	0.000
611.13	608.55	611.13	0.62	0.014	0.528	0.27	0.00192	1.0	0.533
676.66	606.18	676.66	0.99	0.293	0.722	32.78	0.23508	53.5	0.730
751.34	606.46	751.34	0.71	0.611	0.578	41.04	0.52698	116.6	0.584
816.87	605.63	816.87	1.54	0.890	0.971	56.86	0.93142	190.0	0.981
842.74	607.17	842.74	0.00	1.000	0.000	9.64	1.00000	209.8	0.000
Est. Total						140.59			

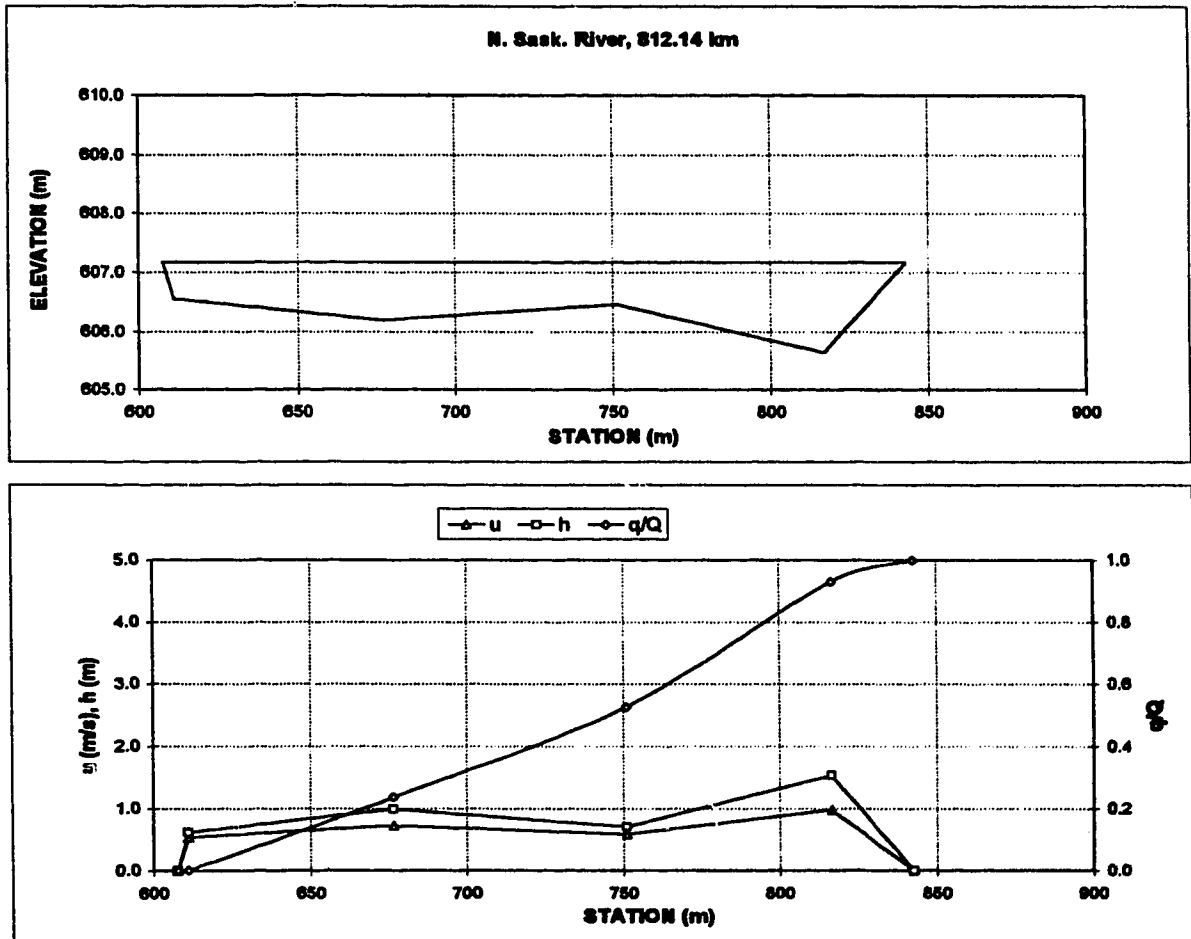


Figure 5.10 Example cross section and flow distribution plot.

5.4.2.3 Model input and results

Beltaos and Anderson (1979) reported that 4.54 L of 20% Rhodamine WT (by weight) was injected into the river about 30 m from the right bank at ARC Section 0 (321.19 km). This corresponds to a total tracer mass of 1.081 kg. Presumably the precise location of the injection was not measured because the study was only intended to determine the transverse mixing coefficient using the method of moments procedure, and to conduct a one dimensional mixing analysis. Tracer samples were collected at ARC Sections 1, 2, 3A, 4A and 5. The sampling schedule at Section 1 was not completed due to an equipment malfunction and was not reported. The dosage distribution measured at each of the sampled sections is shown in Figure 5.11 and the calculated mass recoveries are given in Table 5.9.

Table 5.9 North Saskatchewan River tracer mass recoveries.

Cross section (m) downstream	Mass Recovery (kg)	<u>Mass</u> Reported Mass In	<u>Mass</u> Assumed Mass In
8960	1.963	1.81	0.87
19550	1.211	1.12	0.54
48550	0.901	0.83	0.40

The mass recovery ratio indicated for ARC Section 2 in column two of Table 5.9 indicates there is a discrepancy between the recovered mass and the reported injected mass for the test (i.e. more mass has been recovered than the amount reported as injected). Typically the mass recovery at the initial section in a slug test is in the range of 80 to 100%. It is also known that the tracer was often supplied in 2.5 or 5.0 USGal. containers during the 1970's. With no means to check upon the actual mass injected it seems reasonable to assume that one 2.5 USGal. container was injected rather than the 4.54 L reported. This corresponds to an injected mass of 2.252 kg. Mass recovery ratios based upon this assumption are shown in the last column of Table 5.9. These figures are far more reasonable and all subsequent calculations have been based upon a total injected mass of 2.252 kg.

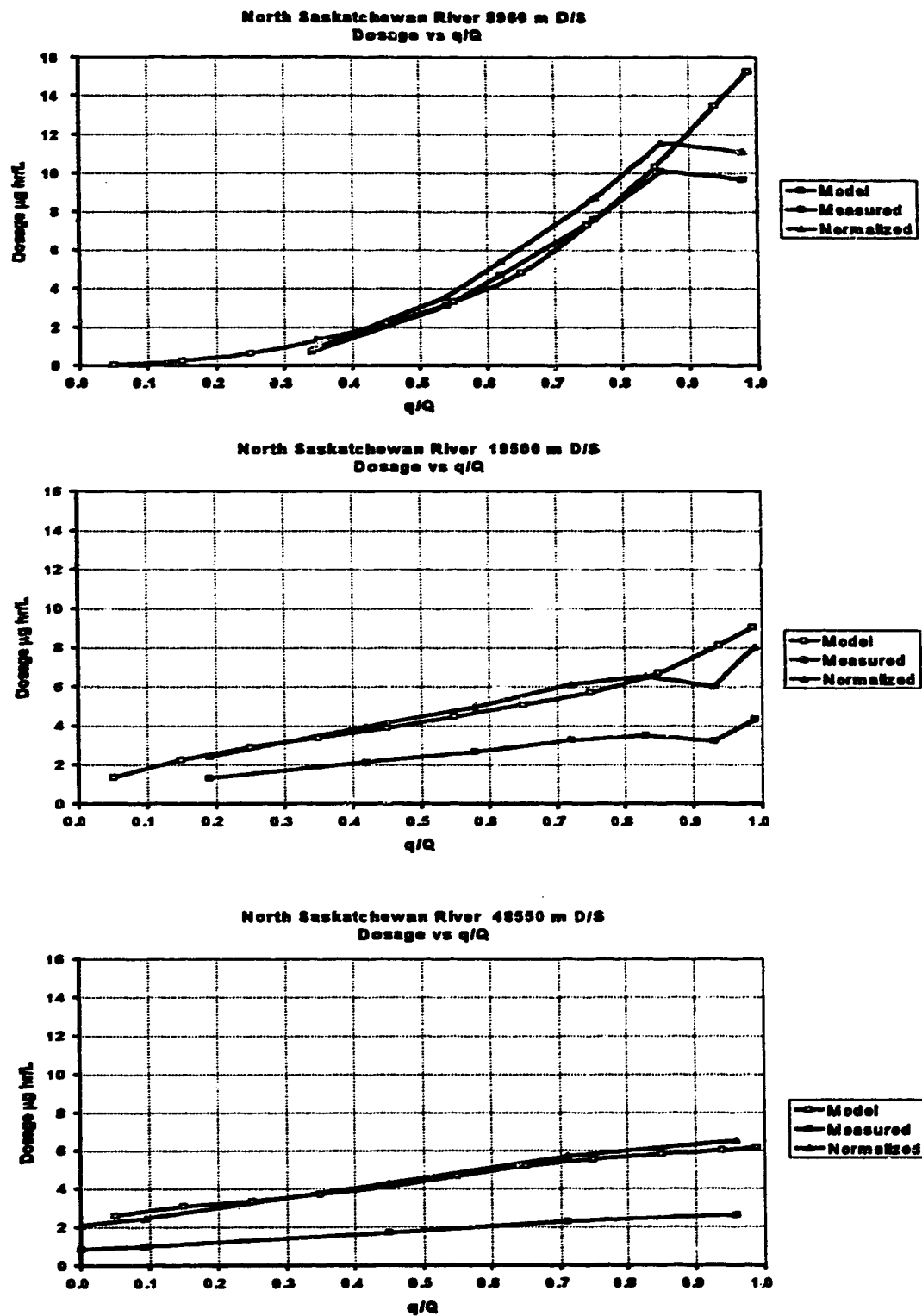


Figure 5.11 North Saskatchewan River dosage distributions, slug input to the model

The river channel was divided into eleven streamtubes with the following boundaries: $q/Q=0.100, 0.200, 0.300, 0.400, 0.500, 0.600, 0.700, 0.800, 0.900, 0.975,$ and 1.00 . A time step of 60 seconds was chosen on the basis of the criteria outlined previously. The injected mass was distributed in streamtube No. 10 (i.e. $q/Q=0.900$ to 0.975) over the initial time step to simulate a slug input. Values for the streamtube local depths, widths and slope, and β , the local dimensionless mixing coefficient, were assembled into the GRIDGEN input file with the aid of STRMTUBE. In general, cross section coverage was sufficient to allow linear interpolation of depths and widths between defined sections. However, at a few locations where linear interpolation was not deemed appropriate, the channel geometry of a single section was used to represent a portion of the reach.

Several computer simulations were conducted varying the magnitude of β . The β value was held constant within each subreach (i.e. between each sampled section) and transversely across the channel. Final values for β were selected by visual comparison of the model output to the normalized measured dosage curve and the normalized C-t curves at each sampled location. The dosage curves generated by the model for the selected β values are shown in Figure 5.11 together with the normalized measured dosage distribution at each sampling location. The C-t curves generated by the model for the selected β values are shown in Figure 5.12 to Figure 5.14 together with the normalized C-t distributions measured at each sampling location.

Comparison of the normalized and simulated dosage curves at each section indicates that there is very good agreement except in the near right bank region at the first measured section (8960 m). Problems in the near right bank region are also quite evident in the C-t plots at 8960 m. The simulated C-t curves in this region have peak concentrations several times that of the normalized measurements. In addition, the time base of the simulated curves in this region are much shorter than that of the measured curves. The simulations at 8960 m improve dramatically towards the centre of the channel. In this region there is good agreement between the peaks and the time base of the concentration waveforms.

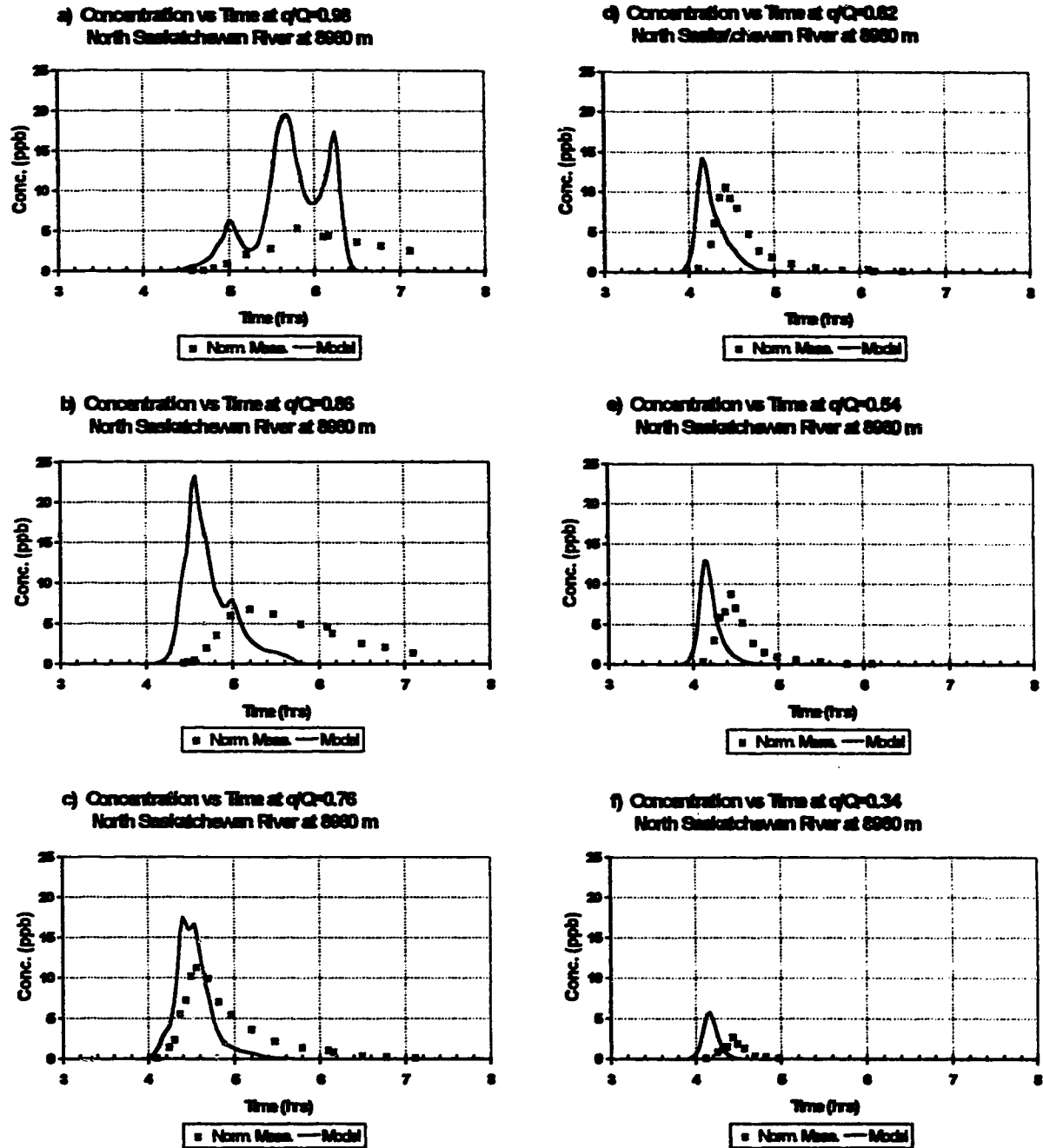


Figure 5.12 North Saskatchewan River, C-t curves at 8960 m, slug input to the model.

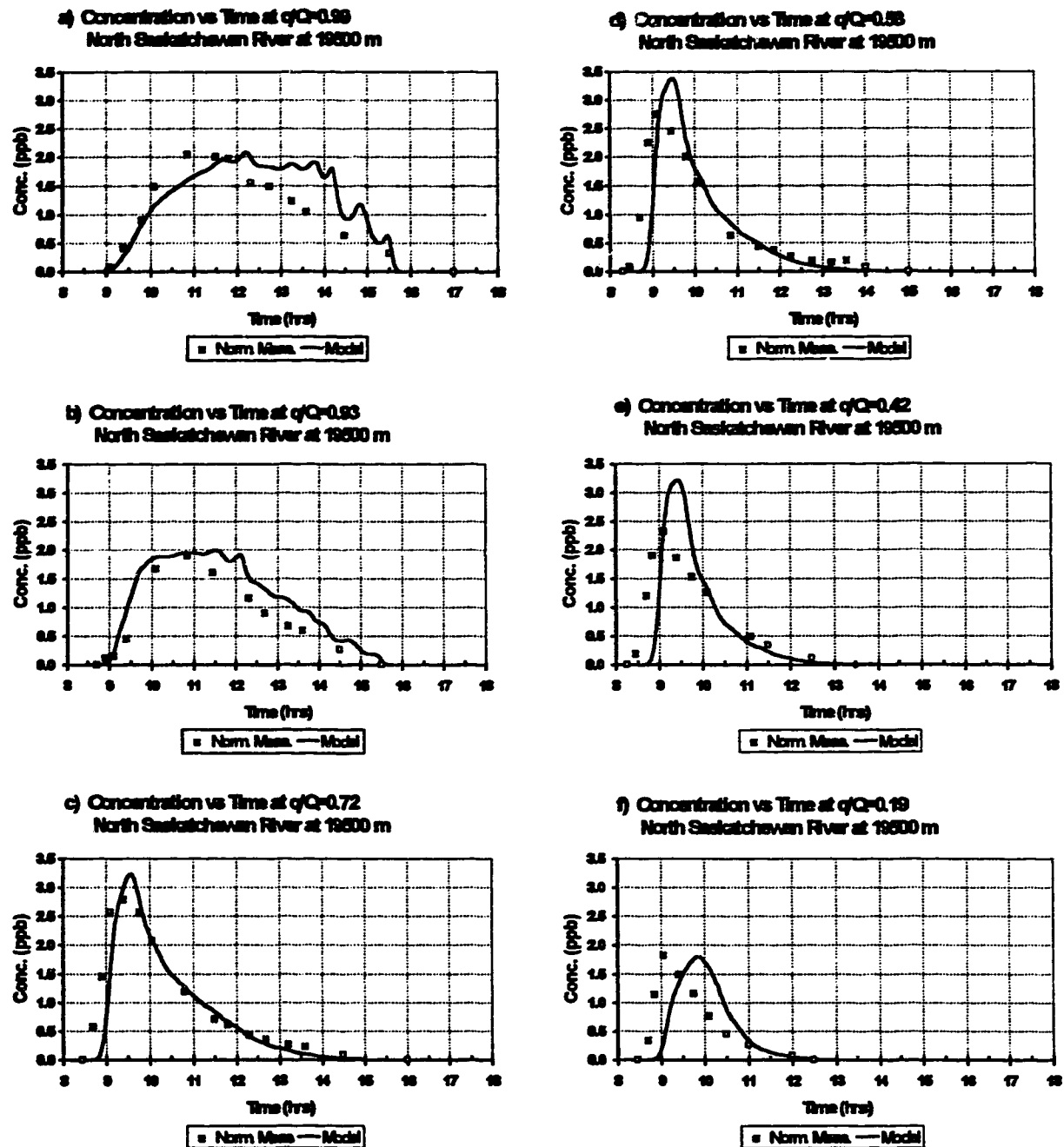


Figure 5.13 North Saskatchewan River, C-t curves at 19500 m, slug input to the model.

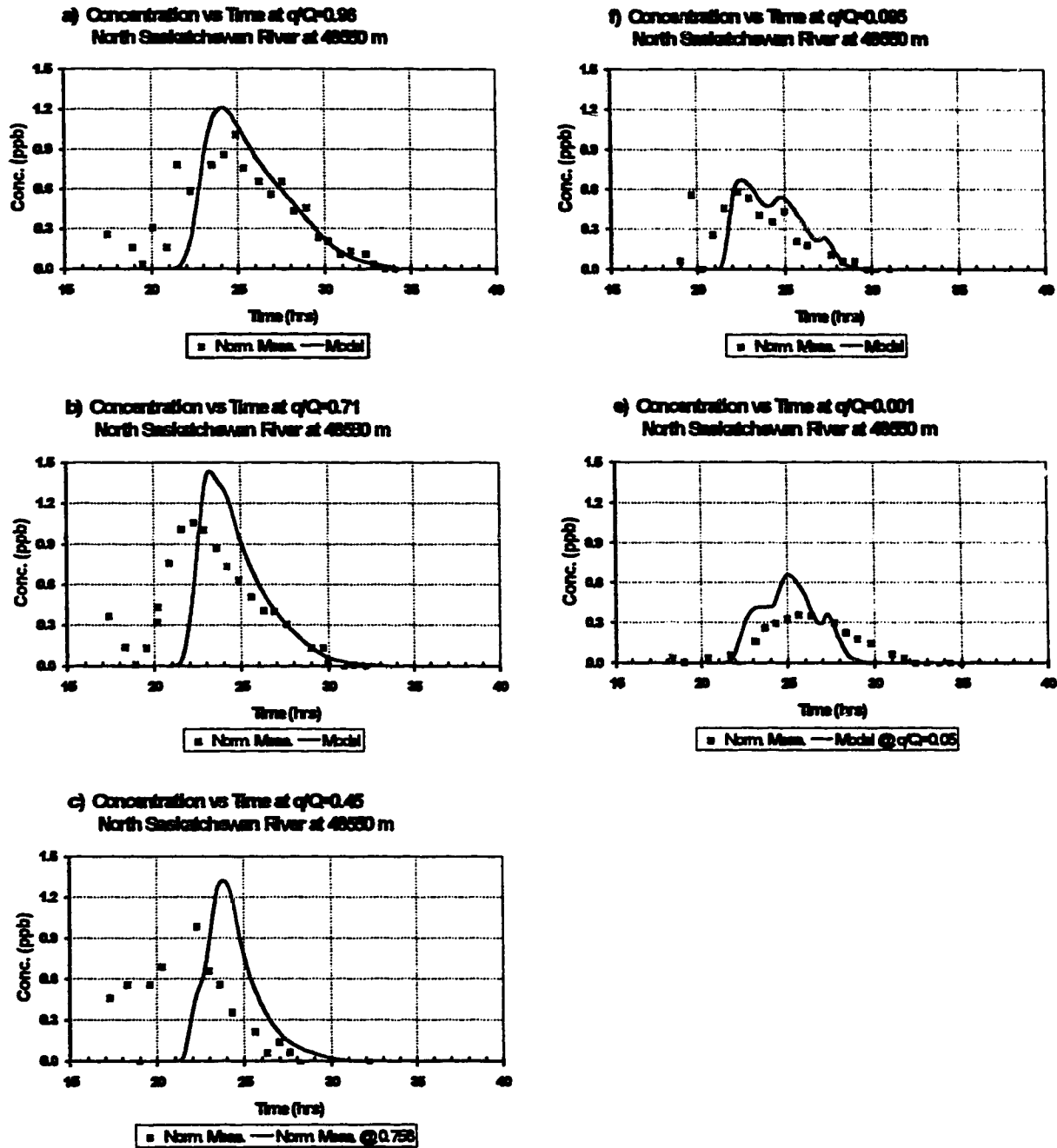


Figure 5.14 North Saskatchewan River, C-t curves at 48550 m, slug input to the model.

It is speculated that the discrepancy in the near right bank region is the result of dead zone effects, hence the extended time base and attenuated peak of the measured curves. As the simulation moves downstream the agreement between the simulated and measured C-t curves in the right bank region improves significantly. Presumably the dead zone effect must be localized between the injection point and the first sampling location. The C-t simulations at 19550 m are very good across the entire channel and those at 48550 m are reasonable.

The following factors may contribute to the poorer match at 48550 m:

1. Fewer cross sections were available in the subreach between 19550 and 48550 m. Therefore, the channel geometry and velocity distributions are not as well defined in this subreach as in the first two subreaches.
2. The concentration measurements at 48550 m are approaching the natural background levels. The scatter displayed by the measurements at this section is evidence of this effect. A small error in background concentration at 48550 m can have a very significant effect upon the peak normalized concentration.

At most locations there are also minor discrepancies between the measured and simulated elapsed time to the peak concentration. However, these discrepancies are small and generally less than 10%. This is well within the accuracy of streamflow measurements and the subsequent generation of the flow distributions at each cross section based upon these measurements.

Although the model can not directly simulate a near-shore dead zone effect, the effect can be crudely approximated by altering the input conditions. If the source is considered to be more dispersed and extended in time rather than an instantaneous point, the extended time base and attenuated peak can be better simulated. The model was rerun placing most of the input mass into streamtube 10 during the first time step, and a portion of the mass into streamtube 11 over a period of 48 minutes. The intention was to simulate the slow release of mass trapped within a near shore dead zone. The output dosage curves for this input condition are shown in Figure 5.15. The corresponding C-t curves are shown in Figure 5.16 to Figure 5.18.

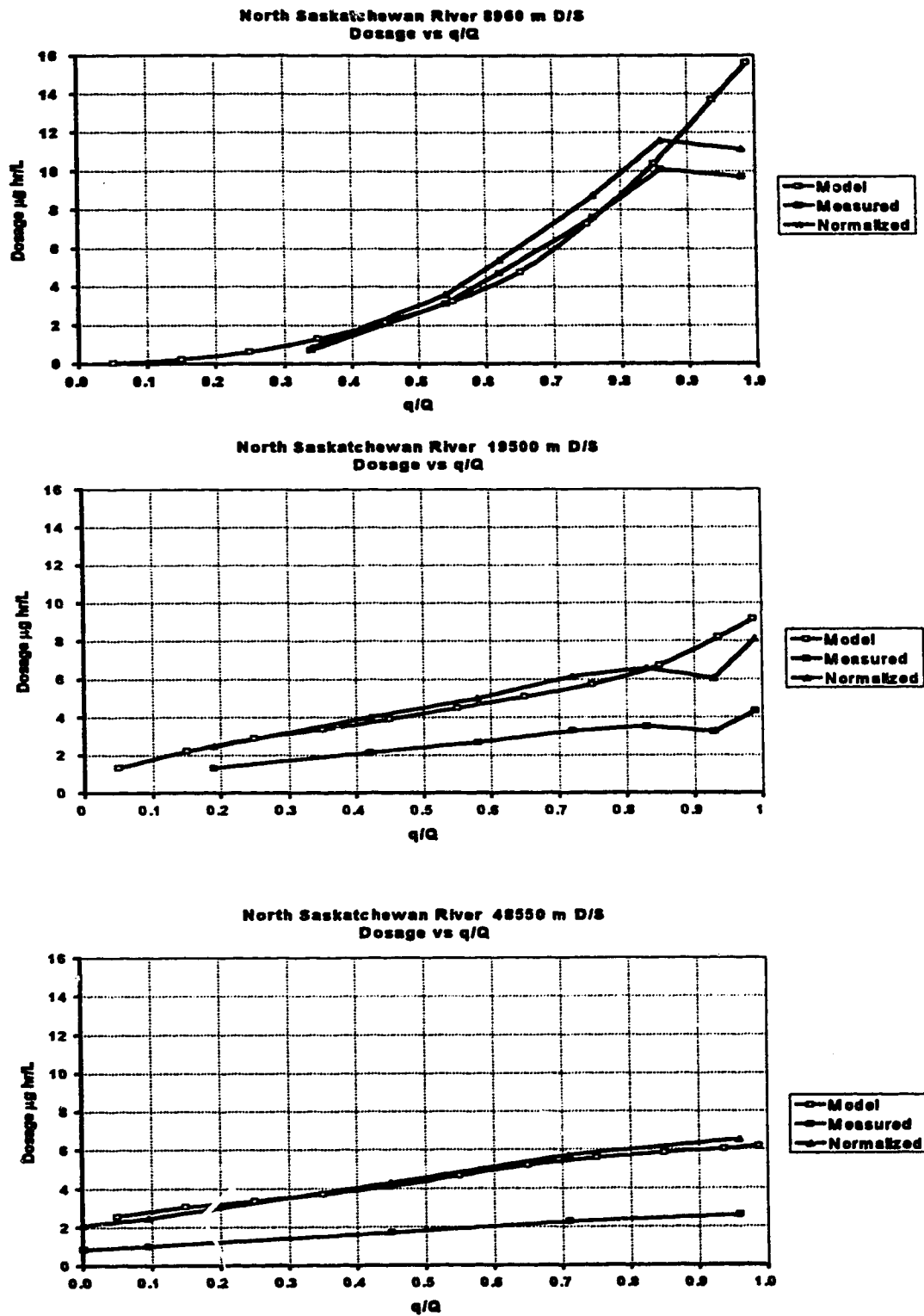


Figure 5.15 North Saskatchewan River dosage distributions, extended slug input to the model

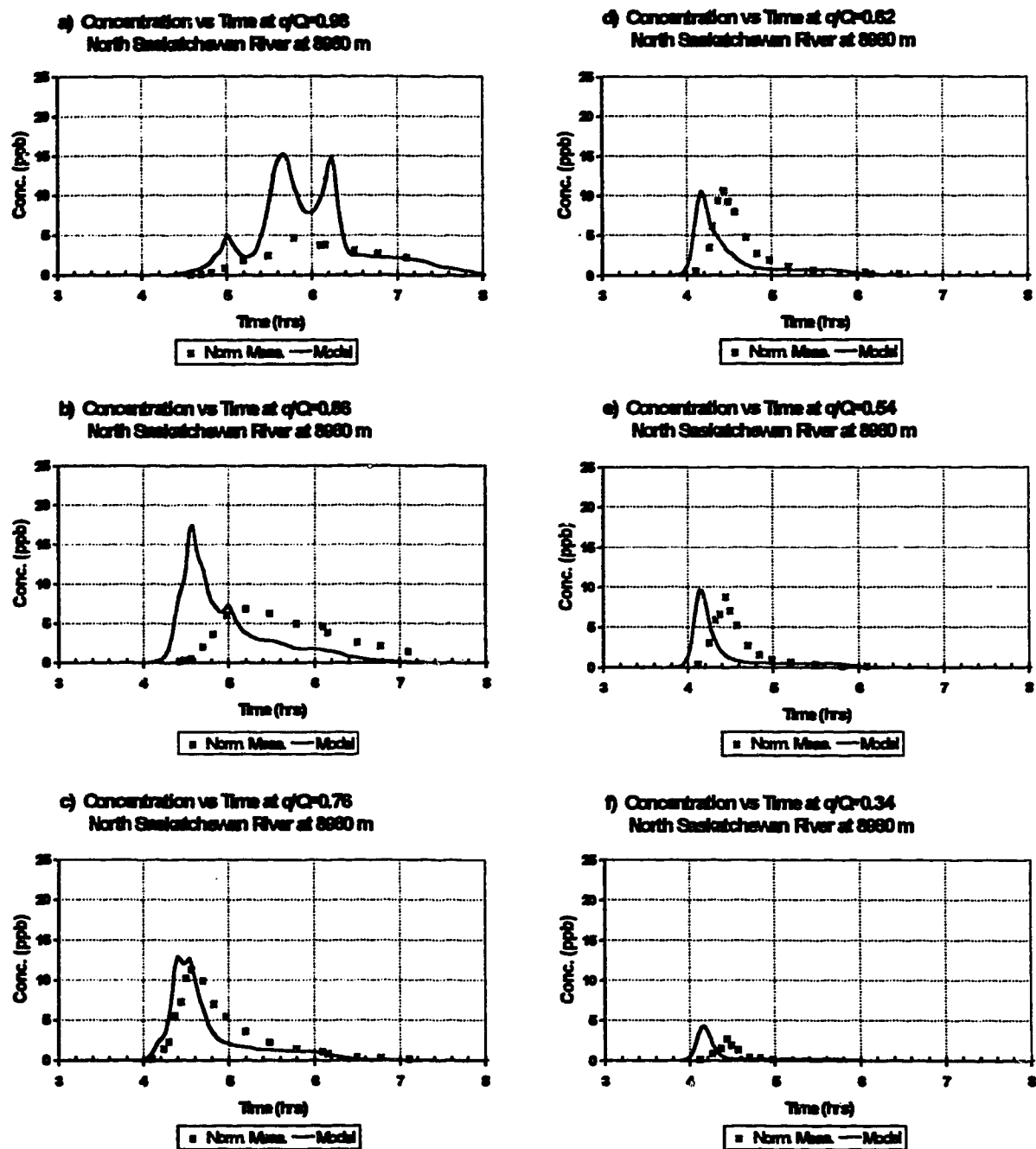


Figure 5.16 North Saskatchewan River, C-t curves at 8960 m, extended slug input to the model.

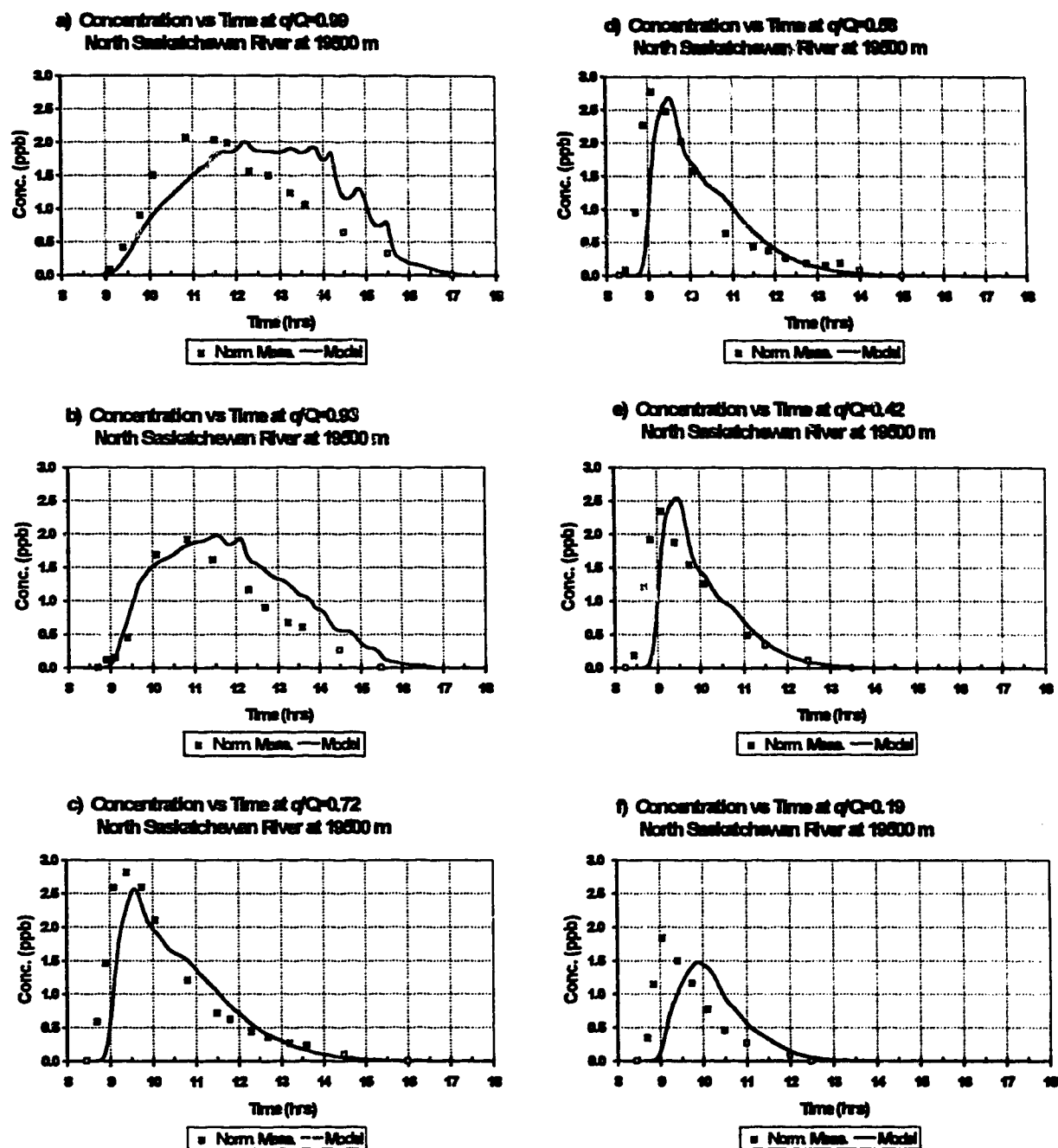


Figure 5.17 North Saskatchewan River, C-t curves at 19500 m, extended slug input to the model.

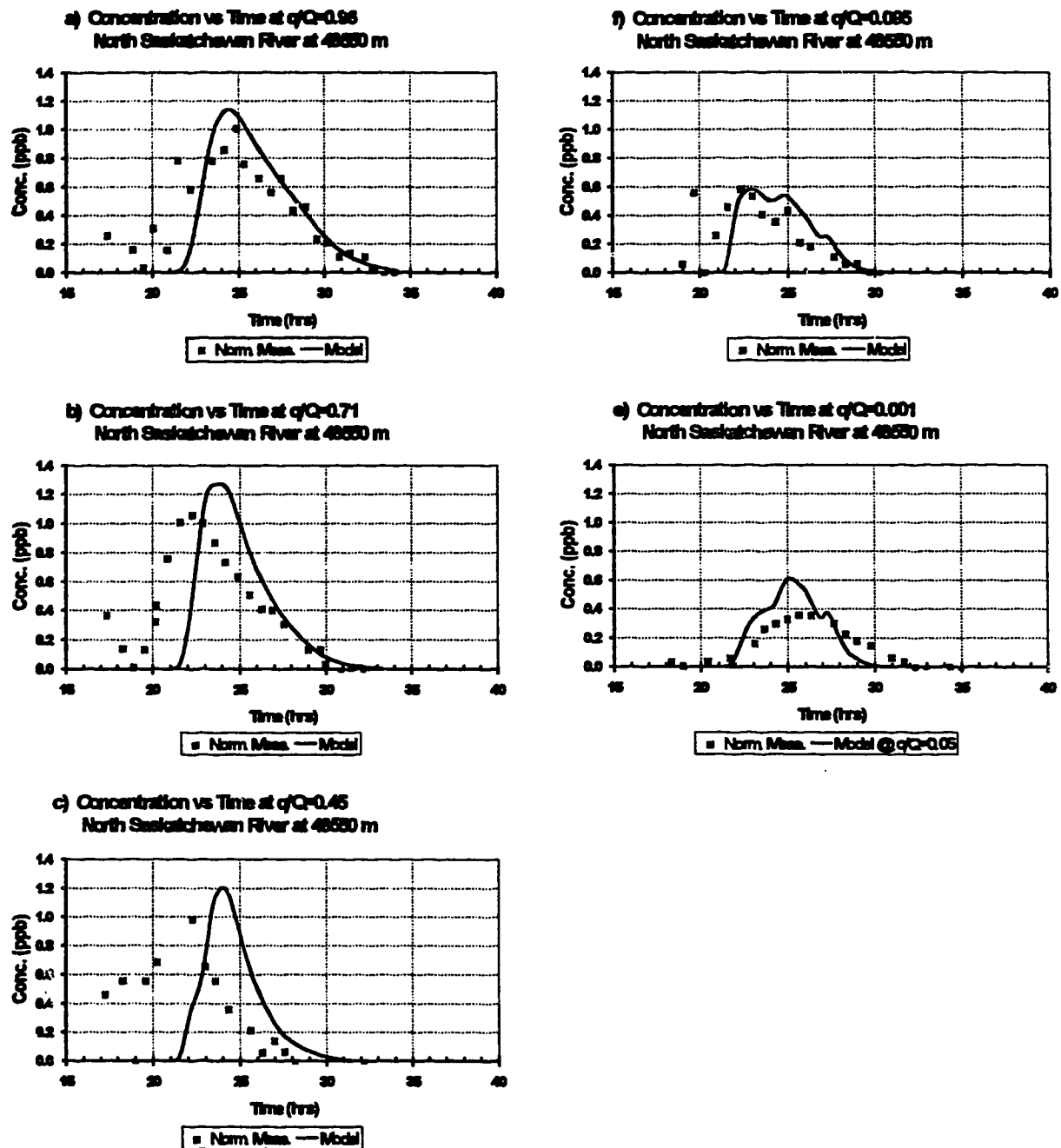


Figure 5.18 North Saskatchewan River, C-t curves at 48550 m, extended slug input to the model.

The modified input condition does not significantly affect the dosage curves. However the modified input condition does improve the C-t curves. At 8960 m the time base match is greatly improved in the near right bank region and the simulation peak concentration has been marginally reduced. The C-t curves toward the centre of the channel at 8960 m, and at the other two downstream sections are also improved. This demonstrates that the input file could be further manipulated to simulate the dead zone effect if more information was available on its location and the relative amount of mass trapped in the dead zone.

The dimensionless mixing coefficients used in the model are given in Table 5.10. Beltaos and Anderson's analysis of the transverse mixing was based upon moment calculations of the plume spread at the measured sections. Their analysis indicated a reach-averaged value of 0.173. They noted that enhanced transverse mixing was evident between Sections 2 and 3A and speculated that this occurred due to the two major bends located within this subreach. This trend is also evident in the numerical results as the value of β increases within this subreach.

Table 5.10 North Saskatchewan River, dimensionless transverse mixing coefficients used in the model.

Subreach	β
0 to 8,960 m	0.30
8,960 to 9,200 m	0.30 to 0.40 (linear increase)
9,200 to 19,500 m	0.400
19,500 to 21,150 m	0.40 to 0.30 (linear decrease)
21,150 to 48,550m	0.30

The question may be asked, why don't the dimensionless mixing coefficients determined using the modeling procedure more closely match the analytically determined average coefficient? One must consider the method by which the coefficients have been determined. In the analytical procedure the average diffusion factor is defined by:

$$D_z = \overline{\psi\beta}(UH^2)(U.H) \quad [113]$$

where U , H , and U_* are reach averaged parameters, $\bar{\Psi}$ is a reach-averaged shape factor and $\bar{\beta}$ is a reach-averaged dimensionless mixing coefficient. In the numerical method a local diffusion factor is calculated as:

$$d_z = \beta(uh^2)(u_*h) \quad [114]$$

where u , h and u_* are local parameters and β is a local dimensionless mixing coefficient.

The amount of plume spread is largely dependent upon the magnitude of the diffusion factor in the region where there is the most significant concentration gradient. In order to characterize the same amount of plume spreading the diffusion factor determined for this region should be equal by either method. In the analytical analysis the plume spread is plotted and the reach-averaged diffusion factor is calculated using the method of moments. $\bar{\beta}$ is then calculated using the reach-averaged depth, velocity and shape factor. These averaged parameters may poorly represent the region where the most significant mixing occurs.

In the numerical method, β is chosen to obtain a match between the output and measured dosage and C-t curves. The diffusion factor is calculated using this value of β and the appropriate local parameters. Given that the local and reach-averaged depths and velocities are similar in magnitude, a better comparison of results may be $\bar{\Psi}\bar{\beta}$ vs. β . The reach-averaged value of $\bar{\Psi}$ reported by Beltraos and Anderson (1979) is 1.73 giving a $\bar{\Psi}\bar{\beta}$ value of 0.30 compared to the numerical results of β in the range of 0.30 to 0.40. Therefore the results of the two procedures are quite comparable.

5.4.3 Peace River at Peace River

5.4.3.1 Background

In February 1993 the Alberta Research Council and Northwest Hydraulic Consultants Ltd. conducted a slug injection tracer study on the Peace River. The study was conducted for the Northern Rivers Basin Study (NRBS) which is a joint initiative of government agencies of Canada, Alberta and the Northwest Territories. The results of the study were presented in March 1994 (Northern Rivers Basin Study, 1994). The 185 km study reach passed through the town of Peace River and was characterized by eight cross-sections surveyed at the time of the test. Tracer concentrations vs. time were measured at several transverse locations across seven of the cross-sections and were presented in the report.

Similar to the ARC study of the North Saskatchewan River, one of the objectives of the NRBS work was to investigate the travel times and the one-dimensional longitudinal mixing characteristics of the Peace River. The NRBS study found that approximately 100 km of travel was required before complete transverse mixing of the tracer was achieved. The transverse mixing characteristics in the upper portion of the reach were also analysed in the NRBS study using dosage calculations and the method of moments procedure. The dosage distributions were then modelled using the analytical solutions developed by Yotsukura and Cobb (1972). No attempt was made to model the two-dimensional transient mixing in the upper portion of the reach. The work presented here focuses on the upper 43 km of the study reach within the two-dimensional mixing zone

5.4.3.2 Hydrometric data

Initial attempts to model the mixing in the upper portion of Peace River study reach, using only the cross-section data available in the NRBS report, proved disappointing. Similar to the North Saskatchewan River study, there was inadequate definition of the channel characteristics for this river reach as well. Fortunately a number of cross-sections were available in the study reach from the River Engineering Branch of

Alberta Environmental Protection (AEP). These AEP cross-sections were used to supplement the four NRBS cross sections documented in the upper portion of the reach.

A plan view of the reach extending from Shaftesbury Ferry to the Daishowa pulp mill is shown in Figure 5.19. Prominent features such as bridges and cairns were used to longitudinally align the AEP and NRBS cross-sections. All the cross-sections were referenced to geodetic elevation. The geodetic water surface of the NRBS sections were specified in the report for the date of the test. Therefore, the water level at each AEP section was estimated by linear interpolation between the NRBS sections. Information on ice cover below the piezometric water surface at the NRBS sections was used to estimate ice cover at the AEP sections.

The mean depth and velocity was determined at each AEP section and the local velocities and flow distribution were then estimated using a resistance relationship. The local velocities and the flow distribution had been measured at each NRBS section. The NRBS also prepared estimated flow distributions at each of their sections using a resistance relationship. Both distributions were presented in the report for comparison, but the synthesized distributions were subsequently used in the NRBS mixing analysis. A tabulation of the calculations for the AEP sections, section plots and flow distributions are presented in Appendix D. A tabulation of the characteristics of the NRBS sections, section plots and the measured flow distributions are also summarized in Appendix D.

5.4.3.3 Model input and results

In order to model the mixing in the upper portion of the NRBS study reach it was necessary to make a number of assumptions regarding the flow conditions under an ice cover. In addition, a number of minor irregularities were discovered in the NRBS report which had to be resolved. Details of these assumptions and the resolution of the irregularities in the report are given in Appendix F.

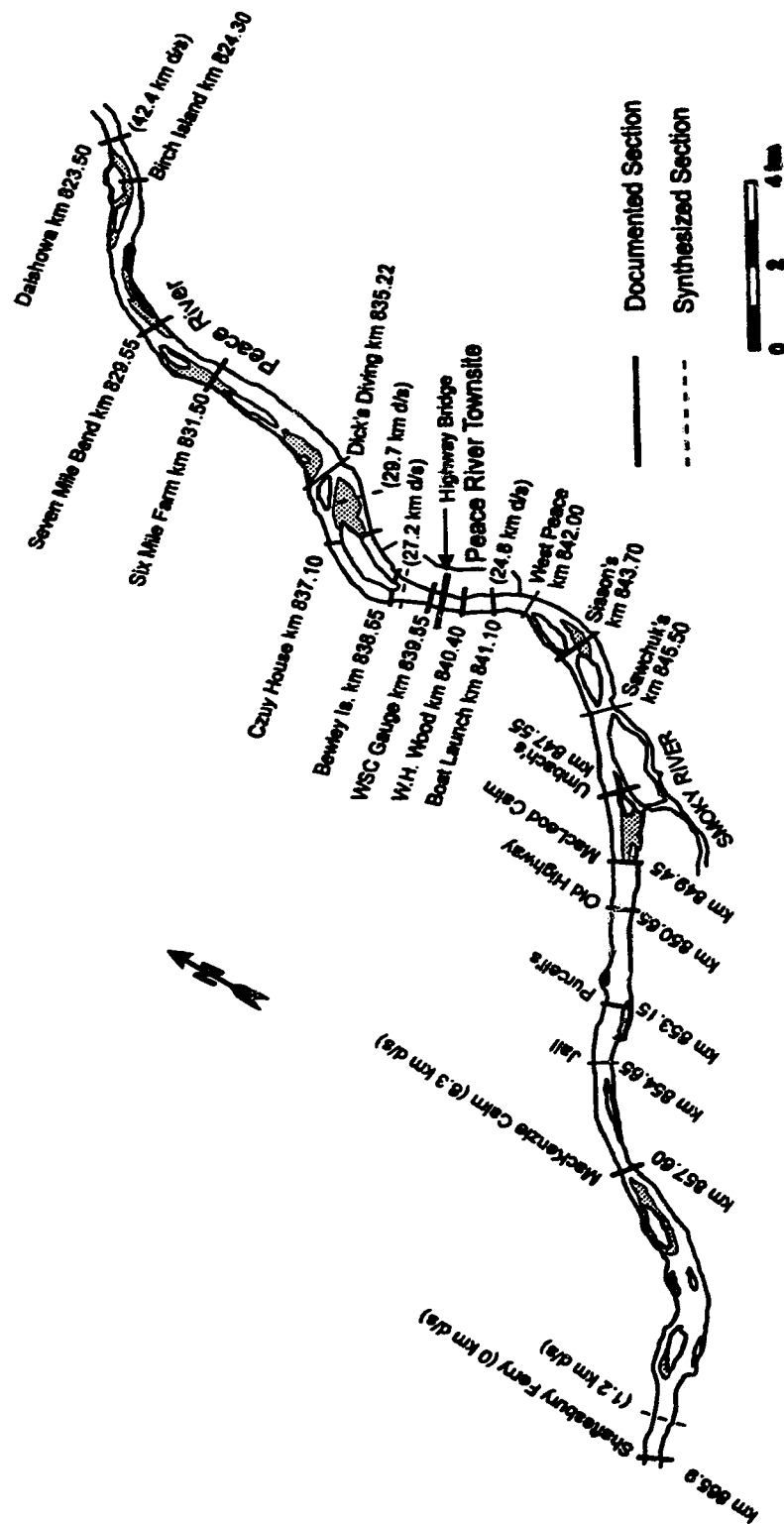


Figure 5.19 Plan of the Peace River study reach

The NRBS report states that 250 kg of 20% Rhodamine WT (by weight) was injected below the ice into the river at approximately mid-flow at the Shaftesbury Ferry cross-section. The tracer was injected through a pipe which was flushed afterwards with clean water to ensure all the dye had entered the flow. Although the report states that the tracer was injected relatively instantaneously it seems more reasonable to assume that some 200 L of liquid would require several minutes to be poured and then flushed through the pipe. For modelling purposes the tracer was assumed to be injected over a six minute interval.

The dosage distribution measured at each of the NRBS sections is shown in Figure 5.20 and the calculated mass recoveries are given in Table 5.11. It should be noted that these plots and mass recoveries are based upon the NRBS measured q/Q distributions, some revisions to the sample hole locations that were specified in the NRBS report (see Appendix F) and the author's integration of the NRBS C-t curves.

Table 5.11 Peace River tracer mass recoveries.

Cross-Section (m) downstream	Mass by Integration (kg)	<u>Mass Recovered</u> Specified Mass In
8300	40.02	0.800
24800	40.58	0.812
42400	38.75	0.775

The river channel was divided into 14 streamtubes with the following boundaries: $q/Q = 0.10, 0.20, 0.30, 0.40, 0.50, 0.55, 0.60, 0.65, 0.70, 0.75, 0.80, 0.90$ and 1.00 . A time step of 60 seconds was chosen on the basis of the criteria outlined previously. The injected mass was distributed in streamtube No. 8 (i.e. 0.55 to 0.60) over the initial six time steps (i.e. six minutes) to simulate an extended slug input. This location is at approximately mid flow as specified in the NRBS report and corresponds to the transverse location of the peak concentration measured at the first sampled section. The streamtube geometric parameters and initial estimates of β were then assembled into the input parameter file for GRIDGEN.

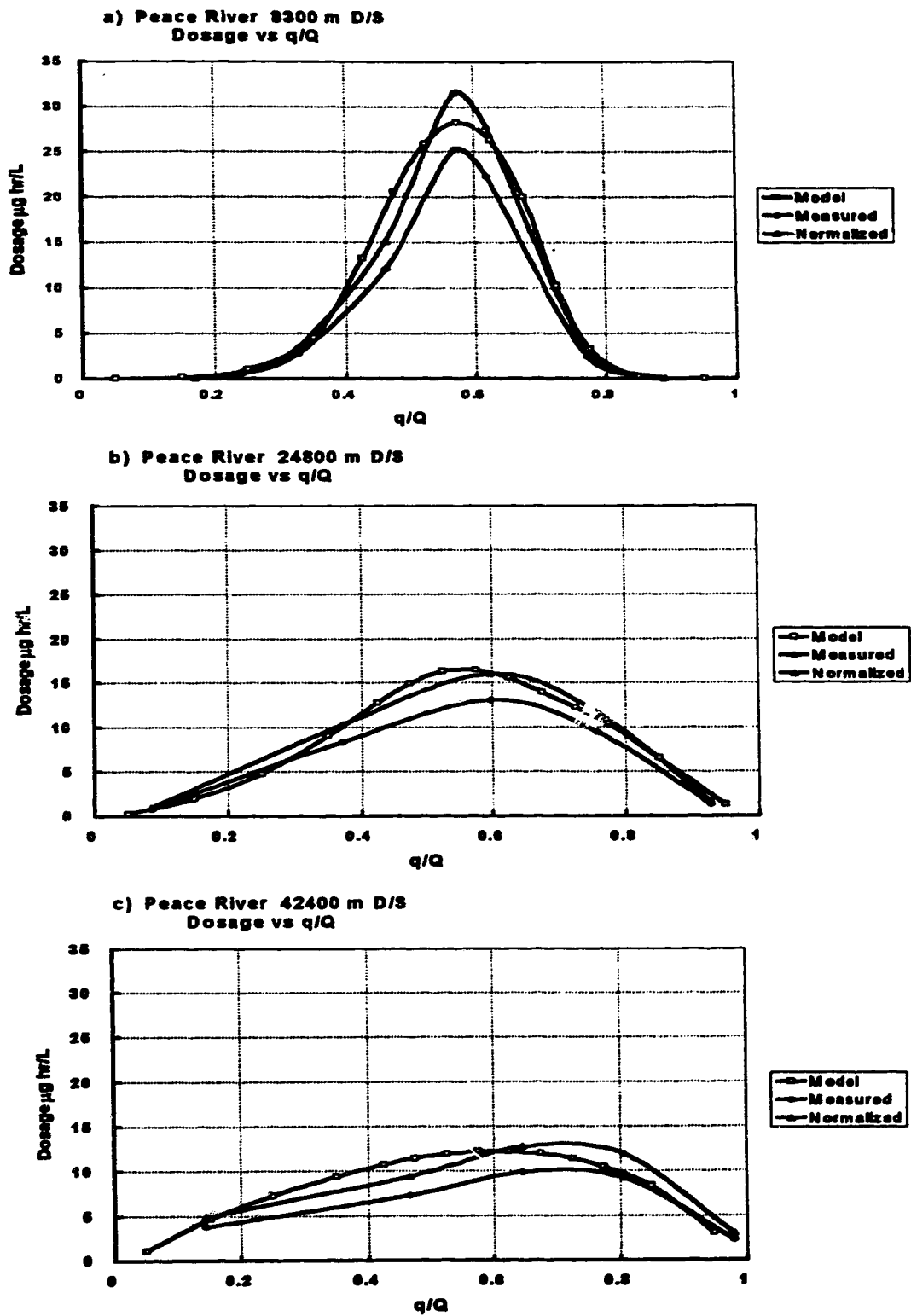


Figure 5.20 Peace River dosage distributions, extended slug input

Initial model runs poorly matched the time of travel indicated by the measured tracer curves (travel times for the measured data were much shorter than would be predicted by the cross section geometries and velocities). This difficulty was also reported by NRBS. They noted the measured times of travel were 40 to 60% less than what would be predicted on the basis of mean channel velocities. NRBS speculated the discrepancy could be due to frazil ice blockage of the near-shore regions of the channel, and in effect reducing the channel area⁴. They repeated their calculations with satisfactory results using an 'effective channel' representing 90% of the original flow distribution curves at each section and approximately 70% of the channel width. A different approach was used to overcome this difficulty in the present study.

In the first subreach there were no AEP cross sections available to supplement the NRBS sections located at the upstream and downstream boundaries. Therefore the channel definition was poor. In order to better represent the channel in this subreach an intermediate section was synthesized as a mirror image of one of the boundary cross sections. In the two remaining subreaches, assumptions were made regarding portions of the river channel that were likely to be cut off by surface ice cover and/or frazil ice accumulation. These assumptions are outlined in Appendix F. The assumptions were also discussed with an AEP representative who regularly observes ice conditions in the Peace River area (Fonstad, 1995).

Several computer simulations were run varying the magnitude of β . As for the North Saskatchewan River simulation, β was held constant in each subreach (i.e. between each sampled section) and varied transversely across the channel. Final values for β were selected by visual comparison of the model output to the normalized measured dosages and the normalized measured C-t distributions at each sampling location. The normalized measured C-t curves and those generated by the model are shown in Figure 5.21 to Figure 5.23. The dosage curves generated by the model are shown in Figure 5.20.

⁴ Frazil ice occurrence and potential effects upon the mixing within the study reach are described in detail in the NRBS report and therefore have not been repeated here.

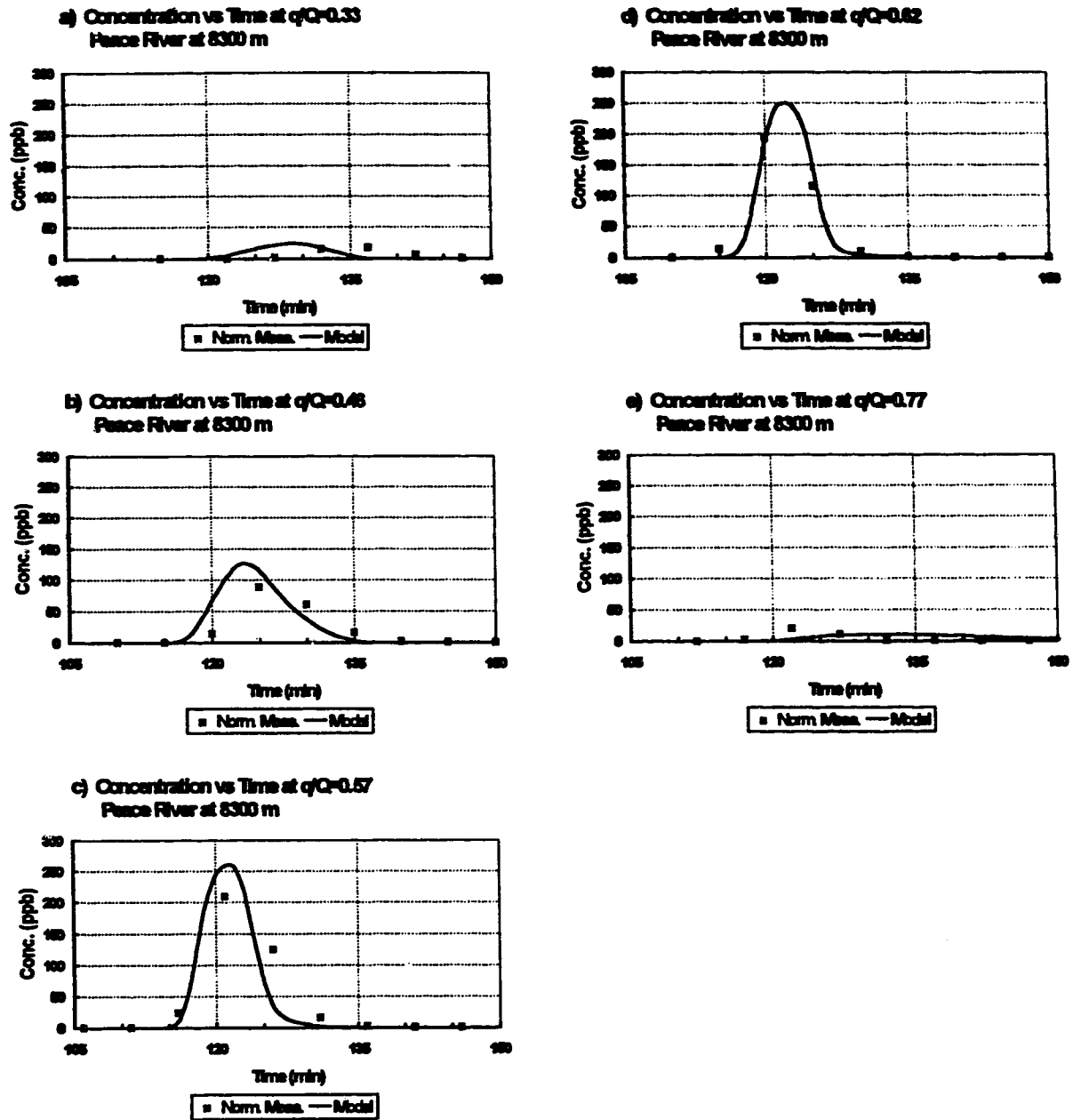


Figure 5.21 Peace River, C-t curves at 8300 m, extended slug input to the model.

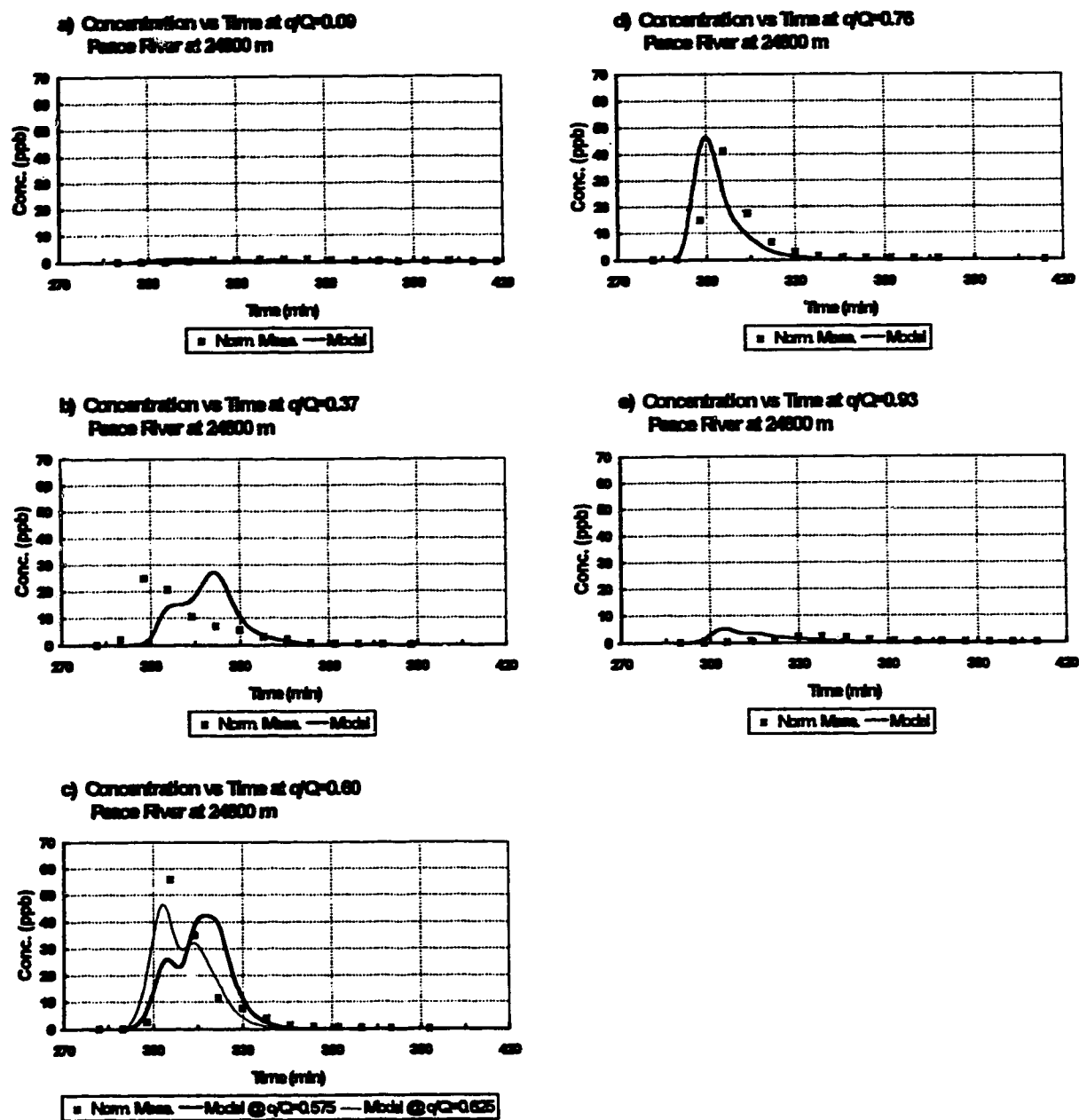


Figure 5.22 Peace River, C-t curves at 24800 m, extended slug input to the model.

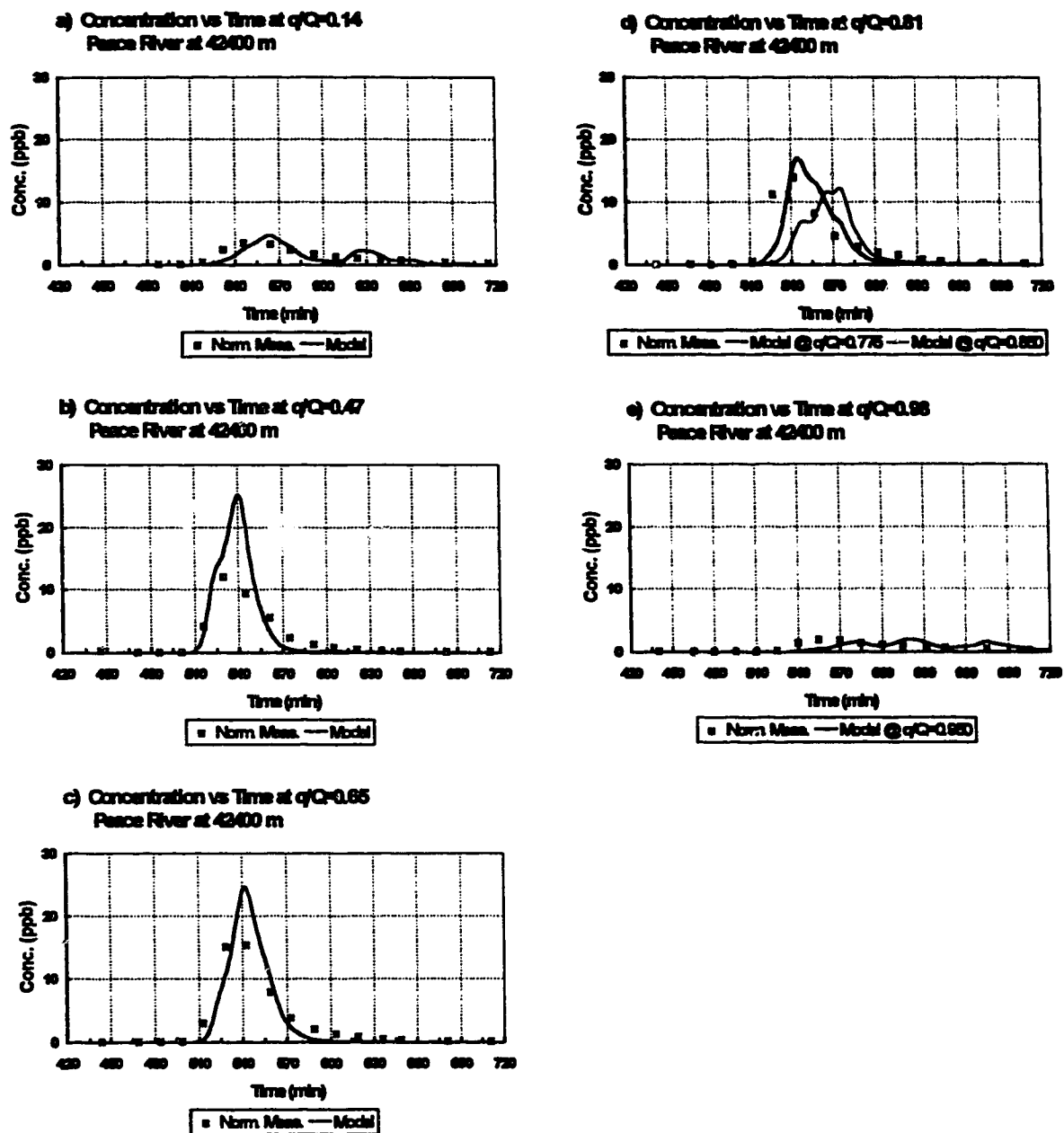


Figure 5.23 Peace River, C-t curves at 42400 m, extended slug input to the model.

Overall the match between the normalized and simulated dosage curves is very good with no major differences. The match between the normalized and simulated C-t curves is not as good as for the dosage curves but overall is quite reasonable. In general there is good agreement between the time bases of the modelled and measured waveforms except in the near-bank regions. This inaccuracy is likely the result of poor streamtube characterization or dead zone effects in these regions due to frazil ice accumulation. However, because this was a central injection, the concentrations are small in this region and therefore the time base shift near the banks is of little consequence. Some over-estimation of the peak concentrations in the central portion of the channel is also evident. This may simply be the result of poor channel definition in the first subreach as discussed above. This initial error is then carried along as the simulation progresses downstream.

It should be noted that the majority of the model output curves presented here represent interpolated values between streamtube centres. Interpolation is necessary because the actual model output is a series of average concentrations within each streamtube. In certain cases where adjacent waveforms have a distinctly different shape it is not appropriate to interpolate between the two. In such cases the two adjacent streamtube average concentrations are plotted (for example see Figure 5.22 c and Figure 5.23 d)).

The dimensionless transverse mixing coefficients used in the model are given in Table 5.12. Also shown in Table 5.12 are the subreach-averaged dimensionless mixing coefficients, channel shape factors and diffusion factors reported by the NRBS. The NRBS analysis of the transverse mixing used the same analytical approach as used by Beltaos and Anderson (1979) but reported on each increment of plume spread rather than one overall reach average.

Table 5.12 Peace River, dimensionless transverse mixing coefficients and shape factors.

Subreach	Numerical Model (local value) β	Analytical Model (subreach avg.) ¹ $\bar{\beta}$	Diffusion Factor m^2/s^2 D_z	Shape Factor (subreach avg.) $\bar{\psi}$
0 to-8.3 km	0.03	0.051	2.49	2.40
8.3 to 24.8 km	0.15	0.053	1.84	2.95
24.8 to 42.4 km	0.18	0.044	1.25	3.05

¹ based upon effective width as defined in the NRBS report

At first glance it again appears that there is poor agreement between the analytical and the numerical approach to determining the dimensionless transverse mixing coefficients. However, the argument presented previously in conjunction with Equation [113] and Equation [114] must be considered (i.e. that the diffusion factor is the unifying connection between the two approaches).

Between the injection point and 8300 m the plume occupies only a small proportion of the channel. For example, at 8300 m the majority of the tracer is contained between $q/Q=0.40$ to 0.70 . Using the geometric parameters and the dimensionless transverse mixing coefficient input into to the model it is possible to calculate the diffusion factor which is applicable to the central region of the channel. The results of these calculations for the four central streamtubes, between 0 and 8300 m, are shown in Table 5.13. The overall average diffusion factor of 2.62 for this region compares very well with the value of 2.49 determined by the analytical procedure. Downstream of 8300 m the plume fills most of the channel, therefore the product $\bar{\psi}\bar{\beta}$ from the analytical analysis should be reasonably comparable to β from the numerical approach. This comparison is shown in Table 5.14.

Table 5.13 Peace River , initial subreach diffusion factor calculations.

Distance (m)	Diffusion Factor d_z (m^2/s)			
	Tube 6 $q/Q = 0.45 - 0.50$	Tube 7 $q/Q = 0.50 - 0.55$	Tube 8 $q/Q = 0.55 - 0.60$	Tube 9 $q/Q = 0.65 - 0.70$
0	1.57	1.59	1.52	1.33
1200	2.76	3.46	2.51	2.07
8300	2.76	3.46	2.51	2.07
Weighted Avg.	2.67	3.33	2.45	2.02
Overall Avg.	2.62			

Table 5.14 Peace River, dimensionless transverse mixing parameters.

Subreach	Numerical Model (local values) β	Analytical Model (subreach average) ¹ $\overline{\psi\beta}$
8300 - 24800 m	0.15	0.16
24800 m - 42400 m	0.18	0.13

¹ based upon effective width as defined in the NRBS report

In summary, both approaches use similar values of the diffusion factor. However they are producing different values for the dimensionless coefficient due to the different choice in length and velocity scales and the use of the shape factor to compensate for not using local values.

5.4.4 Slave River downstream Fort Smith

5.4.4.1 Background

In July 1980 the Environmental Engineering and Science Program of the University of Alberta conducted a slug and a continuous injection tracer test on the Slave River downstream of Fort Smith. The study was conducted for the Northwest Territories Department of Local Government. The results of the continuous injection test were reported by Putz (1983) and Gerard et al. (1985).

The 57 km study reach was characterized by twelve cross-sections surveyed at the time of the tests. The continuous tracer test defined the transverse mixing characteristics of the Slave River at this location. It also demonstrated that the entire study reach was within the two-dimensional mixing zone. The tracer was continuously injected near the left bank and the edge of the resulting plume only spread to approximately half way across the channel by the end of the study reach.

During the slug test, C-t measurements were collected at transverse locations across six sections covering the first 29.1 km of the study reach. Although the samples were analyzed and the results compiled shortly after the test, no attempt was made to model the two-dimensional transient mixing in this portion of the reach. The modeling work presented here uses the slug test data from the first 29.1 kms of the study reach.

5.4.4.2 Hydrometric data

A plan view of the slug injection study reach is shown in Figure 5.24. A more detailed explanation of the collection of hydrometric data at these cross-sections is presented by Putz (1983). The cross-section surveys were referenced to temporary benchmarks established for the duration of the field study. Water surface elevations were then referenced to these temporary benchmarks on the day of the slug test. The average slope of the Slave River through the study reach was taken to be 0.00005 as reported by Northwest Hydraulic Consultants Ltd. (1980) and Shawinigan Stanley (1982). The total streamflow was taken as that measured upstream at Fort Fitzgerald by the Water Survey of Canada gauging station, but accounting for the time of travel to the study reach.

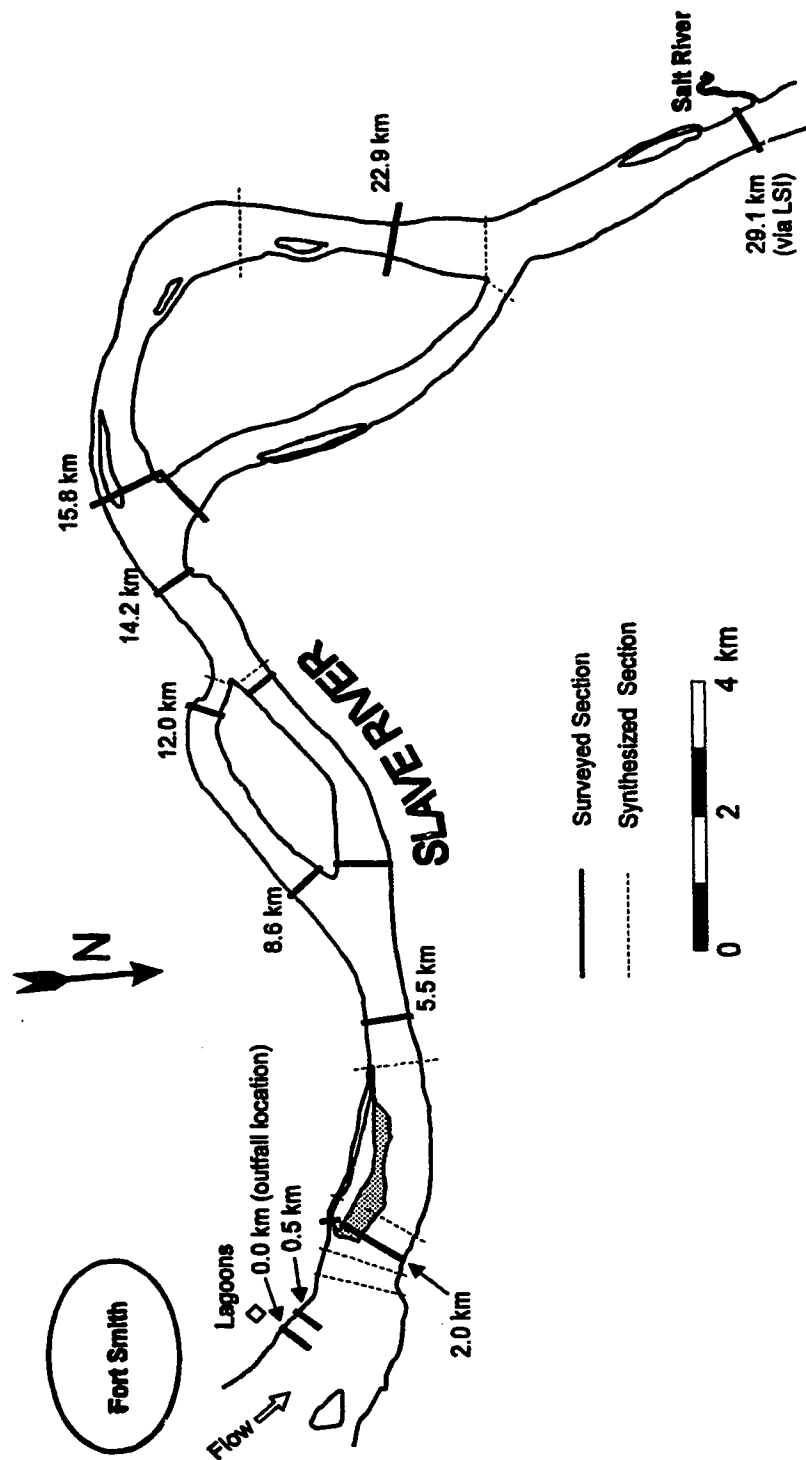


Figure 5.24 Plan of the Slave River study reach.

Velocity and cumulative flow distributions for the sampled cross sections were estimated by one of two procedures depending upon the survey data that was collected. The survey consisted of either :

- 1) cross-section geometry and water level only, or
- 2) cross-section geometry, water level and velocity measurements in the expected plume region.

Where only the section geometry and water level was available the mean depth and velocity was determined, then the local velocities and flow distribution were estimated using a resistance equation approach. Where velocity measurements were available the measured region was divided into transverse intervals, each represented by a measured vertical, and then the flow increment within the interval was calculated. Flow beyond the last measured interval was distributed in the rest of the section using a resistance equation approach.

A tabulation of the calculations for each section, cross-section plots and flow distributions are presented in Appendix D

5.4.4.3 Model input and results

A total of 50 kg of 20% Rhodamine WT (by weight) tracer was injected into the river near the Fort Smith sewage lagoon outfall (see Figure 5.24).

The river channel was divided into 15 streamtubes with the following boundaries: $q/Q = 0.0014, 0.004, 0.008, 0.014, 0.025, 0.040, 0.060, 0.080, 0.100, 0.176, 0.300, 0.3632, 0.600, 0.800$ and 1.00. Note that more streamtubes were placed in the near left bank region of the river where the plume was expected to be observed. The tube boundaries were also chosen to correspond to the location of major islands within the reach. This would allow the 'no flux' boundaries of the islands to be accounted for. A time step of 60 seconds was chosen on the basis of the criteria outlined previously, and the streamtube geometric parameters and initial estimates of β assembled into the GRIDGEN parameter file.

In the initial attempts to model the mixing the mass was distributed in streamtube No. 3 (i.e. 0.040 to 0.060) over the initial time step. As was observed for the North Saskatchewan River simulation, problems were evident in the near-bank region as a result of dead zone effects. For this reach the situation is even worse in that a very complicated flow situation was located on the left bank approximately 1800 m downstream of the injection point. At this location the flow near the left bank enters a dead zone area at the upstream end of an island. The tracer mass was temporarily trapped in this area and the flow distribution distorted (see Figure 5.25). The flow was diverted from the dead zone to either a back channel on the left side of the island, over a large sand bar situated on the right side of the island or to the main channel which is located some distance off the right side of the island

In order to attempt to account for the delay in mass release from the backwater area the input to the model was extended over a short time period, rather than considering it as an instantaneous slug. A period of 8 minutes was found to give the best match to the time base of the measured data.

The dosage distributions measured at sections where there was sufficient definition of the tracer plume to calculate a mass recovery are shown in Figure 5.26 plot a), c) e) and f). The calculated mass recoveries for these sections and for the section at 5500 m are given in Table 5.15. The recovery at 5500 m was very low indicating the entire tracer cloud was probably not sampled. Considering this, the calculated mass recovery at 5500m was not used for normalization purposes. At 5500 m and at 14200 m, where there was obviously incomplete sampling, the C-t curves were normalized using an interpolated recovery between the well sampled sections. The mass recoveries for 5500 m and 14200 m were estimated to be 0.84 and 0.59 respectively. At these locations the dosage distributions were estimated using the results of the steady-state test reported by Putz (1983). These distributions are shown in Figure 5.26 plot b) and d).

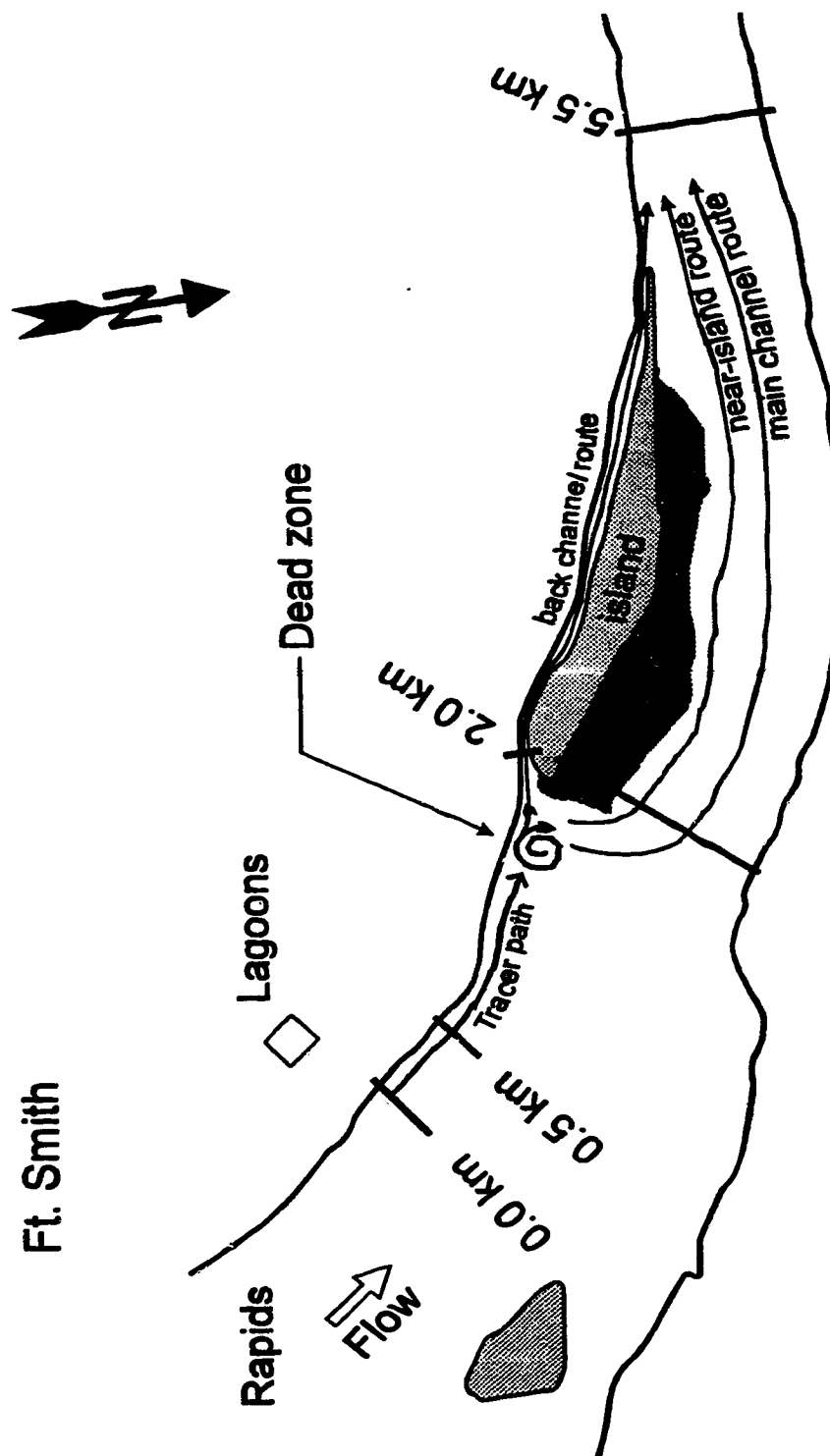


Figure 5.25 Dead zone effect approximately 1800 m downstream of injection.

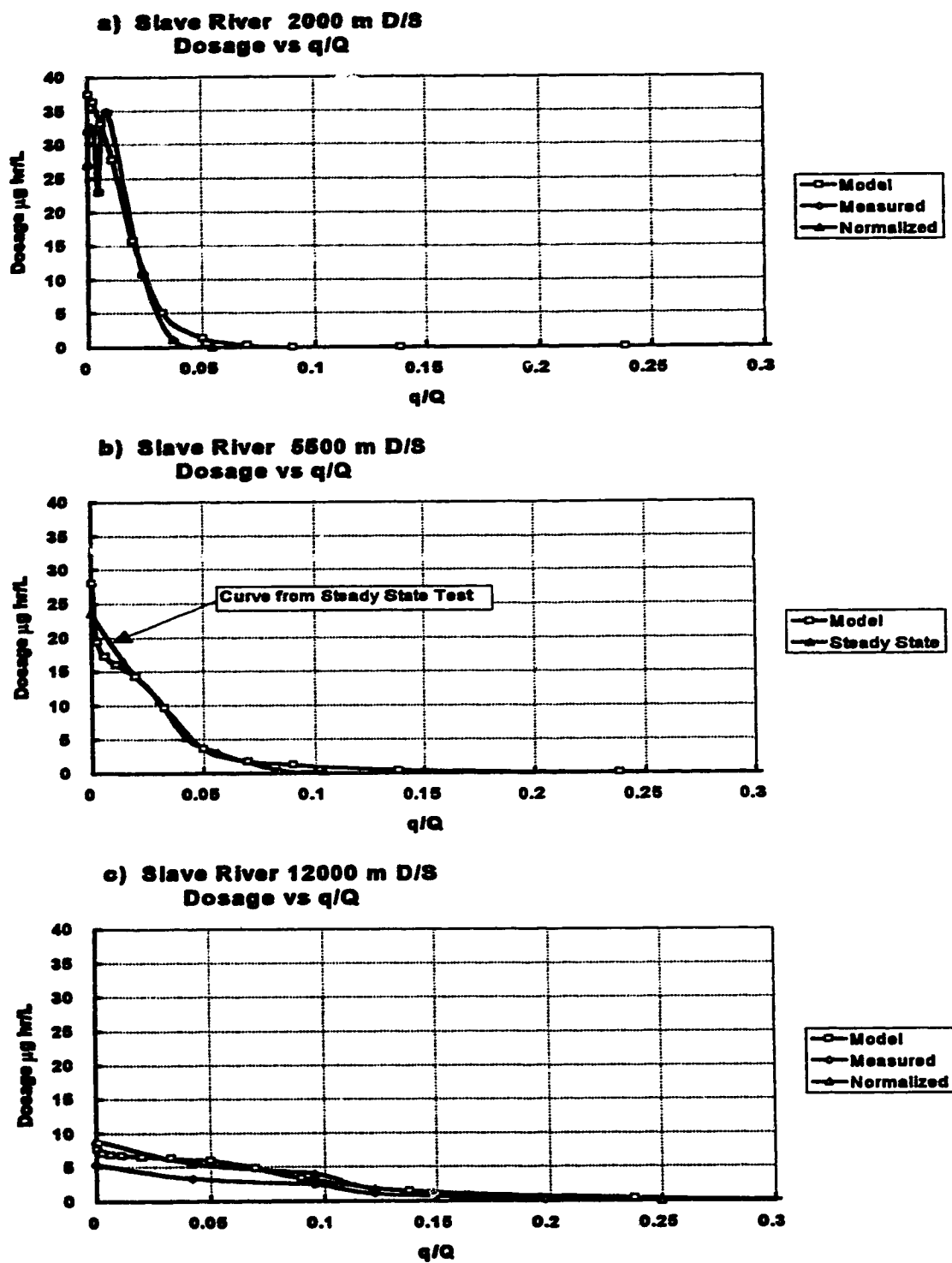


Figure 5.26 Slave River dosage distributions, extended slug input

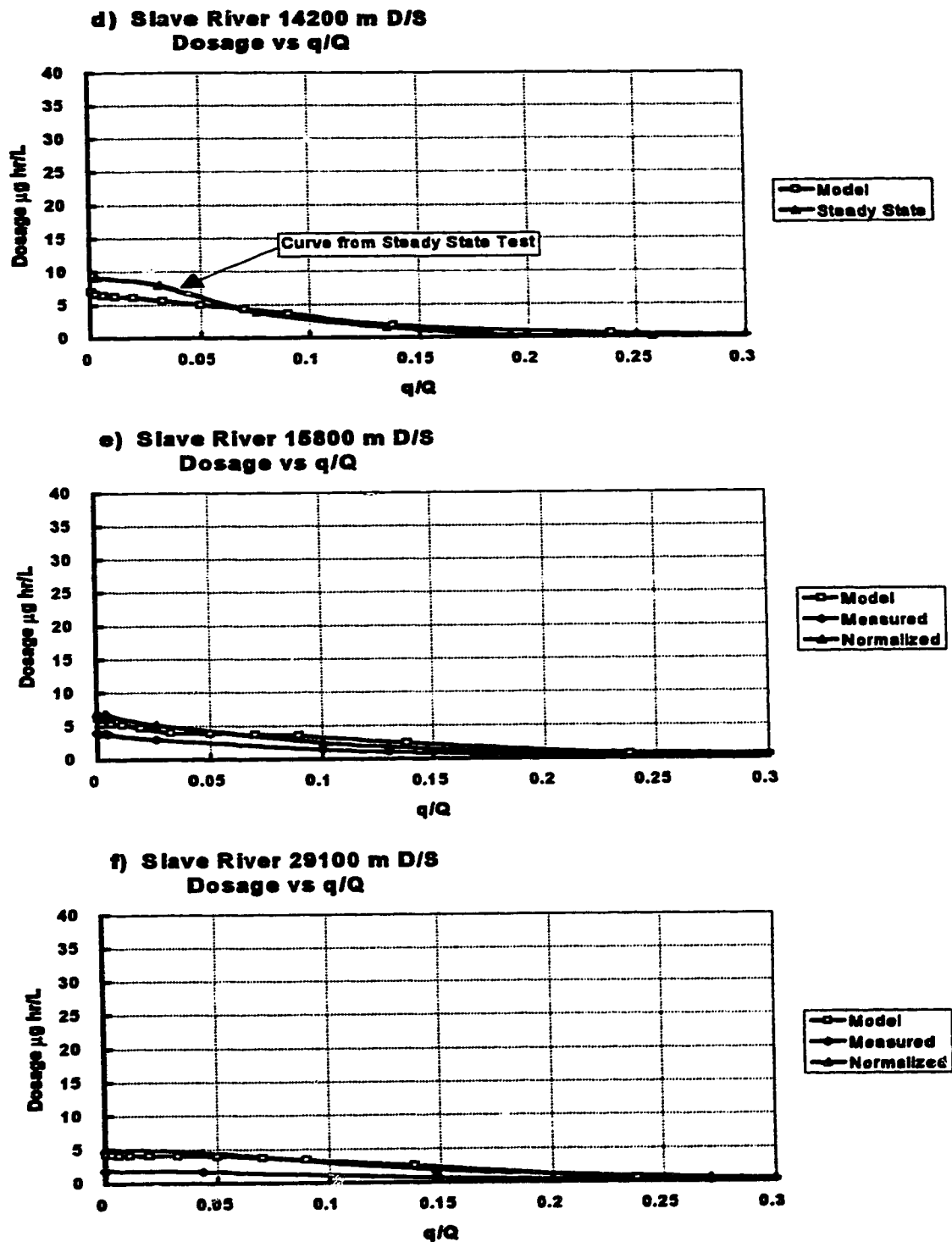


Figure 5.26 cont. Slave River dosage distributions, extended slug input

Table 5.15 Slave River tracer mass recoveries.

Cross-Section (m) downstream	Mass by Integration (kg)	<u>Mass Recovered</u> Specified Mass In
2000	10.01	1.001
5500	3.58	0.358
12000	6.01	0.601
15800	5.81	0.581
29100	3.71	0.371

Several computer simulations were run varying the magnitude of β . Unlike the two studies described previously, β was set at each section⁵ and linearly interpolated between sections. Final values for β were selected by visual comparison of the model output to the normalized measured dosages and the normalized measured C-t distributions at each sampling location. The normalized measured C-t curves and those generated by the model are shown in Figure 5.27 to Figure 5.32. The dosage curves generated by the model are shown in Figure 5.26.

The match between the normalized measured dosage curves and the simulated curves is good considering the complex flow situation present before the first sampled section. However, the effects of the complex flow situation are very evident in the C-t curves at the first two sections. At 2000 m the model over-estimates the peak concentrations. At 5500 m the model seriously over-estimates the peak concentrations.

As shown above a large portion of the mass at 5500 m is unaccounted for because the calculated mass is unreasonable low. The only feasible explanation seems to be that a large portion of the mass has traveled along the bank via the left side of island backchannel and/or over the sand bar on the right side of the island. Evidently this slowly moving mass of tracer was not sampled. This is in fact predicted by the model (see Figure 5.28a), however it seems the tracer is even more skewed to the left than predicted. This may also

⁵ This approach was used because estimates of β from a steady state test were available at each defined cross section. In the previous studies described only subreach estimates of β were available which encompassed several defined cross sections.

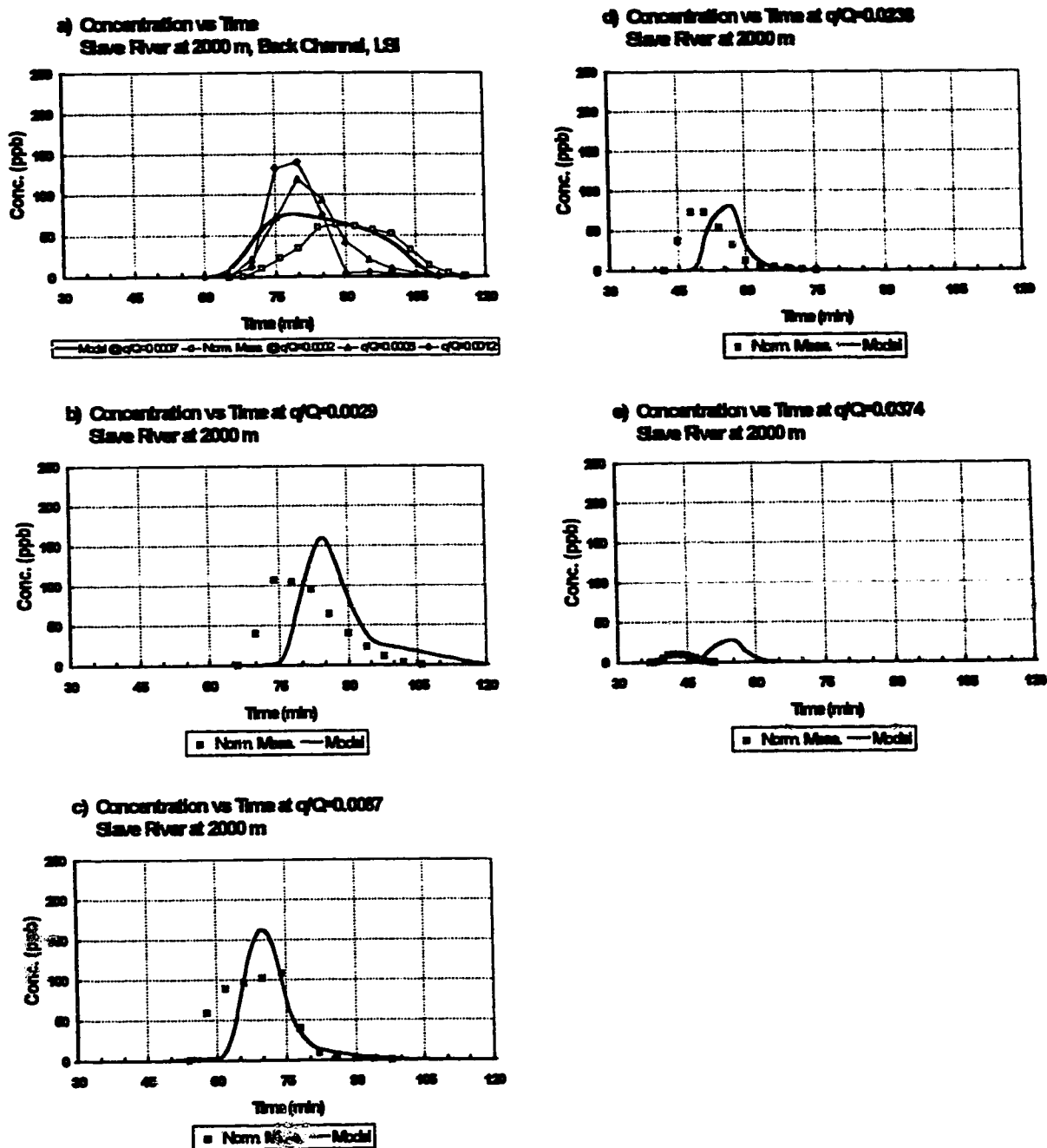


Figure 5.27 Slave River, C-t curves at 2000 m, extended slug input to the model.

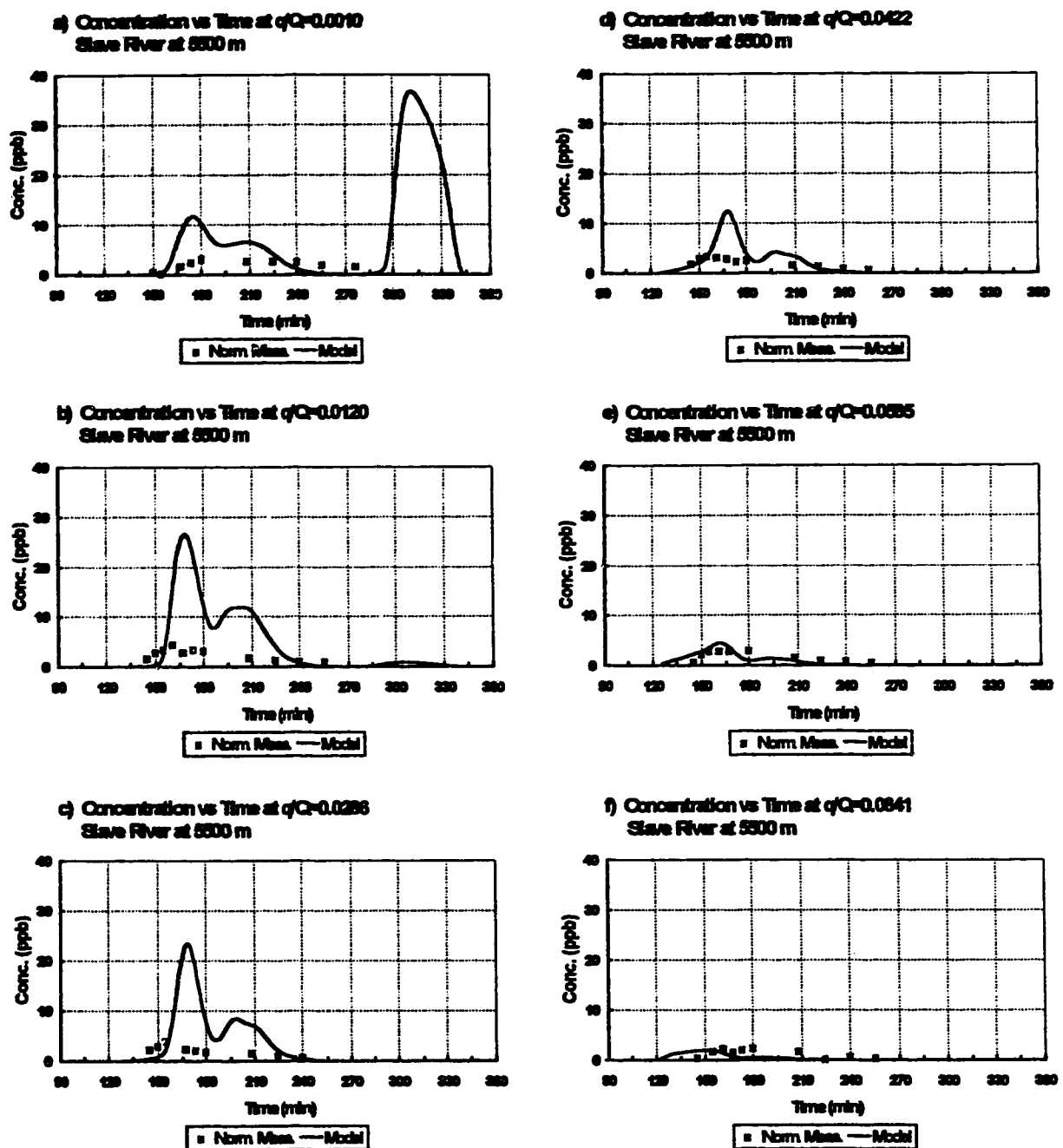


Figure 5.28 Slave River, C-t curves at 5500 m, extended slug input to the model.

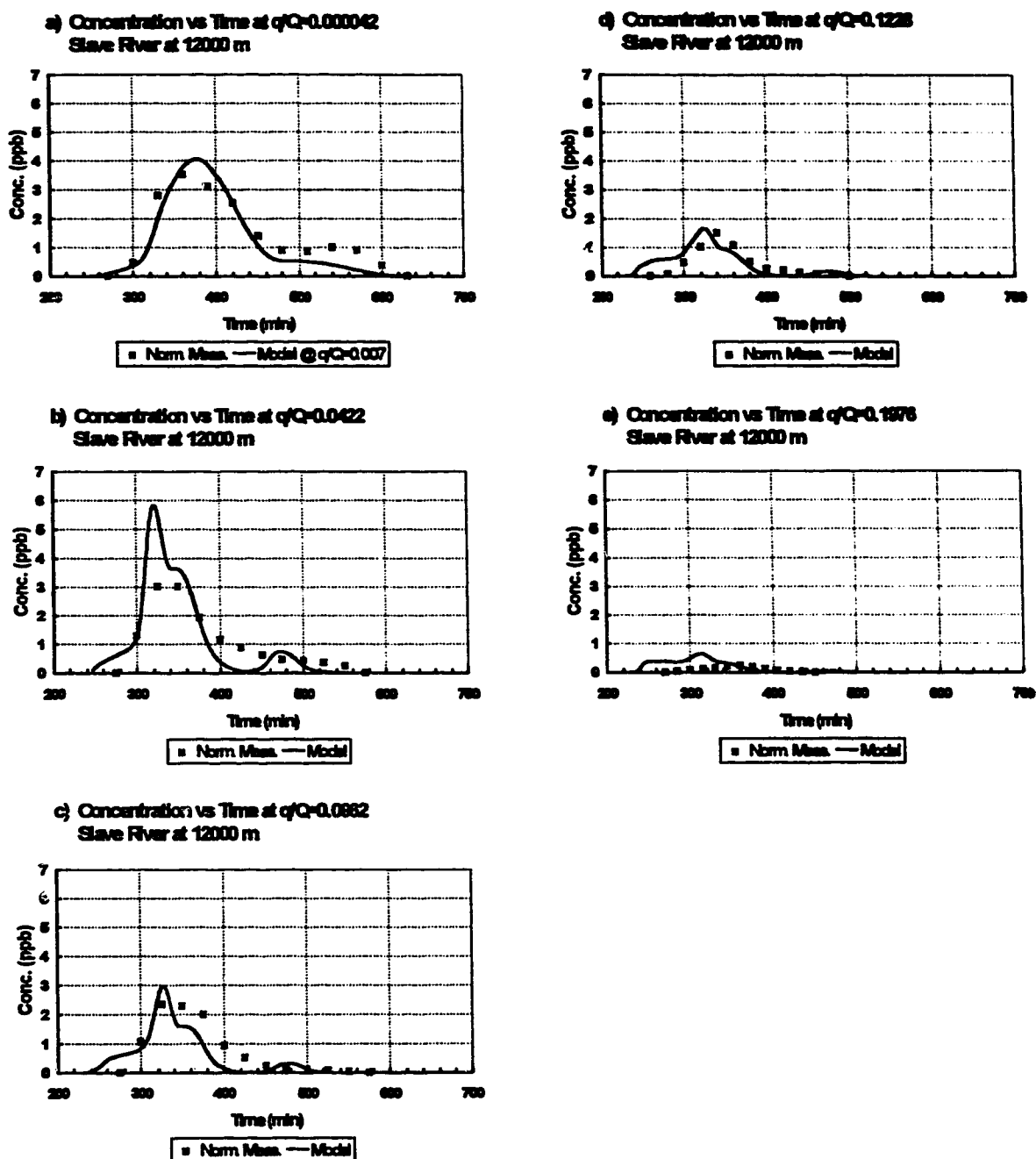


Figure 5.29 Slave River, C-t curves at 12000 m, extended slug input to the model.

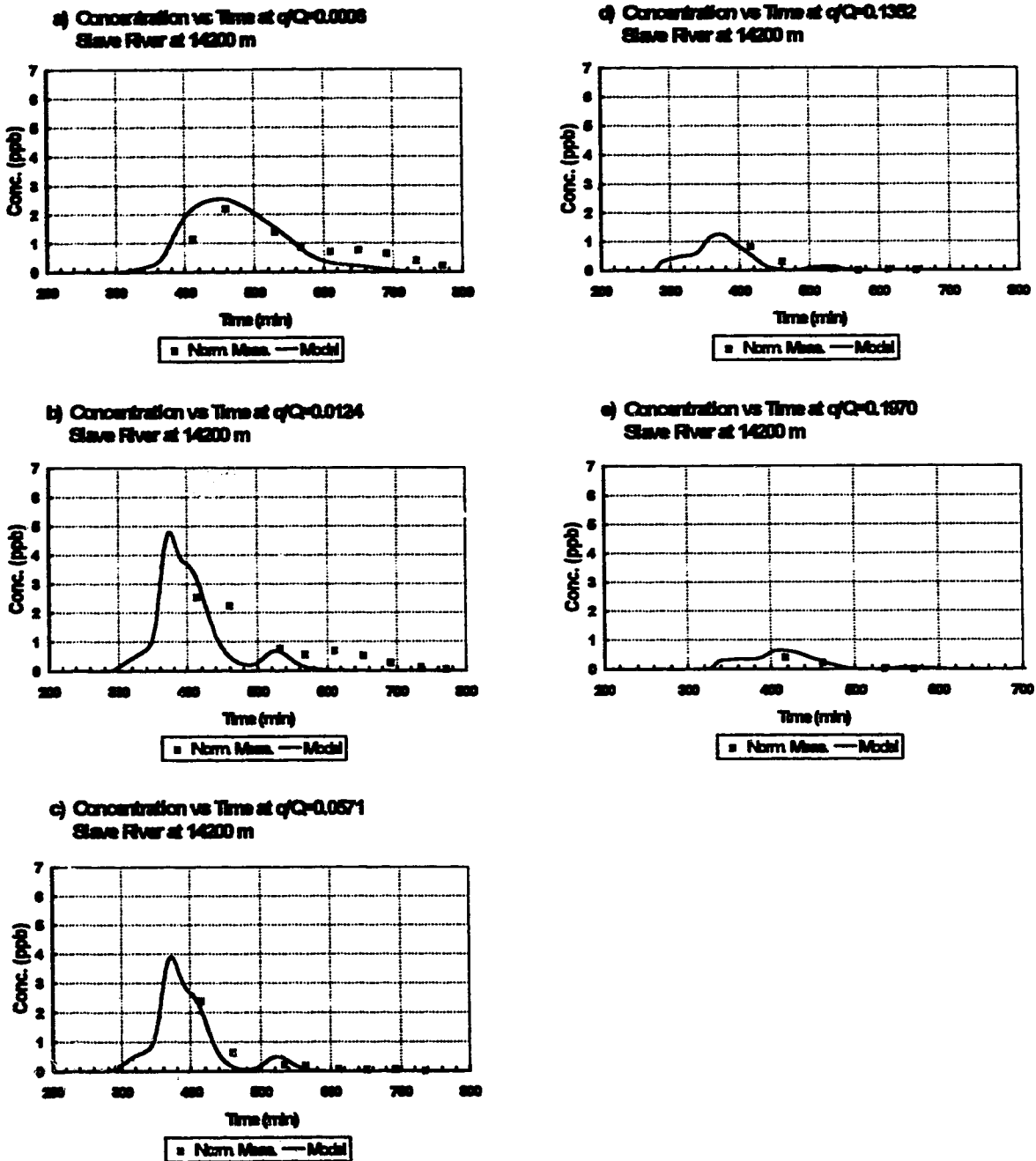


Figure 5.30 Slave River, C-t curves at 14200 m, extended slug input to the model.

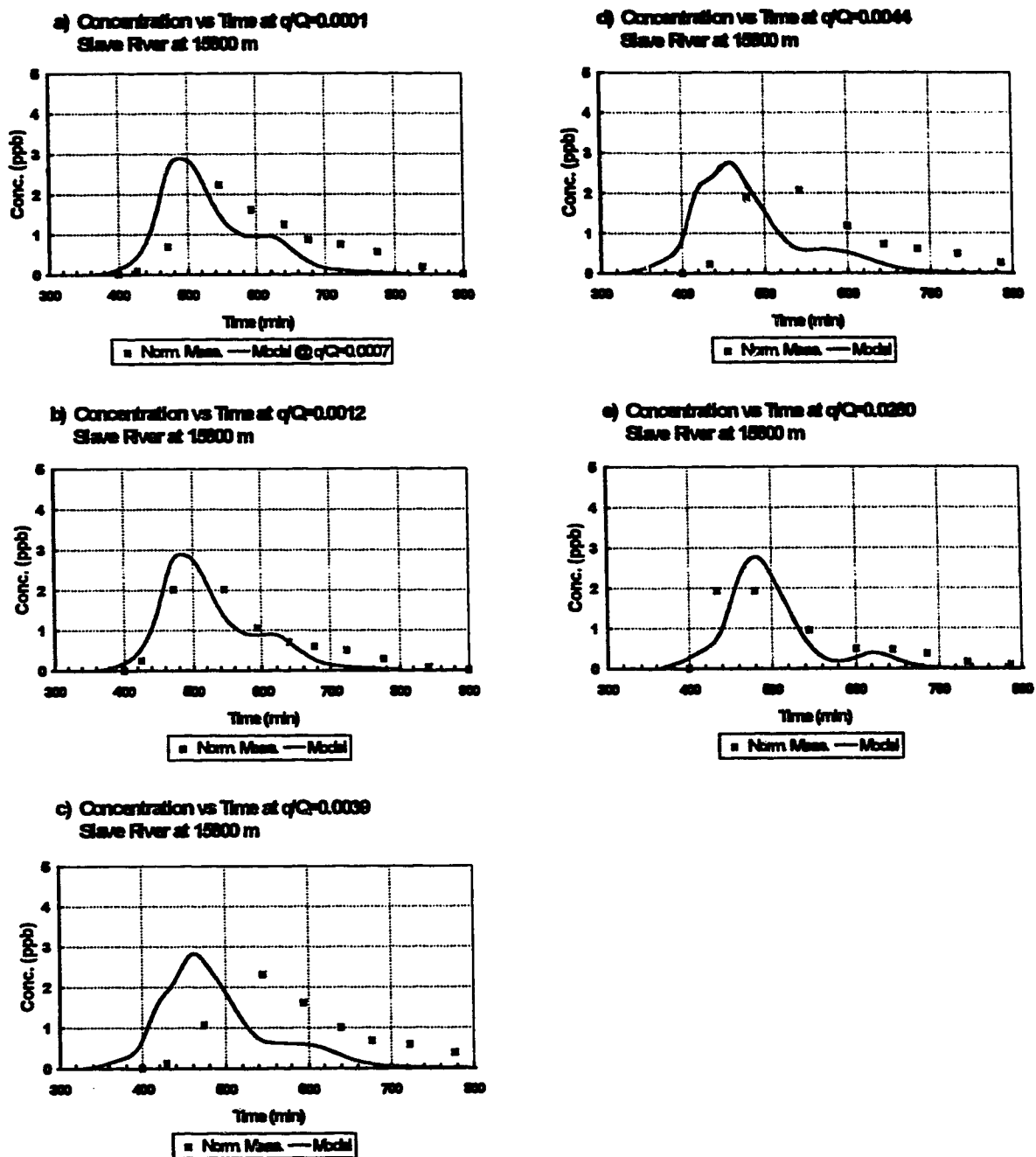


Figure 5.31 Slave River, C-t curves at 15800 m, extended slug input to the model.

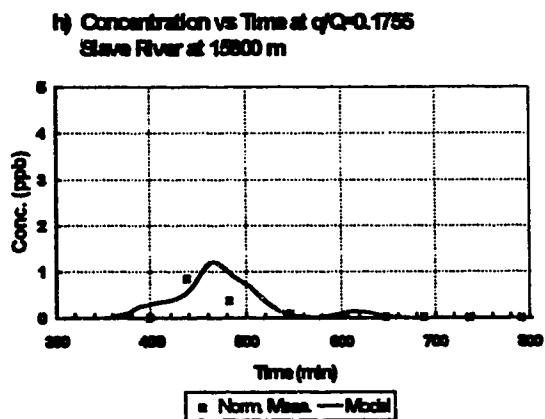
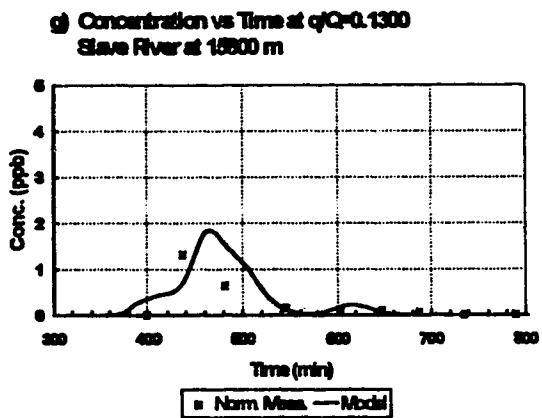
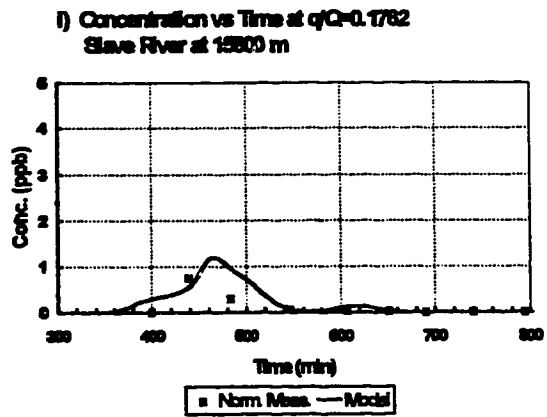
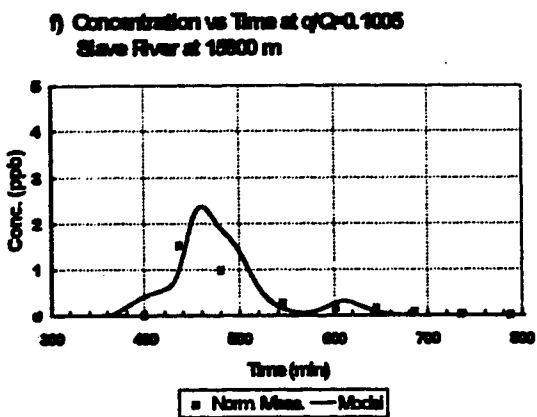


Figure 5.31 cont. Slave River, C-t curves at 15800 m, extended slug input to the model.

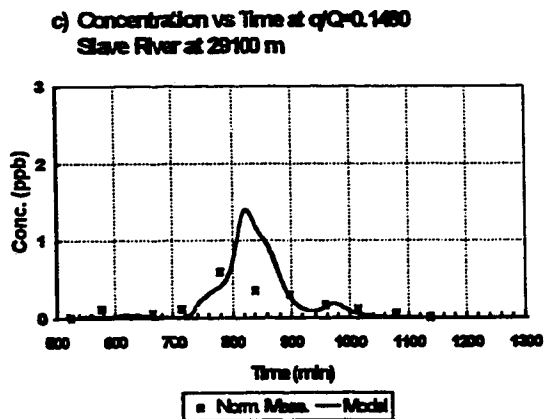
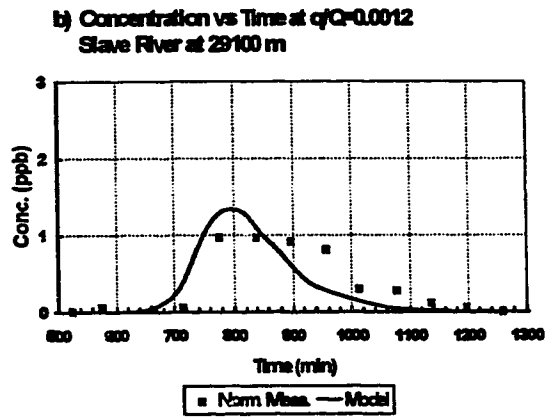
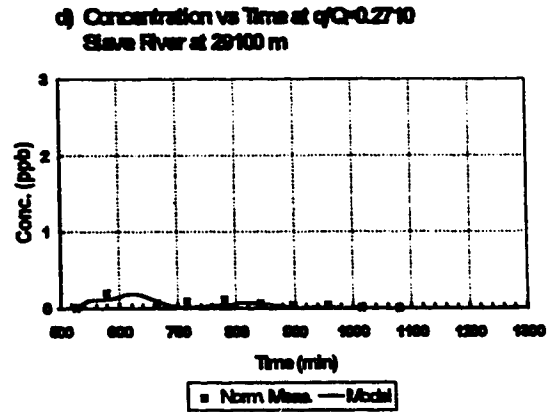
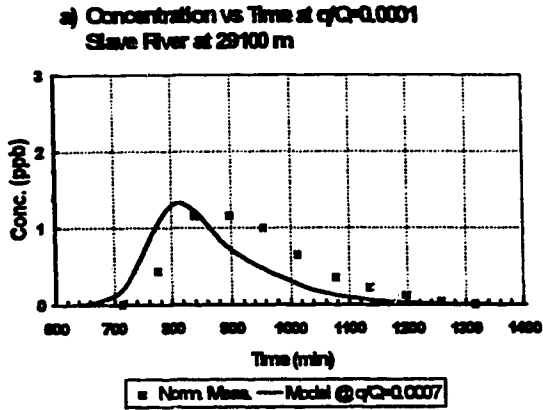


Figure 5.32 Slave River, C-t curves at 29100 m, extended slug input to the model.

explain why the simulated dosage curve agrees reasonable well with the steady-state test curve. In the steady test the near-bank concentrations were sampled, whereas in the slug test the near-bank concentrations were missed.

Beyond 5500 m the model performs very well. The match between the normalized measured and the simulated curves at 12000, 15000 and 29100 m are all very good. This is particularly encouraging when it is considered that the 'no flux' effects of several islands have been accounted for in the model.

The dimensionless transverse mixing coefficients used in the model are given in Table 5.16. Also shown in Table 5.16 are the dimensionless mixing coefficients reported for the reach for the steady state tracer test (Putz, 1983). The steady-state mixing analysis was completed using the numerical model TRSMIX (Putz, 1984).

Table 5.16 Slave River, dimensionless transverse mixing coefficients.

Unsteady Model Cross-Section (m)	Transient Model β	Steady-State Model Subreach (m)	Steady-State Model β
0	0.10		
1700	0.10		
1800	0.10	500 to 900	0.236
2000	5.00	900 to 2000	11.34
2200	9.00	2000 to 2300	9.45
4800	2.45	2300 to 4850	2.45
5500	1.29	4850 to 7800	1.29
8600	1.29	7800 to 10400	0.66
12000	1.25	10400 to 12600	1.25
12600	0.64	12600 to 14200	0.64
14200	0.64	14200 to 15600	1.66
15800	4.58	15600 to 20000	6.58
20000	4.00	20000 to 27500	7.65
27500	1.00	27500 to 29100	1.99
29100	1.00		

The reported values are similar, but not identical. The difference is likely due to the method by which 2DMIX, the transient model, and TRSMIX, the steady state model, handle the dimensionless mixing coefficient and the channel geometric parameters. In the

TRSMIX model the channel is prismatic within each subreach and β is constant. In the transient model the channel parameters and β are linearly interpolated between defined sections. Considering this difference in handling the parameters the results are quite comparable.

5.5 Discussion of Field Verification Results

The three field verification studies discussed in this chapter demonstrate that the AOG method can be applied to two-dimensional, unsteady source mixing problems in natural streams with satisfactory results. At most of the locations examined the model produced representative C-t distributions comparable to the normalized field measurements. The measured transverse dosage distributions were consistently reproduced by the model. In addition the transverse mixing coefficients used in the modeling procedures were of similar magnitude to those previously determined by analytical means on the basis of reach or section-averaged parameters.

Poor prediction of C-t distributions most often occurred near the stream banks where the influence of dead zones or backwater areas would be the most pronounced. However these occurrences are not a drawback specific to the AOG method. All modelling schemes are susceptible to problems created by these complicated flow fields.

The verification studies effectively demonstrated that there is a very large requirement for representative hydrometric data for two-dimensional unsteady source modelling. This requirement is more critical than for steady state modelling. Without an adequate number of cross sections to define the characteristics of the reach, problems will be experienced in modelling the time of travel and longitudinal distribution of mass. Again this is not a specific drawback of the AOG method but rather a requirement for all two-dimensional unsteady source modelling approaches.

On the basis of the study results presented above the AOG model can be considered adequately verified for a conservative tracer and natural stream conditions. Modification of the AOG model and its application to non-conservative water quality parameters is described in the next chapter.

6. Modelling Non-Conservative Substances

6.1 Adaptation of the AOG Method for Non-Conservative Substances

Chapters 3 to 5 have primarily dealt with the modelling of conservative substances (i.e. the reaction term in Equation [22] was assumed equal to zero). Most effluent substances are non-conservative due to environmental reactions such as oxidation, volatilization, adsorption, hydrolysis and photodecomposition. In order to model non-conservative substances appropriate reaction terms describing the attenuating mechanism(s) must be incorporated into the governing mass balance equation.

Many comprehensive one-dimensional steady state mixing models have been developed for non-conservative water quality parameters. McCutcheon (1989) presents a review and evaluation of a number of these models. One example is QUAL2E which can handle fourteen water quality parameters and their associated reaction mechanisms. Despite the sophistication of models such as QUAL2E, they are inappropriate for unsteady sources and simulations within the two-dimensional mixing zone. One-dimensional unsteady models have also been developed for selected non-conservative water quality parameters. Examples are Bedford et al. (1983), McBride and Rutherford (1983), Schoellhamer (1988), Koussis et al. (1990) and Rutherford et al. (1991). While these are improvements over the one-dimensional steady state models in terms of handling unsteady sources they are still not applicable within the transverse mixing zone.

Several field investigation and modelling studies have been reported which deal with non-conservative substances in the transverse mixing zone for steady source conditions. Examples are Putz (1983), Milne (1991) and Smith and Putz (1993). However the model used in these studies can not handle slug, intermittent or variable input conditions. In these situations a model with two-dimensional, time-dependent input capability is required for simulation of water quality parameters in the transverse mixing zone. The adaptation and verification of the AOG method for non-conservative substances represents a major step toward the development of a modelling tool for general application to time-dependent discharges and mixing in the two-dimensional mixing zone.

The fractional time step approach employed by the AOG method is well suited to the incorporation of reaction terms. The mathematical descriptions of the reaction kinetics are handled as an additional substep. During the reaction substep each element is modelled as a completely-mixed batch reactor. Coefficients used in the description of the reaction kinetics are input into the model in similar fashion to the transverse mixing coefficient.

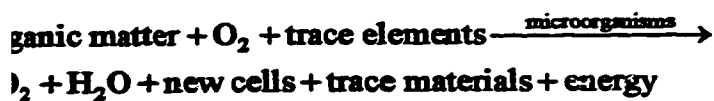
Adaptations of the AOG model to predict biochemical oxygen demand and dissolved oxygen concentrations downstream of a wastewater outfall, and to investigate adsorption of an organic compound to sediments will be demonstrated in the following sections.

6.2 BOD and Dissolved Oxygen Modelling

6.2.1 Background

Organic matter discharged to a water body acts as substrate for bacteria and other microbial populations. Utilization of the organic matter by the microbial population results in the break-down and degradation of these materials. Degradation can occur under aerobic or anaerobic conditions. Aerobic microbes require oxygen in the degradation process, thus an oxygen demand is exerted as the process proceeds. In the absence of oxygen, anaerobic bacteria utilize the organic material and break it down into less complex reduced compounds. Often these reduced compounds are subsequently released to the aerobic environment where they can be utilized by aerobic microbes. The oxygen requirement for the aerobic microbial process is known as biochemical oxygen demand or BOD.

Dissolved oxygen (DO) content is critical for the maintenance of a healthy aquatic environment which is characterized by the presence of a wide diversity of organisms and species. A dissolved oxygen content of at least 4 to 5 mg/L is required to support high order species such as trout and other game fish. Recognizing this, most surface water quality regulations stipulate that DO levels should not fall to below 4 to 5 mg/L as a result of the discharge of effluent containing BOD-causing materials.



[115]

difficult to identify and quantify the wide array of organic compounds present in a waste which contribute to the CBOD. Alternatively the amount of oxygen required for degradation and conversion of the compounds is measured in a standard bottle test (APHA, 1985). The oxygen consumed (the CBOD exerted) in a standard bottle test is characteristic of the strength (the organic content) of the waste. The total amount of oxygen required to complete the reaction is called the ultimate CBOD or CBOD_u.

The degradation process is not instantaneous, rather it proceeds over time. Thus complex kinetic relationships would be required to precisely represent the microorganism-mediated breakdown of the various compounds by the mixed population of organisms. This type of approach is impractical for wastewater engineering purposes. It has been found through experimentation that the following first order empirical relationship adequately represents the CBOD removal kinetics:

$$\frac{dL}{dt} = -K_1 L$$

[116]

where: L is the CBOD concentration remaining (mg O₂ /L), and
 K_1 is the first order rate constant for CBOD exertion in a standard bottle test (/day or /s).

In order to determine K_1 the CBOD exerted must be monitored over time. The expression for CBOD exerted is:

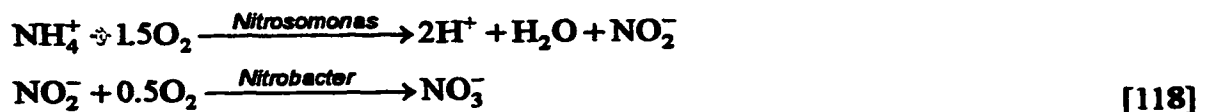
$$y_t = L_0(1 - e^{-K_1 t})$$

[117]

where: $y_t = L_0 - L$ is the CBOD exerted (mg O₂ /L),
 L_0 is the ultimate CBOD concentration (mg O₂ /L),
 K_1 is the first order rate constant for CBOD exertion in a standard bottle test. (/day or /s).

Several methods are available to determine K_1 and L_0 using a set of y vs. t data from bottle tests (Reed and Theriault, 1931; Moore et al., 1950; Thomas, 1950; Fujimoto, 1964). In general the exertion of CBOD within the receiving stream is greater than in the bottle test due to turbulence and the presence of attached biofilms (Thomann and Mueller, 1987). The 'in-stream' reaction kinetics are still assumed to be first order but the rate coefficient is designated K_d to distinguish it from the bottle test rate coefficient. Wright and McDonnell (1979) found that for larger streams ($Q > 23 \text{ m}^3/\text{s}$) K_d approaches K_1 from bottle tests.

Nitrogenous BOD or NBOD results from the nitrification of ammonia released from organic matter or present directly in the wastewater. The ammonia is converted to nitrite and then nitrate as shown in the following equations provided an adequate population of nitrifying bacteria are present:



In a standard bottle test the initiation of the NBOD exertion may lag behind the initiation of the CBOD exertion by several days depending on the amount of CBOD and the nitrifying bacteria present in the sample. In order to quantify the CBOD effect alone the NBOD reactions are often purposely inhibited (APHA, 1985). In order to quantify the NBOD progression two bottle tests must be run, one with NBOD inhibition and one without. The NBOD curve can then be determined by subtraction.

In the natural environment downstream of a continuous wastewater discharge a standing population of acclimated nitrifying bacteria is generally present in attached biofilms. The presence of these microorganisms allows immediate action upon organic nitrogen wastes (Velz, 1984). In such situations a time lag as experienced in the bottle test will not occur before the initiation of the nitrification process.

A series of first order kinetic relationships has been used to describe each step of the organic nitrogen to nitrate degradation process (Thomann et al., 1992). However, for engineering applications a more simplified empirical approach is generally applied. Similar

to CBOD it has been found through experimentation that the following empirical relationship adequately represents the 'in-stream' NBOD reaction kinetics:

$$\frac{dL_N}{dt} = -K_n L_N \quad [119]$$

where: L_N is the NBOD concentration remaining (mg O_2 /L), and
 K_n is a first order rate constant for NBOD exertion (/day or /s).

Unlike CBOD, stoichiometric relationships can be used to reliably predict the NBOD. Stoichiometric calculations indicate NBOD is 4.57 times the total Kjeldahl nitrogen (TKN) content of the wastewater. TKN is a measure of the total organic and ammonia nitrogen of the water (see APHA, 1985). Therefore, NBOD removal kinetics may also be represented by:

$$\frac{dL_N}{dt} = -K_n L_N = -4.57 K_n (\text{TKN}) \quad [120]$$

where: TKN is the total Kjeldahl nitrogen concentration (mg N/L).

CBOD and NBOD are the primary dissolved oxygen sinks resulting from a wastewater discharge. Additional sinks include oxygen demand resulting from biochemical processes occurring in the bottom sediments of the receiving stream and the respiration requirements of aquatic plants and algae. These additional sinks may or may not be significant depending upon the characteristics of the discharged effluent. If the effluent contains large quantities of organic solids, this material will settle and accumulate in the bottom sediments of the river. Within the sediments the organic solids will be subject to the combined action of anaerobic and aerobic processes as mentioned above. This creates a benthic or sediment oxygen demand (SOD).

If the effluent contains significant nitrogen and phosphorus content the receiving stream may become nutrient enriched causing a large seasonal growth of aquatic plants to occur. Although the aquatic plants produce oxygen by photosynthesis during daylight hours, they also continuously consume oxygen due to respiration. During daylight hours the net result is an oxygen source. During darkness respiration is an oxygen sink. In addition to the photosynthesis-respiration effects, the large biomass produced during the

growing season dies over the winter in northern locations. This contributes additional organic solids to the bottom sediments of the stream and increases the SOD. SOD and respiration will be further discussed in Sections 6.2.3.4.3 and 6.2.3.4.4 of this Chapter.

The oxygen sinks created by a wastewater discharge to a stream are opposed by oxygen sources. Sources include atmospheric oxygen input and photosynthetic oxygen production by aquatic plants.

The time rate of exchange of a gas between a water body and the atmosphere is described by 'two-film' theory (see McCutcheon, 1989). The gas must move through a gas film and a liquid film at the gas-liquid interface. For oxygen, the liquid film controls the exchange, and the rate of exchange is given by the following expression (Thomann and Mueller, 1987):

$$V \frac{dC}{dt} = K_L A (C_s - C) \quad [121]$$

where: C is the dissolved oxygen concentration in the water (mg/L or g/m³),
 C_s is the dissolved oxygen saturation concentration (mg/L or g/m³),
 V is the volume of the water body (m³),
 A is the surface area through which the exchange occurs (m²), and
 K_L is the oxygen transfer coefficient (m/s).

Equation [121] assumes there is complete mixing of the oxygen within the volume of water. The dissolved oxygen saturation concentration is a function of the water temperature, salinity and atmospheric pressure (although for fresh water, salinity effects are minor). The saturation concentration can be determined using Henry's Law which is derived from thermodynamic principles (see Snoeyink and Jenkins, 1980). Alternatively, C_s may be determined using equations fit to the results of the thermodynamic equilibrium calculations (this method is used in Section 6.2.3.4.2).

The geometric parameters and the transfer coefficient of Equation [121] are generally combined to give:

$$\frac{dC}{dt} = K_s (C_s - C) \quad [122]$$

where: K_a is called the volumetric reaeration coefficient (despite the fact it describes oxygen transfer) (1/day or 1/s).

The term $(C_s - C)$ is called the oxygen deficit. Analytical oxygen transfer calculations are frequently conducted in terms of the oxygen deficit rather than oxygen concentrations in order to simplify the mathematics. The oxygen deficit term controls the direction of transfer. Under deficit conditions oxygen is transferred to the water column. If the water is supersaturated (e.g. by photosynthetic production) then oxygen will be released to the atmosphere.

The reaeration coefficient is a measure of the geometric and flow conditions which influence the rate at which the water column approaches equilibrium conditions with the atmosphere. Shallow turbulent water will have a much higher exchange rate than deep quiescent water due to the smaller volume and larger surface area involved in the exchange. Numerous equations (over thirty) have been derived to predict the magnitude of K_a as a function of easily measured stream flow parameters. Major reviews of the K_a equations are presented by McCutcheon (1989) and Lau (1972).

McCutcheon (1989) concluded that the best available guidance for selecting a predictive equation for K_a is given by Covar (1976). Covar's method classifies receiving streams into three regimes: shallow, deep with low velocity, and deep with high velocity. According to Covar each of the regimes is best represented by following predictive equations:

Owen's equation for shallow flows, $d < 0.61$ m

$$K_a = \frac{5.32 u^{0.67}}{d^{1.85}} \quad u \text{ in m/s; } d \text{ in m; } K_a \text{ / day, } 20^\circ \text{C} \quad [123]$$

Churchill's equation for deep rivers with high velocity,

$$d \geq 0.61 \text{ m and } \log(d) \leq 2.77 \log(u) + 0.65$$

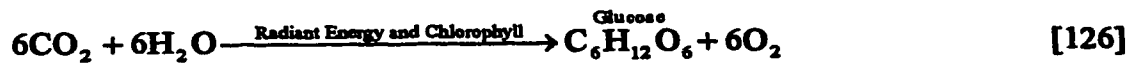
$$K_a = \frac{5.01 u^{0.969}}{d^{1.673}} \quad u \text{ in m/s; } d \text{ in m; } K_a \text{ / day, } 20^\circ \text{C} \quad [124]$$

O'Connor Dobbins equation for deep rivers with low velocity

$$d \geq 0.61 \text{ m and } \log(d) \geq 2.77\log(u) + 0.65$$

$$K_a = \frac{3.90 u^{0.50}}{d^{1.50}} \quad u \text{ in m / s; } d \text{ in m; } K_a \text{ / day, } 20^\circ \text{ C} \quad [125]$$

Algae and aquatic plants which contain chlorophyll capture radiant light energy in order to produce stored energy (sugars) from carbon dioxide and water. Oxygen is a byproduct of the photosynthetic reaction as shown below:



Photosynthetic oxygen production varies depending upon a number of factors which include the amount of incoming radiant energy, water depth, water turbidity, water temperature, nutrient levels and plant species (Di Torro 1992). Production only occurs during daylight hours and typically reaches a peak in mid-afternoon. A plot of oxygen production rate vs. time will generally follow a parabolic shape. If production is significant, dissolved oxygen levels in the receiving water can easily become supersaturated during the day. However, throughout the day the reverse reaction to Equation [126] occurs in order to utilize the stored energy. During daylight the net result is oxygen production. During darkness oxygen is consumed and dissolved oxygen concentrations within the water column can be greatly reduced during the predawn hours.

Methods for predicting the instantaneous photosynthetic oxygen production rate are presented in Section 6.2.3.4.3 of this Chapter.

The rate expressions for sources and sinks of dissolved oxygen discussed above can be combined with advective and diffusive transport terms to formulate a mass balance equation for dissolved oxygen. Based upon the one-dimensional formulation of O'Connor and Di Torro (1970), the governing two -dimensional mass balance equation for dissolved oxygen downstream of a wastewater discharge is:

$$\frac{\partial C}{\partial t} + u \frac{\partial C}{\partial x} = \frac{\partial}{\partial z} \left(E_z \frac{\partial C}{\partial z} \right) + K_a (C_s - C) - K_d L(x, z, t) - K_n L_N(x, z, t) + P(x, z, t) - R(x, z) - S(x, z) \quad [127]$$

in which C is the dissolved oxygen concentration; C_s is the saturated dissolved oxygen concentration; K_a is the reaeration coefficient; $L(x, z, t)$ is the distribution of carbonaceous BOD; K_d is a rate constant for CBOD exertion in the river; $L_N(x, z, t)$ is the distribution of nitrogenous BOD; K_n is a rate constant for NBOD exertion in the river; $P(x, z, t)$ is photosynthetic oxygen production rate resulting from algae and aquatic plants; $R(x, z)$ is respiration rate by algae and aquatic plants; and $S(x, z)$ is the rate of sediment oxygen demand.

Another significant consideration for solving Equation [127] is that the instantaneous concentration distributions of L and L_N (or TKN) must be known in time and space. Therefore the mass balance equations for L and L_N (or TKN) as shown below have to be solved before or at the same time as the dissolved oxygen equation.

$$\frac{\partial L}{\partial t} + u \frac{\partial L}{\partial x} = u \frac{\partial}{\partial z} \left(E_z \frac{\partial L}{\partial z} \right) - K_d L \quad [128]$$

$$\frac{\partial L_n}{\partial t} + u \frac{\partial L_n}{\partial x} = u \frac{\partial}{\partial z} \left(E_z \frac{\partial L_n}{\partial z} \right) - K_n L_n \quad [129]$$

Note that in general K_d and K_n , the 'in-stream' reaction rate constants, do not completely quantify the removal of L and L_N from the receiving stream water. Additional factors such as sedimentation and adsorption to sediments and the bed materials tend to increase the rate of removal. If these additional removal mechanisms are significant they must be considered in the mass balance equations for L and L_N . Typically all the removal mechanisms are considered to be first order and lumped together in one overall rate coefficient (for example K_d would be replaced by K_r in Equation [128], where $K_r > K_d$).

Finally it is important to note that the P , R and S expressions as formulated in Equation [127] are independent of DO and BOD in the water column (i.e. they are zero order). Therefore, the parameters controlling these rate expressions can be determined as

part of the preprocessing routines and the values mapped onto the calculation grid similar to the procedure for the transverse mixing coefficient.

A subroutine describing the BOD-DO reaction kinetics was added to the AOG mixing model as an additional substep. The reaction terms were expressed as explicit finite difference expressions for the change in concentration which occurs in each element during each time step. The expressions are as follows:

$$C^{t+\Delta t} = C^t - K_d L^t \Delta t - 4.57 K_n (\text{TKN})^t \Delta t - \left(\frac{R_{\text{area}}}{h} \right) \Delta t - \left(\frac{S_{\text{area}}}{h} \right) \Delta t + K_r (C_s^t - C^t) \Delta t + \left(\frac{P_{\text{area}}}{h} \right) \Delta t \quad [130]$$

where: P_{area} , R_{area} , S_{area} are areal rates ($\text{g}/(\text{m}^2 \text{day})$), and h is the element average depth (m).

$$L^{t+\Delta t} = L^t - K_d L^t \Delta t \quad [131]$$

$$(\text{TKN})^{t+\Delta t} = (\text{TKN})^t - 4.57 K_n (\text{TKN})^t \Delta t \quad [132]$$

Verification of the reaction substep BOD-DO kinetic equations are presented in the next two sections of this chapter.

6.2.2 Analytical verification

As a first step in the verification process the BOD-DO mixing and reaction model was tested against a steady state and an unsteady analytical solution to the one-dimensional versions of the DO, and CBOD mass balance equations.

The steady state one-dimensional mass balance equation for DO considering only carbonaceous BOD and atmospheric reaeration is:

$$U \frac{\partial C}{\partial x} = K_r (C_s - C) - K_d L(x) \quad [133]$$

where U is the section-averaged velocity and C , C_s and L are section-averaged concentrations. The steady state one-dimensional mass balance equation for CBOD is:

$$U \frac{\partial C}{\partial x} = K_r L(x) \quad [134]$$

where K_r is the in-stream removal rate coefficient.

The analytical solution to Equation [133] is the classic dissolved oxygen sag curve first formulated by Streeter and Phelps (1925). The solution is customarily given in terms of saturation deficit. In terms of dissolved oxygen the solution is (Thomann and Mueller, 1987):

$$C = C_s - \left\{ \frac{K_d}{K_s - K_r} \left[\exp\left(-K_r \frac{x}{U}\right) - \exp\left(-K_s \frac{x}{U}\right) \right] \right\} L_0 - (C_s - C_0) \exp\left(-K_s \frac{x}{U}\right) \quad [135]$$

where C_0 and L_0 are the initial concentrations of DO and CBOD at time zero. The initial concentrations are determined by a mass balance calculation at the outfall assuming instantaneous complete mixing. For example C_0 is given by:

$$C_0 = \frac{C_r Q_r + C_e Q_e}{Q_r + Q_e} \quad [136]$$

where Q_r and C_r are upstream river flow and concentration and Q_e and C_e are effluent flow and concentration.

The flow conditions, effluent input and kinetic parameters used in the verification calculations are shown in Table 6.1. For modelling purposes the hypothetical river channel was divided into three identical streamtubes (with respect to flow velocity, width and depth) in order to properly handle the left and right bank boundary conditions. A time step of 120 seconds was selected for the simulation and the model run for approximately 2500 time steps. The fully mixed DO and CBOD concentrations were continuously placed into the first element of each streamtube to simulate the steady state conditions. The results of the numerical and analytical calculations are shown in Figure 6.1. They indicate there is negligible error associated with the reaction subroutine after the 2500 time steps.

Li (1972) developed an analytical solution for the time dependent DO sag curve resulting from a sinusoidal input of carbonaceous BOD to a channel with known mean

depth, velocity and total flow. Koussis et al. (1990) used Li's solution to test a one-dimensional unsteady substance source mixing and reaction model for BOD and DO. A similar comparison is used here to test the AOG model adapted for BOD-DO kinetics.

Table 6.1 Parameters for model verification against Streeter-Phelps solution.

Parameter	River	Effluent	Fully Mixed
$Q \text{ (m}^3/\text{s)}$	39	1	40
$L \text{ (g/m}^3)$	0.0	200	5
$C \text{ (g/m}^3)$	8.6	2.0	8.44
$C_s \text{ (g/m}^3)$	-	-	8.6
$H \text{ (m)}$	-	-	1
$U \text{ (m/s)}$	-	-	1
$K_d \text{ (/day)}$	-	-	0.3
$K_r \text{ (/day)}$	-	-	0.3
$K_a \text{ (/day)}$	-	-	0.7

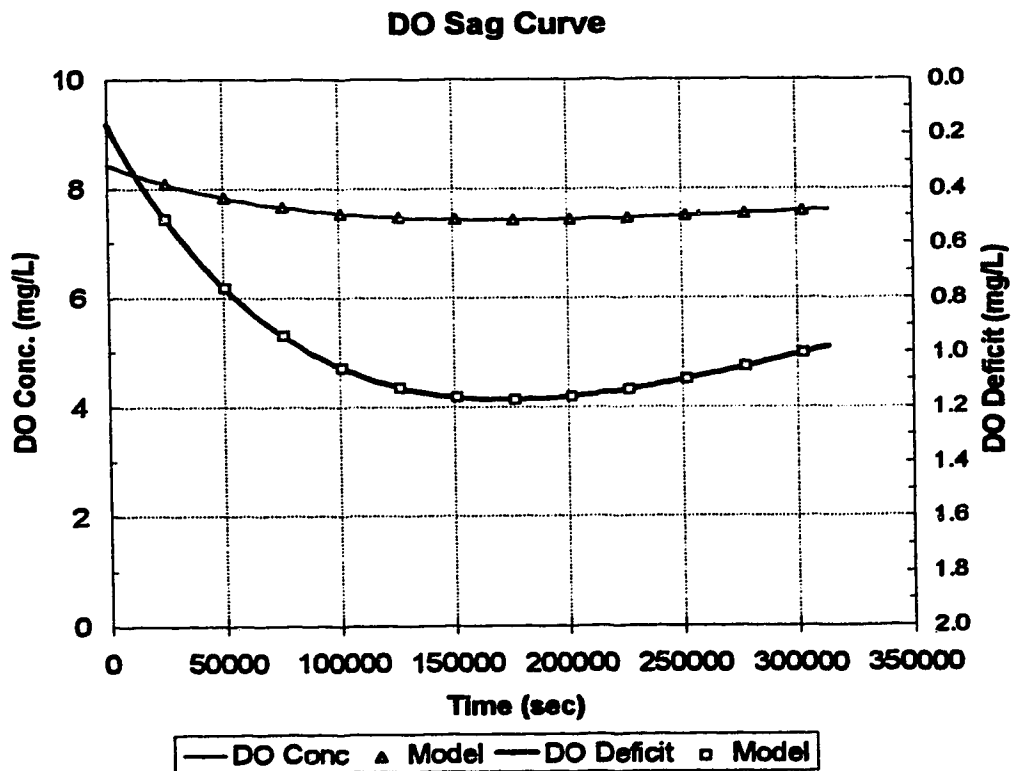


Figure 6.1 Comparison of model output and Streeter-Phelps analysis.

The periodic input of carbonaceous BOD used by Li is given by:

$$L_{(x=0,t)} = L_A \left[1 + A_s \sin\left(\frac{2\pi t}{T}\right) \right] \quad [137]$$

where: $L_{(x=0,t)}$ is the fully mixed CBOD at the discharge point at time t ,
 L_A is the mean fully mixed CBOD over one cycle at the source,
 A_s is amplitude, and
 T is the period.

Li's solution for BOD and the DO deficit downstream of the input are given by:

$$\frac{L_{(x',t')}}{L_A} = \exp(-K_d' \cdot x') \cdot \left\{ 1 + A_s \cdot \sin\left(\pi \cdot \frac{(t' - x')}{2}\right) \cdot \left(1 - \frac{\pi^2 x' \delta}{4}\right) \right\} \quad [138]$$

and

$$\begin{aligned} \frac{D_{(x',t')}}{L_A} = & \left[\frac{K_d}{K_s - K_d} \right] \cdot \left[\exp(-K_d' \cdot x') - \exp(-K_s' \cdot x') \right] \cdot \\ & \cdot \left\{ 1 + N \cdot \sin\left(\pi \cdot \frac{(t' - x')}{2}\right) \cdot \left(1 - \frac{\pi^2 x' \delta}{4}\right) \right\} \end{aligned} \quad [139]$$

where: $L_{(x',t')}$ is the CBOD concentration,
 $D_{(x',t')}$ is the dissolved oxygen deficit = $(C_s - C_{(x',t')})$,
 C_s is the saturation dissolved oxygen concentration,
 $C_{(x',t')}$ is the dissolved oxygen concentration,
 t' is normalized time = $(4t)/T$,
 x' is normalized distance = $(4x)/(UT)$,
 K_d is CBOD exertion rate coefficient,
 K_s is the reaeration rate coefficient,
 K_d' is the normalized CBOD exertion rate coefficient = $(K_d T)/4$,
 K_s' is the normalized reaeration coefficient = $(K_s T)/4$,
 δ = $(4E_x)/(U^2 T)$, and
 E_x is the longitudinal mixing coefficient.

A plot of normalized CBOD concentrations (based upon Li's solution) resulting from a continuous sinusoidal input with $A_s = 1$ for 6 and 12 hour periods is shown in

Figure 6.2. The kinetic parameters and flow characteristics used in the solution are shown in Table 6.1. The Streeter-Phelps solutions which do not account for dispersion are also shown in Figure 6.2. The attenuation of the maximum and minimum BOD concentrations by dispersion effects can be seen in Li's solution in comparison to the Streeter-Phelps solution. It can also be seen that the dispersion effect is more pronounced for the shorter wavelength (input cycle period).

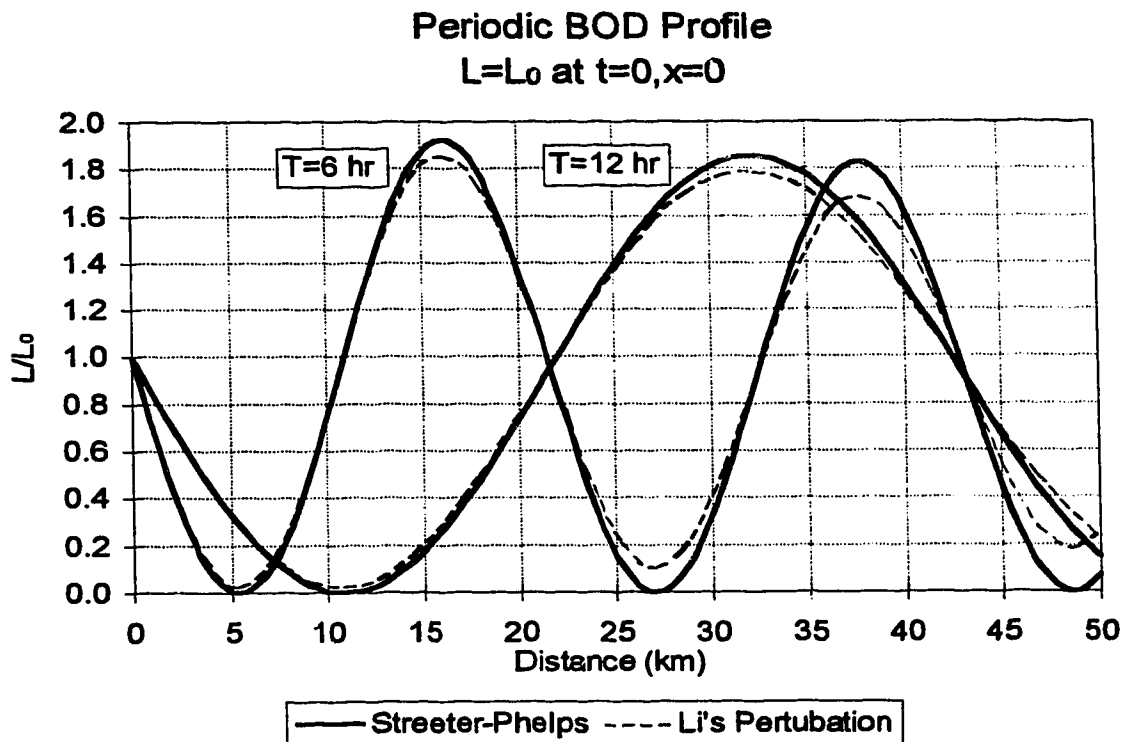


Figure 6.2 Comparison of periodic BOD profiles computed using Li's solution and the Streeter-Phelps model - modified from Koussis et al. (1990).

Table 6.2 Parameters used for periodic BOD calculations.

Parameter	
Amplitude at the source, A_s	1.0
Mean flow velocity, U (m/s)	1.0
Longitudinal mixing coefficient, E_x (m^2/s)	50
CBOD rate constant, K_d (/day)	0.2

Both the AOG method and Li's analytical solution account for longitudinal dispersion. However, it is difficult to make a direct comparison between the results of the two methods due to the manner in which each handles the longitudinal dispersion. The Li solution relies solely on a longitudinal mixing coefficient because it is one-dimensional and can not account for any differential advection. The AOG method assumes longitudinal diffusion is small and relies solely on differential advection to account for longitudinal dispersion.

In order to compare the two methods the varying trapezoidal channel shown in Figure 6.3 was selected for use with the AOG model. The channel geometry was intended to simulate a sinusoidal meander sequence. The flow and streamtube boundaries were chosen so the velocity through each streamtube, over one meander sequence, would be approximately 1.0 m/s. BOD was input to the model as a line source across the channel at $x=0$ according to Equation [137]. The kinetic coefficients and other pertinent parameters used in the simulation are listed in Table 6.3. Li's analytical solution was calculated for comparison using the same kinetic parameters and the mean channel velocity from the numerical simulation (1.0 m/s).

Table 6.3 Parameters used in the AOG model, Li's solution BOD-DO deficit comparisons.

Parameter	
Amplitude at the source, A_s	1.0
Period, T (hrs)	12
Mean flow velocity, U (m/s)	1.0
Longitudinal mixing coefficient, E_x (m^2/s)	50
Dimensionless transverse mixing coefficient, β	0.3
CBOD rate constant, K_d (/day)	0.2
Reaeration rate constant, K_a (/day)	0.7
Time step in numerical solution (secs)	100

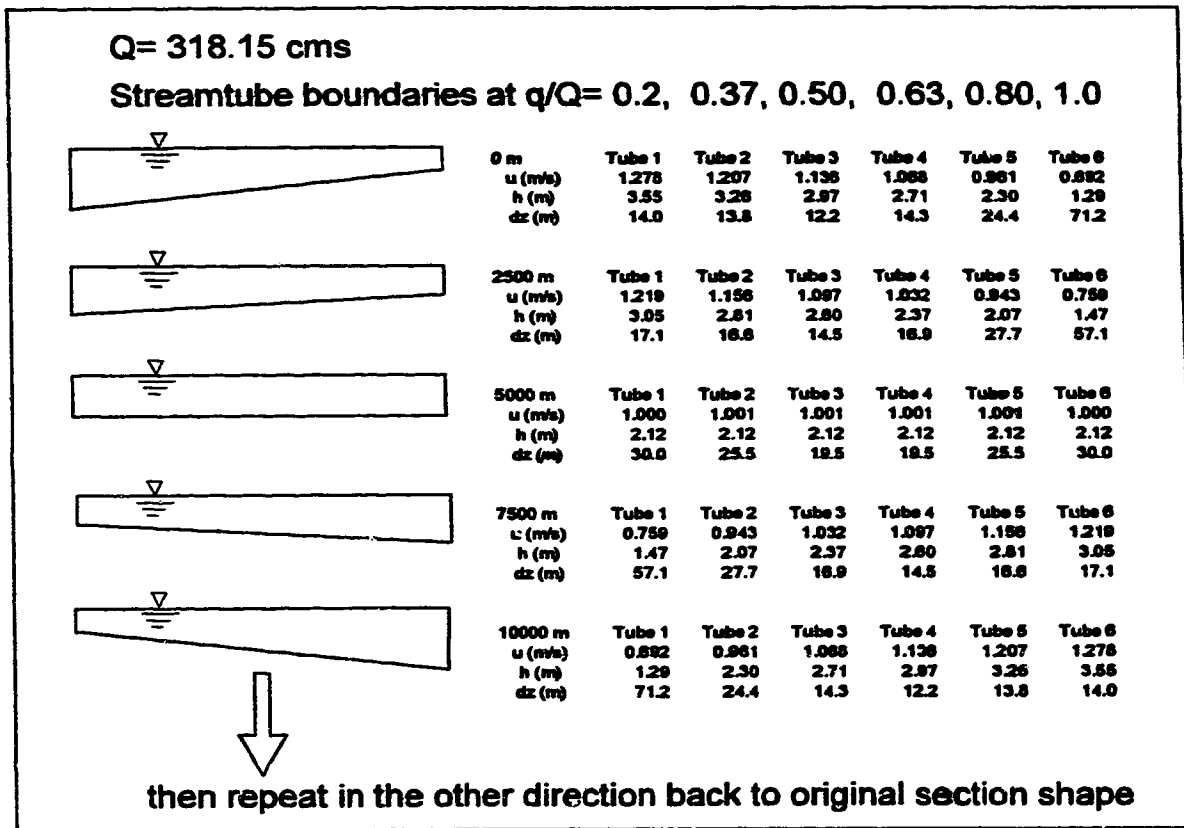


Figure 6.3 Trapezoidal channel sequence used for comparison to Li's solution.

The channel shape and flow characteristics used in the numerical model are reasonably representative of field conditions. Therefore, for the model output to be comparable to Li's solution, the value of the longitudinal mixing coefficient used in Li's solution should fall within the range of coefficients typical for natural streams. A compilation of measured longitudinal dispersion coefficients given by Rutherford (1994) indicates a range of approximately 10 to 100 m²/s is typical.

The results of the model simulation using $\beta = 0.3$ for the dimensionless transverse mixing coefficient are shown in Figure 6.4 and Figure 6.5 in comparison to Li's solution using $E_x = 50$ m²/s. The match between the model mean results and the analytical solution is very good. Some discrepancy in time of travel is evident between the analytical solution and the simulation for tubes 1 and 6 due to the reduced velocity near the boundary. An indication of the sensitivity of the analytical solution to the value selected for E_x is shown in Figure 6.6. It appears that reasonable agreement is obtained for any value of E_x within the typical range for natural streams.

Although these comparisons of the model to analytical solutions are not conclusive evidence that the AOG method can be used to simulate unsteady BOD-DO kinetics in the transverse mixing zone, they are certainly very encouraging. They demonstrate that the BOD-DO kinetics are easily incorporated into the model and are accurate over several thousand time steps. The next step in the verification process is to attempt to use the model to simulate measured DO and BOD levels in the transverse mixing zone downstream of an actual wastewater discharge.

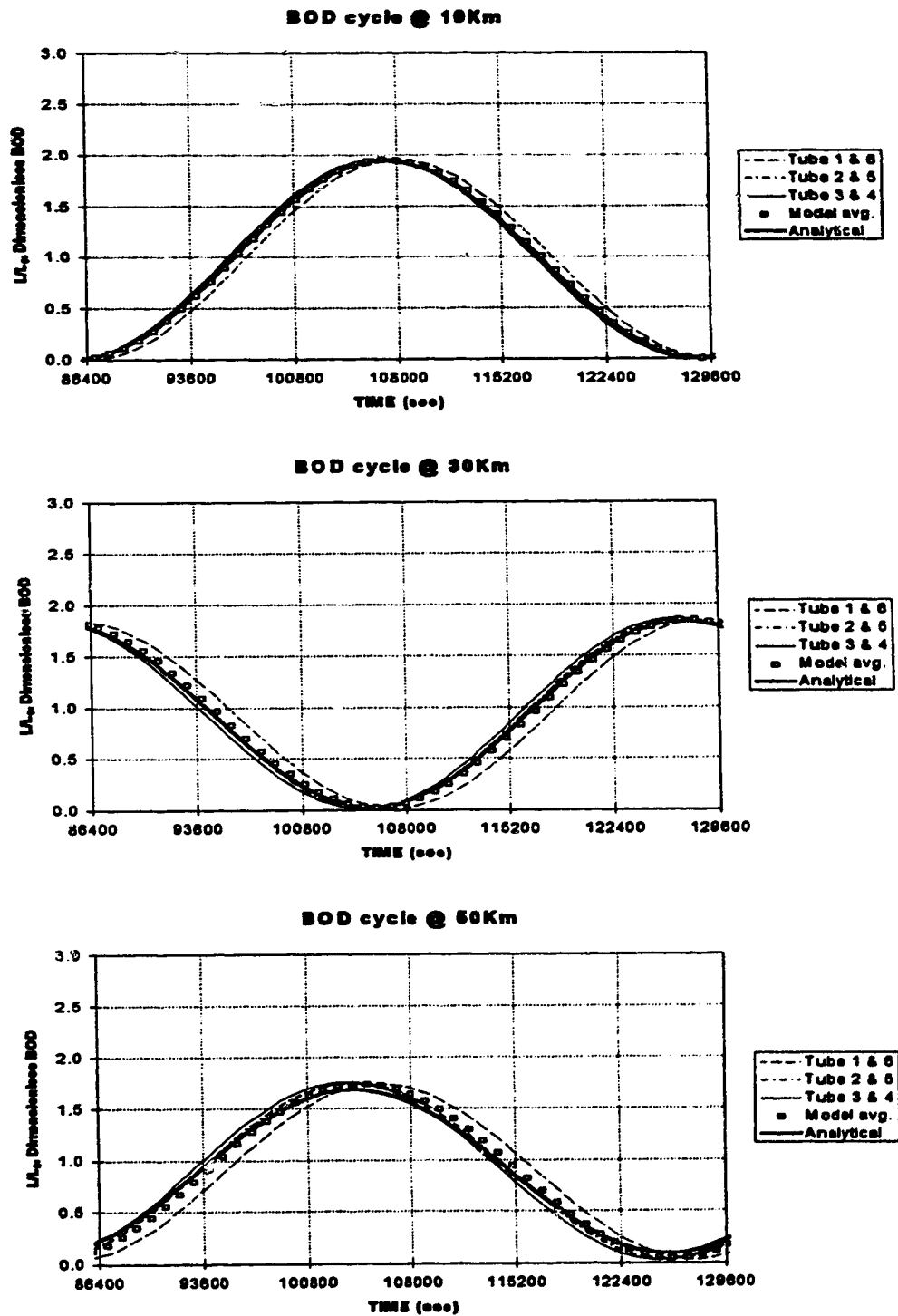


Figure 6.4 Biochemical oxygen demand simulations vs. Li analytical solution, $\beta = 0.30$ for the numerical model, $E_x = 50 \text{ m}^2/\text{s}$ for the analytical model.

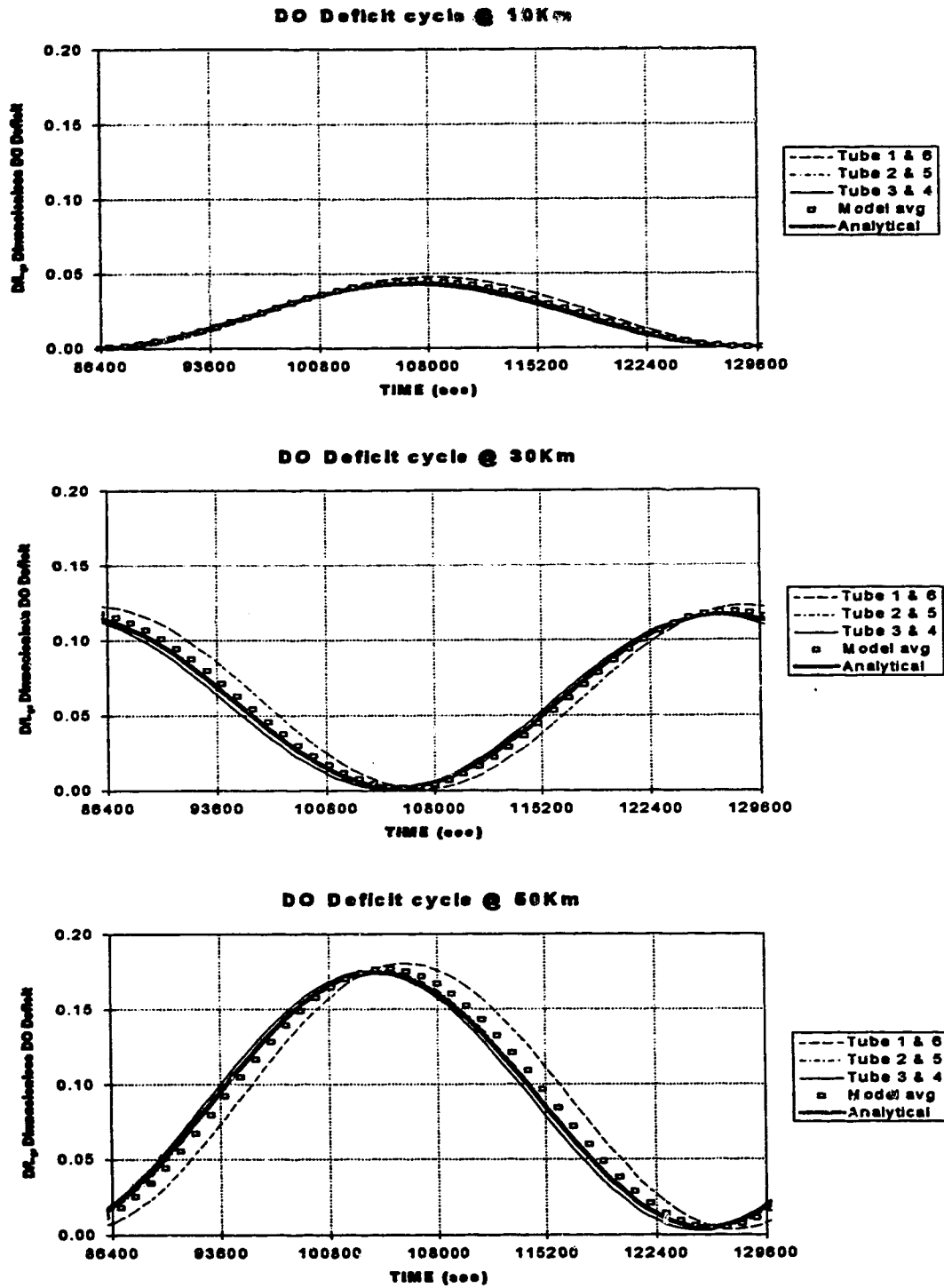


Figure 6.5 Dissolved oxygen deficit simulations vs. Li analytical solution, $\beta = 0.30$ for the numerical model, $E_x = 50 \text{ m}^2/\text{s}$ for the analytical model.

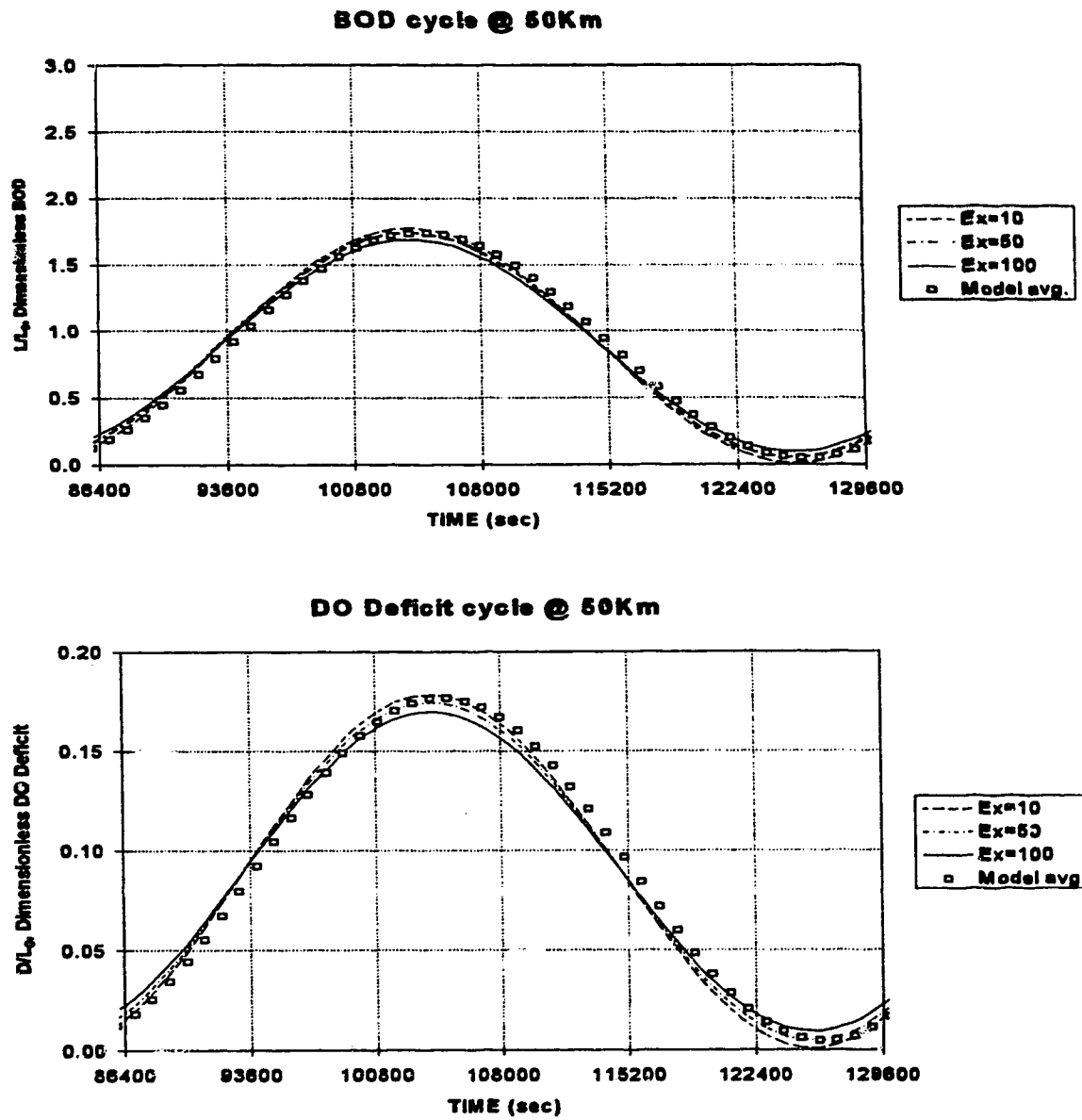


Figure 6.6 BOD and DO analytical solutions for $E_x = 10$ to $100 \text{ m}^2/\text{s}$ vs. numerical solution for $\beta = 0.3$.

6.2.3 Field verification - South Saskatchewan River downstream of Saskatoon

6.2.3.1 Background

The City of Saskatoon (COS) has a population of approximately 190,000 and is located on the South Saskatchewan River. Domestic wastewater is collected at the City's pollution control plant and treated to primary standards before it is discharged to the South Saskatchewan River. The pollution control plant is currently being upgraded to secondary treatment, but before initiating this upgrade the COS conducted a comprehensive study of the river downstream of the plant (City of Saskatoon, 1984, 1985)

During the study period water quality and hydrometric data were collected at several cross sections within the transverse mixing zone downstream of the plant. As part of the study, detailed measurements of DO and BOD variations were taken across several transects over a 48 hour period. This data set, together with the river hydrometric surveys and the plant effluent characteristics and flow, provide an opportunity for further verification of the AOG method adapted for BOD-DO kinetics.

6.2.3.2 Hydrometric data

The relevant portion of the overall COS study reach is shown in Figure 6.7. Transects 5 to 8 are located in the transverse mixing zone. Hydrometric surveys of these sections were conducted in June and July, 1984 approximately one to two months before the 48 hour BOD-DO water quality measurements. However, because the river flow through the Saskatoon is regulated by Gardiner Dam no stage adjustment was required for the sections during the water quality survey. Total river flow during both periods was approximately 50 m³/s. Standard cross section plots, velocity and flow distributions for each of the transects is given in Appendix D.

The flow distributions and channel geometry shown in the Appendix D were scaled from the COS report (City of Saskatoon, 1985). The flow distributions were derived from velocity measurements taken by the COS at each section. The velocity distributions shown in the Appendix D were derived by the author using the COS flow distributions and the channel geometry. The slope of the river downstream of the treatment plant was taken to be 0.0004 on the basis of information presented by Smith and Wigham (1989).

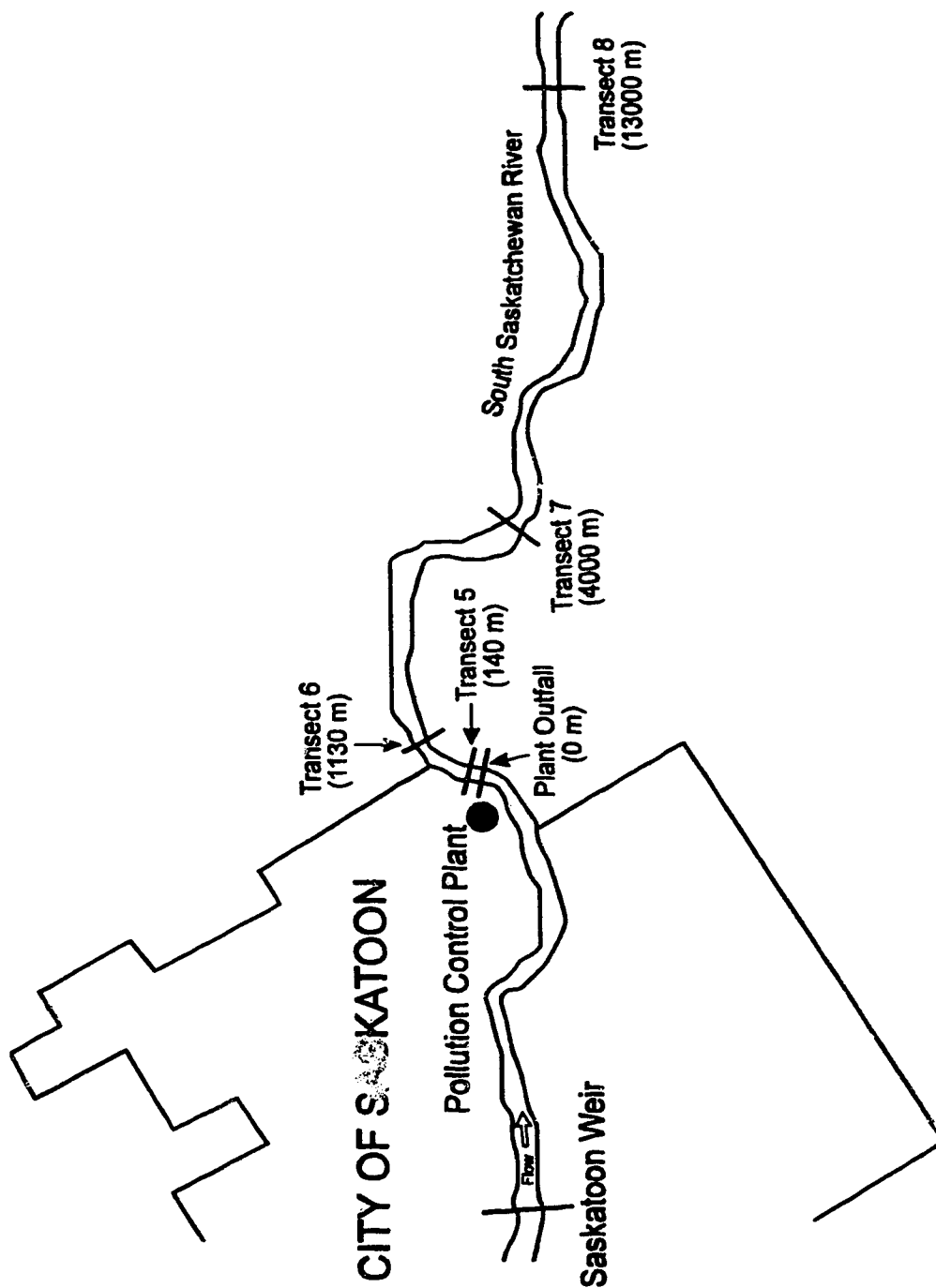


Figure 6.7 South Saskatchewan River downstream of Saskatoon.

6.2.3.3 Transverse mixing

The transverse mixing characteristics of the river reach downstream of the pollution control plant were determined using the chloride content of the effluent as a tracer. Detailed measurements of chloride concentration were taken across each transect and modelled assuming steady state input (City of Saskatoon, 1985). The same approach was used in the present study to determine appropriate values for the transverse mixing coefficient to be used in the BOD-DO mixing and reaction model. The optimum values of β were determined by comparing the predicted chloride distribution to the measured distribution at each transect.

Effluent and river flows, and chloride concentrations, are shown in Figure 6.8 and Figure 6.9. The effluent chloride mass flow is shown in Figure 6.10. Unfortunately the detailed chloride measurements at each transect were not conducted on the same dates as the effluent measurements. However, flow conditions at the plant are reasonably consistent from day to day so the mass flow shown in Figure 6.10 is considered representative. Consequently an average chloride mass flow rate of 94.0 g/s was input into the model. The model results were then scaled in order to compensate for deviations from this average rate due to diurnal variation. The scaling factor used was the ratio of the measured chloride mass flow at each transect over the combination of the assumed input rate and background levels (see Table 6.4).

The river channel was divided into 16 streamtubes with the following boundaries: $q/Q = 0.08, 0.14, 0.20, 0.26, 0.32, 0.36, 0.39, 0.44, 0.50, 0.56, 0.62, 0.68, 0.76, 0.86, 0.94$ and 1.00. Streamtubes were concentrated in the region of the river containing the effluent plume. The average chloride mass flow was continuously placed into streamtube 7 ($q/Q = 0.36$ to 0.39) to simulate the discharge from the plant's submerged outfall. A time step of 60 seconds was chosen on the basis of the criteria outlined previously. All the streamtube geometric parameters, the initial estimates of β , the channel slope and the time step were assembled into the GRIDGEN parameter file in order to run the model.

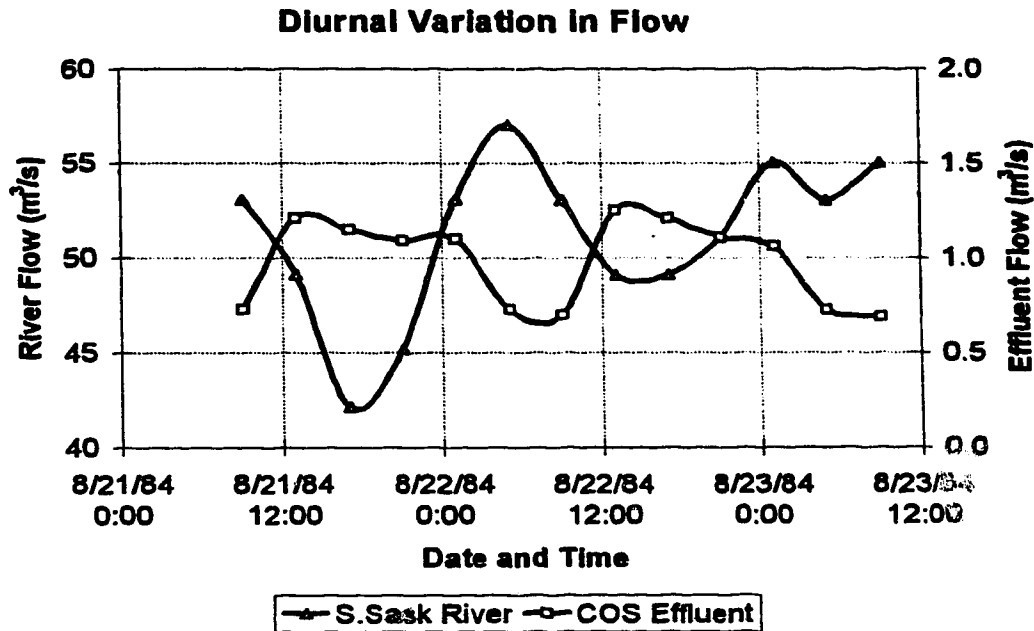


Figure 6.8 Diurnal variations in flow, Saskatoon Pollution Control Plant and South Saskatchewan River.

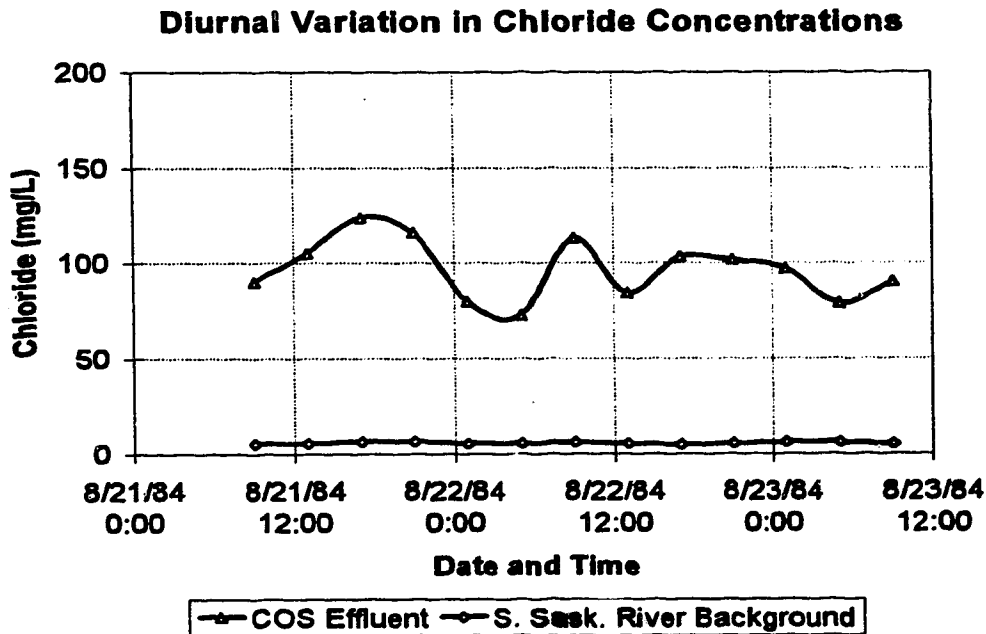


Figure 6.9 Diurnal variations in chloride concentrations, Saskatoon Pollution Control Plant and South Saskatchewan River.

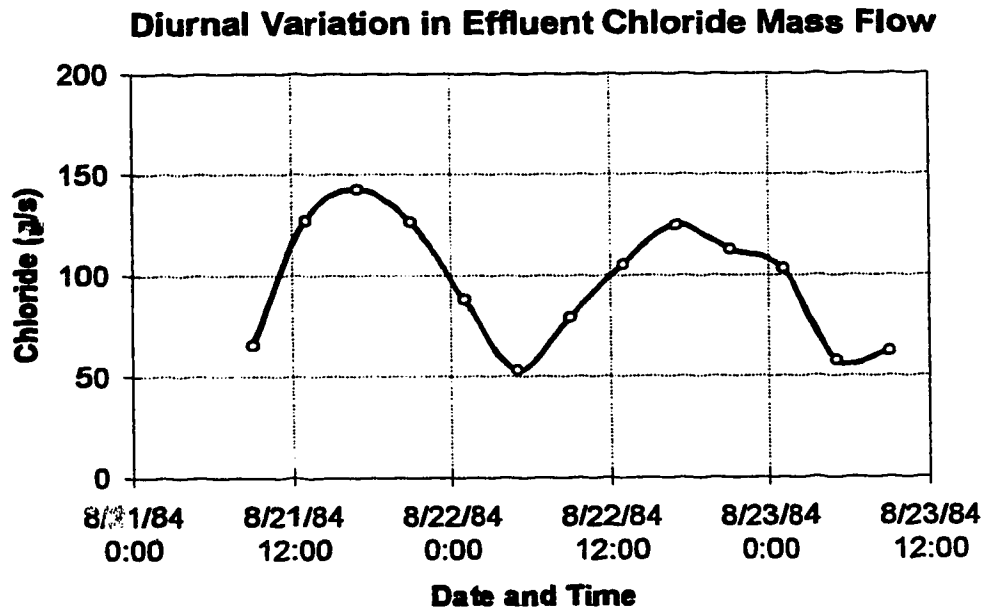


Figure 6.10 Effluent chloride mass flow, Saskatoon Pollution Control Plant.

Table 6.4 South Saskatchewan River chloride mass recovery ratios.

Section	Avg. Chloride Mass Flow ¹ g/m ³ s	Meas. Chloride Mass Flow g/m ³ s	Ratio
Transect 5	391.0	388.7	0.99
Transect 6	391.0	459.9	1.18
Transect 7	391.0	475.3	1.22
Transect 8	391.0	477.9	1.22

¹ Includes chloride input and background readings

The results of the mixing simulations are shown in Figure 6.11. The output distributions give a reasonable representation of the measured concentrations. The distribution at Transect 7 is slightly skewed to the left in comparison to the measured values. It is speculated this shift is the result of the severe bend located just upstream of the section. By Transect 8 the effluent is almost completely mixed across the channel and the distribution is well predicted by the model. The final values selected for β are listed in Table 6.5.

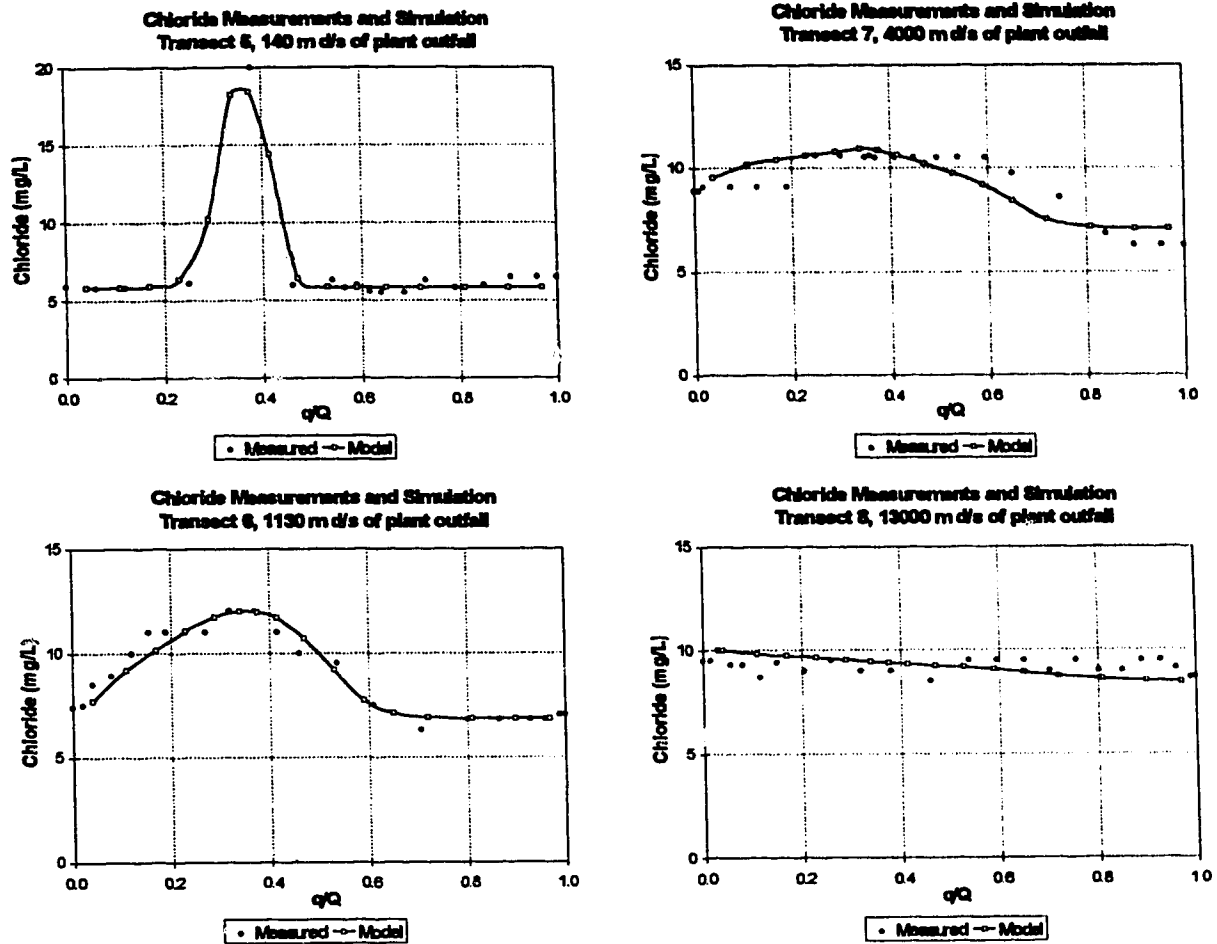


Figure 6.11 Chloride concentration measurements and simulations, South Saskatchewan River downstream of the Saskatoon Pollution Control Plant, input @ $q/Q = 0.36$ to 0.39 .

Table 6.5 South Saskatchewan River dimensionless mixing coefficients.

Section	Location (m)	β
Transect 5	140	0.10
Transect 6	1130	1.00
Transect 7	4000	2.00
Transect 8	13000	2.00

6.2.3.4 Model input

6.2.3.4.1 CBOD and NBOD

The primary effluent discharged to the river contains significant concentrations of CBOD and NBOD. The effluent and river background concentrations of CBOD and TKN were measured every four hours during the 48 hour dissolved oxygen survey (City of Saskatoon, 1984). The results of these measurements are shown in Figure 6.12. The effluent mass flow of CBOD and TKN is shown in Figure 6.13. The CBOD measurements were 20 day standard bottle tests with NBOD inhibition. The 20 day tests were assumed to be a reasonable estimate of the ultimate CBOD of the waste.

The time series of input concentrations was entered into the model from a data file. Each line of the file contained the appropriate CBOD and TKN background concentrations for the first element in streamtubes 1 to 6, and 8 to 16; and the initial CBOD and TKN concentration in streamtube 7. The initial concentration in streamtube 7 was determined assuming the effluent and background mass flow was completely mixed within the first element. The mass flow rates and background levels for each time step were interpolated between the measurement times.

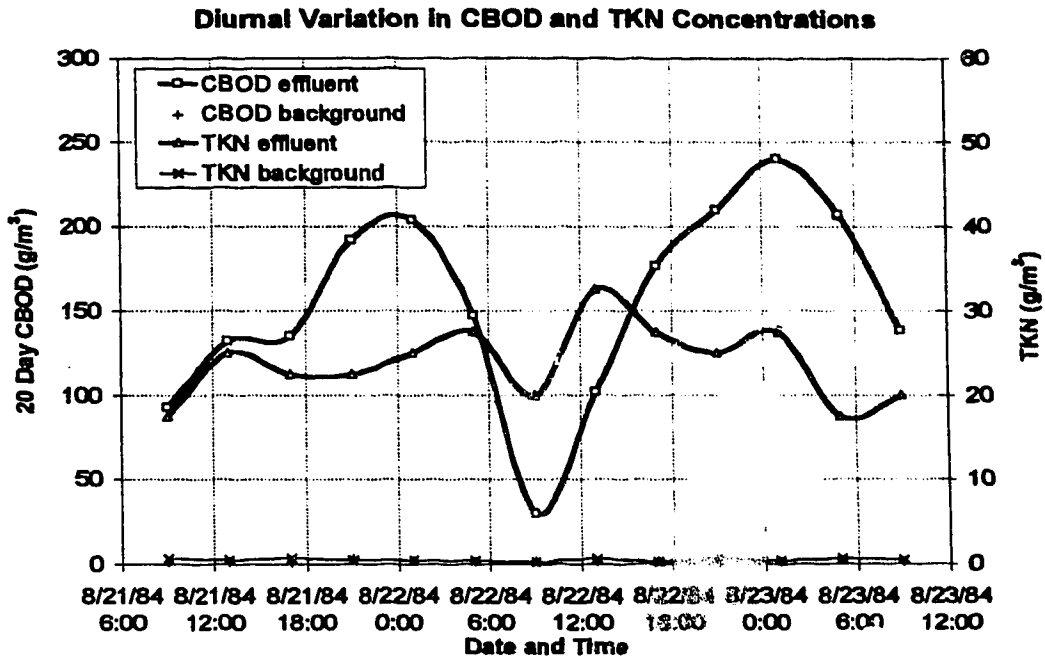


Figure 6.12 Diurnal variation in CBOD and TKN concentration, Saskatoon Pollution Control Plant and South Saskatchewan River.

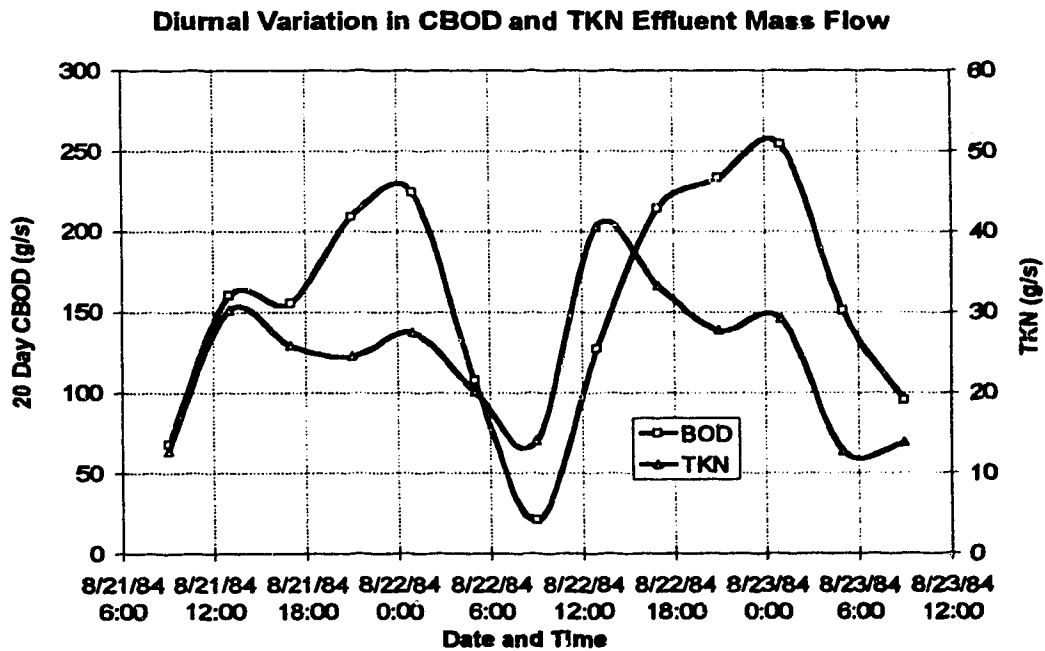


Figure 6.13 Diurnal variation in CBOD and TKN mass flow, Saskatoon Pollution Control Plant.

6.2.3.4.2 Dissolved Oxygen

Background DO concentrations in the river were near saturation values throughout the monitoring period. Measurements taken at Transect 4 (upstream of the outfall) are shown in Figure 6.14 compared to the estimated saturation value. Fresh water saturation concentrations were calculated using the following relationship given by APHA (1985):

$$\ln(C_{s,1atm}) = -139.34411 + \frac{1575701 \times 10^5}{T_K} - \frac{6.642308 \times 10^7}{T_K^2} + \frac{1243800 \times 10^{10}}{T_K^3} - \frac{8.621949 \times 10^{11}}{T_K^4} \quad [140]$$

where: $C_{s,1atm}$ is the saturation concentration (mg/L at 1 atm), and
 T_K is the temperature in °K.

The saturation concentration is corrected for elevation according to the following approximation given by Zison et al. (1978):

$$C_s = C_{s,1atm} \left(\frac{100 - 0.0115Y}{100} \right) \quad [141]$$

where: Y is the height above sea level in metres.

The saturation concentration varies as a function of the diurnal water temperature cycle of the river. Because the reaeration rate is a function of the saturation deficit it is important to be able to predict the saturation value at any time during the day. A composite plot of water temperature vs. time of day measured at all monitoring locations is shown in Figure 6.15. A sinusoidal curve was fit to the data giving the following water temperature vs. time relationship:

$$T_C = T_{cm} \left\{ 1 + T_{ca} \sin \left(2\pi \frac{[t - t_{offset}]}{T} \right) \right\} \quad \begin{aligned} T_{ca} &= 0.07 \text{ for } 0 < t < 720 \\ T_{ca} &= 0.10 \text{ for } 720 \leq t < 1440 \end{aligned} \quad [142]$$

where: T_C is the water temperature in °C,
 T_{cm} is the base water temperature in °C,
 T_{ca} is the temperature offset in °C,
 t is the time in minutes ranging from 0 to 1440,
 t_{offset} is 720 minutes, and
 T is 1440 minutes (1 day).

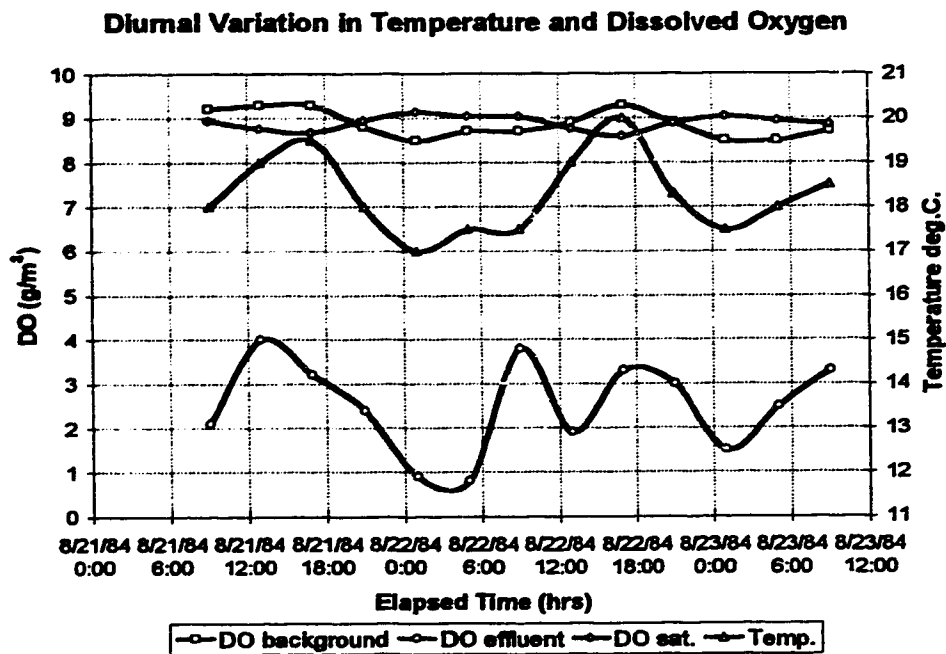


Figure 6.14 Diurnal variation in DO concentration, Saskatoon Pollution Control Plant and South Saskatchewan River.

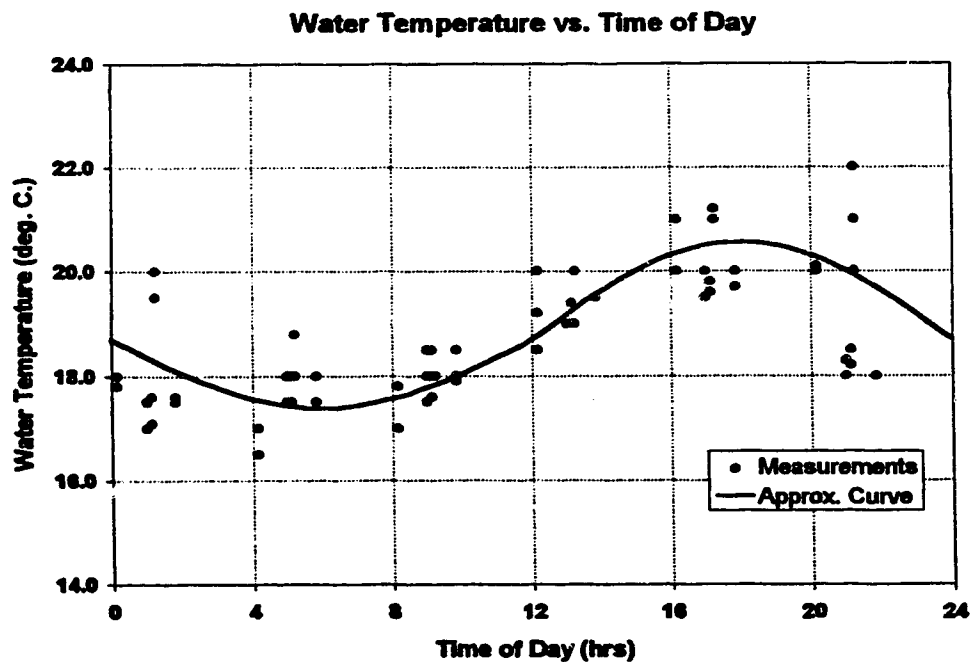


Figure 6.15 Diurnal temperature cycle, South Saskatchewan River downstream of Saskatoon.

Equations [140], [141] and [142] can be used to approximate the dissolved oxygen saturation concentration as a function of time during the survey period.

Dissolved oxygen levels in the effluent are shown in Figure 6.14. The time series of effluent concentrations and the background levels were input to the model from a data file. A mass balance calculation similar to that described for CBOD and TKN was required to determine the initial dissolved oxygen in streamtube 7 for each timestep. The mass flow rates and background levels for each time step were interpolated between the measurement times.

6.2.3.4.3 Photosynthetic oxygen production and respiration rates

A large population of submerged aquatic plants develops downstream of the plant outfall each summer as a result of the nutrient content (nitrogen and phosphorus) of the primary effluent (Landine 1970, City of Saskatoon, 1985). Visual surveys indicated approximately 50 % of the river bottom for the first 20 km downstream of the effluent discharge was covered by the aquatic plants (City of Saskatoon, 1985). The weed growths are so extensive they influenced the velocity distributions in the river. In addition to their physical influence on the river the aquatic plants also produce large quantities of oxygen via photosynthesis during daylight hours. Oxygen is also continuously consumed by the aquatic plants due to respiration. In many river situations photosynthesis and respiration effects are small and can often be ignored. However, in this situation effects are very significant and can not be ignored.

The 48 hour dissolved oxygen surveys conducted on the river provide an opportunity to quantify the level of photosynthetic oxygen production. A typical diurnal cycle is shown schematically in Figure 6.16. Several methods are available to determine P, the rate of photosynthetic oxygen production, over a river reach given diurnal curves similar to Figure 6.16 for the upstream and downstream boundaries (Odum, 1956; Marzolf et al., 1994). These methods produce reach averages between sections and are more suited to cross sectional averaged curves. For two-dimensional mixing analysis a method of quantifying P at a specific point in the river is required.

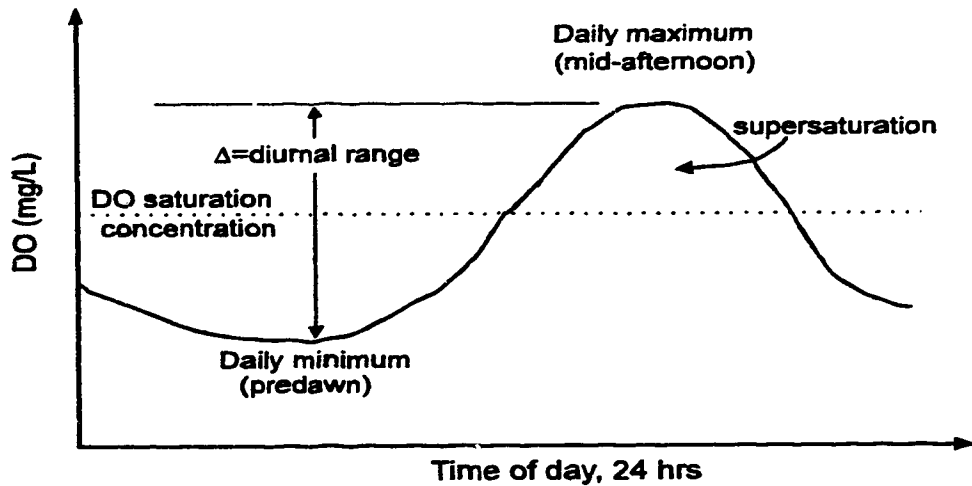


Figure 6.16 Typical diurnal cycle of photosynthetic oxygen production by aquatic plants—modified from Thomann and Mueller (1987).

Di Torro (1992) describes a method well suited for use in mixing analysis. His method estimates P_{avg} on the basis of the difference between the maximum and minimum oxygen concentration measured over a diurnal cycle at a particular location. The relationship for P_{avg} is given as follows:

$$\frac{\Delta}{P_{avg}} = \frac{(1 - e^{-K_a f T})(1 - e^{-K_a T(1-f)})}{f K_a (1 - e^{-K_a T})} \quad [143]$$

where: Δ is the difference between the maximum and minimum dissolved oxygen concentration over one diurnal cycle (mg/L or g/m³),
 P_{avg} is 24 hour average photosynthetic oxygen production (mg/L day),
 T is one day,
 f is the fraction of the day between sunrise and sunset (day), and
 K_a is the reaeration coefficient (/day).

Dissolved oxygen measurements were taken at transects 5 to 8, at transverse locations corresponding to $q/Q = 0.2, 0.4, 0.5, 0.6, 0.8$, over a 48 hour period (City of Saskatoon, 1984). The average Δ value over the two diurnal cycles measured, hydraulic parameters and estimated K_a using the O'Connor Dobbins formula, and the estimated volumetric and areal P_{avg} for each monitoring point are shown in Table 6.6. Plots of the average areal rates of oxygen production across each transect are shown in Figure 6.17.

Table 6.6 Average photosynthetic oxygen production rates, South Saskatchewan River downstream of Saskatoon.

Location	avg. delta (mg/L)	est. depth (m)	est. velocity (m/s)	est. K_a (/day)	est. vol. P_{avg} (mg/L/day)	est. areal P_{avg} (g/m ² /day)
140 m d/s						
q/Q=0.2	0.82	1.75	0.35	0.98	2.796	4.882
q/Q=0.4	0.95	1.62	0.37	1.12	3.236	5.227
q/Q=0.5	0.90	0.89	0.35	2.67	3.360	2.990
q/Q=0.6	0.90	0.35	0.28	9.85	6.551	2.280
q/Q=0.8	1.18	1.09	0.26	1.72	4.115	4.492
1130 m d/s						
q/Q=0.2	1.05	0.57	0.34	5.17	4.928	2.803
q/Q=0.4	0.93	0.65	0.38	4.53	4.077	2.636
q/Q=0.5	1.03	0.80	0.30	2.92	3.903	3.131
q/Q=0.6	0.88	0.95	0.43	2.73	3.281	3.102
q/Q=0.8	1.20	1.08	0.47	2.32	4.364	4.713
4000 m d/s						
q/Q=0.2	3.05	1.02	0.30	2.02	10.874	11.128
q/Q=0.4	3.15	0.64	0.16	3.03	12.099	7.713
q/Q=0.5	3.60	0.83	0.29	2.69	13.459	11.216
q/Q=0.6	2.85	1.00	0.28	2.00	10.149	10.149
q/Q=0.8	1.55	1.26	0.37	1.64	5.407	6.829
13000 m d/s						
q/Q=0.2	10.00	0.86	0.26	2.44	36.699	31.661
q/Q=0.4	9.30	1.04	0.32	2.03	33.185	34.512
q/Q=0.5	9.45	1.04	0.37	2.17	34.031	35.392
q/Q=0.6	9.15	0.89	0.34	2.64	34.059	30.405
q/Q=0.8	7.60	0.85	0.30	2.66	28.335	24.204

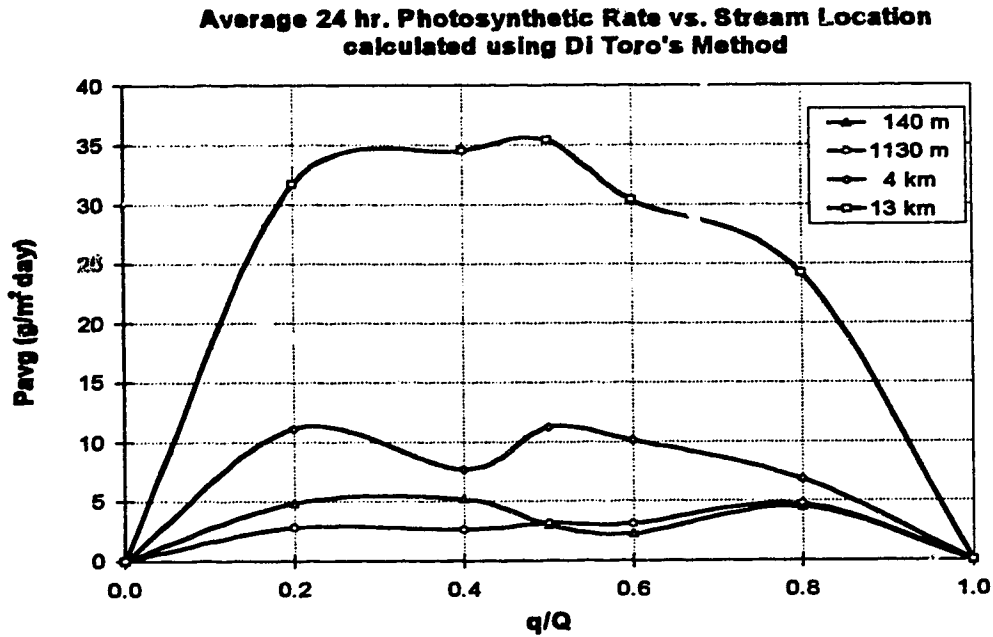


Figure 6.17 Average photosynthetic oxygen areal production rates, South Saskatchewan River downstream of Saskatoon.

P_{avg} values are satisfactory for long term modeling of DO with time increments of one day or more. However for short term simulations $P_{(t)}$ must be predicted throughout the diurnal cycle. The daily photosynthetic cycle is often idealized as a half sine wave or parabolic shape during the photoperiod (sunrise to sunset). During the remainder of the day $P=0$. Di Torro represented this idealization of the photosynthetic cycle using the following Fourier series equation:

$$P_{(t)} = P_{avg} \left\{ 1 + \frac{\pi T}{2f} \sum_{n=1}^{\infty} b_n \cos \left[\frac{2\pi n}{T} \left(t - \frac{f}{2} \right) \right] \right\}$$

$$b_n = \cos \left[\left(\frac{n\pi f}{T} \right) \frac{\frac{4\pi T}{f}}{\left(\frac{\pi T}{f} \right)^2 - (2\pi n)^2} \right] \quad [144]$$

Equation [144] was used in an analytical solution for the one-dimensional steady state oxygen mass balance equation (O'Connor and Di Torro, 1970). The equation allows direct estimation of $P_{(t)}$ from clocktime, however it is somewhat cumbersome to program.

Rutherford (1977) used the following parabolic equation to estimate $P_{(t)}$

$$P_{(t)} = P_{avg} \frac{6T(t_2 - t)(t - t_1)}{f(t_2 - t_1)^2}, \quad \text{for } t_1 \leq t \leq t_2$$

$$P_{(t)} = 0, \quad \text{for } t < t_1 \text{ or } t > t_2 \quad [145]$$

where: t_1 is the sunrise time,
 t_2 is the sunset time.

Rutherford used equation [145] in a one-dimensional numerical solution to the oxygen mass balance equation. The relationship requires a logical operation to test for $t_1 < t < t_2$ but is much easier to program than Di Torro's method. For this reason Rutherford's method was used in the current model.

A comparison of the two methods is shown in Figure 6.18. The curve shapes are very similar. Note also that Rutherford defines P_{avgf} as the mean during the photoperiod rather than over 24 hours, therefore:

$$P_{avgf} = P_{avg} \frac{T}{f} \quad [146]$$

With Rutherford's equation $P_{(t)}$ can be predicted provided P_{avg} is known over the entire grid (t is simply the initial clocktime plus the accumulation of time steps; t_1 and t_2 for a particular date and global position are well documented). The distribution of P_{avg} is known at each of the measured sections (see Figure 6.17 and Table 6.6). P_{avg} is then determined for each element in the grid by interpolation between sections in similar fashion as the hydraulic and mixing parameters.

The respiration rate of photosynthetic plants is generally assumed to be a constant proportion of P_{avg} . Therefore, at any location the respiration rate is given by:

$$R = K P_{avg} \quad [147]$$

where: R is the respiration rate of dissolved oxygen consumption,
 K is a constant.

$K = 0.6$ was used in the simulation on the basis of information presented by Rutherford (1977) and Sculthorpe (1967).

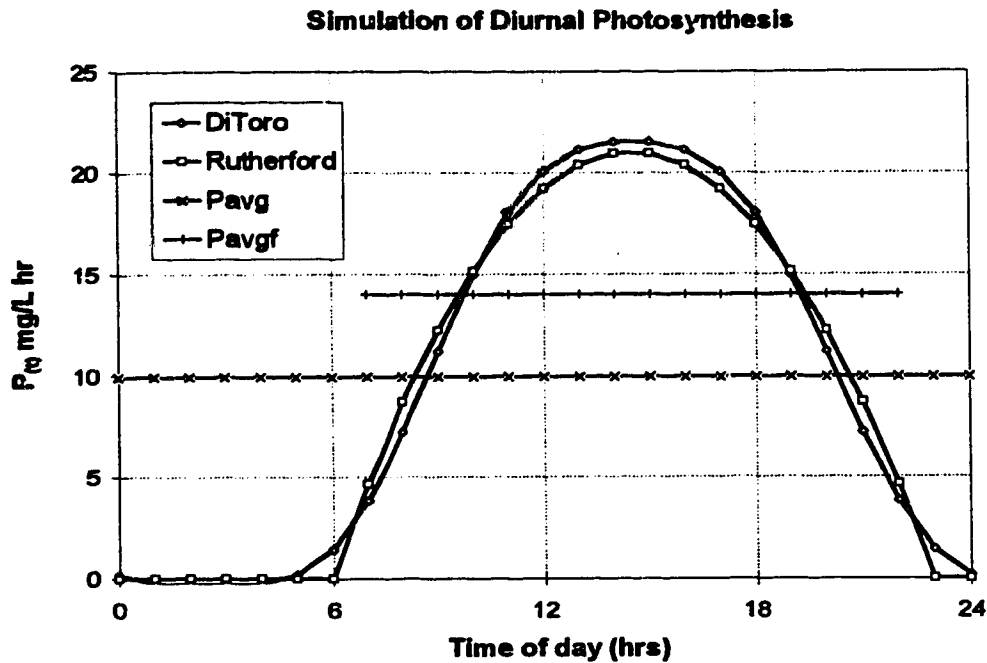


Figure 6.18 Simulation of diurnal photosynthetic oxygen production.

6.2.3.4.4 Sediment Oxygen Demand

No information was available in the COS report regarding sediment oxygen demand. However, the effluent does contain volatile suspended solids (average volatile suspended solids content of the effluent was 43 mg/L with a range of 25 to 59 mg/L). Therefore some of these solids must settle and end up on the bottom of the river. In addition, the large biomass of aquatic plants produced each season dies over the winter providing an additional source of organic solids. Solids from both sources are subject to the degradation processes discussed earlier and therefore will eventually exert some sediment oxygen demand. This demand is generally considered to be zero order, i.e. independent of the BOD concentration in the overlaying water column.

The following approach was utilized to quantify the SOD in the South Saskatchewan River simulation. The model was first run using optimized rate coefficients for CBOD and NBOD and assuming SOD to be zero. The dissolved oxygen results were then compared to the measured dissolved oxygen values and adjustments made to the

SOD rate in order to obtain the best visible match. Finally, the SOD rates were compared to recently published measurements of SOD on other rivers to ensure the rates chosen were not unreasonable.

The SOD rates were entered into the model using the same approach as for the P_{avg} values. Estimates across each section were entered into the parameter file for a modified version of the grid preprocessing program. The modified version of GRIDGEN then interpolates between sections and determines an appropriate estimate for SOD for each element in the grid.

6.2.3.5 Model results for CBOD

Soluble CBOD compounds exert a first order, time-dependent oxygen demand within the river. As noted above particulate organic matter is also present and will settle to the bottom and exert a sediment oxygen demand. Unfortunately insufficient information was available to assess the removal rate of organic particulates via settling within the river. Nor was information available as to what fraction of the CBOD was the result of soluble compounds and what fraction was the result of particulates. Consequently, it had to be assumed the influence of CBOD removal by settling in the river was small and that CBOD removal could be characterized using first order kinetics and a single rate coefficient K_d for CBOD exertion.

Composite CBOD samples had been taken at each transect during the dissolved oxygen survey (City of Saskatoon, 1984). Identical volumes were taken from each transverse location (i.e. $q/Q=0.2, 0.4, 0.5, 0.6, 0.8$) and combined into an overall composite sample for analysis. Presumably insufficient BOD bottles had been available for individual analysis at each location.

The model was run to simulate the mixing and reaction of CBOD only according to Equation [128]. The model output for an assumed value of K_d was compared to the CBOD measurements. The averaged results at the five transverse sampling locations at each transect were used to simulate the composite sample. Several runs were conducted for a range of K_d values. The results of this process are shown in Figure 6.19.

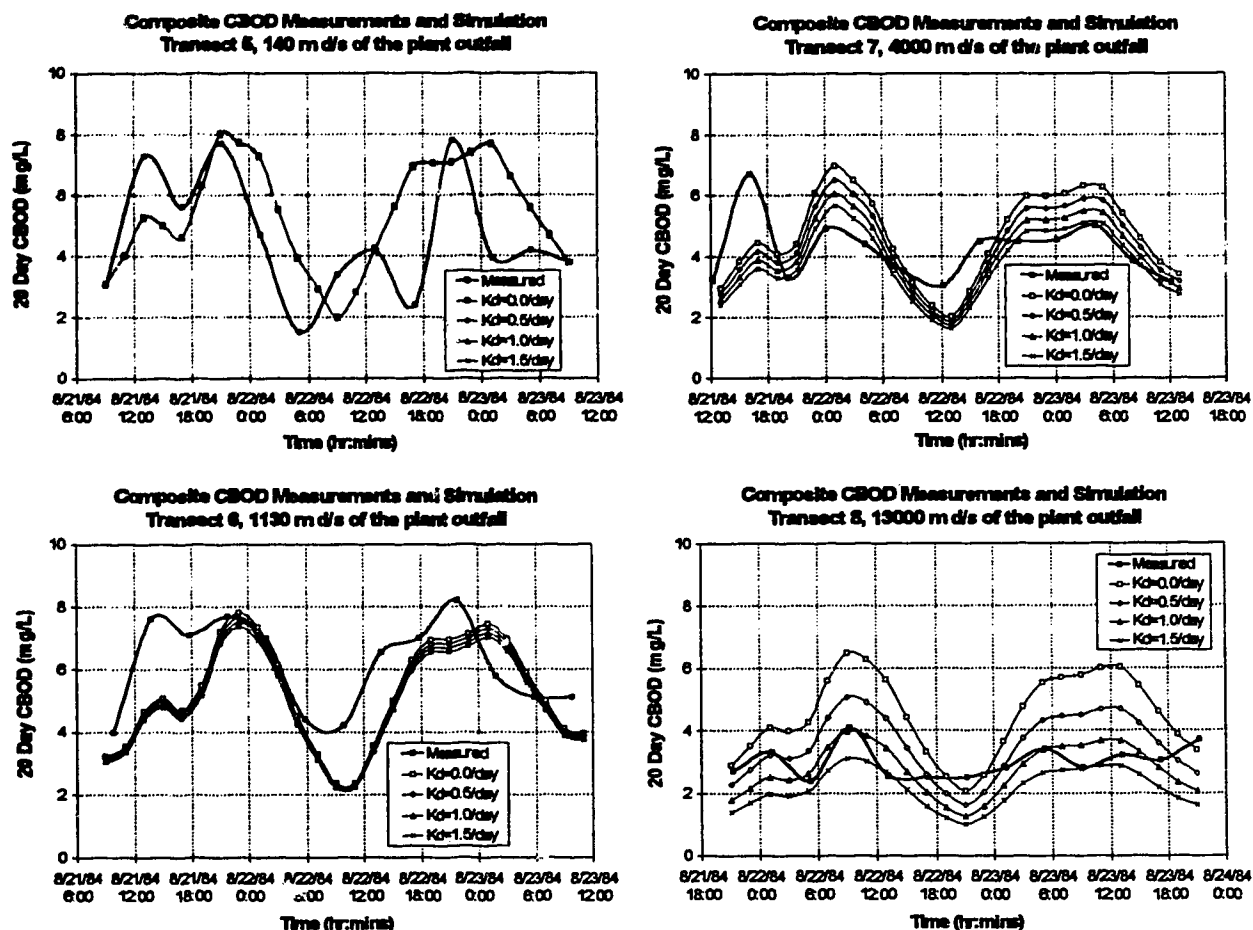


Figure 6.19 CBOD composite concentration measurements and simulations, South Saskatchewan River downstream of the Saskatoon Pollution Control Plant.

There is considerable discrepancy between the model simulations and the measured composite samples however the same general trends are discernible in the plots. This is not unexpected as the results of CBOD bottle tests can be quite variable. Ideally replicate samples should have been taken and analysed rather than relying on the results of a single sample. Despite this problem it appears that a value of $K_d = 1.0$ gives a reasonable fit to the data.

6.2.3.6 Model results for NBOD

As described previously NBOD is determined using the TKN concentration. The comments above regarding soluble and particulate CBOD also apply to the NBOD. In addition, the composite sampling procedure used by the City of Saskatoon was identical to that described for CBOD.

Model runs were conducted to simulate the mixing and decay of TKN according to Equation [129]. The model output for assumed values of K_n was compared to the TKN measurements. The averaged results at the five transverse sampling locations at each transect were used to simulate the composite samples. The results of these simulations are shown in Figure 6.20.

Similar general trends are evident in the measured and simulated curves at Transects 5 and 8, but there is a very large discrepancy between the model results and the measured curves at Transects 6 and 7. It is unlikely this discrepancy is solely the result of experimental error or poor sampling techniques. The curve labeled 'maximum concentration' in the plots for Transects 6 and 7 represents the peak concentrations predicted by the model at each section with K_n set equal to zero. In other words, this is the maximum concentration that would occur at the section for only mixing and transport. Curiously at both transects the diluted composite samples, which presumably have also undergone some degradation in TKN, greatly exceed the predicted maximums. A plausible explanation for this curious finding is that NH_4 , which is measured as a portion of the TKN, is being produced locally as a result of degradation processes in the bottom sediments.

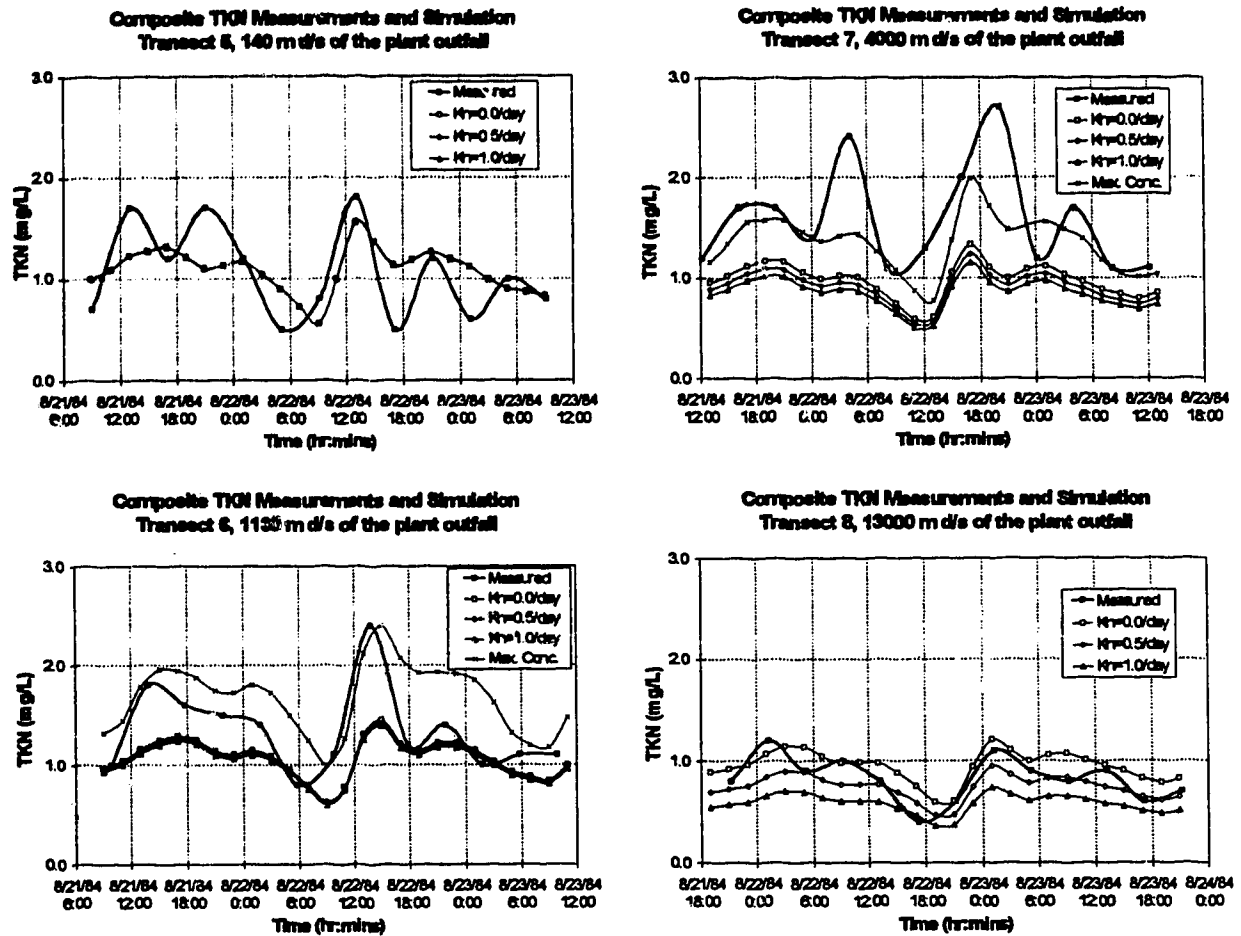


Figure 6.20 TKN composite concentration measurements and simulations, South Saskatchewan River downstream of the Saskatoon Pollution Control Plant.

Di Torro et al. (1990) present a detailed mathematical model describing the conversion of settled organic particulates to NH_4^+ and CH_4 in the anaerobic layers of the bottom sediments. The model is shown schematically in Figure 6.21. The NH_4^+ and CH_4 released to the overlying aerobic layers in the sediment produce an oxygen demand (i.e. SOD). However, not all the NH_4^+ and CH_4 produced is necessarily oxidized in the aerobic layer. A portion is released to the overlying water column in soluble and gaseous form. This source of soluble NH_4^+ could account for the increase in TKN content of the composite samples. The CH_4 is only sparingly soluble so the majority escaping to the water column would be in gaseous form. The gaseous CH_4 and NH_4^+ would travel to the surface and be released to the atmosphere. Unfortunately there is insufficient data available to attempt to incorporate Di Torro's SOD model into the overall mixing model.

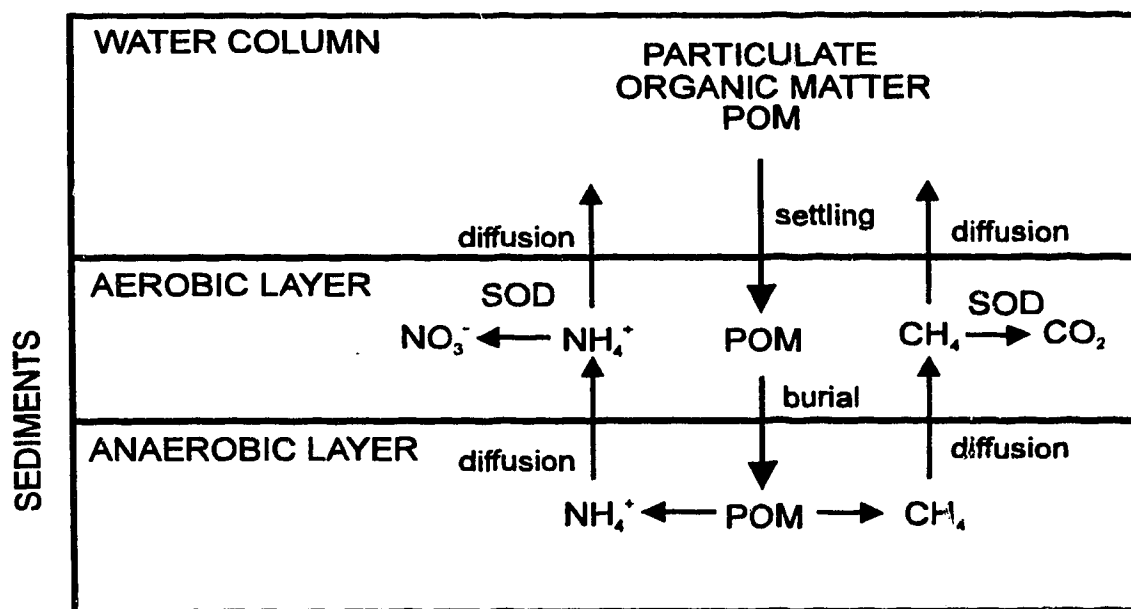


Figure 6.21 Schematic representation of ammonia and methane generation in bottom sediments - modified from Di Torro et al. (1990).

The approach used to model the TKN, and ultimately the NBOD in the dissolved oxygen simulations, was to choose a K_n value consistent with the results at Transect 8. A value of $K_n = 0.5/\text{day}$ was chosen. The excess TKN at Transects 6 and 7 was accounted for as SOD in this region of the reach. Initially attempts were made to incorporate an NH_4^+ flux into the model in this region creating a non-point source of NBOD. However, the results of these efforts always produced an enormous oxygen demand much further downstream due to the first order kinetics. It appeared the oxygen demand was more immediate and local and therefore the SOD zero order kinetics approach proved to be much more successful in simulating the dissolved oxygen profiles at Transects 6 and 7.

6.2.3.7 Model results for Dissolved Oxygen

The mixing and reaction of dissolved oxygen is described by Equation [127]. The followings points summarize the key aspects of running the model for the dissolved oxygen simulations:

1. Simultaneous simulations of DO, CBOD and TKN were required for the DO modelling. Therefore, three sets of element concentrations had to be accounted for during the model run. Mass input of CBOD, TKN and DO were all handled as outlined above.
2. The values for K_d and K_n determined from the CBOD and TKN simulations were used along with CBOD and TKN concentrations to predicted the DO consumption during each time step.
3. The average photosynthetic oxygen production was mapped on the calculation grid and Equation [145] was used to predict instantaneous rates at any element as a function of clocktime.
4. The local respiration rate was determined as a proportion of the local average photosynthetic oxygen production rate using Equation [147].
5. The reaeration term was evaluated for each element at each time step using the local value of K_a and the saturation dissolved oxygen concentration. The local value of K_a was determined using the O'Connor Dobbins equation using the element depth and

flow velocity. The saturation dissolved oxygen concentration was estimated as a function of clocktime using Equations [140], [141] and [142].

6. Estimated local rates of SOD were mapped on the calculation grid using assumed distributions across each of the transects. The SOD was assumed to be concentrated in the region of Transects 6 to 7.

As noted earlier dissolved oxygen measurements were taken at Transects 5 to 8, and at transverse locations corresponding to $q/Q = 0.2, 0.4, 0.5, 0.6, 0.8$, over a 48 hour period (City of Saskatoon, 1984). The measurements were taken with dissolved oxygen sensors and meters which had been calibrated against solutions of known DO determined using the Winkler titrimetric method. APHA (1985).

The model was run for initial estimates of SOD rates in the plume region. These estimates were then revised to obtain the best visual fit possible to the measured C-t curves at each of the transects. The dissolved oxygen measurements and the results of the model simulations are shown in Figure 6.22 to Figure 6.25.

The results of the modelling exercise are quite remarkable considering the number of parameters involved and some of the assumptions that were necessary. The diurnal cycles of oxygen production and the plume influence are well predicted except near the right bank at Transect 7 and at $q/Q = 0.4$ at Transect 5 which is directly downstream of the effluent outlet. The sample results at $q/Q = 0.4$ at Transect 5 appear to represent the background fluctuations only (as indicated by the model results shown for adjacent streamtubes ($q/Q = 0.29$ and 0.47)). It is possible complete vertical mixing may not have been fully established at Transect 5 and therefore DO readings near the surface would not be influenced by the effluent. Another possibility is the transverse location sampled may have been inaccurate. The plume at Transect 5 is quite narrow and therefore any error in transverse location could cause the sample to be taken in a region unaffected by the effluent.

Near the right bank between Transect 6 to 7 the photosynthetic oxygen production may have been much larger than predicted, which would account for the huge supersaturation results recorded during daylight hours.

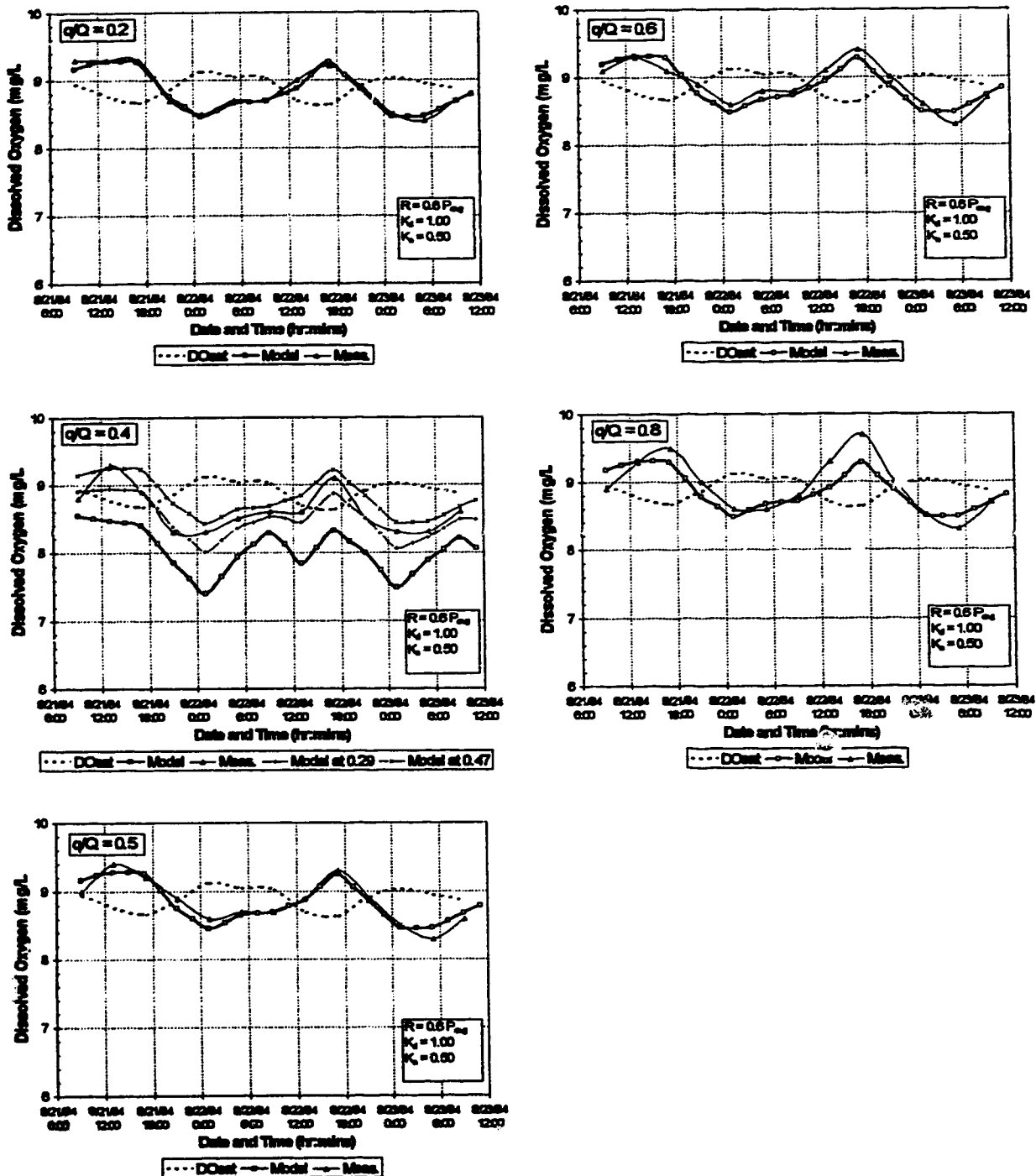


Figure 6.22 Dissolved oxygen measurements and simulations, South Saskatchewan River, Transect 5, 140 m downstream of the Saskatoon Pollution Control Plant.

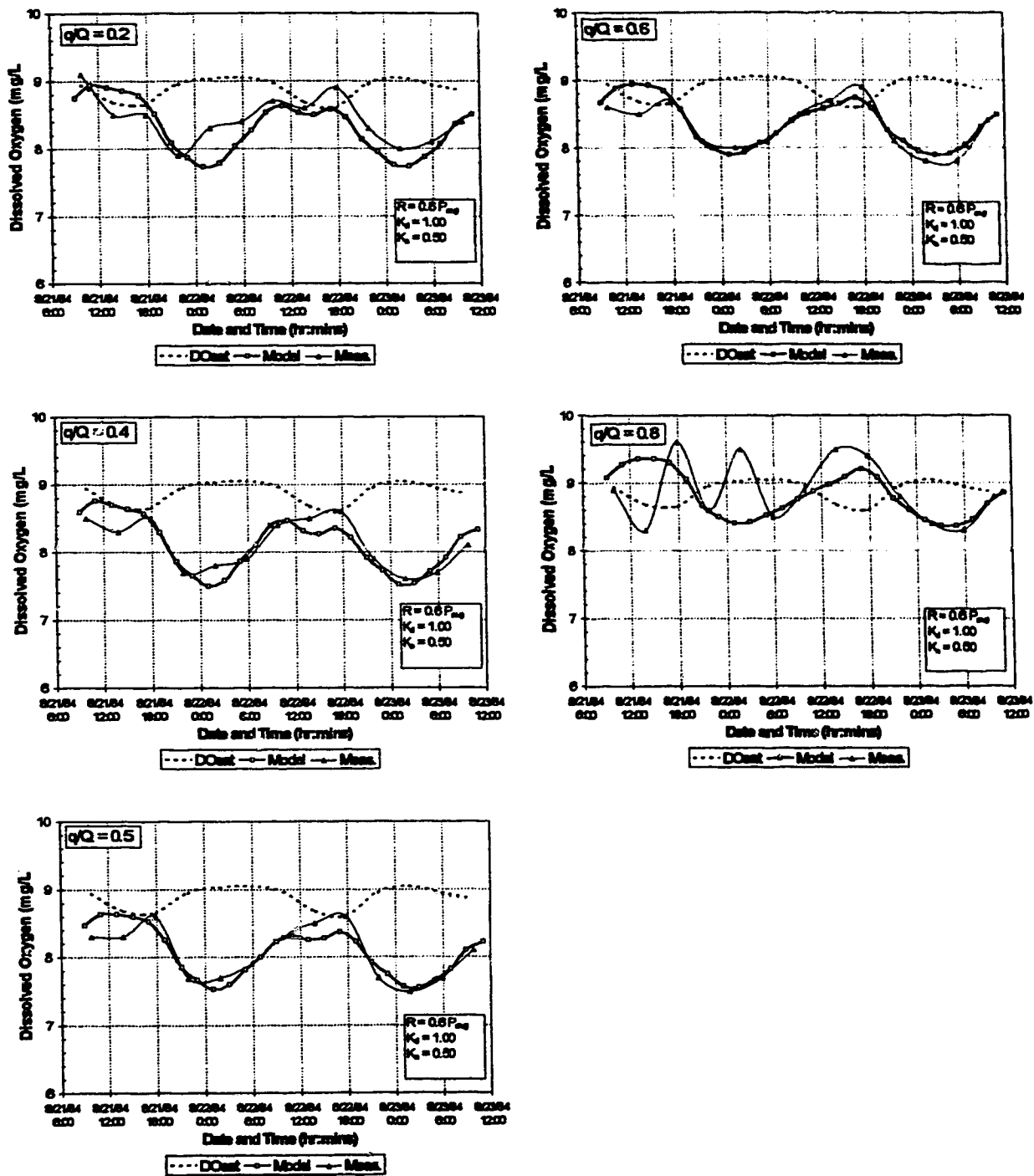


Figure 6.23 Dissolved oxygen measurements and simulations, South Saskatchewan River, Transect 6, 1130 m downstream of the Saskatoon Pollution Control Plant.

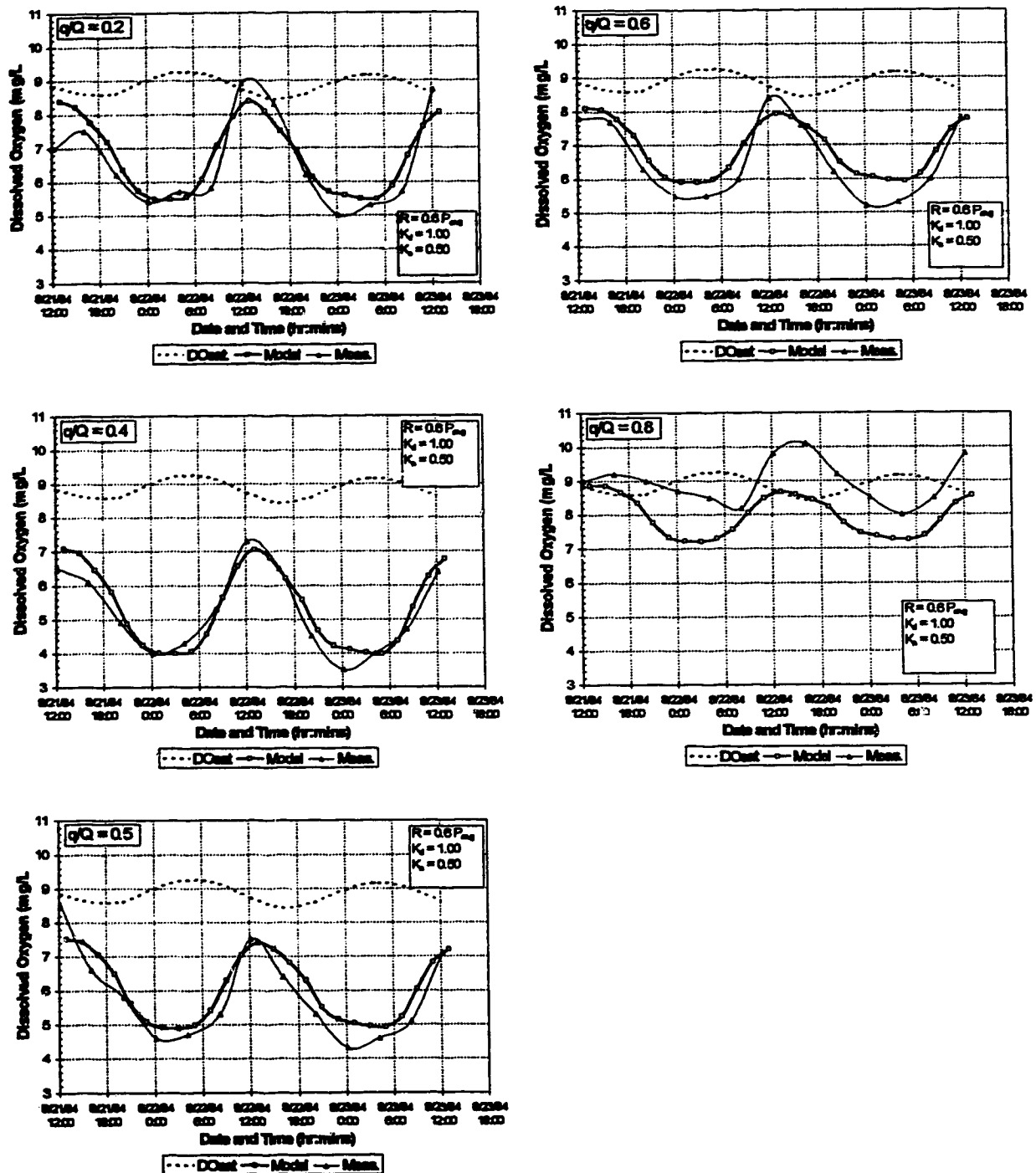


Figure 6.24 Dissolved oxygen measurements and simulations, South Saskatchewan River, Transect 7, 4000 m downstream of the Saskatoon Pollution Control Plant.

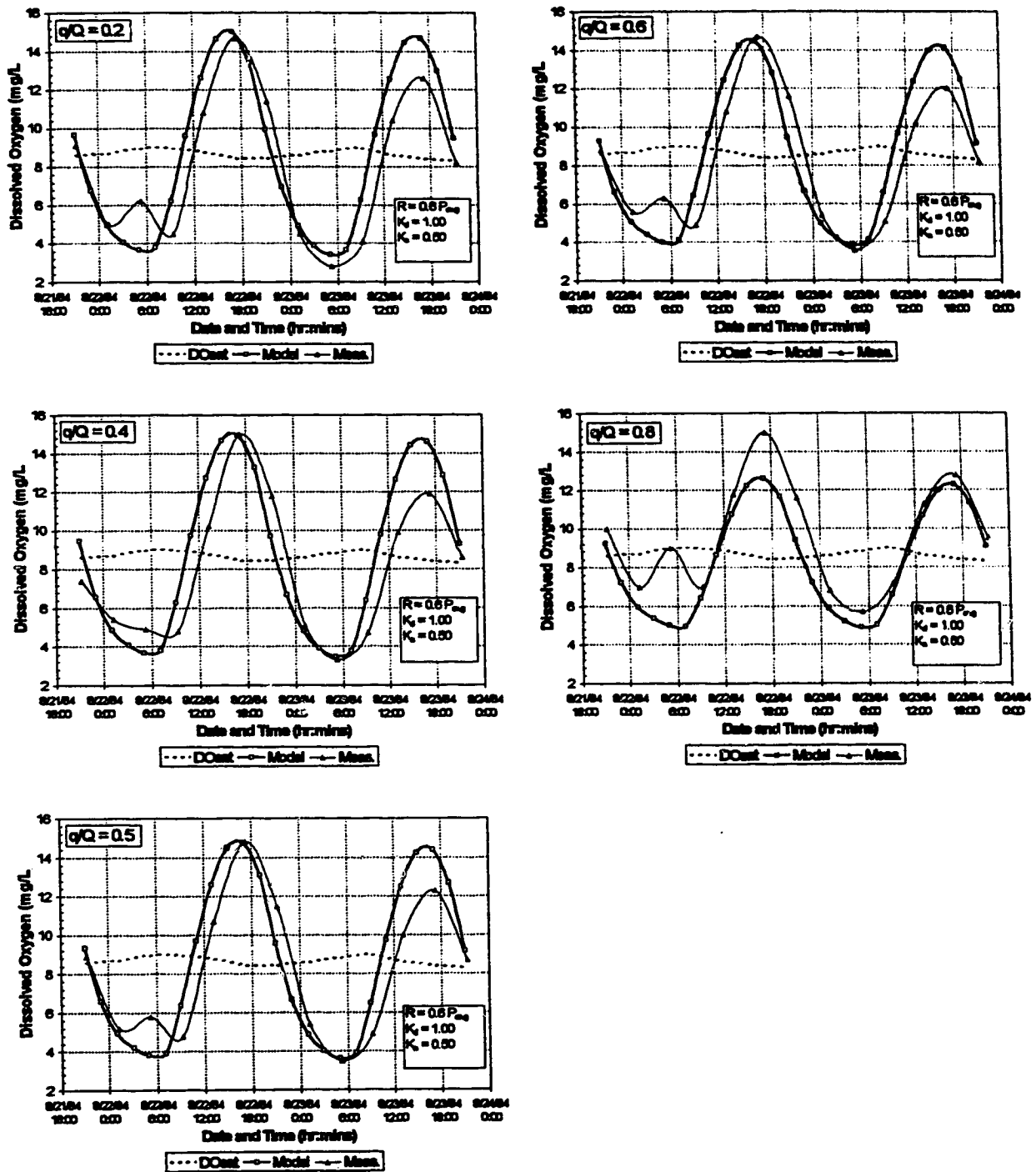


Figure 6.25 Dissolved oxygen measurements and simulations, South Saskatchewan River, Transect 8, 13000 m downstream of the Saskatoon Pollution Control Plant.

6.2.3.8 Model results for Sediment Oxygen Demand

As noted above the SOD estimates were concentrated in the effluent plume region. The final SOD estimates are shown in Table 6.7. Note that an extra section identical to Transect 7 was placed at 5000 m in order to terminate the SOD estimates. Without this extra section values would have been interpolated all the way down to Transect 8 at 13,000 m. With this extra section the modified GRIDGEN preprocessor interpolated values of SOD for elements located in the plume region between Transect 4 (140 m) and 5000 m downstream.

Table 6.7 Sediment oxygen demand estimates.

Streamtube	Sediment Oxygen Demand (g/m ² ·d)				
	Distance downstream (m)				
	0	140	1130	4000	5000
2	0	0	0	0	0
3	0	0	0	25	0
4	0	0	0	25	0
5	0	0	0	30	0
6	0	0	0	30	0
7	0	0	0	35	0
8	0	0	0	35	0
9	0	0	25	40	0
10	0	0	25	40	0
11	0	0	25	40	0
12	0	0	0	0	0

Note: all positions not indicated have SOD = 0

Values used for the SOD rates range from 0 to 40 g/m²·d. The maximum values seem quite high in comparison to some previously published estimates of SOD. For example, SOD resulting from municipal sewage sludge in the vicinity of an outfall was reported to be in the range of 2 to 10 g/m²·d (Thomann and Mueller, 1987). A compilation of SOD values given by Novotny and Olem (1994) are in a range of about 0.3 to 7 g/m²·d. However, SOD is difficult to measure accurately.

The standard measurement procedure for SOD consists of placing a chamber over the sediment layer on the river bed and monitoring changes in the dissolved oxygen over

time. This procedure does not account for any hydrodynamic effects of water flow over the bed surface. An improved measurement method was used by Rutherford et al. (1991) to determine the SOD of the bottom sediments of a mobile bed river in New Zealand downstream of a combined pulp mill and municipal wastewater discharge. The method uses a recirculating chamber with velocity through the chamber matched to actual flow conditions in the river. Using this technique and replicate measurements SOD rates in the range of 15 ± 2 to 32 ± 16 g/m²·d were observed. These measurements are in much closer agreement with the estimates for the South Saskatchewan River. The study reaches also have somewhat similar characteristics as shown in Table 6.8.

Table 6.8 Comparison of study reach characteristics

Parameter	Tawawera River New Zealand	South Sask. River downstream of Saskatoon
Slope	0.0006 to 0.0007	est. 0.0004
Width (m)	21 to 25	180 to 225
Typical summer flow (m ³ /s)	28	50
Mean Velocity (m/s)	0.66 to 0.76	0.28 to 0.37
Mean Depth (m)	1.3 to 1.6	0.7 to 0.8
Bed Material	granular, 0.5 to 1 mm	sandy

Note: the figures shown represent the range of values measured within the study reach

6.2.4 Discussion

Despite some uncertainty in rate coefficients and the SOD rates the AOG model adapted for DO-BOD kinetics was able to very acceptably reproduce the measured DO concentrations vs. time. A more comprehensive data set would allow further verification and development of the model. For instance detailed measurements of suspended solids, CBOD and TKN across each section, similar to the DO measurements on the South Saskatchewan study, would allow better definition of the rate coefficients and allow a consideration of particulate BOD removal by sedimentation.

It would also be preferable to have SOD measurements similar to those described by Rutherford et al. (1991) in order to verify the model. SOD estimates based upon interpolations between measurements could then be directly entered into the model. This

method would involve far less uncertainty and would be preferable to using the curve fitting approach utilized for the South Saskatchewan River data.

Attempts have been made to model aquatic plant biomass as a function of nutrient and solar radiation input (Walker et al. , 1982). This model was reasonably successful but was one-dimensional and involved simulations over an entire growing season. The biomass of aquatic plants and therefore the photosynthetic oxygen production is not simply an immediate response to ambient nutrient levels in the water column. Rather it is a function of nutrient availability from that stored in the bottom sediments and in the plant tissues themselves. Unfortunately the two-dimensional model is not well suited to this type of long term simulation.

For two dimensional modelling the diurnal measurement method of quantifying the photosynthetic oxygen production, as developed by Di Torro (1992), seems more appropriate. Several sets of measurements could be taken over the growing season to determine the worst case scenario to be used in a summer minimum flow situation. This type of measurement would be far easier to obtain than the detailed biomass and nutrient data required to calibrate a biomass production model.

The verification studies with DO-BOD kinetics demonstrates the ease with which the AOG mixing model can be adapted to handle a variety of kinetic calculations. Algorithms previously developed for one-dimensional models and/or continuously mixed batch reactors can be directly utilized in the reaction substep of the AOG model. The time steps requirements for the mixing model appear to be sufficiently small that explicit forward difference expressions can be used for the reaction algorithms without introducing significant error.

6.3 Modelling Methoxychlor-Sediment Interactions

6.3.1 Methoxychlor

Methoxychlor is an organic insecticide that was commonly used as a substitute for DDT after the latter's use was restricted in 1969. Structurally methoxychlor is an analogue of DDT but it is biodegradable and less persistent in aquatic environments. Extensive reviews of methoxychlor chemistry and toxicity are given by Gardner and Bailey (1975) and NRCC (1983).

Methoxychlor was commonly used to control populations of black flies (biting flies) in Western and Northern Canada in the 1970's. The insecticide was generally applied to streams where the flies lay their eggs and the larvae would hatch. The objective was to kill the flies at the larval stage before they emerge as adults. The methoxychlor was generally supplied in a concentrated liquid emulsion of 21 to 25% active ingredient and a petroleum emulsifier. An application would consist of a delivery system to cause the emulsion to mix within the stream to obtain a concentration in the range of 10 to 300 ppb methoxychlor (Gardner and Bailey, 1975).

Several attenuation mechanisms for methoxychlor in aquatic environments are reviewed by Gardner and Bailey (1975). These include photolysis, biological degradation, and adsorption to sediments. The review by the NRCC (1983) states that adsorption to suspended sediments and subsequent deposition is the major removal mechanism. Following deposition, degradation and breakdown of the methoxychlor occurs in the bottom sediments of the water body.

6.3.2 Field Verification Athabasca River downstream of Athabasca

6.3.2.1 Background

Agriculture Canada and the Alberta Research Council (ARC) conducted slug methoxychlor treatment studies of the Athabasca River downstream of Athabasca in the spring of 1974, 1975 and 1976. The results of the associated toxicological and environmental persistence studies, and an analytical analysis of the one-dimensional mixing

and decline of the methoxychlor in this reach of the Athabasca River were reported by Haufe and Croome (1980). The study reach extended from above Athabasca to Fort McMurray and was characterized by approximately forty cross-sections surveyed at various times during the three year program. In 1975 methoxychlor concentrations vs. time were measured at several transverse locations across five of the sections in the first 21.5 km of the study reach (Charnetski et al., 1980). Beyond 21.5 km only a single transverse location was sampled on the assumption that the methoxychlor was uniformly mixed across the channel. The measurements taken in the first 21.5 km will be used for the verification study presented herein.

The ARC also conducted an independent transverse mixing study on the Athabasca River downstream of Athabasca in the fall of 1974 (Beltaos, 1978). The mixing test was not conducted during the period of pesticide treatment as it was feared the fluorescent tracer could influence the effectiveness of the methoxychlor. A two-dimensional analytical analysis of the tracer test was completed to determine the reach-averaged transverse mixing coefficient for the 17 km reach downstream of Athabasca. A one-dimensional analytical analysis of the methoxychlor mixing was also conducted to determine the longitudinal dispersion characteristics of the extended reach all the way down to Fort McMurray (Beltaos and Charnetski, 1980).

6.3.2.2 Hydrometric data

The cross section information available in the blackflies project report (Haufe and Croome, 1980) was supplemented with additional cross-section information obtained from archived records of the Surface Water Engineering Division, Alberta Research Council (ARC, 1975). In total, eighteen cross sections were available from the two sources for the reach of interest. A plan view of the reach and the cross-section locations are shown in Figure 6.26. All the distances shown are from the highway bridge at Athabasca.¹

¹ The distance designations are based upon the ARC unpublished notes which differ slightly from those shown in Haufe and Croome (1980).

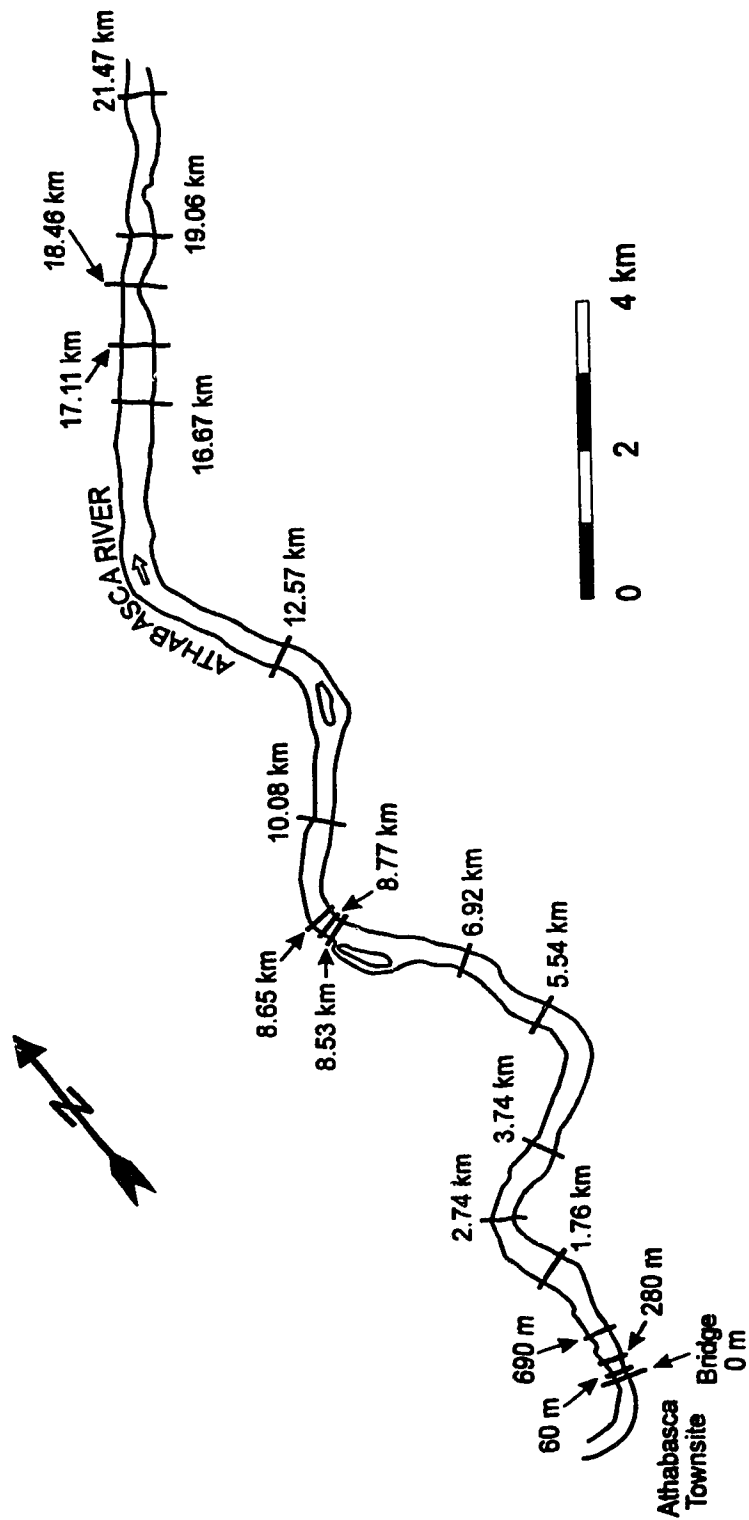


Figure 6.26 Plan view of the Athabasca River study reach.

Unfortunately, none of the sections had been tied to geodetic elevation during surveys and most had not been surveyed on the date of the pesticide injection. In order to use the cross sections the assumed water surface elevation at each location had to be estimated for the date of the injection (June 4, 1975). River discharge records and a gauge discharge relationship were available for the bridge location at Athabasca (Beltaos, 1980c).

As a first estimate, the assumed water surface elevation at each section was adjusted on the basis of the gauging station relationship and the recorded flow for the date of the survey and the date of injection ($484 \text{ m}^3/\text{s}$). This approach was only effective for the sections in the immediate vicinity of the bridge. For the other sections the time of travel indicated by the methoxychlor C-t curves was much shorter than that which was predicted using velocities determined on the basis of the gauge correction. Consequently, the water surface elevations at the other sections was adjusted downward until a reasonable time of travel match was obtained at each section. The flow and date of survey at each of the cross sections together with the final assumed elevation corrections are given in Table 6.9.

Once the water surface elevation at each section was set the mean depth and velocity could be determined. The local velocities and flow distribution were then estimated using a resistance equation relationship. A tabulation of these calculations, a cross section plot, and the estimated flow distribution for each section are presented in Appendix D.

No surveys of the water surface slope through the reach were conducted during the blackfly project or during the ARC tracer study. Instead, Beltaos (1980c) used an average slope of 0.00026 between Athabasca and 91 km downstream which was taken from Kellerhals et al. (1972).

Table 6.9 Athabasca River cross sections.

Location (km) downstream	Date surveyed	Survey flow (m ³ /s)	Gauge height water level adjustment to June 4, 1975 (m)	total water level adjustment to June 4, 1975 (m)
0.06	28/05/74	1048	-1.06	-1.06
0.28	28/05/74	1048	-1.06	-1.06
0.69	28/05/74	1048	-1.06	-1.06
1.76	12/09/75	430	+0.13	+0.13
2.74	17/09/74	521	-0.09	-0.33
3.74	11/09/75	448	+0.09	-0.15
5.54	17/09/74	521	-0.09	-0.33
6.92	17/09/74	521	-0.09	-0.33
8.53	17/09/74	521	-0.09	-0.33
8.65	28/05/74	1048	-1.06	-1.30
8.77	12/09/75	430	+0.13	-0.11
10.08	5/06/74	722	-0.50	-0.74
12.57	17/09/74	521	-0.09	-0.33
16.67	16/09/75	360	+0.13	-0.11
17.11	16/09/75	360	+0.13	-0.11
18.46	16/09/75	360	+0.13	-0.11
19.06	28/05/74	1048	-1.06	-1.30
21.47	11/09/75	448	+0.09	-0.15

Note: the flow on June 4, 1974 was 484 m³/s

6.3.2.3 Mass conservative mixing simulation

Methoxychlor is believed to be a non-conservative parameter due to the potential environmental reactions mentioned above. The principle attenuation mechanism is believed to be adsorption to sediments on the river bed and sediments in suspension. Dissolved methoxychlor and methoxychlor adsorbed to suspended sediments are both toxic to aquatic organisms. Therefore, total water column methoxychlor concentrations (C_t) are reported by Charnetski et al. (1980) which includes both the dissolved (C_w) and the washload (C_m , that adsorbed to the suspended sediment load) components.

Before proceeding to a non-conservative modelling approach to account for adsorption, the standard 2DMIX mass conservative model was run for the methoxychlor input conditions. The results of the conservative model run were intended to be a benchmark against which the attenuation of the methoxychlor could be judged.

Charnetski et al. (1980) reported that 291 L of 21% methoxychlor solution was injected into the river about 100 m downstream from the highway bridge at Athabasca. The injection method involved three boats, each traversing a portion of the river width three times over a period of 7.5 minutes, as described by Depner et al. (1980). Each boat continuously discharged a total volume of methoxychlor solution proportional the flow which they traversed. The theoretical fully mixed line concentration resulting from the injection was 300 ppb over the 7.5 minute injection period..

Methoxychlor samples were collected at 1.76, 3.74, 8.77, 16.67, and 21.47 kms downstream. At 1.76, 3.74 and 21.47 kms samples were taken at transverse locations corresponding to $w/W = 0.25, 0.50$ and 0.75 (where w is the distance from the left bank looking downstream, W is the total width of the stream). At 8.777 and 16.67 kms samples were taken at transverse locations corresponding to $w/W = \approx 0.05, 0.25, 0.50, 0.75$ and ≈ 0.95 . The methoxychlor C-t distributions measured at each of the sampled sections is shown in Figure 6.27 to Figure 6.31

The river channel was divided into ten streamtubes in order to run the computer model. The streamtube boundaries were spaced evenly across the channel in terms of cumulative flow, i.e. $q/Q = 0.100, 0.200, 0.300, 0.400, 0.500, 0.600, 0.700, 0.800, 0.900$, and 1.00 . A time step of 75 seconds was chosen for the simulation on the basis of the criteria outlined previously. Values for the streamtube local depths, widths, slope, and β were assembled into the GRIDGEN input file and the program run to generate the computational grid for the mixing program. The reach-averaged value of $\beta = 0.41$ from the ARC tracer test (Beltaos, 1978) and the average slope of 0.00026 from Kellerhals et al. (1972) was used for each section.

The methoxychlor mass input to the 2DMIX program was distributed to the first element of selected streamtubes in a zigzag pattern. This approach was intended to simulate the movement of the injection boats and was considered far more representative than using a uniform line source across the channel. The C-t curves generated by the mass conservative model are shown in Figure 6.27 to Figure 6.31.

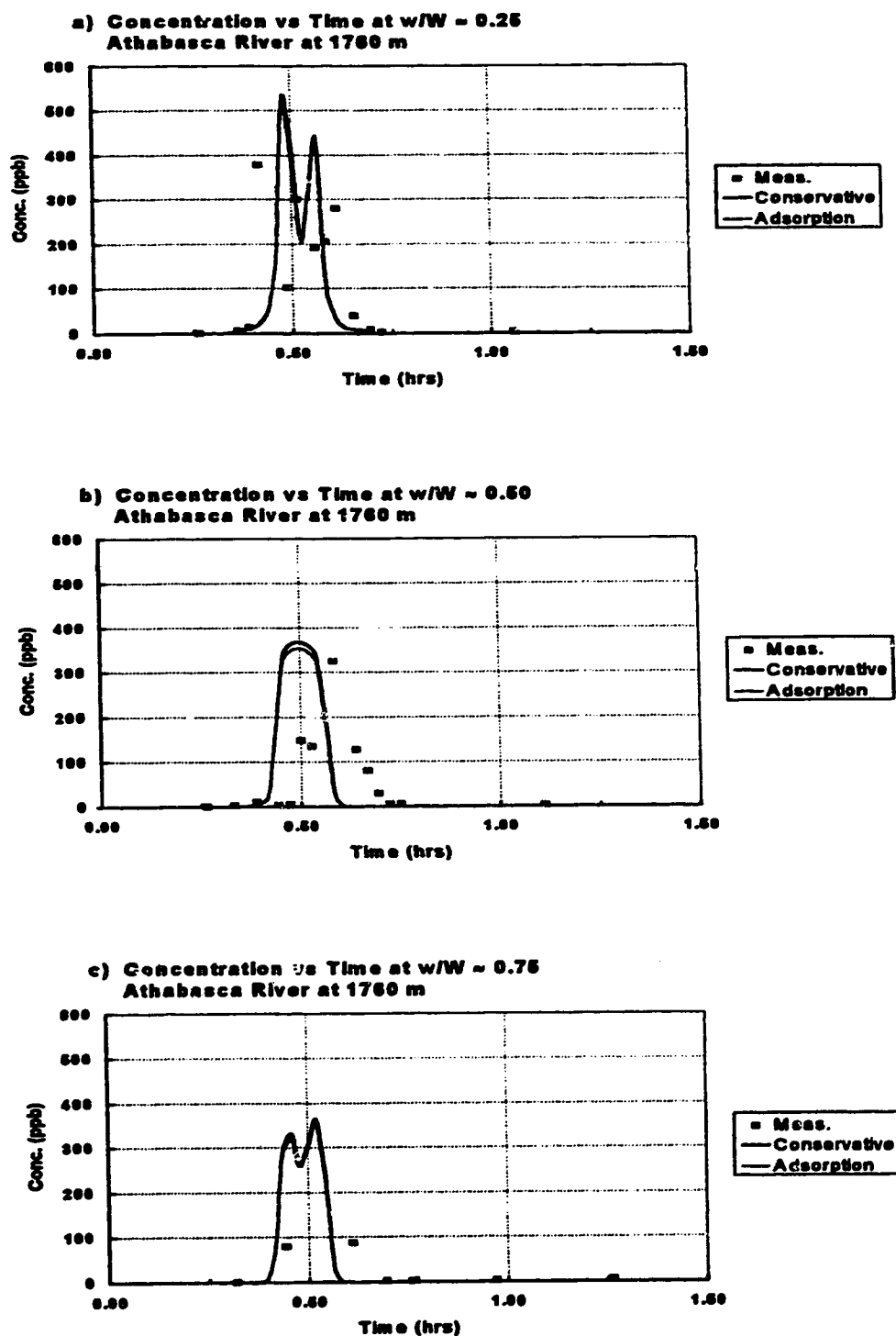


Figure 6.27 Athabasca River, Methoxychlor C-t curves at 1760 m.

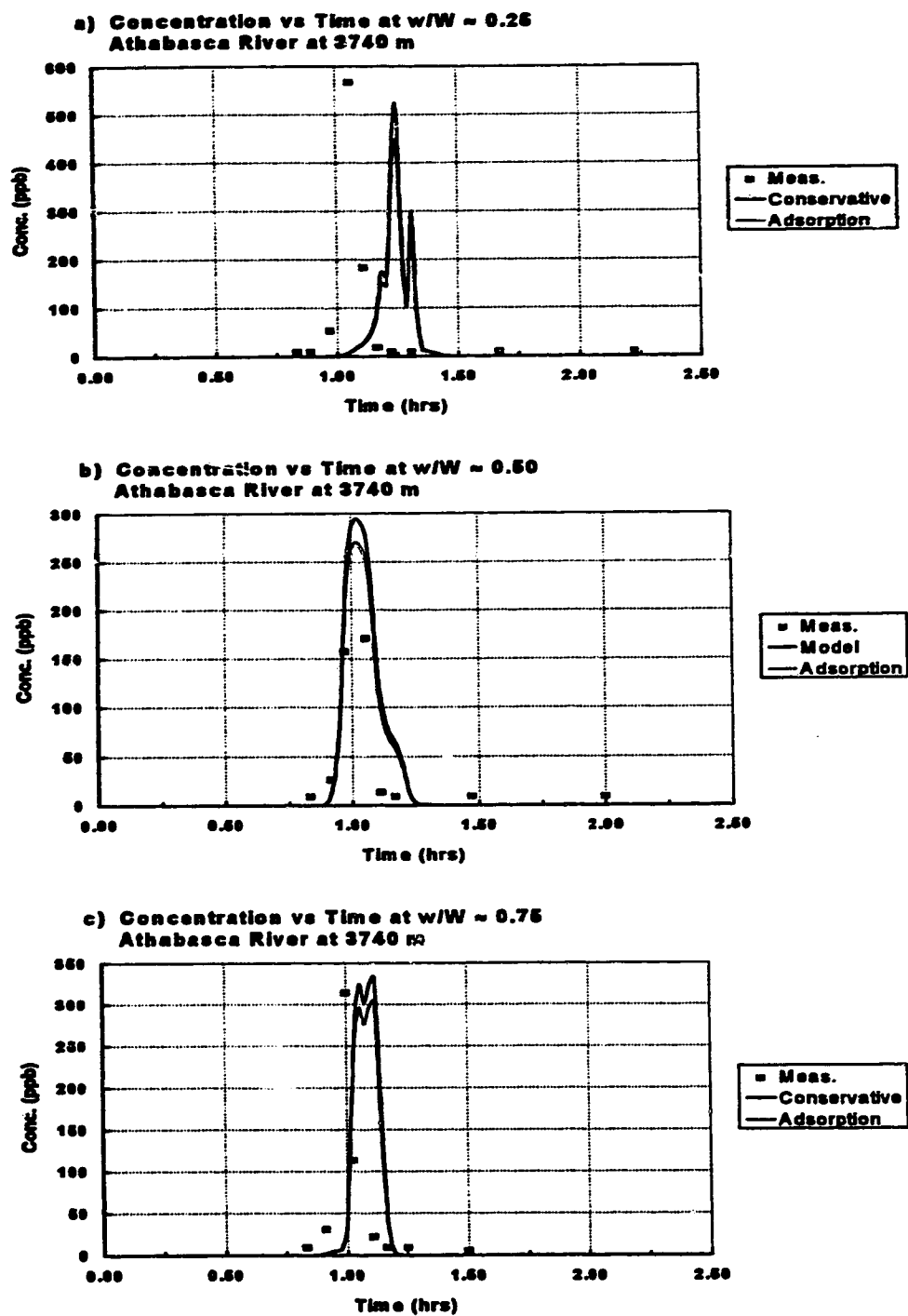


Figure 6.28 Athabasca River, Methoxychlor C-t curves at 3740 m.

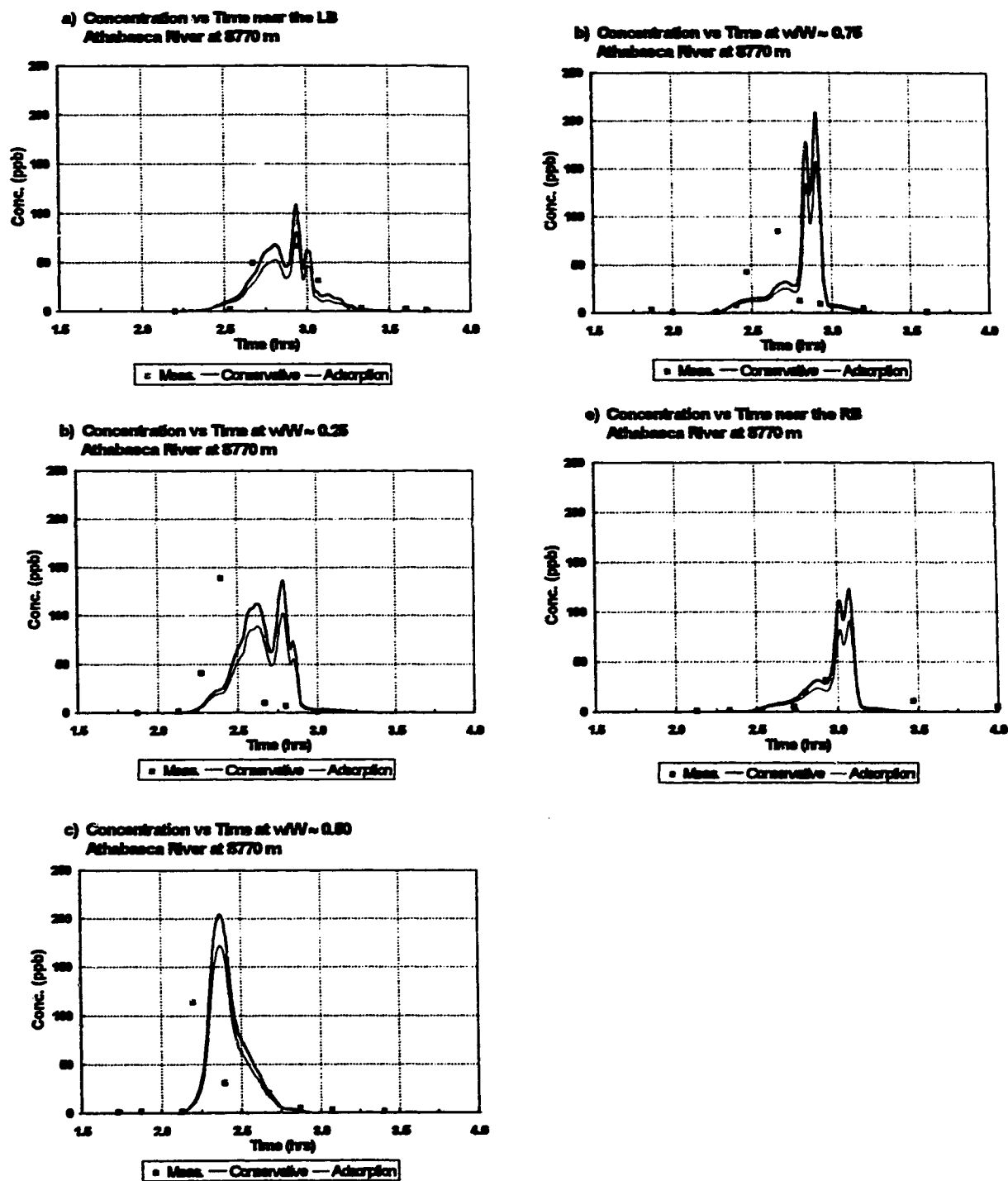


Figure 6.29 Athabasca River, Methoxychlor C-t curves at 8770 m.

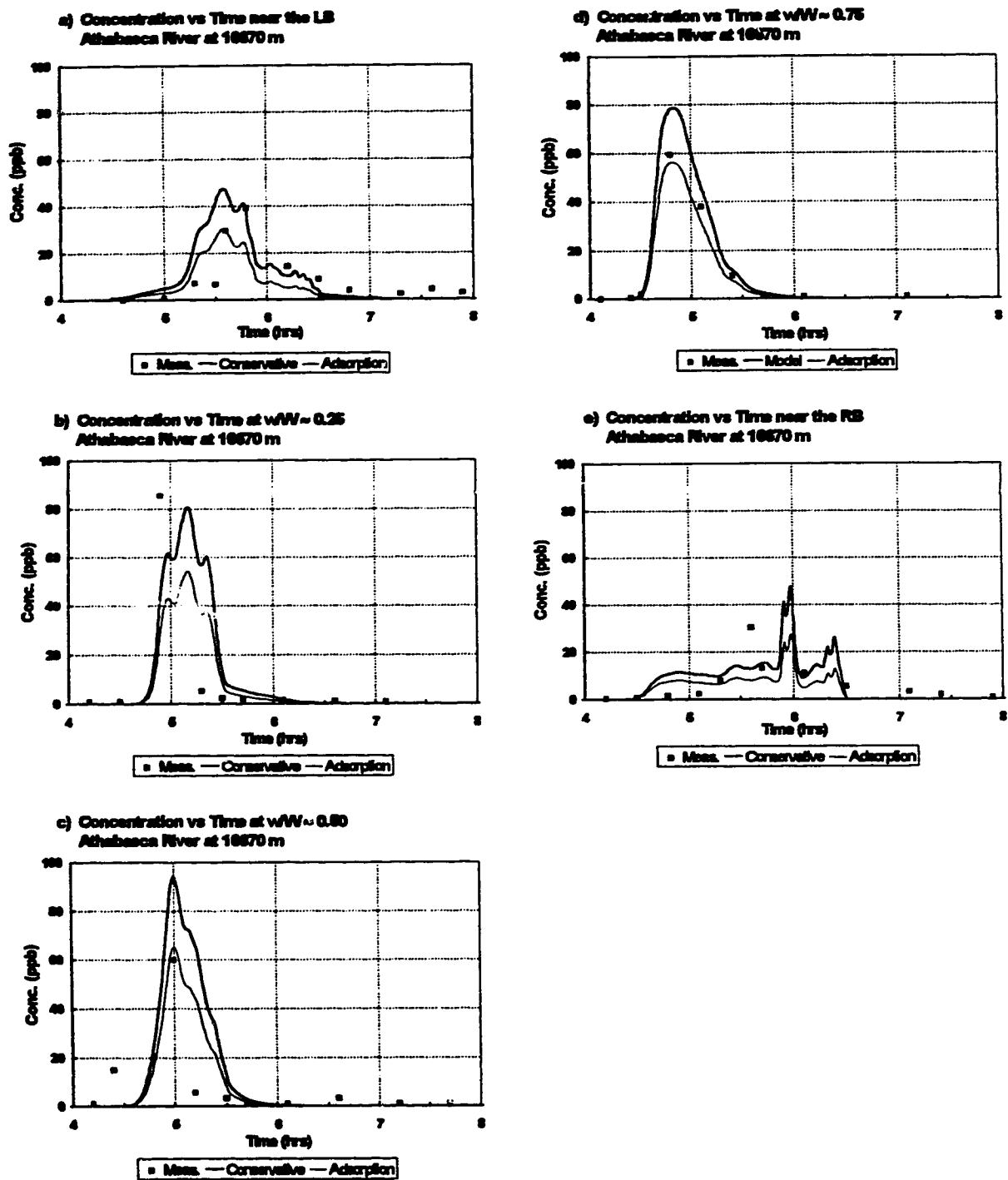


Figure 6.30 Athabasca River, Methoxychlor C-t curves at 16670 m.

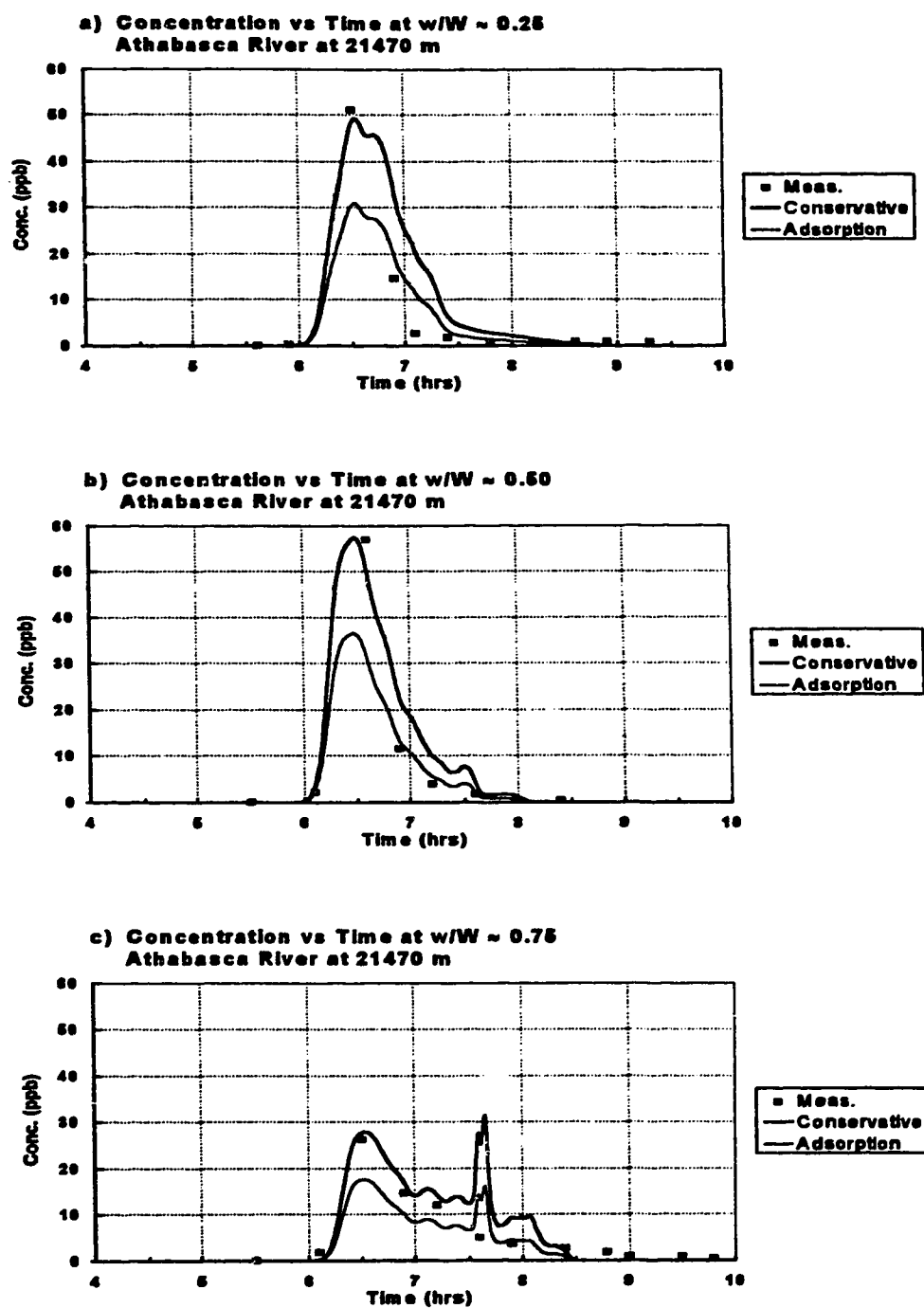


Figure 6.31 Athabasca River, Methoxychlor C-t curves at 21470 m.

6.3.2.4 Adsorption and mixing simulation

Beltaos (1980c) presents an analysis of the mass recovery of methoxychlor for the three blackfly treatment studies. His analysis is based upon one-dimensional C-t curves and is strongly influenced by measurements taken beyond the 21.5 km reach discussed above. The results of the analysis indicate a progressive loss of methoxychlor with distance for all three treatments. The loss within the first 21.5 km was in the order of 30%. As mentioned above the major loss mechanism was expected to be adsorption to the bed material. This was the view of the Agriculture Canada scientists involved in the project which was supported by opinions presented by Gardner and Bailey (1975).

Beltaos determined from the shape of the mass recovery vs. distance curve that the attenuation of the methoxychlor concentrations was not simply a first order relationship. This ruled out the possibility of modeling the adsorption loss rate to the bed as proportional to the total methoxychlor concentration in the water column (dissolved and adsorbed to suspended sediment). Rather Beltaos proposed the following loss mechanism:

1. The areal rate of methoxychlor adsorption to the bed was assumed to be proportional the dissolved methoxychlor concentration in the water column. The rate is given by the following expression:

$$\frac{1}{\Gamma} \frac{dM_b}{dt} = K_b C_w \quad [148]$$

where: M_b is the methoxychlor mass adsorbed to a bed surface area (g),
 Γ is the surface area (m^2),
 C_w is the methoxychlor concentration dissolved within the water column above the bed surface (g/m^3), and
 K_b is the adsorption rate coefficient between the water column and the bed (1/day).

Therefore the rate of loss to the bed is influenced by the exchange of methoxychlor between the dissolved component and that adsorbed to suspended solids in the water column.

2. The rate of adsorption-desorption exchange between the suspended solids and the dissolved phase in the water column is given by the following expression:

$$\frac{1}{V} \frac{dM_{ss}}{dt} = \frac{dC_{ss}}{dt} = K_w C_w - K_{ss} C_{ss} \quad [149]$$

where: M_{ss} is the methoxychlor mass adsorbed to the suspended solids within a given volume of water (g)
 V is the volume of water (m^3)
 C_{ss} is the methoxychlor concentration in sorption on the suspended sediment within a given volume of water (g/m^3)
 C_w is the methoxychlor concentration dissolved within a given volume of water (g/m^3)
 K_w is the adsorption rate coefficient (1/day)
 K_{ss} is the desorption rate coefficient (1/day)

The proposed mechanism assumes there is negligible deposition of suspended solids on the bottom and that there is no desorption of the methoxychlor from the bed after the treatment slug passes.

Beltaos (1980c) determined the values of the three rate coefficients used in Equations [148] and [149] using a best fit approach to the mass recovery data for the three treatment studies. The resulting rate coefficients from his analysis are shown in Table 6.10.

Table 6.10 Summary of methoxychlor sorption and desorption rate coefficients.

River Reach	Coefficient		
	K_w (1/day)	K_{ss} (1/day)	K_b (m/day)
Athabasca to Fort McMurray	0.55	0.20	4.5

Equations [148] and [149] were incorporated into the mixing model as a reaction substep using the following finite difference expressions:

$$C_w^{t+\Delta t} = C_w^t - K_b C_w^t \Delta t - K_w C_w^t \Delta t + K_{ss} C_{ss}^t \Delta t \quad [150]$$

$$C_{ss}^{t+\Delta t} = C_{ss}^t - K_{ss} C_w^t \Delta t \quad [151]$$

The model was then rerun using the rate coefficients shown in Table 6.10 and the same input conditions used for the mass conservative run. Note that at time zero all methoxychlor is dissolved therefore C_w = the input concentration and $C_{ss} = 0$. Both C_w and C_{ss} are carried along in the calculations. The total concentration in the water column is the sum of the two component concentrations, i.e.

$$C_t = C_w + C_{ss} \quad [152]$$

The result of the adsorption modelling are shown in Figure 6.27 to Figure 6.31 together with the conservative model curves and the total methoxychlor concentration measurements.

6.3.3 Discussion

Comparison of the measured total methoxychlor concentrations and the simulated mass conservative C-t curves indicates there is very good agreement in the time base and the peak concentrations of the waveforms. This result is somewhat surprising because it was expected that bed adsorption would have caused a progressive attenuation of the peak concentrations. The curves produced by the proposed adsorption model clearly indicate a reduction in peak concentrations, however this loss is not confirmed by the measurement data. In effect, the two-dimensional mixing analysis indicates the methoxychlor in the water column during the 1975 treatment is conservative over the first 21.5 km of the study reach.

Beltaos's one-dimensional analysis of the adsorption and mixing was based upon section-averaged C-t curves in the first 21.5 km of the reach and single location measurements further downstream. Despite the effort to introduce the methoxychlor as a

uniform line source there are still two-dimensional effects in the river which can not be accounted for in the one-dimensional model. These effects are evident in the measurements taken at 8.8 and 16.9 km where the near-shore peak concentrations are significantly lower than the mid-channel concentrations. These effects and the subsequent averaging of the curves may contribute to a perceived loss. At the sections sampled between 21.5 km and Fort McMurray samples were taken using a pumping apparatus setup on shore (Charnetski et al., 1980). At these locations the single near-shore sample may not have been representative of the channel as a whole which again would influence the one-dimensional analysis. Sampling locations near mid-stream which would be more representative of section averages would have been preferable at these locations.

With the data set available it is impossible to ascertain how much of the methoxychlor loss over the entire 400 km study reach may be perceived due to non representative sampling and how much is real. Undoubtedly real loss has occurred because estimated recoveries at Fort McMurray were only in the order of 10% to 20% of that injected. How much of the actual loss that is attributable to bed adsorption and how much to other mechanisms is also unknown.

Based upon the results of the two-dimensional mixing analysis it reasonable to question whether there was indeed any significant loss of methoxychlor in the first 21.5 km of the reach. The model results clearly demonstrate the importance of using a two-dimensional mixing analysis before attempting to assess the effects of environmental reactions.

7. Conclusions and Recommendations

The following conclusions and recommendations are presented on the basis of the studies presented herein:

- 1. Methods for one-dimensional water quality modelling are well established. However, because the one-dimensional zone is often 10's of kilometres downstream of an outfall or a spill site the value of these models for water quality predictions close to the source are limited.**
- 2. Methods for two-dimensional steady state water quality modelling are also well established. There is uncertainty regarding the prediction of transverse mixing coefficients for use in the existing models.**
- 3. At present the prediction of transverse mixing coefficients using empirical equations is only satisfactory for preliminary mixing calculations. The actual value of the transverse mixing coefficient at any location and flow condition must be verified with a tracer test to reduce this uncertainty. Additional research is required to reliably and accurately predict the transverse mixing coefficient on the basis of easily measured channel geometry and flow parameters.**
- 4. Several models are described in the engineering literature for the simulation of two-dimensional mixing with an unsteady substance source. The explicit method proposed by Fischer (1968) and further developed by Beltaos (1978, which employs an advection optimized grid (AOG), effectively eliminates numerical dispersion and dissipation problems associated with the advective term.**
- 5. Very limited field verifications had been reported for two-dimensional unsteady source mixing models. The microcomputer based AOG model developed for this study was successfully used to simulate unsteady source tracer mixing in three major rivers. On this basis the AOG method is considered verified for the simulation of mixing and transport in natural streams.**

6. The effects of dead zones and backwater areas upon mixing are not well represented by the AOG model. Therefore, simulation inaccuracies can occur in the near-shore region if significant dead zone areas are present.
7. The collection of sufficient hydrometric data to fully represent the study reach is critical to the success of a two-dimensional, unsteady mass input modelling exercise.
8. The AOG based modelling procedure can be easily adapted to account for environmental reactions for non-conservative water quality parameters. Simulation of the mixing and reactions kinetics of BOD and DO downstream of an unsteady wastewater discharge was presented as an example of a practical engineering application of the model. The adapted AOG model was successfully used to simulate the combined effects of mixing, BOD exertion, atmospheric reaeration, photosynthetic oxygen production, aquatic plant respiration and sediment oxygen demand upon DO levels downstream of a primary wastewater treatment plant.
9. Caution should be exercised in interpreting the results of environmental fate studies in rivers and streams without completing a two-dimensional mixing analysis. The methoxychlor mixing simulations presented in this study demonstrate the importance of this consideration.
10. The adapted AOG model for BOD-DO kinetics should be further verified with a more comprehensive data set. The data set should include measurements of sediment oxygen demand. The BOD-DO kinetic subroutine should be further developed to include temperature dependence for rate coefficients and the selection of an atmospheric reaeration relationship based upon Covar's method.
11. Efforts should be made to encourage the use of two-dimensional mixing models as a routine engineering tool to provide information for informed management of wastewater discharges to rivers and streams.

8. Bibliography

- APHA (American Public Health Association). 1985. Standard Methods for the Examination of Water and Wastewater, 16th ed., Washington, D.C.
- ARC (Alberta Research Council). 1975. Unpublished field data, Athabasca River blackflies project. Surface Water Engineering Division, Edmonton, Alberta.
- Bedford, K.W., Sykes, R.M. and Libicki, C. 1983. Dynamic advective water quality model for rivers. *Journal of Environmental Engineering, ASCE*, Vol. 109, EE3, pp. 535-554.
- Beltaos, S. 1975. Evaluation of transverse mixing coefficients from slug tests. *Journal of Hydraulic Research*, Vol. 13, No. 4, pp. 351-360.
- Beltaos, S. 1978. Transverse mixing in natural streams. Alberta Research Council, Report SWE 78-1, Edmonton, Alberta.
- Beltaos, S. 1979. Transverse mixing in natural channels. *Canadian Journal of Civil Engineering, CSCE*, Vol. 6, No. 4, pp. 575-591.
- Beltaos, S. 1980a. Transverse mixing tests in natural streams. *Journal of the Hydraulics Division, ASCE*, Vol. 106, HY10, pp. 1607-1625.
- Beltaos, S. 1980b. Longitudinal dispersion in rivers. *Journal of the Hydraulics Division, ASCE*, Vol. 106, HY1, pp. 151-172.
- Beltaos, S. 1980c. Mixing and effects of insecticides: a working hypothesis for an analytical model. *in: Control of blackflies in the Athabasca River*. Haufe, W.O. and Croome, G.C.R. (ed.), Alberta Environment, Edmonton, Alberta, pp. 97-122.
- Beltaos, S. and Anderson, M.D. 1979. Mixing characteristics of the North Saskatchewan River below Edmonton, Part I. Alberta Research Council, Transportation and Surface Water Engineering Division, Report SWE-79/01.
- Beltaos, S. and Arora, V.K. 1988. An explicit algorithm to simulate transient transverse mixing in rivers. *Canadian Journal of Civil Engineering, CSCE*, Vol. 15, No. 6, pp. 964-976.
- Beltaos, S. and Charnetski, W.A. 1980. Mixing of insecticide: one-dimensional analysis of methoxychlor concentration data. *in: Control of blackflies in the Athabasca River*. Haufe, W.O. and Croome, G.C.R. (ed.), Alberta Environment, Edmonton, Alberta, pp. 123-130.
- Charnetski, W.A., Depner, K.R. and Beltaos, S. 1980. Distribution and persistence of methoxychlor in the Athabasca River. *in: Control of blackflies in the Athabasca River*. Haufe, W.O. and Croome, G.C.R. (ed.), Alberta Environment, Edmonton, Alberta, pp. 39-61.
- City of Saskatoon. 1984. Unpublished field data, South Saskatchewan River Study. Water and Pollution Control Department, Saskatoon, Saskatchewan.

- City of Saskatoon. 1985. South Saskatchewan River Study, Base Line Data Report. Water and Pollution Control Department, Saskatoon, Saskatchewan.
- Covar, A.P. 1976. Selecting the proper reaeration coefficient for use in water quality models. Proceedings, U.S. EPA Conference on Environmental Simulation and Modeling, Cincinnati, OH. *cited in*: McCutcheon, S.C. 1989. Water Quality Modeling, Volume I, Transport and Surface Exchange in Rivers. CRC Press, Boca Raton, Florida.
- Csanady, G.T. 1973. Turbulent Diffusion in the Environment. D. Reidel Publishing Company, Boston, Massachusetts.
- Cunge, J.A., Holly, F.M. and Verwey, A. 1980. Practical Aspects of Computational River Hydraulics. Pitman Advanced Publishing Program, Marshfield, Massachusetts.
- Demetracopoulos, A.C. and Stefan, H.G. 1983. Transverse mixing in a wide and shallow river. Journal of Environmental Engineering, ASCE, Vol. 109, EE3, pp. 685-699.
- Depner, K.R., Charnetski, W.A., and Haufe, W.O. 1980. Population reduction of the black fly simulium articum at breeding sites in the Athabasca River. *in*: Control of blackflies in the Athabasca River. Haufe, W.O. and Croome, G.C.R. (ed.), Alberta Environment, Edmonton, Alberta, pp. 39-61.
- Di Toro, D.M., Paquin, P.R., Subburamu, K. and Gruber, D.A. 1990. Sediment oxygen demand model, methane and ammonia oxidation. Journal of the Environmental Engineering Division, ASCE, Vol. 116, No. 2 pp. 945-986.
- Di Torro, D.M. 1992.. Algae and dissolved oxygen. Notes, Mathematical Modeling of Water Quality: Dissolved Oxygen-Eutrophication, 37th Institute in Water Pollution Control, Manhattan College, Riverdale, New York.
- Elder, J.W. 1959. The dispersion of marked fluid in turbulent shear flow. Journal of Fluid Mechanics, Vol. 5, No. 4, pp. 544-660.
- Elhadi, N., Harrington, A., Hill, I., Lau, Y.L. and Krishnappan, B.G. 1984. River mixing-A state of the art report. Canadian Journal of Civil Engineering, CSCE, Vol. 11, No. 3, pp. 585-609.
- Fischer, H.B. 1966. Longitudinal dispersion in laboratory and natural streams. Ph.D. thesis, California Institute of Technology, Pasadena, California.
- Fischer, H.B. 1967. Transverse mixing in a sand-bed channel. U.S. Geological Survey Professional Paper, 575-D.
- Fischer, H.B. 1968. Methods for predicting dispersion coefficients in natural streams with applications to the lower reaches of the Green and Duwamis Rivers. U.S. Geological Survey, Professional Paper, 582-A.
- Fischer, H.B. 1969. The effect of bends on dispersion in streams. Water Resources Research, Vol. 5, pp. 496-506.

- Fischer, H.B. 1973. Longitudinal dispersion and turbulent mixing in open channel flow. *Annual Review of Fluid Mechanics*, Vol. 5, pp. 59-77.
- Fischer, H.B. 1975. Discussion to simple method of predicting dispersion in streams by R.S. McQuivey and T.N. Keefer. *Journal of the Environmental Engineering Division, ASCE*, Vol. 101, pp. 453-455.
- Fischer, H.B., List, E.J., Koh, R.C.Y., Imberger, J. and Brooks, N.H. 1979. *Mixing in Inland and Coastal Waters*. Academic Press, New York, N.Y.
- Fletcher, C.A.J. 1991. *Computational Techniques in Fluid Dynamics, Volume I*. Springer-Verlag, New York, N.Y.
- Fonstad, G. 1995. Personal Communication, Alberta Environmental Protection, Edmonton, Alberta.
- Fujimoto, Y. 1964. Graphical use of first-stage BOD equation. *Journal of the Water Pollution Control Federation*, Vol. 36, No. 1, pp. 69-71.
- Gardner, D.R. and Bailey, J.R. 1975. Methoxychlor: Its effects on environmental quality. National Research Council Canada, Associate Committee on Scientific Criteria for Environmental Quality, NRCC Publication No. 14102, Ottawa, Canada.
- Gerald, C.F. 1980. *Applied Numerical Analysis*. Addison Wesley, Reading, Massachusetts.
- Gerard, R., Putz, G. and Smith, D.W. 1985. Mixing in the near-bank zone of a large northern river, *Proceedings, 21st Congress of the International Association for Hydraulic Research*, Vol. 2, Melbourne, Australia, pp. 145-148.
- Harden, T.O. and Shen, H.T. 1979. Numerical simulation of mixing in natural rivers. *Journal of the Hydraulics Division, ASCE*, Vol. 105, HY4, pp. 393-408.
- Haufe, W.O. and Croome, G.C.R. (ed.) 1980. *Control of blackflies in the Athabasca River*. Alberta Environment, Edmonton, Alberta.
- Holley, E.R. and Abraham, G. 1973. Field tests on transverse mixing in rivers. *Journal of the Hydraulics Division, ASCE*, Vol. 99, pp. 2313-2331.
- Holly, E.R. and Cunge, J.A. 1975. Prediction of time-dependent mass dispersion in natural streams. *Proceedings of Modelling 75, Hydraulics Division, ASCE*, pp. 1127-1137.
- Holley, E.R., Siemons, J. and Abraham, G. 1972. Some aspects of analysing transverse diffusion in rivers. *Journal of Hydraulic Research*, Vol. 10, No. 1, pp. 27-57.
- Holly, F.M. 1975. Two-dimensional mass dispersion in rivers. *Hydrology papers, No.78* Colorado State University, Fort Collins, CO.
- Holly, F.M. and Nerat, G. 1983. Field calibration of a stream-tube dispersion model. *Journal of Hydraulic Engineering, ASCE*, Vol. 109, No. 11, pp. 1455-1470.

- Holly, F.M. and Preissmann, A. 1977. Accurate calculation of transport in two dimensions. *Journal of Hydraulic Engineering*, ASCE, Vol. 103, HY11, pp. 1259-1277.
- Kellerhals, R., Neill, C.R. and Bray, D.I. 1972. Hydraulic and geomorphic characteristics of rivers in Alberta. Alberta Research Council, River Engineering and Surface Hydrology Division, Report No. 72-1.
- Kolmogoroff, A.N. 1941. Dissipation of energy in locally isotropic turbulence. C.R. (Dokl.) Academy of Science URSS, Vol. 32, No. 16. *cited in:* Krenkel, P.A. and V. Novotny. 1980. *Water Quality Management*. Academic Press, New York, N.Y.
- Koussis, A.D., Kokitkar, P. and Mehta, A. 1990. Modeling DO conditions in streams with dispersion.. *Journal of Environmental Engineering*, ASCE, Vol. 116, No. 3, pp. 601-614.
- Krishnappan, B.G. and Lau, Y.L. 1982. Prediction of transverse mixing in natural streams - RIVMIX. Environment Canada, National Water Research Institute, Study 330, Canada Centre for Inland Waters, Burlington, Ont.
- Krishnappan, B.G. and Lau, Y.L. 1985. User's manual: Prediction of transverse mixing in natural streams model- RIVMIX MK2. Environment Canada, National Water Research Institute, Canada Centre for Inland Waters, Burlington, Ont.
- Landine, R.C. 1970. Prediction of dissolved oxygen levels in the South Saskatchewan River. Sanitary Engineering Report No. 5, Department of Civil Engineering, University of Saskatchewan, Saskatoon, Saskatchewan.
- Lau, Y.L. 1972. A review of conceptual models and prediction equations for reaeration in open-channel flow. Technical Bulletin No. 61, Inland Water Branch, Department of the Environment.
- Lau, Y.L. and Krishnappan, B.G. 1977. Transverse dispersion in rectangular channels. *Journal of the Hydraulics Division*, ASCE, Vol. 103, HY10, pp. 1173-1189.
- Lau, Y.L. and Krishnappan, B.G. 1981. Modelling transverse mixing in natural streams. *Journal of the Hydraulics Division*, ASCE, Vol. 107, HY2, pp. 209-226.
- Lawrence A.L., Anderson, J.C. and Belytschko, T. 1973. Transient hydrothermal analysis of small lakes. *Journal of the Power Division*, ASCE, Vol. 99, PO2, pp. 349-364.
- Li, W.H. 1972. Effects of dispersion on DO-sag in uniform flow. *Journal of Sanitary Engineering*, ASCE, Vol. 98, SA1, pp. 169-182.
- Luk, G.K. 1989. Numerical performance of unsteady-state pollutant mixing algorithms. *Proceedings, Annual Conference of the CSCE*, June 8-10, St. John's Newfoundland.

- Luk, G.Y.K., Lau, Y.L. and Watt, W.E. 1990. Two-dimensional mixing in rivers with unsteady pollutant source. *Journal of Environmental Engineering, ASCE*, Vol. 116, No. 1, pp. 125-143.
- Mackay, J.R. 1970. Lateral mixing of the Liard and Mackenzie Rivers downstream from their confluence. *Canadian Journal of Earth Science*, Vol. 7, pp. 111-124.
- Marzolf, E.R., Mulholland, P.J. and Steinman, A.D. 1994. Improvements to the upstream-downstream dissolved oxygen change technique for determining whole-stream metabolism in small streams. *Canadian Journal of Fisheries and Aquatic Science*, Vol. 51, pp. 1591-1599.
- McBride, G.B. and Rutherford, J.C. 1983. Accurate modeling of river pollutant transport. *Journal of Environmental Engineering, ASCE*, Vol. 110, No. 4, pp. 808-827.
- McCutcheon, S.C. 1989. *Water Quality Modeling, Volume I, Transport and Surface Exchange in Rivers*. CRC Press, Boca Raton, Florida.
- Milne, G.D. 1991. Chlorine decay in a large river. M.Sc. thesis, Department of Civil Engineering, University of Alberta, Edmonton, Alberta.
- Moore, W.E., Thomas, H.A. and Snow, W.B. 1950. Simplified method for analysis of BOD data. *Sewage and Industrial Wastes*, Vol. 22, pp. 1343-1352.
- Nokes, R.I. and Wood, I.R. 1988. Vertical and lateral turbulent dispersion in open channels. *Journal of Fluid Mechanics*, Vol. 187, pp. 373-394.
- Nokes, R.I., McNulty, A.J. and Wood, I.R. 1984. Turbulent dispersion from a steady two dimensional horizontal source. *Journal of Fluid Mechanics*, Vol. 149, pp. 147-159.
- Northern Rivers Basin Study. 1994. Water travel time and mixing characteristics, Peace River: Shaftesbury Ferry to Notikewin River. Edmonton, Alberta.
- Northwest Hydraulic Consultants Ltd. 1980. Summary of hydrological assessments, Slave River hydro feasibility, preliminary report. Edmonton, Alberta.
- Novotny, V. and Olem, H. 1994. *Water Quality, Prevention, Identification, and Management of Diffuse Pollution*. Van Nostrand Reinhold, New York, N.Y.
- NRCC (National Research Council Canada). 1983. Impact assessments in lotic environments - Methoxychlor. Associate Committee on Scientific Criteria for Environmental Quality, NRCC Publication No. 20645, Ottawa, Canada.
- O'Connor, D.J. and Di Torro, D.M. 1970. Photosynthesis and oxygen balance in streams. *Journal of Sanitary Engineering, ASCE*, Vol. 96, SA2, pp. 547-571.
- Odum, H.T. 1956. Primary productivity of flowing waters. *Limnology and Oceanography*, Vol. 2, pp. 85-97.

- Okoye, J. 1970. Characteristics of transverse mixing in open-channel flows. W.M. Keck Laboratory of Hydraulics and Water Resources, Rep KH-R-23, California Institute of Technology, Pasadena, California.
- Peaceman, D.W. and Rachford, H.H. 1955. The numerical solution of parabolic and elliptical differential equations. Journal, Society of Industrial and Applied Mathematics, Vol. 3, No. 1, pp. 28-41.
- Putz, G. 1983. Mixing and microorganism survival, Slave River, N.W.T. M.Sc. thesis, Department of Civil Engineering, University of Alberta, Edmonton, Alberta.
- Putz, G. 1984. TRSMIX (transverse mixing computer model) users manual. Environmental Engineering Technical Report 84-2, Department of Civil Engineering, University of Alberta, Edmonton, Alberta.
- Putz, G., Gerard, R. and D.W. Smith. 1982. Mixing and microorganism survival in an ice-covered river. Proceedings, Annual Conference of the CSCE, Edmonton, Alberta, pp. 1439-1458.
- Putz, G., Gerard, R. and D.W. Smith. 1984. Microorganism survival in an ice-covered river. Canadian Journal of Civil Engineering, CSCE, Vol. 11, No. 2, pp. 177-186.
- Rajaratnam, N. 1980. Course notes, CIV E 531, Environmental fluid mechanics. University of Alberta, Department of Civil Engineering, Edmonton, Alberta.
- Reed, L.J. and Theriault, E.J. 1931. Journal of Physical Chemistry, The statistical treatment of reaction velocity, II, Least squares treatment of the unimolecular expression $y = L(1 - e^{-Kt})$. Vol. 35, No. 4 pp. 950-971.
- Rutherford, J.C. 1977. Modeling effects of aquatic plants in rivers. Journal of Environmental Engineering, ASCE, Vol. 103, EE4, pp. 575-591.
- Rutherford, J.C. 1994. River Mixing. John Wiley and Sons, New York, N.Y.
- Rutherford, J.C., R.J. Wilcock and Hickey, C.W. 1991. Deoxygenation in a mobile-bed river, I. Field studies. Water Research, Vol. 25, No. 12, pp. 1487-1497.
- Sayre, W.W. and Chang, F.M. 1968. A laboratory investigation of open channel dispersion processes for dissolved, suspended and floating dispersants. U.S. Geological Survey, Professional Paper, 433-E, 71 p.
- Sayre, W.W. and Yeh, T.P. 1975. Transverse mixing characteristics of the Missouri River downstream from the Cooper nuclear station. IHR Report 145, Iowa Institute of Hydraulic Research, University of Iowa, Iowa City, Iowa. cited in: Lau, Y.L. and B.G. Krishnappan. 1981. Modelling transverse mixing in natural streams. Journal of the Hydraulics Division, ASCE, Vol. 107, HY2, pp. 209-226.
- Schoellhamer, D.H. 1988. Lagrangian transport modeling with Qual II kinetics. Journal of Environmental Engineering, ASCE, Vol. 114, No. 2, pp. 368-381.
- Sculthorpe, C.D. 1967. Biology of Aquatic Vascular Plants. Arnold, London, England.

- Shawinigan Stanley. 1982. Final report, Slave River hydro feasibility study, Appendix B, Hydrology. Edmonton, Alberta.**
- Smith, C.D. and Wigham, J.M. 1989. A study of erosion and sedimentation in the South Saskatchewan River Basin. a report prepared for the South Saskatchewan River Basin Study, Saskatoon, Saskatchewan.**
- Smith, D.W. and Putz, G. 1993. The simulation of river concentrations of coliform bacteria using a transverse mixing model. Environmental Technology, Vol. 14, pp. 1117-1130.**
- Snoeyink, V.L. and Jenkins, D. 1980. Water Chemistry. John Wiley and Sons, New York, New York.**
- Sobey, R.J. 1984. Numerical alternatives in transient stream response. Journal of Hydraulic Engineering, ASCE, Vol. 110, No. 6, pp. 749-772.**
- Steffler, P.M. 1991. Course notes, CIV E 634, Numerical methods in hydraulics. University of Alberta, Department of Civil Engineering, Edmonton, Alberta.**
- Stone, H.L. and Brian, P.L.T. 1963. Numerical solution of convective transport problems. Journal of the American Institute of Chemical Engineers, Vol. 9, No. 5, pp. 681-688.**
- Streeter, H.W. and Phelps, E.B. 1925. A study of the pollution and natural purification of the Ohio River, III, Factors concerned in the phenomena of oxidation and reaceration, U.S. Public Health Service, Public Health Bulletin No. 146, February, 1925, 75 pp.**
- Taylor, G.I. 1921. Diffusion by continuous movements. Proceedings, London Mathematics Society, Series A, Vol. 20, pp. 196-211.**
- Taylor, G.I.. 1953. Dispersion of solute matter in solvent flowing slowly through a tube. Proceedings, Royal Society of London, Series A, Vol. 219, pp. 186-203.**
- Taylor, G.I. 1954. The dispersion of matter in turbulent flow through a pipe. Proceedings, Royal Society of London, Series A, Vol. 223, pp. 446-468.**
- Thomann, R. and Mueller, J. 1987. Principles of Surface Water Quality Modeling and Control. Harper and Row Publishers, New York, N.Y.**
- Thomann, R.V., Connor, D.J. and Di Torro, D.M. 1992.. Effect of nitrification on the dissolved oxygen of streams and estuaries. Notes, Mathematical Modeling of Water Quality: Dissolved Oxygen-Eutrophication, 37th Institute in Water Pollution Control, Manhattan College, Riverdale, New York.**
- Thomas, H.A. 1950. Graphical determination of BOD curve constants. Water Sewage Works, Vol. 97, p. 123.**
- Velz, C.J. 1984. Applied Stream Sanitation. 2nd. Edition, John Wiley and Sons, New York, New York.**

- Verboom, G.K. 1973. Transverse mixing in rivers; a numerical approach. XVth International Association for Hydraulic Research Congress, Istanbul, Turkey, Vol. 1, pp. 319-326.
- Verboom, G.K. 1975. The advection-dispersion equation for an anisotropic medium solved by fractional-step methods. Proceedings of the International Conference on Mathematical Models for Environmental Problems, University of Southampton, England. Editor: C.A. Brebbia, John Wiley and Sons, New York, pp. 299-312.
- Walker, R., Weatherbe, D.G. and Wilson, K. 1982. Aquatic plant model - derivation and application. Grand River Basin Water Management Study, Technical Report #14, Ontario Ministry of the Environment, Toronto, Ontario.
- Webel, G. and Schatzmann, M. 1984. Transverse mixing in open channel flow. Journal of Hydraulic Engineering, ASCE, Vol. 110, No. 4, pp. 423-435.
- Wright, R.M. and McDonnell, A.J. 1979. In-stream deoxygenation rate prediction. Journal of Environmental Engineering, ASCE, Vol. 105, EE2, pp. 323-391.
- Yotsukura, N. and Cobb, E.D. 1972. Transverse diffusion of solutes in natural streams. United States Geological Survey, Prof. Paper 582-C, pp. c1-c19.
- Yotsukura, N. and Fiering, M.B. 1964. Numerical solution to a dispersion equation. Journal of Hydraulic Engineering, ASCE, Vol. 90, No. 5, pp. 83-104.
- Yotsukura, N. and Sayre, W.W. 1976. Transverse mixing in natural channels. Water Resources Research, Vol. 12, No. 4, pp. 495-497.
- Yotsukura, N., Fischer, H.B. and Sayre, W.W. 1970. Mixing characteristics of the Missouri River between Sioux City, Iowa and Plattsmouth, Nebraska. U.S. Geological Survey, Water Supply Paper, No. 1899-G.
- Zison, S.W., Mills, W.B., Diemer, D. and Chen, C.W. 1978. Rates, constants and kinetic formulations in surface water quality modeling. EPA 600-3-78-105, U.S. EPA, ORD, Athens, GA. *cited in*: Thomann, R. and Mueller, J. 1987. Principles of Surface Water Quality Modeling and Control. Harper and Row Publishers, New York, New York.

Appendix A. Interpolation Procedure for Determining Element Lengths

The streamtube width Δz at a distance x located between sections with defined properties at distances x_u and x_d can be estimated by linear interpolation as follows:

$$\begin{aligned}\Delta z &= \Delta z_u + (\Delta z_d - \Delta z_u) \frac{(x - x_u)}{(x_d - x_u)} \\ \Delta z &= \Delta z_u + \alpha_1 (x - x_u) \\ \Delta z &= \alpha_2 + \alpha_1 x\end{aligned}\tag{A-1}$$

$$\begin{aligned}\text{where: } \alpha_1 &= (\Delta z_d - \Delta z_u) / (x_d - x_u) \\ \alpha_2 &= (\Delta z_u - \alpha_1 x_u)\end{aligned}$$

Similarly the streamtube depth h at a distance x located between sections with defined properties at distances x_u and x_d can be estimated by linear interpolation as follows:

$$\begin{aligned}h &= h_u + (h_d - h_u) \frac{(x - x_u)}{(x_d - x_u)} \\ h &= h_u + \beta_1 (x - x_u) \\ h &= \beta_2 + \beta_1 x\end{aligned}\tag{A-2}$$

$$\begin{aligned}\text{where: } \beta_1 &= (h_d - h_u) / (x_d - x_u) \\ \beta_2 &= (h_u - \beta_1 x_u)\end{aligned}$$

The volume of a length of streamtube extending between distance x and a defined downstream section at distance x_u is determined by integration as follows:

$$\begin{aligned}\text{Volume} &= \int_{x_u}^x \Delta z \cdot h \cdot dx \\ &= \int_{x_u}^x (\alpha_2 + \alpha_1 x)(\beta_2 + \beta_1 x) dx \\ &= \int_{x_u}^x (\alpha_2 \beta_2 + \alpha_2 \beta_1 x + \alpha_1 \beta_2 x + \alpha_1 \beta_1 x^2) dx \\ &= \left[\alpha_2 \beta_2 x + (\alpha_2 \beta_1 + \alpha_1 \beta_2) \frac{x^2}{2} + \alpha_1 \beta_1 \frac{x^3}{3} \right]_{x_u}^x\end{aligned}\tag{A-3}$$

The cumulative volume along the streamtube is the summation of interval volumes between defined sections.

$$\text{cumulative volume to position } m = \sum_{n=1}^m \text{Vol}_n \quad [\text{A-4}]$$

where: Vol_n are interval volumes calculated using Equation A-3, with the upstream and downstream limits set to defined sections and x set equal to x_d , and

m is the number of intervals.

The distance x to the downstream boundary of the i th element in a streamtube is determined as follows:

1. Determine the cumulative volume to each defined section, down streamtube j , using the method outlined above.
2. Determine the cumulative volume to the downstream boundary of the i th element of streamtube j as follows:

$$\text{cumulative volume} = (\Delta q)(dt)(i)$$

where Δq is the streamtube flow, dt is the time step.

3. Solve Equation [A-3] by successive substitution to determine x which gives the appropriate cumulative volume within an acceptable tolerance.
4. Use the calculated x position for the element downstream boundary to determine the streamtube mean depth, right boundary depth, width, and mixing coefficient by linear interpolation between the appropriate upstream and downstream defined sections.
5. Average the upstream and downstream boundary properties for the element to determine the mean properties at the element centroid. Note the downstream boundary properties are known from the previous element calculations.
6. Proceed to each successive element in the streamtube and repeat steps 2 to 5.
7. Proceed to each successive streamtube and repeat steps 1 to 6.

Appendix B. AOG Method Error Analysis

Appendix B.1 Advective Substep

The advective substep governing mass balance equation is:

$$\frac{\partial c}{\partial t} = -u \frac{\partial c}{\partial x} \quad [B-1]$$

The AOG method utilizes the following forward time, backward space, explicit finite difference approximation for Equation B-1:

$$\begin{aligned} \frac{(c_k^{n+1} - c_k^n)}{\Delta t} &= -u \frac{(c_k^n - c_{k-1}^n)}{\Delta x} \\ \text{or} \\ c_k^{n+1} &= c_k^n + C_r [c_{k-1}^n - c_k^n] \end{aligned} \quad [B-2]$$

where Courant No., C_r , is defined as:

$$C_r = u \frac{\Delta t}{\Delta x} \quad [B-3]$$

Appendix B.1.1 Truncation error analysis:

Expressing the node concentrations of Equation B-2 as Taylor series expansions about c_k^n gives:

$$\begin{aligned} c_k^n &= c \\ c_k^{n+1} &= c_k^n + \frac{\partial c}{\partial t} \Delta t + \frac{\partial^2 c}{\partial t^2} \frac{\Delta t^2}{2} + \frac{\partial^3 c}{\partial t^3} \frac{\Delta t^3}{6} + \dots \\ c_{k-1}^n &= c_k^n - \frac{\partial c}{\partial x} \Delta x - \frac{\partial^2 c}{\partial x^2} \frac{\Delta x^2}{2} - \frac{\partial^3 c}{\partial x^3} \frac{\Delta x^3}{6} - \dots \end{aligned} \quad [B-4]$$

Substituting Equation B-4 into Equation B-2 gives:

$$\begin{aligned} \frac{c}{\Delta t} + \frac{\partial c}{\partial t} + \frac{\partial^2 c}{\partial t^2} \frac{\Delta t}{2} - \frac{c}{\Delta t} + \dots &= u \frac{c}{\Delta x} - u \frac{\partial c}{\partial x} - u \frac{\partial^2 c}{\partial x^2} \frac{\Delta x}{2} - u \frac{c}{\Delta x} - \dots \\ \frac{\partial c}{\partial t} &= -u \frac{\partial c}{\partial x} - \left[\frac{\partial^2 c}{\partial t^2} \frac{\Delta t}{2} + u \frac{\partial^2 c}{\partial x^2} \frac{\Delta x}{2} + \dots \right] \end{aligned} \quad [B-5]$$

from which it can be seen the original differential equation is recovered and that the error of the approximation is in the order of Δt and Δx .

Appendix B.1.2 Stability analysis:

The amplification ratio for analytical solution of Equation B-1 is given by:

$$\gamma_{an} = e^{-i\frac{2\pi u \Delta t}{N \Delta x}} = e^{-i\frac{2\pi C_r}{N}} \quad [B-6]$$

from which it can be seen that the amplitude ratio A_{an} and the phase angle error θ_{an} for the analytical solution are respectively:

$$A_{an} = 1 \quad [B-7]$$

$$\theta_{an} = -\frac{2\pi C_r}{N} \quad [B-8]$$

For the numerical solution to Equation B-1 using Equation B-2 as an approximation, the concentration at each node can be given by:

$$\begin{aligned} c_k^n &= A^n e^{i\Omega k \Delta x} \\ c_k^{n+1} &= A^{n+1} e^{i\Omega k \Delta x} \\ c_{k-1}^n &= A^n e^{i\Omega(k-1)\Delta x} \end{aligned} \quad [B-9]$$

where: $\Omega = 2\pi/\lambda$, and

A is the amplitude at a particular time step.

Substituting Equation B-9 into B-2 gives the following expression for the amplification ratio for the numerical solution:

$$\begin{aligned} A^{n+1} e^{i\Omega k \Delta x} &= A^n e^{i\Omega k \Delta x} + C_r \left[A^n e^{i\Omega(k-1)\Delta x} - A^n e^{i\Omega k \Delta x} \right] \\ \frac{c_k^{n+1}}{c_k^n} &= 1 + C_r \left[e^{-i\Omega \Delta x} - 1 \right] \\ \gamma_{num} &= 1 + C_r \left[\cos(\Omega \Delta x) - i \sin(\Omega \Delta x) - 1 \right] \\ \gamma_{num} &= 1 - C_r + C_r \cos(\Omega \Delta x) - i C_r \sin(\Omega \Delta x) \end{aligned} \quad [B-10]$$

Further, defining N as the number of nodes per wavelength:

$$N = \frac{\lambda}{\Delta x} \quad [B-11]$$

and substituting Equation B-11 into Equation B-10 gives:

$$\gamma_{num} = 1 - C_r + C_r \cos\left(\frac{2\pi}{N}\right) - i C_r \sin\left(\frac{2\pi}{N}\right) = a + ib \quad [B-12]$$

From which the phase angle error can be determined to be:

$$\theta_{num} = \tan^{-1}\left(\frac{b}{a}\right) = \tan^{-1}\left[\frac{-C_r \sin\left(\frac{2\pi}{N}\right)}{1 - C_r + C_r \cos\left(\frac{2\pi}{N}\right)}\right] = \tan^{-1}\left[\frac{-C_r \sin\left(\frac{2\pi}{N}\right)}{1 - 2C_r \sin^2\left(\frac{\pi}{N}\right)}\right] \quad [B-13]$$

The ratio of the numerical and the analytical phase angle error is then given by:

$$\frac{\theta_{num}}{\theta_{an}} = \frac{\tan^{-1}\left[\frac{C_r \sin\left(\frac{2\pi}{N}\right)}{1 - C_r + C_r \cos\left(\frac{2\pi}{N}\right)}\right]}{\frac{2\pi C_r}{N}} = \frac{\tan^{-1}\left[\frac{C_r \sin\left(\frac{2\pi}{N}\right)}{1 - 2C_r \sin^2\left(\frac{\pi}{N}\right)}\right]}{\frac{2\pi C_r}{N}} \quad [B-14]$$

From which it can be seen that for $C_r = 1$ and any value of N (greater than the minimum grid resolution), $\theta_{num} = \theta_{an}$ and the numerical scheme produces an exact solution.

The numerical solution amplitude ratio can be determined from B-12 as:

$$\begin{aligned} A_{num} &= (a^2 + b^2)^{\frac{1}{2}} \\ &= \left(\left[1 - C_r + C_r \cos\left(\frac{2\pi}{N}\right) \right]^2 + \left[-C_r \sin\left(\frac{2\pi}{N}\right) \right]^2 \right)^{\frac{1}{2}} \\ &= \left(1 + 2C_r (1 - C_r) \left[\cos\left(\frac{2\pi}{N}\right) - 1 \right] \right)^{\frac{1}{2}} \end{aligned} \quad [B-15]$$

The ratio of the numerical over the analytical amplitude ratio is then given by:

$$\frac{A_{num}}{A_{an}} = \frac{\left(1 + 2C_r (1 - C_r) \left[\cos\left(\frac{2\pi}{N}\right) - 1 \right] \right)^{\frac{1}{2}}}{1} \quad [B-16]$$

From which it can be seen that for $C_r = 1$ and any value of N , $A_{num} = A_{an} = 1$ and the numerical scheme produces an exact solution with no numerical dissipation.

Appendix B.2 Diffusive Substep

The advective substep governing mass balance equation is:

$$\frac{\partial c}{\partial t} = E_z \frac{\partial^2 c}{\partial z^2} \quad [\text{B-17}]$$

The AOG method utilizes the following forward time, centred space, explicit finite difference approximation for Equation B-17:

$$\begin{aligned} \frac{c_j^{n+1} - c_j^n}{\Delta t} &= E_z \frac{(c_{j-1}^n - 2c_j^n + c_{j+1}^n)}{\Delta z^2} \\ \text{or} \\ c_j^{n+1} &= c_j^n + r_r (c_{j-1}^n - 2c_j^n + c_{j+1}^n) \end{aligned} \quad [\text{B-18}]$$

where r_r is defined as:

$$r_r = E_z \Delta t / \Delta z^2 \quad [\text{B-19}]$$

Appendix B.2.1 Truncation Error Analysis

Expressing the node concentrations of Equation B-18 as Taylor series expansions about c_j^n gives:

$$\begin{aligned} c_j^n &= c \\ c_j^{n+1} &= c_j^n + \frac{\partial c}{\partial t} \Delta t + \frac{\partial^2 c}{\partial t^2} \frac{\Delta t^2}{2} + \frac{\partial^3 c}{\partial t^3} \frac{\Delta t^3}{6} + \dots \\ c_{j-1}^n &= c_j^n - \frac{\partial c}{\partial z} \Delta z + \frac{\partial^2 c}{\partial z^2} \frac{\Delta z^2}{2} - \frac{\partial^3 c}{\partial z^3} \frac{\Delta z^3}{6} + \frac{\partial^4 c}{\partial z^4} \frac{\Delta z^4}{12} + \dots \\ c_{j+1}^n &= c_j^n + \frac{\partial c}{\partial z} \Delta z + \frac{\partial^2 c}{\partial z^2} \frac{\Delta z^2}{2} + \frac{\partial^3 c}{\partial z^3} \frac{\Delta z^3}{6} + \frac{\partial^4 c}{\partial z^4} \frac{\Delta z^4}{12} + \dots \end{aligned} \quad [\text{B-20}]$$

Substituting Equation B-20 into Equation B-18 gives:

$$\frac{\partial c}{\partial t} = E_z \frac{\partial^2 c}{\partial z^2} - \left[\frac{\partial^2 c}{\partial t^2} \frac{\Delta t}{2} - E_z \frac{\partial^4 c}{\partial z^4} \frac{\Delta z^2}{6} + \dots \right] \quad [\text{B-21}]$$

from which it can be seen the original differential equation is recovered and that the error of the approximation is in the order of Δt and Δz^2 .

Appendix B.2.2 Stability Analysis

For the numerical solution to Equation B-17 using Equation B-18 as an approximation, the concentration at each node is given by:

$$\begin{aligned} c_j^n &= A^n e^{i\Omega j \Delta z} \\ c_j^{n+1} &= A^{n+1} e^{i\Omega j \Delta z} \\ c_{j-1}^n &= A^n e^{i\Omega (j-1) \Delta z} \\ c_{j+1}^n &= A^n e^{i\Omega (j+1) \Delta z} \end{aligned} \quad [B-22]$$

where: $\Omega = 2\pi/\lambda$, and

A is the amplitude at a particular time step

Substituting Equation B-22 into B-18 gives the following expression for the amplification ratio for the numerical solution:

$$\begin{aligned} A^{n+1} e^{i\Omega j \Delta z} &= A^n e^{i\Omega j \Delta z} + r_r \left[A^n e^{i\Omega (j-1) \Delta z} - 2A^n e^{i\Omega j \Delta z} + A^n e^{i\Omega (j+1) \Delta z} \right] \\ \frac{c_j^{n+1}}{c_j^n} &= 1 + r_r \left[e^{-i\Omega \Delta z} - 2 + e^{i\Omega \Delta z} \right] \\ \gamma_{num} &= 1 + r_r \left[2 \cos(\Omega \Delta z) - 2 \right] \\ \gamma_{num} &= 1 + 2r_r \left[\cos(\Omega \Delta z) - 1 \right] \end{aligned} \quad [B-23]$$

From which it can be seen that the phase error is zero (i.e. there is no imaginary portion).

To ensure stability $|\gamma_{num}| \leq 1$. For the smallest resolvable wavelength $\Omega \Delta z = \pi$, therefore $|1 - 4r_r| \leq 1$ and $r_r \leq \frac{1}{2}$. For longer wavelengths the requirement for r_r is less restrictive, therefore $r_r \leq \frac{1}{2}$ governs.

Appendix C. Program Listings

Appendix C.1 STRMTUBE Program Listing

```

*****
      PROGRAM STRMTUBE
*      Utility program to interpolate cross-section properties
*      given the section flow and geometry.
*****
***** Variable declarations*****
      INTEGER      NPOINTS      ! Number of elev,dist,q/Q points
      INTEGER      I,N          ! Counter(s)
      INTEGER      NTUBES       ! Number of stream tubes for analysis
      INTEGER      IOCHECK      ! Error status variable
      REAL*4       TOTALQ       ! Total river discharge
      REAL*4       SECT         ! Section no., real to accomodate decimals
      REAL*4       LINTERP      ! Linear interpolation function
      REAL*4       BETA         ! Dimensionless mixing coef. for a subreach
      REAL*4       SLOPE        ! Slope of the subreach
      REAL*4       DT           ! Proposed time step
      REAL*4       EXPONENT      ! Exponent for the curve fit near the banks
      REAL*4       SDPTH(0:100) ! X-section survey elevations
      REAL*4       SSTAT(0:100) ! X-section survey distances
      REAL*4       SAREA(0:100) ! X-section survey areas
      REAL*4       SQOVQ(0:100) ! X-section survey cumulative flow
      REAL*4       IDPTH(0:100) ! X-section interpolated elevations
      REAL*4       ISTAT(0:100) ! X-section interpolated distances
      REAL*4       IAREA(0:100) ! X-section interpolated areas
      REAL*4       TWDTH(0:100) ! streamtube width
      REAL*4       TVELC(0:100) ! average streamtube velocity
      REAL*4       TDPH(0:100)  ! average streamtube depth
      REAL*4       ETA(0:100)   ! streamtube eta boundaries
*****
      PARAMETER(EXPONENT=0.5)
      OPEN(UNIT=1,FILE=' ',IOSTAT=IOCHECK,STATUS='OLD')
      OPEN(UNIT=2,FILE=' ',STATUS='UNKNOWN')
      OPEN(UNIT=3,FILE=' ',STATUS='UNKNOWN')

      IF(IOCHECK.GE.0) THEN
        READ(1,*) NTUBES, DT
        WRITE(3,*) '      NO. OF STREAMTUBES = ',NTUBES
        READ(1,*)(ETA(I),I=0,NTUBES-1)
        WRITE(3,*)(ETA(I),I=0,NTUBES-1)
        WRITE(2,2)(ETA(I),I=1,NTUBES-1)
2      FORMAT(8(1X,F8.5))
        ELSE
          WRITE(3,*) 'FILE IS EMPTY'
          STOP
        ENDIF

      READ(1,*,IOSTAT=IOCHECK) SECT,TOTALQ,NPOINTS,BETA,SLOPE

```

```

DOWHILE (IOCHECK.GE.0)
  WRITE(3,5) SECT, TOTALQ, NPOINTS
  FORMAT(5X,F8.2,F10.1,I5)
S  DO I=0,NPOINTS-1
    READ(1,*) SSTAT(I),SDPTH(I),SQOVQ(I)
  ENDDO
  SAREA(0)=0.0
  DO I=1,NPOINTS-1
    SAREA(I)=(SDPTH(I)+SDPTH(I-1))/2.0*(SSTAT(I)-SSTAT(I-1))
+      + SAREA(I-1)
  ENDDO

  WRITE(3,10)
  FORMAT(5X,'STATION',T15,'DEPTH',T30,'q/Q')
10 DO I=0,NPOINTS-1
    WRITE(3,15) SSTAT(I),SDPTH(I),SQOVQ(I),SAREA(I)
15 FORMAT(5X,F8.1,T15,F8.2,T30,F10.6,T45,F8.1)
  ENDDO

  ISTAT(0)=SSTAT(0)
  IDPTH(0)=SDPTH(0)
  DO N=1,NTUBES-1
    I=1
    DOWHILE (SQOVQ(I).LT.ETA(N).AND.I.LE.NPOINTS-1)
      I=I+1
    ENDDO
    IF (I.GT.NPOINTS) THEN
      WRITE(3,*) 'INTERPOLATION ERROR'
    ELSEIF (I.EQ.1) THEN
      ISTAT(N)=SSTAT(I-1)+(SSTAT(I)-SSTAT(I-1))*
+      (ETA(N)/SQOVQ(I))**EXPONENT
    ELSEIF (I.EQ.NPOINTS-1) THEN
      ISTAT(N)=SSTAT(I)-(SSTAT(I)-SSTAT(I-1))*
+      ((1.0-ETA(N))/(ETA(N)-ETA(N-1)))**EXPONENT
    ELSE
      ISTAT(N)=LINTERP(SSTAT,SQOVQ,I,ETA(N))
    ENDIF
    IDPTH(N)=LINTERP(SDPTH,SQOVQ,I,ETA(N))
    IAREA(N)=LINTERP(SAREA,SQOVQ,I,ETA(N))
    TWDTH(N)=ISTAT(N)-ISTAT(N-1)
    TDPH(N)=(IAREA(N)-IAREA(N-1))/TWDTH(N)
    TVELC(N)=(ETA(N)-ETA(N-1))*TOTALQ/
+      (IAREA(N)-IAREA(N-1))
  ENDDO

  WRITE(3,20)
  FORMAT(5X,'TUBE MVEL.',T17,'RB DEPTH',T30,'TUBE WIDTH')
20 WRITE(2,*) '          0.0      0.0      0.0'
  DO I=1,NTUBES-1
    WRITE(3,25) TVELC(I),IDPTH(I),TWDTH(I),ETA(I),
+      TVELC(I)*DT/TWDTH(I),IAREA(I),ISTAT(I)
    WRITE(2,30) TDPH(I),TWDTH(I),IDPTH(I)
25 FORMAT(5X,F8.3,T17,F8.2,T30,F8.1,T45,F10.6,T60,F6.1,1X,2F8.2)
30 FORMAT(5X,T17,F8.2,T30,F8.1,T45,F8.2)
  ENDDO

```

```

        DO I=1,NTUBES-1
            WRITE(2,31) SECT,BETA,SLOPE
31          FORMAT(1X,F10.1,1X,F10.3,1X,F10.6)
        ENDDO
        READ(1,*,IOSTAT=IOCHECK) SECT,TOTALQ,NPOINTS,BETA,SLOPE

        ENDDO

    STOP
    END

*****
    REAL FUNCTION LINTERP(X,Y,I,Z)
    INTEGER I
    REAL*4 X(0:100),Y(0:100),Z

    LINTERP=X(I)-(Y(I)-Z)/(Y(I)-Y(I-1))*(X(I)-X(I-1))

    RETURN
    END
*****

```

Appendix C.2 GRIDGEN Program Listing

```

*****
PROGRAM GRIDGEN
*   Preprocessing program to generate the advection optimized grid
*   given the streamtube flow and geometry at each cross-section.
*****
***** Variable declarations*****
IMPLICIT NONE
INTEGER nsect
INTEGER ntubes
INTEGER nts
INTEGER csect
INTEGER i, j, n
INTEGER maxts
INTEGER mints
INTEGER lasti(25)
real*8 dvol
real*8 xus
real*8 xds
real*8 dx
real*8 interp
real*8 elex
real*8 volume
real*8 qtotal
real*8 dt, cvol, vol
real*8 eta(0:25), deta(0:25)
real*8 sub_x[HUGE](0:50,0:25)
real*8 beta[HUGE](0:50,0:25)
real*8 slp[HUGE](0:50,0:25)
real*8 sub_dh[HUGE](0:50,0:25)
real*8 sub_dr[HUGE](0:50,0:25)
real*8 sub_z[HUGE](0:50,0:25)
real*8 cumvol[HUGE](0:50,0:25)
real*8 ele_dr[HUGE](0:2048,0:25)
real*8 ele_w[HUGE](0:2048,0:25)
real*8 ele_ez[HUGE](0:2048,0:25)
real*8 ele_dh[HUGE](0:2048,0:25)
real*8 ele_x[HUGE](0:2048,0:25)
real*8 dr[HUGE](0:2048,0:25)
real*8 w[HUGE](0:2048,0:25)
real*8 ez[HUGE](0:2048,0:25)
real*8 dh[HUGE](0:2048,0:25)
*****
C   Input of subreach characteristics

OPEN(unit=1, file='parm.dat', status='old')
OPEN(unit=2, file='rchchar.out',
+ status='unknown')
OPEN(unit=3, file='simdims.out',
+ status='unknown', ACCESS='direct', RECL=140, FORM='formatted')

READ(1,*) nsect,ntubes,dt,qtotal
READ(1,*) (eta(i),i=1,ntubes)

```



```

eta(0)=0.0d+00
DO i=1,ntubes
    deta(i)=eta(i)-eta(i-1)
ENDDO
nts=0

DO i=0,nsect
    DO j=0,ntubes
        READ(1,*) sub_dh(i,j),sub_z(i,j),sub_dr(i,j)
    END DO
    DO j=1,ntubes
        READ(1,*) sub_x(i,j),beta(i,j),slp(i,j)
    ENDDO
END DO
CLOSE(1)
WRITE(*,*) "completed read section"

```

C Assign the element characteristics

```

DO j=1,ntubes
    ele_dr(0,j)=sub_dr(0,j)
    ele_w(0,j)=sub_z(0,j)
    ele_dh(0,j)=sub_dh(0,j)
    ele_ez(0,j)=beta(0,j)*ele_dh(0,j)
+
    *sqrt(9.81*slp(0,j)*ele_dh(0,j))
    ele_x(0,j)=sub_x(0,j)
END DO
DO j=1,ntubes
    cumvol(0,j)=0.0d+00
    DO i=1,nsect
        cumvol(i,j)=cumvol(i-1,j)+VOLUME(sub_x(i-1,j),sub_x(i,j),
+
        sub_z(i-1,j),sub_z(i,j),sub_dh(i-1,j),sub_dh(i,j))
        cvol=cumvol(i,j)
        WRITE(*,*) i,j,cvol
    ENDDO
ENDDO

DO j=1,ntubes
    i=1
    csect=1
    vol=0.0d+00
    dvol=deta(j)*qttotal*dt
    DOWHILE (csect.LE.nsect)
        vol=vol+dvol
        IF (vol.LT.cumvol(csect,j)) THEN
            CALL findx(elex,sub_x(csect-1,j),sub_x(csect,j),
+
            sub_z(csect-1,j),sub_z(csect,j),
+
            sub_dh(csect-1,j),sub_dh(csect,j),
+
            0.001d+00,vol-cumvol(csect-1,j))
            ele_x(I,J)=elex
            cvol=cumvol(csect-1,j)
            ele_dr(i,j)=INTERP(ele_x(i,j),sub_x(csect-1,j),
+
            sub_x(csect,j),sub_dr(csect-1,j),sub_dr(csect,j))
            ele_dh(i,j)=INTERP(ele_x(i,j),sub_x(csect-1,j),
+
            sub_x(csect,j),sub_dh(csect-1,j),sub_dh(csect,j))

```

```

ele_ez(i,j)=beta(csect,j)*ele_dh(i,j)*
+      sqrt(9.81*slp(csect,j)*ele_dh(i,j))
dr(i,j)=(ele_dr(i,j)+ele_dr(i-1,j))/2.0d+00
dh(i,j)=(ele_dh(i,j)+ele_dh(i-1,j))/2.0d+00
w(i,j)=dvol/(ele_x(i,j)-ele_x(i-1,j))/dh(i,j)
ez(i,j)=(ele_ez(i,j)+ele_ez(i-1,j))/2.0d+00

IF(ez(i,j)*dt/(ele_x(i,j)-ele_x(i-1,j))**2.GT.0.17) THEN
  WRITE(*,*) i,j,"Diffussion criteria exceeded"
ENDIF

i=i+1

ELSE IF (csect.LT.nsect) THEN
  csect=csect+1
  CALL findx(elex,sub_x(csect-1,j),sub_x(csect,j),
+      sub_z(csect-1,j),sub_z(csect,j),
+      sub_dh(csect-1,j),sub_dh(csect,j),
+      0.001d+00,vol-cumvol(csect-1,j))
  ele_x(I,J)=elex
  cvol=cumvol(CSECT-1,j)
  xus=sub_x(csect-1,j)-ele_x(i-1,j)
  xds=ele_x(i,j)-sub_x(csect-1,j)
  dx=xds+xus
  ele_dr(i,j)=INTERP(ele_x(i,j),sub_x(csect-1,j),
+      sub_x(csect,j),sub_dr(csect-1,j),sub_dr(csect,j))
  ele_dh(i,j)=INTERP(ele_x(i,j),sub_x(csect-1,j),
+      sub_x(csect,j),sub_dh(csect-1,j),sub_dh(csect,j))
  ele_ez(i,j)=beta(csect,j)*ele_dh(i,j)*
+      sqrt(9.81*slp(csect,j)*ele_dh(i,j))
  dr(i,j)=(ele_dr(i-1,j)+sub_dr(csect-1,j))*xus+
+      (ele_dr(i,j)+sub_dr(csect-1,j))*xds)/2.0d+00/dx
  dh(i,j)=(ele_dh(i-1,j)+sub_dh(csect-1,j))*xus+
+      (ele_dh(i,j)+sub_dh(csect-1,j))*xds)/2.0d+00/dx
  w(i,j)=dvol/(ele_x(i,j)-ele_x(i-1,j))/dh(i,j)
  ez(i,j)=(beta(csect-1,j)*sqrt(9.81*slp(csect-1,j))*xus
+      +beta(csect,j)*sqrt(9.81*slp(csect,j))*xds)/dx
+      *dh(i,j)*sqrt(dh(i,j))

  IF(ez(i,j)*dt/(ele_x(i,j)-ele_x(i-1,j))**2.GT.0.17) THEN
    WRITE(*,*) i,j,"Diffussion criteria exceeded"
  ENDIF

  i=i+1

ELSE IF (csect.EQ.nsect) THEN
  ele_x(i,j)=sub_x(csect,j)
  ele_dr(i,j)=sub_dr(csect,j)
  ele_dh(i,j)=sub_dh(csect,j)
  ele_w(i,j)=sub_z(csect,j)
  ele_ez(i,j)=(beta(csect,j)*ele_dh(i,j)
+      *sqrt(9.81*slp(csect,j)*ele_dh(i,j)))

```

```

dr(i,j)=(ele_dr(i,j)+ele_dr(i-1,j))/2.0d+00
dh(i,j)=(ele_dh(i,j)+ele_dh(i-1,j))/2.0d+00
w(i,j)=(ele_w(i,j)+ele_w(i-1,j))/2.0d+00
ez(i,j)=(ele_ez(i,j)+ele_ez(i-1,j))/2.0d+00

IF(ez(i,j)*dt/(ele_x(i,j)-ele_x(i-1,j))**2.GT.0.17) THEN
    WRITE(*,*) i,j,"Diffussion criteria exceeded"
ENDIF

csect=csect+1
END IF
END DO

lasti(j)=i
IF (j.EQ.1) maxts=lasti(j)
IF (j.EQ.1) mints=lasti(j)
IF (lasti(j).GT.maxts) maxts=lasti(j)
IF (lasti(j).LT.mints) mints=lasti(j)
END DO

C    Output the assymetrical grid characteristics

WRITE(2,3) nsect,ntubes,maxts,mints,dt
DO j=1,ntubes
    WRITE(2,1) lasti(j),deta(j)*qtotal*dt
END DO
CLOSE(2)

n=1
DO j=1,ntubes
    DO i=1,lasti(j)
        WRITE(3,2,REC=n) i,j,ele_x(i,j),w(i,j),dh(i,j),
+           ez(i,j), dr(i,j)
        n=n+1
    END DO
END DO
CLOSE(3)
WRITE(*,*) 'Grid Completed!'
1  FORMAT(5X,I5,E14.7)
2  FORMAT(5X,2I5,5E14.7)
3  FORMAT(5X,4I5,2F12.3)
STOP
END

```

```

REAL*8 FUNCTION VOLUME(xus,xds,zus,zds,dhus,dhds)

real*8 xus, xds, zus, zds, dhus, dhds
real*8 a,b,c,x1,x2,dx,alpha1,alpha2,beta1,beta2

x1=0.0d+00      !xus-xus
x2=xds-xus
dx=xds-xus

```

```

alpha1=(zds-zus)/dx
alpha2=zus-alpha1*x1
beta1=(dhds-dhus)/dx
beta2=dhus-beta1*x1
a=(alpha2*beta2)
b=(alpha2*beta1+alpha1*beta2)/2.0d+00
c=alpha1*beta1/3.0d+00

```

```

VOLUME=a*x2+b*x2**2+c*x2**3

```

```

RETURN
END

```

```

*****

```

```

SUBROUTINE findx(ele_x,xus,xds,zus,zds,dhus,dhds,
+               toler,vol)

```

```

real*8 f1,f2,f3,funcx
real*8 vol, ele_x, xus, xds, zus, zds, dhus, dhds
real*8 a,b,c,x1,x2,x3,dx,alpha1,alpha2,beta1,beta2
real*8 toler

```

```

x1=0.0d+00          !xus-xus
x2=xds-xus
dx=xds-xus
alpha1=(zds-zus)/dx
alpha2=zus-alpha1*x1
beta1=(dhds-dhus)/dx
beta2=dhus-beta1*x1
a=(alpha2*beta2)
b=(alpha2*beta1+alpha1*beta2)/2.0d+00
c=alpha1*beta1/3.0d+00
f3=toler

```

```

DOWHILE (ABS(f3).GE.toler)
  f2=funcx(a,b,c,vol,x2)
  f1=funcx(a,b,c,vol,x1)
  x3=x2-f2*(x2-x1)/(f2-f1)
  f3=funcx(a,b,c,vol,x3)
  IF(f3.LT.C.AND.f1.GE.0.OR.f3.GE.0.AND.f1.LT.0) THEN
    x2=x3
  ELSE
    x1=x3
  ENDIF
ENDDO
ele_x=x3+xus
RETURN
END

```

```

*****

```

```

real*8 FUNCTION funcx(a,b,c,d,x)

```

```

real*8 a,b,c,d,x

```

```

funcx=a*x+b*x**2+c*x**3-d

```

```

      RETURN
      END
*****
      REAL*8 FUNCTION INTERP(x,x1,x2,y1,y2)

      REAL*8 x,x1,x2,y1,y2

      INTERP=y1+(x-x1)/(x2-x1)*(y2-y1)

      RETURN
      END
*****

```

Appendix C.3 2DMIX Program Listing

```
*****
PROGRAM 2DMIX
*   Main mixing program.
*****
***** Begin Mainline Program *****
***** Variable declarations*****
IMPLICIT NONE
INTEGER ns
INTEGER ntubes
INTEGER nts
INTEGER maxts
INTEGER mints
INTEGER csect
INTEGER i
INTEGER j
INTEGER jl
INTEGER jr
INTEGER k
INTEGER n
INTEGER r
INTEGER maxi
INTEGER lasti(20)
INTEGER limiti(20)
INTEGER noline(0:2048,20)
REAL*4 x
REAL*4 w
REAL*4 d
REAL*4 ez
REAL*4 bd
REAL*4 dt
REAL*4 deltac
REAL*4 initialx
REAL*4 etime
REAL*4 dvol(20),maxx(20)

STRUCTURE/ptable/
  INTEGER ip
  INTEGER jp
END STRUCTURE
RECORD/ptable/pt(0:2048,20,8)

STRUCTURE/ftable/
  REAL*4 avgd
  REAL*4 avgez
  REAL*4 avgw
  REAL*4 avgl
END STRUCTURE
RECORD/ftable/ft(0:2048,20,8)

STRUCTURE/eleldata/
  REAL*4 x
  REAL*4 d
```

```

END STRUCTURE
RECORD/ele1data/ele1(0:2048,20)

STRUCTURE/ele2data/
  REAL*4 ez
  REAL*4 bd
END STRUCTURE
RECORD/ele2data/ele2(0:2048,20)

STRUCTURE/ele3data/
  REAL*4 w
END STRUCTURE
RECORD/ele3data/ele3(0:2048,20)

STRUCTURE/concdata/
  REAL*4 c1
  REAL*4 c2
END STRUCTURE
RECORD/concdata/elec(0:2048,20)

COMMON ns, ntubes, nts, maxts, csect, i, j, k, dt, deltac, maxi
*****
C
  OPEN(UNIT=1, FILE='rchchar.out', STATUS='old')
  OPEN(UNIT=2, FILE='conc.txt', STATUS='old')
  OPEN(UNIT=7, FILE='simdims.out', STATUS='old',
+ ACCESS='DIRECT', RECL=140, FORM='FORMATTED')
  OPEN(UNIT=3, FILE='timeconc.dat',
+ ACCESS='DIRECT', RECL=4, FORM='UNFORMATTED')
C
  READ(1,*) ns, ntubes, maxts, mints, dt, nts, initialx
  READ(1,*) lasti(1), dvol(1)
  limiti(1)=0
  maxi=lasti(1)
  DO k=2, ntubes
    READ(1,*) lasti(k), dvol(k)
    limiti(k)=0
    IF(lasti(k).GT.maxi) maxi=lasti(k)
  ENDDO
  CLOSE(1)
C
  DO i=0, maxts
    DO j=1, ntubes
      elec(i,j).c1=0.0d+00
      elec(i,j).c2=0.0d+00
    ENDDO
  ENDDO
C
  k=1
  DO WHILE (.NOT.EOF(7))
    READ(7,10,REC=k) i, j, x, w, d, ez, bd
    ele1(i,j).x=x
    ele1(i,j).d=d
    ele3(i,j).w=w
    ele2(i,j).ez=ez

```

```

        ele2(i,j).bd=bd
        k=k+1
    ENDDO
10  FORMAT(5X,2I5,5D14.7)
    CLOSE(7)
C
    DO j=1,ntubes
        ele1(0,j).x=initialx
        ele1(0,j).d=ele1(1,j).d
        ele3(0,j).w=ele3(1,j).w
        ele2(0,j).ez=ele2(1,j).ez
        ele2(0,j).bd=ele2(1,j).bd
    ENDDO

    DO j=1,ntubes
        IF (j.GT.1.AND.j.LT.ntubes) THEN
            DO i=1,lasti(j)
                r=1
                jl=j-1
                CALL FILLTABLE(ele1,ele2,ele3,ft,pt,lasti,jl,r)
                jr=j+1
                CALL FILLTABLE(ele1,ele2,ele3,ft,pt,lasti,jr,r)
                nlines(i,j)=r-1
                IF(r.gt.8) STOP 'Flux table row limit exceeded'
            END DO
        ELSEIF (j.EQ.1) THEN
            DO i=1,lasti(j)
                r=1
                jr=j+1
                CALL FILLTABLE(ele1,ele2,ele3,ft,pt,lasti,jr,r)
                nlines(i,j)=r-1
                IF(r.gt.8) STOP 'Flux table row limit exceeded'
            END DO
        ELSE
            DO i=1,lasti(j)
                r=1
                jl=j-1
                CALL FILLTABLE(ele1,ele2,ele3,ft,pt,lasti,jl,r)
                nlines(i,j)=r-1
                IF(r.gt.8) STOP 'Flux table row limit exceeded'
            END DO
        ENDIF
    ENDDO

    n=1                ! Initilize the record counter

    DO k=1,nts
        IF(.NOT.EOF(2)) THEN
            READ(2,*)etime,(elec(0,j).c1,j=1,ntubes)
        ELSE
            DO j=1,ntubes
                elec(0,j).c1=0.0
            ENDDO
        ENDIF
    ENDDO

```



```

        CALL LIMIT(ele1,limiti,lasti,maxx)
        CALL ADVECTION(elec,limiti)
        CALL DIFFUSION(nolines,elec,ft,pt,limiti,dvol)
        CALL WRTTSTP(n,elec,lasti)
    ENDDO
C
    WRITE(*,*) 'Run Complete! '
    STOP
    END
C***** End Mainline Program *****
C***** Begin Subroutine Filltable *****
    SUBROUTINE FILLTABLE(ele1,ele2,ele3,ft,pt,lasti,l,r)
    IMPLICIT NONE
    INTEGER ns,ntubes,nts,maxts,csect,i,j,k,l,m,r,maxi
    INTEGER lasti(20)
    REAL*4 dt,deltac,back,front

    STRUCTURE/ptable/
    INTEGER ip
    INTEGER jp
    END STRUCTURE
    RECORD/ptable/pt(0:2048,20,8)

    STRUCTURE/ftable/
    REAL*4 avgd
    REAL*4 avgez
    REAL*4 avgw
    REAL*4 avgl
    END STRUCTURE
    RECORD/ftable/ft(0:2048,20,8)

    STRUCTURE/ele1data/
    REAL*4 x
    REAL*4 d
    END STRUCTURE
    RECORD/ele1data/ele1(0:2048,20)

    STRUCTURE/ele2data/
    REAL*4 ez
    REAL*4 bd
    END STRUCTURE
    RECORD/ele2data/ele2(0:2048,20)

    STRUCTURE/ele3data/
    REAL*4 w
    END STRUCTURE
    RECORD/ele3data/ele3(0:2048,20)

    COMMON ns,ntubes,nts,maxts,csect,i,j,k,dt,deltac,maxi

    m=INT((REAL(i)/REAL(lasti(j)))*lasti(l))      !Start position for search
    IF(m.EQ.0) m=1

```

```

IF (ele1(m,1).x.LT.ele1(i-1,j).x) THEN      !Is the position<x current?
  DOWHILE (ele1(m,1).x.LT.ele1(i-1,j).x)
    m=m+1                                     !Increment up
  END DO
ELSE
  IF (ele1(m-1,1).x.GT.ele1(i-1,j).x) THEN !Is the position<x current?
    DO WHILE (ele1(m-1,1).x.GT.ele1(i-1,j).x)
      m=m-1                                     !Increment down
    END DO
  ENDIF
ENDIF
ENDIF

IF (ele1(m,1).x.GE.ele1(i,j).x.AND.ele1(m-1,1).x.LE.ele1(i-1,j).x)
+ THEN
  if(j.lt.1) ft(i,j,r).avgd=ele2(i,j).bd
  if(j.gt.1) ft(i,j,r).avgd=ele2(m,1).bd
  pt(i,j,r).ip=m
  pt(i,j,r).jp=1
  ft(i,j,r).avgw=(ele3(i,j).w+ele3(m,1).w)/2.0d+00
  ft(i,j,r).avgez=(ele2(i,j).ez+ele2(m,1).ez)/2.0d+00
  ft(i,j,r).avgl=ele1(i,j).x-ele1(i-1,j).x
  r=r+1
  RETURN
ELSE
  back=ele1(i-1,j).x
  IF (ele1(m,1).x.LT.ele1(i,j).x) THEN
    front=ele1(m,1).x
    DO WHILE (m.LE.maxts)
      if(j.lt.1) ft(i,j,r).avgd=ele2(i,j).bd
      if(j.gt.1) ft(i,j,r).avgd=ele2(m,1).bd
      pt(i,j,r).ip=m
      pt(i,j,r).jp=1
      ft(i,j,r).avgw=(ele3(i,j).w+ele3(m,1).w)/2.0d+00
      ft(i,j,r).avgez=(ele2(i,j).ez+ele2(m,1).ez)/2.0d+00
      ft(i,j,r).avgl=front-back
      m=m+1
      back=front
      r=r+1
    IF (ele1(m,1).x.GE.ele1(i,j).x) THEN
      if(j.lt.1) ft(i,j,r).avgd=ele2(i,j).bd
      if(j.gt.1) ft(i,j,r).avgd=ele2(m,1).bd
      pt(i,j,r).ip=m
      pt(i,j,r).jp=1
      ft(i,j,r).avgw=(ele3(i,j).w+ele3(m,1).w)/2.0d+00
      ft(i,j,r).avgez=(ele2(i,j).ez+ele2(m,1).ez)/2.0d+00
      ft(i,j,r).avgl=ele1(i,j).x-back
      r=r+1
      RETURN
    ELSE
      front=ele1(m,1).x
    ENDIF
  END DO
  WRITE(*,*)i,j,' Error! dropped out of the search loop.'
ELSE
  WRITE(*,*)i,j,' Error! redundant portion executed'

```

```

        RETURN
    ENDIF
ENDIF
21  FORMAT(10X,3I5,F10.5)
    RETURN
    END
C***** End Subroutine Filltable *****
C***** Begin Subroutine Limit ****
    SUBROUTINE LIMIT(elel,limiti,lasti,maxx)
    IMPLICIT NONE
    INTEGER ns,ntubes,nts,maxts,csect,i,j,k,maxi
    INTEGER limiti(20),lasti(20)
    REAL*4 dt,deltac,maxx(20)

    STRUCTURE/eleldata/
        REAL*4 x
        REAL*4 d
    END STRUCTURE
    RECORD/eleldata/elel(0:2048,20)

    COMMON ns,ntubes,nts,maxts,csect,i,j,k,dt,deltac,maxi
C
    DO j=1,ntubes
        IF(j.EQ.1) THEN
            IF(limiti(j).LT.lasti(j).AND.limiti(j+1).LT.lasti(j+1))THEN
                maxx(j)=MAX(elel(limiti(j+1)+1,j+1).x,
+                 elel(limiti(j)+1,j).x)
            ELSE
                maxx(j)=elel(lasti(j),j).x
            ENDIF
        ELSEIF(j.EQ.ntubes) THEN
            IF(limiti(j).LT.lasti(j).AND.limiti(j-1).LT.lasti(j-1))THEN
                maxx(j)=MAX(elel(limiti(j)+1,j).x,
+                 elel(limiti(j-1)+1,j-1).x)
            ELSE
                maxx(j)=elel(lasti(j),j).x
            ENDIF
        ELSE
            IF(limiti(j).LT.lasti(j).AND.limiti(j+1).LT.lasti(j+1)
+             .AND.limiti(j-1).LT.lasti(j-1))THEN
                maxx(j)=MAX(elel(limiti(j-1)+1,j-1).x,
+                 elel(limiti(j)+1,j).x,elel(limiti(j+1)+1,j+1).x)
            ELSE
                maxx(j)=elel(lasti(j),j).x
            ENDIF
        ENDIF
    ENDDO

    DO j=1,ntubes
        i=limiti(j)
        DOWHILE(elel(i,j).x.LT.maxx(j))
            i=i+1
        ENDDO
        limiti(j)=i
C        WRITE(*,*)limiti(j)

```

```

        ENDDO
        RETURN
    END
C***** End Subroutine Limit *****
C***** Begin Subroutine Advection ****
    SUBROUTINE ADVECTION(elec,limiti)
    IMPLICIT NONE
    INTEGER ns,ntubes,nts,maxts,csect,i,j,k,maxi
    INTEGER limiti(20)
    REAL*4 dt,deltac

    STRUCTURE/concdata/
        REAL*4 c1
        REAL*4 c2
    END STRUCTURE
    RECORD/concdata/elec(0:2048,20)

    COMMON ns,ntubes,nts,maxts,csect,i,j,k,dt,deltac,maxi
C
    DO j=1,ntubes
        DO i=limiti(j),1,-1
            elec(i,j).c1=elec(i-1,j).c1
        ENDDO
    ENDDO
    RETURN
    END
C***** End Subroutine Avection *****
C***** Begin Subroutine Diffusion ****
    SUBROUTINE DIFFUSION(nolines,elec,ft,pt,limiti,dvol)
    IMPLICIT NONE
    INTEGER ns,ntubes,nts,maxts,csect,i,j,k,maxi,r
    INTEGER limiti(20)
    INTEGER nolines(0:2048,20)
    REAL*4 dt,deltac,sum, dsum, tsum
    REAL*4 DVOL(20)
    STRUCTURE/ptable/
        INTEGER ip
        INTEGER jp
    END STRUCTURE
    RECORD/ptable/pt(0:2048,20,8)

    STRUCTURE/ftable/
        REAL*4 avgd
        REAL*4 avgez
        REAL*4 avgw
        REAL*4 avgl
    END STRUCTURE
    RECORD/ftable/ft(0:2048,20,8)

    STRUCTURE/concdata/
        REAL*4 c1
        REAL*4 c2
    END STRUCTURE
    RECORD/concdata/elec(0:2048,20)

```

```

COMMON ns,ntubes,nts,maxts,csect,i,j,k,dt,deltac,maxi
C
tsum=0.0
DO j=1,ntubes
  DO i=1,limiti(j)
    sum=0.0d+00
    DO r=1,nolines(i,j)
      deltac=elec(pt(i,j,r).ip,pt(i,j,r).jp).c1
      -elec(i,j).c1
+      IF (ABS(deltac).GT.0.000001) THEN
        dsum=ft(i,j,r).avgl*ft(i,j,r).avgd
+        *deltac*ft(i,j,r).avgez
+        /ft(i,j,r).avgw
        sum=sum+dsum
      ENDIF
    END DO
    elec(i,j).c2=elec(i,j).c1+sum/dvol(j)*dt
    IF(elec(i,j).c2.lt.0.0) elec(i,j).c2=0.0
  ENDDO
ENDDO

20 FORMAT(1X,3I5)
21 FORMAT(10X,3I5,1X,E18.11)
22 FORMAT(10X,E14.7)
RETURN
END
C***** End Subroutine Diffusion *****
C***** Begin Subroutine Wrttstp ****
SUBROUTINE WRTTSTP(n,elec,lasti)
IMPLICIT NONE
INTEGER ns,ntubes,nts,maxts,csect,i,j,k,n,maxi
INTEGER lasti(20)
REAL*4 dt,deltac,mass

STRUCTURE/concdata/
  REAL*4 c1
  REAL*4 c2
END STRUCTURE
RECORD/concdata/elec(0:2048,20)

COMMON ns,ntubes,nts,maxts,csect,i,j,k,dt,deltac,maxi
C
WRITE(*,10) k, nts
mass=0.0
DO j=1,ntubes
  DO i=1,lasti(j)
    elec(i,j).c1=elec(i,j).c2
    WRITE(3,REC=n) elec(i,j).c1
    n=n+1
  ENDDO
ENDDO
10 FORMAT(' ',10X,'Writing time step ',I4,' of ',I4)
RETURN
END
C***** End Subroutine Wrttstp *****

```

Appendix C.4 XSLICE Program Listing

```

*****
PROGRAM XSLICE
*   Post processing program to interpolate concentrations vs. time in each
*   streamtube at a requested distance downstream .
***** Begin Mainline Program *****
***** Variable declarations*****
INTEGER*4 ns
INTEGER*4 ntubes
INTEGER*4 nts
INTEGER*4 maxts
INTEGER*4 mints
INTEGER*4 recpl
INTEGER*4 tstep
INTEGER*4 cpt
INTEGER*4 stn
INTEGER*4 pt
INTEGER lasti(50)
REAL*4   dt
REAL*4   x
REAL*4   toffset
REAL*4   initialx
REAL*4   sum
REAL*4   xlo
REAL*4   xhi
REAL*4   tempc
REAL*4   farc
REAL*4   interp
REAL*4   t(4096)
REAL*4   dvol(50)
REAL*4   c(50,4096)
LOGICAL loflag
*****
COMMON lasti,initialx

C
OPEN(UNIT=1,FILE='rchchar.out',STATUS='old')
OPEN(UNIT=2,FILE='simdims.out',STATUS='old',
+ ACCESS='DIRECT', RECL=140, FORM='FORMATTED')
OPEN(UNIT=3,FILE='timeconc.dat',STATUS='old',
+ ACCESS='DIRECT', RECL=4, FORM='UNFORMATTED')
OPEN(UNIT=4,FILE='lslice.dat',STATUS='unknown')

C
READ(1,*) ns,ntubes,maxts,mints,dt,nts,initialx,toffset
DO k=1,ntubes
    READ(1,*) lasti(k),dvol(k)
ENDDO
CLOSE(1)
recpl=0
DO j=1,ntubes
    recpl=recpl+lasti(j)
ENDDO

C
WRITE(*,*) 'ENTER the distance downstream'

```

```

      READ(*,*) x
C
      DO stn=1,ntubes

        CALL XSEARCH(x,stn,pt,xlo,xhi,loflag)
C
        DO tstep=1,nts
          cpt=recpl*(tstep-1)+pt
          READ(3,rec=cpt) tempc
          IF(loflag)THEN
            READ(3,rec=cpt-1) farc
            c(stn,tstep)=INTERP(x,xlo,xhi,farc,tempc)
          ELSE
            READ(3,rec=cpt+1) farc
            c(stn,tstep)=INTERP(x,xlo,xhi,tempc,farc)
          ENDIF
        ENDDO
      ENDDO
      sum=0.0
      DO tstep=1,nts
        t(tstep)=real(tstep)*dt+toffset
        WRITE(*,15) t(tstep), (c(stn,tstep),stn=1,ntubes)
        WRITE(4,15) t(tstep), (c(stn,tstep),stn=1,ntubes)
        DO stn=1,ntubes
          sum=sum+c(stn,tstep)*dvol(stn)
        ENDDO
      ENDDO
      WRITE(*,*) sum*1000.0
      ENDDO

15  FORMAT(F12.1,',',50(E12.5,','))
      STOP
      END
C*****Begin Subroutine XSEARCH*
      SUBROUTINE XSEARCH(x,stn,pt,xlo,xhi,loflag)
      INTEGER*4 i,k,n,int,fin,stn,pt
      INTEGER lasti(50)
      REAL*4 x,dxx,usx,xlo,xhi,meanx,farx
      LOGICAL loflag
      COMMON lasti,initialx
C
      k=0
      DO n=1,stn
        k=k+lasti(n)
      ENDDO
      fin=k
      int=k-lasti(stn)
      pt=(int+fin)/2

      READ(2,5,rec=pt) i,n,dxx
      IF (pt.EQ.k-lasti(stn)) THEN
        usx=initialx
      ELSE
        READ(2,5,rec=pt-1) i,n,usx
      ENDIF

```

```

DOWHILE (.NOT. (dsx.GE.x.AND.usx.LT.x))
  IF (dsx.GT.x) THEN
    fin=pt
  ELSE
    int=pt
  ENDIF
  pt=(fin+int)/2
  READ(2,5,rec=pt) i,n,dsx
  IF (pt.EQ.k-lasti(stn)) THEN
    usx=initialx
  ELSE
    READ(2,5,rec=pt-1) i,n,usx
  ENDIF
ENDDO
meanx=((dsx+usx)/2.0d+00)
IF (x.GT.meanx) THEN
  xlo=meanx
  READ(2,5,rec=pt+1) i,n,farx
  xhi=(dsx+farx)/2.0d+00
  loflag=.FALSE.
ELSE
  READ(2,5,rec=pt-2) i,n,farx
  xlo=(farx+usx)/2.0d+00
  xhi=meanx
  loflag=.TRUE.
ENDIF
RETURN
5  FORMAT(5X,2I5,5E14.7)
END
*****End Subroutine Xsearch***
*****Begin Function Interp ***
REAL*4 FUNCTION INTERP(x,x1,x2,y1,y2)
REAL*4 x,x1,x2,y1,y2

INTERP=y1+(x-x1)/(x2-x1)*(y2-y1)

RETURN
END
*****End Function Interp ****

```


Appendix D. Cross Sections

Appendix D.1 North Saskatchewan River

Appendix D.2 Peace River

Appendix D.3 Slave River

Appendix D.4 South Saskatchewan River

Appendix D.5 Athabasca River

Appendix D.1 North Saskatchewan River

X-SECTION N. Sask. River, 813.10 km (ARC Section 0)

DATE October 18, 1977

DISCHARGE m^3/s 142

WIDTH m 187

H MEAN m 1.24

AREA m^2 243.6

U MEAN m/s 0.583

Section from Alberta Research Council Report

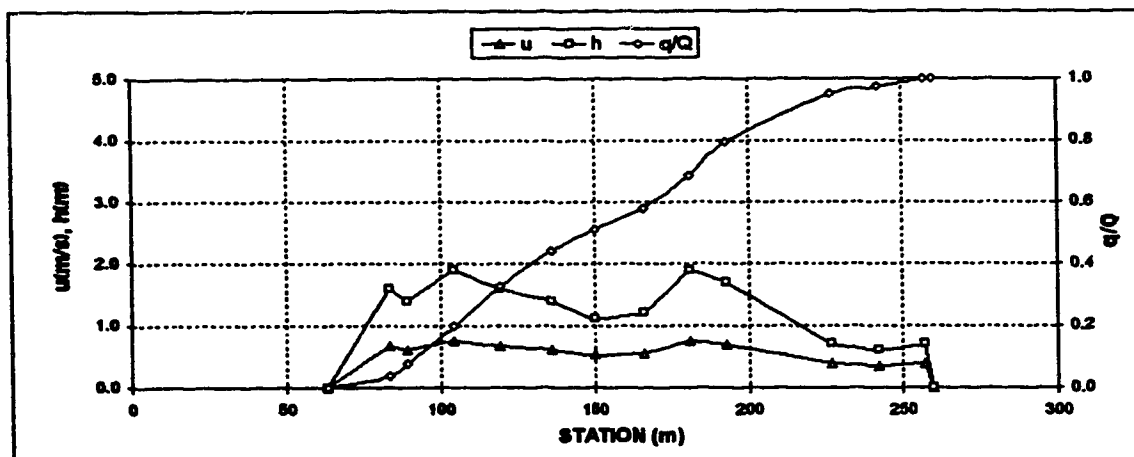
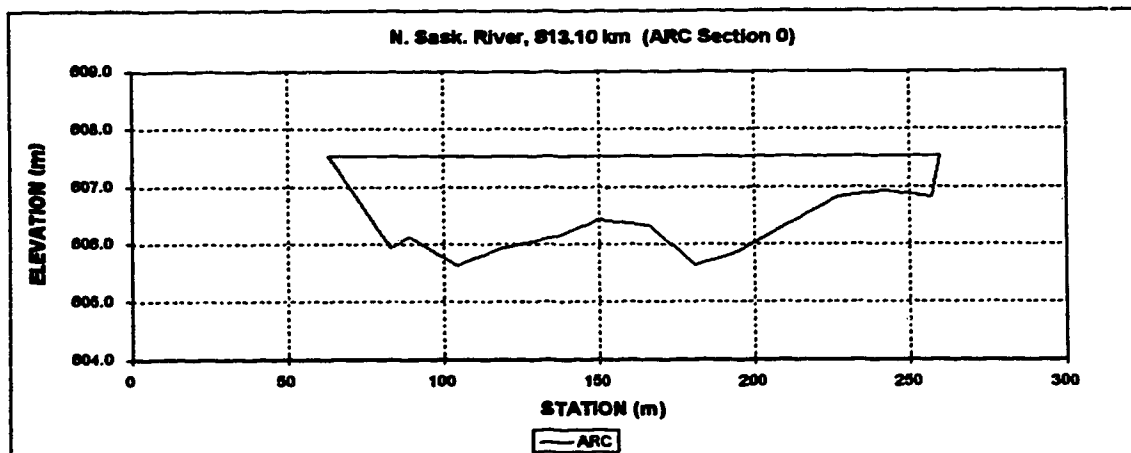
Assumed Water Surface 82.7 m

Est. W.S.E. 10/18/77 607.53 m

Correction to Geodetic 514.828 m

Correction to Station 60 m

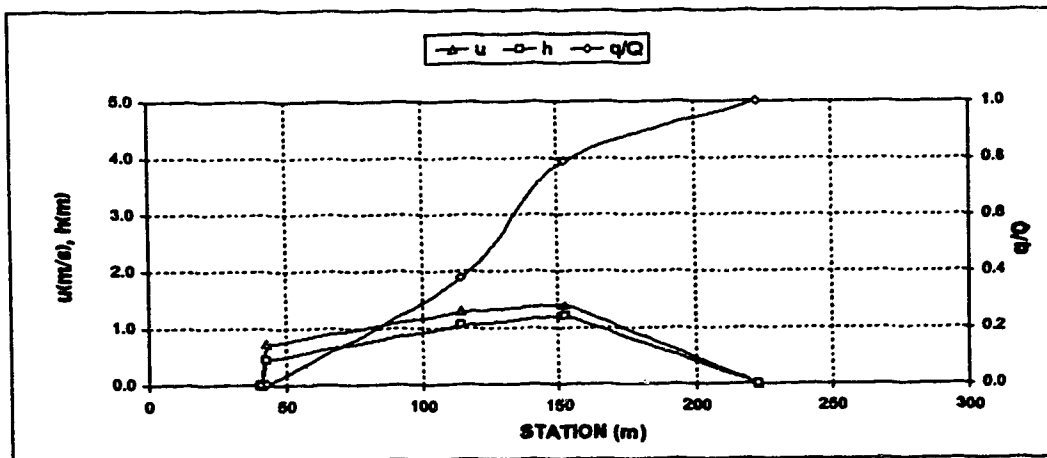
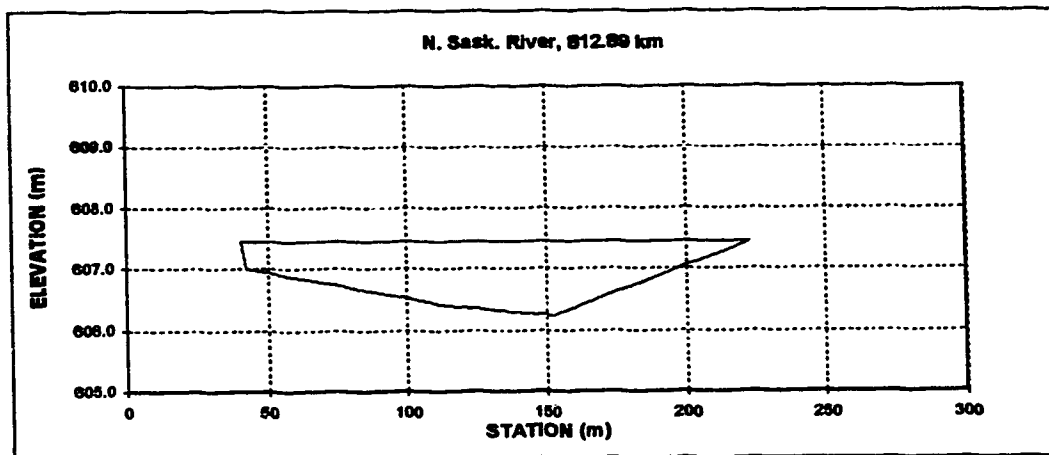
Water's Edge	Assumed Elev	Est. Sta.	Est. Geod.	h	w/W	u	dq est.	norm. q/Q	Area	adj. u
m	m	m	m	m		m/s	m^3		m^2	m/s
3	92.70	83	607.5	0.00	0.000	0.000	0.00	0.00000	0.0	0.000
23	91.10	83	605.9	1.60	0.102	0.892	5.54	0.03745	16.0	0.665
29	91.30	89	606.1	1.40	0.132	0.633	5.96	0.07778	25.0	0.608
44	90.80	104	605.6	1.90	0.208	0.776	17.44	0.19570	49.8	0.745
59	91.10	119	605.9	1.60	0.284	0.692	19.27	0.32808	76.0	0.685
76	91.30	136	606.1	1.40	0.371	0.633	16.90	0.45033	101.5	0.608
90	91.60	150	606.4	1.10	0.442	0.539	10.26	0.50974	119.0	0.518
108	91.50	166	606.3	1.20	0.523	0.571	10.22	0.57083	137.4	0.549
121	90.80	181	605.6	1.90	0.599	0.776	15.67	0.68477	160.7	0.745
133	91.00	193	605.8	1.70	0.660	0.721	16.17	0.76451	182.3	0.692
167	92.00	227	606.8	0.70	0.832	0.399	22.84	0.94856	223.1	0.383
182	92.10	242	606.9	0.60	0.909	0.360	3.70	0.97357	232.8	0.346
197	92.00	257	606.8	0.70	0.985	0.399	3.70	0.99818	242.6	0.383
200	92.70	260	607.5	0.00	1.000	0.000	0.21	1.00000	243.6	0.000
3	92.70	83	607.5							
Est. Total							147.88			



Appendix D.1 North Saskatchewan River

X-SECTION N. Sask. River, 812.89 km
 DATE October 18, 1977
 DISCHARGE m^3/s 142.00
 WIDTH m 182.72
 MEAN DEPTH m 0.78
 AREA m^2 139.55
 MEAN VELOCITY m/s 1.018
 Est. Water Surface Elev. 607.45 m
 LB 40.53 607.45 m
 RB 223.24 607.45 m

Sta. m	Elev. m	h m	w/W	u m/s	dq est. m^3	norm. q/Q	Area adjusted m^2	u m/s
40.53	607.45	0.00	0.000	0.000	0.00	0.00000	0.0	0.000
42.67	607.01	0.44	0.012	0.703	0.16	0.00119	0.5	0.720
114.30	606.40	1.05	0.404	1.257	52.20	0.37758	53.7	1.287
152.40	606.24	1.21	0.612	1.382	56.74	0.78670	96.7	1.415
223.24	607.45	0.00	1.000	0.000	29.58	1.00000	139.6	0.000
Est. Total					138.70			



Appendix D.1 North Saskatchewan River

X-SECTION N. Sask. River, 812.54 km

HEC2 Section from Alberta Env.

DATE October 18, 1977

DISCHARGE m^3/s 142.00

WIDTH m 239.38

MEAN DEPTH m 0.84

AREA m^2 200.32

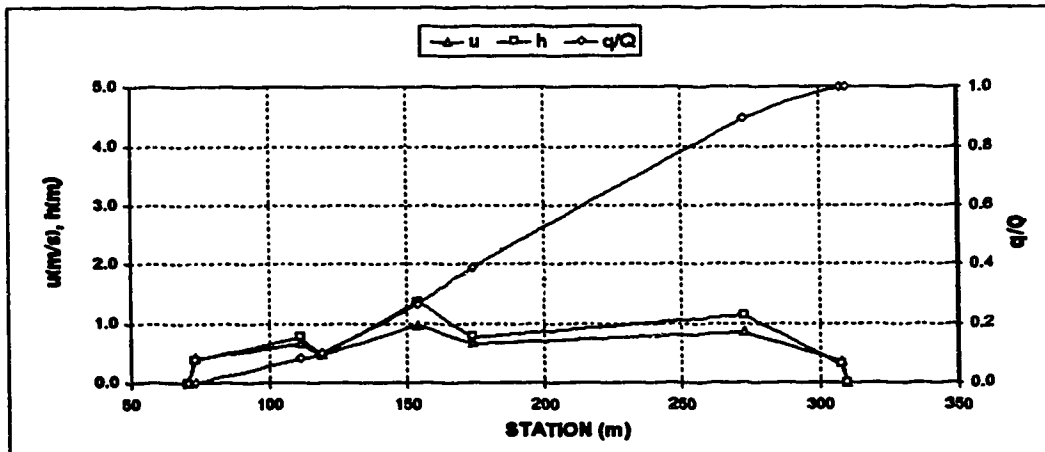
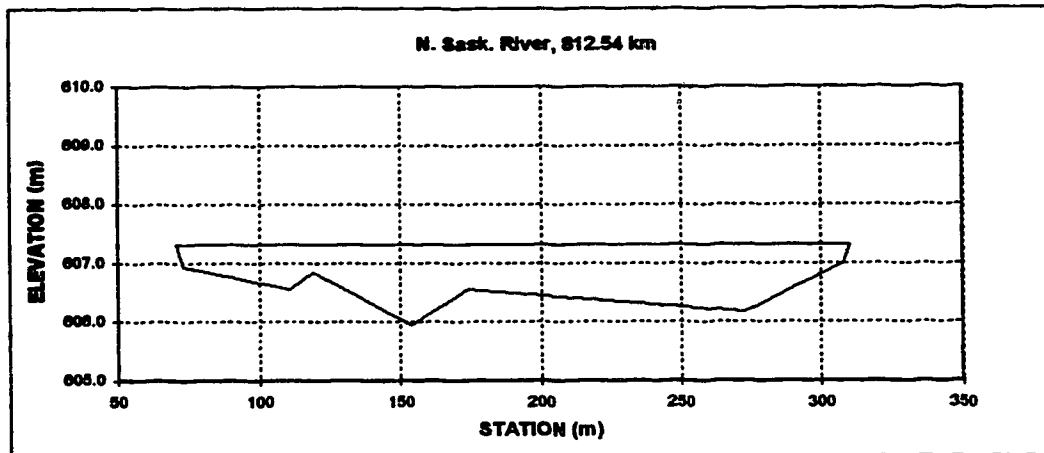
MEAN VELOCITY m/s 0.709

Est. Water Surface Elev. 607.32

LB 70.86 607.32

RB 310.05 607.32

Sta. m	Elev. m	h m	w/W	u m/s	dq est. m^3	norm. q/Q	Area adjusted u m^2	m/s
70.86	607.32	0.00	0.000	0.000	0.00	0.00000	0.0	0.000
73.16	606.94	0.38	0.010	0.416	0.10	0.00068	0.5	0.410
111.28	606.55	0.77	0.170	0.669	11.80	0.08286	22.2	0.659
118.88	606.85	0.47	0.201	0.480	2.70	0.10140	28.9	0.473
153.93	605.94	1.38	0.348	0.988	23.70	0.26801	59.2	0.974
173.74	606.55	0.77	0.431	0.669	17.58	0.38809	80.5	0.659
272.80	606.18	1.14	0.844	0.869	72.47	0.89140	174.7	0.857
307.85	607.01	0.31	0.991	0.363	15.58	0.99958	200.0	0.358
310.05	607.32	0.00	1.000	0.000	0.06	1.00000	200.3	0.000
Est. Total					143.98			



Appendix D.1 North Saskatchewan River

X-SECTION N. Sask. River, 812.14 km

HEC2 Section from Alberta Env.

DATE October 18, 1977

DISCHARGE m^3/s 142.00

WIDTH m 234.83

MEAN DEPTH m 0.89

AREA m^2 209.84

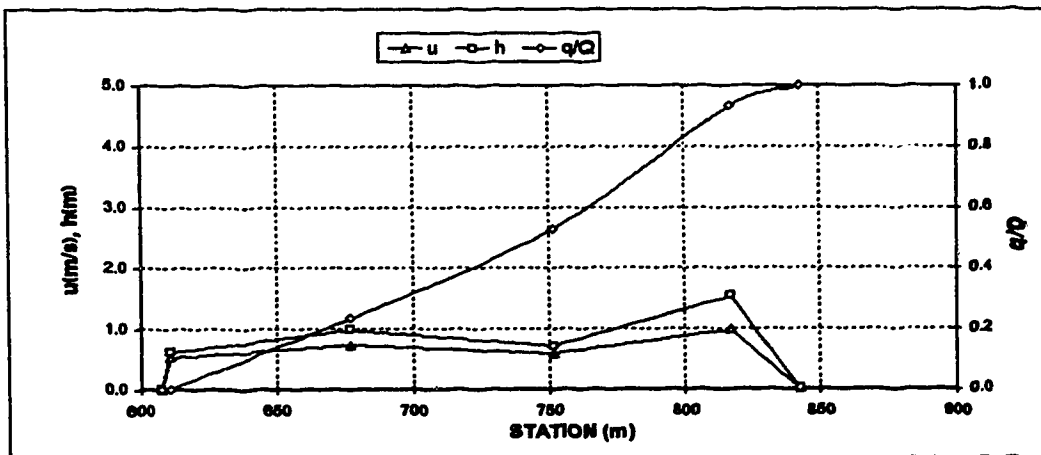
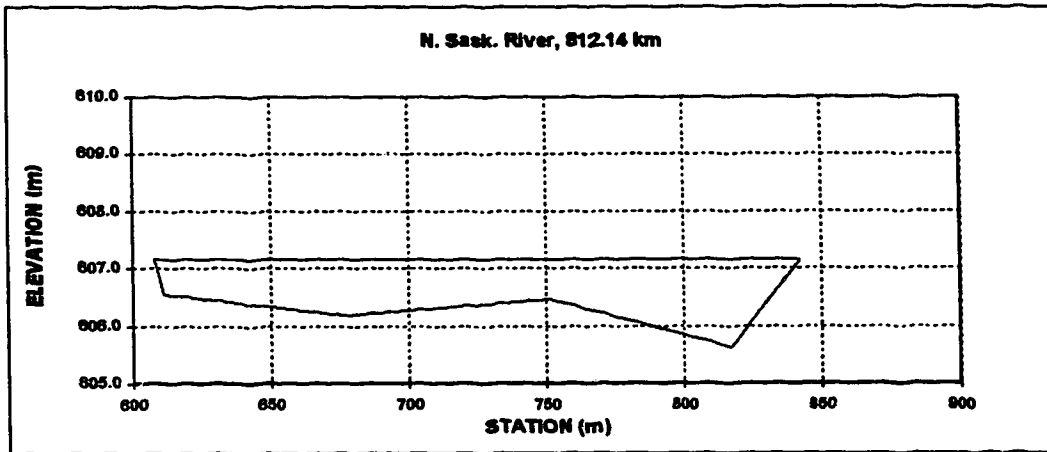
MEAN VELOCITY m/s 0.677

Est. Water Surface Elev. 807.17

LB 807.81 807.17

RB 842.74 807.17

Sta. m	Elev. m	h m	w/W	u m/s	dq est. m^3	norm. q/Q	Area adjusted m^2	u m/s
607.81	807.17	0.00	0.000	0.000	0.00	0.00000	0.0	0.000
611.13	808.55	0.62	0.014	0.528	0.27	0.00192	1.0	0.533
676.66	808.18	0.99	0.263	0.722	32.78	0.23506	53.5	0.730
751.34	808.46	0.71	0.611	0.578	41.04	0.52898	118.6	0.584
816.87	805.63	1.54	0.890	0.971	56.86	0.93142	190.0	0.981
842.74	807.17	0.00	1.000	0.000	9.84	1.00000	209.8	0.000
Est. Total					140.59			



Appendix D.1 North Saskatchewan River

X-SECTION N. Sask. River, 811.81 km

HEC2 Section from Alberta Env.

DATE October 18, 1977

DISCHARGE m^3/s 142.00

WIDTH m 194.10

MEAN DEPTH m 1.48

AREA m^2 286.38

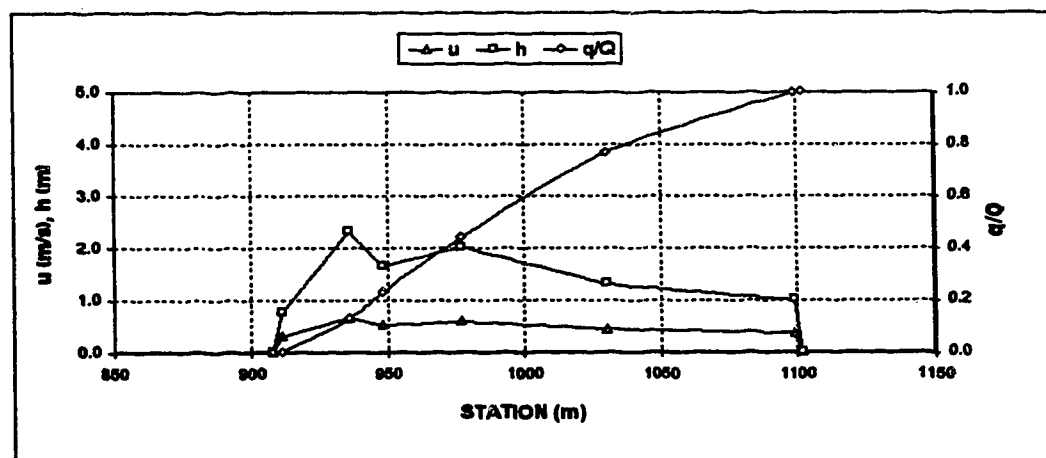
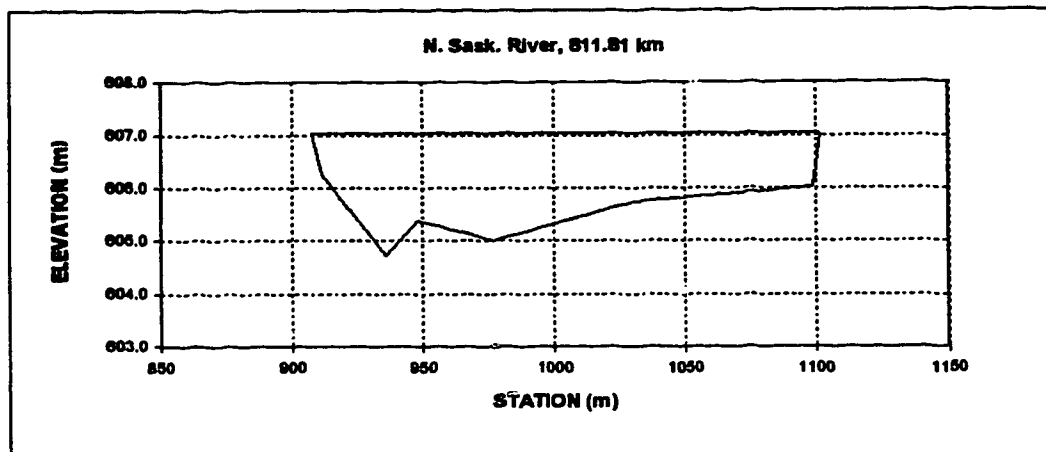
MEAN VELOCITY m/s 0.496

Est. Water Surface Elev. 607.04

LB 907.68 607.04

RB 1101.78 607.04

Sta. m	Elev. m	h m	w/W	u m/s	dq est. m^3	norm. q/Q	Area adjusted m^2	u m/s
907.68	607.04	0.00	0.000	0.000	0.00	0.00000	0.0	0.000
911.35	606.27	0.77	0.019	0.321	0.23	0.00156	1.4	0.314
935.73	604.72	2.32	0.145	0.671	18.69	0.13019	39.1	0.655
947.93	605.39	1.65	0.207	0.534	14.59	0.23082	63.3	0.522
979.88	605.02	2.02	0.357	0.612	30.44	0.44012	116.5	0.598
1030.22	605.73	1.31	0.631	0.458	47.51	0.78707	205.3	0.448
1098.80	606.03	1.01	0.985	0.385	33.56	0.99800	284.9	0.378
1101.78	607.04	0.00	1.000	0.000	0.29	1.00000	286.4	0.000
Est. Total					145.32			



Appendix D.1 North Saskatchewan River

X-SECTION N. Sask. River, 811.40 km

HEC2 Section from Alberta Env.

DATE October 18, 1977

DISCHARGE m^3/s 142.00

WIDTH m 212.65

MEAN DEPTH m 1.37

AREA m^2 291.20

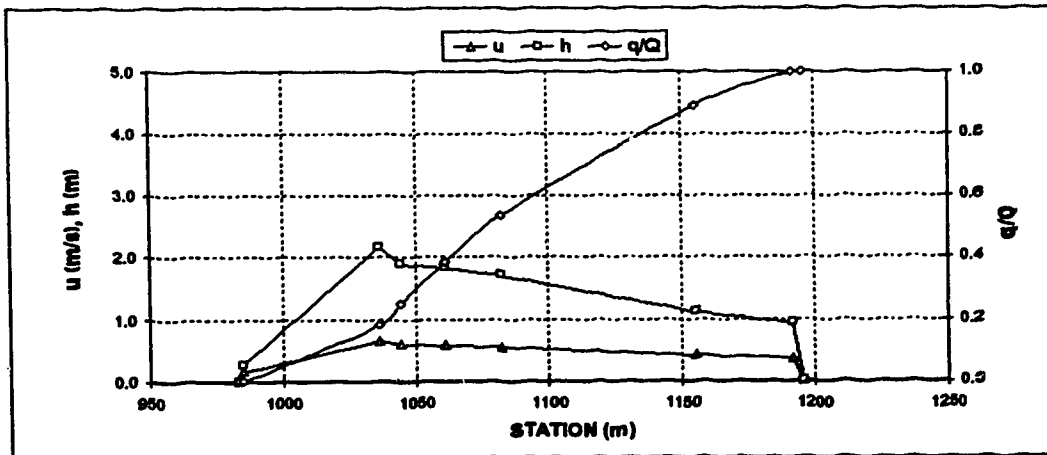
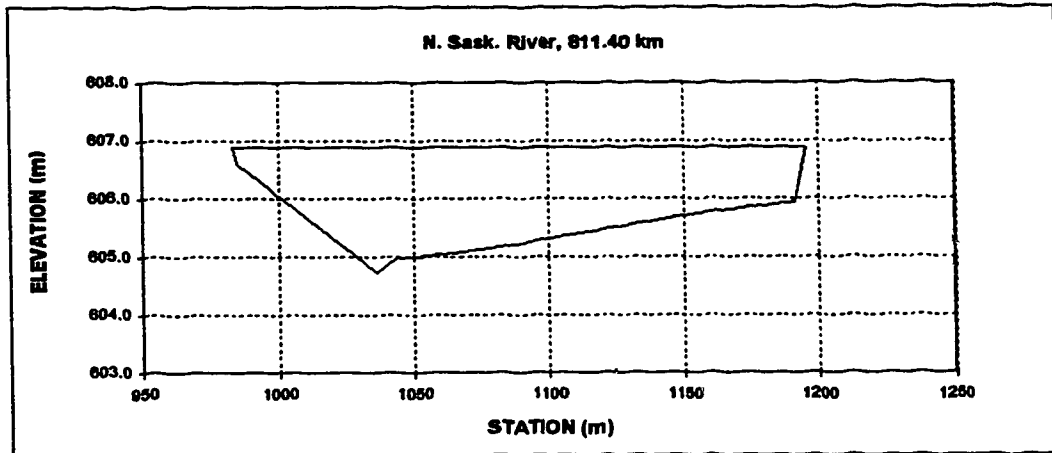
MEAN VELOCITY m/s 0.488

Est. Water Surface Elev. 606.89

LB 982.92 606.89

RB 1195.56 606.89

Sta. m	Elev. m	h m	w/W	u m/s	dq est. m^3	norm. q/Q	Area adjusted m^2	u m/s
982.92	606.89	0.00	0.000	0.000	0.00	0.00000	0.0	0.030
984.51	606.61	0.28	0.007	0.187	0.02	0.00013	0.2	0.185
1036.32	604.72	2.17	0.251	0.662	26.22	0.18262	63.5	0.654
1043.94	604.99	1.90	0.287	0.606	9.81	0.25087	78.9	0.599
1060.71	605.05	1.84	0.366	0.593	18.75	0.38135	110.2	0.586
1082.04	605.18	1.71	0.466	0.565	21.85	0.53345	148.0	0.558
1155.20	605.76	1.13	0.810	0.428	51.38	0.89105	251.5	0.423
1191.77	605.94	0.95	0.982	0.381	15.31	0.9762	289.4	0.376
1195.56	606.89	0.00	1.000	0.000	0.34	1.00000	291.2	0.000
Est. Total					143.69			

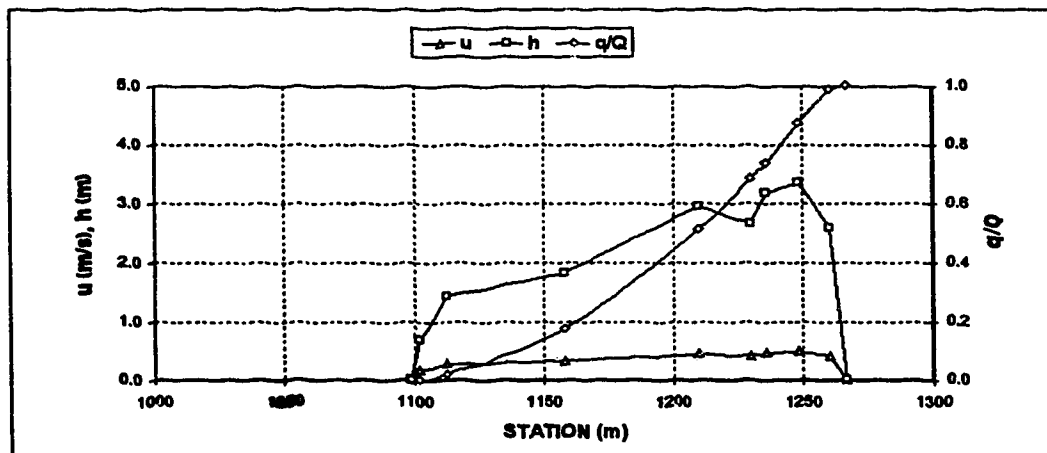
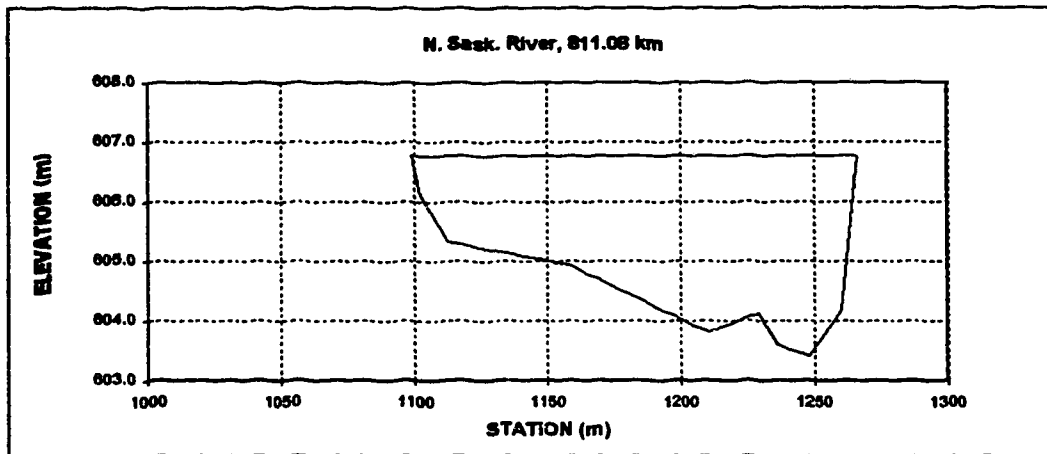


Appendix D.1 North Saskatchewan River

X-SECTION N. Sask. River, 811.08 km
 DATE October 18, 1977
 DISCHARGE m^3/s 142.00
 WIDTH m 168.17
 MEAN DEPTH m 2.19
 AREA m^2 368.78
 MEAN VELOCITY m/s 0.385

HEC2 Section from Alberta Env.
 Est. Water Surface Elev. 606.76
 LB 1098.48 606.76
 RB 1266.65 606.76

Sta. m	Elev. m	h m	w/W	u m/s	dq est. m^3	norm. q/Q	Area adjusted m^2	u m/s
1098.48	606.76	0.00	0.000	0.000	0.00	0.00000	0.0	0.000
1101.85	606.09	0.67	0.020	0.175	0.10	0.00067	1.1	0.167
1112.62	605.33	1.43	0.084	0.290	2.62	0.01825	12.4	0.277
1158.24	604.83	1.83	0.355	0.342	23.62	0.17878	87.1	0.326
1210.06	603.81	2.95	0.683	0.470	50.35	0.51470	211.2	0.448
1229.87	604.11	2.65	0.781	0.437	25.21	0.68394	266.8	0.417
1235.98	603.59	3.17	0.818	0.493	8.26	0.73935	284.5	0.470
1248.15	603.41	3.35	0.890	0.511	18.98	0.87345	324.3	0.487
1260.35	604.17	2.59	0.983	0.431	17.09	0.98819	360.6	0.411
1266.65	606.76	0.00	1.000	0.000	1.76	1.00000	368.8	0.000
Est. Total					148.98			



Appendix D.1 North Saskatchewan River

X-SECTION N. Sask. River, 810.89 km

DATE October 18, 1877

DISCHARGE m^3/s 142.00

WIDTH m 154.38

MEAN DEPTH m 2.42

AREA m^2 373.52

MEAN VELOCITY m/s 0.350

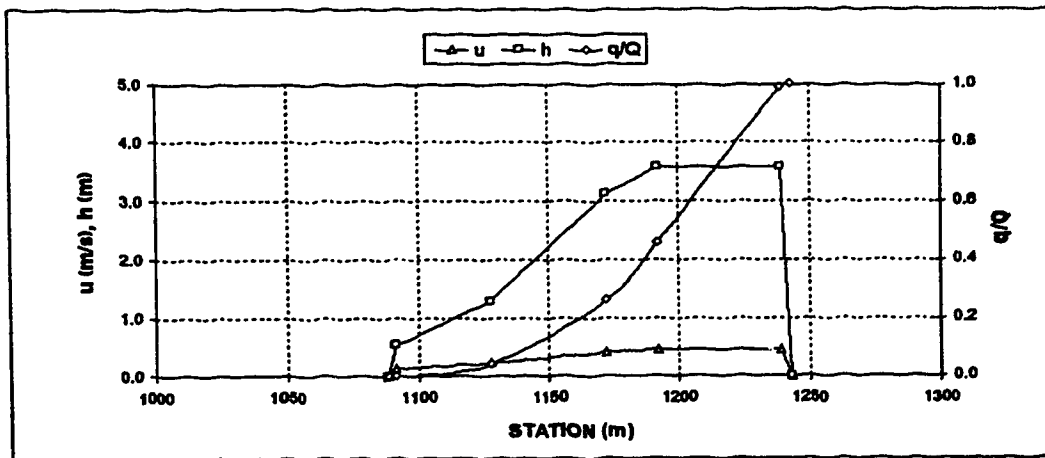
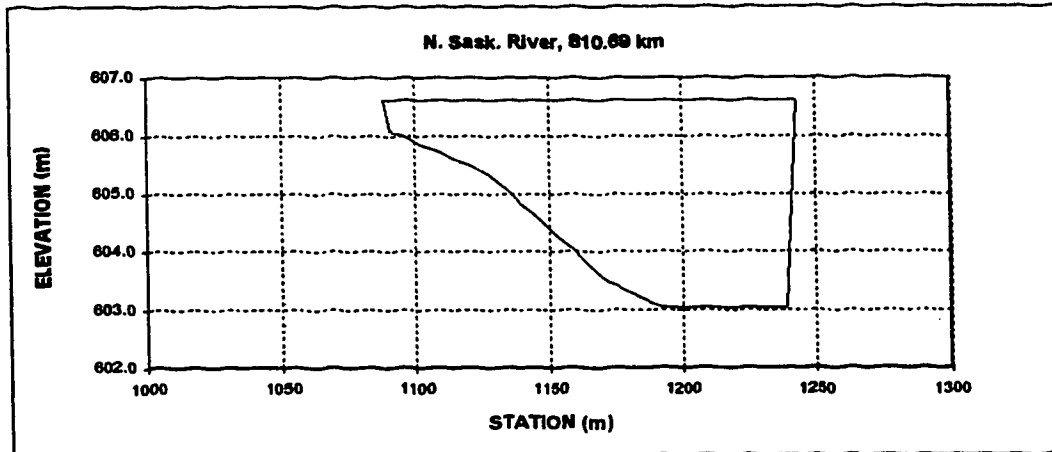
HEC2 Section from Alberta Env.

Est. Water Surface Elev. 606.62

LD 1088.54 606.62

RB 1242.92 606.62

Sta. m	Elev. m	h m	WW	u m/s	dq est. m^3	norm. q/Q	Area adjusted u m^2 m/s
1088.54	606.62	0.00	0.000	0.000	0.00	0.00000	0.0 0.000
1091.18	606.09	0.53	0.017	0.138	0.05	0.00030	0.7 0.124
1127.78	605.33	1.29	0.254	0.250	6.42	0.04124	33.9 0.226
1171.95	603.50	3.12	0.540	0.450	34.05	0.25819	131.2 0.407
1191.78	603.04	3.58	0.669	0.493	31.28	0.45754	197.5 0.446
1239.01	603.04	3.58	0.975	0.493	83.40	0.98900	366.5 0.446
1242.92	606.62	0.00	1.000	0.000	1.73	1.00000	373.5 0.000
Est. Total					156.93		



Appendix D.1 North Saskatchewan River

X-SECTION N. Sask. River, 810.37 km

HEC2 Section from Alberta Env.

DATE October 18, 1977

DISCHARGE m^3/s 142.00

WIDTH m 178.09

MEAN DEPTH m 2.02

AREA m^2 360.21

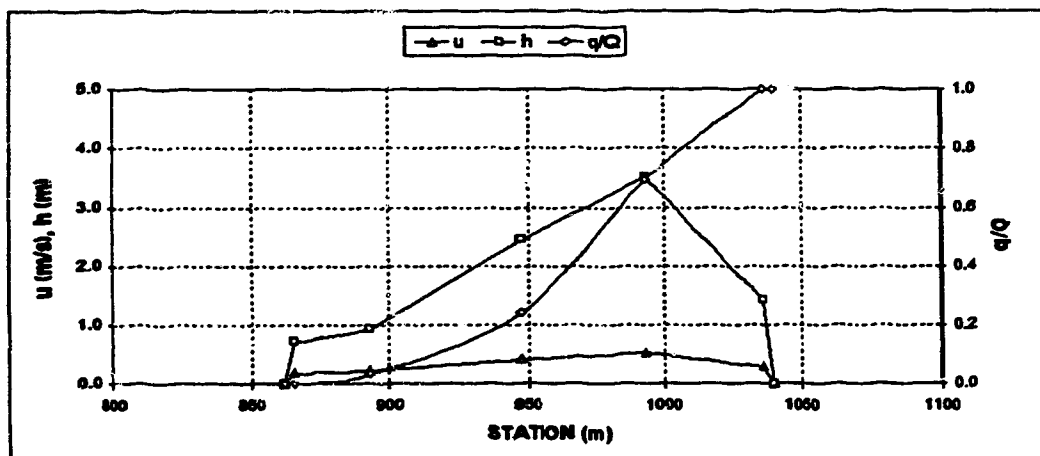
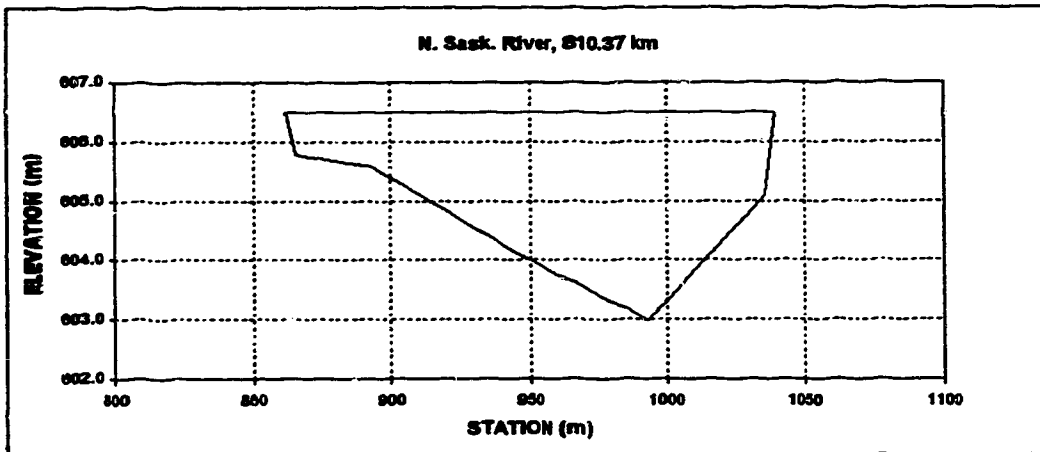
MEAN VELOCITY m/s 0.394

Est. Water Surface Elev. 808.50

LB 862.09 808.50

RB 1040.18 808.50

Sta.	Elev.	h	w/W	u	dq est.	norm. q/Q	Area adjusted u
m	m	m		m/s	m^2		m^2 m/s
862.09	808.50	0.00	0.000	0.000	0.00	0.00000	0.0 0.000
885.83	805.79	0.71	0.020	0.195	0.12	0.00080	1.3 0.182
893.08	805.57	0.93	0.174	0.234	4.81	0.03235	23.6 0.218
947.93	804.05	2.45	0.482	0.448	31.54	0.23928	116.2 0.417
983.66	802.98	3.52	0.738	0.570	69.35	0.99427	252.5 0.531
1036.32	805.09	1.41	0.978	0.309	48.18	0.99725	357.5 0.288
1040.18	808.50	0.00	1.000	0.000	0.42	1.00000	360.2 0.000
Est. Total					152.42		



Appendix D.1 North Saskatchewan River

X-SECTION N. Sask. River, 809.94 km (ARC Section 1)

DATE October 18, 1977

DISCHARGE m^3/s 142

WIDTH m 177

MEAN DEPTH m 1.65

AREA m^2 344.4

MEAN VELOCITY m/s 0.412

Section from Alberta Research Council Report

Assumed Water Surface 94.9

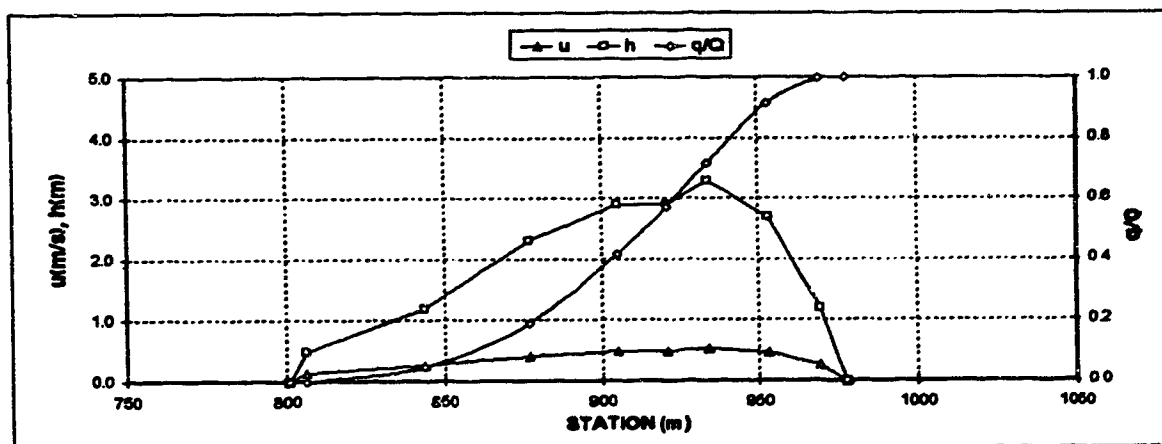
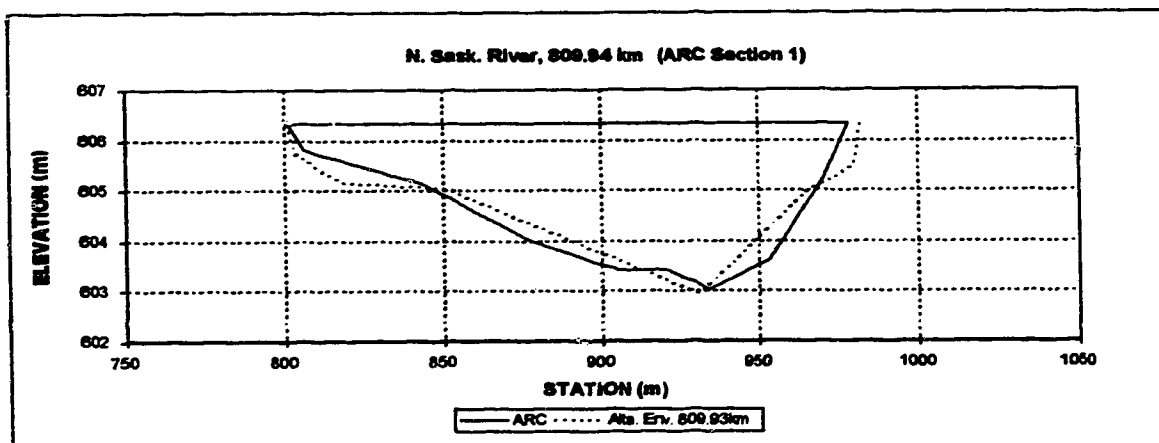
Est. W.S.E. 10/18/77 606.33

Correction to Geodetic 511.43

Correction to Station 801

Water's Edge m	Assumed Elev m	Est. Sta. m	Est. Geod. m	h m	w/W	u m/s	eq est. m^3	norm. q/Q	Area m^2	adj. u m/s
0	94.9	801	606.33	0.00	0.000	0.000	0.00	0.00000	0.0	0.000
5	94.4	806	605.83	0.50	0.028	0.167	0.10	0.00066	1.3	0.149
43	93.7	844	605.13	1.20	0.243	0.299	7.51	0.04811	33.5	0.268
76	92.6	877	604.03	2.30	0.429	0.461	21.94	0.18664	91.3	0.413
104	92.0	905	603.43	2.90	0.588	0.538	36.36	0.41629	164.1	0.483
120	92.0	921	603.43	2.90	0.678	0.538	24.97	0.57395	210.5	0.483
133	91.6	934	603.03	3.30	0.751	0.586	22.66	0.71705	250.8	0.526
152	92.2	953	603.63	2.70	0.859	0.513	31.34	0.91494	307.8	0.460
168	93.7	969	605.13	1.20	0.949	0.299	12.66	0.99491	339.0	0.268
177	94.9	978	606.33	0.00	1.000	0.000	0.81	1.00000	344.4	0.000
		801	606.33							

158.35



Appendix D.1 North Saskatchewan River

X-SECTION N. Sask. River, 809.93 km

HEC2 Section from Alberta Env.

DATE October 18, 1977

DISCHARGE m^3/s 142.00

WIDTH m 181.31

MEAN DEPTH m 1.87

AREA m^2 339.06

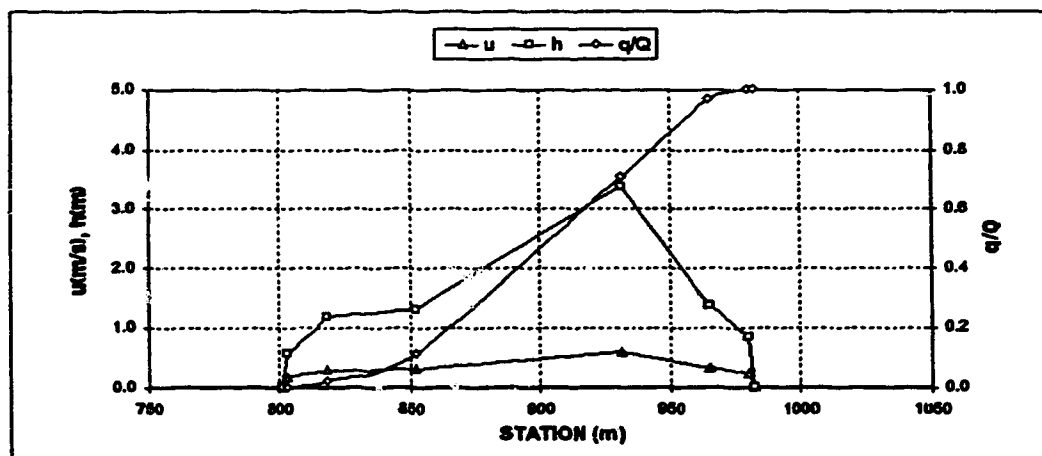
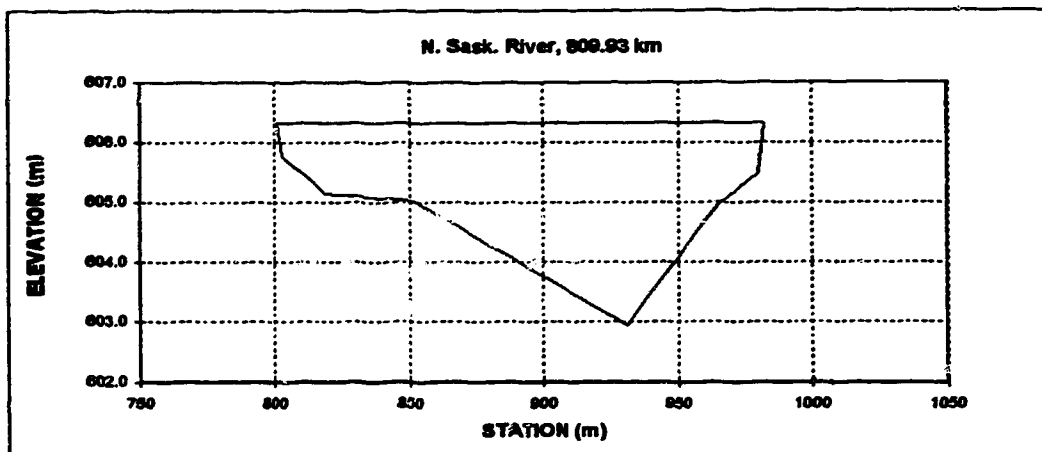
MEAN VELOCITY m/s 0.419

Est. Water Surface Elev. 606.33

LB 600.82 606.33

RB 982.12 606.33

Sta. m	Elev. m	h m	w/W	u m/s	dq est. m^3	norm. q/Q	Area adjusted u m^2	m/s
800.82	606.33	0.00	0.000	0.000	0.00	0.00000	0.0	0.000
803.15	605.76	0.57	0.013	0.190	0.08	0.00042	0.7	0.181
818.39	605.15	1.18	0.067	0.308	3.32	0.02276	14.0	0.295
851.91	605.02	1.31	0.282	0.330	13.32	0.11244	55.7	0.316
931.16	602.95	3.38	0.719	0.622	68.45	0.70791	241.6	0.594
964.99	604.96	1.37	0.904	0.340	38.30	0.98575	321.2	0.325
979.93	605.48	0.85	0.988	0.248	4.97	0.99922	338.1	0.237
982.12	606.33	0.00	1.000	0.000	0.12	1.00000	339.1	0.000
Est. Total					148.53			



Appendix D.1 North Saskatchewan River

X-SECTION N. Sask. River, 809.64 km

HEC2 Section from Alberta Env.

DATE October 18, 1977

DISCHARGE m^3/s

142.00

WIDTH m

169.31

MEAN DEPTH m

1.82

AREA m^2

308.41

MEAN VELOCITY m/s

0.460

Est. Water Surface Elev.

608.22

LS

831.42

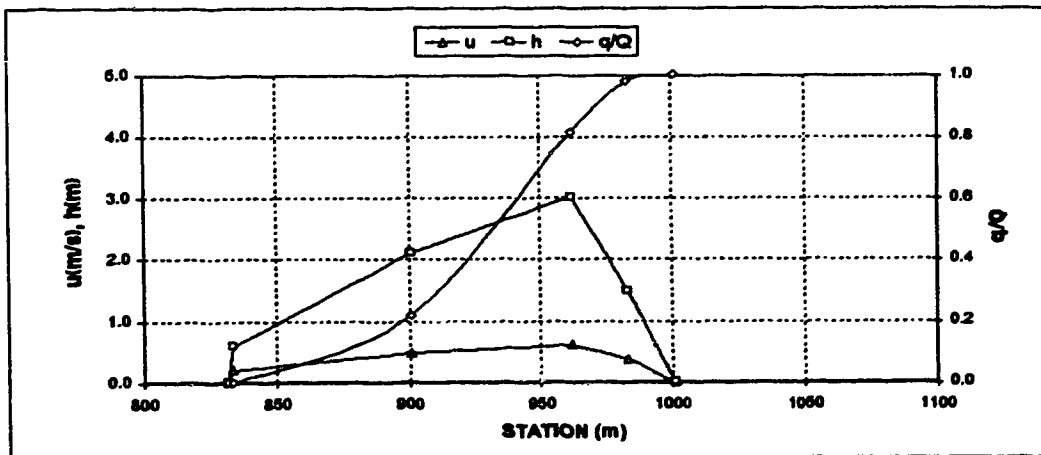
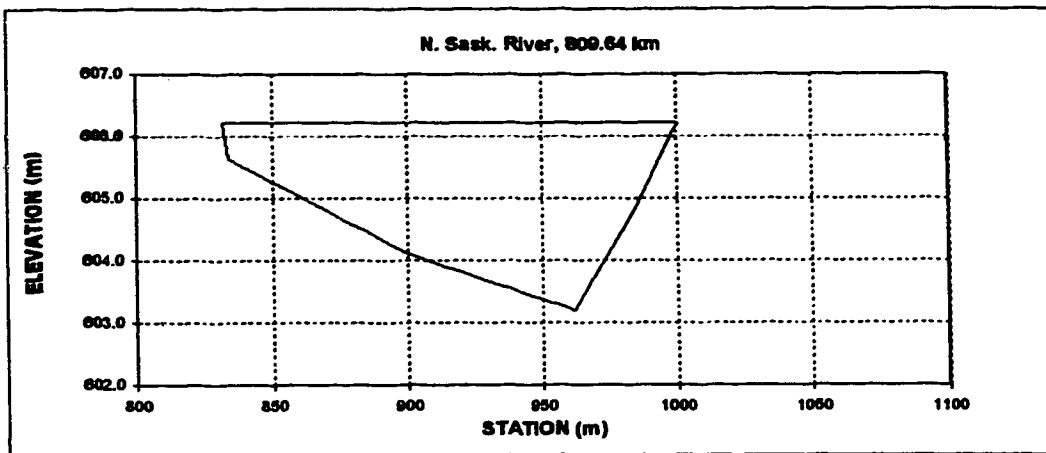
608.22

RB

1000.73

608.22

Sta. m	Elev. m	h m	v/W	u m/s	dq est. m^3	norm. q/Q	Area adjusted m^2	u m/s
831.42	608.22	0.00	0.000	0.000	0.00	0.00000	0.0	0.000
833.62	605.63	0.59	0.013	0.216	0.07	0.00046	0.8	0.204
900.68	604.11	2.11	0.409	0.507	32.63	0.21730	90.9	0.479
981.64	603.20	3.02	0.769	0.644	89.89	0.61456	247.0	0.608
982.98	604.72	1.50	0.895	0.404	25.23	0.86220	295.1	0.381
1000.73	608.22	0.00	1.000	0.000	2.68	1.00000	308.4	0.000
Est. Total					150.50			



Appendix D.1 North Saskatchewan River

X-SECTION N. Sask. River, 809.29 km

HEC2 Section from Alberta Env.

DATE October 18, 1977

DISCHARGE m^3/s 142.00

WIDTH m 170.00

MEAN DEPTH m 1.82

AREA m^2 275.17

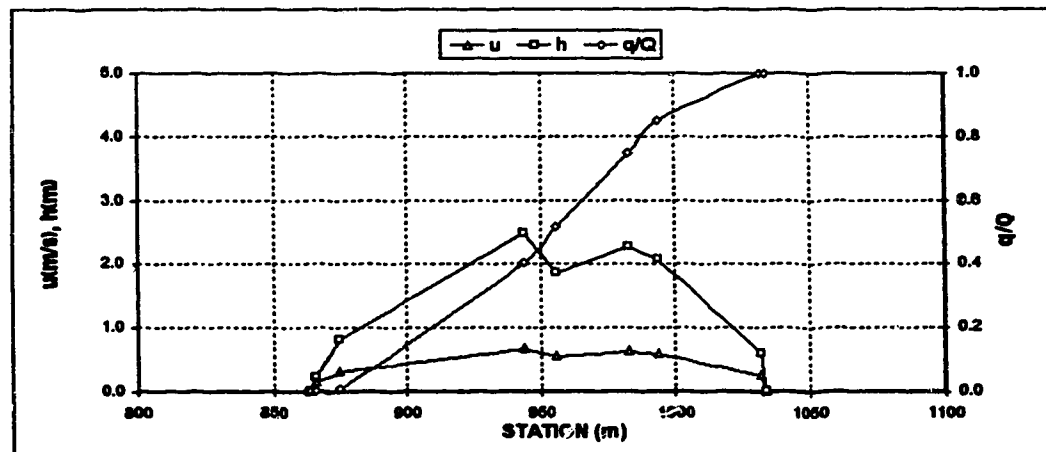
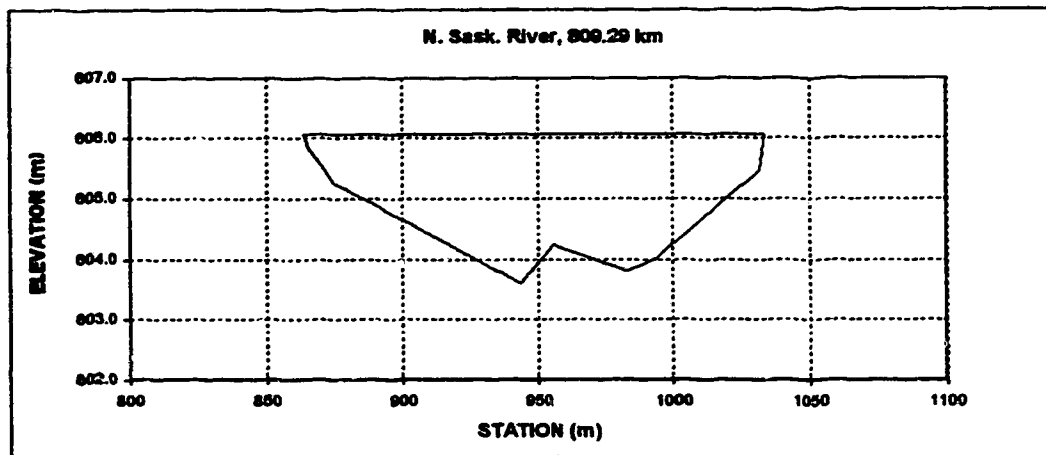
MEAN VELOCITY m/s 0.516

Est. Water Surface Elev. 606.06

LP 863.92 606.06

RB 1033.92 606.06

Sta. m	Elev. m	h m	w/W	u m/s	dq est. m^3	norm. q/Q	Area adjusted m^2	u m/s
863.92	606.06	0.00	0.000	0.000	0.00	0.00000	0.0	0.000
865.63	605.86	0.23	0.010	0.140	0.01	0.00009	0.2	0.136
874.77	605.27	0.81	0.084	0.325	1.10	0.00784	4.9	0.317
943.35	603.59	2.49	0.467	0.687	57.19	0.40050	117.9	0.671
955.55	604.23	1.85	0.539	0.564	16.55	0.51416	144.4	0.550
982.68	603.81	2.27	0.700	0.648	34.15	0.74878	200.8	0.630
993.65	604.02	2.06	0.763	0.606	14.45	0.84800	223.9	0.591
1031.75	605.48	0.60	0.987	0.298	22.04	0.99941	274.5	0.259
1033.92	606.06	0.00	1.000	0.000	0.09	1.00000	275.2	0.000
Est. Total					145.57			



Appendix D.1 North Saskatchewan River

X-SECTION N. Sask. River, 809.04 km

HEC2 Section from Alberta Env.

DATE October 18, 1977

DISCHARGE m^3/s 142.00

WIDTH m 236.97

MEAN DEPTH m 0.71

AREA m^2 168.33

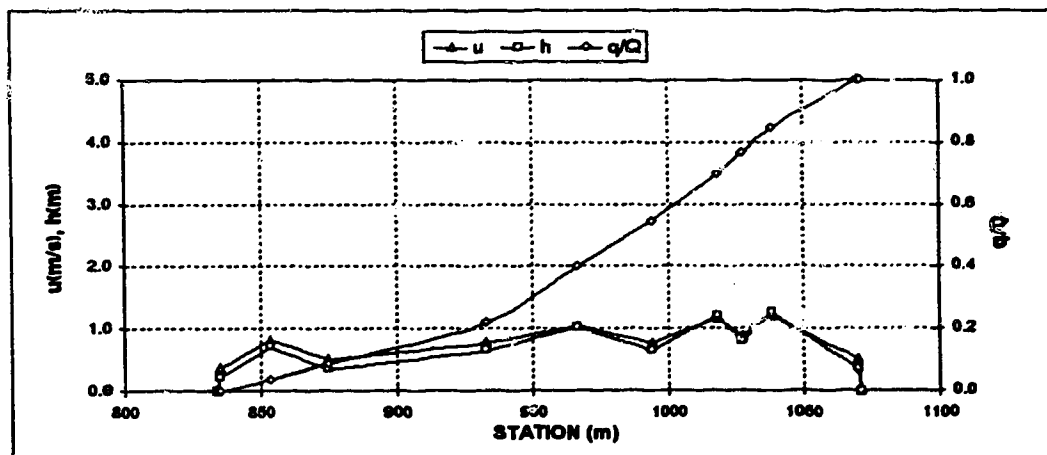
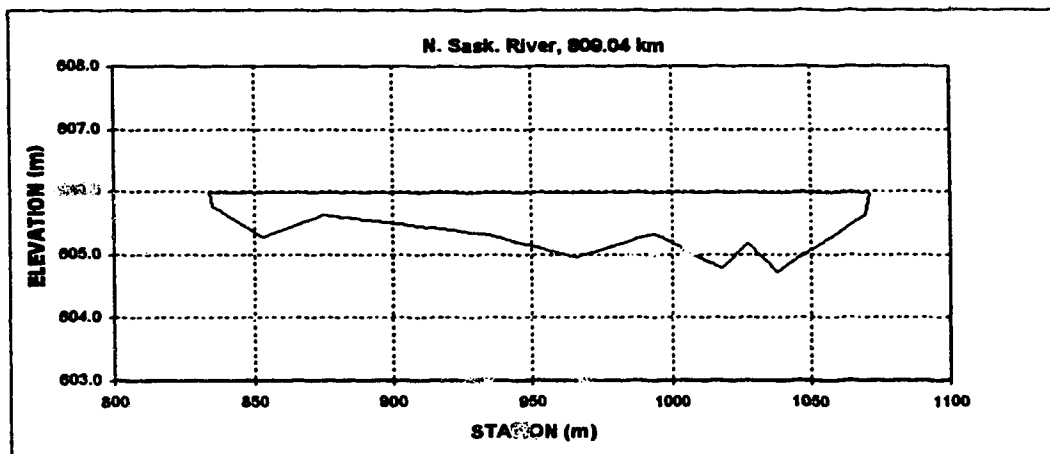
MEAN VELOCITY m/s 0.844

Est. Water Surface Elev. 605.96

LB 834.02 605.96

RB 1070.98 605.96

Sta. m	Elev. m	h m	w/W	u m/s	dq est. m^3	norm. q/Q	Area adjusted m^2	u m/s
834.02	605.96	0.00	0.000	0.000	0.00	0.00000	0.0	0.000
835.15	605.76	0.22	0.005	0.385	0.02	0.00016	0.1	0.374
853.44	605.27	0.71	0.082	0.843	5.22	0.03586	8.6	0.819
874.77	605.63	0.35	0.172	0.526	7.73	0.08872	19.9	0.511
932.69	605.33	0.65	0.416	0.795	19.10	0.21636	48.6	0.772
966.21	604.96	1.02	0.558	1.073	26.13	0.39608	76.6	1.043
993.65	605.33	0.65	0.674	0.795	21.39	0.54438	99.7	0.772
1018.03	604.78	1.20	0.777	1.196	22.44	0.69766	122.3	1.162
1027.17	605.18	0.80	0.815	0.913	9.63	0.76376	131.4	0.887
1037.84	604.72	1.26	0.860	1.236	11.60	0.84449	142.4	1.200
1069.65	605.63	0.35	0.995	0.526	22.66	0.99964	166.1	0.511
1070.98	605.96	0.00	1.000	0.000	0.05	1.00000	166.3	0.000
Est. Total					146.20			



Appendix D.1 North Saskatchewan River

X-SECTION N. Sask. River, 808.70 km

HEC2 Section from Alberta Env.

DATE October 18, 1977

DISCHARGE m^3/s 142.00

WIDTH m 240.72

MEAN DEPTH m 0.78

AREA m^2 183.91

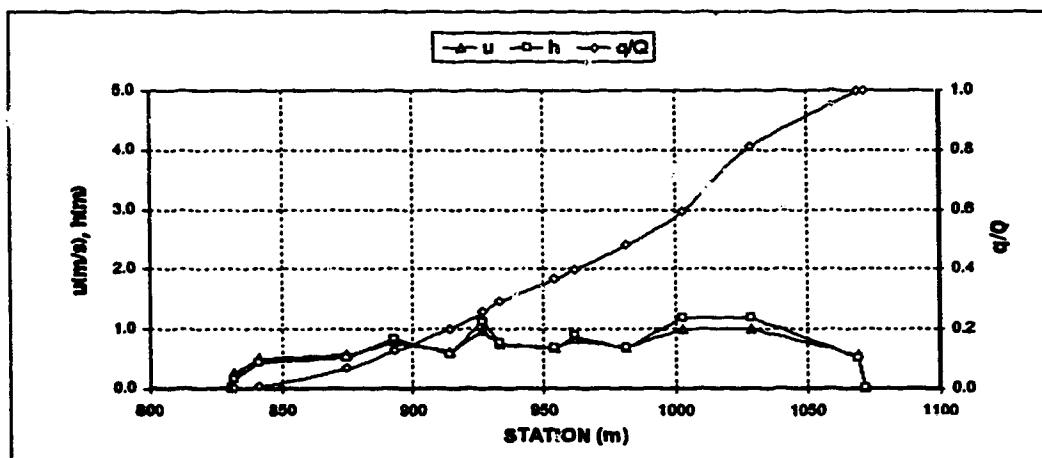
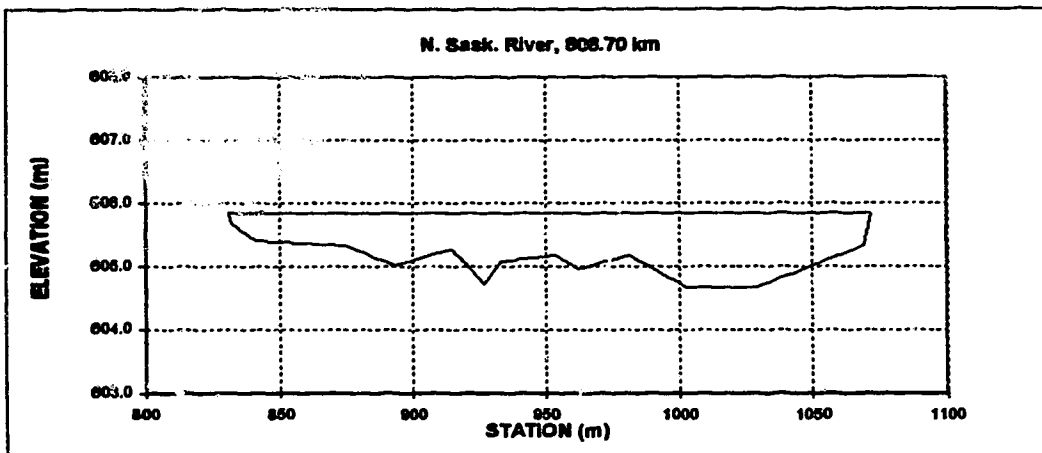
MEAN VELOCITY m/s 0.772

Est. Water Surface Elev. 605.85

LB 831.16 605.85

RS 1071.88 605.85

Sta.	Elev.	h	w/W	u	dq est.	norm. q/Q	Area adjusted u
(%)	m	m		m/s	m^3		m^2 m/s
831.16	605.85	0.00	0.000	0.000	0.00	0.00000	0.0 0.000
832.10	605.69	0.16	0.004	0.287	0.01	0.00007	0.1 0.257
841.25	605.42	0.43	0.042	0.523	1.05	0.00717	2.7 0.502
874.77	605.33	0.52	0.181	0.594	8.81	0.06673	18.5 0.570
883.08	605.02	0.83	0.257	0.813	8.83	0.12508	30.8 0.781
914.40	605.27	0.58	0.346	0.839	10.86	0.18849	45.7 0.814
928.59	604.72	1.13	0.398	1.000	8.50	0.25598	58.1 0.980
932.89	605.09	0.78	0.422	0.788	5.07	0.29022	61.8 0.738
954.02	605.18	0.67	0.510	0.704	11.15	0.36559	77.0 0.678
981.84	604.98	0.89	0.542	0.852	4.80	0.39889	82.9 0.818
981.45	605.18	0.67	0.624	0.704	11.88	0.47754	98.3 0.678
1002.79	604.98	1.19	0.713	1.035	17.18	0.59370	118.0 0.994
1028.70	604.98	1.19	0.821	1.035	31.80	0.80870	148.7 0.994
1069.24	605.33	0.52	0.989	0.594	28.09	0.99863	183.2 0.570
1071.88	605.85	0.00	1.000	0.000	0.20	1.00000	183.9 0.000
Est. Total				147.90			



Appendix D.1 North Saskatchewan River

X-SECTION N. Sask. River, 808.36 km

HEC2 Section from Alberta Env.

DATE October 18, 1977

DISCHARGE m^3/s 142.00

WIDTH m 208.53

MEAN DEPTH m 0.85

AREA m^2 177.53

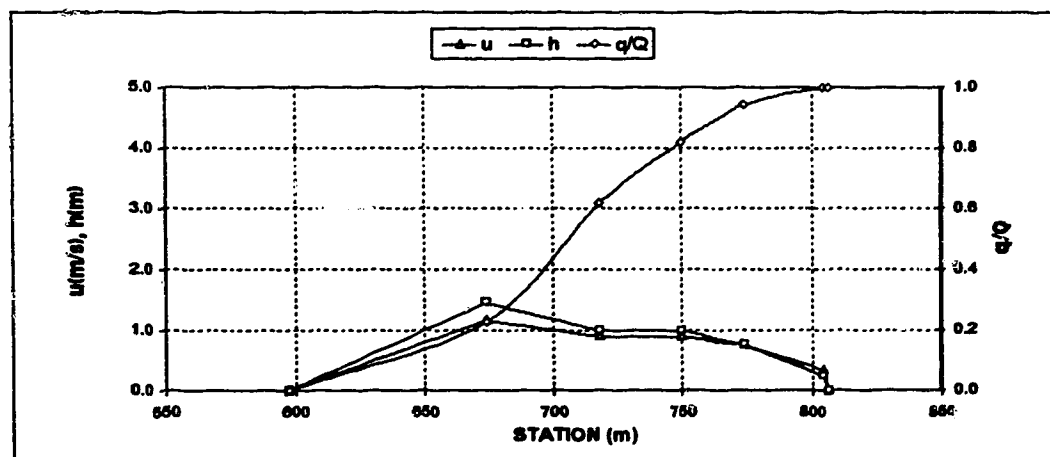
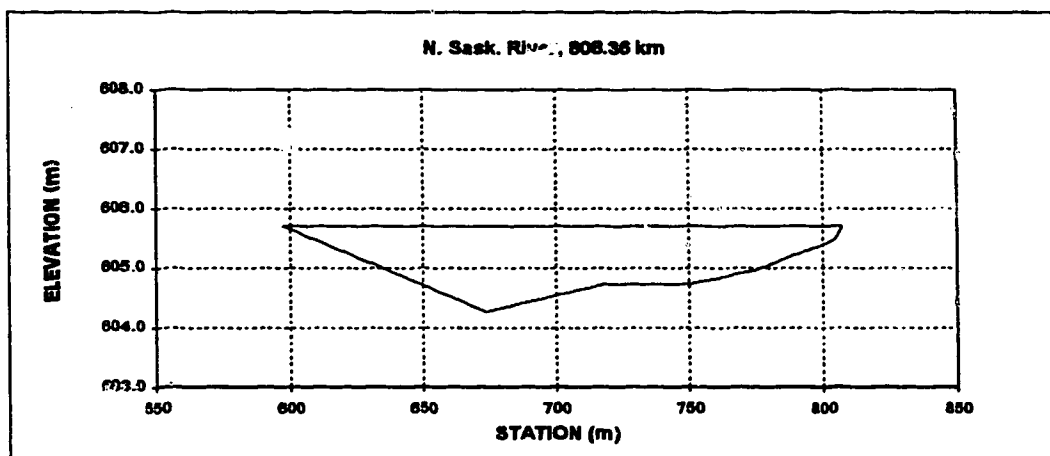
MEAN VELOCITY m/s 0.800

Est. Water Surface Elev. 805.71

LB 597.44 805.71

RB 808.98 805.71

Sta. m	Elev. m	h m	w/W	u m/s	dq est. m^3	norm. q/Q	Area adjusted u m^2	m/s
597.44	805.71	0.00	0.000	0.000	0.00	0.00000	0.0	0.000
673.61	804.28	1.45	0.364	1.146	31.67	0.22591	55.3	1.180
717.80	804.72	0.99	0.574	0.888	54.91	0.61782	109.3	0.900
749.81	804.72	0.99	0.727	0.888	28.20	0.81884	141.0	0.900
774.19	804.98	0.75	0.844	0.739	17.29	0.94218	182.3	0.748
804.67	805.48	0.23	0.989	0.337	8.08	0.99888	177.3	0.341
808.98	805.71	0.00	1.000	0.000	0.04	1.00000	177.5	0.000
Est. Total					140.17			

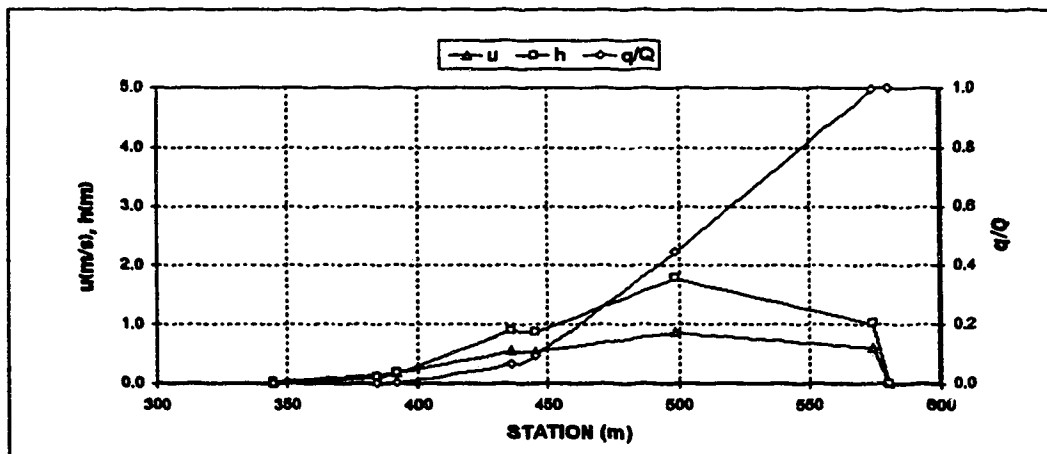
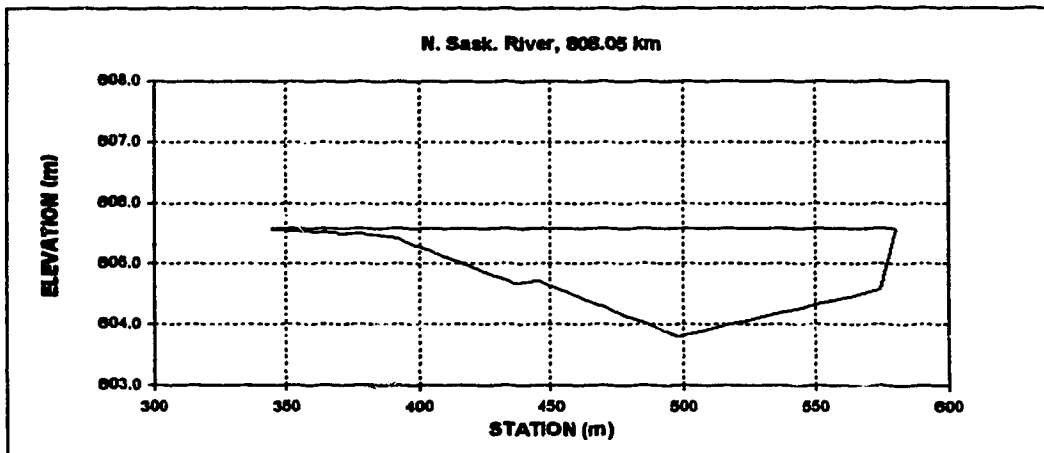


Appendix D.1 North Saskatchewan River

X-SECTION N. Sask. River, 808.05 km
 DATE October 18, 1977
 DISCHARGE m^3/s 142.00
 WIDTH m 236.13
 MEAN DEPTH m 0.91
 AREA m^2 215.65
 MEAN VELOCITY m/s 0.658

HEC2 Section from Alberta Env.
 Est. Water Surface Elev. 605.59
 LB 344.28 605.59
 RB 580.41 605.59

Sta. m	Elev. m	h m	w/W	u m/s	dq est. m^3	norm. q/Q	Area adjusted m^2	u m/s
344.28	605.59	0.00	0.000	0.000	0.00	0.00000	0.0	0.000
344.42	605.57	0.02	0.001	0.051	0.00	0.00000	0.0	0.043
384.65	605.48	0.11	0.168	0.160	0.27	0.00181	2.8	0.135
391.67	605.42	0.17	0.201	0.214	0.20	0.00279	3.6	0.181
435.66	604.65	0.90	0.388	0.652	10.23	0.06356	27.3	0.550
445.61	604.72	0.87	0.427	0.637	5.22	0.04455	35.4	0.537
498.35	603.61	1.78	0.652	1.028	58.62	0.44386	106.0	0.867
574.55	604.57	1.02	0.975	0.709	82.59	0.99371	212.7	0.598
580.41	605.59	0.00	1.000	0.000	1.08	1.00000	215.7	0.000
Est. Total					168.39			

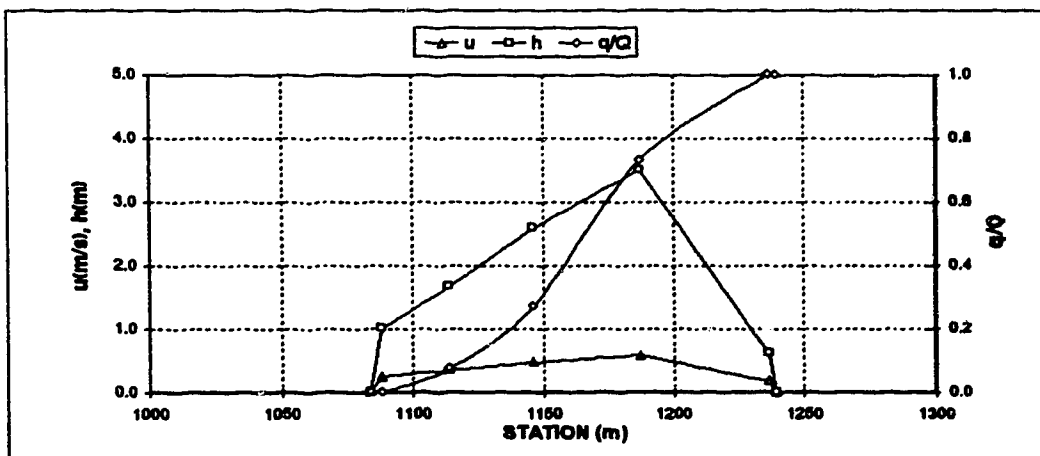
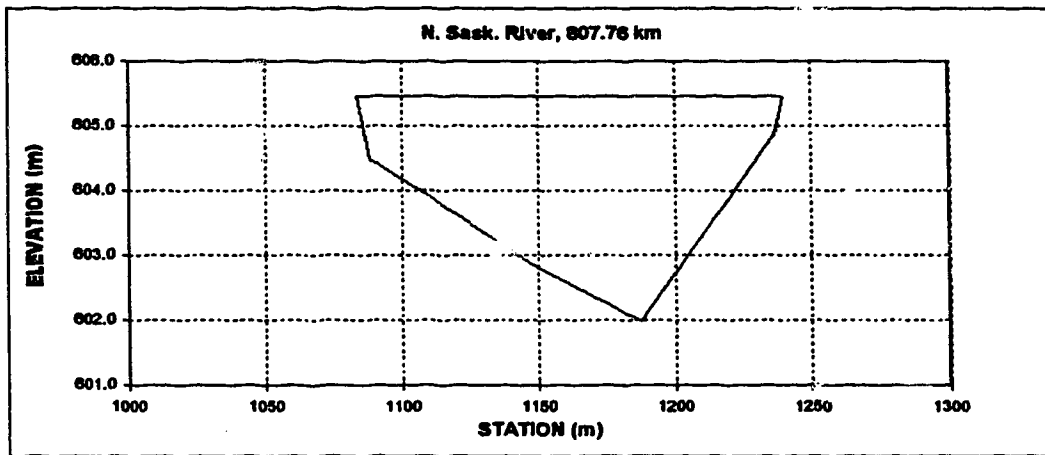


Appendix D.1 North Saskatchewan River

X-SECTION N. Sask. River, 807.76 km
 DATE October 18, 1977
 DISCHARGE m^3/s 142.00
 WIDTH m 155.64
 MEAN DEPTH m 2.13
 AREA m^2 331.69
 MEAN VELOCITY m/s 0.428

HEC2 Section from Alberta Env.
 Est. Water Surface Elev. 605.48
 LB 1083.72 605.48
 RB 1239.36 605.48

Sta. m	Elev. m	h m	w/W	u m/s	dq est. m^3	norm. q/Q	Area adjusted u m^2 m/s
1083.72	605.48	0.00	0.000	0.000	0.00	0.00000	0.0 0.000
1088.14	604.48	1.00	0.028	0.257	0.28	0.00192	2.2 0.249
1114.04	603.81	1.67	0.195	0.363	10.69	0.07459	36.7 0.350
1146.05	602.89	2.59	0.400	0.487	28.89	0.27107	104.7 0.470
1187.20	601.98	3.50	0.685	0.595	67.65	0.73111	229.8 0.574
1236.57	604.87	0.61	0.982	0.185	39.48	0.99947	331.0 0.178
1239.36	605.48	0.00	1.000	0.000	0.08	1.00000	331.9 0.000
Est. Total					147.06		



Appendix D.1 North Saskatchewan River

X-SECTION N. Sask. River, 807.31 km

HEC2 Section from Alberta Env.

DATE October 18, 1977

DISCHARGE m^3/s 142.00

WIDTH m 175.24

MEAN DEPTH m 2.39

AREA m^2 418.23

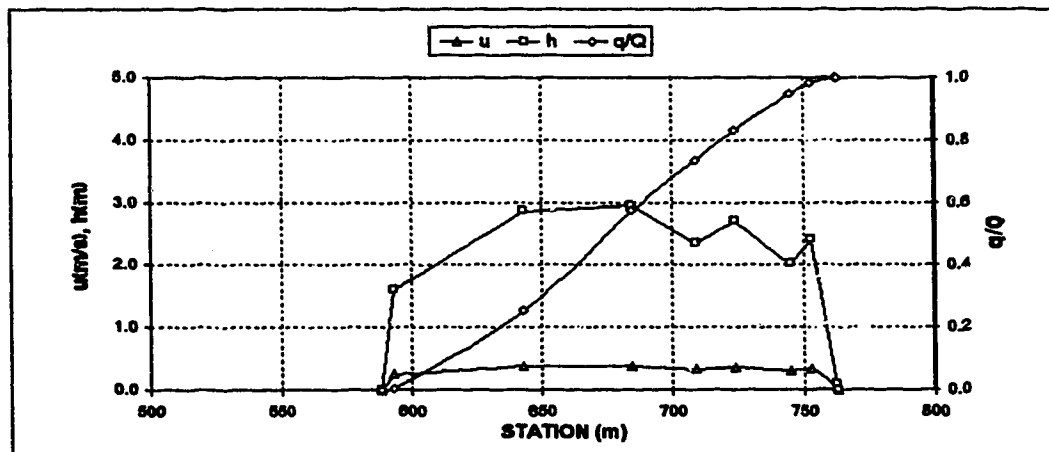
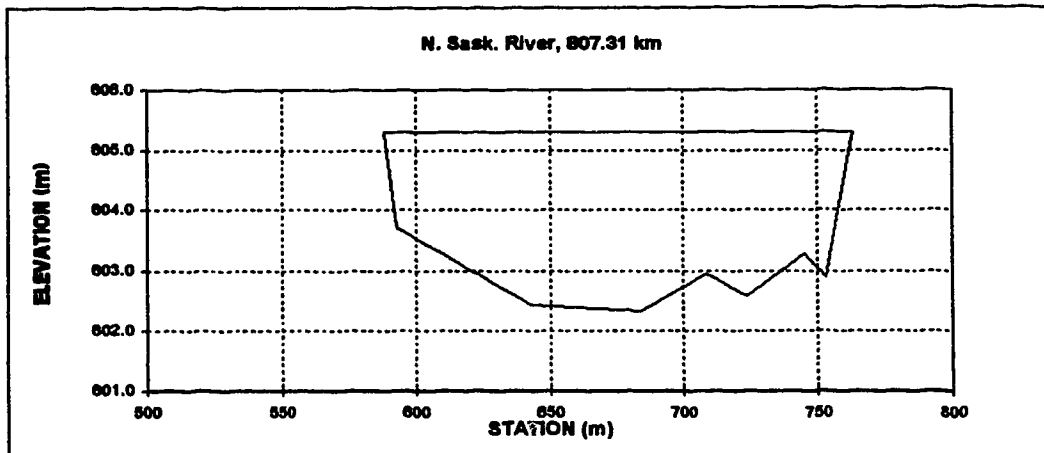
MEAN VELOCITY m/s 0.340

Est. Water Surface Elev. 605.30

LB 588.10 605.30

RB 763.34 605.30

Sta.	Elev.	h	w/W	u	dq est.	norm. q/Q	Area adjusted	u
m	m	m		m/s	m^3		m^2	m/s
588.10	605.30	0.00	0.000	0.000	0.00	0.00000	0.0	0.000
592.84	603.71	1.59	0.027	0.259	0.49	0.00336	3.8	0.254
643.13	602.43	2.87	0.314	0.384	36.00	0.25215	115.8	0.377
684.28	602.34	2.96	0.549	0.392	46.49	0.57340	235.7	0.384
708.66	602.95	2.35	0.688	0.336	23.54	0.73603	300.4	0.330
723.90	602.59	2.71	0.775	0.369	13.59	0.82992	338.9	0.362
744.94	603.29	2.01	0.895	0.303	16.67	0.94512	388.5	0.297
752.88	602.89	2.41	0.940	0.342	5.63	0.98405	408.0	0.335
762.61	605.21	0.09	0.996	0.038	2.31	1.00000	418.2	0.037
763.34	605.30	0.00	1.000	0.000	0.00	1.00000	418.2	0.000
Est. Total					144.72			



Appendix D.1 North Saskatchewan River

X-SECTION N. Sask. River, 808.90 km

HEC2 Section from Alberta Env.

DATE October 18, 1977

DISCHARGE m^3/s 142.00

WIDTH m 179.97

MEAN DEPTH m 1.87

AREA m^2 301.18

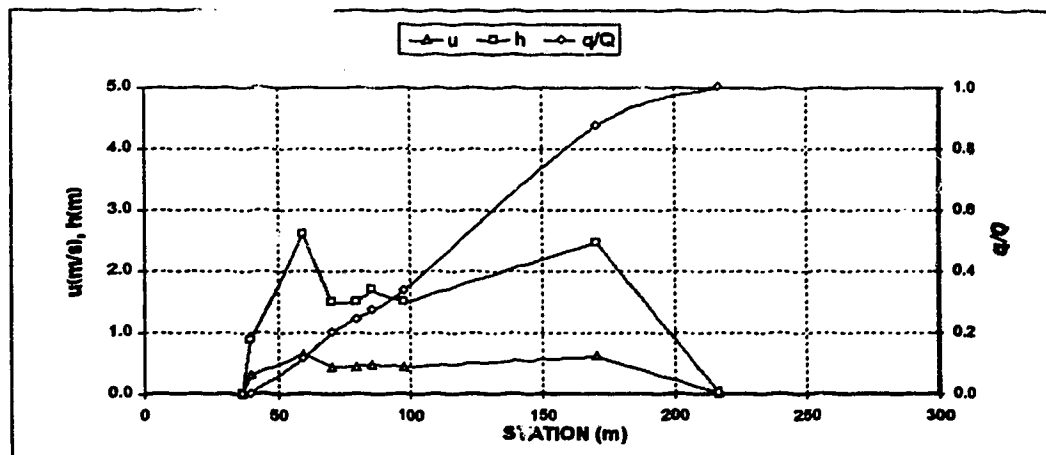
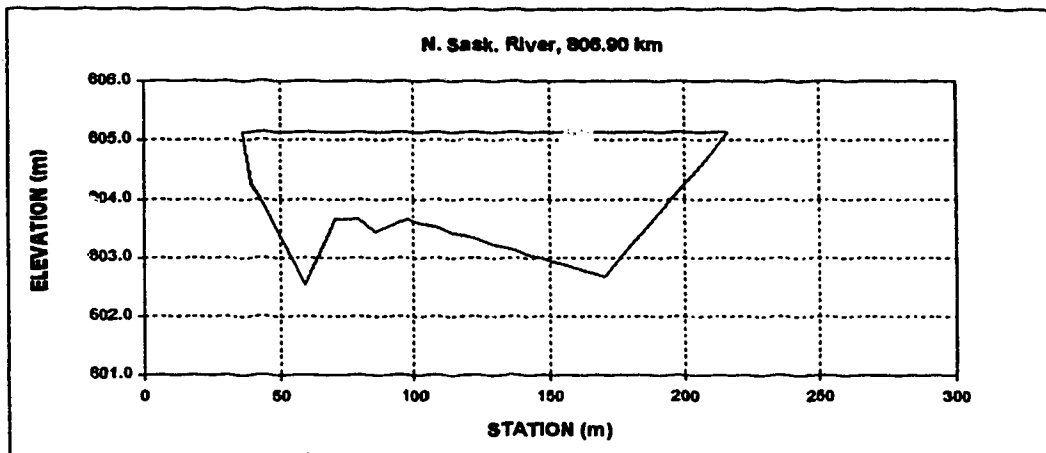
MEAN VELOCITY m/s 0.472

Est. Water Surface Elev. 605.14

LB 36.61 605.14

RB 216.58 605.14

Sta. m	Elev. m	h m	w/W	u m/s	dq est. m^3	norm. q/Q	Area adjusted u m^2 m/s
36.61	605.14	0.00	0.000	0.000	0.00	0.00000	0.0 0.000
39.63	604.28	0.88	0.000	0.308	0.20	0.00144	1.3 0.310
59.44	602.53	2.61	0.127	0.634	16.22	0.11688	35.8 0.640
70.11	603.65	1.49	0.186	0.436	11.68	0.20001	57.7 0.440
79.25	603.65	1.49	0.237	0.436	5.92	0.24216	71.3 0.440
85.35	603.44	1.70	0.271	0.476	4.43	0.27368	81.0 0.481
97.54	603.65	1.49	0.339	0.436	8.85	0.33682	100.4 0.440
170.69	602.68	2.46	0.745	0.609	75.36	0.87300	244.6 0.616
216.41	605.12	0.02	0.999	0.022	17.84	1.00000	301.2 0.022
216.58	605.14	0.00	1.000	0.000	0.00	1.00000	301.2 0.000
Est. Total					140.50		



Appendix D.1 North Saskatchewan River

X-SECTION N. Sask. River, 806.57 km

HEC2 Section from Alberta Env.

DATE October 18, 1977

DISCHARGE m^3/s 142.00

WIDTH m 195.60

MEAN DEPTH m 1.44

AREA m^2 280.87

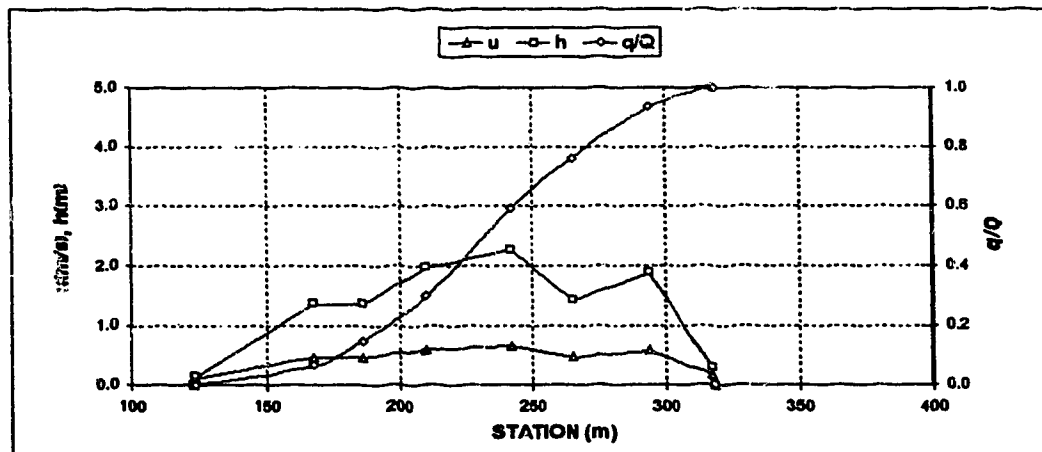
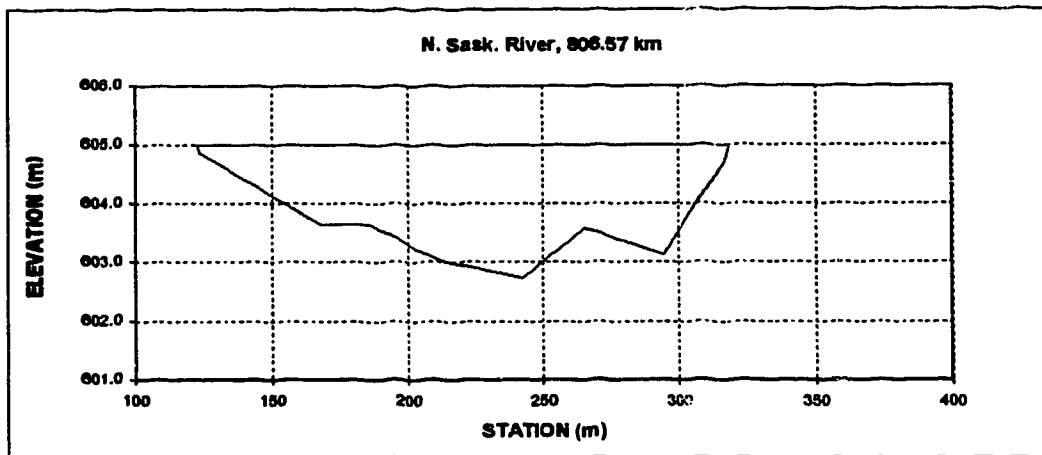
MEAN VELOCITY m/s 0.50

Est. Water Surface Elev. 605.01

LB 122.77 605.01

RB 318.36 605.01

Sta. m	Elev. m	h m	W/W	u m/s	dq est. m^3	norm. q/Q	Area adjusted m^2	u m/s
122.77	605.01	0.00	0.000	0.000	0.00	0.00000	0.0	0.000
123.45	604.87	0.14	0.003	0.105	0.00	0.00002	0.0	0.100
167.64	603.65	1.36	0.229	0.487	9.77	0.06531	33.1	0.462
185.93	603.65	1.36	0.323	0.487	12.08	0.14803	57.9	0.462
210.32	603.04	1.97	0.448	0.624	22.51	0.29839	98.4	0.592
242.32	602.74	2.27	0.611	0.686	44.34	0.59264	166.1	0.650
285.18	603.59	1.42	0.726	0.501	24.98	0.75955	208.2	0.475
294.14	603.13	1.88	0.876	0.604	26.36	0.93568	255.9	0.573
317.00	604.72	0.29	0.993	0.173	9.61	0.99989	280.7	0.164
318.36	605.01	0.00	1.000	0.000	0.02	1.00000	280.9	0.000
Est. Total				149.68				



Appendix D.1 North Saskatchewan River

X-SECTION N. Sask. River, 806.22 km

HEC2 Section from Alberta Env.

DATE October 18, 1977

DISCHARGE m^3/s 142.00

WIDTH m 188.65

MEAN DEPTH m 0.86

AREA m^2 162.78

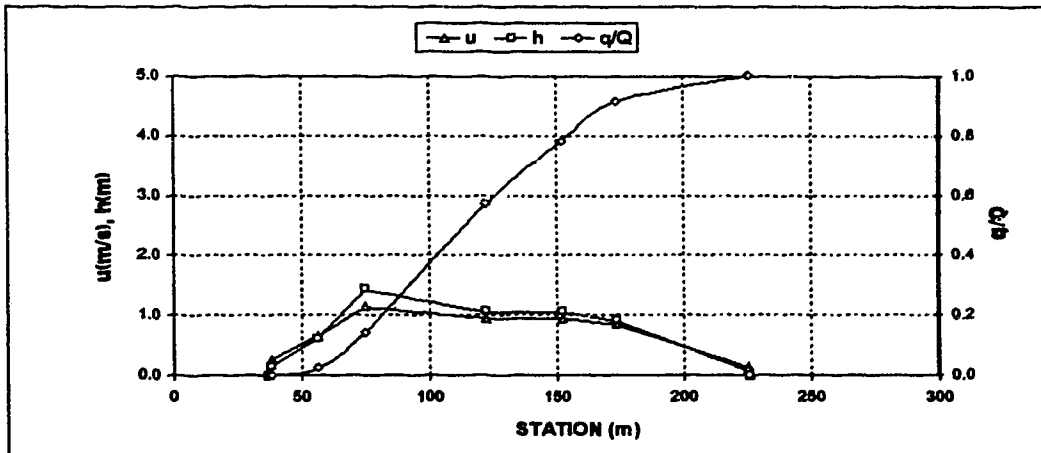
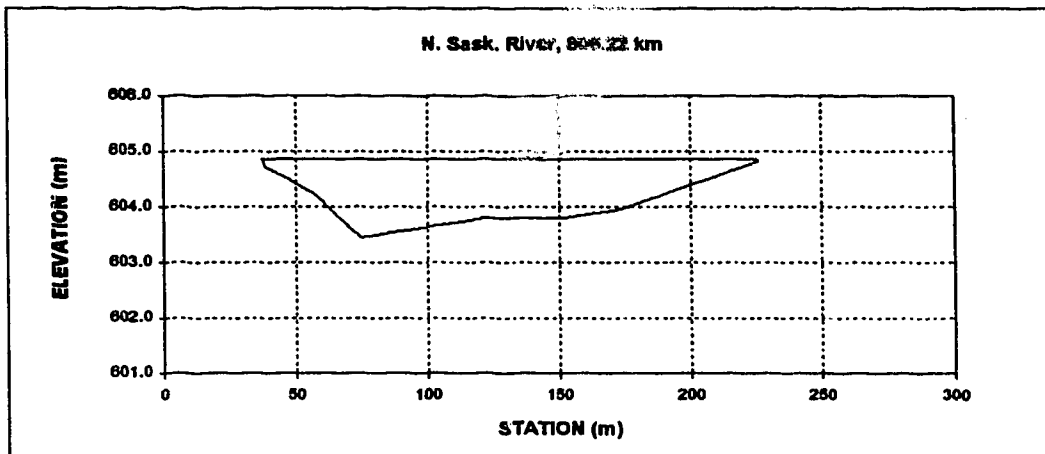
MEAN VELOCITY m/s 0.872

Est. Water Surface Elev. 604.87

LB 37.21 604.87

RB 225.86 604.87

Sta. m	Elev. m	h m	WW	u m/s	dq est. m^3	norm. q/Q	Area adjusted u m^2	m/s
37.21	604.87	0.00	0.000	0.000	0.00	0.00000	0.0	0.000
38.10	604.72	0.15	0.005	0.270	0.01	0.00006	0.1	0.253
56.39	604.28	0.61	0.102	0.692	3.33	0.02202	7.0	0.647
74.68	603.44	1.43	0.189	1.221	17.83	0.13939	25.6	1.142
121.82	603.81	1.06	0.449	1.000	65.28	0.56921	84.4	0.935
152.40	603.81	1.06	0.811	1.000	32.28	0.23178	116.7	0.935
173.74	603.98	0.91	0.724	0.903	19.46	0.13337	137.7	0.845
225.55	604.81	0.06	0.998	0.148	13.59	0.09000	162.8	0.138
225.86	604.87	0.00	1.000	0.000	0.00	1.00000	162.8	0.000
Est. Total					151.67			



Appendix D.1 North Saskatchewan River

X-SECTION N. Sask. River, 805.89 km

HEC2 Section from Alberta Env.

DATE October 18, 1977

DISCHARGE m^3/s 142.00

WIDTH m 211.32

MEAN DEPTH m 0.85

AREA m^2 179.90

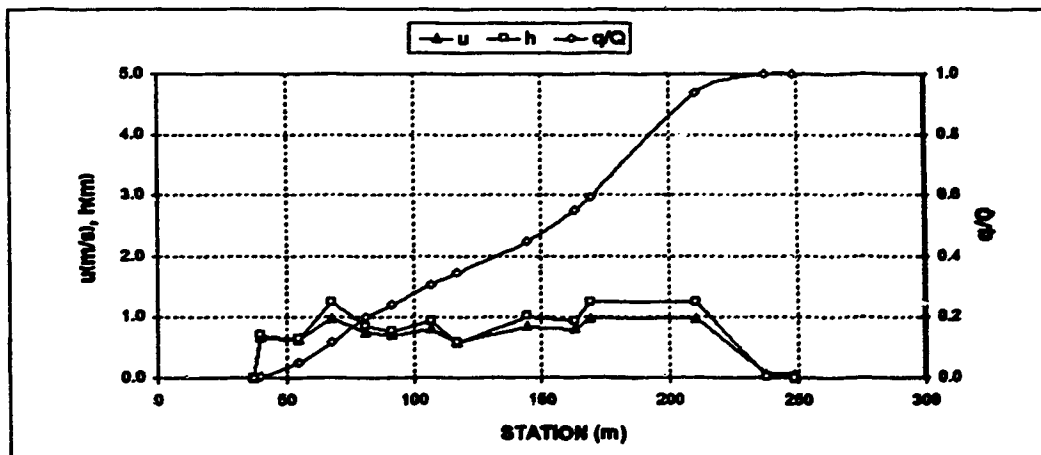
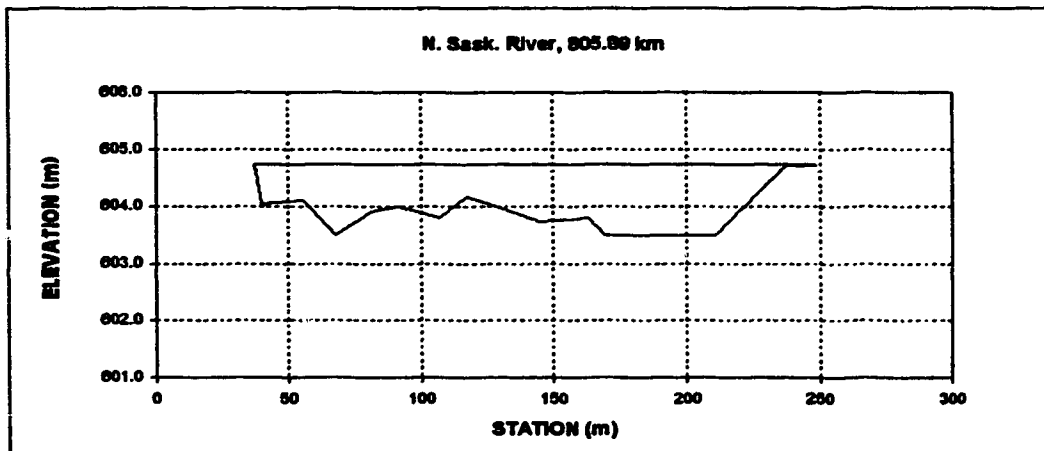
MEAN VELOCITY m/s 0.789

Est. Water Surface Elev. 604.74

LB 37.26 604.74

RB 248.57 604.74

Sta. m	Elev. m	h m	WW	u m/s	dq est. m^3	norm. q/Q	Area adjusted u m^2	m/s
37.26	604.74	0.00	0.000	0.000	0.00	0.00000	0.0	0.000
39.83	604.05	0.69	0.011	0.688	0.28	0.00188	0.8	0.652
54.87	604.11	0.63	0.083	0.645	6.68	0.04681	10.9	0.613
67.67	603.50	1.24	0.144	1.014	9.92	0.11299	22.8	0.964
80.78	603.90	0.84	0.206	0.782	12.23	0.19488	36.4	0.743
91.44	603.99	0.75	0.258	0.725	6.38	0.23754	44.9	0.689
108.68	603.81	0.93	0.329	0.837	9.98	0.30437	57.7	0.795
117.35	604.17	0.57	0.379	0.603	5.78	0.34289	65.7	0.573
144.78	603.74	1.00	0.509	0.878	15.93	0.44654	87.2	0.835
163.07	603.81	0.93	0.595	0.837	15.12	0.55075	104.8	0.795
169.17	603.50	1.24	0.624	1.014	6.12	0.59171	111.4	0.984
210.32	603.50	1.24	0.819	1.014	51.70	0.93774	162.4	0.984
237.75	604.72	0.02	0.949	0.063	9.29	0.99991	179.7	0.080
248.42	604.72	0.02	0.999	0.063	0.01	1.00000	179.9	0.080
248.57	604.74	0.00	1.000	0.000	0.00	1.00000	179.9	0.000
Est. Total					149.41			



Appendix D.1 North Saskatchewan River

X-SECTION N. Sask. River, 805.53 km

DATE October 18, 1977

DISCHARGE m^3/s 142.00

WIDTH m 197.27

MEAN DEPTH m 0.26

AREA m^2 51.32

MEAN VELOCITY m/s 2.767

HEC2 Section from Alberta Env.

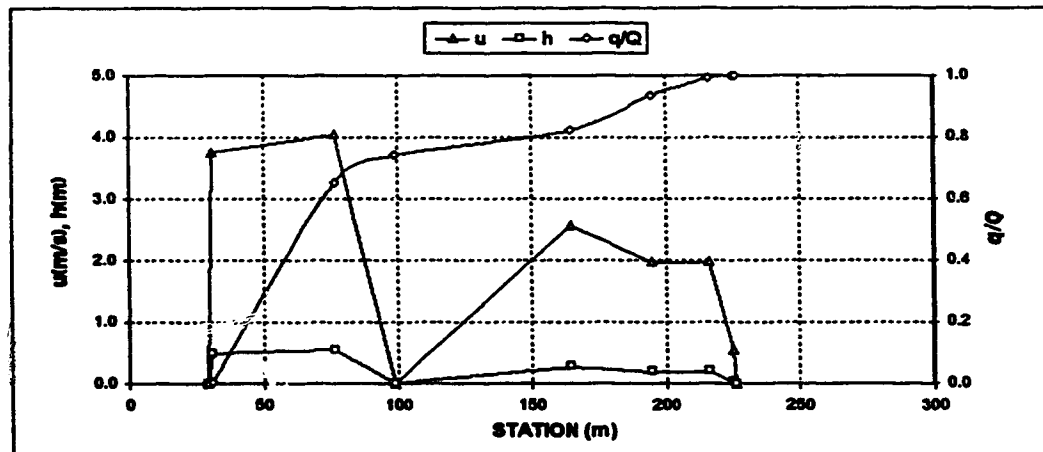
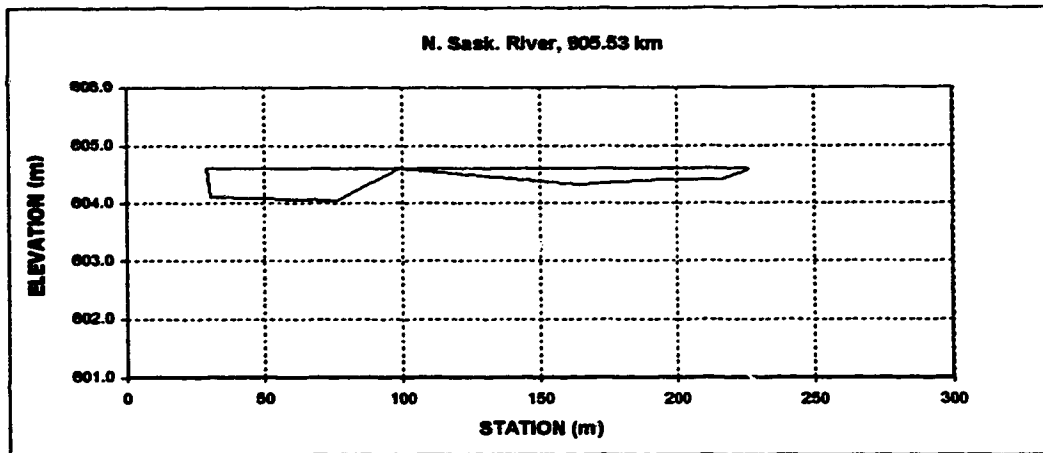
One high point at mid channel omitted

Est. Water Surface Elev. 604.60

LB 29.21 604.60

RB 226.48 604.60

Sta. m	Elev. m	h m	w/W	u m/s	dq est. m^3	norm. q/Q	Area adjusted m^2	u m/s
29.21	604.60	0.00	0.000	0.000	0.00	0.00000	0.0	0.000
30.48	604.11	0.49	0.006	4.206	0.65	0.00407	0.3	3.740
76.20	604.05	0.55	0.238	4.544	103.48	0.65222	24.0	4.042
86.61	604.60	0.00	0.352	0.000	13.93	0.73950	30.1	0.000
184.59	604.32	0.28	0.686	2.888	13.21	0.82224	39.2	2.568
195.07	604.41	0.19	0.841	2.223	18.10	0.93559	46.3	1.977
216.41	604.41	0.19	0.949	2.223	8.89	0.99125	50.3	1.977
226.55	604.57	0.03	0.995	0.616	1.39	0.99998	51.3	0.548
226.48	604.60	0.00	1.000	0.000	0.00	1.00000	51.3	0.000
Est. Total					159.66			



Appendix D.1 North Saskatchewan River

X-SECTION N. Sask. River, 805.12 km

DATE October 18, 1977

DISCHARGE m^3/s 142.00

WIDTH m 182.50

MEAN DEPTH m 0.52

AREA m^2 94.44

MEAN VELOCITY m/s 1.504

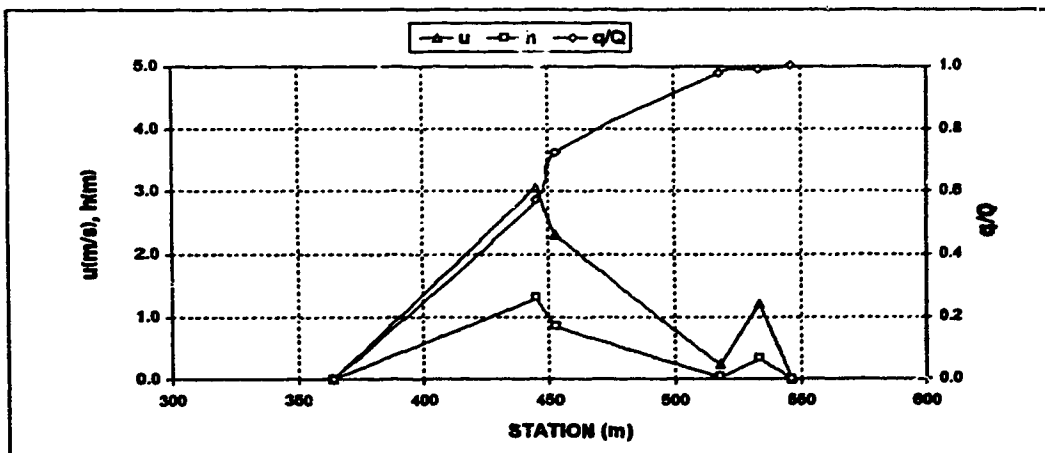
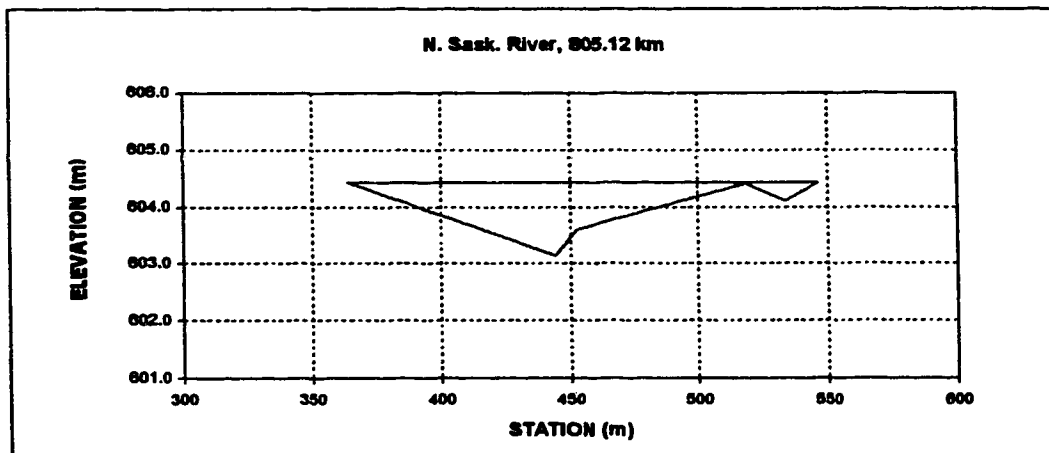
HEC2 Section from Alberta Env.

Est. Water Surface Elev. 604.436

LB 364.07 604.44

RS 546.57 604.44

Sta. m	Elev. m	h m	w/W	u m/s	dq est. m^3	norm. q/Q	Area adjusted u m^2	m^3/s
364.07	604.44	0.00	0.000	0.000	0.00	0.00000	0.0	0.000
445.00	603.13	1.31	0.443	2.788	73.66	0.56967	52.8	3.062
452.62	603.59	0.85	0.485	2.087	19.98	0.72420	61.0	2.292
518.16	604.41	0.03	0.844	0.204	32.73	0.97727	89.6	0.224
533.40	604.11	0.33	0.928	1.105	1.75	0.99084	92.3	1.213
546.57	604.44	0.00	1.000	0.000	1.18	1.00000	94.4	0.000
Est. Total					129.31			

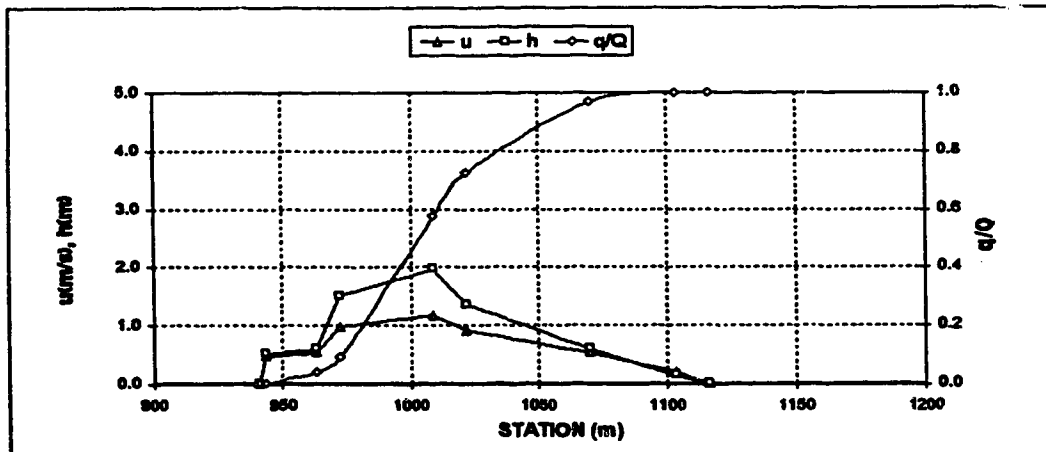
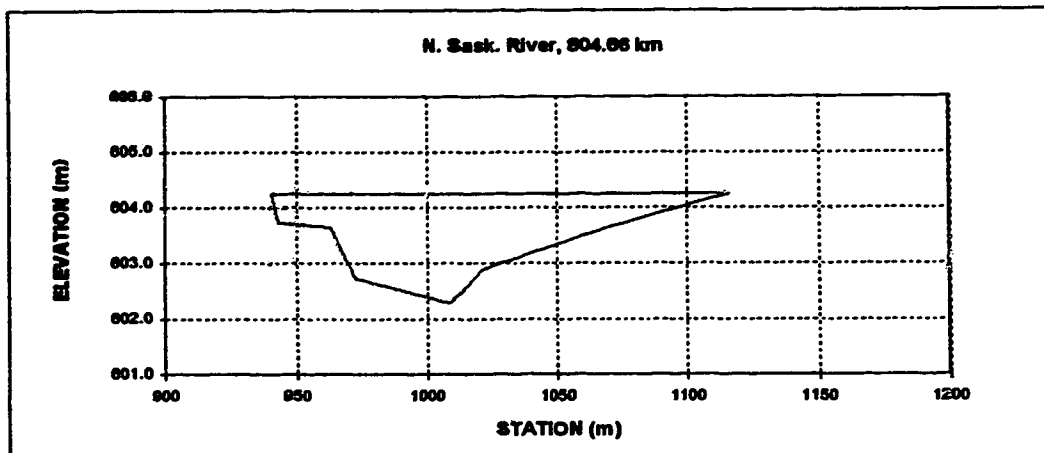


Appendix D.1 North Saskatchewan River

X-SECTION N. Sask. River, 804.88 km
 DATE October 18, 1977
 DISCHARGE m^3/s 142.00
 WIDTH m 175.81
 MEAN DEPTH m 0.95
 AREA m^2 167.16
 MEAN VELOCITY m/s 0.849

HEC2 Section from Alberta Env.
 Est. Water Surface Elev. 804.25
 LB 940.84 804.25
 RB 1116.25 804.25

Sta. m	Elev. m	h m	w/W	u m/s	dq est. m^3	norm. q/Q	Area m^2	adjusted u m/s
940.84	804.25	0.00	0.000	0.000	0.00	0.00000	0.0	0.000
943.38	803.74	0.51	0.016	0.564	0.20	0.00118	0.7	0.476
963.17	803.65	0.60	0.128	0.628	6.60	0.04046	11.8	0.530
972.31	802.74	1.51	0.180	1.158	8.65	0.09189	21.5	0.978
1006.89	802.28	1.97	0.369	1.382	81.05	0.57393	85.3	1.167
1021.08	802.89	1.36	0.458	1.080	25.06	0.72295	105.7	0.912
1069.85	803.65	0.60	0.736	0.628	41.01	0.98684	153.7	0.530
1103.38	804.11	0.14	0.927	0.242	5.46	0.99933	166.2	0.204
1116.25	804.25	0.00	1.000	0.000	0.11	1.00000	167.2	0.000
Est. Total					168.13			



Appendix D.1 North Saskatchewan River

X-SECTION N. Sask. River, 804.21 km

HEC2 Section from Alberta Env.

DATE October 18, 1977

DISCHARGE m^3/s 142.00

WIDTH m 170.83

MEAN DEPTH m 1.53

AREA m^2 260.93

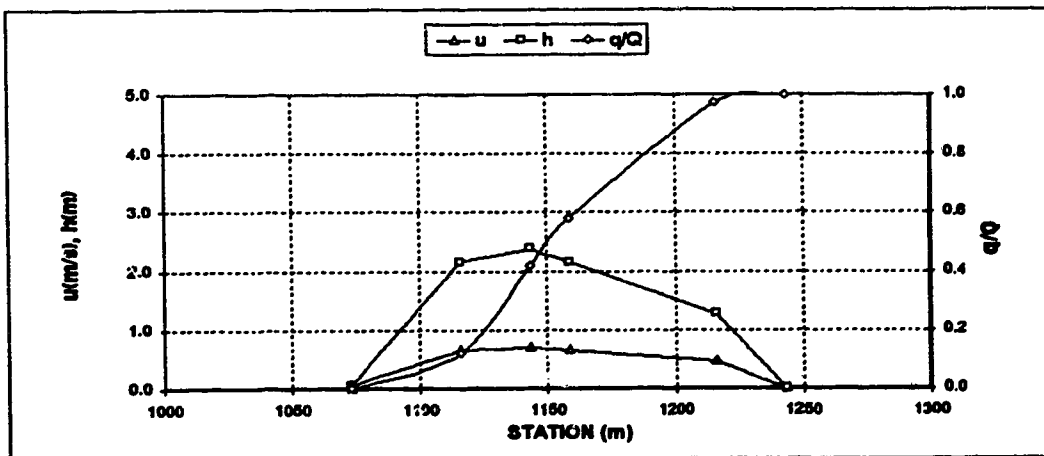
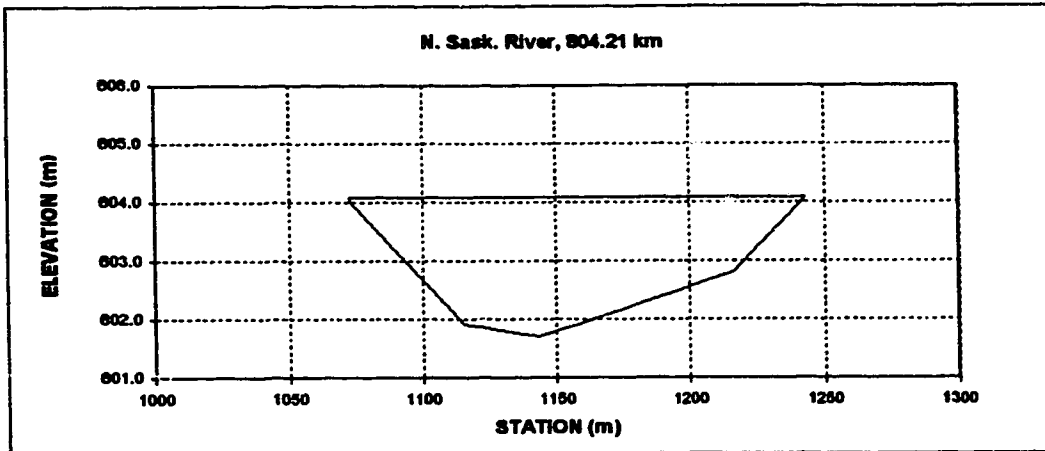
MEAN VELOCITY m/s 0.544

Est. Water Surface Elev. 604.08

LB 1072.60 604.08

RB 1243.43 604.08

Sta.	Elev.	h	w/W	u	dq est	norm. q/Q	Area adjusted	u
m	m	m		m/s	m^3		m^2	m/s
1072.60	604.08	0.00	0.000	0.000	0.00	0.00000	0.0	0.000
1072.89	604.02	0.06	0.002	0.061	0.00	0.00000	0.0	0.058
1115.57	601.92	2.16	0.252	0.685	17.64	0.11881	47.3	0.655
1143.00	601.70	2.38	0.412	0.731	44.05	0.41548	109.5	0.899
1158.24	601.92	2.16	0.501	0.685	24.47	0.58031	144.0	0.655
1216.15	602.80	1.28	0.840	0.483	58.10	0.97165	243.5	0.462
1243.43	604.08	0.00	1.000	0.000	4.21	1.00000	260.9	0.000
Est. Total					148.47			



Appendix D.1 - North Saskatchewan River

X-SECTION N. Sask. River, 804.14km (ARC Section 2)

Section from Alberta Research Council Report

DATE

October 18, 1977

DISCHARGE m^3/s

142

Assumed Water Surface

95.3

WIDTH m

170

Water Surface

604.05

MEAN DEPTH m

1.59

Correction to Geodetic

508.75

AREA m^2

269.9

Correction to Station

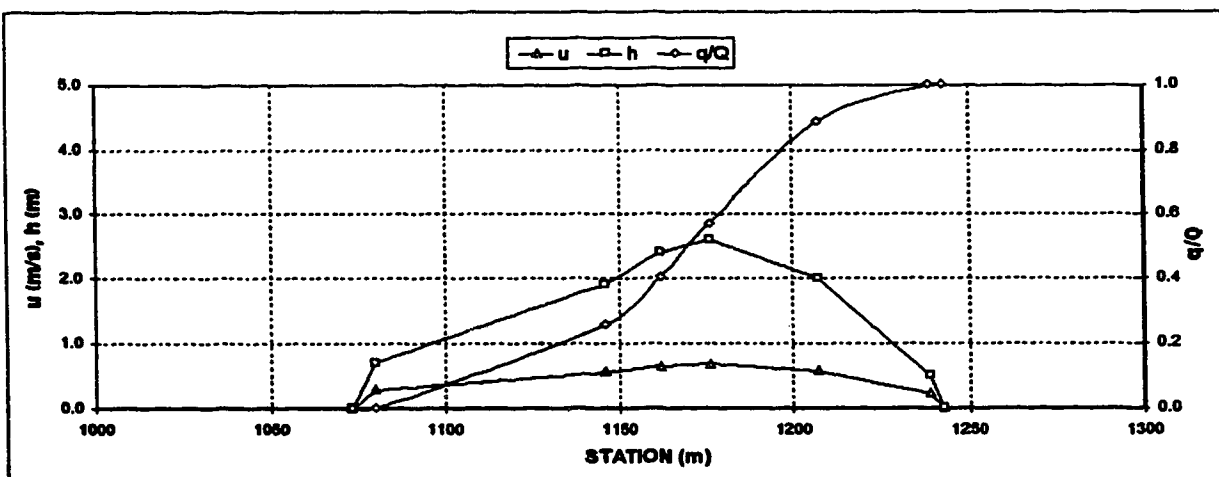
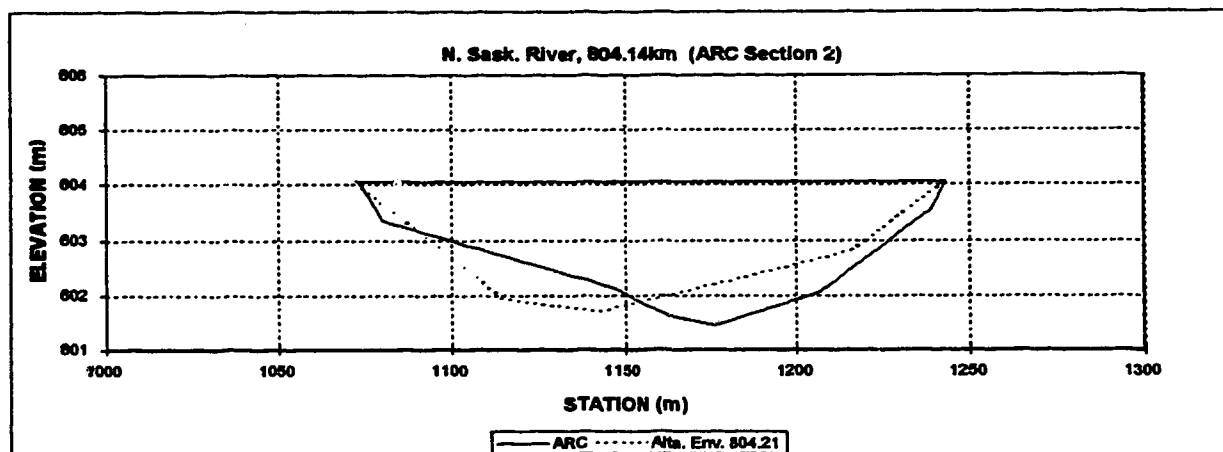
1073

MEAN VELOCITY m/s

0.526

Water's Edge	Assumed Elev	Est. Sta.	Est. Geod.	h	v/W	u	dq est.	norm. q/Q	Area	adj. u
m	m	m	m	m		m/s	m^3		m^2	m/s
0	95.3	1073	604.05	0.00	0.000	0.000	0.00	0.00000	0.0	0.000
7	94.6	1080	603.35	0.70	0.041	0.305	0.37	0.00247	2.4	0.286
73	93.4	1148	602.15	1.90	0.429	0.593	38.50	0.25730	88.2	0.557
89	92.9	1182	601.65	2.40	0.524	0.693	22.12	0.40386	122.6	0.651
103	92.7	1178	601.45	2.60	0.606	0.731	24.92	0.56858	157.6	0.687
134	93.3	1207	602.05	2.00	0.788	0.614	47.93	0.88577	228.9	0.577
166	94.8	1239	603.55	0.50	0.976	0.243	17.14	0.99919	268.9	0.229
170	95.3	1243	604.05	0.00	1.000	0.000	0.12	1.00000	269.9	0.000
		1073	604.05							

151.09

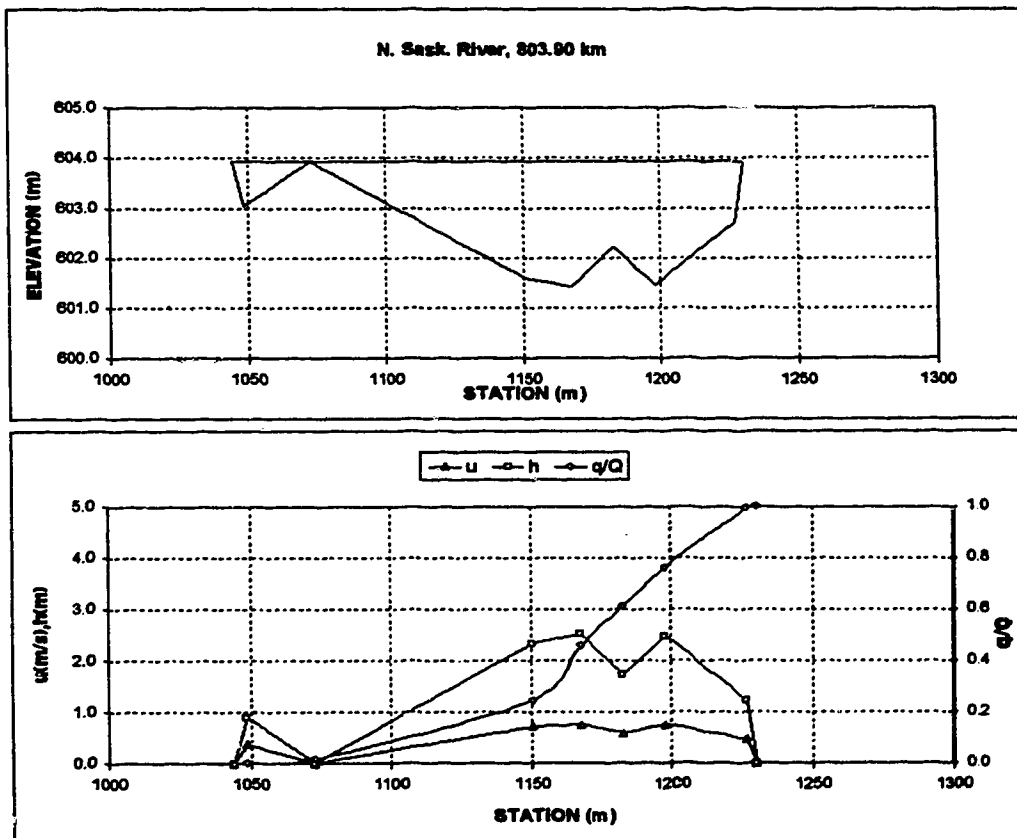


Appendix D.1 - North Saskatchewan River

X-SECTION N. Sask. River, 803.90 km HEC2 Section from Alta Env. Prot.
 DATE October 18, 1977
 DISCHARGE m^3/s 142.00
 WIDTH m 186.03
 MEAN DEPTH m 1.42
 AREA m^2 264.86
 MEAN VELOCITY m/s 0.536

Est. Water Surface Elev. 603.94
 LB 1044.42
 RB 1230.45

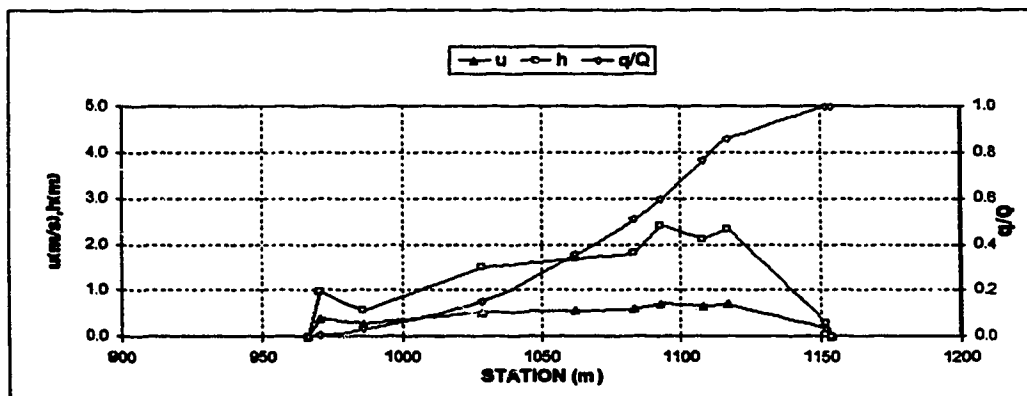
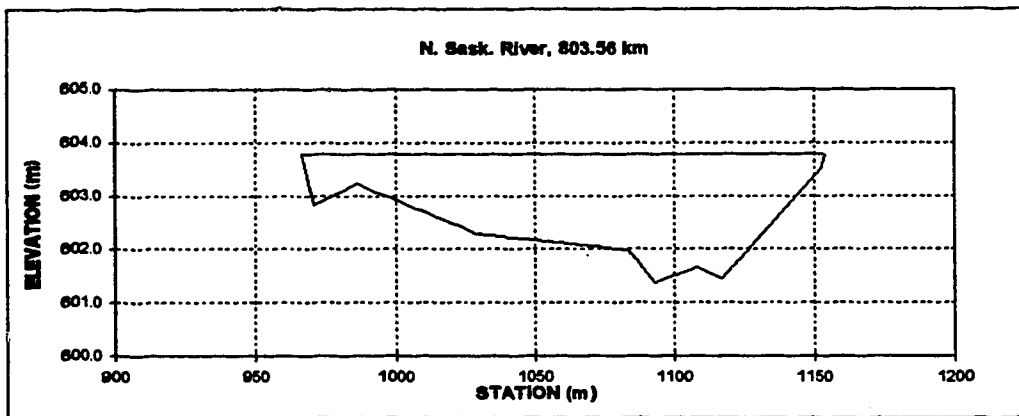
Sta.	Elev.	h	w/W	u	dq est	norm. q/Q	Area	adj. u
m	m	m		m/s	m^3		m^2	m/s
1044.42	603.94	0.00	0.000	0.000	0.00	0.00000	0.0	0.000
1048.52	603.04	0.90	0.022	0.396	0.37	0.00249	1.9	0.383
1072.48	603.94	0.00	0.151	0.000	2.14	0.01707	12.7	0.000
1150.62	601.61	2.33	0.571	0.745	33.98	0.24860	103.8	0.721
1167.39	601.43	2.51	0.661	0.783	31.06	0.46020	144.5	0.758
1182.63	602.22	1.72	0.743	0.609	22.47	0.61329	176.8	0.599
1197.87	601.46	2.48	0.825	0.777	22.21	0.76462	208.6	0.752
1226.82	602.71	1.23	0.980	0.487	34.00	0.99628	262.6	0.471
1230.45	603.94	0.00	1.000	0.000	0.55	1.00000	264.9	0.000
Est. Total					146.78			



Appendix D.1 - North Saskatchewan River

X-SECTION N. Sask. River, 803.56 km HEC2 Section from Alta Env. Prot.
 DATE October 18, 1977
 DISCHARGE m^3/s 142.00
 WIDTH m 187.22 Est. Water Surface Elev. 603.79
 MEAN DEPTH m 1.44 LB 986.58 603.79
 AREA m^2 269.58 RB 1153.80 603.79
 MEAN VELOCITY m/s 0.527

Sta. m	Elev. m	h m	w/W	u m/s	dq est. m^3	norm. q/Q	Area m^2	adjusted u m/s
986.58	603.79	0.00	0.000	0.000	0.00	0.00000	0.0	0.000
970.79	602.83	0.96	0.023	0.403	0.41	0.00275	2.0	0.385
986.03	603.23	0.56	0.104	0.281	3.97	0.02947	13.6	0.269
1028.70	602.28	1.51	0.332	0.544	18.28	0.15239	57.9	0.520
1082.23	602.10	1.69	0.511	0.587	30.37	0.35680	111.6	0.581
1063.57	601.98	1.81	0.625	0.614	22.45	0.50786	149.0	0.587
1092.71	601.37	2.42	0.674	0.745	13.15	0.59636	168.3	0.712
1107.95	601.67	2.12	0.755	0.882	24.71	0.76268	203.0	0.652
1117.10	601.46	2.33	0.804	0.727	14.35	0.85929	223.4	0.694
1152.15	603.50	0.29	0.991	0.182	20.89	0.99985	269.3	0.174
1153.80	603.79	0.00	1.000	0.000	0.02	1.00000	269.6	0.000
Est. Total					148.59			

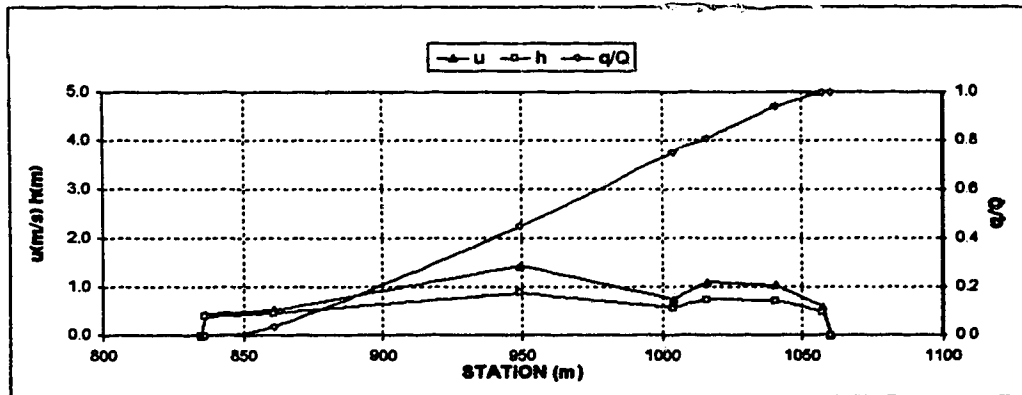
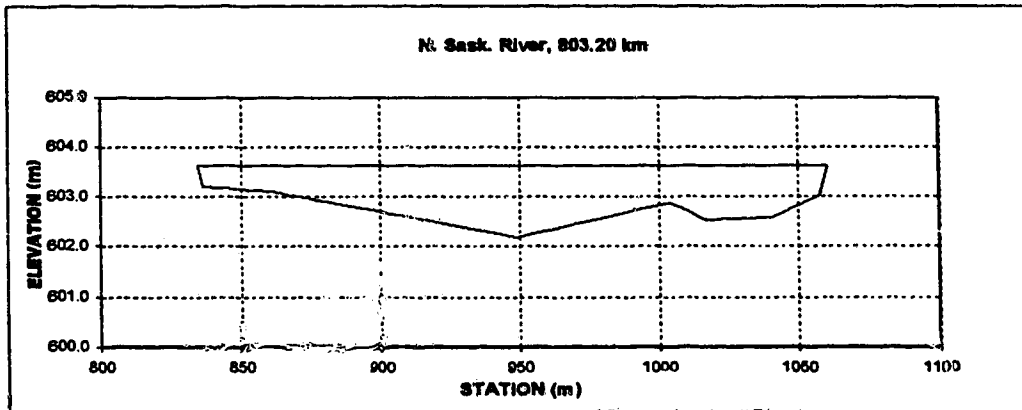


Appendix D.1 - North Saskatchewan River

X-SECTION N. Sask. River, 803.20 km HEC2 Section from Alta Erv. Prot.
 DATE October 18, 1977
 DISCHARGE m^3/s 142.00
 WIDTH m 225.68
 MEAN DEPTH m 0.94
 AREA m^2 211.22
 MEAN VELOCITY m/s 0.672

Est. Water Surface Elev. 603.63
 LB 534.82 603.63
 RB 1060.49 603.63

Sta. m	Elev. m	h m	w/W	u m/s	rq est. m^3	norm. q/Q	Area m^2	adjusted u m/s
834.82	603.63	0.00	0.000	0.000	0.00	0.00000	0.0	0.000
836.63	603.20	0.43	0.008	0.401	0.08	0.00055	0.4	0.397
861.02	603.10	0.53	0.116	0.481	5.07	0.03582	12.1	0.456
949.41	602.19	1.44	0.508	0.897	59.24	0.44797	99.4	0.886
1004.27	602.89	0.74	0.751	0.576	44.11	0.75486	159.3	0.569
1016.46	602.53	1.10	0.805	0.750	7.45	0.80688	170.5	0.741
1040.85	602.59	1.04	0.913	0.722	19.24	0.94054	196.7	0.713
1057.61	603.04	0.59	0.987	0.495	8.33	0.69853	210.4	0.489
1060.49	603.63	0.00	1.000	0.000	0.21	1.00000	211.2	0.000
Est. Total					143.74			

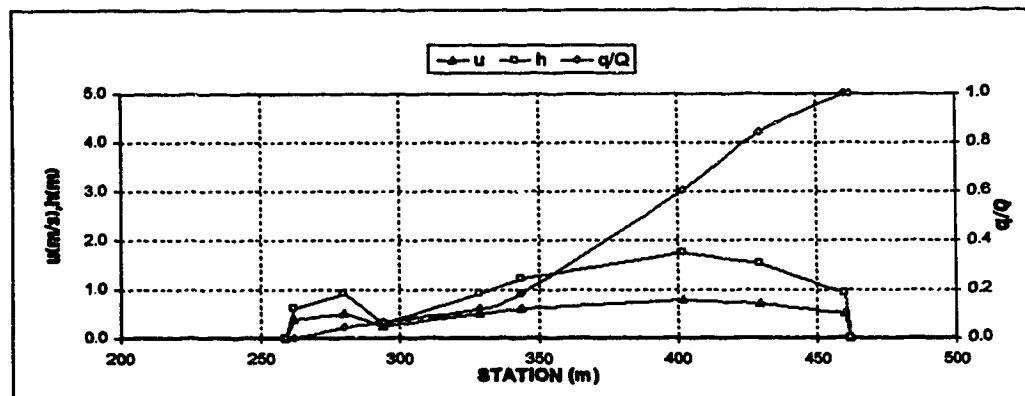
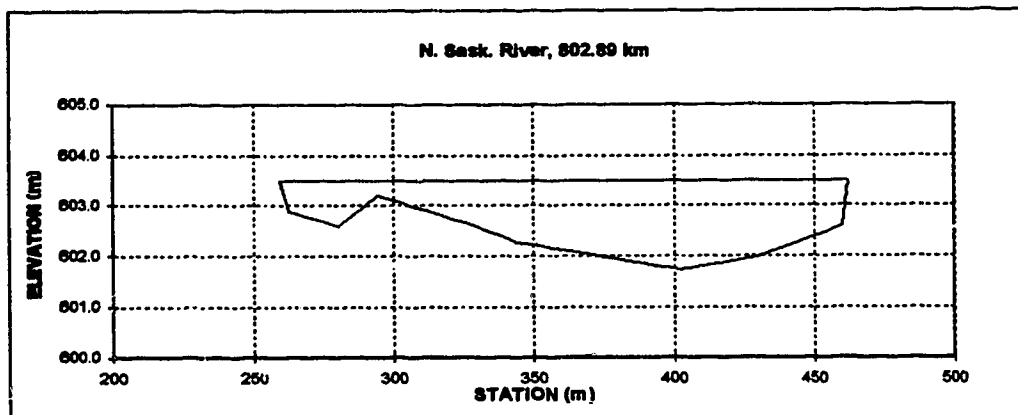


Appendix D.1 - North Saskatchewan River

X-SECTION N. Sask. River, 802.89 km HEC2 Section from Alta Env. Prot.
 DATE October 18, 1977
 DISCHARGE m^3/s 142.00
 WIDTH m 203.01
 MEAN DEPTH m 1.13
 AREA m^2 228.98
 MEAN VELOCITY m/s 0.620

Est. Water Surface Elev. 603.49
 LB 259.21 603.49
 RB 462.21 603.49

Sta. m	Elev. m	h m	w/W	u m/s	dq est. m3	norm. q/Q	Area m2	adjusted u m/s
259.21	603.49	0.00	0.000	0.000	0.00	0.00000	0.0	0.000
262.08	602.89	0.60	0.014	0.409	0.18	0.00117	0.9	0.383
280.37	602.59	0.90	0.104	0.535	6.51	0.04410	14.7	0.501
294.09	603.20	0.29	0.172	0.263	3.24	0.08545	22.9	0.237
329.14	602.59	0.90	0.344	0.535	8.27	0.12001	43.9	0.501
344.38	602.28	1.21	0.420	0.651	9.58	0.18315	60.0	0.610
402.29	601.73	1.76	0.705	0.838	64.12	0.60593	146.3	0.782
429.72	601.98	1.51	0.840	0.755	35.75	0.84168	191.2	0.707
460.20	602.59	0.90	0.990	0.535	23.77	0.99839	228.1	0.501
462.21	603.49	0.00	1.000	0.000	0.24	1.00000	229.0	0.000
Est. Total					151.66			

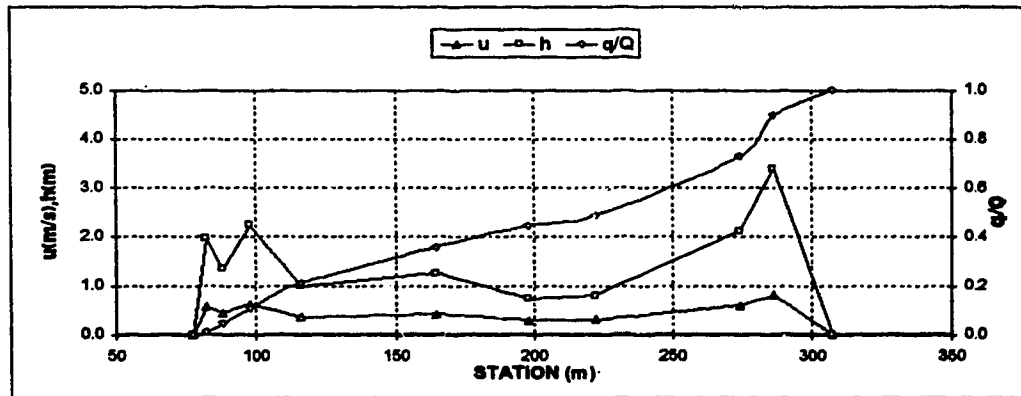
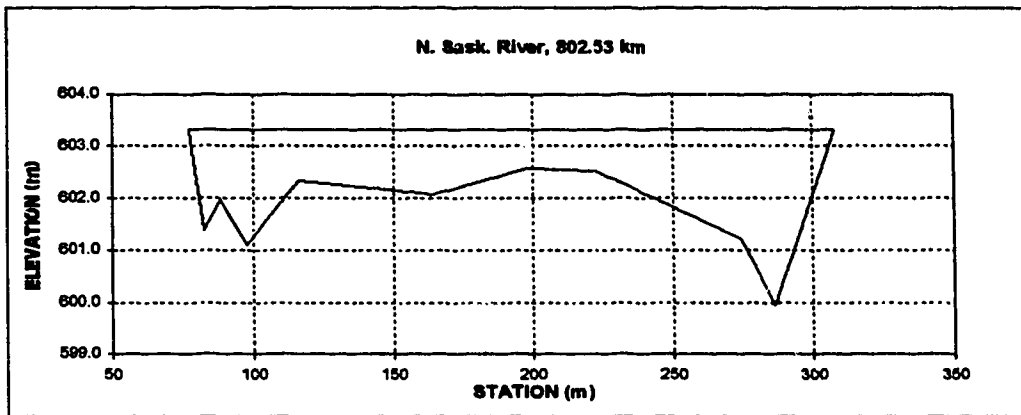


Appendix D.1 - North Saskatchewan River

X-SECTION N. Sask. River, 802.53 km
 DATE October 18, 1977
 DISCHARGE m^3/s 142.00
 WIDTH m 230.07
 MEAN DEPTH m 1.36
 AREA m^2 313.88
 MEAN VELOCITY m/s 0.452

HEC2 Section from Alta Env. Prot.
 Est. Water Surface Elev. 603.33
 LB 77.51 603.33
 RB 307.57 603.33

Sta. m	Elev. m	h m	w/W	u m/s	dq est m ³	norm. q/Q	Area m ²	adjusted u m/s
77.51	603.33	0.00	0.000	0.000	0.00	0.00000	0.0	0.000
82.29	601.37	1.96	0.021	0.577	1.36	0.00837	4.7	0.567
88.39	601.98	1.35	0.047	0.450	5.20	0.04531	14.8	0.442
97.53	601.09	2.24	0.087	0.630	8.88	0.10876	31.3	0.619
115.82	602.34	0.99	0.167	0.366	14.76	0.20883	60.9	0.360
164.59	602.07	1.26	0.379	0.430	21.92	0.36044	115.9	0.422
198.12	602.59	0.74	0.524	0.302	12.32	0.44565	149.6	0.297
222.50	602.53	0.80	0.630	0.318	5.85	0.46610	168.5	0.312
274.32	601.21	2.12	0.855	0.608	35.12	0.72697	244.3	0.597
286.51	599.93	3.40	0.908	0.832	24.26	0.89679	278.0	0.818
307.57	603.33	0.00	1.000	0.000	14.92	1.00000	313.9	0.000
Est. Total					144.58			



Appendix D.1 - North Saskatchewan River

X-SECTION N. Sask. River, 802.10 km

HEC2 Section from Alta Env. Prot.

DATE October 18, 1977

DISCHARGE m^3/s 142.00

WIDTH m 191.27

MEAN DEPTH m 1.09

AREA m^2 208.33

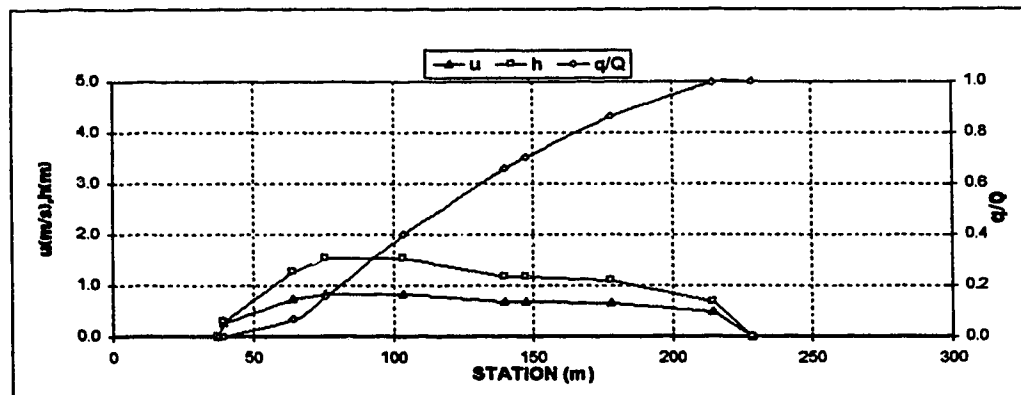
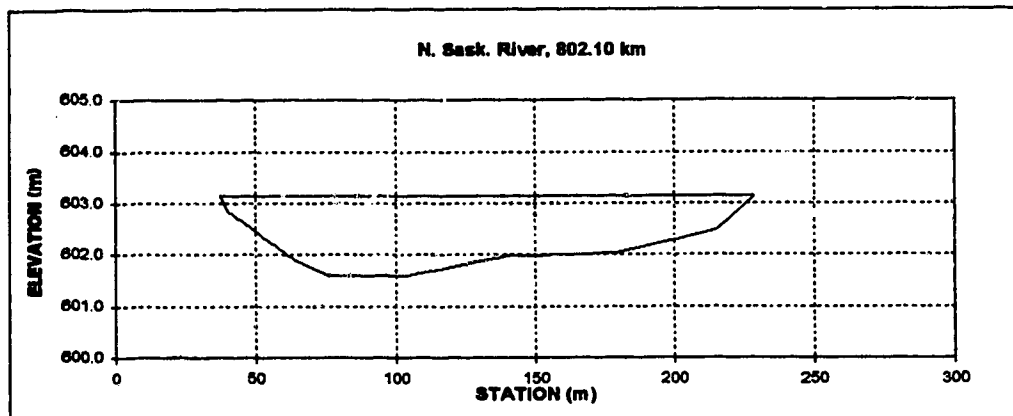
MEAN VELOCITY m/s 0.682

Est. Water Surface Elev. 603.14

LB 37.60 603.14

RB 228.87 603.14

Sta. m	Elev. m	h m	w/W	u m/s	dq est. m^3	norm. q/Q	Area m^2	adjusted u m/s
37.60	603.14	0.00	0.000	0.000	0.00	0.00000	0.0	0.000
39.63	602.86	0.28	0.011	0.277	0.04	0.00027	0.3	0.284
64.01	601.88	1.26	0.138	0.762	9.70	0.06531	19.1	0.716
76.20	601.61	1.53	0.202	0.856	13.70	0.15720	36.2	0.815
103.63	601.61	1.53	0.345	0.856	35.99	0.39857	78.2	0.815
140.21	601.98	1.16	0.536	0.712	38.65	0.65779	127.5	0.678
147.83	601.98	1.16	0.576	0.712	6.31	0.70009	136.4	0.678
178.31	602.04	1.10	0.736	0.687	24.16	0.86209	170.9	0.654
214.89	602.46	0.68	0.927	0.499	19.37	0.99201	203.6	0.475
228.87	603.14	0.00	1.000	0.000	1.19	1.00000	208.3	0.000
Est. Total					149.11			

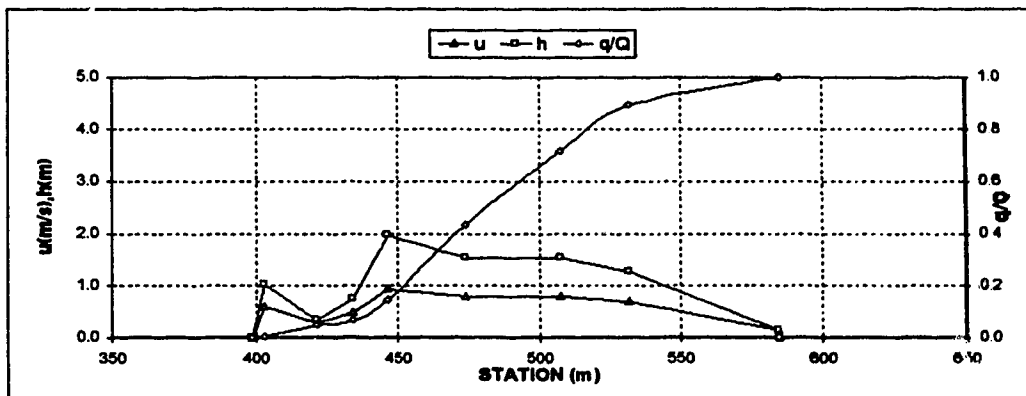
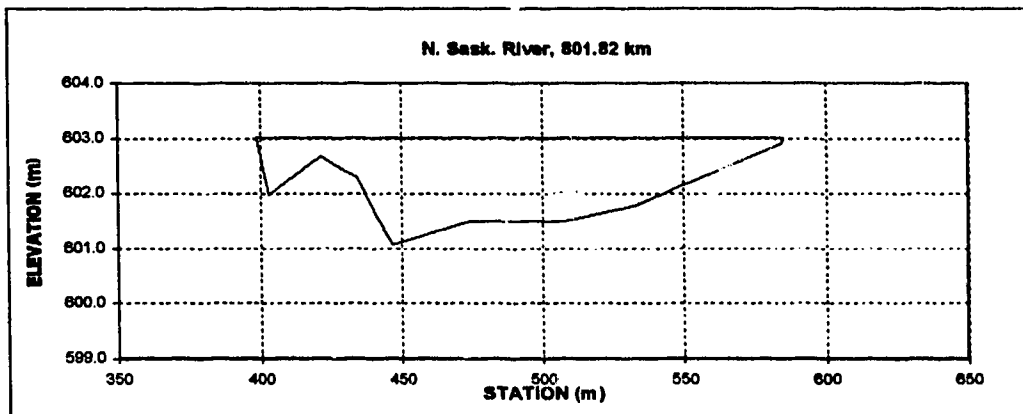


Appendix D.1 - North Saskatchewan River

X-SECTION N. Sask. River, 801.82 km HEC2 Section from Alta Enw. Prot.
 DATE October 18, 1977
 DISCHARGE m^3/s 142.00
 WIDTH m 186.89
 MEAN DEPTH m 1.11
 AREA m^2 208.05
 MEAN VELOCITY m/s 0.683

Est. Water Surface Elev. 603.02
 LB 398.54 603.02
 RB 585.23 603.02

Sta. m	Elev. m	h m	w/W	u m/s	dq est. m^3	norm. q/Q	Area m^2	adjusted u m/s
398.54	603.02	0.00	0.000	0.000	0.00	0.00000	0.0	0.000
402.95	601.98	1.04	0.024	0.651	0.75	0.00488	2.3	0.606
421.34	602.68	0.34	0.123	0.308	6.14	0.04509	15.1	0.287
434.34	602.28	0.74	0.192	0.519	2.85	0.06375	22.0	0.483
446.53	601.06	1.96	0.257	0.994	12.43	0.14520	38.4	0.925
473.96	601.49	1.53	0.404	0.843	43.91	0.43292	86.2	0.784
507.49	601.49	1.53	0.584	0.843	43.18	0.71582	137.5	0.784
531.88	601.76	1.28	0.714	0.740	26.89	0.89201	171.5	0.689
584.81	602.89	0.13	0.997	0.161	16.48	0.99998	208.0	0.150
585.23	603.02	0.00	1.000	0.000	0.00	1.00000	208.1	0.000
Est. Total					152.62			

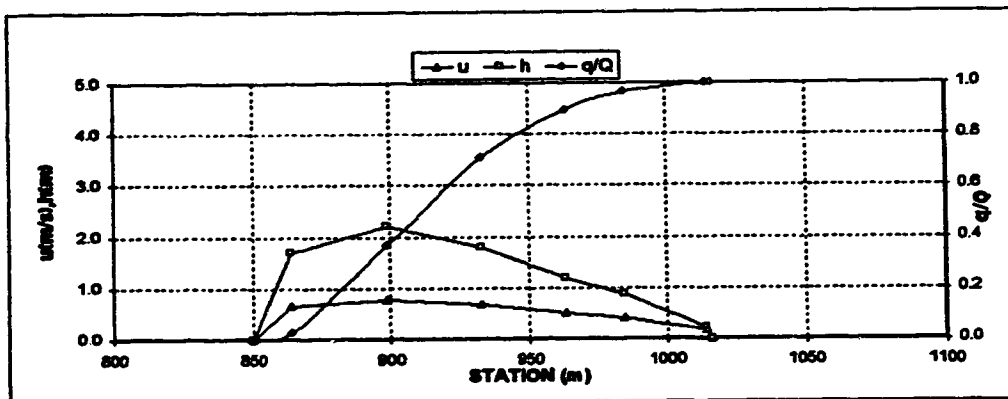
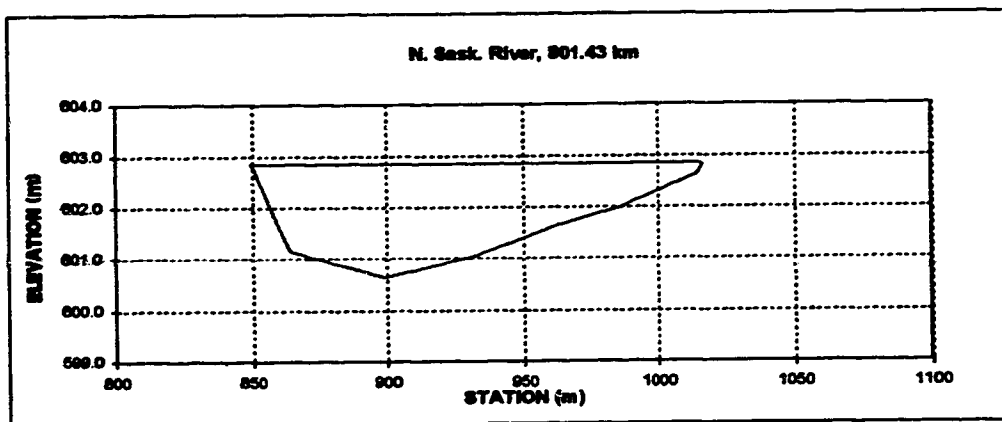


Appendix D.1 - North Saskatchewan River

X-SECTION N. Sask. River, 801.43 km HEC2 Section from Alta Env. Prot.
 DATE October 18, 1977
 DISCHARGE m^3/s 142.00
 WIDTH m 166.26
 MEAN DEPTH m 1.39
 AREA m^2 230.86
 MEAN VELOCITY m/s 0.616

Est. Water Surface Ele 602.84
 LB 649.82 602.84
 RB 1016.06 602.84

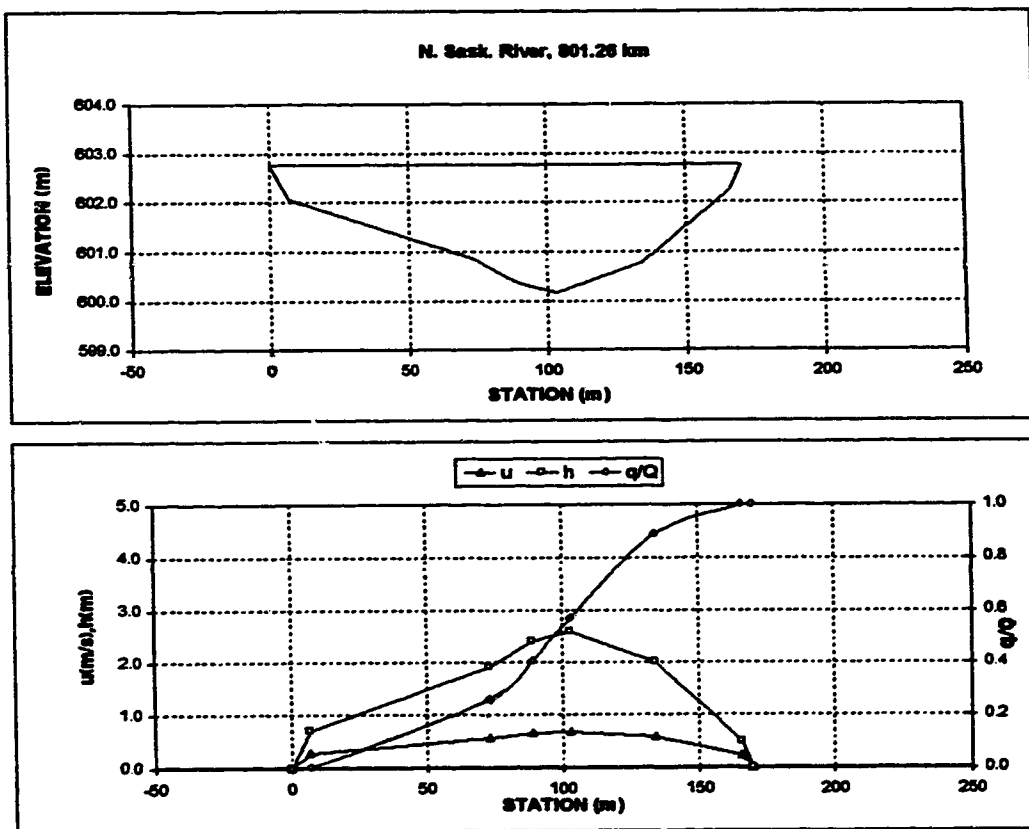
Sta. m	Elev. m	h m	w/W	u m/s	dq est. m^3	norm. q/Q	Area m^2	adjusted u m/s
849.82	602.84	0.00	0.000	0.000	0.00	0.00000	0.0	0.000
854.11	601.15	1.69	0.086	0.704	4.26	0.02761	12.1	0.648
859.16	600.64	2.20	0.297	0.838	52.69	0.36925	80.4	0.772
932.62	601.06	1.78	0.496	0.728	52.40	0.70696	147.3	0.670
963.17	601.67	1.17	0.682	0.551	28.85	0.89601	192.4	0.507
984.50	601.88	0.86	0.810	0.449	10.86	0.98654	214.2	0.414
1014.37	602.62	0.22	0.990	0.183	5.14	0.99989	230.5	0.168
1016.06	602.84	0.00	1.000	0.000	0.02	1.00000	230.7	0.000
Est. Total					154.24			



Appendix D.1 - North Saskatchewan River

X-SECTION	N. Sask. River, 801.26 km	HEC2 Section from Alta Env. Prot.
DATE	October 18, 1977	
DISCHARGE m^3/s	142.00	
WIDTH m	170.00	Est. Water Surface Elev. 602.77
MEAN DEPTH m	1.59	LB 0.00 602.77
AREA m^2	269.95	RB 170.00 602.77
MEAN VELOCITY m/s	0.526	

Sta. m	Elev. m	h m	w/W	u m/s	dq est. m^3	norm. q/Q	Area m^2	
0.00	602.77	0.00	0.000	0.000	0.00	0.00000	0.0	0.000
7.00	602.07	0.70	0.041	0.305	0.37	0.00247	2.4	0.286
73.00	600.87	1.90	0.429	0.583	38.50	0.25730	88.2	0.557
89.00	600.37	2.40	0.524	0.683	22.12	0.40366	122.6	0.651
103.00	600.17	2.60	0.606	0.731	24.92	0.56856	157.6	0.687
134.00	600.77	2.00	0.788	0.614	47.93	0.88577	228.9	0.577
168.00	602.27	0.50	0.976	0.243	17.14	0.99919	268.9	0.229
170.00	602.77	0.00	1.000	0.000	0.12	1.00000	269.9	0.000
Est. Total					151.09			

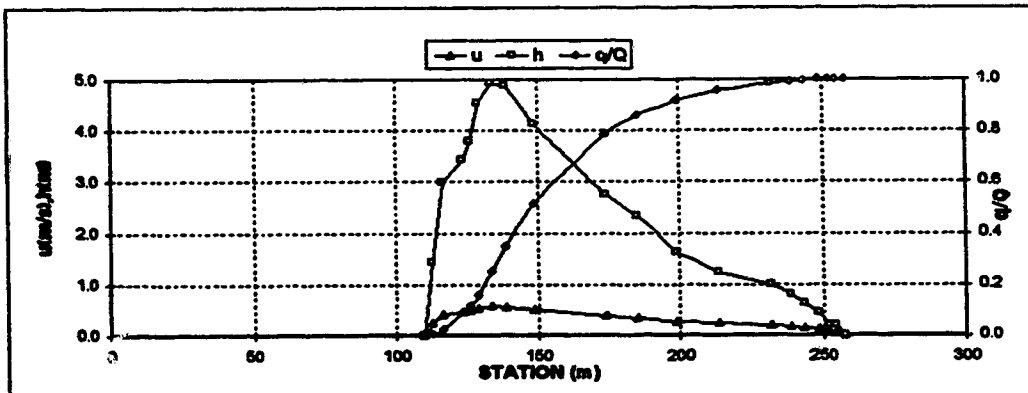
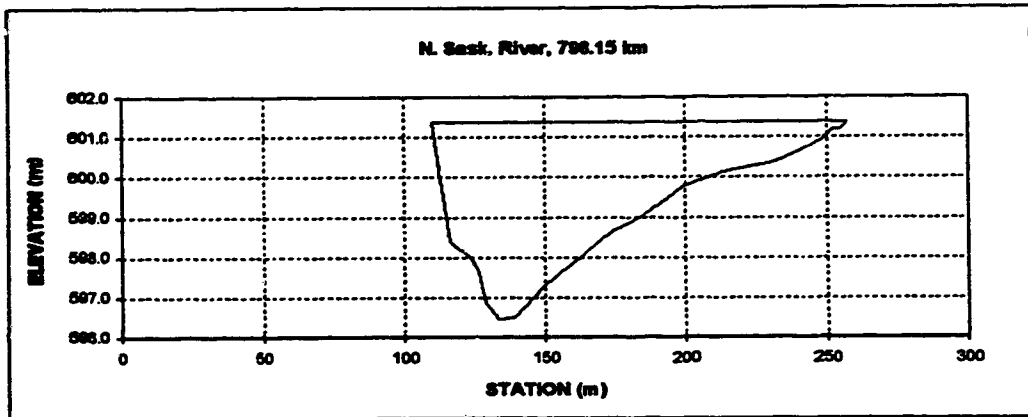


Appendix D.1 - North Saskatchewan River

X-SECTION N. Sask. River, 798.15 km
 DATE October 18, 1977
 DISCHARGE m^3/s 142.00
 WIDTH m 147.91
 MEAN DEPTH m 2.33
 AREA m^2 344.30
 MEAN VELOCITY m/s 0.412

HEC2 Section from Alta Env. Prot.
 Est. Water Surface Elev. 601.39
 LB 109.68 601.39
 RB 257.79 601.39

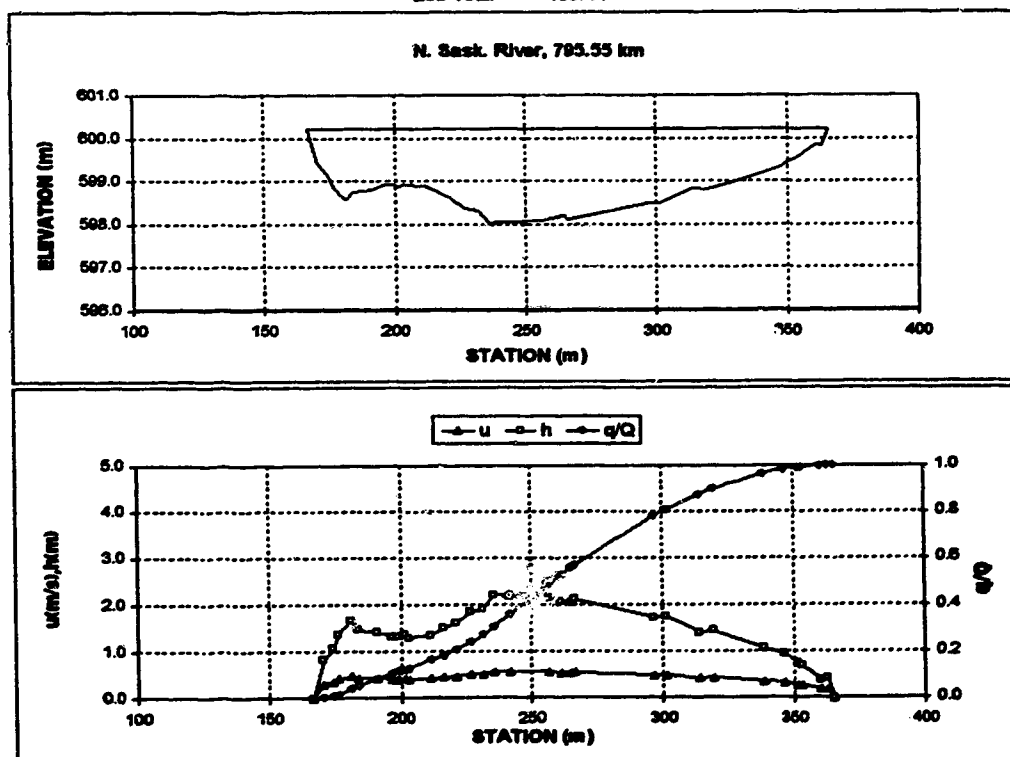
Sta. m	Elev. m	h m	w/W	u m/s	dq tot. m ³	norm. q/Q	Area m ²	adjusted u m/s
109.68	601.39	0.00	0.000	0.000	0.00	0.00000	0.0	0.000
112.76	599.95	1.44	0.019	0.299	0.31	0.00181	2.1	0.249
116.50	598.40	2.99	0.045	0.487	1.25	0.00886	10.3	0.405
123.76	597.95	3.44	0.084	0.535	11.91	0.08069	33.7	0.445
126.00	597.60	3.79	0.109	0.571	4.47	0.11690	41.7	0.475
128.76	596.85	4.54	0.128	0.644	6.97	0.15778	53.2	0.536
133.76	596.45	4.94	0.161	0.681	15.88	0.24973	76.9	0.567
138.76	596.50	4.89	0.195	0.676	16.66	0.34743	101.5	0.563
148.76	597.25	4.14	0.263	0.605	28.91	0.51690	146.6	0.504
173.76	596.65	2.74	0.432	0.459	45.73	0.78499	232.5	0.382
185.00	596.05	2.34	0.508	0.413	12.44	0.85794	261.0	0.344
199.00	596.75	1.84	0.603	0.328	10.28	0.91821	288.8	0.271
213.76	600.15	1.24	0.702	0.270	6.32	0.95528	310.0	0.225
232.00	600.40	0.99	0.826	0.233	5.10	0.98516	330.3	0.194
238.76	600.60	0.79	0.871	0.200	1.30	0.99276	336.3	0.166
243.76	600.75	0.64	0.905	0.174	0.66	0.99666	339.8	0.145
248.76	600.95	0.44	0.939	0.135	0.41	0.99908	342.5	0.112
252.00	601.20	0.19	0.961	0.077	0.11	0.99971	343.5	0.064
254.76	601.20	0.19	0.980	0.077	0.04	0.99994	344.0	0.064
257.79	601.39	0.00	1.000	0.000	0.01	1.00000	344.3	0.000
Est. Total					170.56			



Appendix D.1 - North Saskatchewan River

X-SECTION	N. Sask. River, 795.55 km	HEC2 Section from Alta Env. Prot.
DATE	October 18, 1977	
DISCHARGE m^3/s	142.00	
WIDTH m	198.85	Est. Water Surface Ele 600.23
MEAN DEPTH m	1.52	LB 599.78 600.23
AREA m^2	301.39	RB 599.62 600.23
MEAN VELOCITY m/s	0.471	

Sta. m	Elev. m	h m	w/W	u m/s	dq est. m^3	norm. q/Q	Area m^2	q/estd u m/s
166.78	599.78	0.00	0.000	0.000	0.00	0.00000	0.0	0.000
170.59	599.41	0.82	0.019	0.313	0.24	0.00182	1.8	0.295
174.65	599.16	1.07	0.040	0.373	1.32	0.01038	5.4	0.353
176.59	598.85	1.38	0.049	0.443	0.97	0.01682	1.0	0.418
181.59	598.56	1.67	0.074	0.503	3.60	0.04077	18.0	0.474
183.94	598.76	1.47	0.086	0.482	1.78	0.05260	19.1	0.436
191.59	598.81	1.42	0.125	0.451	5.04	0.08613	30.1	0.426
196.59	598.91	1.32	0.150	0.430	3.02	0.10618	37.0	0.406
198.09	598.92	1.31	0.162	0.427	1.41	0.11554	40.3	0.403
201.59	598.87	1.36	0.175	0.438	1.44	0.12515	43.6	0.414
203.02	598.93	1.30	0.182	0.425	0.82	0.13061	45.5	0.401
211.59	598.88	1.35	0.225	0.436	4.89	0.16312	56.9	0.412
216.59	598.74	1.49	0.251	0.466	3.20	0.18440	64.0	0.440
221.59	598.61	1.62	0.276	0.453	3.73	0.20916	71.8	0.465
226.59	598.38	1.85	0.301	0.536	4.47	0.23888	80.4	0.506
231.59	598.32	1.91	0.326	0.550	5.11	0.27266	89.8	0.519
235.97	598.02	2.21	0.348	0.606	5.21	0.30752	98.8	0.572
241.59	598.04	2.19	0.376	0.602	7.47	0.35716	111.2	0.568
256.59	598.07	2.16	0.452	0.597	19.56	0.48716	143.8	0.563
261.59	598.17	2.06	0.477	0.578	6.20	0.52835	154.4	0.546
265.23	598.20	2.03	0.495	0.573	4.28	0.55682	161.8	0.540
266.59	598.11	2.12	0.502	0.589	1.64	0.56772	164.7	0.556
296.59	598.50	1.73	0.653	0.515	31.88	0.77959	222.4	0.486
301.59	598.49	1.74	0.678	0.517	4.47	0.80832	231.1	0.488
314.39	598.83	1.40	0.742	0.447	9.68	0.87367	251.2	0.422
319.72	598.79	1.44	0.769	0.455	3.41	0.88636	258.7	0.430
339.09	599.16	1.07	0.867	0.373	10.07	0.96332	283.1	0.363
346.59	599.29	0.94	0.904	0.343	2.70	0.98128	290.6	0.323
351.59	599.49	0.74	0.929	0.292	1.33	0.99012	294.8	0.276
353.19	599.54	0.69	0.937	0.279	0.33	0.99229	295.9	0.263
360.59	599.85	0.38	0.975	0.187	0.92	0.99842	298.9	0.177
362.92	599.61	0.42	0.986	0.200	0.18	0.99962	300.8	0.169
365.62	600.23	0.00	1.000	0.000	0.06	1.00000	301.4	0.000
Est. Total					150.44			



Appendix D.1 - North Saskatchewan River

X-SECTION N. Sask. River, 794.10 km

HEC2 Section from Alta Erv. Prot.

DATE October 18, 1977

DISCHARGE m^3/s

142.00

WIDTH m

178.00

MEAN DEPTH m

1.42

AREA m^2

252.10

MEAN VELOCITY m/s

0.563

Est. Water Surface Elev.

599.68

LB

0.00

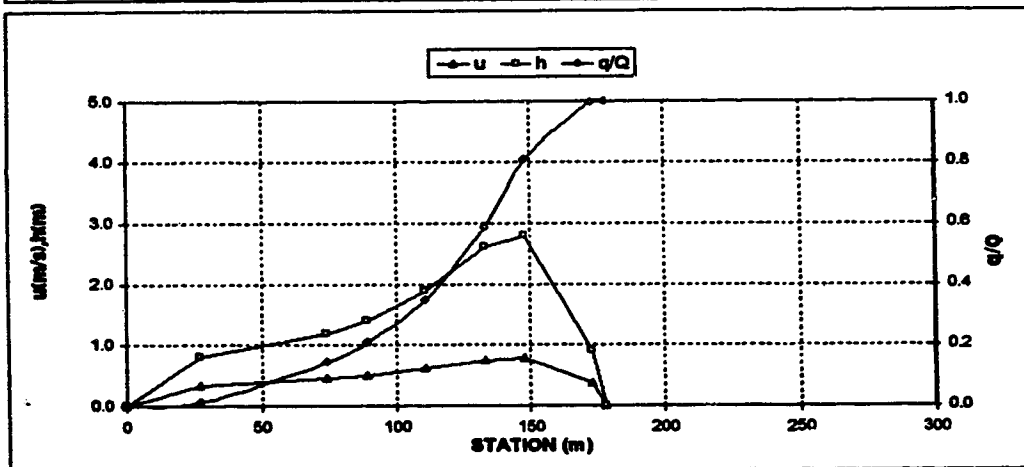
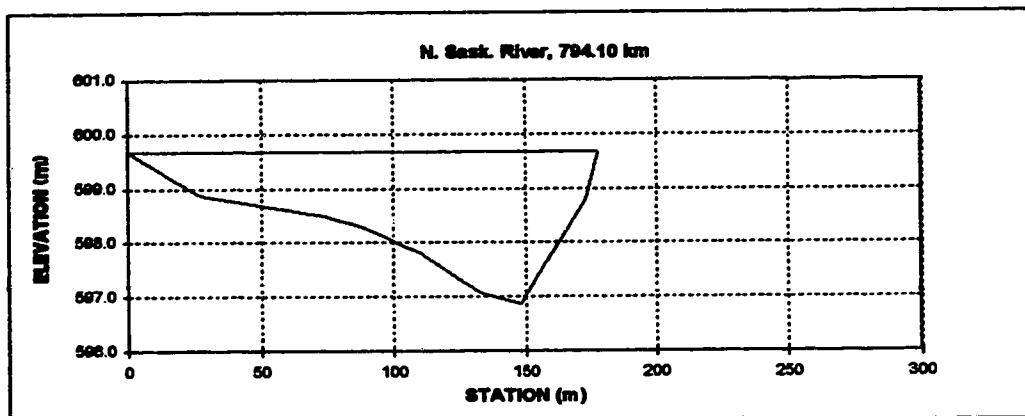
599.68

RB

178.00

599.68

Sta. m	Elev. m	h m	w/W	u m/s	dq est. m^3	norm. q/Q	Area m^2	adjusted u m/s
0.00	599.68	0.00	0.000	0.000	0.00	0.00000	0.0	0.000
27.00	598.68	0.80	0.152	0.385	2.06	0.01303	10.8	0.343
74.00	598.48	1.20	0.416	0.504	20.89	0.14405	57.8	0.449
89.00	598.28	1.40	0.500	0.559	10.37	0.20906	77.3	0.498
111.00	597.78	1.90	0.624	0.685	22.58	0.35065	113.6	0.610
133.00	597.08	2.60	0.747	0.845	37.86	0.58808	163.1	0.752
148.00	596.68	2.80	0.831	0.887	35.08	0.80802	203.6	0.790
173.00	596.78	0.90	0.972	0.410	30.15	0.99706	249.8	0.371
178.00	599.68	0.00	1.000	0.000	0.47	1.00000	252.1	0.000
Est. Total					159.48			

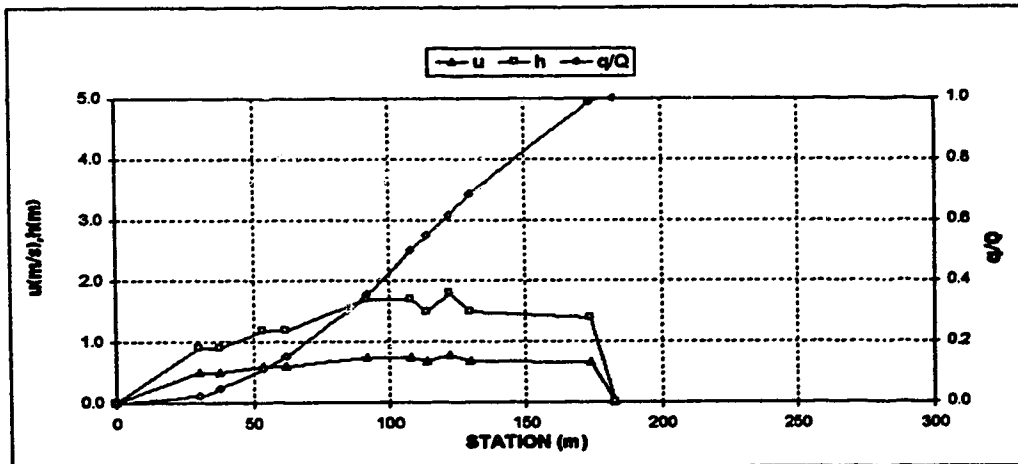
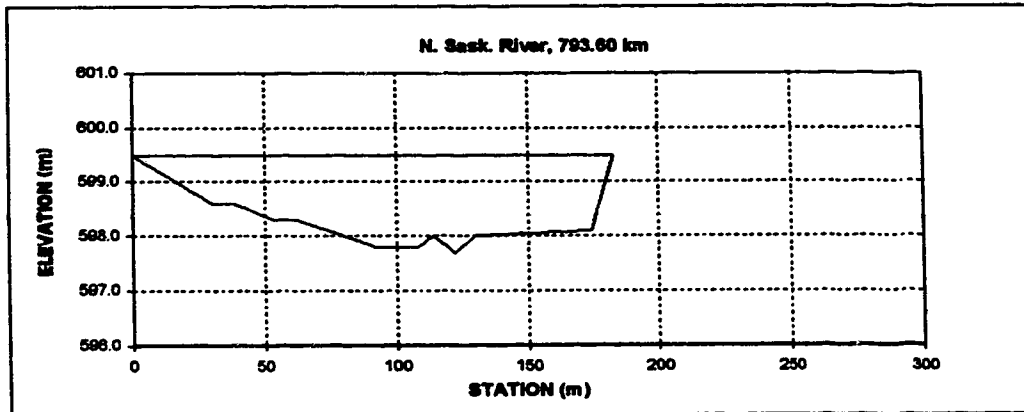


Appendix D.1 - North Saskatchewan River

X-SECTION N. Sask. River, 793.60 km HEC2 Section from Alta. Enw. Prot.
 DATE October 18, 1977
 DISCHARGE m^3/s 142.00
 WIDTH m 183.00
 MEAN DEPTH m 1.22
 AREA m^2 223.90
 MEAN VELOCITY m/s 0.634

Est. Water Surface Elev. 599.48
 LB 0.00 599.48
 RB 183.00 599.49

Sta. m	Elev. m	h m	w/W	u m/s	dq est. m^3	norm. q/Q	Area m^2	adjusted u m/s
0.00	599.49	0.00	0.000	0.000	0.00	0.00000	0.0	0.000
30.00	598.59	0.90	0.184	0.517	3.49	0.02321	13.5	0.468
38.00	598.59	0.90	0.208	0.517	3.72	0.04796	20.7	0.488
54.00	598.29	1.20	0.295	0.628	9.60	0.11184	37.5	0.592
62.00	598.29	1.20	0.339	0.628	6.01	0.15183	47.1	0.592
92.00	597.79	1.70	0.503	0.790	30.79	0.35673	90.6	0.746
108.00	597.79	1.70	0.590	0.790	21.48	0.49957	117.8	0.746
114.00	597.99	1.50	0.623	0.727	7.28	0.54810	127.4	0.686
122.00	597.69	1.80	0.667	0.820	10.21	0.61603	140.6	0.775
130.00	597.99	1.50	0.710	0.727	10.21	0.68397	153.8	0.686
174.00	598.09	1.40	0.951	0.694	45.31	0.98546	217.6	0.656
183.00	599.49	0.00	1.000	0.000	2.19	1.00000	223.9	0.000
Est. Total					150.29			



Appendix D.1 - North Saskatchewan River

X-SECTION N. Sask. River, 791.95 km

HEC2 Section from Alta Env. Prot.

DATE October 18, 1977

DISCHARGE m^3/s 142.00

WIDTH m 213.43

MEAN DEPTH m 1.23

AREA m^2 262.02

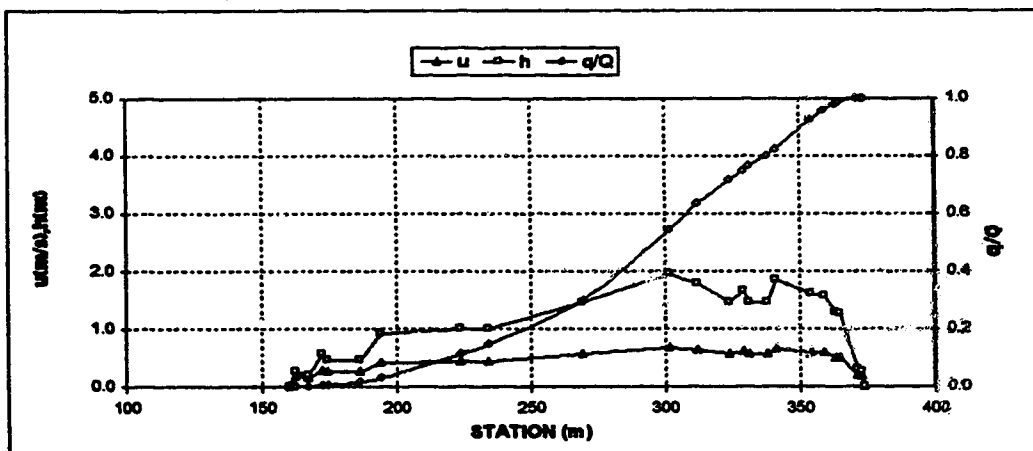
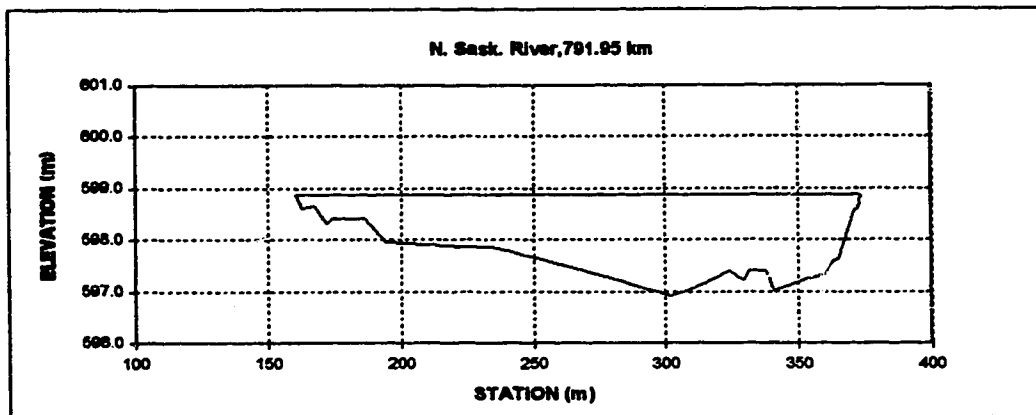
MEAN VELOCITY m/s 0.542

Est. Water Surface Elev. 598.87

LB 160.43 598.87

RS 373.87 598.87

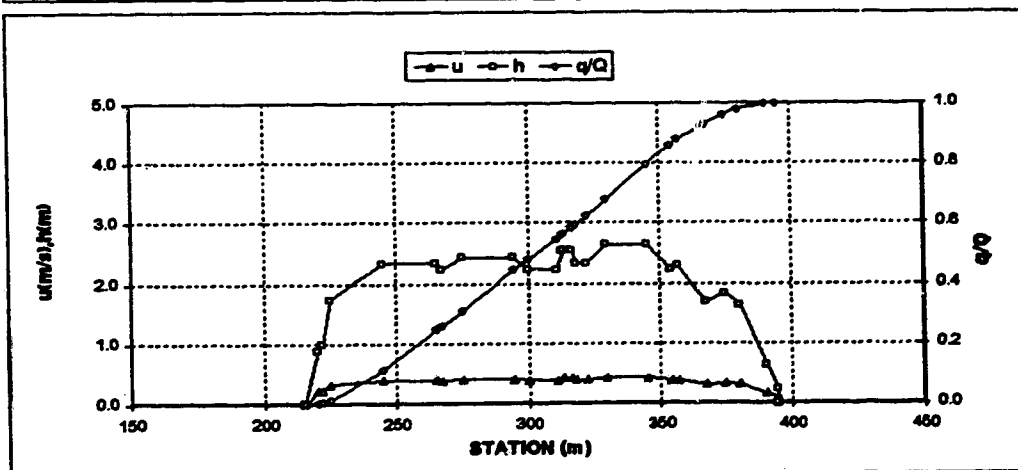
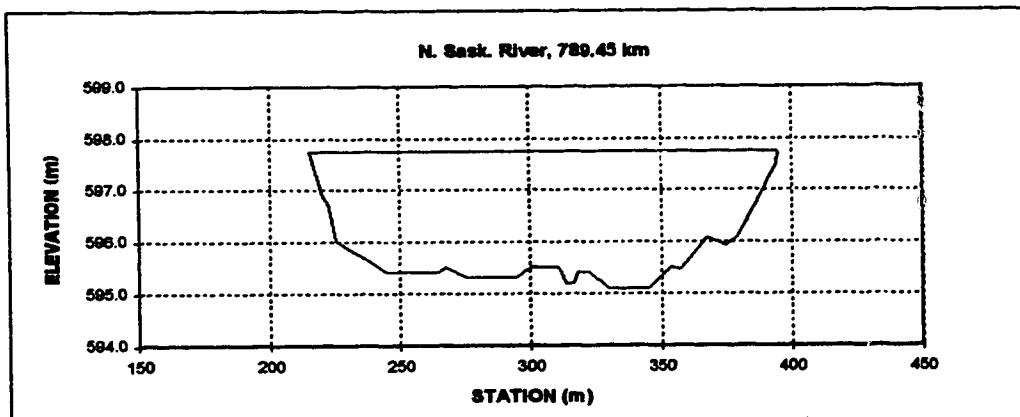
Sta. m	Elev. m	h m	w/W	u m/s	dq est. m^3	norm. q/Q	Area m^2	adjusted u m/s
160.43	598.87	0.00	0.000	0.000	0.00	0.00000	0.0	0.000
162.67	598.61	0.26	0.010	0.182	0.03	0.00018	0.3	0.178
167.17	598.66	0.21	0.032	0.167	0.19	0.00142	1.3	0.154
172.17	598.31	0.56	0.055	0.321	0.47	0.00447	3.3	0.297
174.17	598.41	0.46	0.064	0.282	0.31	0.00647	4.3	0.260
186.37	598.41	0.46	0.122	0.282	1.58	0.01675	9.9	0.260
194.17	597.96	0.91	0.158	0.444	1.94	0.02936	15.2	0.410
224.17	597.86	1.01	0.299	0.476	13.24	0.11551	44.0	0.440
234.17	597.86	1.01	0.345	0.476	4.81	0.14677	54.1	0.440
289.17	597.41	1.46	0.509	0.608	23.43	0.29920	97.4	0.582
301.77	596.91	1.96	0.662	0.740	37.60	0.54376	153.1	0.684
312.00	597.09	1.78	0.710	0.694	13.72	0.63303	172.2	0.641
324.17	597.41	1.46	0.767	0.608	12.84	0.71657	182.0	0.582
329.17	597.21	1.66	0.791	0.663	4.96	0.74882	199.8	0.612
331.47	597.41	1.46	0.801	0.608	2.28	0.76366	203.4	0.582
338.00	597.41	1.46	0.832	0.608	5.80	0.80139	212.9	0.562
341.00	597.01	1.86	0.846	0.715	3.30	0.82282	217.9	0.660
354.17	597.26	1.61	0.906	0.649	15.59	0.92423	240.7	0.600
359.17	597.31	1.56	0.931	0.636	5.09	0.95736	248.6	0.587
363.00	597.59	1.28	0.949	0.557	3.24	0.97846	254.1	0.515
364.77	597.61	1.26	0.957	0.551	1.25	0.98657	256.3	0.509
371.27	598.56	0.31	0.988	0.216	1.96	0.99931	261.4	0.200
372.87	598.61	0.26	0.995	0.192	0.09	0.99992	261.9	0.178
373.87	598.87	0.00	1.000	0.000	0.01	1.00000	262.0	0.000
Est. Total					153.73			



Appendix D.1 - North Saskatchewan River

X-SECTION	N. Sask. River, 789.45 km	HEC2 Section from Alta Env. Prot.
DATE	October 18, 1977	
DISCHARGE m^3/s	142.00	
WIDTH m	179.41	Est. Water Surface Elev.
MEAN DEPTH m	2.09	LB 215.26 597.75
AREA m^2	374.78	RB 394.68 597.75
MEAN VELOCITY m/s	0.379	

Sta.	Elev.	h	w/W	u	dq est.	norm. q/Q	Area	adjusted u
m	m	m		m/s	m^3		m^2	m/s
215.26	597.75	0.00	0.000	0.000	0.00	0.00000	0.0	0.000
220.00	596.86	0.89	0.026	0.214	0.22	0.00152	2.1	0.206
221.70	596.76	0.99	0.036	0.230	0.35	0.00382	3.7	0.221
225.00	596.01	1.74	0.054	0.335	1.27	0.01252	8.2	0.322
245.00	595.41	2.34	0.166	0.408	15.14	0.11516	48.9	0.393
265.00	595.41	2.34	0.277	0.408	19.09	0.24452	95.7	0.393
267.50	595.51	2.24	0.291	0.397	2.30	0.26012	101.4	0.382
275.00	595.31	2.44	0.333	0.420	7.16	0.30862	118.9	0.404
295.00	595.31	2.44	0.444	0.420	20.47	0.44734	167.7	0.404
300.00	595.51	2.24	0.472	0.397	4.77	0.47968	179.4	0.382
311.00	595.51	2.24	0.534	0.397	9.76	0.54583	204.0	0.382
313.50	595.21	2.54	0.548	0.431	2.47	0.56257	209.9	0.415
316.50	595.21	2.54	0.564	0.431	3.28	0.58482	217.5	0.415
318.00	595.41	2.34	0.573	0.408	1.53	0.59522	221.2	0.393
322.50	595.41	2.34	0.598	0.408	4.29	0.62433	231.7	0.393
330.00	595.11	2.64	0.640	0.443	7.94	0.67812	250.4	0.426
345.00	595.11	2.64	0.723	0.443	17.51	0.79678	289.9	0.426
354.00	595.51	2.24	0.773	0.397	9.20	0.85916	311.9	0.382
357.00	595.46	2.29	0.790	0.403	2.71	0.87754	318.6	0.387
367.50	596.06	1.69	0.849	0.329	7.63	0.92923	339.5	0.316
375.00	595.91	1.84	0.890	0.348	4.47	0.95952	352.7	0.335
380.00	596.11	1.64	0.918	0.322	2.91	0.97923	361.4	0.310
390.00	597.11	0.64	0.974	0.172	2.81	0.99826	372.8	0.165
394.50	597.51	0.24	0.999	0.089	0.26	0.99999	374.8	0.085
394.68	597.75	0.00	1.000	0.000	0.00	1.00000	374.8	0.000
Est. Total					147.56			

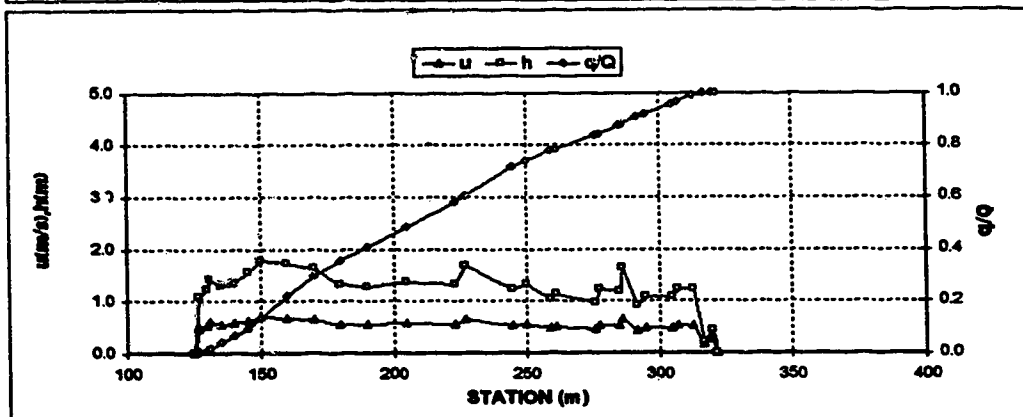
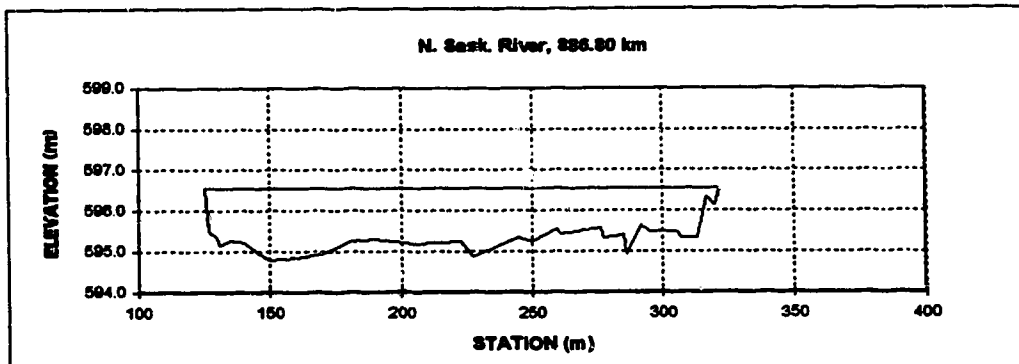


Appendix D.1 - North Saskatchewan River

X-SECTION N. Sask. River, 886.80 km
 DATE October 18, 1977
 DISCHARGE m^3/s 142.00
 WIDTH m 186.71
 MEAN DEPTH m 1.28
 AREA m^2 252.48
 MEAN VELOCITY m/s 0.562

HEC2 Section from Alta Env. Prot.
 Est. Water Surface Elev. 596.56
 LB 125.09 596.56
 RB 321.79 596.56

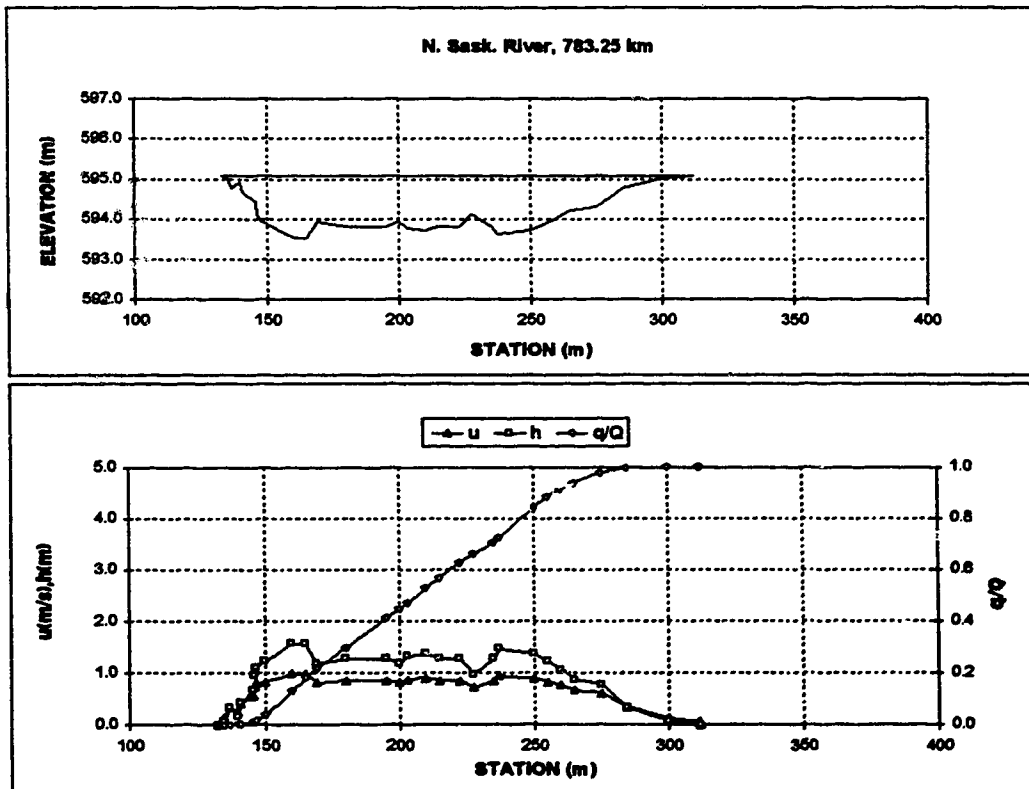
Sta. m	Elev. m	h m	w/W	u m/s	dq est. m^3	norm. q/Q	Area m^2	adjusted u m/s
125.09	596.56	0.00	0.000	0.000	0.00	0.00000	0.0	0.000
127.00	595.49	1.07	0.010	0.497	0.25	0.00174	1.0	0.485
130.00	595.34	1.22	0.025	0.543	1.78	0.01399	4.4	0.530
131.00	595.14	1.42	0.030	0.601	0.75	0.01917	5.8	0.586
135.00	595.27	1.29	0.050	0.563	3.15	0.04080	11.2	0.550
140.00	595.22	1.34	0.076	0.578	3.74	0.06653	17.7	0.564
145.00	594.99	1.57	0.101	0.643	4.43	0.09698	25.0	0.627
150.00	594.79	1.77	0.127	0.696	5.58	0.13533	33.3	0.679
160.00	594.84	1.72	0.177	0.683	12.01	0.21788	50.7	0.686
170.00	594.94	1.62	0.228	0.656	11.16	0.29459	67.4	0.640
180.00	595.24	1.32	0.279	0.572	9.01	0.35651	82.1	0.558
190.00	595.29	1.27	0.330	0.558	7.30	0.40867	95.0	0.544
205.00	595.19	1.37	0.406	0.587	11.30	0.48435	114.8	0.572
223.00	595.24	1.32	0.498	0.572	14.00	0.58054	138.9	0.558
227.00	594.89	1.67	0.518	0.670	3.71	0.60601	144.9	0.653
245.00	595.34	1.22	0.610	0.543	15.73	0.71415	170.1	0.530
250.00	595.24	1.32	0.635	0.572	3.53	0.73843	177.2	0.558
259.00	595.54	1.02	0.681	0.482	5.53	0.77646	187.7	0.470
261.00	595.44	1.12	0.691	0.513	1.06	0.78375	189.8	0.500
276.20	595.59	0.97	0.768	0.406	7.75	0.83700	205.7	0.454
277.40	595.34	1.22	0.774	0.543	0.86	0.84154	207.0	0.530
284.70	595.39	1.17	0.811	0.528	4.66	0.87356	215.7	0.515
285.80	594.84	1.62	0.817	0.656	0.91	0.87979	217.2	0.640
292.00	595.64	0.92	0.849	0.449	4.34	0.90963	225.1	0.439
295.00	595.49	1.07	0.864	0.497	1.41	0.91931	228.0	0.485
305.00	595.49	1.07	0.915	0.497	5.31	0.95578	238.7	0.485
307.00	595.34	1.22	0.925	0.543	1.19	0.96394	241.0	0.530
313.00	595.34	1.22	0.955	0.543	3.96	0.99118	248.3	0.530
317.00	596.24	0.22	0.976	0.172	1.02	0.99823	251.2	0.168
320.00	596.14	0.42	0.991	0.286	0.21	0.99966	252.1	0.259
321.79	596.56	0.00	1.000	0.000	0.05	1.00000	252.5	0.000
Est. Total					145.49			



Appendix D.1 - North Saskatchewan River

X-SECTION	N. Sask. River, 783.25 km	HEC2 Section from Alta Env. Prot.
DATE	October 18, 1977	
DISCHARGE m^3/s	142.00	
WIDTH m	179.43	Est. Water Surface Elev.
MEAN DEPTH m	0.97	LB 132.60 595.09
AREA m^2	174.27	RB 312.03 595.09
MEAN VELOCITY m/s	0.815	

Sta.	Elev.	h	w/W	u	dq est.	norm. q/Q	Area	adjusted u
m	m	m		m/s	m^3		m^2	m/s
132.67	595.09	0.00	0.000	0.000	0.00	0.00000	0.0	0.000
135.00	595.02	0.07	0.013	0.147	0.01	0.00004	0.1	0.129
136.80	594.77	0.32	0.023	0.392	0.10	0.00084	0.4	0.343
140.00	594.92	0.17	0.041	0.260	0.26	0.00225	1.2	0.227
141.00	594.67	0.42	0.047	0.469	0.11	0.00292	1.5	0.411
145.50	594.42	0.67	0.072	0.639	1.37	0.01137	4.0	0.539
146.00	594.12	0.97	0.075	0.817	0.30	0.01322	4.4	0.715
147.00	593.97	1.12	0.080	0.899	0.90	0.01677	5.5	0.786
150.00	593.87	1.22	0.097	0.951	1.20	0.03885	9.0	0.832
160.00	593.52	1.57	0.153	1.125	14.53	0.12838	23.0	0.984
165.00	593.52	1.57	0.181	1.125	8.86	0.18295	30.9	0.984
169.00	593.92	1.17	0.203	0.925	5.64	0.21768	36.4	0.809
180.00	593.62	1.27	0.264	0.977	12.81	0.29663	49.9	0.855
195.00	593.82	1.27	0.348	0.977	18.68	0.41173	69.0	0.855
200.00	593.92	1.17	0.376	0.925	5.82	0.44762	75.1	0.809
203.00	593.77	1.32	0.392	1.002	3.61	0.46988	78.9	0.877
210.00	593.72	1.37	0.431	1.027	9.59	0.52896	88.3	0.899
215.00	593.82	1.27	0.459	0.977	6.64	0.56987	94.9	0.855
222.50	593.82	1.27	0.501	0.977	9.34	0.62742	104.5	0.855
227.50	594.12	0.97	0.529	0.817	5.04	0.65850	110.1	0.715
235.00	593.82	1.27	0.571	0.977	7.57	0.70512	118.6	0.855
237.00	593.62	1.47	0.582	1.077	2.82	0.72251	121.3	0.942
250.00	593.72	1.37	0.654	1.027	19.49	0.84258	139.8	0.899
255.00	593.87	1.22	0.582	0.951	6.43	0.88219	146.3	0.832
260.00	594.02	1.07	0.710	0.872	5.24	0.91448	152.1	0.763
265.00	594.22	0.87	0.738	0.760	3.98	0.93898	156.9	0.665
275.00	594.32	0.77	0.794	0.701	6.02	0.97610	165.2	0.613
285.00	594.77	0.32	0.849	0.392	3.01	0.99463	170.7	0.343
300.00	595.02	0.07	0.933	0.147	0.81	0.99961	173.7	0.129
311.50	595.07	0.02	0.997	0.071	0.06	1.00000	174.3	0.062
312.03	595.09	0.00	1.000	0.000	0.00	1.00000	174.3	0.000
Est. Total					162.30			

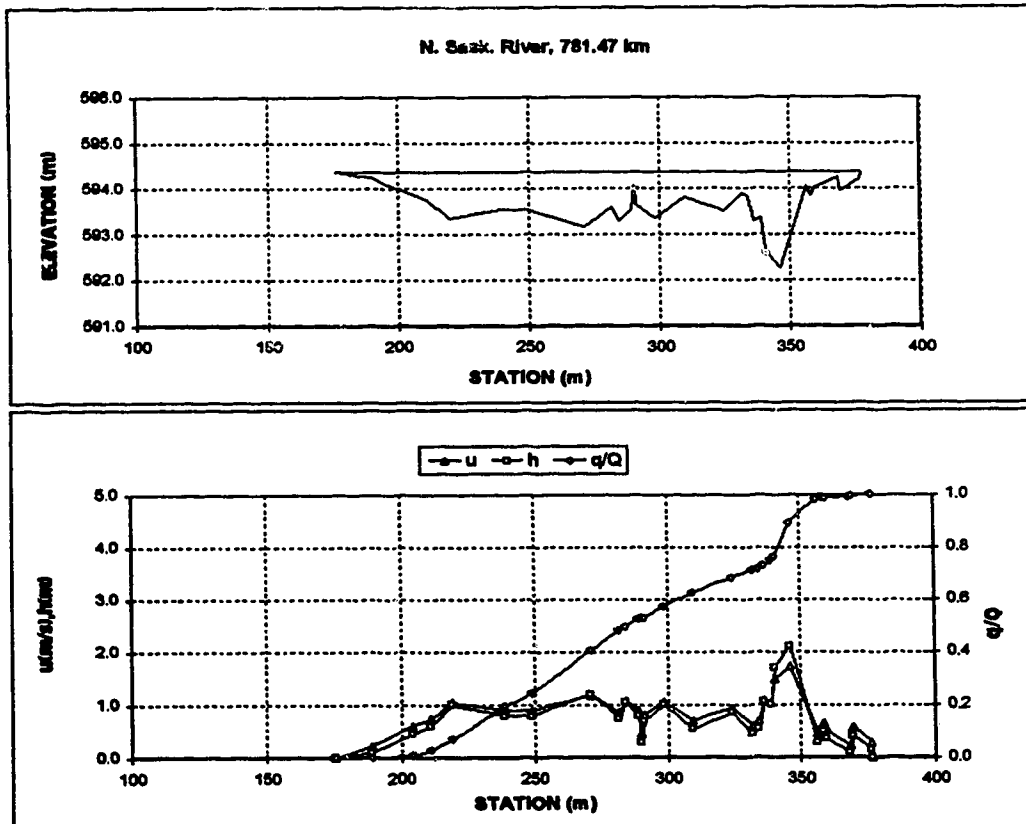


Appendix D.1 - North Saskatchewan River

X-SECTION N. Sask. River, 781.47 km HEC2 Section from Alta Env. Prot.
 DATE October 18, 1977
 DISCHARGE m^3/s 142.00
 WIDTH m 201.06
 MEAN DEPTH m 0.73
 AREA m^2 147.54
 MEAN VELOCITY m/s 0.962

Est. Water Surface Elev. 594.36
 LB 175.77 594.36
 RB 376.83 594.36

Sta. m	Elev. m	h m	w/W	u m/s	dq est. m^3	norm. q/Q	Area m^2	adjusted u m/s
175.77	594.36	0.00	0.000	0.000	0.00	0.00000	0.0	0.000
189.34	594.28	0.10	0.087	0.258	0.09	0.00055	0.7	0.227
204.34	593.91	0.45	0.142	0.696	1.98	0.01282	4.8	0.813
211.00	593.76	0.60	0.175	0.843	2.70	0.02856	8.4	0.742
219.34	593.36	1.00	0.217	1.184	6.78	0.07156	15.0	1.042
239.34	593.66	0.80	0.316	1.021	19.89	0.19480	33.1	0.898
249.34	593.66	0.80	0.386	1.021	8.19	0.24552	41.1	0.898
271.00	593.16	1.20	0.474	1.337	25.59	0.40406	62.8	1.177
281.84	593.61	0.75	0.528	0.978	12.28	0.48002	73.4	0.861
284.34	593.31	1.05	0.540	1.224	2.48	0.49540	75.6	1.077
289.00	593.66	0.80	0.563	1.021	4.85	0.52543	80.7	0.898
290.00	594.06	0.30	0.568	0.532	0.43	0.52808	80.5	0.468
291.00	593.66	0.70	0.573	0.934	0.37	0.53036	81.0	0.822
296.34	593.36	1.00	0.610	1.184	6.62	0.57140	87.3	1.042
309.34	593.61	0.55	0.684	0.796	8.46	0.62382	95.8	0.700
324.34	593.51	0.85	0.739	1.063	9.78	0.68444	106.3	0.935
331.84	593.91	0.45	0.776	0.696	4.30	0.71109	111.2	0.613
334.34	593.61	0.55	0.769	0.796	0.94	0.71689	112.5	0.700
336.50	593.31	1.05	0.799	1.224	1.75	0.72772	114.2	1.077
339.00	593.36	1.00	0.812	1.184	3.09	0.74687	116.8	1.042
340.50	592.66	1.70	0.819	1.687	2.91	0.78491	118.8	1.484
346.34	592.26	2.10	0.848	1.942	20.15	0.88976	129.9	1.708
356.50	594.06	0.30	0.899	0.532	15.10	0.98334	142.1	0.468
358.34	593.66	0.50	0.908	0.747	0.47	0.98627	142.9	0.657
359.34	594.01	0.35	0.915	0.589	0.29	0.98803	143.3	0.519
368.50	594.26	0.10	0.959	0.258	0.88	0.99349	145.4	0.227
369.34	593.96	0.40	0.963	0.644	0.10	0.99408	145.6	0.567
376.34	594.21	0.15	0.988	0.336	0.95	0.99996	147.5	0.296
376.83	594.36	0.00	1.000	0.000	0.01	1.00000	147.5	0.000
Est. Total					161.39			

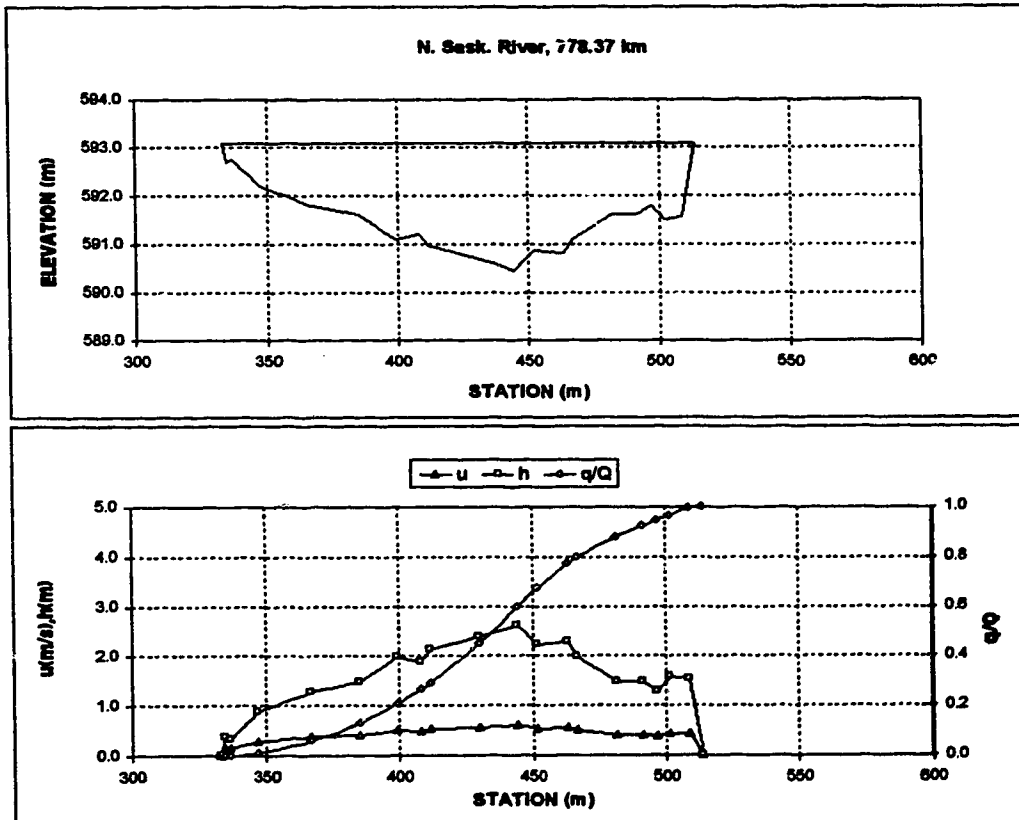


Appendix D.1 - North Saskatchewan River

X-SECTION N. Sask. River, 778.37 km
 DATE October 18, 1977
 DISCHARGE m^3/s 142.00
 WIDTH m 180.36
 MEAN DEPTH m 1.66
 AREA m^2 300.04
 MEAN VELOCITY m/s 0.473

HEC2 Section from Alta Env. Prot.
 Est. Water Surface Elev. 593.09
 LB 333.33 593.09
 RB 513.68 593.09

Sta. m	Elev. m	h m	w/W	u m/s	dq est. m^3	norm. q/Q	Area m^2	adjusted u m/s
333.33	593.09	0.00	0.000	0.000	0.00	0.00000	0.0	0.000
334.57	592.71	0.38	0.007	0.175	0.02	0.00014	0.2	0.165
336.77	592.76	0.33	0.019	0.159	0.13	0.00099	1.0	0.150
346.77	592.21	0.88	0.075	0.308	1.40	0.01028	7.0	0.290
366.74	591.81	1.28	0.185	0.396	7.56	0.06036	28.5	0.373
385.00	591.81	1.48	0.287	0.437	10.48	0.12962	53.6	0.411
399.00	591.11	1.98	0.384	0.531	11.88	0.20698	77.7	0.499
408.00	591.21	1.88	0.414	0.513	9.04	0.26682	95.1	0.482
411.77	590.96	2.13	0.435	0.557	4.03	0.29353	102.6	0.524
430.00	590.71	2.38	0.536	0.600	28.74	0.45070	143.6	0.584
444.27	590.46	2.63	0.615	0.642	22.15	0.59737	179.3	0.603
451.77	590.86	2.23	0.657	0.575	11.06	0.67061	187.5	0.540
463.50	590.81	2.28	0.722	0.583	15.28	0.77177	223.9	0.548
468.77	591.11	1.98	0.740	0.531	3.87	0.79740	230.8	0.499
481.77	591.61	1.48	0.823	0.437	12.52	0.88028	256.7	0.411
491.77	591.61	1.48	0.878	0.437	6.44	0.92294	271.4	0.411
496.77	591.81	1.28	0.906	0.396	2.86	0.94191	278.3	0.373
501.77	591.51	1.58	0.934	0.456	3.04	0.96202	285.4	0.429
508.77	591.56	1.53	0.973	0.447	4.90	0.99448	290.3	0.420
513.68	593.09	0.00	1.000	0.000	0.84	1.00000	300.0	0.000
Est. Total					151.01			

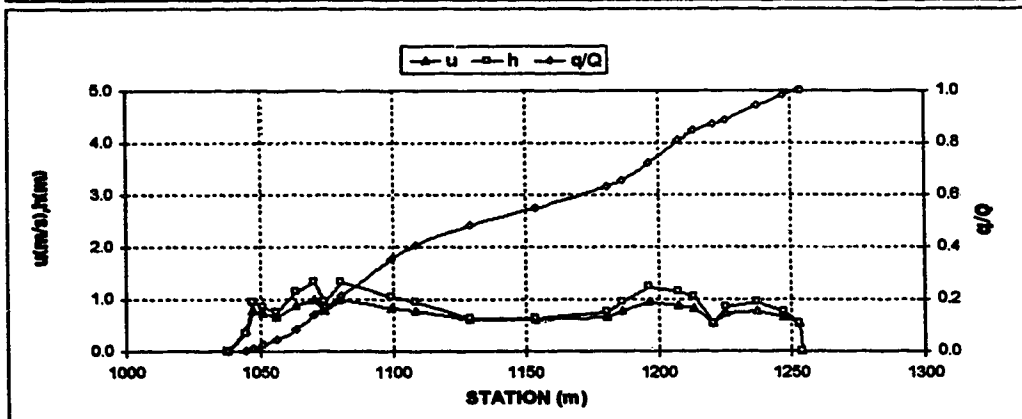
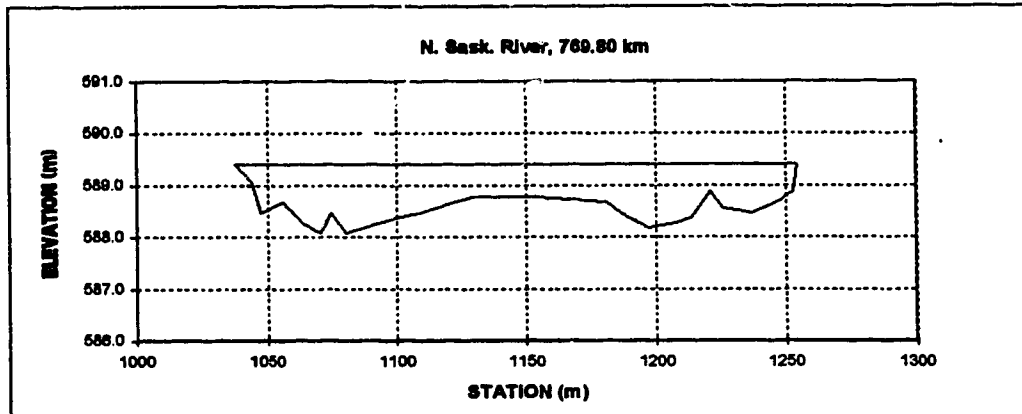


Appendix D.1 - North Saskatchewan River

X-SECTION N. Sask. River, 769.80 km HEC2 Section from Alta Env. Prot.
 DATE October 18, 1977
 DISCHARGE m^3/s 142.00
 WIDTH m 216.19
 MEAN DEPTH m 0.66
 AREA m^2 186.40
 MEAN VELOCITY m/s 0.762

Est. Water Surface Elev. 589.41
 LB 1037.94 589.41
 RB 1254.14 589.41

Sta. m	Elev. m	h m	w/W	u m/s	dq est. m^3	norm. q/Q	Area m^2	adjusted u m/s
1037.94	589.41	0.00	0.000	0.000	0.00	0.00000	0.0	0.000
1044.53	589.07	0.34	0.030	0.410	0.23	0.00155	1.1	0.393
1047.56	588.47	0.94	0.044	0.807	1.18	0.00953	3.1	0.775
1051.19	588.57	0.84	0.061	0.749	2.51	0.02652	6.3	0.719
1056.25	588.67	0.74	0.085	0.688	2.87	0.04594	10.3	0.661
1063.49	588.27	1.14	0.118	0.918	5.48	0.08289	17.1	0.681
1070.72	588.07	1.34	0.152	1.022	8.70	0.14170	28.1	0.962
1074.34	588.47	0.94	0.168	0.807	3.77	0.16723	30.2	0.775
1080.62	588.07	1.34	0.197	1.022	6.55	0.21151	37.3	0.982
1099.45	588.37	1.04	0.285	0.863	21.13	0.35438	59.8	0.829
1108.45	588.47	0.94	0.328	0.807	7.44	0.40470	68.7	0.775
1128.92	588.77	0.64	0.421	0.624	11.57	0.48297	84.8	0.600
1153.87	588.77	0.64	0.536	0.624	9.97	0.55041	100.8	0.600
1180.65	588.67	0.74	0.660	0.688	12.13	0.63241	119.3	0.661
1186.51	588.47	0.94	0.687	0.807	3.68	0.65729	124.2	0.775
1196.76	588.17	1.24	0.735	0.971	9.93	0.72445	135.4	0.932
1207.74	588.27	1.14	0.785	0.918	12.34	0.80789	148.4	0.881
1213.43	588.37	1.04	0.812	0.863	5.52	0.84524	154.6	0.829
1220.75	588.67	0.54	0.816	0.558	4.11	0.87302	160.4	0.535
1225.63	588.57	0.84	0.838	0.749	2.20	0.88789	163.8	0.719
1237.02	588.47	0.94	0.821	0.807	7.89	0.94122	173.9	0.775
1247.06	588.67	0.74	0.867	0.688	6.30	0.96185	182.4	0.661
1252.80	588.67	0.54	0.894	0.558	2.29	0.99132	186.0	0.535
1254.14	589.41	0.00	1.000	0.000	0.10	1.00000	186.4	0.000
Est. Total					147.88			

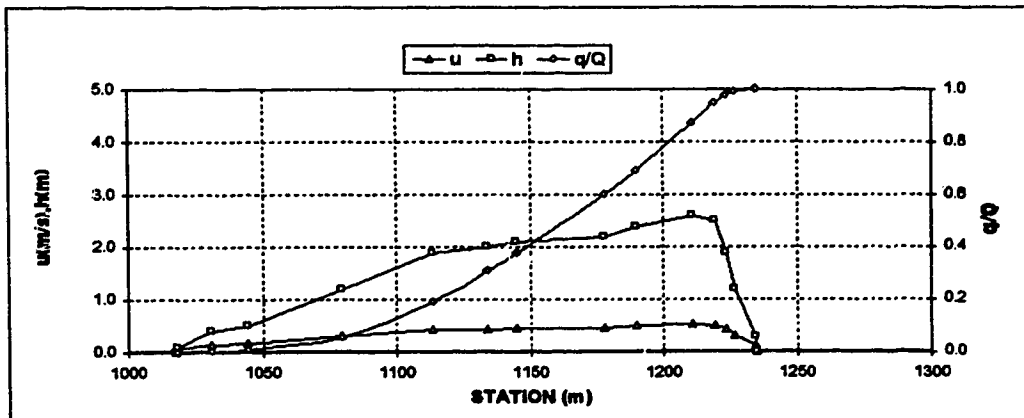
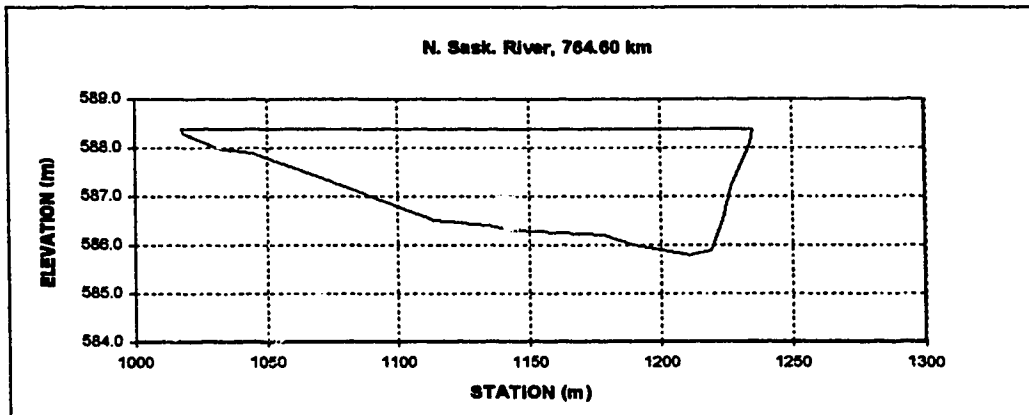


Appendix D.1 - North Saskatchewan River

X-SECTION N. Sask. River, 764.60 km HEC2 Section from Alta Env. Prot.
 DATE October 18, 1977
 DISCHARGE m^3/s 142.00
 WIDTH m 217.12
 MEAN DEPTH m 1.59
 AREA m^2 344.44
 MEAN VELOCITY m/s 0.412

Est Water Surface Elev. 588.39
 LP 1017.87 588.39
 R/B 1234.99 588.39

Sta. m	Elev. m	h m	w/W	u m/s	dq est. m^3	norm. q/Q	Area m^2	adjusted u m/s
1017.87	588.39	0.00	0.000	0.000	0.00	0.00000	0.0	0.000
1018.10	588.30	0.09	0.001	0.081	0.00	0.00000	0.0	0.054
1030.63	588.00	0.39	0.059	0.162	0.33	0.00211	3.0	0.144
1044.42	587.90	0.49	0.122	0.188	1.06	0.00579	9.1	0.168
1079.62	587.20	1.19	0.284	0.340	7.81	0.05794	38.7	0.304
1113.65	586.50	1.89	0.441	0.483	21.06	0.19039	91.1	0.414
1134.10	586.40	1.99	0.535	0.480	18.70	0.30803	130.7	0.428
1144.70	586.30	2.09	0.584	0.495	10.54	0.37433	152.4	0.443
1177.98	586.20	2.19	0.737	0.511	35.85	0.59980	223.6	0.457
1189.90	586.00	2.39	0.792	0.542	14.37	0.69019	260.9	0.484
1210.92	585.80	2.59	0.889	0.572	29.14	0.87348	303.2	0.511
1219.39	585.90	2.49	0.928	0.557	12.14	0.94884	321.7	0.497
1223.59	586.50	1.89	0.948	0.463	4.69	0.97935	333.9	0.414
1226.79	587.20	1.19	0.962	0.340	1.98	0.99181	338.9	0.304
1234.19	588.10	0.29	0.996	0.133	1.30	0.99995	344.3	0.119
1234.99	588.39	0.00	1.000	0.000	0.01	1.00000	344.4	0.000
Est. Total					158.99			



Appendix D.1 - North Saskatchewan River

X-SECTION N. Sask. River, 784.6 km (ARC Section 4)

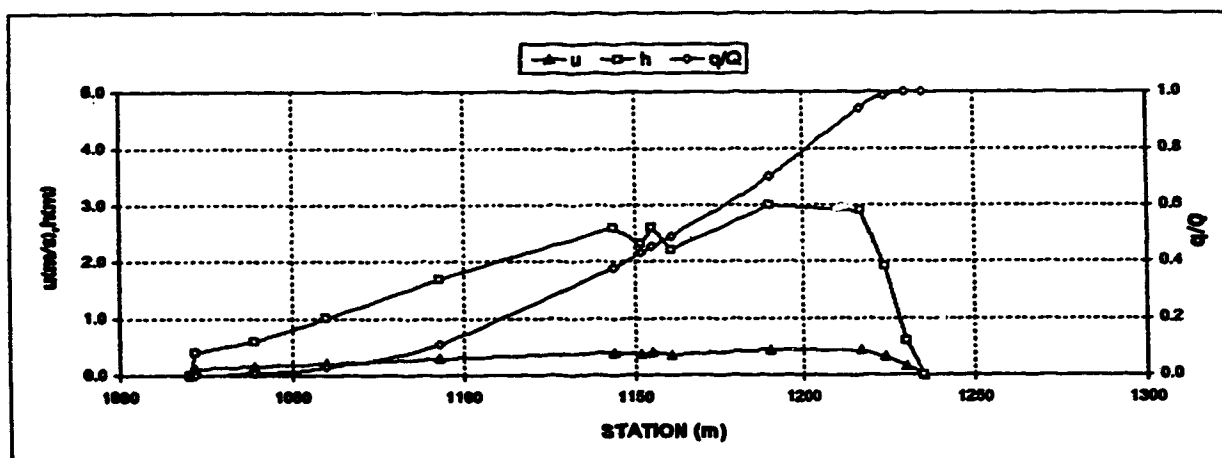
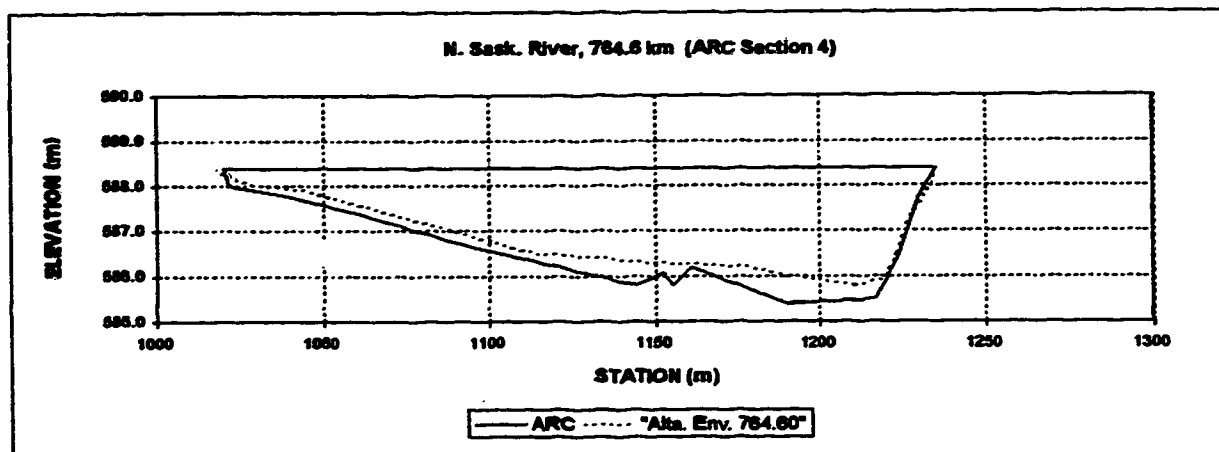
HEC2 Section from Alta Env. Prot.

DATE October 18, 1977

DISCHARGE m^3/s	142		99.8
WIDTH m	215	Est. Water Surface Elev.	588.39
MEAN DEPTH m	1.87	LB	488.59
AREA m^2	402.1	RB	1020
MEAN VELOCITY m/s	0.353		

Water's Edge	Assumed Elev	Est. Sta.	Est. Geod.	h	w/W	u	dq est.	norm. q/Q	Area	adj. u
m	m	m	m	m		m/s	m^3		m^2	m/s
0	99.8	1020	588.39	0.00	0.000	0.000	0.00	0.00000	0.0	0.000
2	99.4	1022	587.99	0.40	0.009	0.128	0.03	0.00016	0.4	0.114
19	99.2	1039	587.79	0.60	0.068	0.185	1.24	0.00805	8.9	0.150
40	98.8	1080	587.39	1.00	0.186	0.233	3.34	0.02933	25.7	0.210
73	98.1	1093	586.89	1.70	0.340	0.331	12.56	0.10829	70.3	0.300
124	97.2	1144	585.79	2.60	0.577	0.440	42.29	0.37845	179.9	0.368
132	97.5	1152	586.09	2.30	0.614	0.405	8.26	0.43118	199.5	0.368
135	97.2	1155	585.79	2.80	0.628	0.440	3.11	0.45095	208.9	0.368
141	97.6	1161	586.19	2.20	0.656	0.394	6.00	0.46915	221.3	0.356
170	96.8	1190	585.39	3.00	0.791	0.484	33.06	0.69973	296.7	0.437
197	96.9	1217	585.49	2.90	0.916	0.473	38.12	0.94236	376.3	0.428
204	97.9	1224	586.49	1.80	0.949	0.357	6.97	0.98574	383.1	0.323
210	99.2	1230	587.79	0.60	0.977	0.165	1.96	0.99921	400.6	0.150
215	99.8	1235	588.39	0.00	1.000	0.000	0.12	1.00000	402.1	0.000
		1020	588.39							

157.11



Appendix D.2 Peace River

X-SECTION

DATE

SHAFTESBURY FERRY, 0.0 km downstream

DISCHARGE m^3/s

1740

WIDTH m

388.5

Ice Bottom Elev.

320.80

MEAN DEPTH m

5.33

AREA m^2

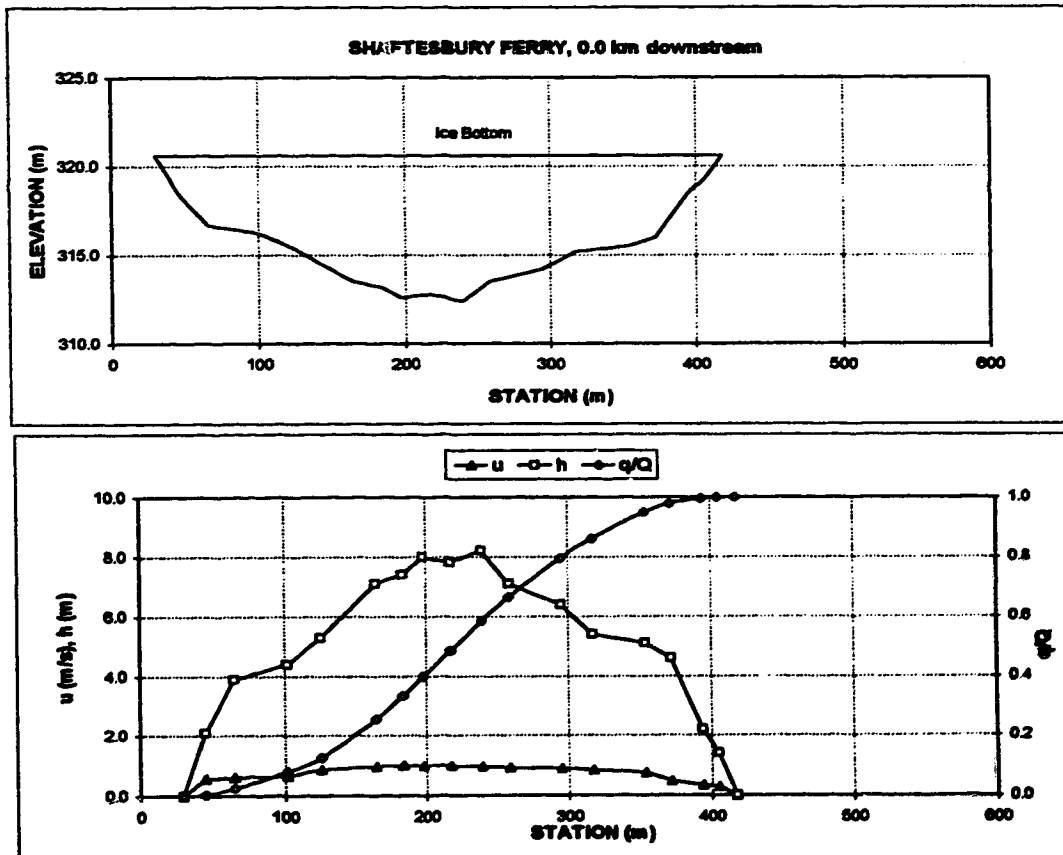
2072.1

MEAN VELOCITY m/s

0.840

Sta. m	Elev. m	h m	w/W	u m/s	dq m ³	q/Q	area m ²
29.8	320.80	0.00	0.00	0.000	0.00	0.00000	0.0
45.2	318.50	2.10	0.04	0.567	8.70	0.00500	16.2
65.4	316.70	3.90	0.09	0.615	34.80	0.02500	76.7
101.9	316.20	4.40	0.19	0.849	95.70	0.08000	228.4
126.0	315.30	5.30	0.25	0.858	78.30	0.12500	345.0
164.4	313.50	7.10	0.35	0.967	228.20	0.25500	583.4
183.7	313.20	7.40	0.40	1.000	139.20	0.33500	722.8
188.1	312.60	8.00	0.43	0.982	111.36	0.38900	833.9
217.3	312.80	7.80	0.48	0.984	149.64	0.48500	885.8
239.4	312.40	8.20	0.54	0.967	174.00	0.58500	1162.7
258.7	313.50	7.10	0.59	0.828	139.20	0.63500	1309.9
295.2	314.20	6.40	0.68	0.900	228.20	0.79500	1558.5
317.3	315.20	5.40	0.74	0.837	113.10	0.86000	1687.0
353.8	315.50	5.10	0.83	0.745	158.60	0.95000	1878.8
372.1	316.00	4.60	0.88	0.478	52.20	0.98000	1967.4
394.2	318.40	2.20	0.94	0.345	26.10	0.99500	2042.6
405.8	319.20	1.40	0.97	0.295	6.96	0.99900	2063.4
418.3	320.80	0.00	1.00	0.000	1.74	1.00000	2072.1
29.8	320.80						

Total flow 1740.00



Appendix D.2 Peace River

X-SECTION

MACKENZIE CAIRN, 8300 m downstream

DATE

Feb 27, 1993

DISCHARGE m^3/s

1740

WIDTH m

317.307692

Ice Bottom Elev.

318.00

MEAN DEPTH m

5.94

AREA m^2

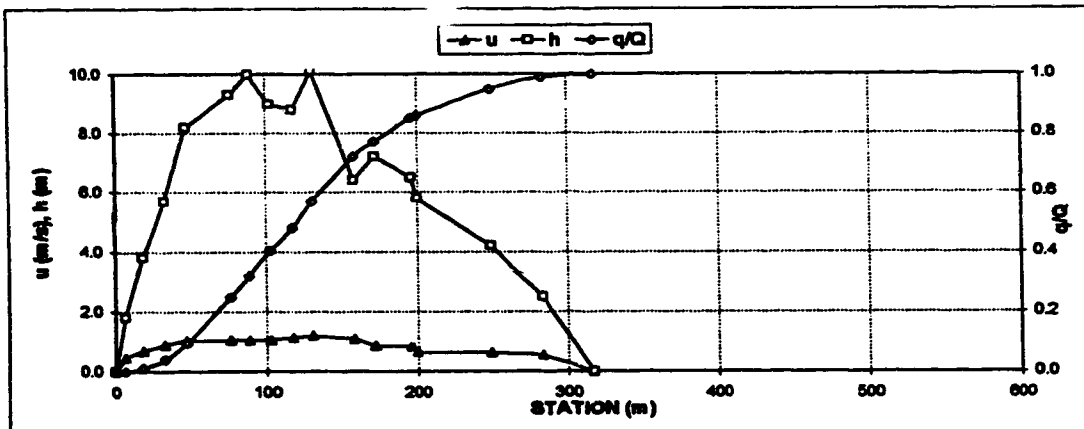
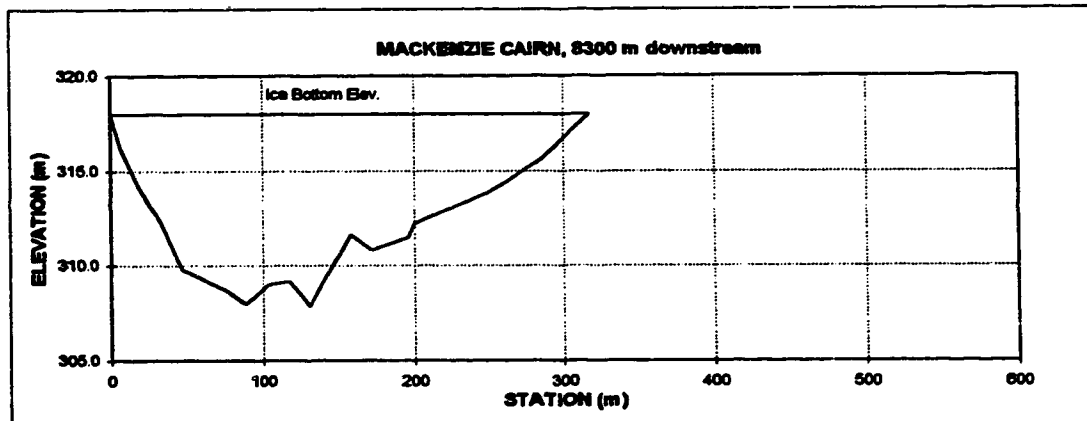
1884.5

MEAN VELOCITY m/s

0.923

Sta. m	Elev. m	h m	w/W	u m/s	dq m ³	q/Q	area m ²
0.0	318.00	0.00	0.000	0.000	0.00	0.00000	0.0
6.7	316.20	1.80	0.021	0.454	1.74	0.00100	6.1
18.3	314.20	3.80	0.058	0.673	15.86	0.01000	38.4
32.7	312.30	5.70	0.103	0.876	52.20	0.04000	106.9
47.1	309.80	8.20	0.148	1.021	95.70	0.09500	207.1
76.0	308.70	6.30	0.239	1.050	284.48	0.24700	459.5
88.5	308.00	10.00	0.279	1.054	127.02	0.32000	580.1
102.9	309.00	9.00	0.324	1.058	144.42	0.40300	717.2
117.3	309.20	8.80	0.370	1.137	135.72	0.48100	845.5
130.8	307.90	10.10	0.412	1.180	154.86	0.57000	972.7
157.7	311.80	6.40	0.497	1.087	281.00	0.72000	1194.9
172.1	310.80	7.20	0.542	0.861	87.00	0.77000	1292.9
196.2	311.50	6.50	0.616	0.832	139.20	0.85000	1457.6
200.0	312.20	5.80	0.630	0.847	17.40	0.86000	1481.3
249.0	313.80	4.20	0.785	0.828	156.60	0.95000	1728.4
283.7	315.50	2.50	0.894	0.551	69.60	0.99000	1842.4
317.3	318.00	0.00	1.000	0.000	17.40	1.00000	1884.5
0	318.00						

Total flow 1740.00



Appendix D.2 Peace River

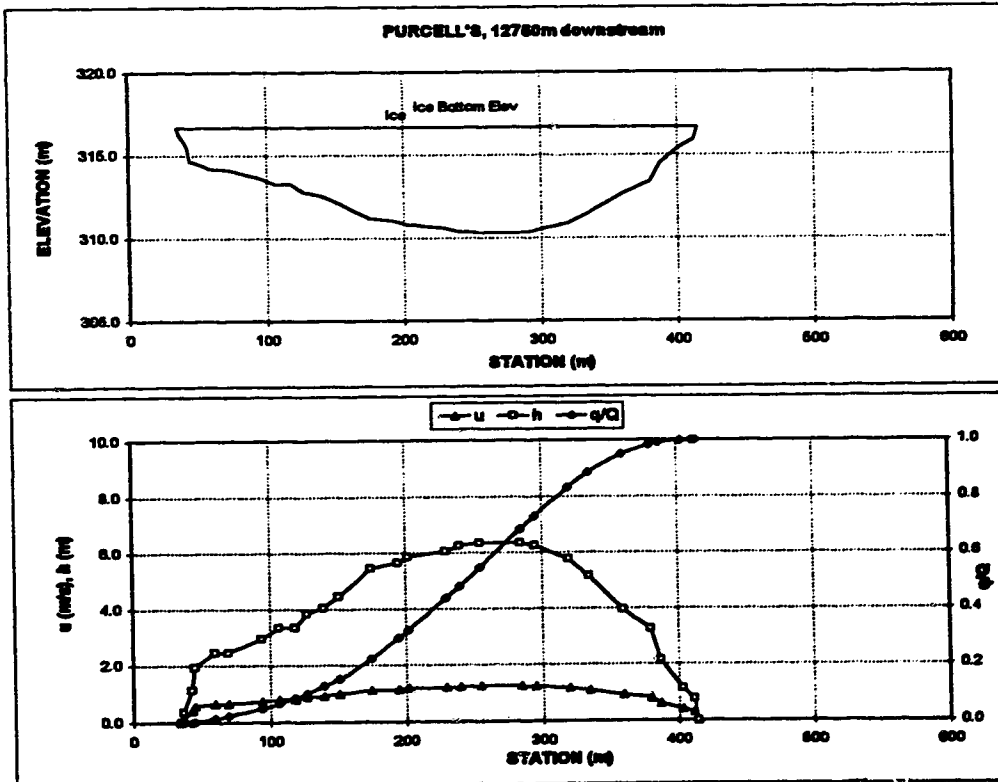
X-SECTION
DATE
DISCHARGE m^3/s
WIDTH m
MEAN DEPTH m
AREA m^2
MEAN VELOCITY m/s

PURCELL'S, 12750m downstream
Feb 27, 1993
1740
380
4.38
1656.8
1.050

HEC2 Section from Alberta Env.
Ice Bottom Elev
316.85

Sta.	Elev.	h	w/W	u	dq	q/Q	area	adj. u
m	m	m		m/s	m^3		m^2	m/s
35	316.65	0.00	0.000	0.000	0.00	0.00000	0.0	0.000
37	316.3	0.35	0.005	0.185	0.03	0.00002	0.3	0.180
43	315.52	1.13	0.021	0.427	1.38	0.00075	4.8	0.363
45	314.7	1.95	0.028	0.614	1.60	0.00180	7.8	0.585
60	314.2	2.45	0.068	0.715	21.83	0.01319	40.8	0.868
70	314.2	2.45	0.082	0.715	17.52	0.02245	65.4	0.868
84	313.7	2.95	0.155	0.809	49.39	0.04856	130.2	0.744
107	313.3	3.35	0.189	0.881	34.81	0.06686	171.1	0.810
118	313.3	3.35	0.218	0.881	32.46	0.06402	208.0	0.810
127	312.8	3.85	0.242	0.967	29.83	0.06684	240.4	0.889
140	312.8	4.05	0.278	1.006	50.49	0.12853	291.7	0.928
151	312.2	4.45	0.305	1.065	48.28	0.15204	338.5	0.979
175	311.2	5.45	0.368	1.219	135.83	0.22375	457.3	1.121
195	311	5.85	0.421	1.248	136.83	0.29813	568.3	1.148
202	310.8	5.85	0.439	1.278	80.84	0.32301	608.5	1.175
230	310.6	6.05	0.513	1.307	215.28	0.43662	775.1	1.202
240	310.4	6.25	0.539	1.335	81.24	0.47977	838.6	1.228
255	310.3	6.35	0.579	1.350	126.88	0.54684	931.1	1.241
285	310.3	6.35	0.658	1.350	257.09	0.88275	1121.8	1.241
295	310.4	6.25	0.684	1.335	84.57	0.72746	1184.6	1.228
320	310.9	5.75	0.750	1.283	184.88	0.83049	1334.9	1.162
335	311.5	5.15	0.789	1.174	99.60	0.88315	1416.4	1.080
360	312.7	3.95	0.855	0.983	122.87	0.94800	1530.1	0.904
380	313.4	3.25	0.908	0.863	66.48	0.96314	1602.1	0.794
387	314.5	2.15	0.828	0.655	14.35	0.99073	1621.0	0.603
403	315.522	1.13	0.868	0.426	14.18	0.99823	1647.2	0.382
412	315.9	0.75	0.962	0.325	3.17	0.99990	1655.7	0.289
415	316.85	0.00	1.000	0.000	0.18	1.00000	1656.8	0.000
35	316.7							

Est. flow 1881.53



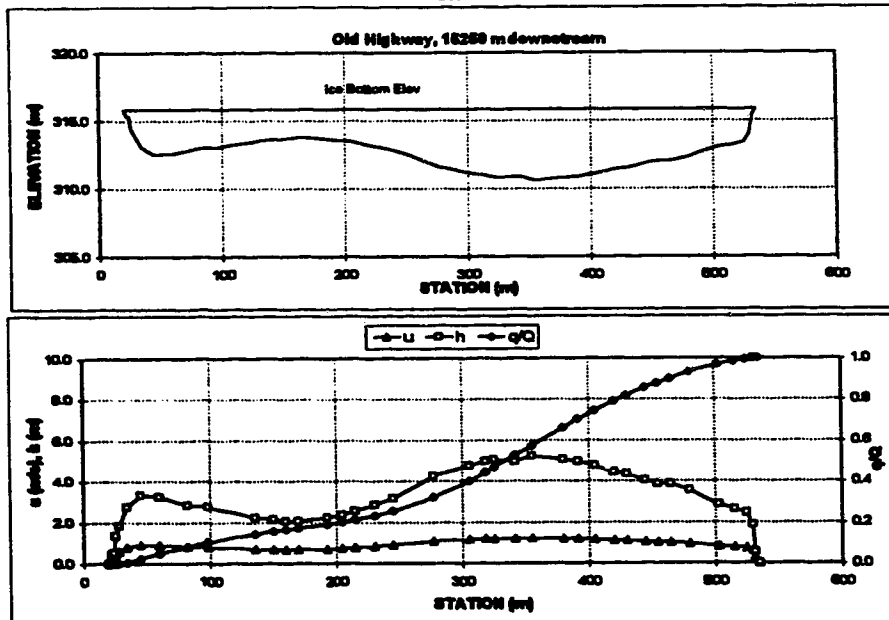
Appendix D.2 Peace River

X-SECTION
DATE Old Highway, 18250 m downstream
Feb 27, 1993
DISCHARGE m^3/s 1740
WIDTH m 515
MEAN DEPTH m 3.43
AREA m^2 1768.4
MEAN VELOCITY m/s 0.985

HEC2 Section from Alberta Env.
Ice Bottom Elev 315.84

Sta.	Elev.	h	w/W	U	dq	q/Q	area	adj. u
m	m	m		m/s	m^2		m^2	m/s
20	315.84	0.00	0.000	0.000	0.00	0.00000	0.0	0.000
22	315.4	0.44	0.004	0.250	0.06	0.00003	0.4	0.237
24	315.3	0.52	0.006	0.279	0.25	0.00017	1.4	0.284
26	314.5	1.34	0.010	0.528	0.37	0.00037	2.3	0.487
28	314.0	1.84	0.016	0.650	2.81	0.00189	7.1	0.615
34	313.1	2.74	0.027	0.848	10.29	0.00749	20.8	0.802
46	312.5	3.34	0.049	0.988	30.36	0.02388	54.3	0.915
60	312.6	3.24	0.078	0.948	47.28	0.04886	103.6	0.886
82	313.0	2.84	0.120	0.869	60.76	0.06288	170.5	0.821
86	313.1	2.74	0.151	0.848	38.32	0.10347	215.1	0.802
138	313.8	2.24	0.225	0.741	75.20	0.14432	309.8	0.701
160	313.7	2.14	0.252	0.719	22.39	0.15648	340.4	0.680
160	313.8	2.04	0.272	0.697	14.79	0.16451	361.3	0.658
170	313.8	2.04	0.291	0.697	14.21	0.17223	381.7	0.658
182	313.8	2.24	0.334	0.741	33.85	0.19082	428.8	0.701
205	313.5	2.34	0.359	0.763	22.40	0.20278	458.6	0.721
215	313.3	2.64	0.379	0.808	19.15	0.21318	483.0	0.762
230	313.0	2.84	0.408	0.869	33.79	0.23154	523.3	0.821
245	312.7	3.14	0.437	0.829	40.30	0.25343	568.2	0.878
277	311.6	4.24	0.499	1.135	121.83	0.31980	689.3	1.072
306	311.1	4.74	0.553	1.222	148.17	0.40006	812.0	1.155
318	310.9	4.94	0.579	1.256	77.98	0.44244	874.9	1.188
325	310.8	5.04	0.592	1.273	44.18	0.46644	909.8	1.203
342	310.9	4.94	0.625	1.256	107.31	0.52472	994.7	1.188
366	310.8	5.24	0.650	1.307	84.81	0.57079	1080.8	1.235
380	310.8	5.04	0.699	1.273	165.78	0.69084	1189.3	1.203
382	310.9	4.94	0.722	1.256	75.75	0.70188	1249.2	1.188
405	311.1	4.74	0.748	1.222	77.98	0.74434	1312.1	1.155
420	311.4	4.44	0.777	1.170	82.26	0.78907	1381.0	1.108
430	311.5	4.34	0.798	1.153	50.98	0.81676	1424.9	1.089
445	311.8	4.04	0.825	1.099	70.75	0.85519	1487.7	1.038
456	312.0	3.84	0.845	1.062	42.57	0.87831	1527.1	1.004
465	312.0	3.84	0.864	1.062	40.79	0.90047	1565.5	1.004
480	312.3	3.54	0.893	1.006	57.24	0.93156	1620.9	0.951
503	313.0	2.84	0.938	0.869	68.77	0.98591	1694.2	0.821
515	313.2	2.64	0.961	0.827	27.88	0.98405	1727.1	0.782
525	313.4	2.44	0.961	0.785	20.48	0.99518	1752.5	0.742
530	314.0	1.84	0.990	0.650	7.88	0.99935	1763.2	0.615
532	315.3	0.52	0.994	0.279	1.09	0.99994	1765.6	0.284
535	315.84	0.00	1.000	0.000	0.11	1.00000	1768.4	0.000
20	315.84							

Est. flow 1841.07

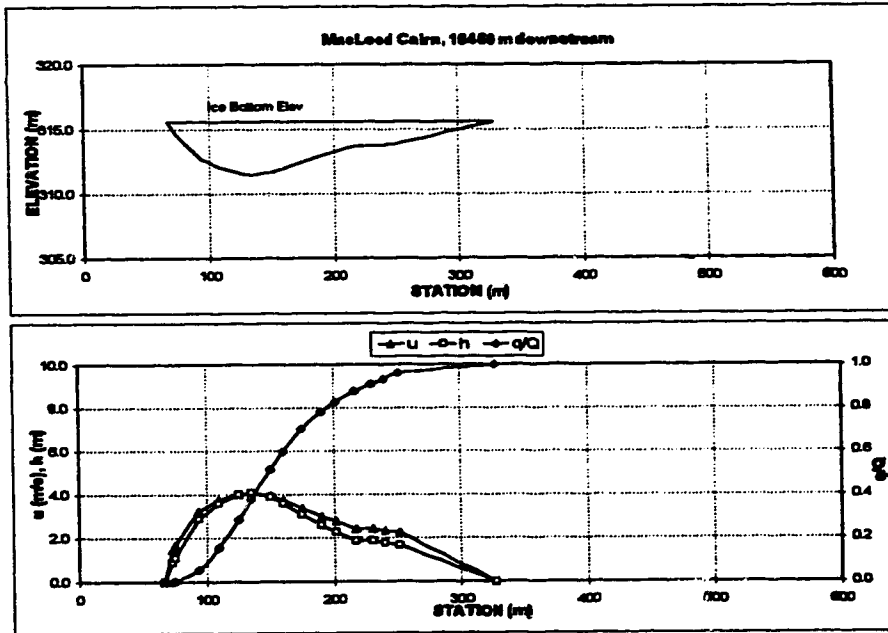


Appendix D.2 Peace River

X-SECTION MacLeod Cairn, 18450 m d 18450m Section truncated at Sta. 327
 DATE Feb 27, 1993
 DISCHARGE m^3/s 1740
 WIDTH m 280
 MEAN DEPTH m 2.18
 AREA m^2 567.4
 MEAN VELOCITY m/s 3.067
 HEC2 Section from Alberta Env.
 Ice Bottom Elev 315.58

Sta.	Elev.	h	wtW	u	dq	q/Q	area	adj. u
m	m	m		m/s	m^3		m^2	m/s
67.0	315.58	0.00	0.000	0.000	0.00	0.00000	0.0	0.000
73.0	314.70	0.88	0.023	1.673	2.21	0.00111	2.6	1.482
75.0	314.50	1.08	0.031	1.918	3.52	0.00288	4.6	1.876
94.0	312.70	2.88	0.104	3.690	105.50	0.05586	42.2	3.225
110.0	312.00	3.58	0.165	4.287	205.61	0.15912	83.9	3.728
125.0	311.60	3.98	0.223	4.579	250.78	0.28506	150.6	4.001
135.0	311.50	4.08	0.282	4.655	186.08	0.37851	180.9	4.068
150.0	311.70	3.88	0.319	4.502	273.35	0.51578	250.6	3.934
160.0	312.00	3.58	0.358	4.287	163.54	0.59791	287.9	3.728
175.0	312.50	3.08	0.415	3.859	202.95	0.69063	337.8	3.372
190.0	313.00	2.58	0.473	3.429	154.70	0.77782	380.3	2.997
202	313.3	2.28	0.519	3.158	96.04	0.82575	409.5	2.759
218	313.7	1.88	0.581	2.771	98.76	0.87535	442.7	2.428
230	313.7	1.88	0.627	2.771	62.64	0.90681	465.3	2.428
240	313.8	1.78	0.685	2.677	49.90	0.93187	483.6	2.339
252	313.9	1.68	0.712	2.576	54.53	0.95625	504.4	2.251
327	315.58	0.00	1.000	0.000	81.14	1.00000	567.4	0.000
67.0	315.58							

Est. flow 1991.23781



Appendix D.2 Peace River

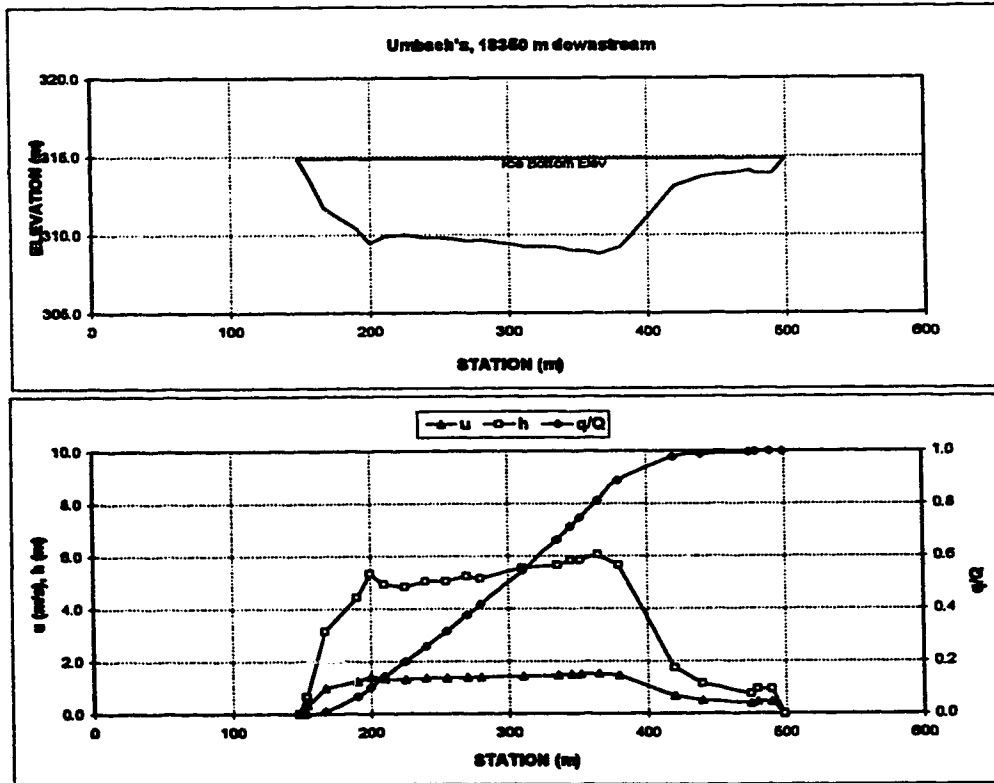
X-SECTION
DATE
Discharge m^3/s
WIDTH m
MEAN DEPTH m
AREA m^2
MEAN VELOCITY m/s

Umbach's, 18350 m downstream
Feb 27, 1983
1740
361
3.87
1357.8
1.282

HEC2 Section from Alberta Env.
Ice Bottom Elev 314.84

Sta.	Elev.	h	w/W	u	dq	q/Q	area	adj. u
m	m	m		m/s	m^3		m^2	m/s
148	314.84	0.00	0.000	0.000	0.00	0.00000	0.0	0.000
153	314.2	0.84	0.014	0.398	0.31	0.00016	1.8	0.341
167	311.7	3.14	0.054	1.115	19.88	0.01025	28.1	0.986
180	310.4	4.44	0.120	1.405	109.83	0.06805	115.2	1.242
200	309.5	5.34	0.148	1.589	73.20	0.10325	184.1	1.405
210	309.9	4.94	0.177	1.509	79.61	0.14369	215.5	1.334
225	310.0	4.84	0.219	1.488	109.90	0.19954	288.9	1.316
240	309.8	5.04	0.282	1.529	111.78	0.25833	363.0	1.352
255	309.8	5.04	0.305	1.529	115.58	0.31508	438.6	1.352
270	309.8	5.24	0.348	1.589	119.43	0.37574	515.7	1.387
280	309.7	5.14	0.378	1.549	80.82	0.41685	567.6	1.369
310	309.3	5.54	0.462	1.628	254.52	0.54817	727.8	1.440
335	309.2	5.64	0.533	1.648	228.94	0.66249	867.5	1.457
345	309.0	5.84	0.561	1.687	95.71	0.71112	924.9	1.491
362	309.0	5.84	0.581	1.687	68.95	0.74615	985.8	1.491
385	308.8	6.04	0.618	1.725	131.73	0.81308	1043.0	1.525
380	309.2	5.64	0.661	1.648	147.74	0.88815	1130.9	1.457
420	313.1	1.74	0.775	0.752	177.13	0.97815	1278.2	0.885
440	313.7	1.14	0.832	0.567	19.00	0.98780	1307.0	0.502
475	314.1	0.74	0.832	0.425	16.33	0.99610	1339.9	0.376
480	313.9	0.94	0.946	0.499	1.94	0.99708	1344.1	0.441
480	313.9	0.84	0.974	0.499	4.69	0.99948	1353.5	0.441
499	314.84	0.00	1.000	0.000	1.05	1.00000	1357.8	0.000
148	314.84							

Est. flow 1968.16



Appendix D.2 Peace River

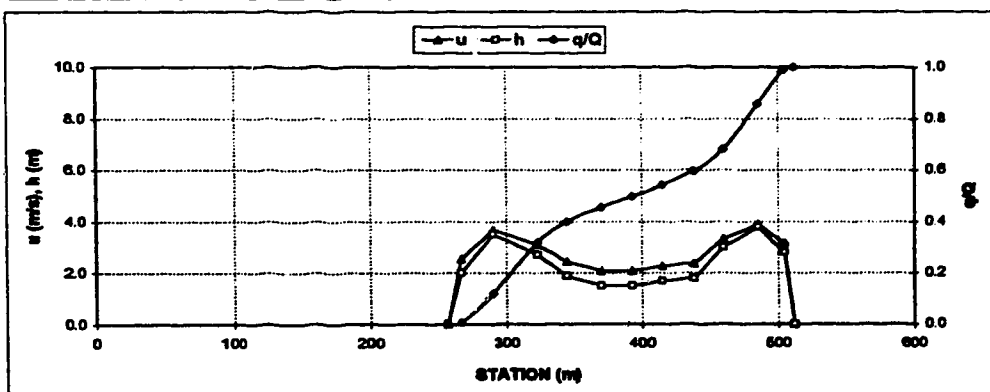
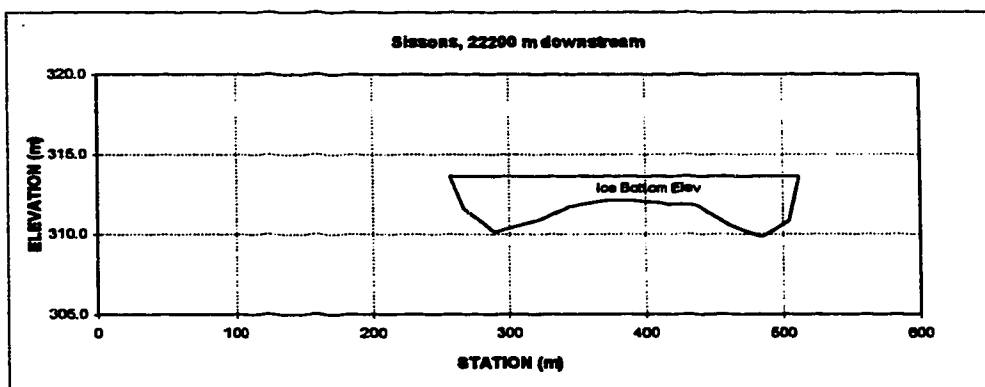
X-SECTION
DATE
DISCHARGE m^3/s
WIDTH m
MEAN DEPTH m
AREA m^2
MEAN VELOCITY m/s

Sissons, 22200 m downstream
Feb 27, 1993

truncated at Sta. 512m, i.e. just LBI
HEC2 Section from Alberta Env.
Ice Bottom Elev 313.00

Sta. m	Elev. m	h m	w/W	u m/s	dq m^3	q/Q	area m^2	adj. u m/s
257	313.6	0.00	0.000	0.000	0.00	0.00000	0.0	0.000
287	311.6	2.00	0.039	2.859	13.30	0.00728	10.0	2.534
290	310.1	3.50	0.129	3.863	208.27	0.12025	73.3	3.681
323	310.9	2.70	0.259	3.249	363.76	0.31947	175.6	3.086
345	311.7	1.90	0.345	2.570	147.22	0.40010	228.2	2.449
370	312.1	1.50	0.443	2.195	101.28	0.45556	288.7	2.082
393	312.1	1.50	0.533	2.195	75.73	0.48703	303.2	2.082
415	311.9	1.70	0.620	2.386	80.63	0.54119	338.4	2.274
438	311.8	1.80	0.710	2.479	97.91	0.59482	378.6	2.362
460	310.8	3.00	0.798	3.485	157.48	0.88105	431.4	3.321
485	309.8	3.80	0.894	4.081	321.55	0.85716	516.4	3.889
505	310.8	2.80	0.973	3.329	244.50	0.99107	582.4	3.172
512	313.6	0.00	1.000	0.000	16.31	1.00000	582.2	0.000
257	313.6							

Est. flow 1825.90



Appendix D.2 Peace River

X-SECTION

PEACE RIVER, 24800m downstream

DATE

Feb 18, 1993

DISCHARGE m^3/s

1740

WIDTH m

400

Ice Bottom Elev

312.88

MEAN DEPTH m

4.56

AREA m^2

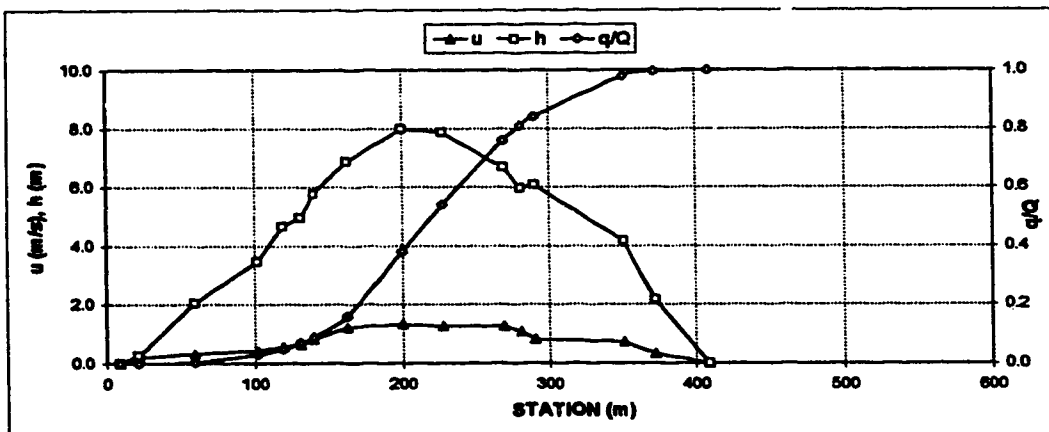
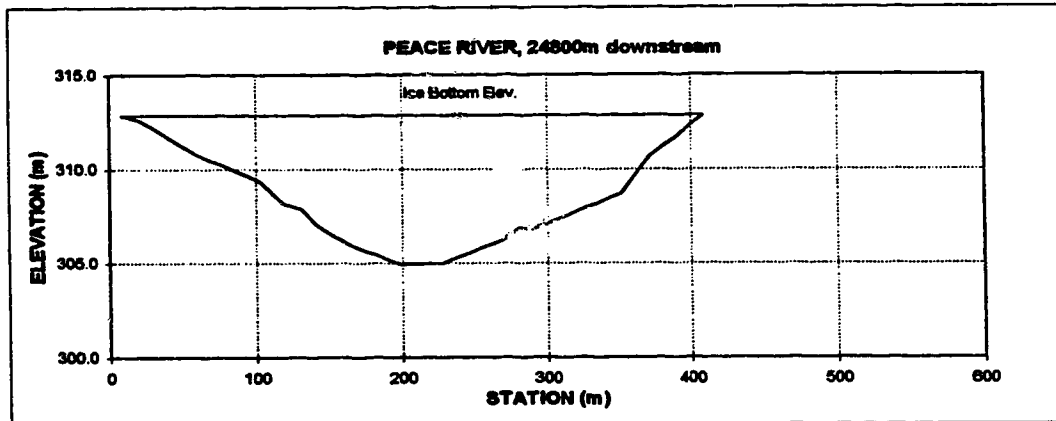
1824.9

MEAN VELOCITY m/s

0.953

Sta. m	Elev. m	h m	w/W	u m/s	dq m ³	q/Q	area m ²
8.7	312.88	0.00	0.00	0.000	0.00	0.00000	0.0
21.2	312.80	0.28	0.03	0.188	0.00	0.00000	1.8
59.8	310.80	2.08	0.13	0.323	8.70	0.00500	46.2
101.9	309.40	3.48	0.23	0.419	43.50	0.03000	163.0
119.2	308.20	4.68	0.28	0.533	34.80	0.05000	233.3
130.8	307.90	4.98	0.31	0.650	34.80	0.07000	288.8
140.4	307.10	5.78	0.33	0.820	34.80	0.09000	340.3
162.5	306.00	6.88	0.38	1.209	121.80	0.18000	479.9
200.0	304.90	7.98	0.48	1.327	382.80	0.38000	757.7
227.9	305.00	7.88	0.55	1.283	278.40	0.54000	878.3
289.2	306.20	6.68	0.65	1.280	379.32	0.75800	1278.5
280.8	306.90	5.98	0.68	1.093	90.48	0.81000	1351.3
290.4	306.80	6.68	0.70	0.805	52.20	0.84000	1409.1
351.0	308.70	4.18	0.88	0.717	243.60	0.98000	1718.8
372.1	310.70	2.18	0.91	0.327	28.10	0.99500	1785.5
408.7	312.88	0.00	1.00	0.700	8.70	1.00000	1824.9
8.7	312.88						

Total flow 1740.00



Appendix D.2 Peace River

X-SECTION

DATE

DISCHARGE m^3/s

WIDTH m

MEAN DEPTH m

AREA m^2

MEAN VELOCITY m/s

W.D. WOOD, 25500 m downstream

Feb 27, 1983

1740

366.3684

5.59

2041.0

0.853

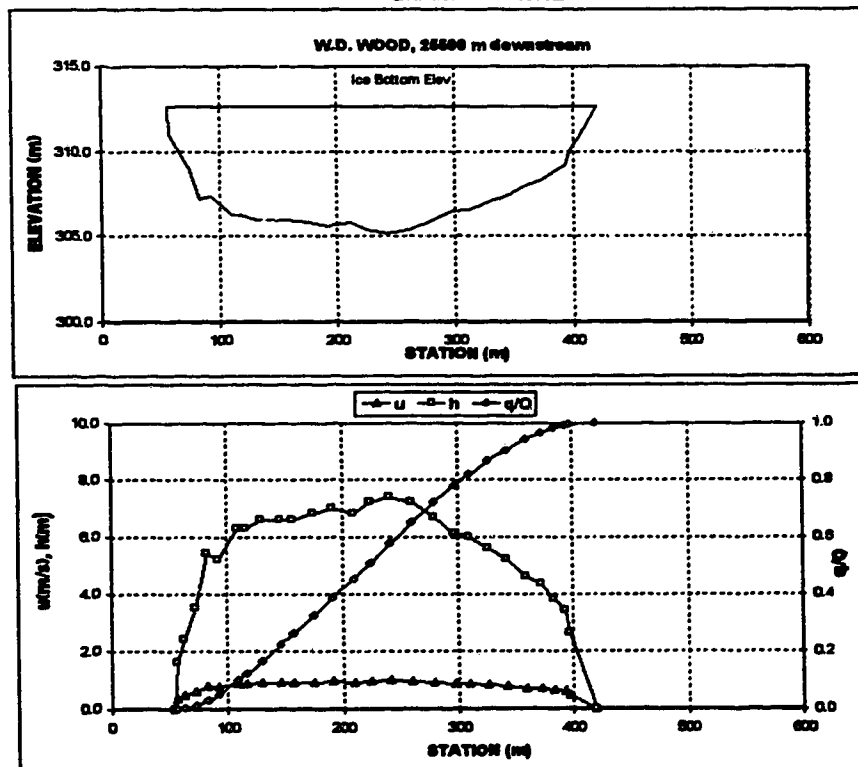
HEC2 Section from Alberta Env.

Ice Bottom Elev

312.61

Sta.	Elev.	h	w/W	u	dq	q/Q	area	adj. u
m	m	m		m/s	m^3		m^2	m/s
55.28	312.61	0.00	0.000	0.000	0.00	0.00000	9.0	0.000
57	311.0	1.61	0.005	0.372	0.26	0.00014	1.4	0.363
64	310.2	2.41	0.024	0.487	6.04	0.00343	18.6	0.462
73	309.1	3.51	0.049	0.825	14.81	0.01151	42.1	0.563
83	307.2	5.41	0.076	0.834	32.55	0.02927	86.7	0.782
92	307.4	5.21	0.101	0.814	39.38	0.05075	134.5	0.772
110	306.3	6.31	0.150	0.825	90.12	0.09991	236.2	0.878
117	306.3	6.31	0.189	0.925	40.84	0.12219	282.3	0.878
130	306.0	6.61	0.206	0.964	78.88	0.16621	366.3	0.906
147	306.0	6.61	0.251	0.964	107.17	0.22368	478.7	0.906
158	306.0	6.61	0.281	0.964	69.35	0.26150	561.4	0.906
175	305.8	6.81	0.328	0.973	109.89	0.32144	686.6	0.923
182	305.8	7.01	0.374	0.982	115.40	0.35439	782.9	0.941
210	305.8	6.81	0.423	0.973	122.19	0.45108	907.3	0.923
225	305.4	7.21	0.465	1.011	104.29	0.50783	1012.6	0.959
242	305.2	7.41	0.511	1.029	126.75	0.57707	1136.7	0.977
260	305.4	7.21	0.560	1.011	134.21	0.60628	1268.3	0.969
279	305.9	6.71	0.612	0.983	130.52	0.72146	1400.6	0.914
297	306.6	6.11	0.662	0.906	107.79	0.78627	1516.9	0.839
310	306.6	6.01	0.697	0.895	70.91	0.81896	1594.7	0.850
327	307.0	5.61	0.744	0.856	88.43	0.86969	1693.5	0.811
342	307.4	5.21	0.785	0.814	67.71	0.90302	1774.6	0.772
360	308.0	4.61	0.834	0.750	69.10	0.94072	1863.0	0.712
373	308.3	4.31	0.870	0.717	42.63	0.96382	1921.0	0.681
384	308.8	3.81	0.900	0.690	30.76	0.98069	1965.7	0.627
393	309.2	3.41	0.924	0.613	20.69	0.99198	1998.1	0.582
397	310.0	2.61	0.935	0.513	6.78	0.99568	2010.2	0.487
420.64	312.61	0.00	1.000	0.000	7.92	1.00000	2041.0	0.000
55.28	312.61							

Est. flow 1833.27



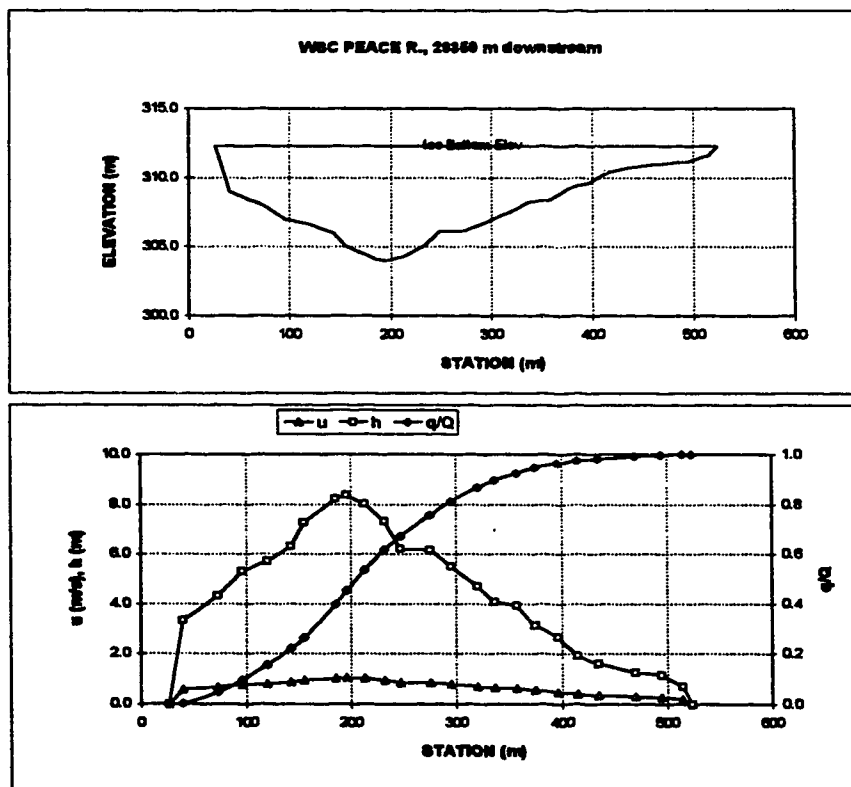
Appendix D.2 Peace River

X-SECTION
 DATE Feb 27, 1993
 DISCHARGE m^3/s 1740
 WIDTH m 487.118
 MEAN DEPTH m 4.42
 AREA m^2 2195.5
 MEAN VELOCITY m/s 0.783

WBC PEACE R., 28350 m downstream
 HEC2 Section from Alberta Env.
 Ice Bottom Elev 312.31

Sta. m	Elev. m	h m	w/W	u m/s	dq m^3	q/Q	area m^2	adj. u m/s
26.76	312.31	0.00	0.000	0.000	0.00	0.00000	0.0	0.000
40	308.00	3.31	0.027	0.884	7.16	0.00386	21.9	0.566
73	308.00	4.31	0.083	0.780	90.12	0.04837	147.6	0.875
98	307.00	5.31	0.138	0.898	82.70	0.08447	258.3	0.775
120	308.80	8.71	0.188	0.941	121.45	0.18485	390.5	0.814
143	308.00	6.31	0.234	1.005	134.50	0.22173	828.7	0.870
185	305.05	7.26	0.258	1.104	85.88	0.28443	610.2	0.955
185	304.10	8.21	0.318	1.188	287.14	0.38728	842.2	1.037
198	303.95	8.36	0.340	1.213	109.68	0.45190	933.3	1.049
213	304.30	8.01	0.376	1.179	166.40	0.53464	1072.5	1.020
232	305.00	7.31	0.413	1.109	166.49	0.61743	1218.0	0.960
247	308.10	6.21	0.443	0.995	108.67	0.67047	1319.4	0.861
275	308.15	6.16	0.499	0.989	171.81	0.75590	1482.6	0.856
296	308.80	5.51	0.540	0.919	111.33	0.81125	1609.3	0.795
320	307.80	4.71	0.590	0.827	111.51	0.86670	1737.1	0.718
337	308.25	4.06	0.624	0.749	58.76	0.88592	1811.6	0.648
357	308.40	3.91	0.664	0.731	58.97	0.92324	1891.3	0.632
375	309.20	3.11	0.701	0.627	42.89	0.94657	1954.5	0.543
395	309.65	2.66	0.743	0.585	36.12	0.96453	2015.1	0.489
415	310.41	1.90	0.781	0.452	22.02	0.97548	2058.4	0.391
435	310.71	1.60	0.821	0.403	14.85	0.98291	2093.4	0.348
470	311.05	1.28	0.892	0.343	18.67	0.98219	2143.4	0.297
495	311.15	1.18	0.942	0.325	10.11	0.99722	2173.7	0.281
515	311.60	0.71	0.982	0.234	5.23	0.99982	2192.4	0.203
523.88	312.31	0.00	1.000	0.000	0.37	1.00000	2195.5	0.000
26.76	312.31							

Est. flow 2011.12



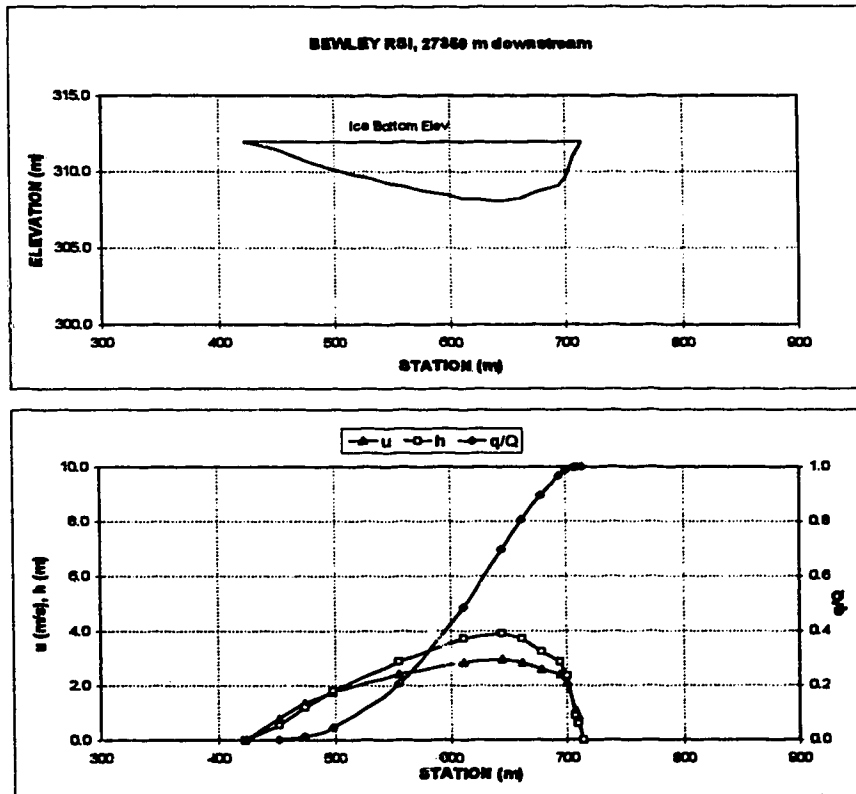
Appendix D.2 Peace River

X-SECTION BEVLEY R81, 27350 m downstream
 DATE Feb 27, 1993
 DISCHARGE m^3/s 1740
 WIDTH m 290.8284
 MEAN DEPTH m 2.44
 AREA m^2 709.7
 MEAN VELOCITY m/s 2.452

HEC2 Section from Alberta Env.
 Ice Bottom Elev 311.96

Sta. m	Elev. m	h m	w/W	u m/s	dq m^3	q/Q	area m^2	adj. u m/s
422.70	311.96	0.00	0.000	0.000	0.00	0.00000	0.0	0.000
452.33	311.42	0.54	0.102	0.897	3.59	0.00182	8.0	0.791
473.73	310.74	1.22	0.175	1.544	22.98	0.01346	26.8	1.362
498.13	310.16	1.80	0.259	2.002	65.32	0.04657	63.7	1.765
555.73	309.09	2.87	0.457	2.732	318.33	0.29789	188.2	2.409
611.43	308.24	3.72	0.649	3.248	648.79	0.48601	381.7	2.884
644.33	308.06	3.91	0.762	3.358	414.88	0.39611	507.2	2.961
661.63	308.24	3.72	0.822	3.248	218.00	0.20659	573.2	2.884
677.93	308.72	3.24	0.878	2.962	176.14	0.16565	629.9	2.612
694.53	309.09	2.87	0.935	2.732	144.39	0.09903	680.7	2.409
700.33	309.61	2.38	0.955	2.391	38.78	0.03668	695.8	2.108
707.03	311.07	0.89	0.978	1.251	19.77	0.00670	706.6	1.103
709.43	311.36	0.60	0.988	0.962	1.98	0.00070	708.4	0.848
713.53	311.96	0.00	1.000	0.000	0.59	1.00000	709.7	0.000
422.70	311.96							

Est. flow 1973.23

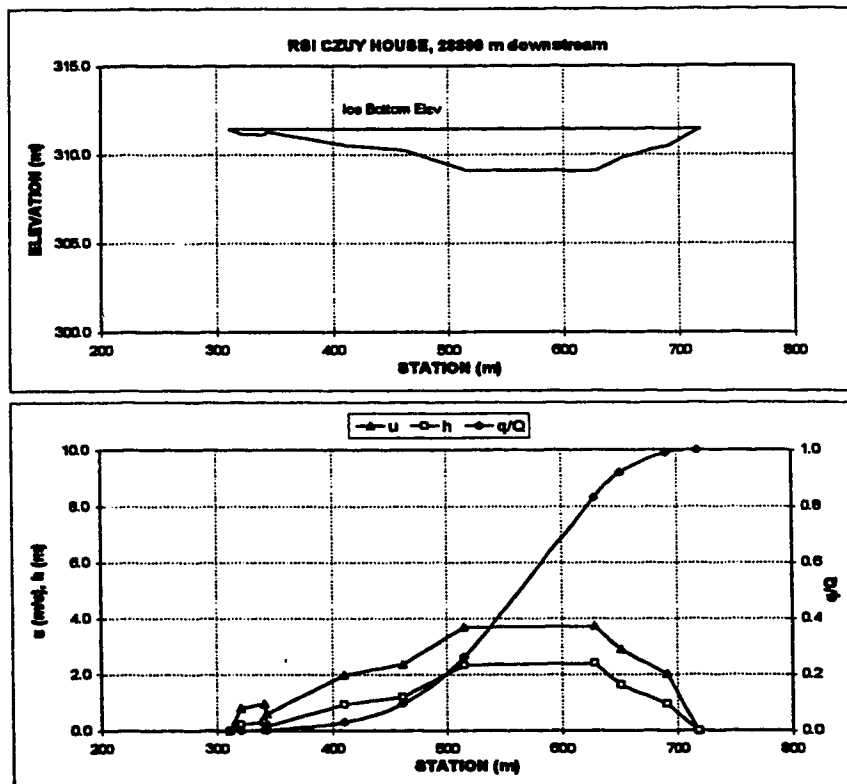


Appendix D.2 Peace River

X-SECTION RSI CZUY HOUSE, 28800 m downstream
 DATE Feb 27, 1993
 DISCHARGE m^3/s 1740 HEC2 Section from Alberta Env.
 WIDTH m 407.7066 Ice Bottom Elev 311.45
 MEAN DEPTH m 1.40
 AREA m^2 570.0
 MEAN VELOCITY m/s 3.062

Sta.	Elev.	h	w/W	u	dq	q/Q	area	adj. u
m	m	m		m/s	m^3		m^2	m/s
311.39	311.45	0.00	0.000	0.000	0.00	0.00000	0.0	0.000
321.17	311.22	0.23	0.024	0.924	0.53	0.00028	1.1	0.792
341.17	311.14	0.31	0.073	1.125	5.60	0.00302	6.6	0.984
343.17	311.39	0.15	0.075	0.896	0.43	0.00323	7.1	0.599
410.27	310.53	0.92	0.243	2.314	54.39	0.03002	43.2	1.983
461.77	310.25	1.20	0.369	2.761	138.95	0.08846	87.9	2.367
515.27	309.12	2.33	0.500	4.285	333.75	0.28285	182.5	3.681
628.17	309.06	2.39	0.777	4.368	1155.72	0.63209	459.3	3.744
651.07	309.83	1.62	0.833	3.372	177.98	0.91975	505.3	2.890
690.87	310.50	0.95	0.931	2.364	147.04	0.99217	555.6	2.025
719.10	311.45	0.00	1.000	0.000	15.90	1.00000	570.0	0.000
311.39	311.45							

Est. flow 2030.29

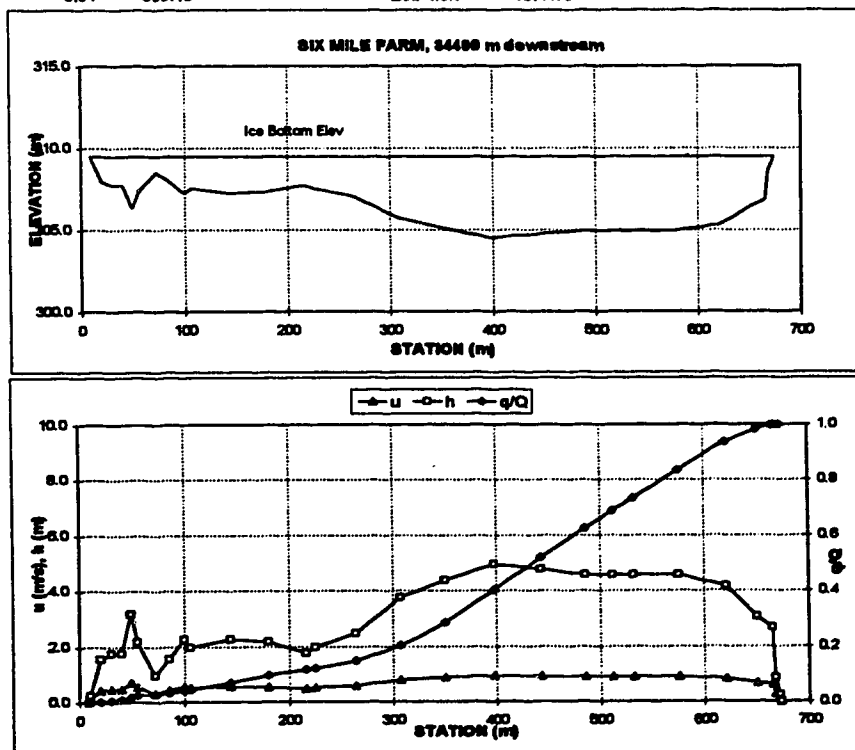


Appendix D.2 Peace River

X-SECTION SIX MILE FARM, 34400 m downstream
 DATE Feb 27, 1993
 DISCHARGE m^3/s 1740
 WIDTH m 683.741
 MEAN DEPTH m 3.33
 AREA m^2 2211.4
 MEAN VELOCITY m/s 0.787

HEC2 Section from Alberta Env.
 Ice Bottom Elev 309.48

Sta.	Elev.	h	w/V	u	dq	q/Q	area	adj. u
m	m	m		m/s	m^3		m^2	m/s
9.54	309.48	0.00	0.000	0.000	0.00	0.00000	0.0	0.000
10	309.3	0.18	0.001	0.108	0.00	0.00000	0.0	0.088
11	309.2	0.25	0.002	0.142	0.03	0.00001	0.2	0.131
20	307.9	1.58	0.018	0.478	2.82	0.00138	8.4	0.440
30	307.7	1.78	0.031	0.518	8.23	0.00874	28.1	0.477
40	307.7	1.78	0.048	0.518	9.08	0.01067	42.7	0.477
49	308.3	3.18	0.089	0.780	14.13	0.01810	84.9	0.704
55	307.3	2.18	0.088	0.690	10.79	0.02384	80.9	0.548
72	308.5	0.98	0.084	0.344	12.41	0.03044	107.4	0.319
85	307.9	1.58	0.114	0.478	8.73	0.03403	123.9	0.440
100	307.2	2.28	0.138	0.608	15.54	0.04230	182.6	0.563
108	307.5	1.98	0.145	0.583	7.38	0.04822	188.3	0.512
144	307.2	2.28	0.203	0.608	46.83	0.07104	248.8	0.563
180	307.3	2.18	0.257	0.690	47.73	0.08844	328.3	0.548
218	307.7	1.78	0.311	0.518	39.08	0.11723	388.0	0.477
225	307.5	1.98	0.328	0.583	8.86	0.12199	412.7	0.512
285	307.0	2.48	0.385	0.843	82.97	0.15019	501.3	0.598
308	305.7	3.78	0.450	0.853	100.20	0.20382	635.2	0.790
350	305.1	4.38	0.513	0.942	183.22	0.28807	808.8	0.872
398	304.5	4.98	0.585	1.028	220.32	0.40238	1029.7	0.951
443	304.7	4.78	0.653	0.999	221.82	0.52031	1248.5	0.925
486	304.9	4.58	0.718	0.971	197.45	0.62541	1449.1	0.899
512	304.9	4.58	0.757	0.971	115.18	0.68871	1867.7	0.899
532	304.9	4.58	0.787	0.971	88.58	0.73388	1859.0	0.899
575	304.9	4.58	0.852	0.971	190.46	0.83523	1856.2	0.899
621	305.3	4.18	0.821	0.913	189.03	0.93585	2056.0	0.848
650	306.4	3.08	0.985	0.744	86.82	0.98208	2180.8	0.889
685	306.8	2.68	0.988	0.678	30.53	0.99831	2203.7	0.828
688	308.6	0.88	0.992	0.320	2.84	0.99872	2209.0	0.298
672	309.23	0.25	0.998	0.142	0.82	0.99999	2211.3	0.131
673.28	309.48	0.00	1.000	0.000	0.01	1.00000	2211.4	0.000
9.54	309.48			Est. flow	1878.73			



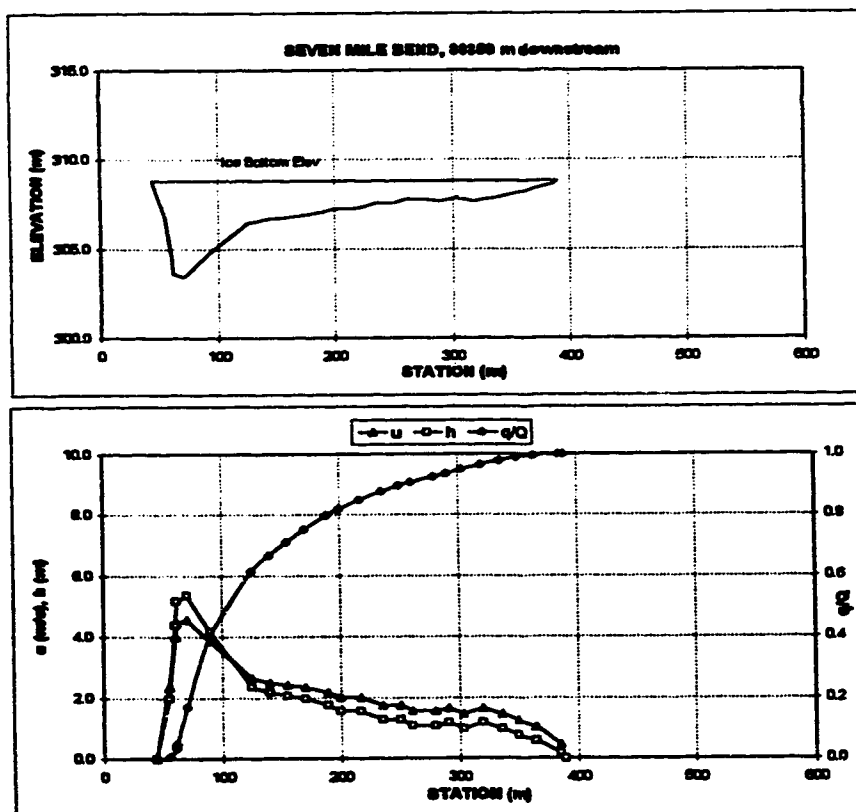
Appendix D.2 Peace River

X-SECTION
DATE Feb 27, 1993
DISCHARGE m^3/s 1740
WIDTH m 344.8298
MEAN DEPTH m 1.63
AREA m^2 632.5
MEAN VELOCITY m/s 2.761

SEVEN MILE BEND, 36360 m downstream
HEC2 Section from Alberta Env.
Ice Bottom Elev 306.80

Sta.	Elev.	h	vel	u	dq	q/Q	area	adj. u
m	m	m	m/s	m/s	m^3		m^2	m/s
44.33	306.80	0.00	0.000	0.000	0.00	0.00000	0.0	0.000
55	306.8	1.97	0.031	2.883	15.14	0.00705	10.5	2.338
60	304.4	4.37	0.046	4.907	61.70	0.03580	28.3	3.979
61	303.8	8.17	0.046	8.480	24.79	0.04735	31.1	4.481
70	303.4	8.37	0.074	8.631	283.82	0.17018	78.5	4.565
80	304.6	4.17	0.132	4.796	485.25	0.40084	173.9	3.856
125	306.4	2.37	0.234	3.282	458.55	0.61480	288.2	2.645
140	306.6	2.17	0.277	3.678	107.79	0.08483	322.3	2.494
155	306.7	2.07	0.321	2.990	86.19	0.70805	354.0	2.416
170	306.8	1.97	0.384	2.883	88.74	0.76080	384.3	2.338
180	307.0	1.77	0.422	2.684	103.99	0.79845	421.7	2.176
200	307.2	1.57	0.451	2.478	43.05	0.81951	438.3	2.008
217	307.2	1.57	0.501	2.478	68.04	0.86028	465.0	2.008
235	307.5	1.27	0.563	2.150	59.06	0.87727	490.5	1.744
250	307.5	1.27	0.586	2.150	40.90	0.88686	508.5	1.744
260	307.7	1.07	0.625	1.918	23.76	0.90782	521.2	1.555
280	307.7	1.07	0.683	1.918	40.96	0.92700	542.8	1.555
289	307.8	1.17	0.712	2.036	22.10	0.93736	553.7	1.551
303	307.8	0.97	0.750	1.796	26.60	0.94880	567.6	1.456
320	307.8	1.17	0.789	2.036	34.78	0.96590	585.8	1.551
336	307.8	0.97	0.843	1.796	30.69	0.98020	601.8	1.456
350	308.0	0.77	0.886	1.539	21.71	0.99031	614.8	1.248
365	308.2	0.57	0.930	1.299	14.01	0.99684	624.8	1.020
385	308.6	0.17	0.988	0.558	6.68	0.99995	632.2	0.453
399.25	308.88	0.00	1.000	0.000	0.10	1.00000	632.5	0.000
44.33	306.80							

Est. Row 2146.17



Appendix D.2 Peace River

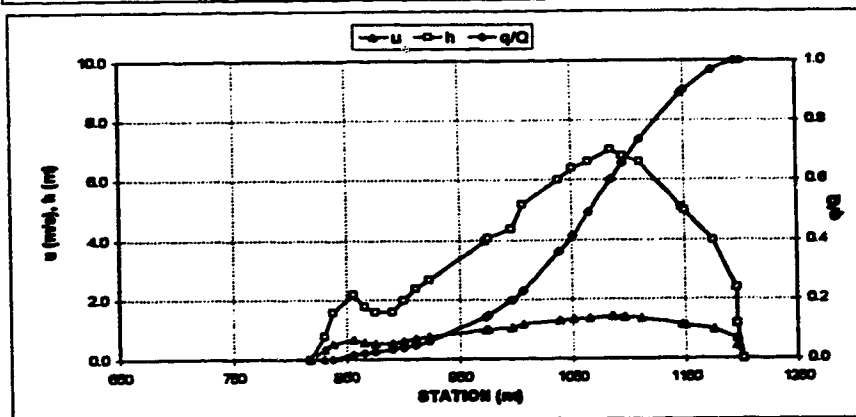
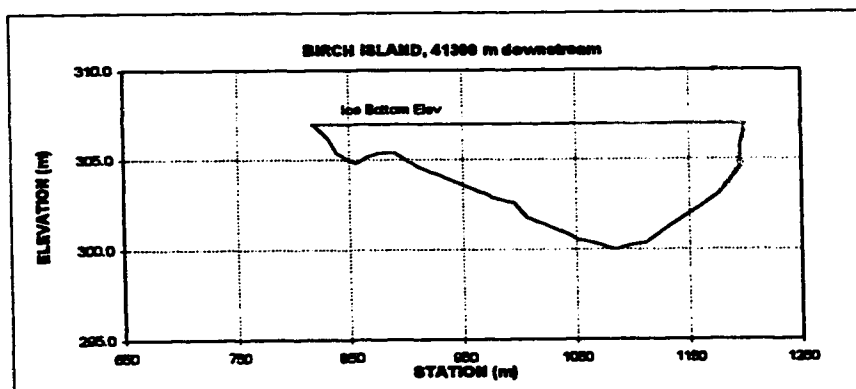
X-SECTION
DATE
DISCHARGE m^3/s
WIDTH m
MEAN DEPTH m
AREA m^2
MEAN VELOCITY m/s

BIRCH ISLAND, 41000 m downstream
Feb 27, 1993
1740
383
4.07
1557.2
1.117

HEC2 Section from Alberta Env.
Ice Bottom Elev
306.95

Sta. m	Elev. m	h m	w/W	u m/s	eq m^2	q/Q	area m^2	adj. u m/s
818	306.95	0.00	0.000	0.000	0.00	0.00000	0.0	0.000
831	306.2	0.78	0.034	0.371	0.84	0.00048	8.1	0.330
839	305.4	1.58	0.065	0.595	4.88	0.00281	14.5	0.528
858	304.8	2.18	0.098	0.737	21.29	0.01368	46.5	0.666
866	305.2	1.78	0.125	0.844	13.68	0.02086	66.3	0.672
876	305.4	1.58	0.151	0.885	10.41	0.02398	83.1	0.628
891	305.4	1.58	0.191	0.895	14.10	0.03317	108.8	0.628
901	305.0	1.98	0.217	0.882	11.45	0.03802	124.6	0.614
911	304.6	2.38	0.243	0.782	16.06	0.04722	146.4	0.606
923	304.3	2.68	0.274	0.846	24.71	0.05884	176.7	0.782
973	303.0	3.98	0.405	1.102	592.16	0.14263	343.2	0.979
976	302.9	4.08	0.413	1.120	13.43	0.14849	395.3	0.986
996	302.6	4.38	0.465	1.174	87.05	0.18804	438.9	1.043
1006	301.6	5.18	0.481	1.313	69.45	0.22839	487.7	1.167
1039	301.0	5.98	0.577	1.445	293.98	0.38807	671.9	1.284
1051	300.8	6.38	0.608	1.509	109.55	0.41501	746.0	1.341
1066	300.4	6.88	0.648	1.541	148.22	0.48068	843.2	1.369
1086	300.0	6.98	0.700	1.602	213.09	0.58848	876.8	1.424
1096	306.2	6.78	0.726	1.572	168.16	0.65523	1047.8	1.398
1111	300.4	6.58	0.765	1.541	165.92	0.73483	1147.8	1.369
1148	301.9	5.08	0.862	1.296	305.98	0.89105	1363.5	1.182
1151	302.0	4.98	0.869	1.279	18.43	0.90068	1378.8	1.137
1176	303.0	3.98	0.935	1.102	133.33	0.98905	1490.6	0.979
1196	304.6	2.38	0.987	0.782	69.89	0.98963	1554.2	0.695
1196	305.8	1.18	0.987	0.490	0.00	0.98963	1554.2	0.435
1201	306.95	0.00	1.000	0.000	0.72	1.00000	1557.2	0.000
818	306.95							

Est. flow 1055.61



Appendix D.2 Peace River

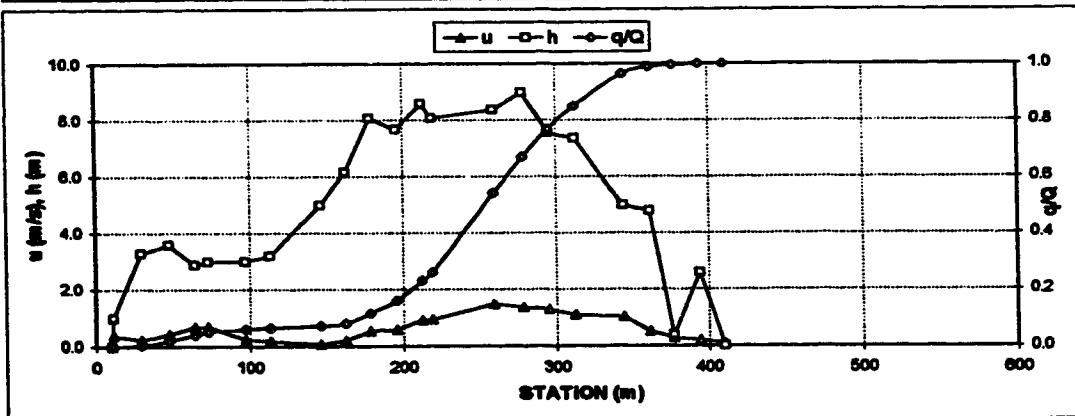
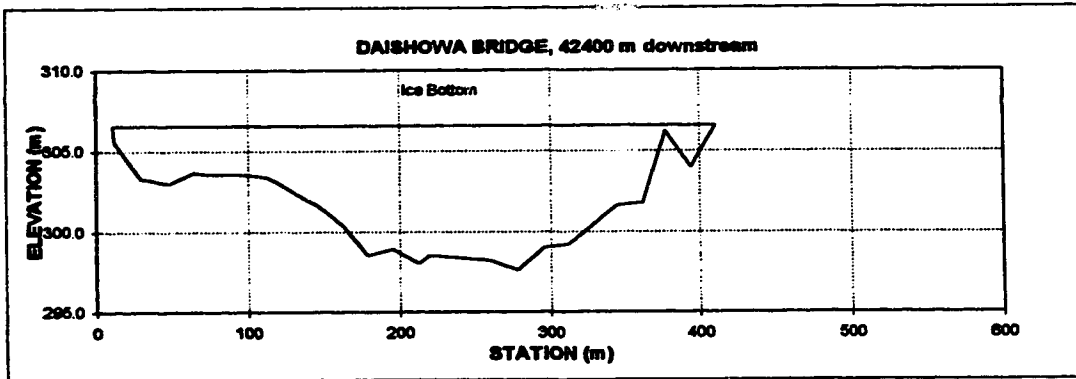
X-SECTION
DATE
DISCHARGE m^3/s
WIDTH m
MEAN DEPTH m
AREA m^2
MEAN VELOCITY m/s

DAISHOWA BRIDGE, 424 42.4 km
Feb 27, 1993
1740
400.0
5.24
2095.8
0.830

Ice Bottom Elev 306.57

Sta. m	Elev. m	h m	w/W	u m/s	dq m ³	q/Q	area m ²
10.8	306.57	0.00	0.00	0.000	0.00	0.00000	0.0
11.5	305.80	0.87	0.00	0.373	0.17	0.00010	0.5
29.8	303.30	3.27	0.05	0.220	8.53	0.00500	39.2
48.1	303.00	3.57	0.09	0.418	28.10	0.02000	101.7
64.4	303.70	2.87	0.13	0.631	34.80	0.04000	154.3
73.1	303.80	2.97	0.16	0.889	17.40	0.05000	179.8
87.1	303.80	2.97	0.22	0.244	17.40	0.06000	251.0
113.5	303.40	3.17	0.28	0.173	8.70	0.06500	301.2
146.2	301.80	4.97	0.34	0.065	8.70	0.07000	434.2
162.5	300.40	6.17	0.38	0.191	17.40	0.08000	525.3
178.8	298.50	8.07	0.42	0.523	60.90	0.11500	841.6
198.2	298.90	7.67	0.46	0.575	78.30	0.16000	777.9
212.5	298.00	8.57	0.50	0.818	121.80	0.23000	910.8
219.2	298.50	8.07	0.52	0.932	52.20	0.28000	986.6
259.6	298.20	8.37	0.62	1.468	487.20	0.54000	1298.6
276.6	297.80	8.97	0.67	1.357	228.20	0.67000	1465.3
295.2	299.00	7.57	0.71	1.287	174.00	0.77000	1600.5
312.5	299.20	7.37	0.75	1.077	139.20	0.85000	1729.8
344.2	301.80	4.97	0.83	1.022	200.10	0.96500	1925.5
361.5	301.80	4.77	0.88	0.516	43.50	0.99000	2009.8
378.9	306.20	0.37	0.92	0.284	10.44	0.99800	2049.4
394.2	304.00	2.57	0.96	0.205	5.22	0.99900	2074.8
410.6	306.57	0.00	1.00	0.083	1.74	1.00000	2095.8
10.6	306.57						

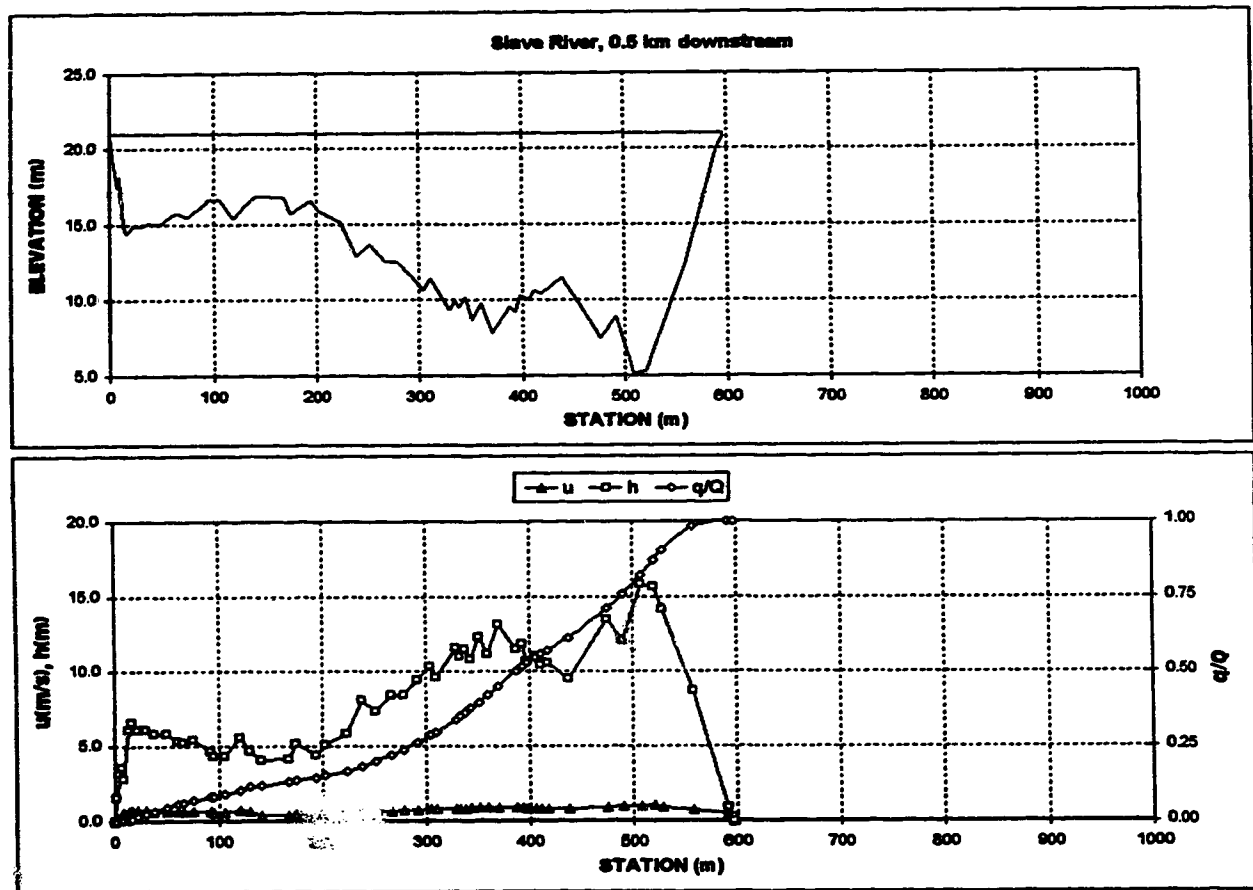
Total flow 1740.00



Appendix D.3 Slave River

X-SECTION		Slave River, 0.5 km downstream					
DATE	July, 1980						
DISCHARGE m ³ /s		3820		Assumed Water Surface		20.97	
WIDTH m		596.7		Water Surface Elev.		20.97	
DMEAN m		8.28		Correction to Geodetic		n/a	
AREA m ²		4928.1		Correction to Station		0	
VMEAN m/s		0.775					
Est. Sta. m	assumed Elev m	h m	w/W	u m/s	dq m ³	q/Q	area m ²
0.0	20.97	0	0.000	0.000	0.00	0	0.0
2.0	19.44	1.53	0.003	0.346	0.38	0.0001	1.5
7.5	17.44	3.53	0.013	0.388	4.97	0.0014	15.4
9.0	18.14	2.83	0.015	0.541	2.29	0.002	20.2
13.5	14.94	6.03	0.023	0.631	11.08	0.0049	40.2
16.5	14.44	6.53	0.028	0.723	13.37	0.0084	59.0
22.5	14.94	6.03	0.038	0.711	27.50	0.0156	96.7
30.5	14.94	6.03	0.051	0.696	33.62	0.0244	144.9
38.0	15.14	5.83	0.064	0.684	30.94	0.0325	189.4
50.0	15.14	5.83	0.084	0.672	47.37	0.0449	259.3
61.0	15.64	5.33	0.102	0.657	40.67	0.0556	320.7
66.0	15.74	5.23	0.111	0.640	16.61	0.06	347.1
78.5	15.54	5.43	0.128	0.625	35.91	0.0694	403.1
91.5	16.34	4.63	0.153	0.606	46.22	0.0815	478.5
94.5	16.64	4.33	0.158	0.557	7.84	0.0835	492.0
105.5	16.64	4.33	0.177	0.584	28.36	0.0904	539.6
120.0	15.44	5.53	0.201	0.723	43.17	0.1017	611.1
130.0	16.29	4.68	0.218	0.666	45.46	0.1136	662.1
141.0	16.89	4.08	0.236	0.421	20.63	0.119	710.3
168.0	16.79	4.18	0.282	0.429	46.60	0.1312	821.8
175.0	15.79	5.18	0.283	0.464	15.28	0.1352	854.6
194.0	16.59	4.38	0.325	0.464	42.02	0.1462	945.4
203.2	15.89	5.08	0.341	0.498	20.25	0.1515	988.9
223.0	15.19	5.78	0.374	0.558	54.63	0.1658	1096.4
238.0	12.89	8.08	0.399	0.629	63.03	0.1823	1200.4
252.0	13.69	7.28	0.422	0.654	69.91	0.2006	1307.9
267.0	12.59	8.38	0.447	0.672	77.16	0.2208	1425.4
278.0	12.59	8.38	0.466	0.709	63.79	0.2375	1517.5
292.5	11.59	9.38	0.490	0.746	92.83	0.2618	1646.3
304.0	10.69	10.28	0.509	0.775	87.48	0.2847	1759.4
310.0	11.39	9.58	0.520	0.804	46.22	0.2968	1818.9
328.0	9.39	11.58	0.550	0.822	154.71	0.3373	2009.4
333.0	9.99	10.98	0.558	0.849	48.13	0.3499	2065.8
338.0	9.49	11.48	0.566	0.842	47.37	0.3623	2121.9
344.0	10.19	10.78	0.577	0.855	56.15	0.377	2188.7
351.0	8.69	12.28	0.588	0.869	69.91	0.3953	2269.4
360.0	9.79	11.18	0.603	0.884	92.06	0.4194	2375.0
370.0	7.79	13.18	0.620	0.901	108.87	0.4479	2496.6
387.9	9.49	11.48	0.650	0.896	199.79	0.5002	2717.5
393.0	9.19	11.78	0.659	0.857	51.19	0.5136	2776.8
398.0	10.29	10.68	0.667	0.835	47.75	0.5281	2833.0
406.0	9.99	10.98	0.680	0.824	71.43	0.5448	2919.6
411.0	10.59	10.38	0.689	0.814	43.63	0.5563	2973.0
418.0	10.39	10.58	0.701	0.789	59.21	0.5718	3046.4
436.0	11.49	9.48	0.734	0.836	157.00	0.6129	3247.0
476.0	7.49	13.48	0.798	0.880	375.51	0.7112	3683.2
491.0	8.89	12.08	0.823	0.974	177.25	0.7578	3674.9
508.0	5.19	15.78	0.851	1.020	240.28	0.8205	4111.7
520.0	5.29	15.68	0.871	1.028	193.67	0.8712	4300.5
528.0	6.79	14.18	0.885	0.902	123.00	0.9034	4418.8
558.0	12.28	8.68	0.935	0.732	284.14	0.9804	4762.8
591.6	20.99	0.68	0.991	0.459	74.49	0.9999	4823.4
596.6	20.78	0.19	1.000	0.142	0.38	0.999999	4828.1
596.7	20.97	0	1.000	0.000	0.00	1	4828.1
0.0	20.97						
Est. Total				3820.00			

Appendix D.3 Slave River

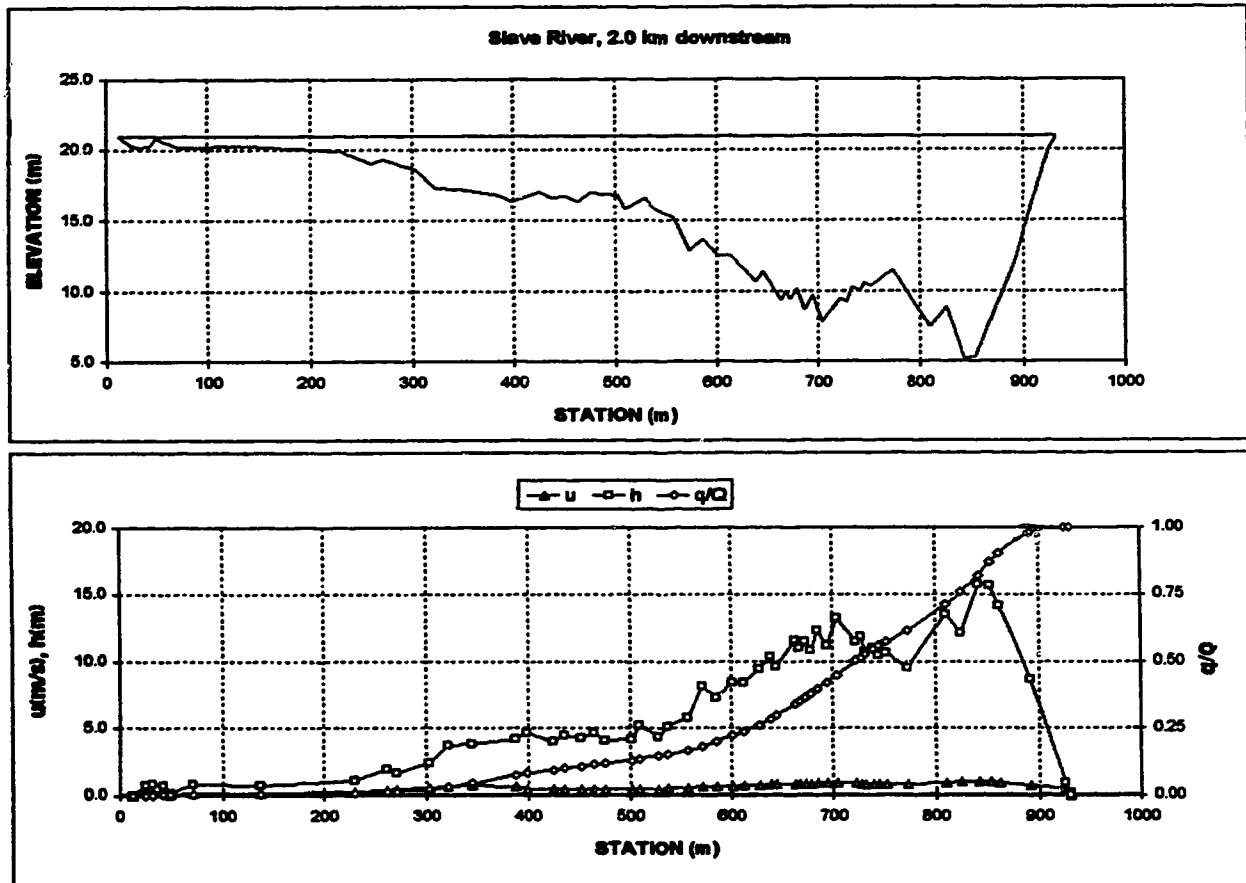


Appendix D.3 Slave River

X-SECTION		Slave River, 2.0 km downstream						
DATE	July, 1980							
DISCHARGE m³/s		3820	Assumed Water Surface				20.97	
WIDTH m		918	Water Surface Elev.				20.97	
DMEAN m		5.67	Correction to Geodetic				n/a	
AREA m²		5202.2	Correction to Station				0	
VMEAN m/s		0.734						
Est. Sta.	ssumed Elev	h	w/W	u	dq	q/Q	area	
m	m	m		m/s	m²		m²	
13.0	20.97	0	0.000	0.000	0.00	0	0.0	
25.1	20.22	0.75	0.013	0.228	0.76	0.0002	4.5	
32.3	20.19	0.78	0.021	0.300	1.53	0.0006	10.0	
43.5	20.23	0.74	0.033	0.277	2.67	0.0013	18.6	
50.3	20.97	0	0.041	0.151	0.36	0.0014	21.1	
50.4	20.76	0.19	0.041	0.072	0.00	0.0014	21.1	
72.3	20.19	0.78	0.065	0.151	0.76	0.0016	31.7	
137.3	20.29	0.63	0.135	0.187	8.02	0.0037	79.2	
229.3	19.89	1.08	0.236	0.245	16.04	0.0079	160.1	
261.0	18.99	1.98	0.270	0.349	15.66	0.012	208.6	
271.0	19.29	1.68	0.281	0.419	7.64	0.014	228.9	
303.3	18.59	2.38	0.316	0.490	27.50	0.0212	292.5	
322.3	17.29	3.68	0.337	0.629	32.85	0.0298	350.1	
345.6	17.19	3.78	0.362	0.689	58.06	0.045	437.0	
367.3	16.79	4.18	0.408	0.841	116.13	0.0754	602.9	
398.3	16.29	4.68	0.420	0.434	21.39	0.081	651.7	
425.3	16.99	3.98	0.449	0.430	50.42	0.0942	766.6	
436.6	16.54	4.43	0.461	0.432	20.25	0.0995	816.1	
452.3	16.69	4.28	0.479	0.441	29.80	0.1073	884.5	
464.3	16.29	4.68	0.492	0.438	24.07	0.1136	938.2	
475.3	16.89	4.08	0.504	0.421	20.63	0.119	986.4	
502.3	16.79	4.18	0.533	0.429	46.60	0.1312	1097.9	
509.3	15.79	5.18	0.541	0.464	15.28	0.1352	1130.7	
528.3	16.59	4.38	0.561	0.464	42.02	0.1462	1221.5	
537.5	15.89	5.08	0.571	0.496	20.25	0.1515	1265.0	
557.3	15.19	5.78	0.593	0.556	54.63	0.1656	1372.5	
572.3	12.89	8.08	0.609	0.629	63.03	0.1823	1476.5	
586.3	13.69	7.28	0.625	0.654	69.91	0.2006	1584.0	
601.3	12.59	8.38	0.641	0.672	77.16	0.2206	1701.4	
612.3	12.59	8.38	0.653	0.709	63.79	0.2375	1793.6	
626.6	11.59	9.38	0.669	0.746	92.63	0.2618	1922.4	
636.3	10.69	10.28	0.681	0.775	87.48	0.2847	2035.4	
644.3	11.39	9.58	0.688	0.804	46.22	0.2966	2095.0	
662.3	9.39	11.58	0.707	0.822	154.71	0.3373	2265.4	
667.3	9.99	10.98	0.713	0.849	46.13	0.3499	2341.8	
672.3	9.49	11.48	0.718	0.842	47.37	0.3623	2398.0	
678.3	10.19	10.78	0.725	0.855	56.15	0.377	2464.8	
685.3	8.69	12.28	0.732	0.869	69.91	0.3953	2546.5	
694.3	9.79	11.18	0.742	0.884	92.06	0.4194	2651.1	
704.3	7.79	13.18	0.753	0.901	106.67	0.4479	2772.9	
722.2	9.49	11.48	0.773	0.896	199.79	0.5002	2993.6	
727.3	9.19	11.78	0.778	0.857	51.19	0.5136	3052.9	
732.3	10.29	10.68	0.784	0.835	47.75	0.5261	3109.0	
740.3	9.99	10.98	0.792	0.824	71.43	0.5448	3196.7	
745.3	10.59	10.38	0.798	0.814	43.93	0.5563	3249.1	
752.3	10.39	10.58	0.805	0.789	59.21	0.5718	3322.4	
772.3	11.49	9.48	0.827	0.836	157.00	0.6129	3523.0	
810.3	7.49	13.48	0.869	0.880	375.51	0.7112	3959.3	
825.3	8.69	12.08	0.885	0.974	177.25	0.7676	4151.0	
842.3	5.19	15.78	0.903	1.020	240.28	0.8205	4367.6	
854.3	5.29	15.68	0.916	1.028	193.67	0.8712	4576.5	
862.3	6.79	14.18	0.925	0.902	123.00	0.9034	4696.0	
892.3	12.29	8.68	0.958	0.732	284.14	0.9604	5036.9	
925.9	20.09	0.88	0.994	0.459	74.49	0.9999	5199.5	
930.9	20.76	0.19	1.000	0.142	0.36	0.9999999	5202.2	
931.0	20.97	0	1.000	0.000	0.00	1.00000	5202.2	
13.0	20.97							

Est. Total 3620.00

Appendix D.3 Slave River

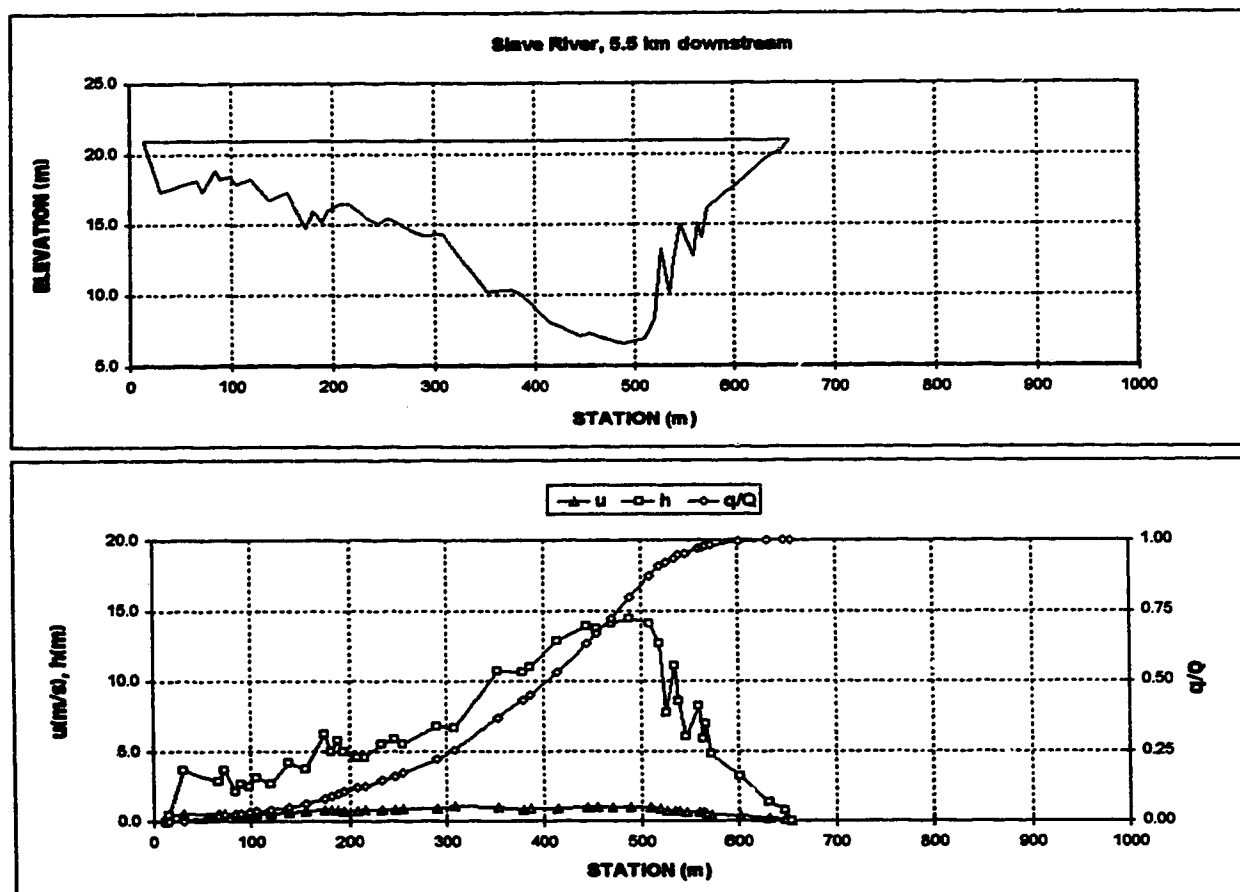


Appendix D.3 Slave River

X-SECTION		Slave River, 5.5 km downstream					
DATE	July, 1980						
DISCHARGE m ³ /s		3820	Assumed Water Surface		20.97		
WIDTH m		841	Water Surface Elev.		20.97		
DMEAN m		6.95	Correction to Geodetic		n/a		
AREA m ²		4452.1	Correction to Station		0		
VMEAN m/s		0.858					
Est. Sta.	assumed Elev	h	w/W	u	dq	q/Q	area
m	m	m		m/s	m ³		m ²
14.0	20.97	0	0.000	0.000	0.00	0	0.0
15.5	20.54	0.43	0.002	0.385	0.04	0.00001	0.3
30.0	17.34	3.63	0.025	0.524	11.42	0.003	29.8
66.0	18.14	2.83	0.081	0.563	64.94	0.02	146.0
72.0	17.34	3.63	0.090	0.567	11.46	0.023	165.4
84.0	18.84	2.13	0.109	0.572	19.10	0.028	200.0
89.0	18.24	2.73	0.117	0.427	7.64	0.03	212.1
98.0	18.44	2.53	0.131	0.439	7.64	0.032	235.8
105.0	17.84	3.13	0.142	0.539	11.46	0.035	255.6
120.0	18.24	2.73	0.165	0.573	22.92	0.041	299.6
138.0	16.74	4.23	0.193	0.645	38.20	0.051	362.2
155.0	17.24	3.73	0.220	0.753	45.84	0.063	429.9
174.0	14.74	6.23	0.250	0.798	76.40	0.083	524.5
181.0	15.94	5.93	0.261	0.830	30.56	0.091	563.9
189.0	15.1	5.83	0.273	0.866	38.20	0.101	607.3
194.0	15.34	5.03	0.281	0.768	22.92	0.107	634.5
207.1	16.44	4.53	0.301	0.742	45.84	0.119	697.1
216.0	16.44	4.53	0.315	0.788	30.56	0.127	737.4
234.0	15.44	5.53	0.343	0.815	72.58	0.146	828.0
246.0	15.04	5.93	0.362	0.857	57.30	0.161	896.7
255.0	15.44	5.53	0.376	0.883	45.84	0.173	948.3
289.5	14.19	6.78	0.430	0.928	187.18	0.222	1160.6
308.0	14.24	6.73	0.459	1.128	126.08	0.255	1285.6
352.0	10.24	10.73	0.527	1.022	446.94	0.372	1969.7
378.0	10.34	10.63	0.568	0.828	229.86	0.43212	1947.4
385.0	10.04	10.93	0.579	0.880	62.84	0.44857	2022.9
415.0	8.14	12.83	0.628	0.930	317.21	0.53161	2379.3
445.0	7.04	13.93	0.672	0.972	387.69	0.6331	2760.7
455.0	7.24	13.73	0.688	0.990	136.68	0.66888	2919.0
489.9	6.94	14.03	0.711	1.000	204.87	0.72251	3125.8
489.9	6.54	14.43	0.742	1.008	286.77	0.79758	3410.4
509.9	6.94	14.03	0.774	0.994	286.77	0.87285	3695.0
519.9	8.34	12.63	0.789	0.907	128.43	0.90627	3828.3
528.9	13.24	7.73	0.800	0.777	57.03	0.9212	3899.5
534.9	9.94	11.03	0.813	0.764	56.69	0.93604	3974.6
539.9	12.44	8.53	0.820	0.706	38.05	0.946	4023.5
546.5	14.94	6.03	0.831	0.628	30.45	0.95397	4071.5
559.5	12.74	8.23	0.851	0.624	57.91	0.96913	4164.2
563.5	15.04	5.93	0.857	0.602	17.57	0.97373	4192.5
567.5	14.04	6.93	0.863	0.562	14.94	0.97784	4218.2
572.5	16.14	4.83	0.871	0.441	16.04	0.98184	4247.6
601.5	17.74	3.23	0.917	0.361	48.48	0.99463	4364.5
631.5	19.64	1.33	0.963	0.244	18.45	0.99936	4432.9
647.5	20.24	0.73	0.988	0.127	2.29	0.99998	4449.4
655.0	20.97	0	1.000	0.000	0.15	1	4452.1
14.0	20.97						

Est. Total 3820.00

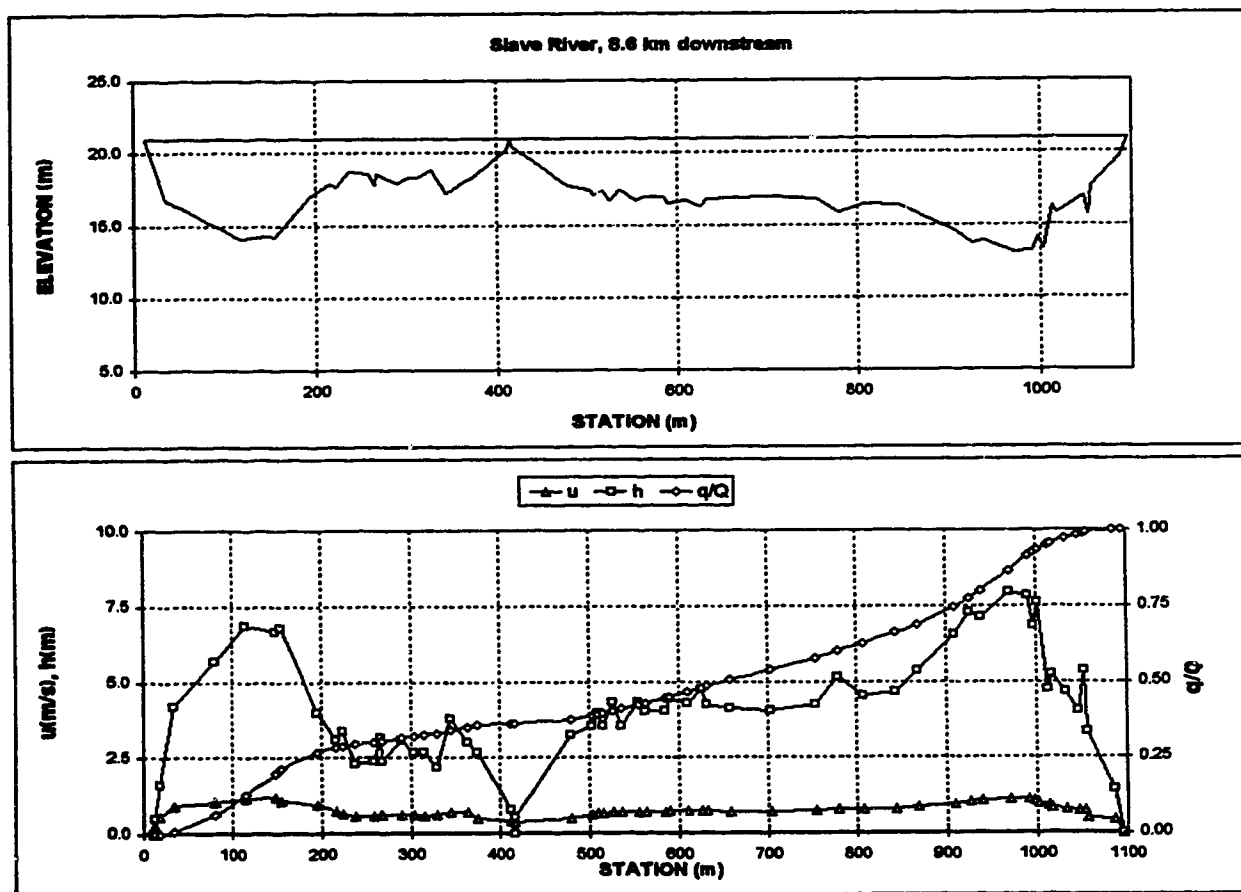
Appendix D.3 Slave River



Appendix D.3 Slave River

X-SECTION		Slave River, 8.6 km downstream					
DATE	July, 1980						
DISCHARGE m ³ /s		3820		Assumed Water Surface		20.97	
WIDTH m		1082.8		Water Surface Elev.		20.97	
DMEAN m		4.28		Correction to Geodetic		n/a	
AREA m ²		4809.7		Correction to Station		0	
VMEAN m/s		0.829					
Est. Sta. m	Assumed Elev m	h m	w/W	u m/s	dq m ²	q/Q	area m ²
12.0	20.97	0	0.000	0.000	0.00	0	0.0
13.0	20.50	0.47	0.001	0.283	0.00	0	0.2
20.0	19.39	1.58	0.007	0.585	1.95	0.00051	7.4
35.0	18.79	4.18	0.021	0.897	27.54	0.00772	60.6
80.0	15.29	5.68	0.063	1.036	210.14	0.06273	272.5
115.0	14.09	6.88	0.095	1.157	247.46	0.12751	492.3
147.4	14.29	6.68	0.125	1.188	281.10	0.19586	711.9
155.0	14.19	6.78	0.132	1.042	80.51	0.2117	763.1
195.0	16.99	3.98	0.169	0.941	217.09	0.28553	978.3
216.0	17.89	3.08	0.188	0.732	55.05	0.28294	1052.4
223.0	17.59	3.38	0.195	0.853	15.78	0.28707	1075.0
237.9	18.69	2.28	0.209	0.582	26.51	0.29401	1117.2
258.0	18.59	2.38	0.227	0.564	25.33	0.30084	1164.0
285.0	17.79	3.18	0.234	0.820	12.07	0.3038	1183.5
288.0	18.59	2.38	0.236	0.813	5.16	0.30515	1191.8
290.0	17.89	3.08	0.257	0.821	36.75	0.31477	1251.9
303.0	18.29	2.68	0.269	0.822	23.84	0.32101	1289.3
314.0	18.29	2.68	0.279	0.580	17.76	0.32586	1318.8
328.0	18.79	2.18	0.292	0.817	19.08	0.33065	1352.8
345.0	17.19	3.78	0.308	0.890	33.16	0.33933	1403.5
363.0	17.99	2.98	0.324	0.889	43.74	0.35078	1464.3
374.0	18.29	2.68	0.334	0.491	19.63	0.35592	1485.5
411.7	20.20	0.77	0.369	0.417	27.62	0.36315	1560.5
416.0	20.97	0	0.373	0.115	0.19	0.3632	1562.1
417.3	20.44	0.53	0.374	0.381	0.04	0.36321	1562.5
479.0	17.74	3.23	0.431	0.472	44.31	0.37481	1678.5
503.0	17.44	3.53	0.453	0.612	48.82	0.38759	1759.6
509.0	17.04	3.93	0.459	0.648	14.48	0.39138	1782.0
518.0	17.44	3.53	0.465	0.663	16.92	0.39581	1803.1
528.0	18.64	4.33	0.475	0.673	28.43	0.40273	1847.4
536.0	17.44	3.53	0.484	0.673	28.43	0.40985	1886.7
554.0	18.64	4.33	0.501	0.683	47.60	0.42211	1957.4
562.3	18.94	4.03	0.508	0.691	24.41	0.4285	1992.1
584.0	18.94	4.03	0.528	0.690	59.94	0.44419	2079.6
589.0	18.54	4.43	0.533	0.722	15.01	0.44812	2100.7
609.0	18.69	4.28	0.551	0.734	63.18	0.46466	2187.8
625.0	18.24	4.73	0.566	0.743	53.63	0.4767	2259.9
632.0	18.74	4.23	0.573	0.713	23.26	0.48479	2291.3
658.4	18.64	4.13	0.597	0.697	77.74	0.50514	2401.6
704.0	18.94	4.03	0.639	0.695	128.77	0.53885	2567.7
754.2	18.74	4.23	0.685	0.722	144.78	0.57675	2795.0
779.0	15.84	5.13	0.708	0.774	88.74	0.59998	2911.1
807.0	18.44	4.53	0.734	0.766	105.81	0.62768	3046.3
844.0	18.34	4.63	0.788	0.773	127.51	0.66106	3215.8
869.0	15.64	5.33	0.791	0.869	99.59	0.68713	3340.3
909.0	14.44	6.53	0.828	0.941	214.84	0.74337	3577.5
927.0	13.69	7.28	0.845	1.021	125.33	0.77618	3701.7
939.0	13.84	7.13	0.858	1.063	89.81	0.79989	3788.2
970.8	13.04	7.93	0.885	1.086	256.70	0.86689	4027.7
991.0	13.14	7.83	0.904	1.093	176.14	0.913	4186.8
998.0	14.14	6.83	0.911	1.048	54.01	0.92714	4238.1
1003.0	13.34	7.63	0.915	0.973	37.63	0.93699	4274.3
1013.0	16.24	4.73	0.924	0.900	57.64	0.95208	4336.1
1017.0	15.74	5.23	0.928	0.784	15.89	0.95624	4356.0
1032.0	16.34	4.63	0.942	0.780	58.68	0.9716	4430.0
1047.0	16.94	4.03	0.956	0.734	46.91	0.98388	4494.9
1052.0	15.84	5.33	0.960	0.751	17.62	0.98857	4518.3
1055.0	17.64	3.33	0.963	0.502	9.40	0.99103	4531.3
1085.0	18.54	1.43	0.991	0.437	32.93	0.99985	4602.7
1094.8	20.97	0	1.000	0.000	1.34	1	4609.7
12.0	20.97			Est. Total	3820.00		

Appendix D.3 Slave River



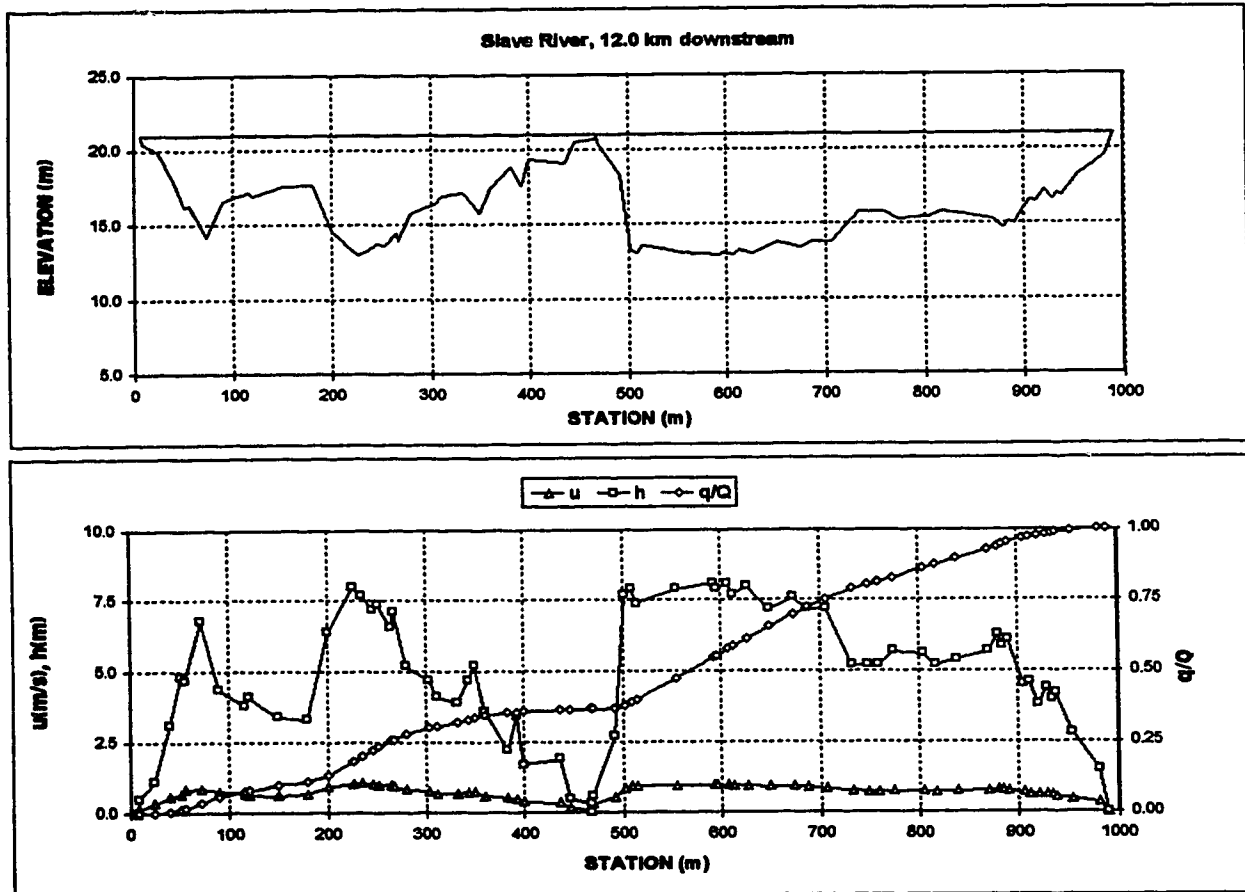
Appendix D.3 Slave River

X-SECTION Slave River, 12.0 km downstream							
DATE July, 1980							
DISCHARGE m ³ /s		3820		Assumed Water Surface		20.97	
WIDTH m		982		Water Surface Elev.		20.97	
DMEAN m		4.96		Correction to Geodetic		n/a	
AREA m ²		4872.0		Correction to Station		0	
VMEAN m/s		0.784					
Est. Sta.	ssumed Elev	h	w/W	u	dq	q/Q	area
m	m	m		m/s	m ³		m ²
7.0	20.97	0	0.000	0.000	0.00	0	0.0
9.0	20.49	0.48	0.002	0.153	0.04	0.00001	0.5
25.0	19.89	1.08	0.018	0.328	1.95	0.00052	13.0
40.0	17.89	3.08	0.034	0.543	12.30	0.00374	44.2
52.0	16.19	4.78	0.046	0.668	30.25	0.01186	91.3
58.0	16.29	4.68	0.050	0.824	13.90	0.0153	110.2
72.0	14.19	6.78	0.066	0.834	77.24	0.03552	201.9
90.0	16.59	4.38	0.085	0.742	83.05	0.05726	302.4
115.0	17.19	3.78	0.110	0.656	67.19	0.07485	404.4
120.0	16.89	4.08	0.115	0.620	12.57	0.07814	424.0
150.0	17.59	3.38	0.146	0.593	66.99	0.0962	535.9
180.0	17.69	3.28	0.176	0.655	56.61	0.11102	635.8
200.0	14.59	6.38	0.197	0.906	72.05	0.12988	732.4
226.0	12.99	7.98	0.223	1.006	184.62	0.17621	919.1
235.0	13.29	7.68	0.232	1.031	74.11	0.19761	989.6
246.0	13.79	7.18	0.243	1.008	82.78	0.21928	1071.3
252.0	13.59	7.38	0.249	0.979	43.62	0.2307	1115.0
285.0	14.39	6.58	0.263	0.967	88.01	0.25374	1205.7
287.0	13.89	7.08	0.265	0.895	12.99	0.25714	1219.4
280.0	15.79	5.18	0.278	0.809	70.52	0.2756	1299.1
303.0	16.29	4.68	0.301	0.740	85.78	0.29805	1412.5
312.0	16.89	4.08	0.311	0.683	27.39	0.30522	1451.9
332.0	17.09	3.88	0.331	0.660	51.49	0.3187	1531.5
343.0	16.29	4.68	0.342	0.714	32.09	0.3271	1578.6
350.0	15.79	5.18	0.349	0.722	26.13	0.33394	1613.1
360.0	17.39	3.58	0.359	0.584	30.41	0.3419	1656.9
382.0	18.79	2.18	0.382	0.504	32.20	0.35033	1720.2
392.0	17.59	3.38	0.392	0.480	13.71	0.35392	1746.0
400.0	19.29	1.68	0.400	0.373	9.36	0.35637	1768.3
437.0	19.09	1.88	0.436	0.330	22.77	0.36233	1834.1
447.0	20.49	0.48	0.446	0.169	2.87	0.36308	1845.9
467.0	20.69	0.28	0.466	0.059	0.42	0.36319	1853.5
468.0	20.97	0	0.469	0.121	0.04	0.3632	1853.7
469.7	20.39	0.58	0.471	0.283	0.04	0.36321	1854.2
492.0	18.29	2.68	0.494	0.527	10.39	0.36593	1890.5
502.0	13.29	7.68	0.504	0.816	36.06	0.37537	1942.3
509.0	13.09	7.88	0.511	0.924	50.62	0.38862	1996.8
514.0	13.59	7.38	0.516	0.917	34.99	0.39776	2034.9
554.0	13.09	7.88	0.557	0.932	279.82	0.47103	2340.1
583.0	12.89	8.08	0.597	0.946	294.45	0.54811	2651.3
585.0	13.09	7.88	0.599	0.946	15.13	0.55207	2667.3
607.0	12.89	8.08	0.611	0.944	90.61	0.57579	2763.1
612.0	13.29	7.68	0.616	0.934	36.94	0.58546	2802.5
627.0	12.89	7.98	0.631	0.921	109.60	0.61415	2919.9
650.0	12.79	7.18	0.655	0.904	159.10	0.6558	3094.2
674.0	13.39	7.58	0.679	0.895	158.61	0.69732	3271.4
688.0	13.79	7.18	0.693	0.886	92.52	0.72154	3374.7
706.0	13.79	7.18	0.712	0.828	113.49	0.75125	3503.9
734.0	15.79	5.18	0.740	0.761	136.72	0.76704	3677.0
749.0	15.79	5.18	0.756	0.696	54.09	0.8012	3754.7
759.0	15.79	5.18	0.766	0.710	36.06	0.81064	3806.5
774.0	15.29	5.68	0.781	0.733	58.60	0.82596	3887.9
804.0	15.39	5.58	0.812	0.732	124.84	0.85866	4056.8
817.0	15.79	5.18	0.825	0.709	50.04	0.87178	4126.8
839.0	15.59	5.38	0.847	0.720	81.98	0.89322	4242.9
869.0	15.29	5.68	0.878	0.741	120.98	0.92469	4408.8
879.0	14.69	6.28	0.888	0.775	46.18	0.93698	4468.6
884.0	15.09	5.88	0.893	0.775	23.72	0.94319	4499.0
890.0	14.89	6.08	0.899	0.728	27.66	0.95043	4534.9
905.0	16.49	4.48	0.914	0.687	55.92	0.96507	4614.1
911.0	16.39	4.58	0.921	0.610	17.16	0.96959	4641.3

Appendix D.3 Slave River

920.0	17.19	3.78	0.930	0.590	22.39	0.97542	4678.9
928.0	16.59	4.38	0.938	0.590	19.08	0.98041	4711.5
934.0	16.99	3.98	0.944	0.592	14.97	0.98433	4736.6
938.0	16.79	4.18	0.948	0.534	9.55	0.98683	4752.9
954.0	18.19	2.78	0.964	0.438	28.92	0.9944	4808.6
981.0	19.49	1.48	0.992	0.337	20.44	0.99975	4888.1
989.0	20.97	0	1.000	0.000	0.95	1.00000	4872.0
7.0	20.97						

Est. Total 3620.00

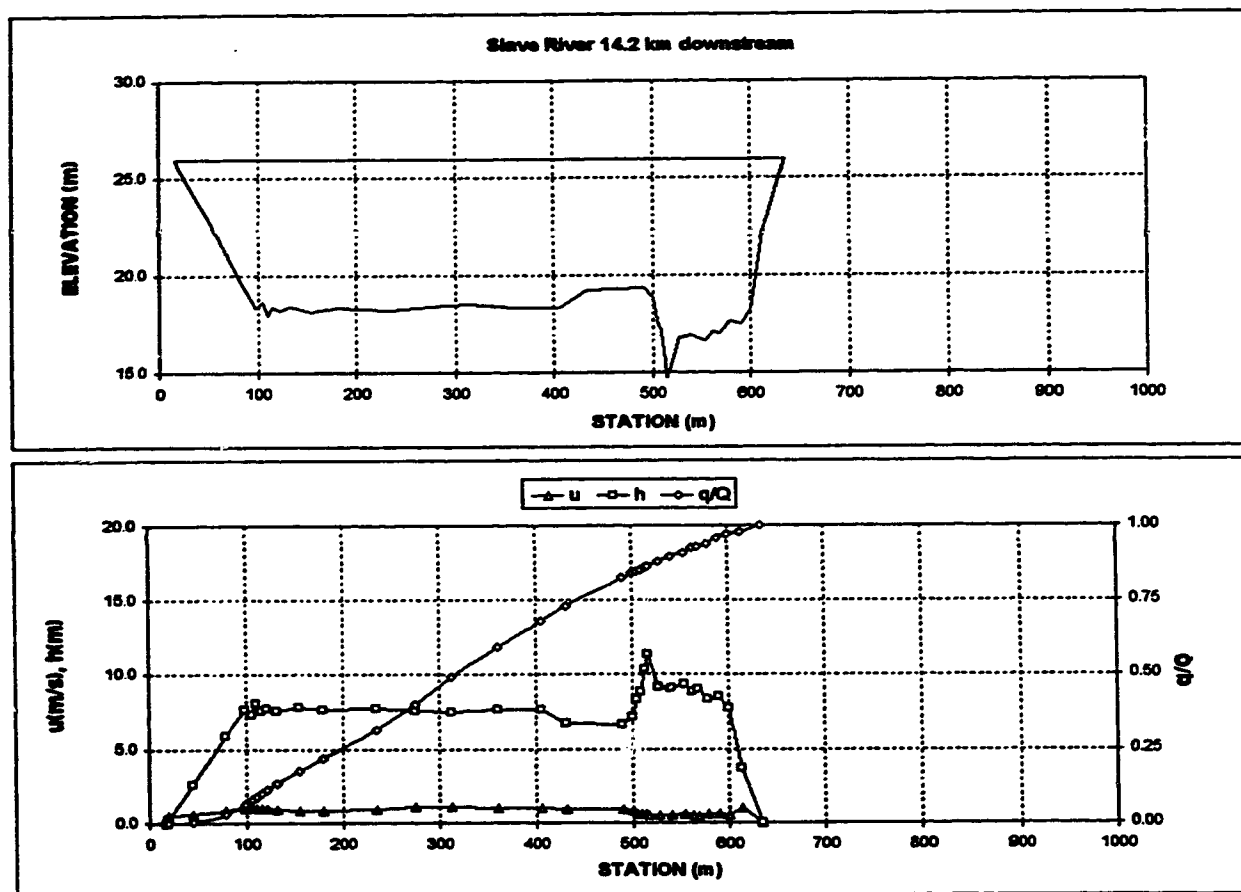


Appendix D.3 Slave River

X-SECTION		Slave River 14.2 km downstream					
DATE	July, 1980						
DISCHARGE m ³ /s		3520		Assumed Water Surface		25.96	
WIDTH m		618		Water Surface Elev.		25.96	
DMEAN m		6.99		Correction to Geodetic		n/a	
AREA m ²		4320.4		Correction to Station		0	
VMEAN m/s		0.884					
Est. Sta. m	ssumed Elev m	h m	w/W	u m/s	dq m ³	q/Q	area m ²
17.0	26.0	0.00	0.000	0.000	0.00	0.000000	0.0
18.2	25.7	0.24	0.002	0.493	0.04	0.000010	0.1
45.0	25.3	2.64	0.045	0.842	19.08	0.005000	30.7
78.0	20.1	5.84	0.099	0.834	95.50	0.030000	178.7
98.0	18.3	7.64	0.131	1.020	133.70	0.065000	313.5
105.0	18.6	7.34	0.142	1.051	57.30	0.080000	365.9
110.0	17.9	8.04	0.150	0.987	38.20	0.090000	404.3
115.0	18.4	7.54	0.159	1.033	38.20	0.100000	443.3
122.0	18.2	7.74	0.170	1.029	57.30	0.115000	496.8
132.0	18.4	7.54	0.186	0.983	76.40	0.135000	573.2
153.0	18.1	7.84	0.220	0.876	152.80	0.17500	734.7
180.0	18.3	7.64	0.284	0.854	171.90	0.22000	943.6
234.3	18.2	7.74	0.352	0.944	362.90	0.31500	1361.2
275.0	18.4	7.54	0.417	1.117	324.70	0.40000	1672.2
313.4	18.5	7.44	0.480	1.136	343.80	0.49000	1959.8
360.0	18.3	7.64	0.555	1.024	362.00	0.59000	2311.1
405.8	18.3	7.64	0.629	0.994	336.16	0.67800	2681.0
432.0	19.2	6.74	0.672	0.974	198.64	0.73000	2849.4
490.0	19.3	6.64	0.765	0.920	362.90	0.82500	3237.4
500.0	18.8	7.14	0.762	0.842	57.30	0.84000	3306.3
504.0	17.6	8.34	0.788	0.643	26.74	0.84700	3337.3
508.7	17.1	8.84	0.796	0.631	19.10	0.85200	3377.7
512.7	15.6	10.34	0.802	0.604	30.56	0.86000	3416.0
515.0	14.8	11.34	0.806	0.491	7.64	0.86200	3441.0
527.0	16.8	9.14	0.825	0.523	64.94	0.87900	3563.8
540.0	16.9	9.04	0.846	0.514	61.12	0.89500	3662.0
553.0	16.6	9.34	0.867	0.569	61.12	0.91100	3801.5
562.0	17.1	8.84	0.882	0.537	53.48	0.92500	3883.3
568.0	17.0	8.94	0.892	0.410	19.10	0.93000	3936.6
578.0	17.6	8.34	0.906	0.613	36.20	0.94000	4029.0
590.0	17.5	8.44	0.927	0.631	76.40	0.96000	4129.7
600.0	18.2	7.74	0.943	0.491	36.20	0.97000	4204.6
613.0	22.2	3.74	0.964	0.990	36.20	0.98000	4279.2
635.0	26.0	0.00	1.000	0.000	76.40	1.00000	4320.4
17.0	26.0						

Est. Total 3520.00

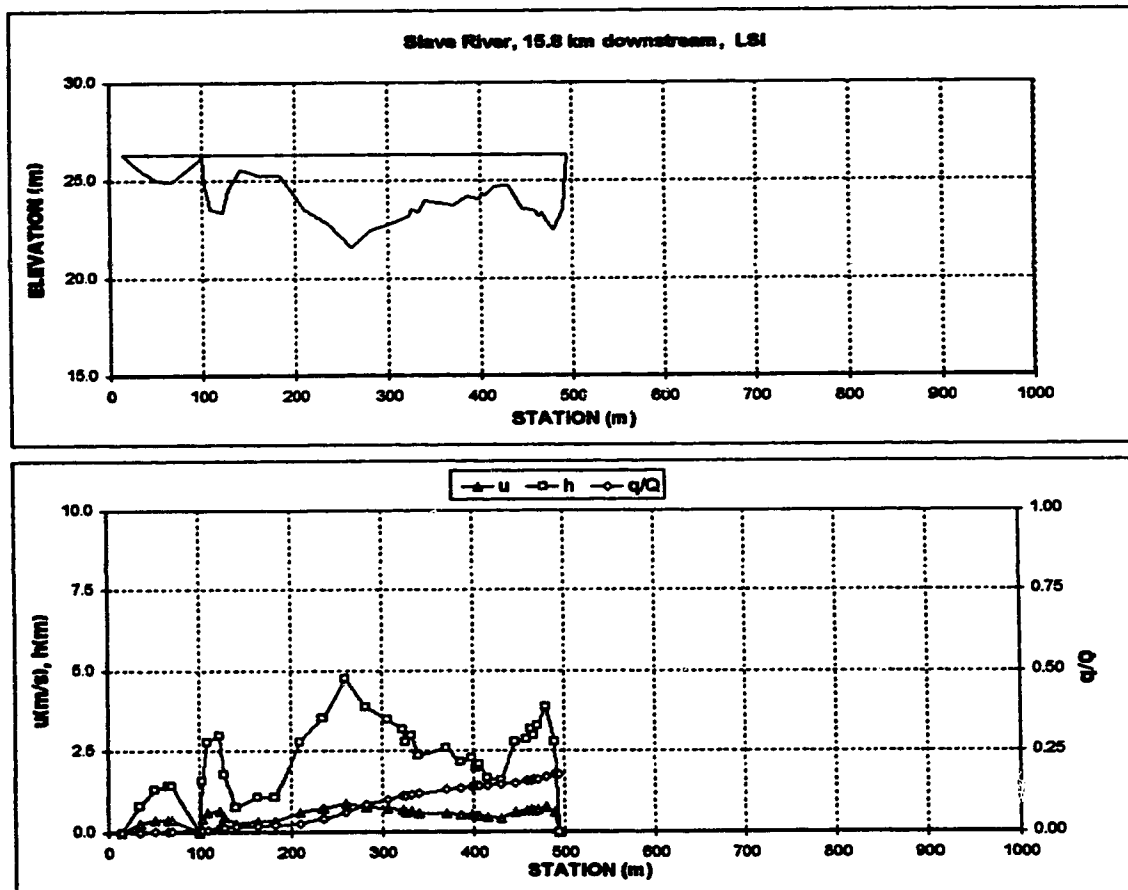
Appendix D.3 Slave River



Appendix D.3 Slave River

X-SECTION			Slave River, 15.8 km downstream, LSI					
DATE July, 1980								
CHANNEL Q m³/s			672.32		TOTAL Q m³/s		3820	
WIDTH m			478.50		Avg. Water Surface Elev.		28.31	
DMEAN m			2.28		LB		15.00	
AREA m²			1091.61		RB		483.50	
VMEAN m/s			0.618				28.31	
Est. Sta.	assumed Elev	h	w/W	u	dq	q/Q	area	adj. u
m	m	m		m/s	m³		m²	m/s
15.00	28.31	0.00	0.000	0.000	0.90	0.00000	0.0	0.000
34.70	25.50	0.81	0.041	0.309	1.23	0.00029	8.0	0.273
49.90	25.00	1.31	0.073	0.425	5.91	0.00168	24.1	0.377
66.10	24.90	1.41	0.107	0.447	9.61	0.00388	46.1	0.398
69.60	24.90	1.41	0.115	0.447	2.33	0.00442	51.3	0.398
100.00	26.19	0.00	0.178	0.000	4.76	0.00553	72.6	0.000
102.90	24.74	1.57	0.184	0.480	0.55	0.00565	74.9	0.425
109.00	23.54	2.77	0.198	0.701	7.82	0.00746	88.1	0.621
123.00	23.34	2.97	0.228	0.734	26.84	0.01415	128.3	0.650
128.00	24.54	1.77	0.236	0.520	7.43	0.01587	140.2	0.480
140.00	25.54	0.77	0.281	0.298	6.24	0.01731	155.4	0.264
164.00	25.24	1.07	0.311	0.372	7.40	0.01903	177.5	0.329
183.00	25.24	1.07	0.351	0.372	7.56	0.02078	197.8	0.329
210.30	23.54	2.77	0.408	0.701	28.11	0.02729	250.2	0.621
235.00	22.79	3.52	0.460	0.823	59.17	0.04101	327.9	0.728
260.00	21.54	4.77	0.512	1.007	94.61	0.06298	431.5	0.892
282.00	22.44	3.87	0.558	0.876	89.50	0.08372	526.6	0.776
306.30	22.84	3.47	0.609	0.815	75.40	0.10119	615.8	0.721
323.00	23.14	3.17	0.644	0.767	43.85	0.11136	671.2	0.679
325.00	23.54	2.77	0.648	0.701	4.36	0.11237	677.2	0.621
332.00	23.34	2.97	0.682	0.734	14.42	0.11571	697.2	0.650
340.00	23.94	2.37	0.679	0.632	14.59	0.11909	718.6	0.559
370.50	23.74	2.57	0.743	0.667	48.92	0.13042	793.9	0.590
385.00	24.14	2.17	0.773	0.596	21.69	0.13545	828.3	0.527
398.00	24.04	2.27	0.800	0.614	17.45	0.13950	857.2	0.543
402.00	24.34	1.97	0.809	0.558	4.97	0.14065	865.6	0.494
405.00	24.24	2.07	0.815	0.577	3.44	0.14145	871.7	0.511
415.90	24.64	1.67	0.836	0.500	10.07	0.14378	890.4	0.443
430.00	24.74	1.57	0.867	0.480	11.91	0.14654	914.7	0.425
446.00	23.54	2.77	0.901	0.701	20.50	0.15129	949.4	0.621
458.00	23.44	2.87	0.928	0.718	24.01	0.15685	983.3	0.635
463.00	23.14	3.17	0.936	0.767	11.21	0.15945	998.4	0.679
466.00	23.34	2.97	0.943	0.734	6.91	0.16105	1007.6	0.650
470.00	23.04	3.27	0.951	0.783	9.47	0.16325	1020.1	0.693
479.00	22.44	3.87	0.970	0.876	26.66	0.16943	1052.2	0.776
489.00	23.54	2.77	0.991	0.701	26.18	0.17649	1085.4	0.621
493.50	26.31	0.00	1.000	0.000	2.18	0.17800	1091.6	0.000
Est. Total					759.46			

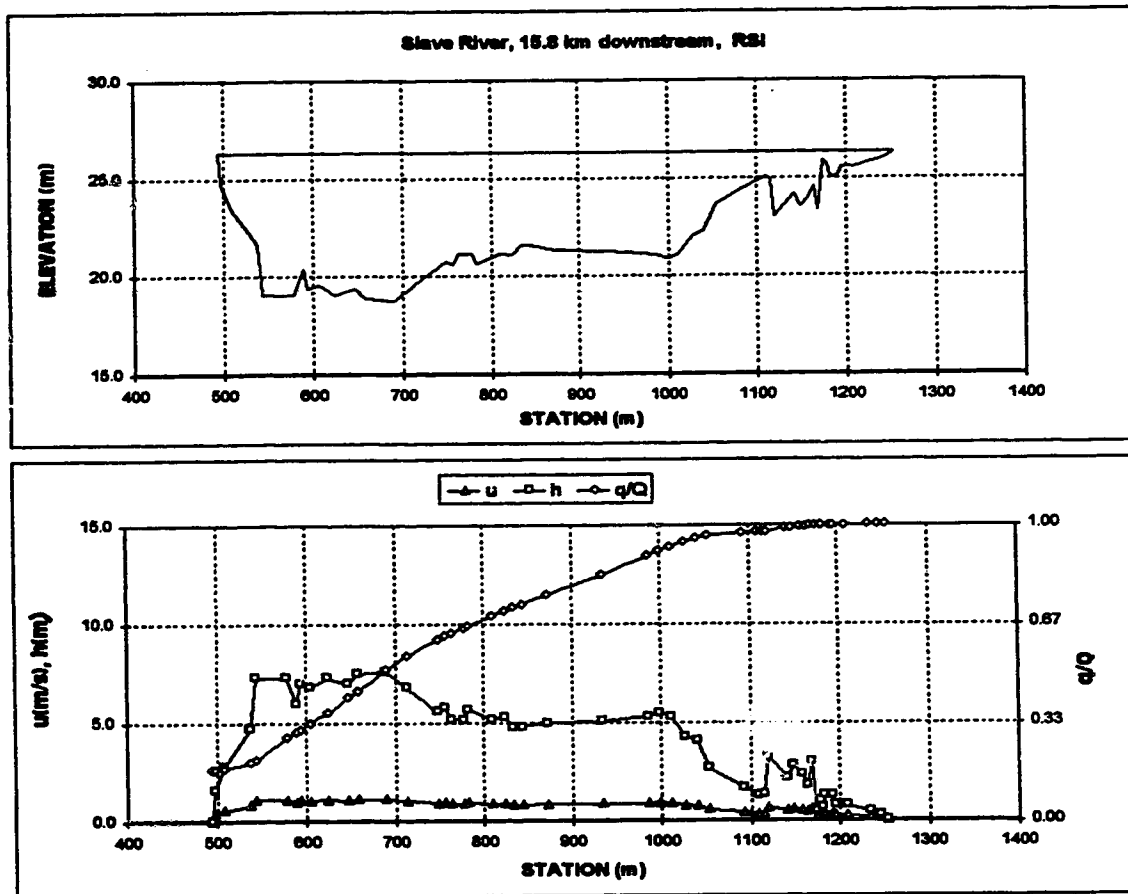
Appendix D.3 Slave River



Appendix D.3 Slave River

X-SECTION			Slave River, 15.8 km downstream, RSI					
DATE July, 1980								
CHANNEL Q m³/s			3147.68		TOTAL Q m³/s		3820	
WIDTH m			759.50		Avg. Water Surface Elev.		26.31	
DMEAN m			4.54		LB		493.50	
AREA m²			3450.72		RB		26.31	
VMEAN m/s			0.912					
Est. Sta.	assumed Elev	h	w/W	u	dq	q/Q	area	adj. u
m	m	m		m/s	m³		m²	m/s
493.50	26.31	0.00	0.000	0.000	0.00	0.17600	0.0	0.000
497.40	24.74	1.57	0.005	0.449	0.69	0.17616	3.1	0.398
508.00	23.54	2.77	0.019	0.656	12.71	0.17911	26.1	0.582
536.00	21.64	4.67	0.056	0.929	82.54	0.19828	130.2	0.824
543.00	19.04	7.27	0.065	1.248	45.49	0.20884	172.0	1.107
578.00	19.04	7.27	0.111	1.248	317.58	0.28258	426.5	1.107
588.00	20.34	5.97	0.124	1.094	77.54	0.30059	492.7	0.971
593.00	19.34	6.97	0.131	1.214	37.33	0.30925	525.0	1.076
605.00	19.54	6.77	0.147	1.190	99.08	0.33226	607.5	1.056
623.00	19.04	7.27	0.171	1.248	154.05	0.36803	733.8	1.107
647.00	19.34	6.97	0.202	1.214	210.32	0.41687	904.7	1.076
658.00	18.84	7.47	0.217	1.271	98.66	0.43978	984.1	1.127
689.90	18.74	7.57	0.259	1.282	306.23	0.51088	1224.0	1.137
713.00	19.54	6.77	0.289	1.190	204.75	0.55843	1389.6	1.056
748.00	20.74	5.57	0.335	1.045	241.34	0.61447	1605.6	0.927
756.00	20.54	5.77	0.346	1.070	47.96	0.62560	1650.9	0.949
763.00	21.14	5.17	0.355	0.994	39.52	0.63478	1689.2	0.882
778.00	21.14	5.17	0.375	0.994	77.11	0.65268	1768.8	0.882
783.00	20.84	5.67	0.381	1.057	27.80	0.65914	1793.9	0.938
809.20	21.14	5.17	0.416	0.994	145.67	0.69297	1935.9	0.882
823.00	21.04	5.27	0.434	1.007	72.08	0.70970	2007.9	0.893
833.00	21.54	4.77	0.447	0.942	48.93	0.72107	2058.1	0.836
843.00	21.54	4.77	0.460	0.942	44.95	0.73150	2105.8	0.836
872.70	21.34	4.97	0.499	0.968	138.18	0.76359	2250.5	0.859
933.00	21.24	5.07	0.579	0.981	295.12	0.83212	2553.2	0.871
986.00	21.04	5.27	0.648	1.007	272.43	0.89537	2827.2	0.893
998.00	20.84	5.47	0.684	1.032	65.71	0.91063	2891.6	0.916
1010.00	21.04	5.27	0.680	1.007	65.71	0.92589	2956.1	0.893
1027.00	22.04	4.27	0.702	0.875	76.32	0.94361	3037.1	0.776
1040.00	22.24	4.07	0.720	0.848	46.70	0.95445	3091.4	0.752
1053.00	23.64	2.67	0.737	0.640	32.58	0.96202	3135.2	0.568
1093.30	24.64	1.67	0.790	0.468	48.44	0.97327	3222.6	0.415
1109.00	25.04	1.27	0.810	0.390	9.90	0.97557	3245.7	0.346
1115.00	24.94	1.37	0.816	0.410	3.17	0.97630	3253.6	0.364
1120.00	23.04	3.27	0.825	0.733	6.63	0.97784	3265.2	0.650
1142.00	24.14	2.17	0.854	0.557	38.59	0.98680	3325.1	0.494
1148.00	23.54	2.77	0.862	0.658	8.99	0.98889	3339.9	0.582
1157.00	23.94	2.37	0.874	0.591	14.42	0.99224	3363.0	0.524
1163.00	24.54	1.77	0.882	0.486	6.69	0.99379	3375.4	0.431
1168.00	23.34	2.97	0.888	0.687	6.95	0.99540	3387.3	0.609
1175.00	25.84	0.47	0.897	0.201	5.34	0.99664	3399.3	0.178
1180.00	25.69	0.62	0.904	0.242	0.60	0.99678	3402.0	0.214
1182.00	25.04	1.27	0.907	0.390	0.60	0.99692	3403.9	0.346
1191.00	25.04	1.27	0.918	0.390	4.46	0.99796	3416.4	0.346
1195.00	25.54	0.77	0.924	0.279	1.36	0.99827	3419.4	0.248
1208.00	25.54	0.77	0.941	0.279	2.79	0.99892	3429.4	0.248
1234.00	25.84	0.47	0.975	0.201	3.87	0.99982	3445.6	0.178
1245.00	26.04	0.27	0.989	0.139	0.69	0.99998	3449.6	0.123
1253.00	26.31	0.00	1.000	0.000	0.07	1.00000	3450.7	0.000
Est. Total				3548.62				

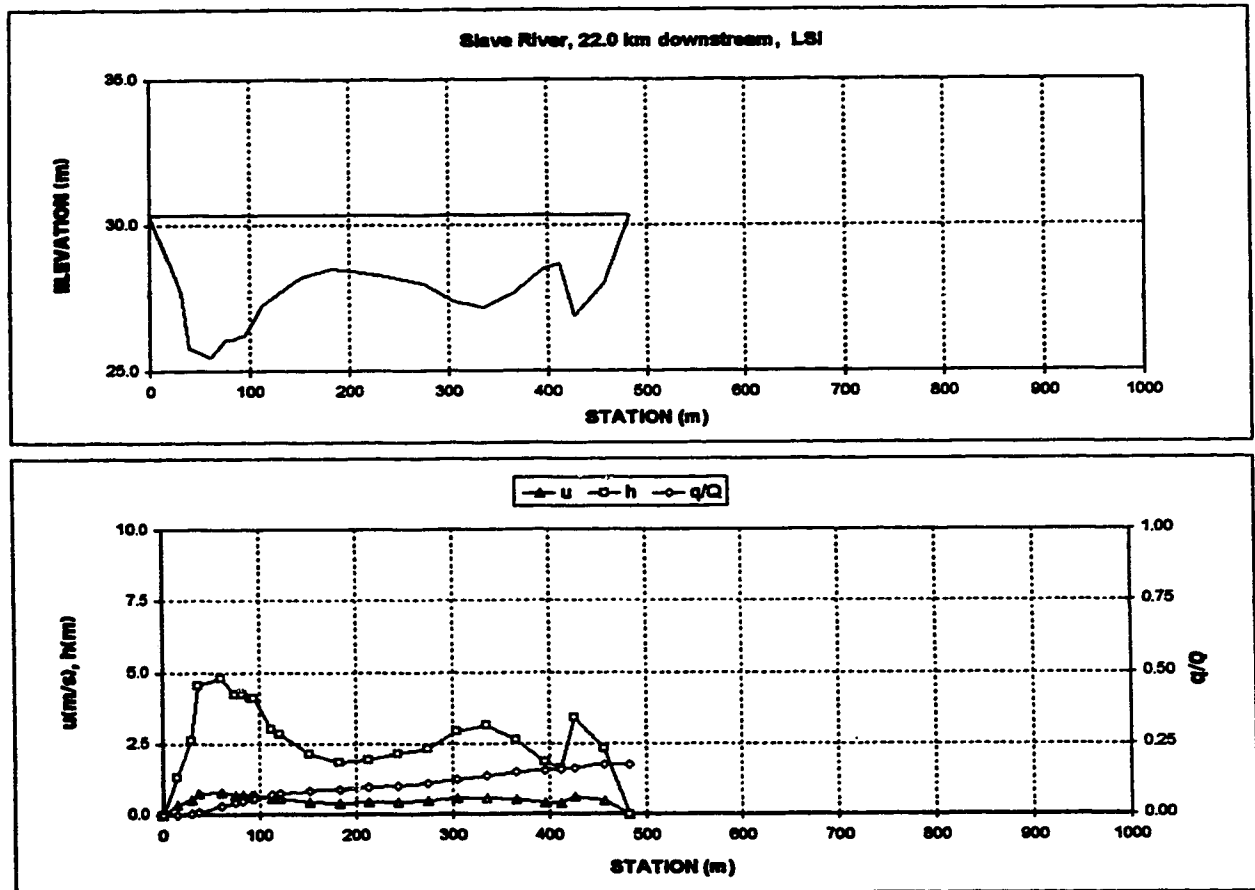
Appendix D.3 Slave River



Appendix D.3 Slave River

X-SECTION				Slave River, 22.0 km downstream, LSI					
DATE July, 1980									
CHANNEL Q m³/s				872.32		TOTAL Q m³/s		3820	
WIDTH m				483.00		Avg. Water Surface Elev.		30.30	
DMEAN m				2.57		LB		0.00 30.30	
AREA m²				1241.48		RB		483.00 30.30	
VMEAN m/s				0.542					
Est. Sta.	assumed Elev		h	ww	u	dq	q/Q	area	adj. u
m	m		m		m/s	m³		m²	m/s
0.00	30.30	0.00	0.00	0.000	0.000	0.00	0.00000	0.0	0.000
15.20	28.98	15.20	1.32	0.031	0.347	1.74	0.00043	10.0	0.328
30.50	27.68	30.50	2.62	0.063	0.549	13.50	0.00375	40.2	0.515
38.60	25.78	38.60	4.52	0.080	0.789	19.34	0.00850	89.1	0.741
61.00	25.48	61.00	4.82	0.128	0.824	84.38	0.02823	173.7	0.773
76.20	26.08	76.20	4.22	0.158	0.754	54.19	0.04255	242.4	0.708
82.30	26.08	82.30	4.22	0.170	0.754	19.40	0.04732	288.1	0.708
91.40	26.18	91.40	4.12	0.189	0.742	28.38	0.05429	306.1	0.696
94.50	26.18	94.50	4.12	0.198	0.742	9.47	0.05882	318.9	0.696
112.80	27.28	112.80	3.02	0.234	0.603	43.83	0.06742	384.2	0.586
121.90	27.48	121.90	2.82	0.252	0.576	15.87	0.07127	410.8	0.541
152.40	28.18	152.40	2.12	0.316	0.478	39.64	0.08101	486.1	0.447
182.90	28.48	182.90	1.82	0.379	0.430	27.23	0.08770	546.2	0.404
213.40	28.38	213.40	1.92	0.442	0.448	24.98	0.09384	603.2	0.419
243.80	28.18	243.80	2.12	0.505	0.478	28.31	0.10080	684.8	0.447
274.30	27.98	274.30	2.32	0.568	0.508	33.25	0.10897	732.3	0.475
304.80	27.38	304.80	2.92	0.631	0.590	43.77	0.11972	812.2	0.554
335.30	27.18	335.30	3.12	0.694	0.618	55.54	0.13337	904.4	0.579
365.80	27.68	365.80	2.62	0.757	0.549	50.88	0.14590	991.9	0.515
396.20	28.48	396.20	1.82	0.820	0.430	33.02	0.15402	1059.4	0.404
411.50	28.68	411.50	1.62	0.852	0.398	10.90	0.15870	1085.7	0.374
426.70	28.88	426.70	3.42	0.883	0.655	20.17	0.16185	1124.0	0.615
457.20	27.98	457.20	2.32	0.947	0.506	50.81	0.17414	1211.5	0.475
483.00	30.30	483.00	0.00	1.000	0.000	7.57	0.17800	1241.5	0.000
Est. Total						716.16			

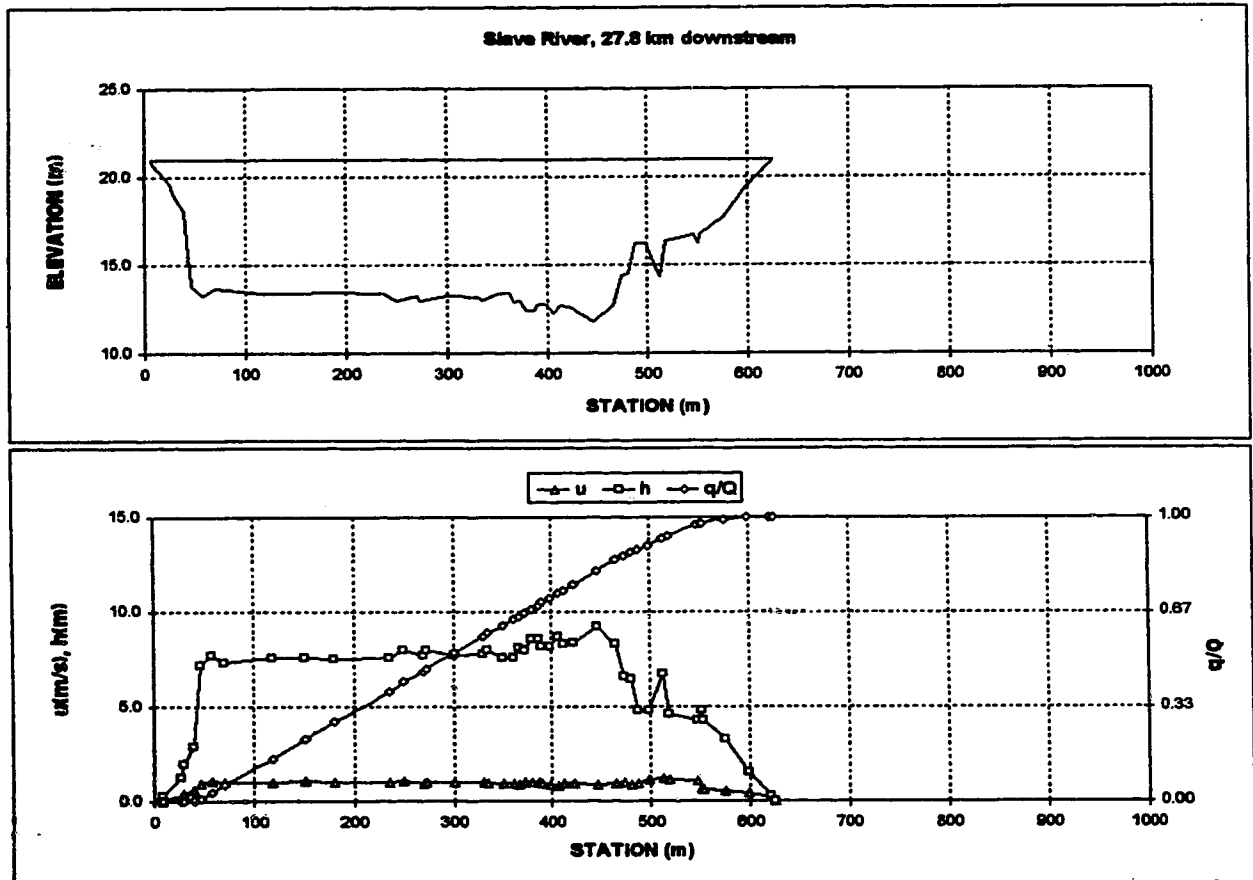
Appendix D.3 Slave River



Appendix D.3 Slave River

X-SECTION		Slave River, 27.8 km downstream						
DATE	July, 1980							
DISCHARGE m ³ /s		3820	Assumed Water Surface				20.97	
WIDTH m		617	Water Surface Elev.				20.97	
DMEAN m		6.46	Correction to Geodetic				n/a	
AREA m ²		3984.9	Correction to Station				0	
VMEAN m/s		0.959						
Est. Sta.	ssumed Elev	h	w/W	u	dq	q/Q	area	
m	m	m		m/s	m ³		m ²	
8.0	20.97	0.00	0.000	0.000	0.00	0.00000	0.0	
8.4	20.69	0.28	0.001	0.166	0.04	0.00001	0.1	
26.0	19.69	1.28	0.029	0.225	2.25	0.00060	13.8	
30.0	18.99	1.98	0.036	0.417	2.29	0.00120	20.3	
39.0	18.09	2.88	0.050	0.622	9.55	0.00370	42.2	
46.0	13.79	7.18	0.062	0.912	25.98	0.01050	77.4	
58.0	13.29	7.68	0.081	1.057	87.48	0.03340	166.5	
70.0	13.69	7.28	0.100	0.982	101.61	0.06000	256.3	
117.9	13.39	7.58	0.178	1.007	336.16	0.14800	612.2	
151.0	13.39	7.58	0.232	1.058	275.04	0.22000	863.1	
181.0	13.49	7.48	0.260	0.996	229.20	0.28000	1089.0	
235.0	13.39	7.58	0.368	1.022	401.10	0.38500	1485.6	
250.0	12.99	7.98	0.392	1.050	133.70	0.42000	1612.3	
269.0	13.29	7.68	0.423	0.954	146.16	0.45800	1761.1	
272.0	12.99	7.98	0.426	0.976	19.10	0.46300	1784.6	
300.0	13.29	7.68	0.473	0.991	217.74	0.52000	2003.8	
330.0	13.19	7.78	0.522	0.988	229.20	0.58000	2235.7	
334.9	12.99	7.98	0.530	0.906	38.20	0.59000	2274.3	
350.0	13.39	7.58	0.554	0.951	103.14	0.61700	2391.8	
361.0	13.39	7.58	0.572	0.967	87.88	0.64000	2475.2	
367.0	12.89	8.08	0.582	0.877	38.20	0.65000	2522.2	
372.0	12.99	7.98	0.590	0.975	38.20	0.66000	2562.3	
379.0	12.44	8.53	0.601	0.975	57.30	0.67500	2620.1	
386.0	12.44	8.53	0.613	1.025	57.30	0.69000	2679.8	
390.0	12.79	8.18	0.619	0.966	38.20	0.70000	2713.2	
398.0	12.79	8.18	0.632	0.962	57.30	0.71500	2776.7	
406.0	12.29	8.68	0.645	0.807	57.30	0.73000	2846.1	
412.0	12.69	8.28	0.655	0.911	38.20	0.74000	2897.0	
422.0	12.59	8.38	0.671	0.909	84.04	0.76200	2980.3	
446.0	11.79	9.18	0.710	0.893	183.36	0.81000	3191.0	
465.0	12.69	8.28	0.741	0.932	152.80	0.85000	3356.9	
473.0	14.39	6.58	0.754	0.981	57.30	0.86500	3416.3	
480.0	14.49	6.48	0.765	0.898	45.84	0.87700	3462.0	
487.0	16.19	4.78	0.776	0.955	30.56	0.88500	3501.4	
496.0	16.19	4.78	0.784	1.151	57.30	0.90000	3554.0	
512.0	14.29	6.68	0.817	1.173	95.50	0.92500	3634.2	
516.0	16.39	4.58	0.827	1.154	36.20	0.93500	3668.0	
547.0	16.69	4.28	0.874	1.087	146.98	0.97400	3796.5	
552.0	16.19	4.78	0.882	0.691	15.26	0.97800	3819.1	
553.1	16.69	4.28	0.883	0.609	3.82	0.97900	3824.1	
575.0	17.69	3.28	0.919	0.544	49.66	0.99200	3906.9	
599.0	19.44	1.53	0.958	0.390	26.74	0.99900	3964.6	
620.7	20.69	0.28	0.993	0.189	3.44	0.99990	3984.3	
625.0	20.97	0.00	1.000	0.000	0.38	1.00000	3984.9	
8.0	21.0							
Est. Total				3820.00				

Appendix D.3 Slave River



Appendix D.4 South Saskatchewan River

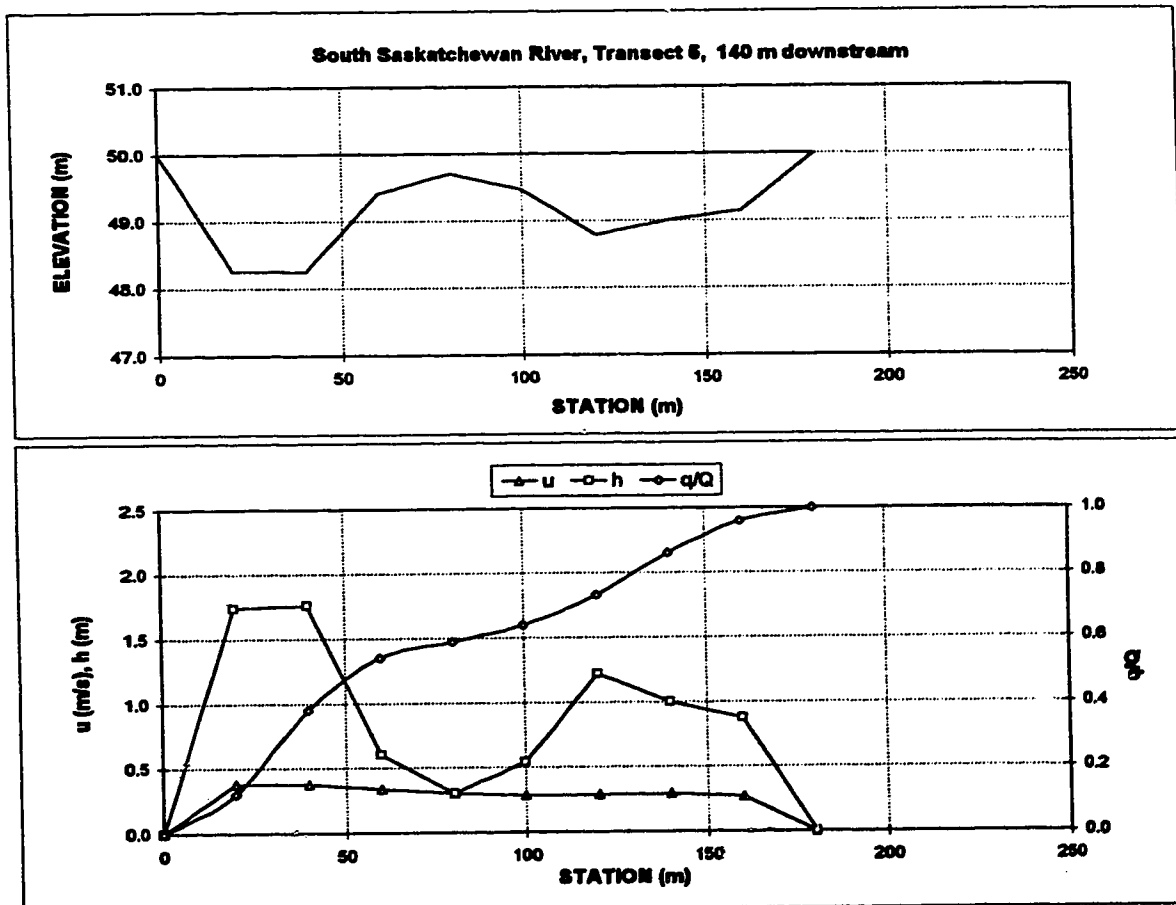
X-SECTION
DATE
DISCHARGE m³/s
WIDTH m
DMEAN m
AREA m²
VMEAN m/s

South Saskatchewan River, Transect 5, 140 m downstream
August, 1984
52
180.0
0.89
180.6
0.324

Assumed Water Surf. Elev. 50.00

Sta. m	Elev. m	h m	w/W	est. u m/s	dq m ³	q/Q	area m ²
0.0	50.00	0.00	0.00	0.000	0.00	0.00000	0.0
20.0	48.26	1.74	0.11	0.377	8.24	0.12000	17.4
40.0	48.24	1.76	0.22	0.373	13.52	0.38000	52.4
60.0	49.40	0.60	0.33	0.335	8.32	0.54000	78.0
80.0	49.70	0.30	0.44	0.299	2.60	0.59000	85.0
100.0	49.46	0.54	0.56	0.280	2.60	0.64000	93.4
120.0	48.78	1.22	0.67	0.287	4.68	0.73000	111.0
140.0	49.00	1.00	0.78	0.292	6.76	0.86000	133.2
160.0	49.13	0.87	0.89	0.266	5.20	0.98000	151.9
180.0	50.00	0.00	1.00	0.000	2.08	1.00000	180.6
0	50.00						

Total Flow 52.00

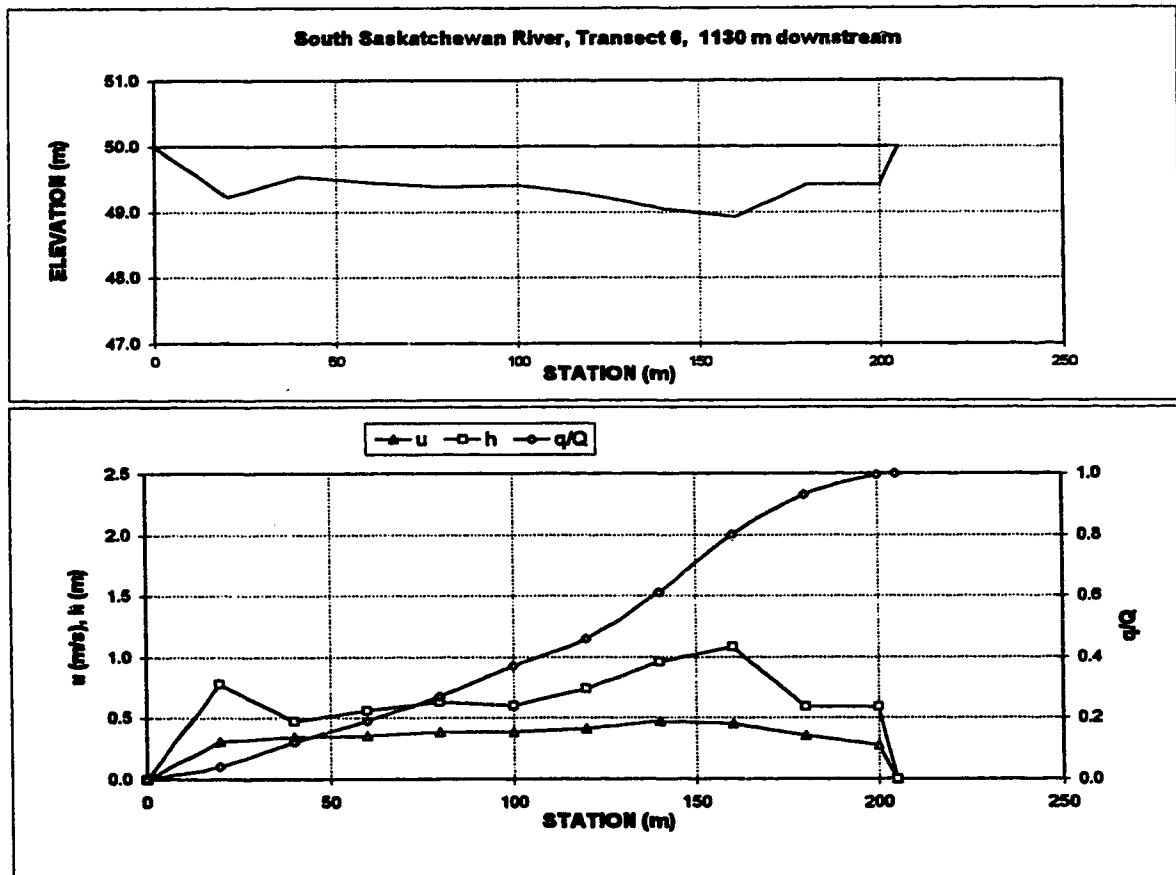


Appendix D.4 South Saskatchewan River

X-SECTION South Saskatchewan River, Transect 6, 1130 m downstream
 DATE August, 1984
 DISCHARGE m³/s 52
 WIDTH m 205.0 Assumed Water Surf. Elev. 50.00
 DMEAN m 0.68
 AREA m² 135.6
 VMEAN m/s 0.384

Sta. m	Elev. m	h m	w/W	est. u m/s	dq m ³	q/Q	area m ²
0.0	50.00	0.00	0.00	0.000	0.00	0.00000	0.0
20.0	49.22	0.78	0.10	0.307	2.08	0.04000	7.8
40.0	49.53	0.47	0.20	0.342	4.16	0.12000	20.3
60.0	49.44	0.56	0.29	0.351	3.84	0.19000	30.6
80.0	49.37	0.63	0.39	0.387	4.16	0.27000	42.5
100.0	49.40	0.60	0.49	0.384	5.20	0.37000	54.8
120.0	49.26	0.74	0.59	0.411	4.68	0.48000	68.2
140.0	49.04	0.96	0.68	0.473	7.80	0.61000	85.2
160.0	48.92	1.08	0.78	0.449	9.88	0.80000	105.6
180.0	49.41	0.59	0.88	0.356	6.76	0.93000	122.3
200.0	49.41	0.59	0.98	0.274	3.38	0.99500	134.1
205.0	50.00	0.00	1.00	0.000	0.26	1.00000	135.6
0	50.00						

Total Flow 52.00



Appendix D.4 South Saskatchewan River

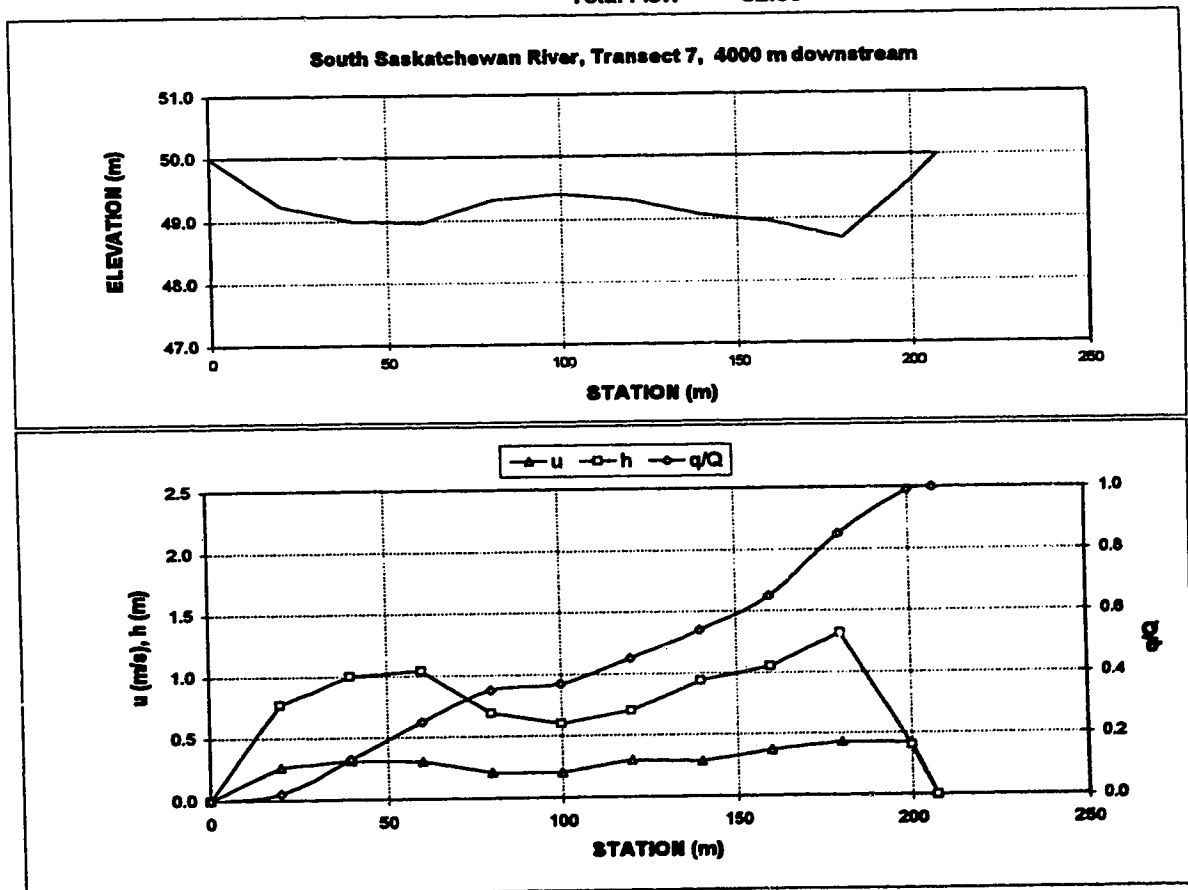
X-SECTION
 DATE
 DISCHARGE m³/s
 WIDTH m
 DMEAN m
 AREA m²
 VMEAN m/s

South Saskatchewan River, Transect 7, 4000 m downstream
 August, 1984
 52
 207.0
 0.81
 167.6
 0.310

Assumed Water Surf. Elev. 50.00

Sta. m	Elev. m	h m	w/W	est. u m/s	dq m ³	q/Q	area m ²
0.0	50.00	0.00	0.00	0.000	0.00	0.00000	0.0
20.0	49.23	0.77	0.10	0.266	1.04	0.02000	7.7
40.0	49.00	1.00	0.19	0.314	5.72	0.13000	25.4
60.0	48.96	1.04	0.29	0.303	6.24	0.25000	45.8
80.0	49.31	0.69	0.39	0.207	5.20	0.35000	63.1
100.0	49.40	0.60	0.48	0.201	1.04	0.37000	76.0
120.0	49.30	0.70	0.58	0.301	4.16	0.45000	89.0
140.0	49.06	0.94	0.68	0.287	4.68	0.54000	105.4
160.0	48.95	1.05	0.77	0.370	5.72	0.65000	125.3
180.0	48.68	1.32	0.87	0.432	10.40	0.85000	149.0
200.0	49.60	0.40	0.97	0.419	7.28	0.99000	166.2
207.0	50.00	0.00	1.00	0.000	0.52	1.00000	167.6
0	50.00						

Total Flow 52.00

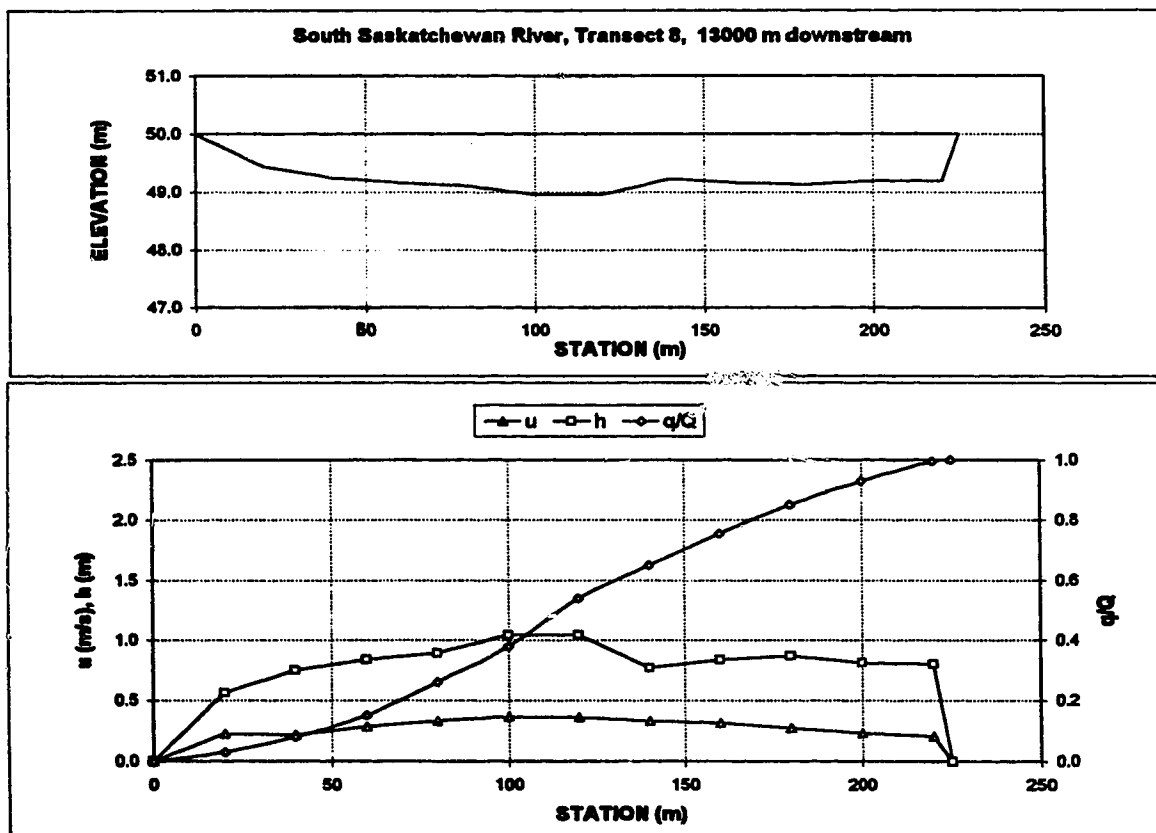


Appendix D.4 South Saskatchewan River

X-SECTION	South Saskatchewan River, Transect 8, 13000 m downstream		
DATE	August, 1984		
DISCHARGE m³/s	52		
WIDTH m	225.0	Assumed Water Surf. Elev.	50.00
DMEAN m	0.79		
AREA m²	178.2		
VMEAN m/s	0.292		

Sta. m	Elev. m	h m	w/W	est. u m/s	dq m ³	q/Q	area m ²
0.0	50.00	0.00	0.00	0.000	0.00	0.00000	0.0
20.0	49.44	0.56	0.09	0.222	1.56	0.03000	5.6
40.0	49.25	0.75	0.18	0.215	2.60	0.08000	18.7
60.0	49.16	0.84	0.27	0.282	3.64	0.15000	34.6
80.0	49.11	0.89	0.36	0.327	5.72	0.28000	51.9
100.0	48.96	1.04	0.44	0.363	6.24	0.38000	71.2
120.0	48.96	1.04	0.53	0.361	8.32	0.54000	92.0
140.0	49.23	0.77	0.62	0.327	5.72	0.65000	110.1
160.0	49.16	0.84	0.71	0.313	5.46	0.75500	126.2
180.0	49.13	0.87	0.80	0.268	4.94	0.85000	143.3
200.0	49.19	0.81	0.89	0.229	4.16	0.93000	160.1
220.0	49.20	0.80	0.98	0.201	3.38	0.99500	176.2
225.0	50.00	0.00	1.00	0.000	0.26	1.00000	178.2
0	50.00						

Total Flow 52.00



Appendix D.5 Athabasca River

X-SECTION Athabasca River, 60 m downstream

ORIGINAL SURVEY 28-May-74

TREATMENT DATE 4-Jun-75

DISCHARGE m^3/s 484.00

Assumed

WIDTH m 188.04

Water Surface Elev.

101.64

MEAN DEPTH m 3.34

LB

7.58

101.64

AREA m^2 627.39

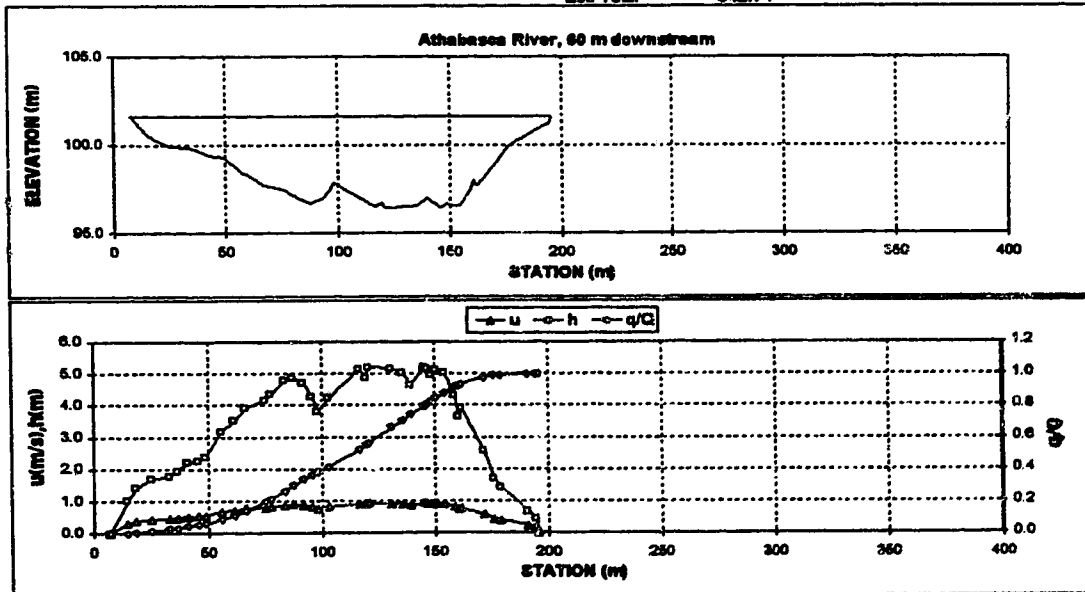
RB

195.61

101.64

MEAN VELOCITY m/s 0.771

Sta.	Elev.		h	w/W	u	dq est.	norm. q/Q	Area	adjusted u
m	m		m		m/s	m^3		m^2	m/s
7.58	101.64	7.58	0.00	0.000	0.000	0.00	0.00000	0.0	0.000
14.80	100.63	14.80	1.01	0.038	0.348	0.63	0.00117	3.6	0.310
18.46	100.24	18.46	1.40	0.058	0.432	1.72	0.00434	8.1	0.385
25.47	99.93	25.47	1.71	0.085	0.484	5.05	0.01364	19.0	0.440
33.40	99.87	33.40	1.77	0.137	0.505	8.89	0.02634	32.8	0.451
37.36	99.69	37.36	1.95	0.158	0.539	3.85	0.03343	40.1	0.481
41.32	99.45	41.32	2.19	0.179	0.583	4.80	0.04190	48.3	0.520
45.59	99.38	45.59	2.28	0.202	0.595	5.59	0.05221	57.8	0.531
48.84	99.26	48.84	2.38	0.220	0.616	4.70	0.06087	65.6	0.549
56.56	98.47	56.56	3.17	0.261	0.746	14.39	0.08739	86.7	0.665
61.74	98.13	61.74	3.51	0.288	0.798	13.35	0.11200	104.0	0.712
66.62	97.74	66.62	3.90	0.314	0.856	14.85	0.13855	122.1	0.763
75.16	97.49	75.16	4.15	0.359	0.892	30.05	0.19491	156.5	0.786
77.90	97.31	77.90	4.33	0.374	0.918	10.52	0.21428	168.1	0.819
83.99	96.85	83.99	4.79	0.408	0.982	26.38	0.26289	195.9	0.876
87.65	96.76	87.65	4.88	0.428	0.994	17.48	0.29510	213.8	0.887
92.22	96.92	92.22	4.72	0.450	0.972	21.57	0.33484	235.5	0.867
95.58	97.37	95.58	4.27	0.468	0.909	14.21	0.36102	250.6	0.811
98.02	97.86	98.02	3.78	0.481	0.838	8.58	0.37683	260.4	0.748
103.50	97.43	103.50	4.21	0.510	0.901	19.04	0.41191	282.3	0.803
116.91	96.49	116.91	5.15	0.581	1.030	60.80	0.52357	345.1	0.919
119.66	96.76	119.66	4.88	0.596	0.994	13.98	0.54929	358.9	0.887
121.18	96.46	121.18	5.18	0.604	1.034	7.75	0.56358	366.5	0.923
131.24	96.49	131.24	5.15	0.658	1.030	53.65	0.66243	418.5	0.919
135.81	96.81	135.81	5.03	0.682	1.014	23.78	0.70825	441.7	0.905
139.77	97.01	139.77	4.63	0.703	0.980	18.88	0.74104	460.9	0.856
145.56	96.46	145.56	5.18	0.734	1.034	28.32	0.79321	489.3	0.923
147.09	96.49	147.09	5.15	0.742	1.030	8.16	0.80825	497.2	0.919
148.92	96.79	148.92	4.94	0.752	1.002	9.38	0.82554	506.4	0.894
151.05	96.65	151.05	5.09	0.763	1.022	10.81	0.84546	517.1	0.912
154.71	96.81	154.71	5.03	0.782	1.014	18.86	0.88021	535.6	0.905
158.67	97.34	158.67	4.30	0.804	0.914	17.81	0.91302	554.1	0.815
160.80	98.01	160.80	3.83	0.815	0.816	7.30	0.92648	562.5	0.728
162.02	97.71	162.02	3.93	0.821	0.860	3.87	0.93360	567.1	0.767
171.47	99.08	171.47	2.56	0.872	0.848	23.11	0.97618	597.8	0.577
176.35	99.93	176.35	1.71	0.898	0.494	5.94	0.98712	608.2	0.440
179.40	100.21	179.40	1.43	0.914	0.438	2.23	0.99123	613.0	0.391
190.98	100.97	190.98	0.67	0.975	0.264	4.27	0.99911	625.2	0.236
194.64	101.21	194.64	0.43	0.995	0.197	0.46	0.99996	627.2	0.175
195.61	101.64	195.61	0.00	1.000	0.000	0.02	1.00000	627.4	0.000
Est. Total						542.74			



Appendix D.5 Athabasca River

X-SECTION Athabasca River, 280 m downstream

ORIGINAL SURVEY 28-May-74

TREATMENT DATE 4-Jun-75

DISCHARGE m^3/s 484.00

Assumed

WIDTH m 220.88

Avg. Water Surface Elev.

MEAN DEPTH m 2.87

LS

101.64

AREA m^2 880.72

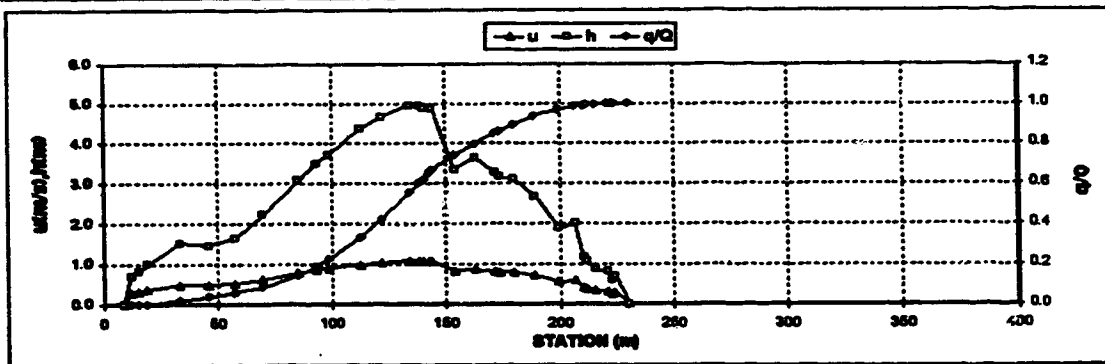
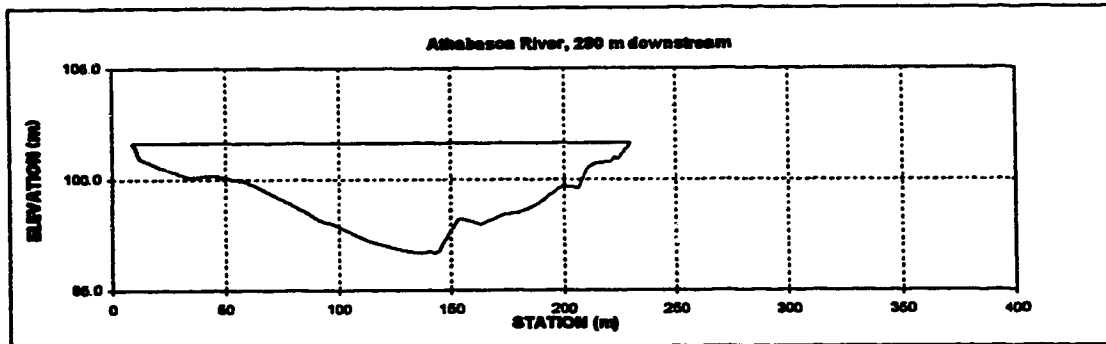
RS

229.88

101.64

MEAN VELOCITY m/s 0.816

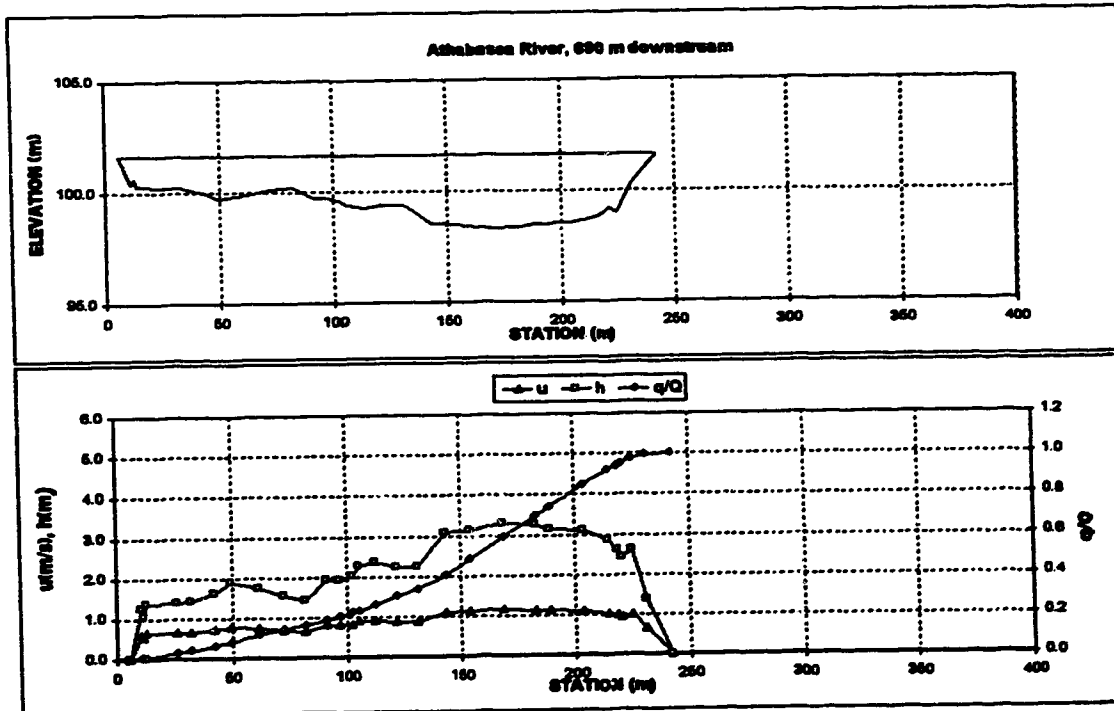
Sta.	Elev.	h	w/W	u	dq est.	norm. q/Q	Area	adjusted u
m	m	m		m/s	m^3		m^2	m/s
8.86	101.64	8.86	0.00	0.000	0.00	0.00000	0.0	0.000
12.03	100.84	12.03	0.70	0.014	0.335	0.18	0.00032	1.1
18.08	100.82	15.08	0.82	0.028	0.373	0.82	0.00181	3.4
19.04	100.83	18.04	1.01	0.046	0.428	1.45	0.00443	7.0
33.38	100.12	33.38	1.52	0.110	0.882	8.97	0.02086	25.1
45.86	100.18	45.86	1.48	0.188	0.547	10.09	0.03851	43.3
57.75	99.99	57.75	1.85	0.221	0.584	10.82	0.05849	62.3
69.94	99.41	69.94	2.23	0.276	0.726	15.61	0.08673	85.9
85.18	98.56	85.18	3.08	0.345	0.901	32.91	0.14828	126.4
92.80	98.13	92.80	3.51	0.379	0.983	23.84	0.18006	151.5
98.90	97.82	98.90	3.72	0.407	1.021	22.10	0.22804	173.5
112.61	97.28	112.61	4.38	0.489	1.135	58.73	0.33713	228.9
121.76	96.96	121.76	4.86	0.510	1.187	47.92	0.42384	270.2
133.85	96.70	133.85	4.94	0.586	1.234	70.83	0.55202	328.7
138.52	96.70	138.52	4.94	0.586	1.234	27.86	0.60244	351.3
140.04	96.76	140.04	4.88	0.563	1.224	8.17	0.61804	358.7
143.08	96.73	143.08	4.81	0.607	1.229	18.31	0.65218	373.7
144.31	96.78	144.31	4.88	0.612	1.224	7.33	0.68543	378.6
163.78	96.29	163.78	3.36	0.855	0.952	42.32	0.74201	418.5
182.80	97.96	182.80	3.88	0.867	1.010	31.44	0.78890	450.6
171.54	98.35	171.54	3.29	0.736	0.941	28.29	0.85191	480.6
173.27	98.47	173.27	3.17	0.743	0.918	5.19	0.86131	486.2
179.67	98.53	179.67	3.11	0.772	0.806	18.33	0.89449	506.3
188.91	98.86	188.91	2.68	0.814	0.821	23.10	0.93629	533.0
189.48	98.75	189.48	1.83	0.862	0.850	17.78	0.98843	557.2
208.49	98.63	208.49	2.01	0.884	0.877	8.07	0.98485	570.8
210.15	100.48	210.15	1.18	0.910	0.469	3.33	0.99087	576.6
211.62	100.57	211.62	1.07	0.917	0.445	0.75	0.99223	578.3
215.02	100.78	215.02	0.88	0.932	0.390	1.58	0.99473	581.6
220.51	100.82	220.51	0.82	0.957	0.373	1.78	0.99795	586.3
222.64	101.03	222.64	0.61	0.967	0.308	0.52	0.99889	587.8
223.86	100.84	223.86	0.70	0.972	0.335	0.28	0.99835	588.6
229.88	101.64	229.88	0.00	1.000	0.000	0.36	1.00000	590.7
Est. Total					552.62			



Appendix D.5 Athabasca River

X-SECTION Athabasca River, 680 m downstream		ORIGINAL SURVEY 28-May-74	
TREATMENT DATE	4-Jun-75		
DISCHARGE m^3/s	484.00	Assumed	
WIDTH m	238.20	Water Surface Elev.	101.64
MEAN DEPTH m	2.21	LB	101.64
AREA m^2	521.61	RB	101.64
MEAN VELOCITY m/s	0.928		

Sta.	Elev.	h	w/W	u	eq est.	norm. q/Q	Area	adjusted u
m	m	m		m/s	m^3		m^2	m/s
5.85	101.64	5.85	0.00	0.000	0.00	0.00000	0.0	0.000
10.73	100.39	10.73	1.25	0.021	0.635	0.97	0.00187	3.1
11.95	100.60	11.95	1.04	0.026	0.562	0.84	0.00349	4.4
13.15	100.27	13.15	1.37	0.031	0.675	0.89	0.00522	5.9
26.55	100.24	26.55	1.40	0.068	0.685	12.62	0.02886	24.5
32.65	100.21	32.65	1.43	0.113	0.694	5.95	0.04117	33.1
42.15	100.02	42.15	1.82	0.154	0.755	10.50	0.06150	47.6
48.45	99.75	48.45	1.89	0.185	0.836	10.19	0.06123	60.4
61.65	99.90	61.65	1.74	0.236	0.792	18.02	0.11613	82.5
72.25	100.09	72.25	1.55	0.281	0.733	13.29	0.14186	100.0
82.05	100.21	82.05	1.43	0.323	0.694	10.42	0.16203	114.6
91.15	99.72	91.15	1.82	0.361	0.845	11.73	0.18475	129.8
96.95	99.72	96.95	1.82	0.396	0.845	9.41	0.20296	140.9
102.15	99.63	102.15	2.01	0.408	0.871	8.77	0.21996	151.2
105.25	99.38	105.25	2.26	0.421	0.942	6.00	0.23158	157.8
112.55	99.29	112.55	2.35	0.452	0.967	16.07	0.28269	174.6
121.65	99.41	121.65	2.23	0.490	0.934	19.51	0.30104	185.4
130.85	99.41	130.85	2.23	0.526	0.934	19.16	0.33614	216.0
143.05	98.56	143.05	3.08	0.581	1.158	33.89	0.40376	248.4
154.25	98.50	154.25	3.14	0.626	1.173	40.61	0.46239	283.2
168.95	98.35	168.95	3.29	0.691	1.211	56.33	0.59147	330.4
182.65	98.38	182.65	3.26	0.749	1.203	54.15	0.69631	375.3
188.75	98.50	188.75	3.14	0.774	1.173	23.20	0.74122	394.8
203.95	98.53	203.95	3.11	0.839	1.166	55.56	0.84880	442.3
214.95	98.77	214.95	2.87	0.885	1.105	37.35	0.82111	475.2
218.65	99.02	218.65	2.62	0.901	1.040	10.89	0.94220	486.4
221.05	99.23	221.05	2.41	0.911	0.984	6.11	0.96403	491.4
225.25	99.02	225.25	2.62	0.929	1.040	10.69	0.97472	502.0
231.45	100.27	231.45	1.37	0.955	0.675	10.61	0.96326	514.3
242.05	101.64	242.05	0.00	1.000	0.000	2.45	1.00000	521.6
Est. Total					516.47			



Appendix D.5 Athabasca River

X-SECTION Athabasca River, 1760 m downstream

ORIGINAL SURVEY 12-Sep-75

TREATMENT DATE 4-Jun-77

DISCHARGE m^3/s 484.66

Assumed

WIDTH m 374.06

Water Surface Elev.

MEAN DEPTH m 1.72

LB

3.27

AREA m^2 642.41

RB

377.36

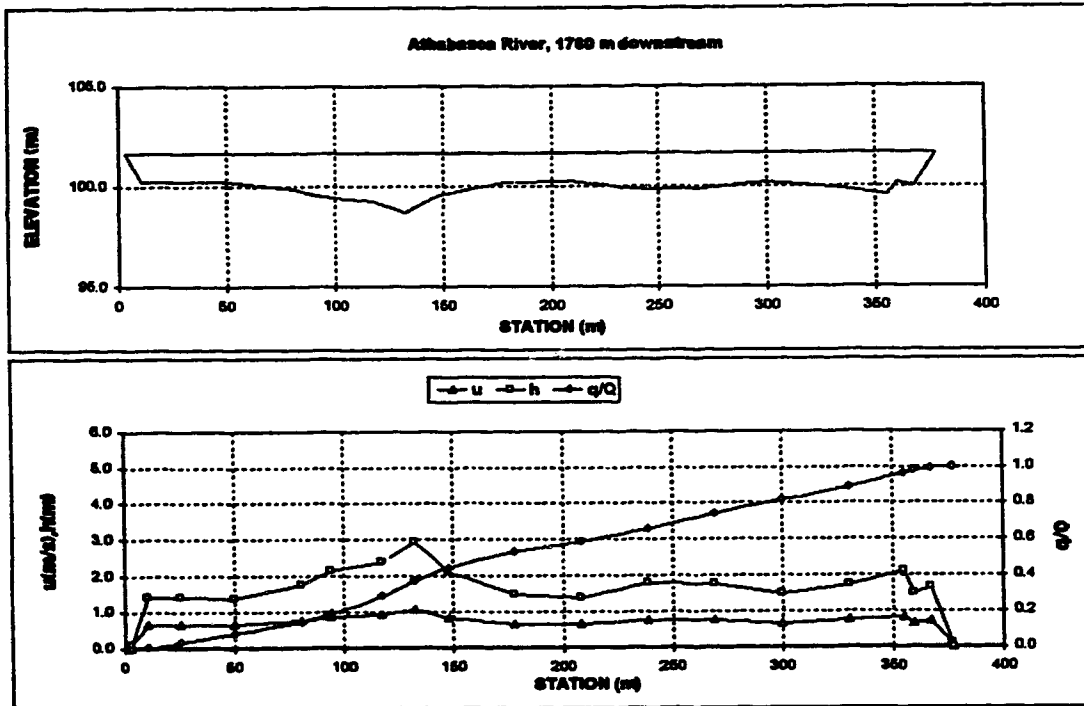
MEAN VELOCITY m/s 0.753

101.84

101.84

101.84

Sta. m	Elev. m	t m	w/W	u m/s	dq est. m^3	norm. q/Q	Area m^2	adjusted u m/s
3.27	101.84	3.27	0.00	0.000	0.00	0.00000	0.0	0.000
3.53	101.55	3.53	0.06	0.001	0.00	0.00000	0.0	0.098
11.15	100.21	11.16	1.43	0.021	0.095	2.20	5.8	0.649
25.78	100.21	25.78	1.43	0.080	0.685	13.88	28.6	0.649
50.18	100.24	50.18	1.39	0.125	0.856	22.72	61.0	0.639
80.84	99.87	80.84	1.78	0.207	0.766	34.19	109.1	0.747
94.36	99.48	94.36	2.16	0.243	0.677	22.07	136.0	0.855
117.22	99.23	117.22	2.40	0.305	0.942	47.39	188.1	0.918
132.46	98.99	132.46	2.95	0.345	1.061	41.23	228.8	1.054
147.70	98.52	147.70	2.10	0.386	0.867	37.32	267.3	0.839
178.18	98.17	178.18	1.48	0.468	0.684	42.17	321.9	0.967
208.06	97.84	208.06	1.39	0.549	0.656	29.42	365.8	0.839
239.14	97.57	239.14	1.78	0.631	0.775	34.74	414.3	0.755
269.82	97.27	269.82	1.78	0.712	0.766	41.71	468.5	0.747
300.10	96.15	300.10	1.49	0.793	0.684	35.89	518.0	0.967
330.58	99.90	330.53	1.73	0.875	0.757	35.33	567.0	0.736
354.96	99.54	354.96	2.10	0.940	0.861	37.73	613.6	0.839
369.54	100.15	369.54	1.48	0.952	0.684	6.33	621.8	0.967
367.16	99.97	367.16	1.57	0.973	0.739	8.56	633.8	0.721
376.91	101.55	376.91	0.08	0.999	0.101	3.59	642.4	0.098
377.36	101.84	377.36	0.00	1.000	0.000	1.00000	642.4	0.000
Est. Total					486.46			



Appendix D.5 Athabasca River

X-SECTION Athabasca River, 2740 m downstream

ORIGINAL SURVEY 17-Sep-74

TREATMENT DATE 4-Jun-75

DISCHARGE m^3/s 484.00

Assumed

WIDTH m 313.88

Water Surface Elev.

101.30

MEAN DEPTH m 1.71

LS 28.85

101.30

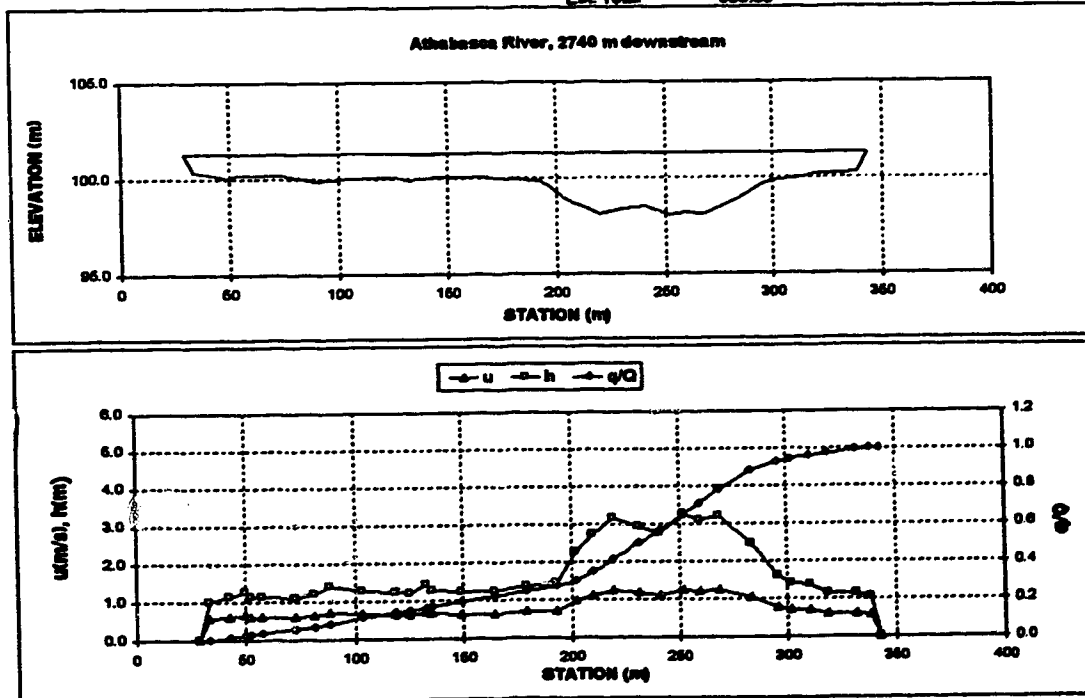
AREA m^2 538.44

RS 342.83

101.30

MEAN VELOCITY m/s 0.898

Sta.	Elev.		h	w/W	u	sq est.	norm. q/Q	Area	adjusted u
m	m		m		m/s	m^2		m^2	m/s
28.95	101.30	28.95	0.00	0.000	0.000	0.00	0.00000	0.0	0.000
33.53	100.30	33.53	1.01	0.015	0.829	0.72	0.00135	2.3	0.898
42.55	100.18	42.53	1.13	0.044	0.678	6.34	0.01318	12.0	0.813
50.05	100.02	50.03	1.29	0.087	0.742	6.33	0.02500	20.9	0.870
52.43	100.18	52.43	1.13	0.075	0.678	2.05	0.02884	23.8	0.813
57.93	100.18	57.93	1.13	0.082	0.678	4.20	0.03867	30.0	0.813
73.13	100.21	73.13	1.10	0.141	0.888	11.35	0.05788	48.9	0.802
81.33	100.09	81.33	1.22	0.167	0.714	6.84	0.07006	86.3	0.845
88.43	99.90	88.43	1.41	0.189	0.787	6.98	0.08310	85.8	0.711
103.63	100.02	103.63	1.29	0.238	0.742	15.82	0.11227	88.1	0.870
118.83	100.06	118.83	1.24	0.288	0.728	14.11	0.13881	105.3	0.888
125.53	100.09	125.53	1.22	0.308	0.714	5.93	0.14988	113.5	0.845
132.93	99.87	132.93	1.44	0.331	0.788	7.41	0.16383	123.3	0.721
135.63	100.02	135.63	1.29	0.340	0.742	2.83	0.16880	127.0	0.870
149.33	100.06	149.33	1.24	0.383	0.728	12.72	0.19254	144.4	0.888
164.63	100.06	164.63	1.24	0.432	0.728	13.83	0.21836	163.4	0.888
179.83	99.93	179.83	1.38	0.481	0.778	14.85	0.24828	183.3	0.701
182.93	99.87	182.93	1.44	0.522	0.788	14.48	0.27332	201.7	0.721
202.43	99.05	202.43	2.28	0.552	1.079	16.45	0.30403	219.2	0.875
210.33	98.56	210.33	2.74	0.578	1.230	22.60	0.34890	239.0	1.112
219.43	98.13	219.43	3.18	0.607	1.358	34.83	0.41181	285.9	1.225
231.03	98.38	231.03	2.83	0.644	1.283	48.88	0.49877	301.3	1.160
240.83	98.53	240.83	2.77	0.675	1.239	35.23	0.58454	329.2	1.120
252.03	98.04	252.03	3.27	0.710	1.381	44.31	0.64728	363.1	1.248
259.73	98.20	259.73	3.11	0.735	1.338	33.31	0.70848	387.6	1.207
268.53	98.10	268.53	3.21	0.763	1.384	37.48	0.77842	415.4	1.233
283.43	98.84	283.43	2.47	0.810	1.145	53.00	0.87836	457.6	1.036
295.63	99.69	295.63	1.81	0.849	0.884	25.00	0.82502	482.5	0.780
301.73	99.90	301.73	1.41	0.889	0.787	7.80	0.93821	491.7	0.711
318.93	99.93	310.93	1.38	0.898	0.778	9.98	0.95787	504.5	0.701
319.13	100.18	319.13	1.13	0.824	0.879	7.45	0.97178	514.7	0.813
332.23	100.18	332.23	1.13	0.886	0.879	10.00	0.99045	529.5	0.813
338.33	100.27	338.33	1.04	0.985	0.842	4.35	0.99857	536.1	0.580
342.83	101.30	342.83	0.00	1.000	0.000	0.77	1.00000	538.4	0.000
Est. Total						535.66			



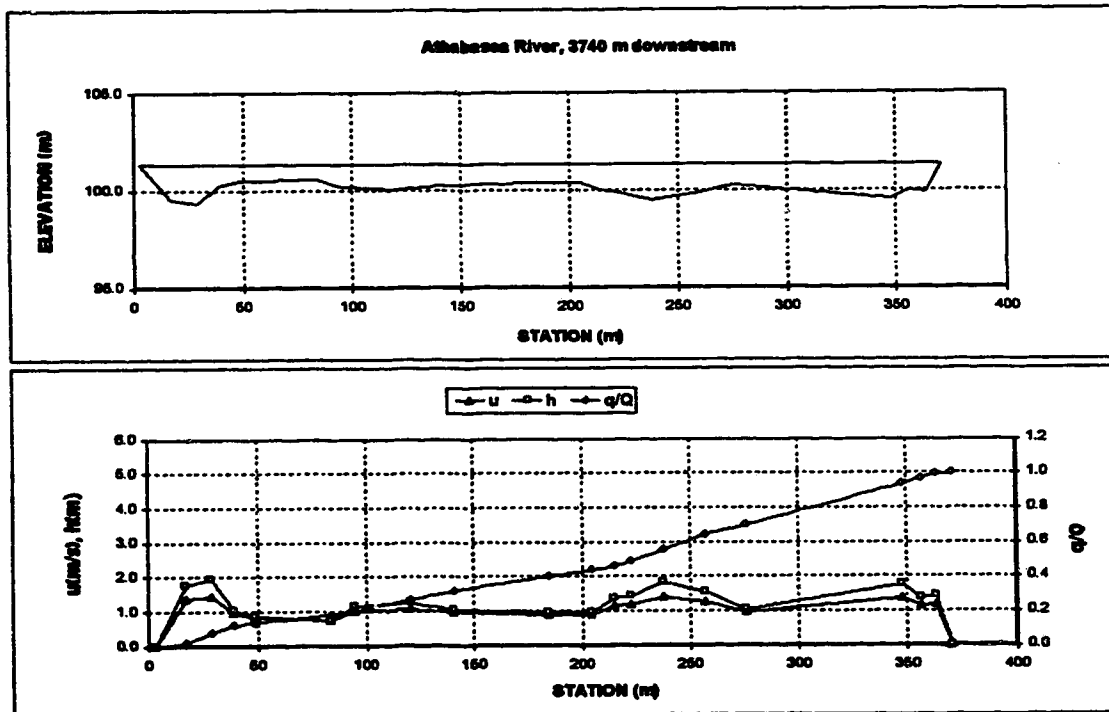
Appendix D.5 Athabasca River

X-SECTION Athabasca River, 3740 m downstream
TREATMENT DATE 4-Jun-75
DISCHARGE m^3/s 484.00
WIDTH m 387.88
MEAN DEPTH m 1.22
AREA m^2 447.62
MEAN VELOCITY m/s 1.081

ORIGINAL SURVEY 11-Sep-75

Assumed
Water Surface Elev. 101.30
LB 3.00 101.30
RB 370.88 101.30

Sta. m	Elev. m	h m	w/W	u cm/s	dq est. m^3	norm. q/Q	Area m^2	adjusted u m/s
3.00	101.30	3.00	0.00	0.000	0.00	0.00000	0.0	0.000
17.00	99.55	17.00	1.75	0.038	1.377	0.01704	12.3	1.347
29.00	99.35	29.00	1.95	0.071	1.480	0.08113	34.5	1.448
38.00	100.25	38.00	1.05	0.088	0.980	0.11840	49.5	0.958
48.00	100.45	48.00	0.85	0.125	0.851	0.13598	59.0	0.832
84.00	100.55	84.00	0.75	0.220	0.783	0.18217	86.9	0.765
88.00	100.15	88.00	1.15	0.250	1.041	0.20141	97.4	1.018
121.00	100.05	121.00	1.25	0.321	1.101	0.28890	128.8	1.076
141.00	100.25	141.00	1.05	0.375	0.980	0.31723	151.8	0.958
185.00	100.35	185.00	0.95	0.485	0.916	0.40149	185.6	0.896
205.00	100.35	205.00	0.95	0.549	0.916	0.43087	214.6	0.896
215.00	99.95	215.00	1.35	0.577	1.158	0.46077	228.1	1.133
223.00	99.85	223.00	1.45	0.598	1.215	0.48782	237.3	1.188
238.00	99.45	238.00	1.85	0.639	1.429	0.55372	282.1	1.388
257.00	99.75	257.00	1.55	0.691	1.270	0.64180	284.4	1.242
278.00	100.25	278.00	1.65	0.743	0.980	0.69793	319.1	0.958
348.00	99.55	348.00	1.75	0.938	1.377	0.93792	419.8	1.347
358.00	99.95	358.00	1.35	0.980	1.158	0.98988	432.2	1.133
363.00	99.55	363.00	1.45	0.979	1.215	0.98317	442.0	1.188
370.88	101.30	370.88	0.00	1.000	0.000	1.00000	447.6	0.000
Est. Total					495.03			



Appendix D.5 Athabasca River

X-SECTION Athabasca River, 5540 m downstream

ORIGINAL SURVEY 17-Sep-74

TREATMENT DATE 4-Jun-75

DISCHARGE m^3/s 484.00

Assumed

WIDTH m 304.11

Water Surface Elev.

MEAN DEPTH m 1.71

LB

0.00 101.40

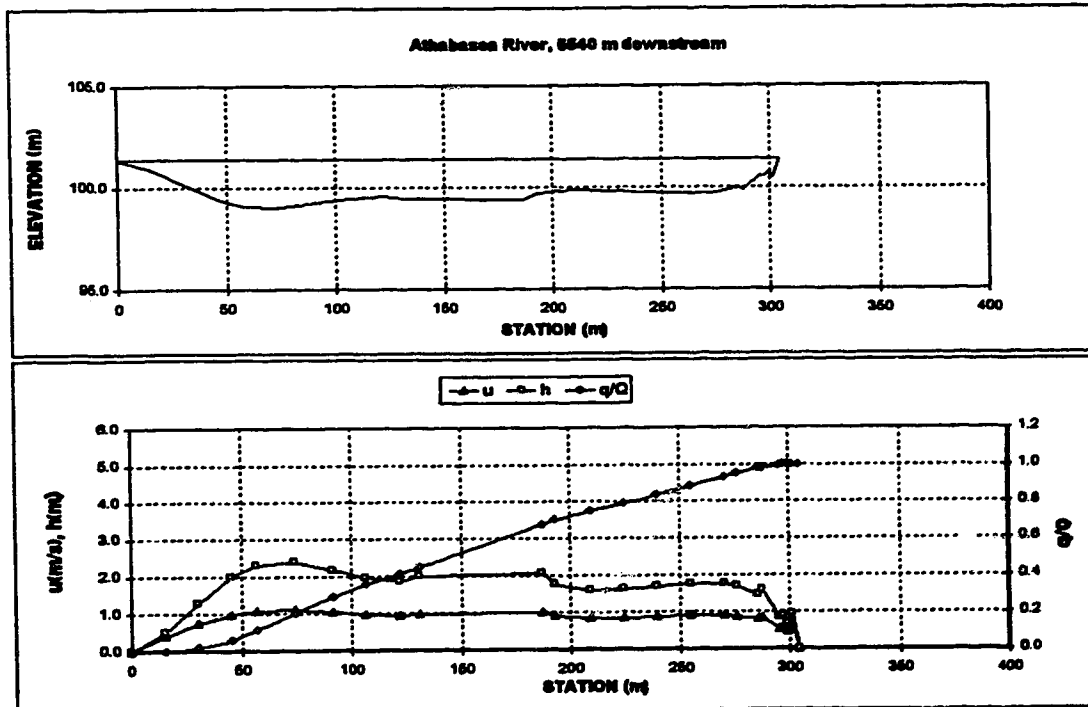
AREA m^2 521.27

RB

304.11 101.40

MEAN VELOCITY m/s 0.929

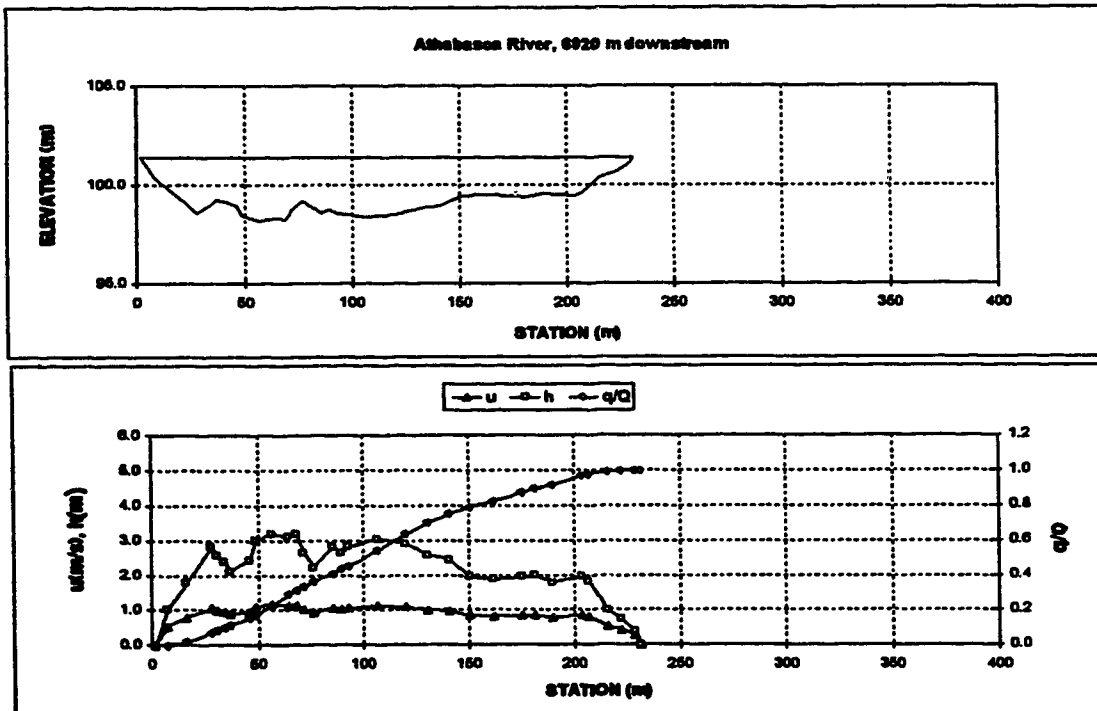
Sta. m	Elev. m	h m	w/W	u m/s	dq est. m^3	norm. q/Q	Area m^2	adjusted u m/s
0.00	101.40	0.00	0.000	0.000	0.00	0.00000	0.0	0.000
15.20	100.91	15.20	0.050	0.405	0.76	0.00150	3.8	0.389
30.50	100.12	30.50	1.29	0.100	0.766	0.01719	17.4	0.730
45.70	99.41	45.70	2.00	0.150	1.027	0.06117	42.3	0.978
57.30	99.10	57.30	2.31	0.188	1.131	0.11413	67.2	1.077
74.40	99.02	74.40	2.39	0.245	1.157	0.20441	107.3	1.102
91.40	99.26	91.40	2.15	0.301	1.078	0.28908	145.9	1.027
106.70	99.45	106.70	1.98	0.351	1.014	0.35362	177.2	0.985
121.90	99.54	121.90	1.87	0.401	0.982	0.41082	208.2	0.935
131.40	99.41	131.40	2.00	0.432	1.027	0.44687	224.6	0.878
167.10	99.35	167.10	2.06	0.615	1.048	0.67712	337.4	0.968
192.90	99.66	192.90	1.75	0.634	0.940	0.69867	348.4	0.895
209.40	99.84	209.40	1.57	0.689	0.874	0.74738	375.7	0.832
224.30	99.78	224.30	1.63	0.738	0.896	0.78875	399.5	0.853
239.90	99.72	239.90	1.69	0.789	0.918	0.83482	425.3	0.874
255.10	99.66	255.10	1.75	0.839	0.940	0.88245	451.4	0.895
270.70	99.66	270.70	1.75	0.890	0.940	0.93277	478.6	0.895
276.50	99.72	276.50	1.69	0.909	0.918	0.95085	488.5	0.874
285.70	99.86	285.70	1.45	0.936	0.829	0.97588	502.9	0.789
287.70	99.84	287.70	1.57	0.948	0.874	0.98073	505.9	0.832
295.40	100.57	295.40	0.84	0.971	0.575	0.98389	515.2	0.547
297.40	100.54	297.40	0.87	0.978	0.588	0.98584	516.9	0.560
299.30	100.73	299.30	0.88	0.984	0.499	0.99740	518.3	0.475
301.40	100.48	301.40	0.93	0.991	0.615	0.99924	520.0	0.598
304.11	101.40	304.11	0.00	1.000	0.000	1.00000	521.3	0.000
Est. Total					508.31			



Appendix D.5 Athabasca River

X-SECTION Athabasca River, 6820 m downstream		ORIGINAL SURVEY		17-Sep-74
TREATMENT DATE	4-Jun-78			
DISCHARGE m ³ /s	484.00	Assumed		
WIDTH m	229.82	Water Surface Elev.		101.40
MEAN DEPTH m	2.20	LB	2.07	101.40
AREA m ²	504.82	RB	231.90	101.40
MEAN VELOCITY m/s	0.958			

Sta.	Elev.		h	w/W	u	dq est.	norm. q/Q	Area	adjusted u
m	m		m		m/s	m ³		m ²	m/s
2.07	101.40	2.07	0.00	0.000	0.000	0.00	0.00000	0.0	0.000
8.00	100.38	8.00	1.02	0.028	0.573	0.86	0.00168	3.0	0.540
16.50	99.83	16.50	1.78	0.083	0.832	8.33	0.01791	14.8	0.784
28.10	98.59	28.10	2.82	0.113	1.132	28.15	0.08882	41.5	1.087
31.20	98.84	31.20	2.57	0.127	1.084	9.16	0.08885	49.8	1.003
34.20	98.99	34.20	2.42	0.140	1.022	7.79	0.10182	57.3	0.983
38.70	98.29	38.70	2.12	0.151	0.935	5.54	0.11281	63.0	0.882
48.10	98.98	48.10	2.45	0.192	1.030	21.07	0.15363	24.4	0.971
48.90	98.41	48.90	3.00	0.204	1.180	8.42	0.17002	82.0	1.112
58.50	98.20	58.50	3.21	0.237	1.234	28.44	0.22539	115.8	1.183
68.00	98.29	68.00	3.12	0.274	1.211	32.84	0.28834	142.4	1.141
68.70	98.23	68.70	3.18	0.280	1.227	14.18	0.31898	154.1	1.156
72.00	98.74	72.00	2.87	0.304	1.091	11.17	0.33871	163.7	1.029
76.90	98.17	76.90	2.24	0.328	0.971	12.38	0.38281	179.7	0.915
88.00	98.58	88.00	2.85	0.385	1.140	24.39	0.41031	190.8	1.074
90.00	98.77	90.00	2.64	0.383	1.083	12.18	0.43403	209.5	1.021
93.10	98.58	93.10	2.82	0.398	1.132	9.38	0.45225	218.2	1.067
108.80	98.35	108.80	3.08	0.458	1.198	48.79	0.54337	258.4	1.127
120.80	98.90	120.80	2.91	0.515	1.158	48.00	0.63883	208.3	1.088
131.20	98.81	131.20	2.80	0.582	1.072	32.78	0.70067	328.7	1.010
140.80	98.86	140.80	2.45	0.604	1.030	25.70	0.75071	353.8	0.971
150.70	99.45	150.70	1.98	0.647	0.888	20.68	0.78087	374.7	0.837
161.90	99.51	161.90	1.90	0.695	0.889	18.94	0.82785	386.3	0.819
175.40	99.45	175.40	1.98	0.754	0.888	22.83	0.87231	422.2	0.837
181.40	99.41	181.40	2.00	0.780	0.900	10.59	0.88293	434.1	0.848
188.70	98.80	188.70	1.81	0.818	0.842	13.73	0.91867	449.9	0.783
204.00	99.45	204.00	1.98	0.879	0.888	23.25	0.98483	476.7	0.837
207.00	99.57	207.00	1.84	0.892	0.851	4.94	0.97455	482.4	0.802
215.80	100.42	215.80	0.98	0.929	0.582	8.57	0.99123	494.6	0.530
222.80	100.86	222.80	0.75	0.980	0.468	3.11	0.99730	500.6	0.440
228.70	101.03	228.70	0.38	0.988	0.285	1.30	0.99983	504.0	0.278
231.90	101.40	231.90	0.00	1.000	0.000	0.00	1.00000	504.6	0.000
Est. Total						513.56			



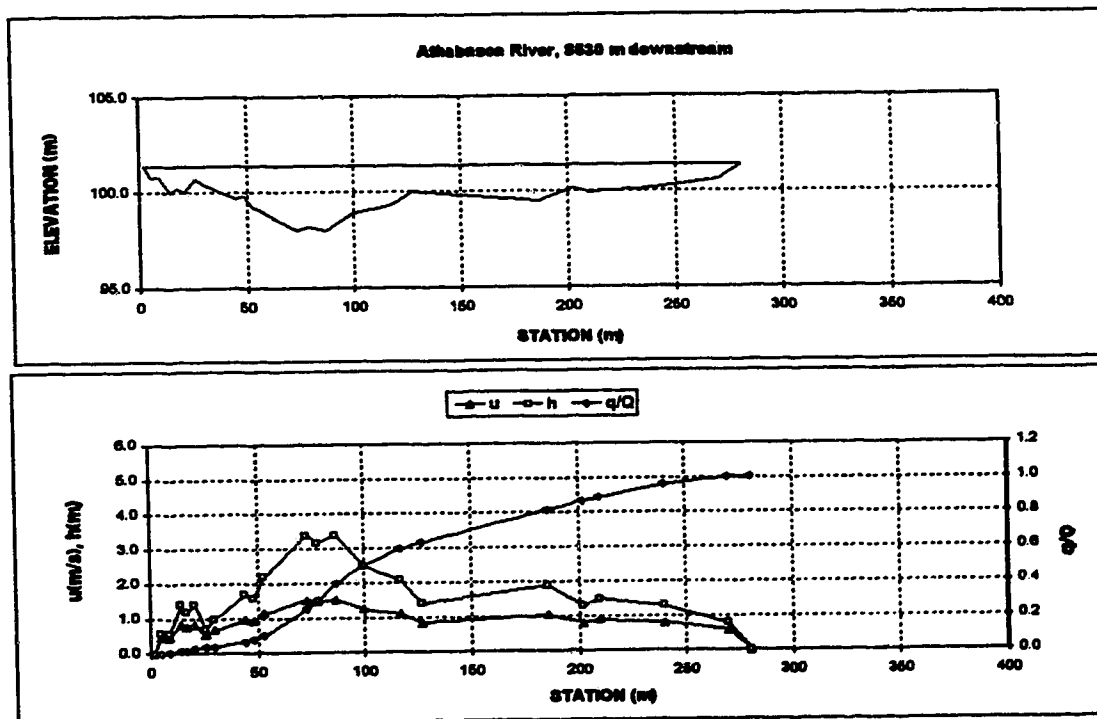
Appendix D.5 Athabasca River

X-SECTION Athabasca River, 8530 m downstream
TREATMENT DATE 4-Jun-75
DISCHARGE m^3/s 484.73
WIDTH m 278.88
MEAN DEPTH m 1.67
AREA m^2 464.73
MEAN VELOCITY m/s 1.641

ORIGINAL SURVEY 17-Sep-74

Assumed
Water Surface Elev. 101.40
LB 1.78 101.40
RB 280.64 101.40

Sta. m	Elev. m	h m	w/W	u m/s	dq est. m^3	norm. q/Q	Area m^2	adjusted u m/s
1.78	101.40	1.78	0.00	0.000	0.00	0.00000	0.0	0.000
5.00	100.82	5.00	0.58	0.012	0.515	0.00045	0.9	0.470
9.00	100.82	9.00	0.58	0.028	0.515	0.00270	3.3	0.470
14.00	100.02	14.00	1.38	0.044	0.918	0.00630	8.2	0.837
17.00	100.22	17.00	1.18	0.055	0.827	0.01563	12.0	0.784
21.00	100.02	21.00	1.38	0.069	0.918	0.02405	17.1	0.837
28.00	100.72	28.00	0.68	0.087	0.573	0.03128	22.3	0.822
30.00	100.42	30.00	0.88	0.101	0.731	0.03538	25.8	0.888
44.00	99.72	44.00	1.68	0.151	1.047	0.06954	44.2	0.955
46.00	99.82	46.00	1.58	0.166	1.005	0.07915	50.7	0.916
53.00	99.22	53.00	2.18	0.184	1.248	0.09907	60.1	1.136
73.00	98.02	73.00	3.38	0.255	1.669	0.25173	118.7	1.622
78.00	98.22	78.00	3.18	0.273	1.603	0.30226	132.1	1.481
87.00	98.02	87.00	3.38	0.306	1.669	0.36323	161.6	1.622
100.00	98.92	100.00	2.48	0.352	1.356	0.50182	196.7	1.238
117.00	99.32	117.00	2.08	0.413	1.207	0.59547	238.5	1.101
127.00	100.02	127.00	1.38	0.449	0.918	0.63011	256.8	0.837
186.00	99.52	186.00	1.88	0.661	1.129	0.81553	362.0	1.029
202.00	100.12	202.00	1.28	0.716	0.873	0.86320	377.2	0.798
210.00	99.92	210.00	1.48	0.747	0.982	0.88228	388.3	0.877
240.00	100.12	240.00	1.28	0.854	0.873	0.95386	429.7	0.798
270.00	100.82	270.00	0.78	0.982	0.628	0.96755	460.6	0.572
280.64	101.40	280.34	0.00	1.000	0.000	1.00000	464.7	0.000
Est. Total					530.84			



Appendix D.5 Athabasca River

X-SECTION Athabasca River, 8850 m downstream

ORIGINAL SURVEY 28-May-74

TREATMENT DATE 4-Jun-75

DISCHARGE m^3/s 484.00

Assumed

WIDTH m 310.52

Water Surface Elev.

MEAN DEPTH m 1.58

LB 4.72

AREA m^2 491.01

RB 315.24

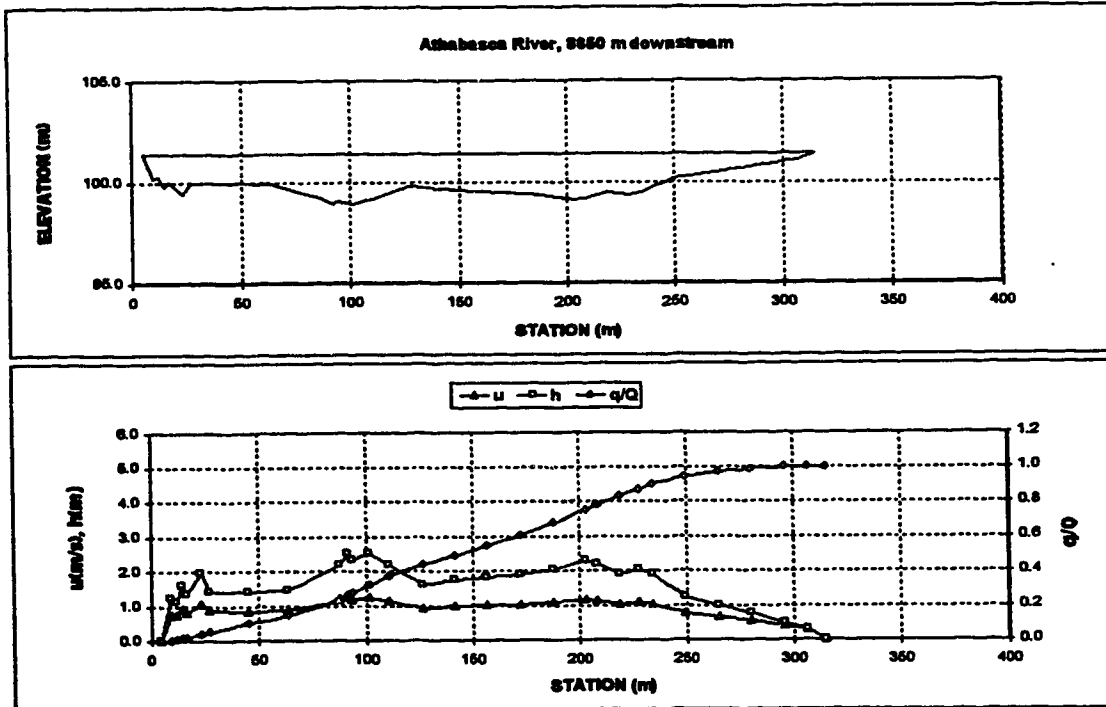
MEAN VELOCITY m/s 0.986

101.40

101.40

101.40

Sta.	Elev.	h	w/W	u	dq est.	norm. q/Q	Area	adjusted u	
m	m	m		m/s	m ³		m ²	m/s	
4.72	101.40	4.72	0.00	0.000	0.00	0.00000	0.0	0.000	
9.35	100.15	9.35	1.28	0.015	0.845	1.23	0.00237	2.9	0.789
12.05	100.27	12.05	1.14	0.024	0.790	2.64	0.00748	6.1	0.738
14.56	99.81	14.55	1.00	0.032	0.891	3.04	0.01332	9.5	0.925
16.65	100.06	16.65	1.35	0.038	0.885	2.90	0.01890	12.6	0.828
23.05	99.45	23.05	1.96	0.059	1.136	10.67	0.03948	23.2	1.060
26.75	99.96	26.75	1.48	0.071	0.928	6.49	0.05199	29.5	0.866
45.85	99.99	45.85	1.42	0.132	0.915	24.91	0.10004	56.5	0.854
63.85	99.93	63.85	1.48	0.190	0.941	24.41	0.14711	82.8	0.878
67.65	99.20	67.65	2.21	0.287	1.230	47.55	0.23881	126.6	1.149
91.95	98.90	91.95	2.51	0.281	1.340	13.01	0.26390	136.7	1.251
93.75	98.08	93.75	2.33	0.267	1.275	5.68	0.27486	141.1	1.190
101.35	98.90	101.35	2.51	0.311	1.340	23.99	0.32113	159.4	1.251
110.55	99.20	110.55	2.21	0.341	1.230	27.84	0.37483	181.1	1.149
126.65	99.81	126.65	1.60	0.393	0.991	33.98	0.44037	211.7	0.925
141.65	99.66	141.65	1.75	0.441	1.053	25.60	0.48974	236.7	0.983
156.65	99.57	156.65	1.84	0.490	1.089	28.13	0.54592	263.9	1.016
172.45	99.51	172.45	1.90	0.540	1.112	32.01	0.60766	293.0	1.038
187.95	99.35	187.95	2.08	0.590	1.174	34.99	0.67514	323.6	1.096
203.15	99.11	203.15	2.30	0.639	1.264	40.30	0.73285	356.7	1.180
208.35	99.20	208.35	2.21	0.656	1.230	14.59	0.78099	368.4	1.149
218.75	99.51	218.75	1.90	0.689	1.112	24.97	0.82915	389.7	1.038
228.15	99.35	228.15	2.06	0.720	1.174	21.22	0.87008	408.3	1.096
234.25	99.51	234.25	1.90	0.739	1.112	13.77	0.89664	420.3	1.038
249.85	100.15	249.85	1.28	0.789	0.845	24.04	0.94300	444.9	0.789
265.05	100.42	265.05	0.98	0.838	0.719	13.31	0.98867	461.9	0.671
280.65	100.63	280.65	0.78	0.889	0.613	9.14	0.98630	475.7	0.572
296.15	100.91	296.15	0.50	0.939	0.454	5.25	0.99642	485.5	0.424
308.25	101.09	308.25	0.32	0.971	0.336	1.62	0.99954	489.6	0.314
315.24	101.40	315.24	0.00	1.000	0.000	0.24	1.00000	491.0	0.000
Est. Total					518.54				



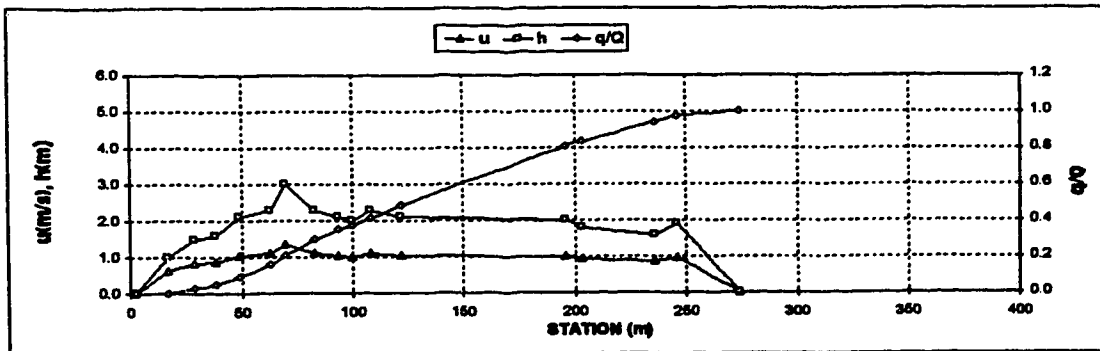
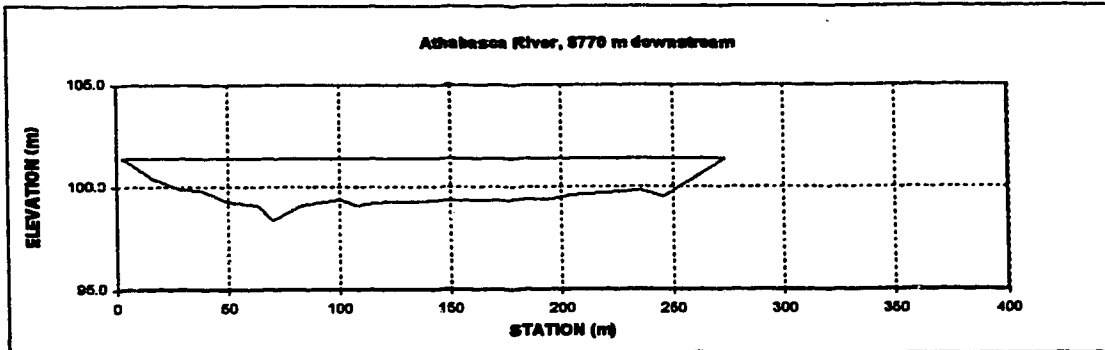
Appendix D.5 Athabasca River

X-SECTION Athabasca River, 8770 m downstream
TREATMENT DATE 4-Jun-75
DISCHARGE m^3/s 484.00
WIDTH m 271.87
MEAN DEPTH m 1.80
AREA m^2 488.82
MEAN VELOCITY m/s 0.990

ORIGINAL SURVEY 12-Sep-75

Assumed
Water Surface Elev. 101.40
LB 101.40
RB 274.41 101.40

Sta. m	Elev. m		h m	w/W	u m/s	dq est. m^3	norm. q/Q	Area m^2	adjusted u m/s
2.54	101.40	2.54	0.00	0.000	0.000	0.00	0.00000	0.0	0.000
17.00	100.41	17.00	0.99	0.053	0.987	2.40	0.00475	7.2	0.840
29.00	99.91	29.00	1.49	0.087	0.875	11.50	0.02759	22.1	0.840
38.00	99.81	38.00	1.59	0.130	0.913	12.42	0.05228	38.0	0.878
49.00	99.31	49.00	2.09	0.171	1.088	20.38	0.08270	56.3	1.053
63.00	99.11	63.00	2.29	0.222	1.184	34.71	0.18181	87.0	1.119
70.00	98.41	70.00	2.99	0.248	1.391	23.65	0.20855	105.5	1.336
83.00	99.11	83.00	2.29	0.298	1.184	43.91	0.29572	159.9	1.119
94.00	99.31	94.00	2.09	0.338	1.088	27.27	0.34988	184.0	1.053
100.00	99.41	100.00	1.99	0.358	1.081	13.22	0.37811	176.3	1.019
108.00	99.11	108.00	2.29	0.388	1.184	18.08	0.41389	183.4	1.119
122.00	99.31	122.00	2.09	0.439	1.088	34.71	0.48289	224.2	1.053
198.00	99.41	198.00	1.99	0.712	1.081	183.07	0.80081	375.4	1.019
203.00	99.81	203.00	1.79	0.737	0.988	13.58	0.83357	388.7	0.950
236.00	99.81	236.00	1.59	0.859	0.913	53.18	0.83909	444.6	0.878
248.00	99.51	248.00	1.89	0.898	1.025	18.90	0.87284	482.0	0.985
274.41	101.40	274.41	0.00	1.000	0.000	13.79	1.00000	488.9	0.000
Est. Total						503.76			



Appendix D.5 Athabasca River

X-SECTION Athabasca River, 10080 m downstream

ORIGINAL SURVEY

5-Jun-74

TREATMENT DATE

4-Jun-75

DISCHARGE m^3/s

484.00

Assumed

WIDTH m

243.99

Water Surface Elev.

101.40

MEAN DEPTH m

2.86

LB

6.86

101.40

AREA m^2

649.37

RB

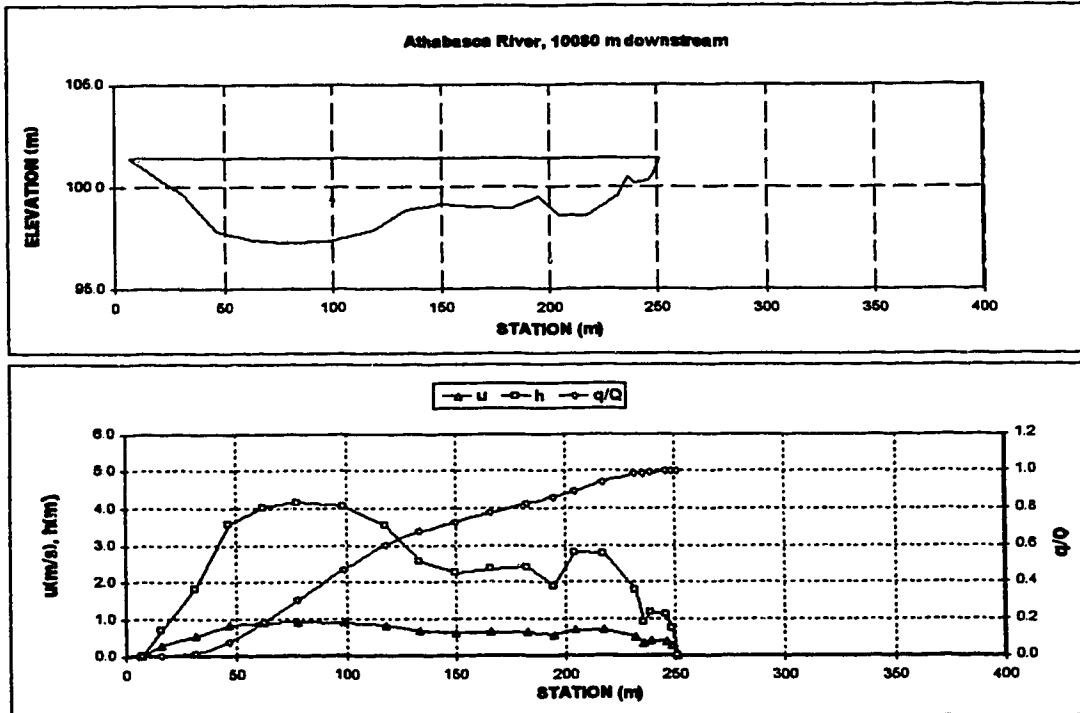
250.85

101.40

MEAN VELOCITY m/s

0.745

Sta. m	Elev. m		h m	w/V	u m/s	dq est. m^3	norm. q/Q	Area m^2	adjusted u m/s
6.86	101.40	6.86	0.00	0.000	0.000	0.00	0.00000	0.0	0.000
16.04	100.69	16.04	0.72	0.038	0.310	0.51	0.00097	3.3	0.286
31.24	99.57	31.24	1.84	0.100	0.582	8.64	0.01742	22.7	0.536
46.54	97.83	46.54	3.58	0.163	0.907	30.81	0.07608	64.0	0.836
62.34	97.37	62.34	4.04	0.227	0.984	56.85	0.18430	124.2	0.906
77.64	97.25	77.64	4.16	0.290	1.003	62.25	0.30280	186.8	0.924
98.94	97.34	98.94	4.07	0.377	0.989	87.19	0.46877	274.4	0.911
118.44	97.86	118.44	3.55	0.457	0.902	70.16	0.60232	348.6	0.831
133.34	98.83	133.34	2.58	0.518	0.729	37.19	0.67312	394.2	0.672
149.84	99.14	149.84	2.27	0.586	0.669	27.92	0.72627	434.1	0.617
166.04	99.05	166.04	2.36	0.652	0.687	25.38	0.77458	471.5	0.633
182.74	98.99	182.74	2.42	0.721	0.699	27.59	0.82710	511.3	0.644
194.94	99.50	194.94	1.91	0.771	0.586	17.06	0.85958	537.7	0.549
204.44	98.59	204.44	2.62	0.810	0.774	15.36	0.88682	560.1	0.713
217.24	98.62	217.24	2.79	0.862	0.768	27.63	0.94142	595.9	0.708
231.84	99.60	231.84	1.81	0.922	0.575	22.51	0.98427	629.5	0.530
235.84	100.48	235.84	0.93	0.938	0.368	2.58	0.98918	634.9	0.339
239.14	100.21	239.14	1.20	0.952	0.437	1.41	0.99186	638.4	0.403
245.84	100.30	245.84	1.11	0.979	0.415	3.28	0.99810	646.1	0.382
248.34	100.66	248.34	0.75	0.990	0.319	0.85	0.99972	648.4	0.294
250.85	101.40	250.85	0.00	1.000	0.000	0.15	1.00000	649.4	0.000
Est. Total						525.31			



Appendix D.5 Athabasca River

X-SECTION Athabasca River, 12570 m downstream

ORIGINAL SURVEY

8-May-74

TREATMENT DATE 4-Jun-75

DISCHARGE m^3/s 484.00

Assumed

WIDTH m 297.92

Water Surface Elev.

101.40

MEAN DEPTH m 1.92

LB

0.00 101.40

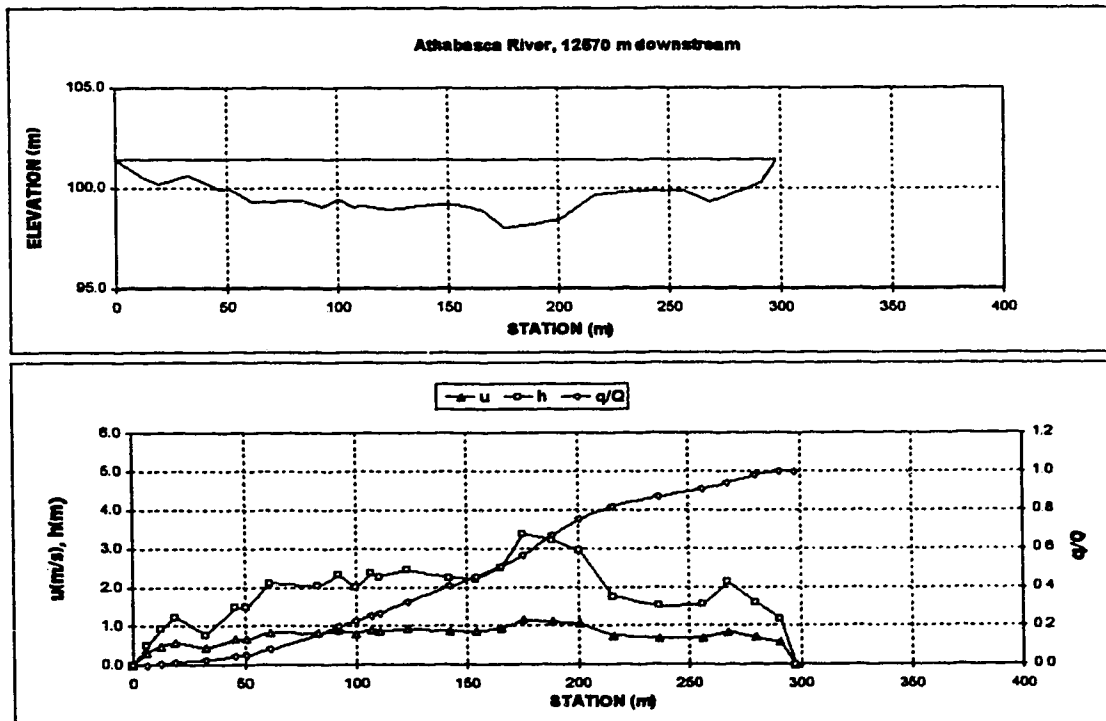
AREA m^2 572.46

RB

297.92 101.40

MEAN VELOCITY m/s 0.845

Sta. m	Elev. m		h m	w/w	u m/s	dq est. m^3	norm. q/Q	Area m^2	adjusted u m/s
0.00	101.40	0.00	0.00	0.000	0.000	0.00	0.00000	0.0	0.000
6.10	101.91	6.10	0.50	0.020	0.342	0.28	0.00050	1.5	0.320
12.50	101.48	12.50	0.93	0.042	0.519	1.06	0.00428	6.1	0.486
18.90	100.18	18.90	1.23	0.063	0.628	3.94	0.01190	12.9	0.586
32.30	100.63	32.30	0.78	0.108	0.461	7.29	0.02599	26.3	0.432
46.00	99.93	46.00	1.48	0.154	0.709	9.02	0.04343	41.7	0.663
50.90	99.93	50.90	1.48	0.171	0.709	5.12	0.05333	49.0	0.663
61.30	99.29	61.30	2.12	0.206	0.901	15.03	0.08239	67.6	0.844
83.20	99.38	83.20	2.03	0.279	0.876	40.28	0.16027	113.0	0.819
92.70	99.09	92.70	2.32	0.311	0.957	18.89	0.19880	133.6	0.898
100.30	99.41	100.30	2.00	0.337	0.867	14.94	0.22569	150.0	0.811
107.00	99.05	107.00	2.36	0.359	0.988	13.37	0.25155	164.5	0.906
110.60	99.14	110.60	2.27	0.371	0.943	7.95	0.26692	172.9	0.883
123.40	98.98	123.40	2.45	0.414	0.993	29.18	0.32335	203.0	0.929
142.30	99.17	142.30	2.24	0.478	0.935	42.63	0.40579	247.2	0.875
154.20	99.20	154.20	2.21	0.518	0.927	24.59	0.45334	273.6	0.867
165.80	98.90	165.80	2.51	0.557	1.009	28.44	0.50447	301.0	0.944
175.30	98.04	175.30	3.37	0.588	1.229	31.20	0.56479	328.8	1.150
188.70	98.20	188.70	3.21	0.633	1.189	53.22	0.66769	372.9	1.113
200.60	98.47	200.60	2.94	0.673	1.122	42.21	0.74931	409.4	1.050
216.10	99.66	216.10	1.75	0.725	0.793	34.72	0.81644	445.7	0.742
236.80	99.89	236.80	1.52	0.795	0.722	25.55	0.86584	479.4	0.675
256.00	99.87	256.00	1.54	0.859	0.728	21.22	0.90687	508.7	0.681
267.60	99.28	267.60	2.13	0.898	0.904	17.32	0.94037	529.9	0.846
280.40	99.81	280.40	1.60	0.941	0.747	19.65	0.97837	553.7	0.699
291.10	100.24	291.10	1.17	0.977	0.606	9.98	0.99767	568.5	0.567
297.92	101.40	297.92	0.00	1.000	0.000	1.20	1.00000	572.5	0.000
Est. Total						517.16			

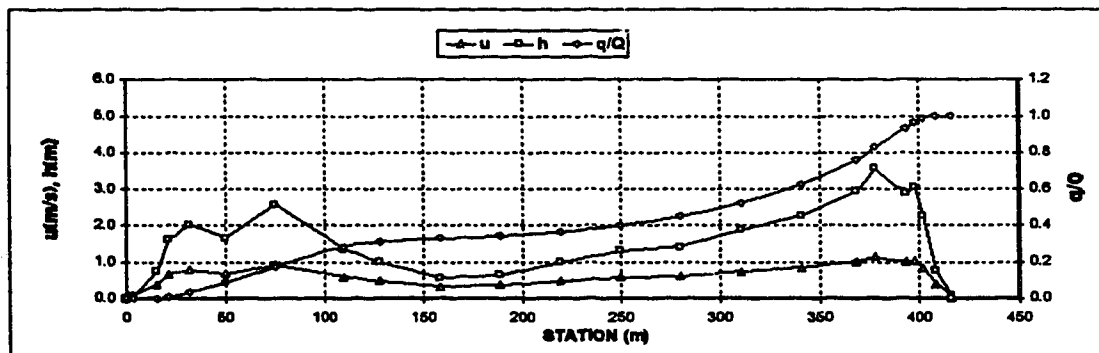
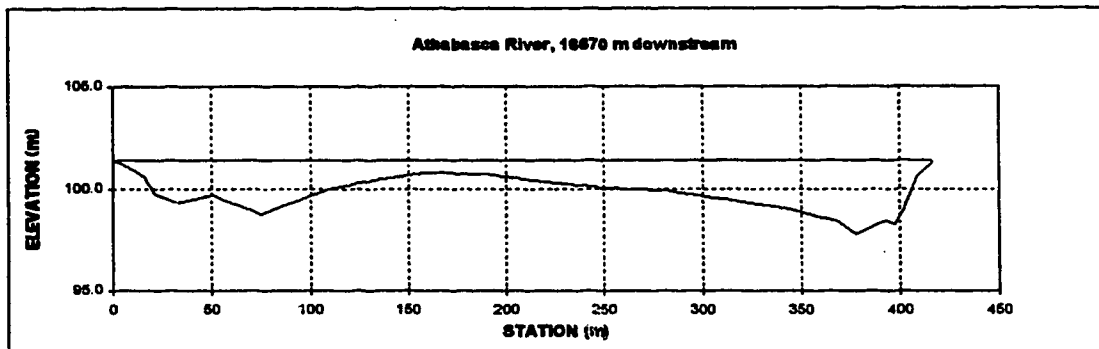


Appendix D.5 Athabasca River

X-SECTION Athabasca River, 16670 m downstream
TREATMENT DATE 4-Jun-75
DISCHARGE m^3/s 484.00
WIDTH m 416.42
MEAN DEPTH m 1.57
AREA m^2 651.84
MEAN VELOCITY m/s 0.743

ORIGINAL SURVEY 16-Sep-75
Assumed
Water Surface Elev. 101.40
LB 0.00
RB 416.42 101.40

Sta. m	Elev. m	h m	w/W	u m/s	dq est. m^3	norm. q/Q	Area m^2	adjusted u m/s
0.00	101.40	0.00	0.000	0.000	0.00	0.00000	0.0	0.000
3.66	101.33	3.66	0.009	0.098	0.01	0.00001	0.1	0.087
15.24	100.85	15.24	0.75	0.453	1.31	0.00241	4.9	0.401
21.34	99.80	21.34	1.80	0.753	4.31	0.01029	12.0	0.667
32.00	99.37	32.00	2.03	0.882	15.81	0.03823	31.4	0.781
50.29	99.74	50.29	1.66	0.121	0.772	0.09025	65.1	0.684
74.68	98.83	74.68	2.57	0.179	1.035	0.17582	118.7	0.917
109.73	100.04	109.73	1.36	0.284	0.674	0.28336	185.6	0.598
128.02	100.41	128.02	0.99	0.307	0.547	0.30732	207.0	0.484
158.50	100.84	158.50	0.56	0.381	0.375	0.32728	230.7	0.332
188.98	100.75	188.98	0.65	0.454	0.415	0.34070	248.2	0.368
219.46	100.41	219.46	0.99	0.527	0.547	0.38274	274.2	0.484
249.94	100.11	249.94	1.29	0.600	0.654	0.40099	309.1	0.579
280.42	99.98	280.42	1.42	0.673	0.695	0.45198	350.4	0.615
310.90	99.53	310.90	1.87	0.747	0.837	0.52225	400.5	0.742
341.38	99.13	341.38	2.27	0.820	0.951	0.62559	463.6	0.843
368.81	98.46	368.81	2.94	0.886	1.131	0.78175	535.1	1.002
377.85	97.85	377.85	3.55	0.908	1.282	0.82727	584.8	1.136
393.19	98.52	393.19	2.88	0.944	1.115	0.93474	613.7	0.988
397.78	98.34	397.78	3.06	0.955	1.162	0.96304	627.3	1.029
402.34	99.13	402.34	2.27	0.906	0.951	0.98861	639.5	0.843
408.43	100.85	408.43	0.75	0.881	0.453	0.99842	648.7	0.401
416.05	101.33	416.05	0.08	0.999	0.098	1.00000	651.8	0.087
416.42	101.40	416.42	0.00	1.000	0.000	1.00000	651.8	0.000
Est. Total					546.28			

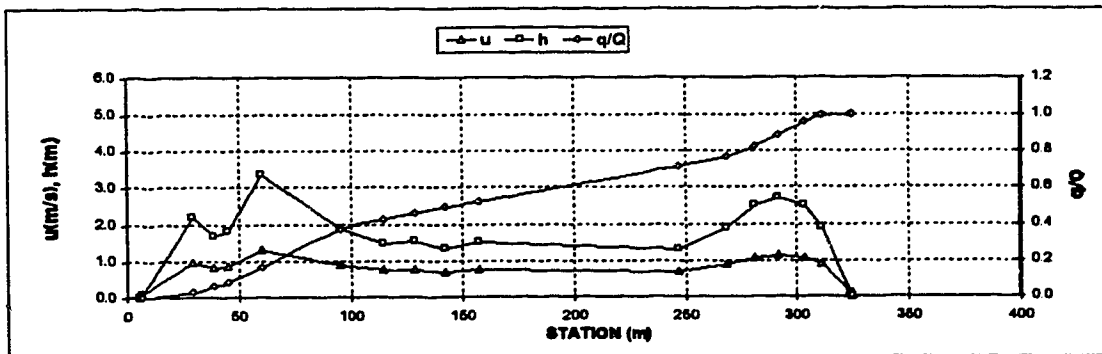
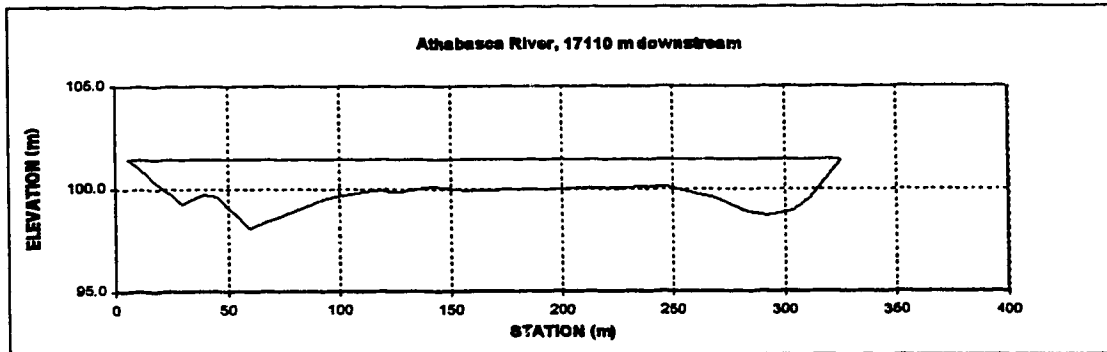


Appendix D.5 Athabasca River

X-SECTION Athabasca River, 17110 m downstream
TREATMENT DATE 4-Jun-75
DISCHARGE m^3/s 484.00
WIDTH m 319.41
MEAN DEPTH m 1.73
AREA m^2 554.16
MEAN VELOCITY m/s 0.873

ORIGINAL SURVEY 16-Sep-75
Assumed
Water Surface Elev. 101.40
LB 101.40
RB 324.96 101.40

Sta. m	Elev. m	h m	w/W	u m/s	dq est m^3	norm. q/Q	Area m^2	adjusted u m/s
5.55	101.40	5.55	0.00	0.000	0.00	0.00000	0.0	0.000
6.57	101.33	6.57	0.07	0.107	0.00	0.00000	0.0	0.103
29.43	99.22	29.43	2.18	1.016	14.47	0.02869	25.8	0.975
38.58	99.71	38.58	1.89	0.103	16.58	0.06156	43.5	0.824
45.28	99.59	45.28	1.81	0.124	10.32	0.02202	55.2	0.863
59.91	98.06	59.91	3.34	0.170	42.37	0.16301	82.9	1.296
94.96	99.53	94.96	1.87	0.280	103.64	0.37145	184.2	0.882
114.78	99.92	114.78	1.48	0.342	28.27	0.42750	217.4	0.753
128.49	99.86	128.49	1.54	0.385	16.44	0.48029	238.1	0.773
142.21	100.08	142.21	1.32	0.428	15.07	0.48997	257.7	0.700
157.45	99.89	157.45	1.51	0.478	16.45	0.52259	279.3	0.763
247.36	100.11	247.36	1.29	0.757	95.32	0.71153	405.2	0.689
268.70	99.53	268.70	1.87	0.824	27.67	0.78639	439.0	0.882
280.89	98.92	280.89	2.48	0.862	26.93	0.81979	485.6	1.064
291.56	98.70	291.56	2.70	0.895	31.51	0.88225	493.2	1.124
303.75	98.92	303.75	2.48	0.934	36.01	0.95364	524.8	1.064
311.37	99.53	311.37	1.87	0.957	16.83	0.98701	541.4	0.882
324.48	101.33	324.48	0.07	0.999	6.55	1.00000	554.1	0.103
324.96	101.40	324.96	0.00	1.000	0.00	1.00000	554.2	0.000
Est. Total					504.47			

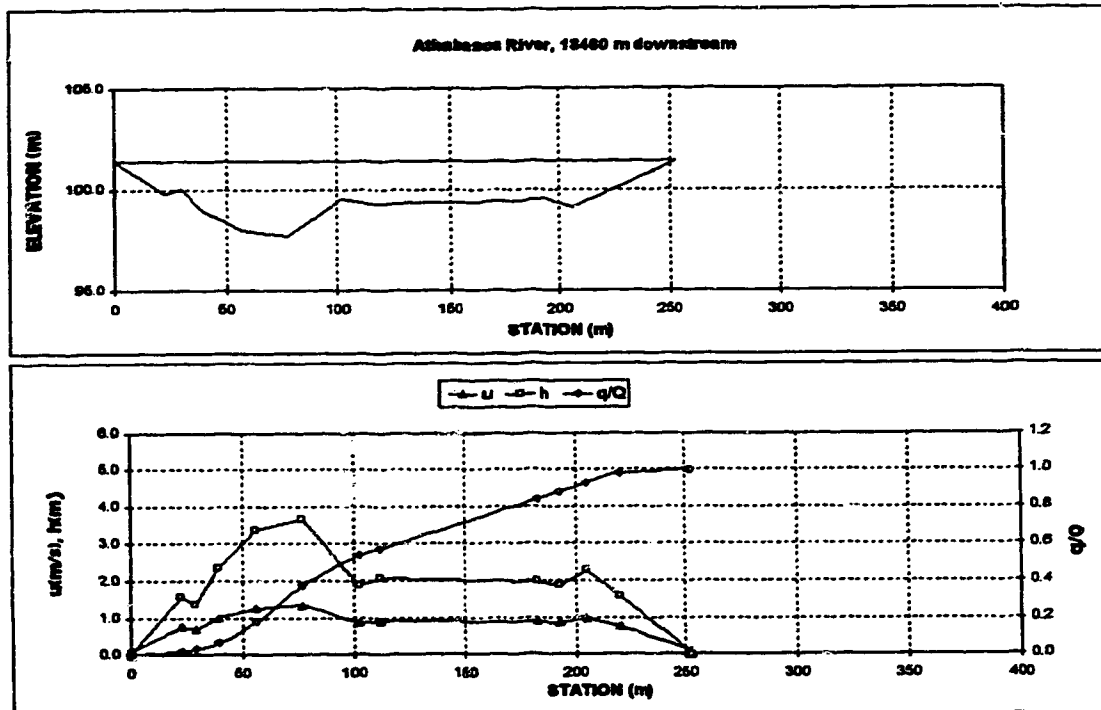


Appendix D.5 Athabasca River

X-SECTION Athabasca River, 18480 m downstream
TREATMENT DATE 4-Jun-75
DISCHARGE m^3/s 484.00
WIDTH m 252.84
MEAN DEPTH m 1.88
AREA m^2 501.18
MEAN VELOCITY m/s 0.966

ORIGINAL SURVEY 16-Sep-75
Assumed
Water Surface Elev. 101.40
LB 0.53 101.40
RB 253.17 101.40

Sta. m	Elev. m	h m	w/W	u m/s	dq est. m^3	norm. q/Q	Area m^2	adjusted u m/s
0.53	101.40	0.53	0.00	0.00	0.00	0.00000	0.0	0.000
0.70	101.33	0.70	0.07	0.108	0.00	0.00000	0.0	0.100
22.50	99.83	22.50	0.087	0.828	8.40	0.01606	18.0	0.786
25.57	100.03	29.50	0.115	0.756	8.17	0.03167	28.3	0.889
36.50	98.03	38.50	0.154	1.089	17.28	0.06470	47.0	1.007
98.50	98.03	58.50	0.222	1.378	60.21	0.17979	95.9	1.273
77.50	97.73	77.50	0.305	1.457	104.83	0.38014	169.9	1.348
102.50	98.53	102.50	0.404	0.830	82.75	0.53830	239.2	0.880
112.50	99.33	112.50	0.443	0.985	19.60	0.57400	259.0	0.920
182.50	98.43	182.50	0.720	0.983	138.68	0.83962	400.7	0.880
193.50	99.53	193.50	0.784	0.930	20.02	0.87789	421.8	0.860
205.50	98.13	205.50	0.811	1.058	24.73	0.92516	448.7	0.979
220.50	99.83	220.50	0.871	0.828	27.21	0.97716	475.6	0.786
251.50	101.33	251.50	0.983	0.108	11.85	0.99899	501.1	0.100
253.17	101.40	253.17	0.00	1.000	0.00	1.00000	501.2	0.000
Est. Total					523.21			



Appendix D.5 Athabasca River

X-SECTION Athabasca River, 19060 m downstream

ORIGINAL SURVEY

28-May-74

TREATMENT DATE

4-Jun-75

DISCHARGE m^3/s

484.00

Assumed

WIDTH m

298.04

Water Surface Elev.

MEAN DEPTH m

2.27

LS

8.94

AREA m^2

677.86

RS

308.94

MEAN VELOCITY m/s

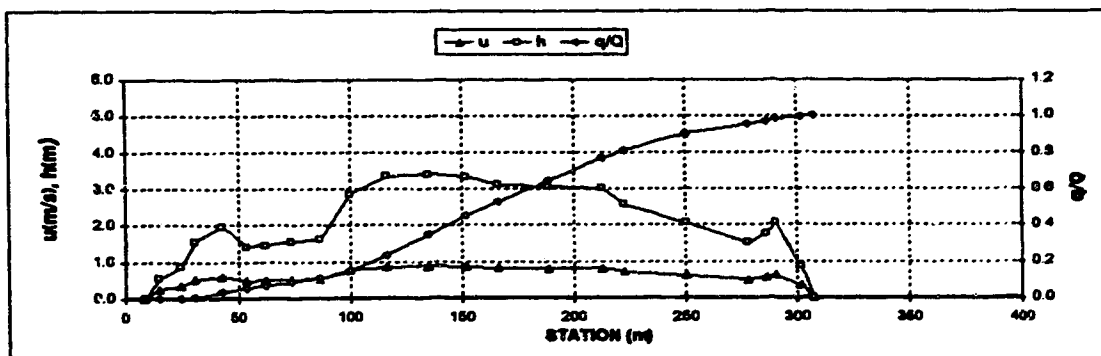
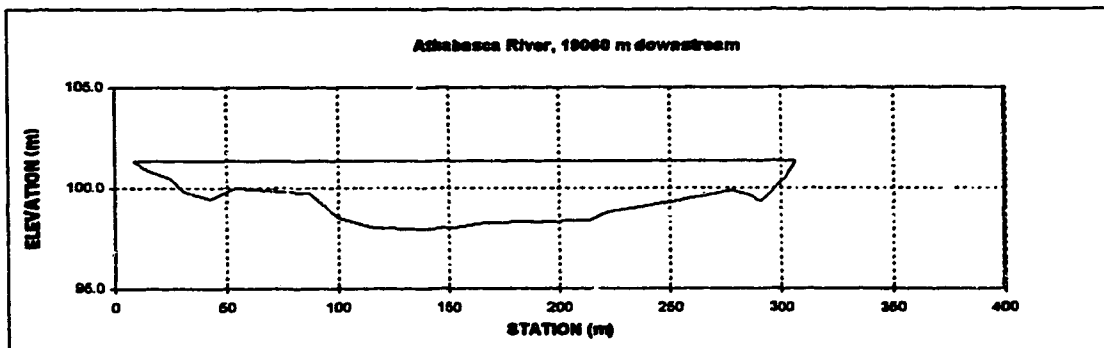
0.714

101.40

101.40

101.40

Sta.	Elev.		h	w/W	u	dq est.	norm. q/Q	Area	adjusted u
m	m		m		m/s	m^3		m^2	m/s
8.94	101.40	8.94	0.00	0.000	0.000	0.00	0.00000	0.0	0.000
14.95	100.86	14.95	0.55	0.020	0.276	0.23	0.00043	1.6	0.266
24.35	100.54	24.35	0.87	0.052	0.375	2.16	0.00456	6.3	0.348
30.95	99.84	30.95	1.57	0.074	0.557	3.74	0.01172	16.3	0.516
42.55	99.44	42.55	1.97	0.113	0.648	12.34	0.03536	36.8	0.601
53.95	99.99	53.95	1.42	0.151	0.521	11.26	0.05664	56.0	0.483
61.95	99.94	61.95	1.47	0.178	0.533	6.07	0.06857	67.5	0.494
74.15	99.84	74.15	1.57	0.219	0.557	10.07	0.06786	66.0	0.516
86.75	99.79	86.75	1.82	0.291	0.599	11.27	0.10947	106.1	0.527
100.35	98.54	100.35	2.87	0.307	0.833	21.38	0.16040	136.5	0.773
116.75	98.04	116.75	3.37	0.362	0.928	44.99	0.23661	187.6	0.861
135.35	97.99	135.35	3.42	0.424	0.937	58.80	0.34829	250.7	0.899
152.35	98.07	152.35	3.34	0.481	0.822	53.34	0.45151	308.0	0.855
168.35	98.29	168.35	3.12	0.528	0.881	40.72	0.52954	353.2	0.817
189.15	98.33	189.15	3.08	0.605	0.874	61.82	0.64820	423.8	0.810
212.95	98.39	212.95	3.02	0.684	0.862	62.91	0.76876	486.2	0.800
222.55	98.84	222.55	2.57	0.717	0.774	21.82	0.81076	523.0	0.718
250.55	99.34	250.55	2.07	0.811	0.670	46.81	0.90045	587.8	0.621
277.75	99.89	277.75	1.52	0.902	0.545	29.57	0.95713	636.5	0.505
285.95	99.64	285.95	1.77	0.929	0.603	7.72	0.97192	650.9	0.566
290.35	99.34	290.35	2.07	0.944	0.670	5.36	0.98220	658.4	0.621
301.95	100.54	301.95	0.87	0.983	0.375	8.68	0.99622	675.4	0.348
308.98	101.40	308.98	0.00	1.000	0.000	0.41	1.00000	677.6	0.000
Est. Total						521.83			



Appendix D.5 Athabasca River

X-SECTION Athabasca River, 21470 m downstream

ORIGINAL SURVEY

11-Sep-75

TREATMENT DATE

4-Jun-75

DISCHARGE m^3/s

484.00

Assumed

Water Surface Elev.

101.40

WIDTH m

221.11

LS

15.75

101.40

MEAN DEPTH m

2.49

RB

236.86

101.40

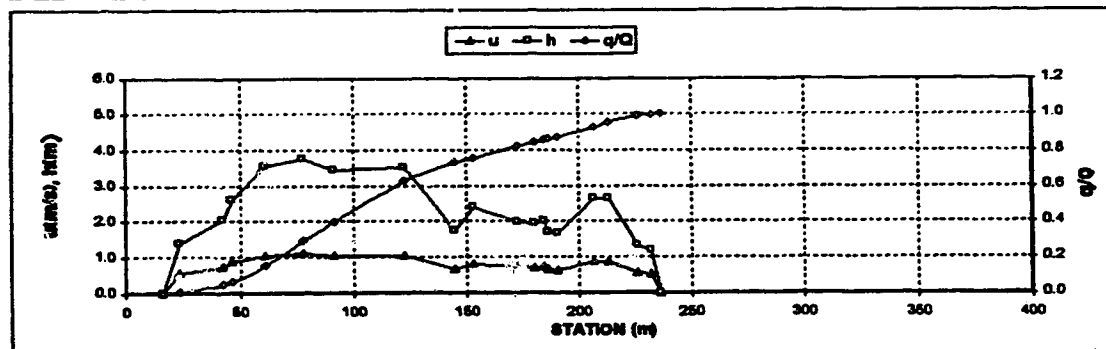
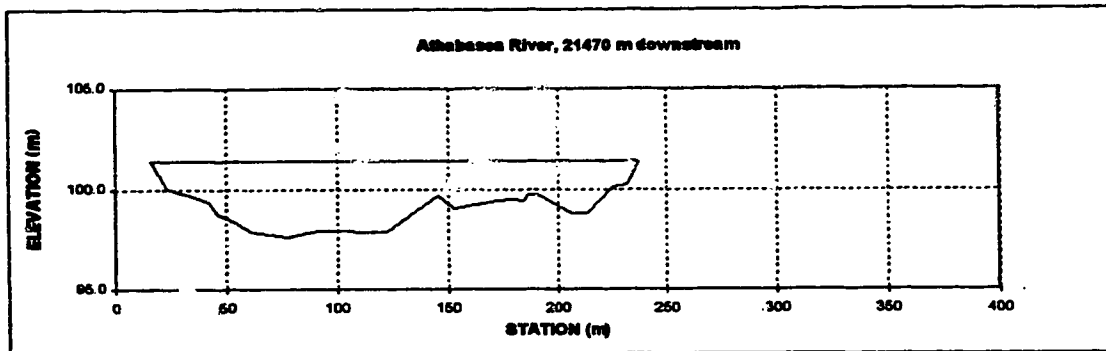
AREA m^2

550.47

MEAN VELOCITY m/s

0.879

Sta.	Elev.		h	w/W	u	dq est.	norm. q/Q	Area	adjusted u
m	m		m		m/s	m^3		m^2	m/s
15.75	101.40	15.75	0.00	0.000	0.000	0.00	0.00000	0.0	0.000
23.19	100.02	23.19	1.38	0.034	0.593	1.52	0.00297	5.1	0.580
42.40	98.35	42.40	2.05	0.121	0.772	22.47	0.04678	38.1	0.729
48.05	98.80	48.05	2.60	0.137	0.905	7.13	0.08068	48.6	0.854
61.28	97.88	61.28	3.54	0.208	1.113	47.20	0.15272	83.3	1.050
78.06	97.64	78.06	3.76	0.262	1.157	69.43	0.28810	154.5	1.082
91.77	97.95	91.77	3.45	0.344	1.093	55.62	0.38654	204.0	1.032
122.25	97.89	122.25	3.51	0.482	1.108	116.72	0.62415	310.1	1.044
145.11	99.86	145.11	1.74	0.585	0.894	54.08	0.72960	370.2	0.855
152.73	99.02	152.73	2.38	0.620	0.854	12.18	0.75335	385.9	0.806
172.55	99.41	172.55	1.99	0.708	0.757	34.90	0.82140	429.2	0.714
180.17	99.47	180.17	1.93	0.744	0.741	11.18	0.84320	444.2	0.700
184.74	99.38	184.74	2.02	0.784	0.765	6.79	0.85645	453.2	0.722
186.28	99.72	186.28	1.68	0.771	0.677	2.03	0.86041	456.0	0.639
190.83	99.75	190.83	1.65	0.792	0.669	5.14	0.87043	463.6	0.632
206.88	98.77	206.88	2.63	0.864	0.912	28.82	0.92273	497.6	0.860
213.69	98.77	213.69	2.63	0.895	0.912	16.80	0.95549	516.0	0.860
225.89	100.08	225.89	1.32	0.950	0.575	17.69	0.98037	540.1	0.543
231.98	100.23	231.98	1.17	0.978	0.530	4.18	0.98853	547.6	0.500
236.86	101.40	236.86	0.00	1.000	0.000	0.75	1.00000	550.5	0.000
Est. Total						512.83			



Appendix E. Concept of Dosage

The concept of dosage can be used to determine the transverse mixing coefficient from a slug injection of tracer. Dosage is defined as the time integral of depth-averaged concentration at a given location downstream of a slug injection, i.e.

$$\Theta = \int_0^{\infty} c \, dt \quad [A-1]$$

where Φ is the dosage. Therefore the dosage is the area under a C-t plot.

Beltaos (1975) showed that dosage at a point downstream of a slug injection is analogous to concentration at a point downstream of a steady state injection. Therefore the distribution of dosage across the channel at several locations can be used to determine the transverse mixing coefficient using the method of moments or simulation techniques.

Dosage distributions can also be used to determine M , the total mass passing a section by integrating over the total flow as follows:

$$M = \int_0^Q \Theta_{(q)} \, dq \quad [A-2]$$

where: q is the cumulative flow coordinate
 $\Theta_{(q)}$ is the dosage at a given cumulative flow
 Q is the total streamflow

The result of the integration can be compared to the mass input to assess the mass recovery at the cross section.

Appendix F. Notes and Assumptions Regarding the Peace River Mixing Simulation

Several assumptions were made in order to complete the Peace River mixing simulation. These included assumptions required to resolve some irregularities in the NRBS report on the study (Northern Rivers Basin Study, 1994). The assumptions and other pertinent notes regarding the simulation are listed below.

Appendix F.1 Shaftesbury Ferry Injection Site

- The location of the tracer injection as specified in the NRBS report and designated in NRBS Figure 3.4a does not correspond with the q/Q coordinate for peak dosage in NRBS Figure 4.5 ($q/Q \approx 0.36$ compared to $q/Q \approx 0.55$).
- It is unlikely that the maximum dosage location can shift to a different streamtube in such a short distance. Therefore the input location was assumed to correspond to the peak dosage location.
- Interestingly, if the 190 m from the bank specified for the injection location was taken from the RB rather than the LB, then the injection location would correspond to the peak on the dosage plots.
- The injection consisted of 250 kg of 20% Rhodamine WT, i.e. 50 kg of tracer. Assuming this mass is initially mixed into a volume defined by three time steps between $q/Q = 0.55$ to 0.60 gives the following initial concentration:

$$\frac{50000000 \text{ mg}}{[0.05][1740 \text{ m}^3/\text{sec}][360 \text{ sec}]} = 1596.4 \text{ ppb}$$

Appendix F.2 Shaftesbury Ferry to MacKenzie Cairn Reach

- The only cross sections available in this reach are those at Shaftesbury Ferry and MacKenzie Cairn. No intermediate sections were available from Alberta Environmental Protection.

- After many unsuccessful simulation attempts using just the NRBS sections at Shaftesbury Ferry and MacKenzie Cairn it was concluded there was inadequate definition of the channel geometry (input location, length of subreaches, duration of slug injection were all varied with little success). An “effective cross-sectional area” approach was also attempted as used in the NRBS report. This also met with little success. The time of travel to the MacKenzie Cairn section could only be matched by synthesizing an intermediate section.
- Observing the channel curvature it was decided to attempt to use a mirror image of the MacKenzie Cairn section to represent a portion of the reach.
- Using this synthesized section and some trial and error in subdividing the reach into subreaches the concentration profiles at MacKenzie Cairn were modelled with reasonable results.

Appendix F.3 MacKenzie Cairn Concentration Profiles

- Some discrepancy exists between the hole locations labeled on NRBS Figure 3.5a and NRBS Figure 3.4a (see Table F.1 and Table F.2 below).
- The NRBS Figure 3.4a locations appear to be correct in that:
 1. they correspond reasonably well to an even spacing of 20 holes across the section (as specified in the report)
 2. the q/Q locations of the holes correspond to the q/Q values which are listed in NRBS Figure 3.5a.
- The interpolated values from the measured q/Q curve in NRBS Figure 4.1d (based upon the transverse locations indicated in NRBS Figure 3.4a) were used for replotting the concentration results.

Table F.1 Hole locations at MacKenzie Cairn based upon NRBS Figure 3.5a.

Hole No.	Dist from LB (from Fig 3.5a)	w/W	interp q/Q (from Fig 4.1b)	reported q/Q (from Fig 3.5a)
4	76.0	0.239	0.247	-
5	85.5	0.279	0.320	0.24
6	102.9	0.324	0.403	0.32
7.5	124.0	0.391	0.526	0.44
9	145.2	0.458	0.651	0.57
10	157.7	0.497	0.720	0.66
12	186.5	0.588	0.818	0.77

Table F.21 Hole locations at MacKenzie Cairn based upon NRBS Figure 3.4a.

Hole No.	Dist from LB (from Fig 3.4a)	w/W	interp q/Q (from Fig 4.1b)	reported q/Q (from Fig 3.5a)
5	75.0	0.236	0.241	0.24
6	89.4	0.282	0.326	0.32
7.5	113.4	0.358	0.461	0.44
9	130.8	0.412	0.570	0.57
10	140.5	0.440	0.619	0.66
12	172.1	0.543	0.771	0.77

Appendix F.4 MacKenzie Cairn Dosage Distribution

The dosage distribution was determined by integrating the C-t curves rather than using Figure 4.5a in the NRBS report. The results are shown in Table F.2. The dosages were normalized using the mass recovery ratio (0.800) determined by integrating the transverse dosage distribution with respect q. The mass recovery determined by integration was used rather than the value shown in Table 2.5 of the NRBS report.

Table F.2 Dosage distribution at MacKenzie Cairn.

Hole No.	w/W	interp q/Q (from Fig 4.1b)	Measured Dosage ($\mu\text{g hr/L}$)	Normalized Dosage ($\mu\text{g hr/L}$)
5	0.236	0.241	0.52	0.65
6	0.282	0.326	2.78	3.47
7.5	0.358	0.461	12.10	15.12
9	0.412	0.570	25.26	31.58
10	0.440	0.619	22.31	27.89
12	0.543	0.771	2.42	3.03

Appendix F.5 MacKenzie Cairn to Peace River Boat Launch Reach.

- A number of sections were available in this reach as indicated in Table F.3. Attempts to use all the sections 'as is' met with limited success. Some sections were eliminated and some were modified as follows:
 1. The Jail section was considered unrepresentative due to the influence of a sand bar extending from the RB.
 2. In the vicinity of the Smoky R. confluence much of the RB consists of bars and shallow braided channels. It was assumed much of this area would be isolated by ice cover and frazil ice. Therefore, the Macleod Cairn section was truncated and the Sawchuck's section was not used.
 3. The RSI portion of the Sisson's section was assumed to be blocked by ice and all the flow channeled through the LSI portion of the section.
 4. The West Peace section appears to be influenced by a large bar on the LB so it was also eliminated.
- Seven sections were ultimately used to represent the reach in the mixing simulations.
- The water level elevations were obtained at the intermediate sections by linear interpolation between the surveyed elevations at MacKenzie Cairn and the Peace River boat launch. The ice bottom elevations were estimated by subtracting the average ice thickness.

Table F.3 Cross sections MacKenzie Cairn to Peace River Boat Launch.

X-Section	Source	km	Water Level m	Ice Bot. m	Distance m
MacKenzie Cairn	NRBS	857.60	319.18	318.00	8300
Jail	AEP not used	854.65	318.23	317.13	11250
Purcell's	AEP used	853.15	317.75	316.65	12750
Old Highway	AEP used	850.65	316.94	315.84	15250
MacLeod Cairn	AEP used	849.45	316.55	315.45	16450
	truncated				
Umbach's	AEP used	847.55	315.94	314.84	18350
Sawchucks	AEP not used	845.50	315.28	314.18	20400
Sisson's	AEP used	843.70	314.70	313.60	22200
	truncated				
West Peace	AEP not used	842.00	314.15	313.05	23900
Peace River Boat Launch	NRBS	841.10	313.86	312.86	24800

NRBS Northern River Basin Study

AEP Alberta Environment Protection HEC2 file

Appendix F.6 Peace River Boat Launch Concentration Profiles

Minor discrepancies exist between the q/Q hole locations labeled on NRBS Figure 3.5b and those scaled from NRBS Figure 4.1c (see Table F.4). Some of the difference may be due the use of either the measured or estimated q/Q curve for interpolation. In other cases the NRBS report seems to have misinterpreted the q/Q curves. The measured curves were used for the interpolations performed by the author.

- The interpolated values from the measured q/Q curve in NRBS Figure 4.1c were used for replotting of the concentration results.

Table F.4 Hole locations at Peace River Boat Launch.

Hole No.	Dist from LB (from Fig 3.5b)	w/W	interp q/Q (from Fig 4.1c)	reported q/Q (from Fig3.5b)
8	130	0.325	0.086	0.11
14	190	0.475	0.372	0.34
18	230	0.575	0.597	0.55
21	260	0.650	0.758	0.69
27	320	0.800	0.928	0.89

Appendix F.7 Peace River Dosage Distribution

- The dosage distribution was determined by integrating the C-t curves rather than using Figure 4.5a in the NRBS report. The results are shown in Table F.5. The dosages were normalized using the mass recovery ratio (0.812) determined by integrating the transverse dosage distribution with respect q. The mass recovery determined by integration was used rather than the value shown in Table 2.5 of the NRBS report.

Table F.5 Dosage distribution at Peace River Boat Launch.

Hole No.	w/W	interp q/Q (from Fig 4.1c)	Measured Dosage ($\mu\text{g hr/L}$)	Normalized Dosage ($\mu\text{g hr/L}$)
8	0.325	0.086	0.72	0.96
14	0.475	0.372	8.34	11.12
18	0.575	0.597	12.99	17.32
21	0.650	0.758	9.42	12.56
27	0.800	0.928	1.30	1.73

Appendix F.8 Peace River Boat Launch to Daishowa Plant Reach

- A number of sections were available in this reach as indicated in Table F.6.
 1. The section designated as Dick's Diving was not used because it was badly skewed across the channel.
 2. Attempts to use the remaining sections "as is" met with limited success. If flow occurred in the right and left channels around Bewley Island a division in the tracer plume results and there is a velocity difference ~~in~~ the two paths. In the simulation attempts this resulted in a multiple peaked waveform. However this type of waveform is not evident in the concentration measurements at the Daishowa Plant. The left channel near the end of the island is very shallow in comparison to the right. Considering this only the right channel around Bewley Island was used. In effect the left channel was considered blocked due to ice accumulation in the shallows.
- Nine sections were used to represent the reach in the mixing simulations.
- The water level elevations were obtained at the intermediate sections by linear interpolation between the surveyed elevations at the Peace River boat launch and the

Daishowa Plant. The ice bottom elevations were estimated by subtracting the average ice thickness.

Table F.6 7 Cross sections Peace River Boat Launch to Daishowa.

X-Section	Source	km	Water Level m	Ice Bot. m	Distance m
Peace R.	NRBS	841.10	313.86	312.86	24800
Wood	AEP used	840.40	313.61	312.61	25500
PeaceR WSC	AEP used	839.55	313.31	312.31	26350
Bewley Is.	AEP used	838.55	312.96	311.96	27350
	truncated				
Czuy House	AEP used	837.10	312.45	311.45	28800
	truncated				
Dick's Diving	AEP not used	835.22	311.79	310.79	30680
Six Mile Farm	AEP used	831.50	310.48	309.48	34400
Seven Mile Bend	AEP used	829.55	309.80	308.80	36350
Birch Is.	AEP used	824.30	307.95	306.95	41600
Daishowa	NRBS	823.50	307.67	306.67	42400

NRBS Northern River Basin Study

AEP Alberta Environmental Protection HEC2 file

Appendix F.9 Daishowa Concentration Profiles

- Minor discrepancies exists between the q/Q hole locations labeled on NRBS Figure 3.5c and those scaled from Figure 4.1d (see Table F.8). Some of the difference may again be due the use of either the measured or estimated q/Q curve for interpolation (quite a larger deviation is evident in the central region of the channel for the two curves). In other cases the NRBS report seems to have misinterpreted the q/Q curves. The measured curves were used for the interpolations performed by the author.
- The interpolated values from the measured q/Q curve in Figure 4.1d were used for replotting the concentration results.

Table F.8 Hole locations at Daishowa.

Hole No.	Dist from LB (from Fig 3.5c)	w/W	interp q/Q (from Fig 4.1d)	reported q/Q (from Fig3.5c)
6	190	0.449	0.144	0.18
9	249	0.596	0.467	0.38
11	272	0.654	0.646	0.54
13	303	0.731	0.807	0.70
16	355	0.861	0.981	0.91

Appendix F.10 Daishowa Dosage Distribution

- The dosage distribution was determined by integrating the C-t curves rather than using Figure 4.5b in the NRBS report. The results are shown in Table F.9. The dosages were normalized using the mass recovery ratio (0.775) determined by integrating the transverse dosage distribution with respect q. The mass recovery determined by integration was used rather than the value shown in Table 2.5 of the NRBS report.

Table F.9 Dosage distribution at Daishowa

Hole No.	w/W	interp q/Q (from Fig 4.1d)	Measured Dosage ($\mu\text{g hr/L}$)	Normalized Dosage ($\mu\text{g hr/L}$)
6	0.449	0.144	3.82	5.31
9	0.596	0.467	7.26	10.08
11	0.654	0.646	9.82	13.64
13	0.731	0.807	9.18	12.75
16	0.861	0.981	2.31	3.21